iconst est'22

September 7-9, 2022
5th International Conferences on Science and Technology
Budva, Montenegro

Engineering Science and Technology

Abstracts & Proceedings Book

ICONST EST 2022

International Conferences on Science and Technology

Engineering Science and Technology

September 7-9, 2022 in Budva, MONTENEGRO

ABSTRACTS
&
PROCEEDINGS BOOK

ICONST EST 2022

International Conferences on Science and Technology

Engineering Science and Technology

September 7-9, 2022 in Budva, MONTENEGRO

Editors

Dr. Mustafa Karaboyacı
Dr. Kubilay Taşdelen
Dr. Abdullah Beram
Dr. Hamza Kandemir
Dr. Ergin Kala
Dr. Serkan Özdemir

Technical Editors

MSc. Şerafettin Atmaca
MSc. Doğan Akdemir
Ma. Fıratcan Çınar

Cover design & Layout
Dr. Okan Dağ

Copyright © 2022

Published by

ICONST EST 2022

International Conferences on Science and Technology

Engineering Science and Technology

September 7-9, 2022 in Budva, MONTENEGRO

Scientific Honorary Committee

Prof. Dr. Rade RATKOVIC, Fakultet za biznis i turizam Budva University, MONTENEGRO
Prof. Dr. İlker Hüseyin ÇARIKÇI, Suleyman Demirel University, TURKEY
Prof. Dr. İbrahim DİLER, Isparta University of Applied Sciences, TURKEY
Prof. Dr. Edmond HAJRİZİ, University of Business and Technology, KOSOVO
Prof. Dr. Bujar DEMJAHA, Rector of AAB College, KOSOVO
Prof. Dr. Vujadin VEŠOVİĆ, Faculty of Transport Communications and Logistics, MONTENEGRO
Prof. Dr. Samedin KRRABAJ, University of Prizren, KOSOVO
Prof. Dr. Fadıl HOCA, International Vision University, MACEDONIA
Prof. Dr. Ahmad Umar, Editor of Science of Advanced Materyals, KINGDOM OF SAUDI ARABIA
Prof. Dr. Kürşad Özkan, Isparta University of Applied Sciences, TURKEY
Prof.Dr. Harun Parlar, Parlar Research & Technology-PRT, GERMANY
Prof. Dr. Naime BRAJSHORİ, Kolegji Heimerer, KOSOVO
Prof. Dr. Nermina HADŽİGRAHİĆ, University of Tuzla, BOSNIA AND HERZEGOVINA
Prof. Dr. Kseanela SOTİROFSK, University of Durres, ALBANIA

Organizing Committee

Dr. Mustafa Karaboyacı, Suleyman Demirel University, TURKEY
Dr. Hamza Kandemir, Isparta University of Applied Science, TURKEY
Dr. Serkan Özdemir, Isparta University of Applied Science, TURKEY
Dr. Abdullah Beram, Pamukkale University, TURKEY
Dr. Kubilay Taşdelen, Isparta University of Applied Sciences, TURKEY
Dr. Ergin Kala, University of Prizren, KOSOVO
Dr. Joanna Machnik-Slomka, Silesian University of Technology, POLAND
Dr. Elzbieta Pawlowska, Silesian University of Technology, POLAND
Dr. Fatmir Mehmeti, Prizren University, KOSOVO
Prof Dr. Indrit Bimi, Durres University, ALBANIA

Technical Committee

MSc. Kubilay Yatman, Isparta University of Applied Sciences, TURKEY
MSc. Doğan Akdemir, Balıkesir University, TURKEY
MSc. Şerafettin Atmaca, Isparta University of Applied Sciences, TURKEY
MSc. Tunahan Çınar, Düzce University, TURKEY
Ma. Fıratcan Çınar, Isparta University of Applied Sciences, TURKEY

ICONST EST 2022

International Conferences on Science and Technology

Engineering Science and Technology

September 7-9, 2022 in Budva, MONTENEGRO

Scientific Committee

Dr. Alev Akpınar Borazan, Bilecik Seyh Edebali University, Turkey
Dr. Amer Kanan, Al-Quds University, Palestine
Dr. Andrea G. Capodaglio, University of Pavia, Italy
Dr. Aybeyan Selim, International Vision University, North Macedonia
Dr. Apostolos Kiritsakis, Alexander Tech. Educational Ins. of Thessaloniki, Greece
Dr. Ayodeji Olalekan Salau, Obafemi Awolowo University, Nigeria
Dr. Bülent Derviş, International Vision University, North Macedonia
Dr. Cristian Fosalau, Technical University of Iasi, Romania
Dr. Driton Vela, University of Business and Technology, Kosovo
Dr. Eda Mehmeti, University of Business and Technology, Kosovo
Dr. Elvida Pallaska, University of Business and Technology, Kosovo
Dr. Ermek A. Aubakirov, Al – Farabi Kazakh National University, Kazakhstan
Dr. Fecir Duran, Gazi University, Turkey
Dr. Gauss M. Cordeiro, Federal University of Pernambuco, Brazil
Dr. Gholamhossein Hamedani, Marquette University, USA
Dr. Gülcan Özkan, Süleyman Demirel University, Turkey
Dr. Hamid Doost Mohammadian,FHM University of Applied Sciences, Germany
Dr. Ines Bula, University of Business and Technology, Kosovo
Dr. Izabela Zimoch, Silesian Universum of Technology, Poland
Dr. Joanna Boguniewicz-Zabłocka, Opole University of Technology, Poland
Dr. Kari Heliövaara, University of Helsinki, Finland
Dr. Kłosok-Bazan Iwona, Opole University of Technology, Poland
Dr. Kubilay Akçaözoğlu, Niǧde Ömer Halisdemir University, Turkey
Dr. Leyla Tavacıoğlu, Istanbul Technical University, Turkey
Dr. Lulzim Beqiri, University for Business and Technology, Kosovo
Dr. Mathew Ademola Jayeola, Obafemi Awolowo University, Nigeria
Dr. Mehmet Kitiş, Suleyman Demirel University, Turkey
Dr. Merita Barani, University for Business and Technology, Kosovo
Dr. Meruyert Kaygusuz, Pamukkale University, Turkey
Dr. Mirosław Kwiatkowski, AGH- University of Science And Technology, Poland
Dr. Mohd Aswadi Bin Alias, Unıversıty Kuala Lumpur- Bmı, Malaysia
Dr. Muhamet Ahmeti, University of Business and Technology, Kosovo
Dr. Naushad Ali Mamode Khan, University of Mauritius, Mauritius
Dr. Nicholas Baldacchino, Malta College of Arts, Science & Technology, Malta
Dr. Nuray Benli Yıldız, Duzce University, Turkey
Dr. Rahmon Ariyo Badru, Obafemi Awolowo University, Nigeria
Dr. Ramazan Şenol, Suleyman Demirel University, Turkey
Dr. Salina Muhamad, Universiti Selangor, Malasıa
Dr. Sami Makolli, University of Business and Technology, Kosovo
Dr. Serhat Oğuzhan Kıvrak, Hitit University, Turkey
Dr. Shpend Dragusha, University of Business and Technology, Kosovo
Dr. Şule Sultan Uğur, Suleyman Demirel University, Turkey
Dr. Valmir Hoxha, University of Business and Technology, Kosovo
Dr. Vehebi Sofiu, University of Business and Technology, Kosovo
Dr. Vincenzo Naddeo, University of Salerno, Italy
Dr. Zhandos T. Mukayev, Shakarim State University of Semey, Kazakhstan

ICONST 2022

International Conferences on Science and Technology
Engineering Science and Technology
Life Science and Technology
Natural Science and Technology
September 7-9, 2022 in Budva, MONTENEGRO

Dear Readers;

The fifth of ICONST organizations was held in Budva/Montenegro between 7-9 September 2022 with the theme of '***science for sustainable technology***' again. In recent years, weather changes due to climate change have reached a perceptible level for everyone and have become a major concern. For this reason, scientific studies that transform technological progress into a sustainable one is seen as the only solution for humanity's salvation. Here we ask ourselves "which branch of science is responsible for sustainability?". Sustainability science is an interdisciplinary field of study that covers all basic sciences with social, economic, ecological dimensions. If we consider technology as the practical application of scientific knowledge, the task of scientists under these conditions is to design products that consume less energy, require less raw materials, and last longer.

ICONST organizations organize congresses on sustainability issues of three main fields of study at the same time in order to present different perspectives to scientists. This year, 129 papers from 27 different countries presented by scientists in **ICONST Organizations**.

72 papers from 19 countries presented in our **International Conference on Engineering Science and Technology** organized under ICONST organizations. The total rate of countries excluding Türkiye is 52%. Türkiye is the country with the highest participation with 48%, followed by Poland 7%, Montenegro 5%, India 4%, Italy 4%, Kosovo 4%, Hungary 4%, Slovakia 4%, Afghanistan 2%, Czech Republic 2%, Iran 2%, Algeria 2%, Ethiopia 2%, Central African Republic 2%, Romania 2%, Russia 2%, Serbia 2%, North Macedonia 2% and Moldova %2.

31 papers from 9 countries presented in our **International Conference on Life Science and Technology** organized under ICONST organizations. The total rate of countries excluding Türkiye is 58%. Türkiye is the country with the highest participation with 42%, followed by Poland 16%, Bulgaria 12%, Slovakia 8%, Philippines 6%, Czech Republic 3%, Tunisia 3%, Algeria 3% and Switzerland 3%.

Finally, 26 papers from 10 countries presented in our **International Conference on Natural Science and Technology** organized under ICONST organizations. The total rate of countries excluding Türkiye is 65%. Türkiye is the country with the highest participation with 35%, followed by Serbia 19%, Slovakia 11.5%, Algeria 8%, India 8%, Croatia 3.8%, Ethiopia 3.8%, Hungary 3.8%, Kosovo 3.8%, South Africa 3.8%.

As ICONST organizations, we will continue to organize organizations with the value you deserve in order to exchange ideas against the greatest threat facing humanity, to inspire each other and to contribute to science. See you at your future events.

ICONST Organizing Committee

ICONST EST 2022

International Conferences on Science and Technology

Engineering Science and Technology

September 7-9, 2022 in Budva, MONTENEGRO

Contents

Comparison of Mechanical Properties of Hemp Fiber Reinforced Biocomposite Material and Plastic Materials: The Example of Çanakkale Furniture Industry

Ceren Ceylan[1], Emin Yakar[2*]

Abstract: Although the use of natural fibers as filling material or strengthening material in composite materials is a common and effective method, the structural properties of natural fibers appear as negative effects in composites. The main challenges of applying natural fibers in composites are: limited mechanical properties, excess water absorption, low fire resistance and processing and homogeneity. To overcome these difficulties with natural fiber-polymer composites (NFPCs), a number of chemical and physical modification methods must be applied for polymer matrices and natural fibers. The aim of this study is to investigate the mechanical properties of plastic materials produced with hemp fiber reinforced composite materials and ABS raw materials used in Çanakkale Furniture Industry. If it is necessary to determine the limits of the study, only the comparison of the mechanical properties will be made. Fourier transfer infrared spectroscopy (FTIR), tensile tests, contact angle method, bending and impact tests, scanning electron microscopy (SEM), polarized microscope and optical microscopy will be used for these comparisons.

Keywords: NFPC, Composites, ABS raw materials, Hemp Fiber

[1] Çanakkale Onsekiz Mart University, Graduate School of Natural And Applied Science, Department of Bioengineering and Material Engineering, Çanakkale, Türkiye
[2] Çanakkale Onsekiz Mart University, The Faculty of Engineering, Department of Material Science and Engineering, Çanakkale, Türkiye
* Corresponding author: eyakar@comu.edu.tr

Classification of Earthquake Magnitudes in the Aegean Region into Seismic Zones by Clustering Analysis

Hasan Hüseyin Pay[1], Ecir Uğur Küçüksille[1*], Hatice Öncel Çekim[2], Gamze Özel Kadılar[2], Senem Tekin[3]

Abstract: All over the world, earthquakes cause great loss of life and property. For this reason, a large number of studies have been made and continue to be done on the estimation of earthquake magnitudes. For this purpose, both statistical methods and artificial intelligence techniques are used. In order to estimate the magnitude of earthquakes occurring in a region more effectively, examining that region by dividing it into sub-clusters gives more effective and accurate results. In this study, clustering analysis carried out using the data compiled from three different earthquake catalogs, which took place within the Aegean Region + 200 km buffer zone. K-Means algorithm was used in cluster analysis and k value was determined as three with the help of Silhouette Score scale. The statistical properties of the obtained clusters were evaluated, as a result of normality tests for within clusters and Kendall's correlation test for inter-cluster relations. As a result, it was determined that clusters other than cluster1 did not have a normal distribution and there was no relationship between clusters.

Keywords: Earthquake, K-Means, Clustering, Cluster Analysis

[1] Suleyman Demirel University, Faculty of Engineering, Computer Engineering, Isparta, Türkiye
[2] Hacettepe University, Faculty of Science, Statistics, Ankara, Türkiye
[3] Adıyaman University, School of Technical Sciences, Mining and Mineral Extraction, Adıyaman, Türkiye
* Corresponding author: ecirkucuksille@sdu.edu.tr

Heritage and Society

Fernanda Cantone[1*]

Abstract: Regeneration is a process referred to the "formation of new, to reproduce" and in particular to the "process that restores a previous condition of dignity, glory, greatness, returns initial properties"; it becomes a scenario of action based on the commonality with other disciplines, most notably sociology. The field of action is the existing buildings that was constructed through the overlap of cultures, native also: to restore what Salvatore Settis called the sick man: the Italian building heritage. The concept of regeneration also includes the idea of continuity, to prolong the useful life of an asset or urban building, by returning the values lost in time. It means, above all, restore the quality of urban life and social relationships that define a built environment. The regeneration process put into play the user requests, to involve them in decision-making, to share and discuss with them the architectural and redevelopment choises. This is not to be subjugated by the will of the users but use their experience, their knowledge of the place as a living space for the definition of the scenarios project. Users are the community, made up of older people whose knowledge is helpful to identify the changes, young people to understand what they would like in the future, the adults to understand the problems of the place. The task of regeneration is to improve the quality of the urban environment and return to the place its identity, restore a lost soul in time, through forms of association and social experimentation, areas of innovation and research. In this sense, the project intervention productions a decisive role in the process of developing a strategy: you have to work for projects, to identify local factors, for the decay of urban quality. The case study is an area next to the historical center of Adrano, interesting town area of Catania, full of history and buildings of cultural value. It is a zone defined as La Linea, for the presence of the railroad and, subsequently, for the burying of the same. The vacuum left by the railroad is unused, full of rubbish and meeting place for drug addicts and drug dealers. n this context, so near to the historical center, there are both buildings of the past and new buildings, in a chaotic and indefinite mix. The inhabitants are relegated to public spaces confined, no green, no possibility of aggregation. The unfinished defines the district. he research aims to identify strategies for a political project of regeneration and improvement of urban and construction quality, relating to recovery of buildings and spaces, their connection to the historic center, the regeneration.

* Corresponding author: fcantone@unict.it
[1] University of Catania, SDS Architecture, DICAR Department, Italy

Structural and Morphological Properties of Ns.BioChar/ZnO Adsorption

H. Rahali, H. Menasra, S. Djebabra

Abstract: A novel Biochar/ZnO composite has been synthesized in a single step from charcoal. The chemical activation of the Bio-carbon with a solution of ZnCl2 at 0.136 mole and neutral pH gives a pure composite at T= 600°C which is characterized by XRD, SEM, BET, FTR, and UV-Visible for the study of copper adsorption. The adsorption kinetics appropriate to the Experimental data is the pseudo-second order kinetics. The maximum adsorption capacity for copper (II) based on the Langmuir model is 1272 mg g-1 at 20°C. Thus, the low cost synthesis of the ZnO Bio-composite is a promoter axis for the absorption of heavy metals such as copper.

Keywords: Biochar, Composite, Copper, DRX.

* Corresponding author: s.djebabra@univ-biskra.dz
[1] University of Biskra, Algeria

In Vitro Meat in the Light of Natural/Artificial Argument

Luca Lo Sapio[1*]

Abstract: The growing demand of food supplies within the developed and developing countries confronts us with the need to find new ways to satisfy our nutritional urges. In particular, the livestock farming causes a great amount of GHG (nearly 10% of all anthropogenic emissions), the exploitation of soil and water, the mistreatment of non-human animals, and various troubles for human health. Plant-based meat, in vitro meat, insects, and algae were suddenly considered an intriguing new opportunity for and eco-sustainable food system.

The very aim of this contribution is to focus on in vitro meat. This technique is opposed by a vast array of arguments ranging from the safeness of a synthetic product as such to the very nature of cultured meat. According to most of the natural/artificial argument advocates, synthetic meat has nothing to do with natural product. In my intervention I shall argue that the appeal to nature is flawed for several serious reasons so as the vigorous contrast to artificial. First, I will show that the natural/artificial argument, regarding in vitro meat, seems to be not so different from the arguments raised against in vitro fertilization or the use of genome editing techniques in agriculture (OGMs). Second, I will discuss a thought experiment, alien genesis, through which I hope to dismantle the idea that a valuable moral assessment could be grounded in the concept of essence. All in all, the nature of something lies in its properties, not in an alleged essence. Finally, I will show that the concept of nature is not suitable even for the traditional way of producing meat.

Keywords: In vitro meat, Sustainable food system, Natural, Artificial.

* Corresponding author: luca.losapio@unito.it
[1] University of Turin, Italy.

Formulation of Novel Culture Propagation Media with Dairy By-Products for Fermented Milk Products Industry: Experiments on Yogurt Cultures

Hale İnci Öztürk[1*], Nihat Akın[2]

Abstract: TW60 is a culture growth medium designed for the safe propagation of starter cultures used in the dairy industry and is often used on a commercial scale in the manufacture of fermented milk products. This study aimed to develop an alternative growth medium to TW60 medium for yogurt cultures by using dairy industry by-products to reduce the production cost. Buttermilk (BM), cheese whey, and yogurt whey (YW) are by-products obtained after the production of butter, various types of cheese, and strained yogurt, respectively. These products were used in the design of the media. A total of 4 different formulations were prepared: 10% BM (I), 5% BM and 5% YW (II), 10% YW (III), and TW60 (IV). Except for TW60, 7% whey powder and 0.25% buffer containing vitamin C and yeast extract were added to each formulation. Afterward, the acid-forming abilities and viable cell numbers (when pH 4.6 was reached) of Streptococcus (S.) thermophilus and Lactobacillus (L.) bulgaricus in each sterilized media (45 min at 95 °C) were determined and the results were compared with the commercial medium, TW60. In terms of its cell counts, the best growth for S. thermophilus was observed in TW60 and medium containing 10% BM. Increases in colony counts for L. bulgaricus were significantly higher than TW60 in new formulations. The highest number of L. bulgaricus was determined in medium containing 10% BM. . Regarding the acidification kinetics, the maximum acidification rate (Vmax) of S. thermophilus was determined in TW60 and medium containing 5% BM and 5% YW (12.95 and 14.38, respectively), and the shortest TpH4.6 was detected in these media. For L. bulgaricus, on the other hand, the highest Vmax (22.33) was determined in the medium containing 10% BM while the lowest Vmax (10.50) was detected in TW60.

Keywords: Yogurt Cultures, Acidification Kinetics, Growth Media, TW60, Buttermilk, Yogurt Whey.

[1] Konya Food and Agriculture University, Konya, Türkiye
* Corresponding author: inci.ozturk@gidatarim.edu.tr

Structural Characterization Analysis of Architect Sinan's Şehzade Mosque

Esra Şahin[1*]

Abstract: One of the greatest masters in the history of world architecture and engineering is undoubtedly Architect Sinan. There are many works that he has built. When Architect Sinan is mentioned, the first building type that comes to mind is mosques. Architect Sinan's Şehzade Mosque is his apprenticeship, Süleymaniye Mosque is his journeyman's work, and Selimiye Mosque is his master's work, and these mosques have been a touchstone for him. For this reason, Architect Sinan Mosques have been the subject of many studies in terms of artistic and engineering. Walls, columns, buttresses, arches, domes and foundations are the main bearing elements of historical mosque-like structures. It is seen that many valuable studies have been done on these elements in the general literature. Columns and walls in historical buildings are vital load-bearing elements for carrying vertical and horizontal loads. In this study, the structural characterization analysis of the Şehzade Mosque, one of the mosques designed by Sinan, was examined. Structural characterization analysis includes the examination of columns, one of the structural elements of the Şehzade Mosque. The load bearing capacities of the columns were determined by the classical stress equation. High vertical load capacity values were determined for all columns. As a result, it has been understood that the Şehzade Mosque has designed and built its columns to withstand vertical loads with a very high level of safety and to have a significant level of strength against horizontal loads.

Keywords: Architect Sinan, Şehzade Mosque, Column Properties, Analysis

[1]İstanbul Aydın University, Türkiye.
* Corresponding author: esrasahin3@aydin.edu.tr

The Geometry of The Railway Transition Curves Between Theory and Practice

Orban Zsolt Laszlo[1*]

Abstract: In time, with the passage of traffic, the railway track deforms and especially the railway curves lose their original designed shape. This degradation process is a self-generating one. In order to restore the geometric elements of a railway track, respectively realign the railway curves to their original shape, continuous monitoring and intervention is necessary.
The paper presents a curve realignment method used in Romanian railways maintenance as well as theoretical aspects of the railway transition curves geometry compared with in situ measurements collected for a period of ten years. The aim of the paper is to highlight certain aspects regarding the deformation in time of the geometry of the railway curves which may lead to the reconsideration of the design criteria of these curves.

Keywords: Railway, Track, Curve, Transition, Versine, Realignment.

* Corresponding author: zsolt.orban@cfdp.utcluj.ro
[1]Technical University of Cluj-Napoca, Romania

Isolation of Essential Oil from Lavandula angustifolia by Using Supercritical Carbondioxide Extraction, and Evaluation of Antimicrobial and Antioxidant Activities

Ayça Gedikoğlu[1*]

Abstract: Lavandula angustifolia also commonly known as lavender is an aromatic plant with strong fragrance. Essential oil of lavender has been used in food, cosmetic, and pharmaceutical industries. Bioactivity and chemical composition of lavender essential oil depends on many factors such as geography, climatic conditions, extraction techniques etc. Therefore, the aim of this study was to determine the chemical composition, yield (%), antimicrobial and antioxidant activity of lavender essential oil obtained by one of the green extraction techniques called supercritical carbondioxide extraction. The chemical composition of the lavender essential oil was analyzed by Gas Chromatography Mass Spectrometry (GC-MS). Disk diffusion assay and minimum inhibitory concentrations (MIC) of the lavender essential oil was determined for 4 bacteria. The antioxidant activity of lavender essential was carried out according to the ferric reducing antioxidant power (FRAP) assay. The results of the gas chromatograph-mass spectrometry analysis showed that chemicals found in lavender the highest in order were linalyl acetate (28.72%), lavandulol (27.48%), 3-Cyclohexen-1-ol, 4-methyl-1-(1-methylethyl) (6.26%), lavandulyl acetate (5.59%), and caryophyllene oxide (4.51%). Essential oil yield was 2.94% and demonstrated moderate antimicrobial activity against all tested bacteria. The highest antimicrobial activity was shown against Bacillus cereus. The ferric reducing power of lavender essential oil was 5.086 μM Fe+2/g. The results suggested that chemical composition of the lavender essential oil was very diverse and its bioactivity was related to the chemical composition and their amount.

Keywords: Aromatic plant, Salmonella enteritidis, Pathogen, Volatile compounds, Terpenes.

1 Konya Food and Agriculture University, Konya, Türkiye.
* Corresponding author: ayca.gedikoglu@gidatarim.edu.tr

Lane Detection on Model Electric Vehicle Using Deep Learning Algorithm

Mustafa Tumbek[1]*, Selami Kesler[1], Omer Boyaci[1]

Abstract: In recent years, oil prices have been increasing as fossil fuel reserves have become increasingly depleted. In addition, the use of oil in fossil fuel vehicles is damaging the environment. Therefore, interest in electric vehicles has been growing rapidly in recently. Electric vehicles provide many advantages. In particular, self-driving electric vehicles will solve problems such as traffic accidents and traffic jams. The vehicle that will drive autonomously must have the ability to detect lanes and objects on the road. Lane detection on electric vehicle aids in vehicle positioning. However, lane detection remains a problem that must be completely solved before autonomous cars can be used. Many studies on lane detection, which have been going on for many years, show that deep learning-based algorithms in artificial intelligence have achieved high performance.

In this study, lane detection algorithms, one of the most important and indispensable tasks of autonomous driving, are tested and improved. In this context, Nvidia Jetson TX2 control card and two webcams in different directions were installed on the mini electric vehicle Racecar. The purpose of using more than one camera here is to combine the images from the cameras to create a wide-angle view. Also, a 50 meters long road and traffic scenario was designed for a small-scale vehicle model. In addition, in order to investigate whether accurate lane detection is achieved, poor light and unclear lanes are added to design as noise in a real environment. The results show that deep learning-based algorithms can perform lanes detection more accurately than many methods. However, there are a number of important issues that need to be resolved. In future work, a faster algorithm can be developed for faster vehicle response. Also, the effectiveness of the algorithms can be compared in bad weather conditions, high speed driving and on different types of roads.

Keywords: Line Detection, Model Electric Vehicle, Deep Learning, Autonomous Vehicle.

* Corresponding author: mustafatumbek@pau.edu.tr
[1] Department of Electric and Electronics Engineering, Pamukkale University, 20160 Denizli, Türkiye.

Characterization of Soil for Road Shoulders Mixed with Reclaimed Asphalt Pavement Waste

Saber Shah Saberi[1], Dr. Azman Mohamed[2]*

Abstract: The use of recovered asphalt pavement can reduce the amount of new bitumen and aggregates used in pavement construction and rehabilitation (RAP). RAP is a waste product that results from the removal of an old or damaged pavement surface. Although it has been used since the 1970s, and numerous recommendations for using RAP in the new mixture have been made, there is only a little research available. Because the materials used are recycled, it is also cost-effective and environmentally friendly. The purpose of this study is to characterize soil that has been blended with reclaimed asphalt pavement (RAP) for use on the local road shoulder. RAP is one of the rehabilitation procedures used to repair a deteriorated surface by removing the upper pavement and replacing it with new pavement. According to an earlier study, mixing dirt with different materials improves the finding. The goals of this study are to establish the material qualities of soil and RAP, determine the optimum moisture content of material and degree of compaction for road shoulders, and determine the appropriate mix proportion of soil and RAP for road shoulders using the California Bearing Ratio (CBR) test. The Atterberg limit, liquid limit, and plastic limit for soil were evaluated on a sample of soil and RAP. For soil and RAP, a sieve analysis was performed. Compaction tests for soil and RAP were carried out with a mixture of 10S, 2S8RAP, 4S6RAP, 6S4RAP, 8S2RAP, and 10RAP, as well as CBR tests for soil and RAP. According to the results of the laboratory test, 20% of RAP (8S2RAP) had a better-mixed proportion for the road shoulder. As a result, repurposed materials like RAP can be used as road shoulder material.

Keywords: Reclaimed asphalt, Reuse asphalt

1 Shaikh Zayed University, Afghanistan.
* Corresponding author: azmanmohamed.kl@utm.my

Ink Material Based on Alginate/Psyllium Husk Powder Blends for 3D Printing Applications

Sevil Cikrikci Erunsal[1]*, Erinc Bahcegul[2], Gokce Bahcegul[3]

Abstract: 3D printing (3DP) has opened a way to fabricate complex geometrical structures for different applications such as food, chemical or biomedical related studies. Different than conventional techniques, 3DP can transform computer-aided models into physical objects via layer-by-layer printing. Hydrogels are one of the most suitable classes of ink materials used in extrusion-based 3D printing. Utilization of natural polymers offers a non-toxic nature, but they can also be used as a blend of two or more polymers to enhance their properties like mechanical and rheological features. There are so many factors affecting printability success such as material and printing parameters. The aim of this study was to investigate printability of alginate (ALG) gel solution replaced with psyllium husk powder (PSY). First, blends of ALG (2.5%, 5%, 7.5%) and PSY (2.5%, 5%, 7.5%) at equal concentrations were studied with a custom-made 3D printer to obtain optimum combination in terms of viscosity and printability. Blend with equal portion of 5% ALG and 5% PSY was found as the most acceptable formulation to be printed. Then, the effect of different layer height (0.1, 0.2 and 0.3 mm), extrusion multiplier (EM) (between 1.5 and 3), CaCI2 concentration (between 2 and 10%) as post-process gelling agent and washing with ethanol after printing were analyzed for printability. Temperature, printing speed, infill percentage, number of layers and inner nozzle diameter were kept constant as room temperature, 1500 mm/min, 41%, 3 and 0.84 mm, respectively. Viscosities of 5% ALG, 5% PSY and total 5% ALG/PSY blend solutions were obtained as 940 ± 5 mPa.s, 1134 ± 5.3 and 1877 ± 6.08 mPa.s in vibro-viscometer, respectively. Among blends, grid models printed from ALG/PSY blends by using EM as 2, layer height as 0.3 mm and postprocess with 2% CaCl2 solution had the best overall appearance with a printability value of 0.891 ± 0.057. The total area of the cells inside this grid model reached to around 93% of the ideal (intended) area. This study promoted future studies about the use of PSY-ALG combinations as ink material in different areas for different purposes like carrier systems for bioactive agent/drugs.

Keywords: 3D printing, printability, alginate, psyllium

[1] Konya Food and Agriculture University, Faculty of Engineering and Architecture, Department of Food Engineering, 42080, Konya, Turkey
[2] Konya Food and Agriculture University, Faculty of Engineering and Architecture, Department of Bioengineering, 42080, Konya, Turkey
[3] Middle East Technical University, Department of Polymer Science and Technology, 06800, Ankara, Turkey
* Corresponding author: sevil.cikrikci@gidatarim.edu.tr

Analysis and Modeling of Biological Processes with the Use of The Micro-Flow System

Student Sebastian[1]*, Staśczak Alicja[2], Fujarewicz Krzsztof[3]

Abstract: Microfluidics seems to be particularly important as most processes involve micro-flow, from transport through cell walls, through oxygen diffusion into the lungs, to blood flow in the capillaries. Microfluidic perfusion cultures for mammalian cells provide an alternative to standard macroscale cell culture systems in single cells analysis. The aim is to provide a near-real cell culture environment, which is one that can be ensured by a microreactor. The functional principle of this solution was to produce a microchip. Its main premise was the application of a hydropneumatic system to control the microcircuit by manipulating the channels supplying fluids to the reaction chamber. In the project, a microchip created from a PDMS gel was applied as part of the environment for cell growth. Prepared HELA tumor cells with fluorescently labeled histone H2B were introduced into the system to assess their cell cycle length and to record monitoring of the movements of individual daughter cells. Thus, the growth characteristics of the cells can be determined. The experiment made observations using a fluorescence microscope with automatic image acquisition software. The resulting images were analyzed using an algorithm. It allows for automatic cell counting and labeling. The precisely controlled cell culture conditions are important to cell division analysis, particularly the total cell cycle duration for mother-daughter, sisters cousins cells. In our study, we have analyzed the cell cycle duration in HeLa cells.

Keywords: Mathematical biology, Bioengineering, Microfluidics.

1 Silesian University of Technology, Poland.
* Corresponding author: sebastian.student@polsl.pl

Changes in Use of Educational Computer and Communication Technologies and Approach of Instructors to Changes

Fehmi Skender[1*], Yalçin İşler[2]

Abstract: The use of computer and internet technologies has increased rapidly in recent years. Especially the technologies used in industrial production processes are developing at a dizzying pace due to the increasingly serious competition conditions. Thus, human and technology interaction has become indispensable in all areas of life. This rapid change in technology affects other sectors as well. For example, all educational levels, especially vocational education, are also affected by these changes. Due to the rapid increase in the need for trained human resources to use these current technologies in production, it is natural that the use of computer and internet technologies in education will increase.

Under normal circumstances, some people find it difficult to accept innovations, but they must adapt in the face of compelling events. Especially with the effect of the pandemic that has come to the fore, the contribution of computers and different technological tools in education has increased recently, and the use of these technologies by the entire society has become mandatory. This study gives information about educational software, which is being used more and more effectively in education. While conducting the study, the thoughts and attitudes of teachers working in the Republic of North Macedonia and the parents of the students were compiled with the electronic survey method. The collected data were analyzed by processing with data visualization tools. The results show that the current software used in education is directly affected by the development of technology. The collected information serves as a scientific basis for further research.

Keywords: Computer Supported Education, Visual data analysis, Interaction.

1 International Vizyon University, Gostivar, North Macedonia
* Corresponding author: fehmi.skender@vizyon.edu.mk

Simultaneous Removal of Heavy Metals and Cyanide by Photoelectrocoagulation

Ahmad Shahedi[1], Ahmad Jamshidi[2], Taghipour[3], Ahmad Khodadadi Darban[4]*

Abstract: One of the new methods used to remove contaminants from the effluent is the electrocoagulation method, which is sometimes combined with other methods to increase the removal efficiency of contaminants. In this study, in order to simultaneously remove nickel, cyanide, zinc, and copper, the combined method of photo-electrocoagulation was used along with an oxidizing agent, namely hydrogen peroxide (Hp). In addition, the effects of factors affecting the removal efficiency were investigated, including pH, electrode arrangement, and current intensity. Due to the low efficiency of conventional methods in removing cyanide and heavy metals simultaneously, this new combined method (photo-electrocoagulation oxidation) was employed. Optimum conditions required for performing the photo- electrocoagulation-oxidation technique included the use of an electric current of 300 mA at pH=10 for 60 minutes, Fe-SS electrodes with an electrode distance of 5 cm, and hydrogen peroxide at a rate of 4 mg/l. According to these study findings, when the combined method of photocatalyst-electrocoagulation-oxidation (Hp) was used, the highest removal efficiencies of nickel, cyanide, zinc, and copper were 85, 96, 94, and 98%, respectively. The results showed that the use of combined photo-electrocoagulation-oxidation method increased the efficiency of simultaneous removal of pollutants by 10% compared to conventional electrocoagulation method. The reason for the increase in removal efficiency is the production of hydroxyl radicals simultaneously with the formation of coagulants produced by the electrocoagulation process. In general, the results revealed the effectiveness of this method in the simultaneous removal of cyanide and meta.

Keywords: Zinc, Nickel, Copper, Cyanide, Photo electrocoagulation.

1 Tarbiat Modares University, Tehran, Iran
* Corresponding author: akdarban@modares.ac.ir

Influence of Steel Scrap in the Charge on Metallurgical Quality and Cast Iron Properties

Alena Pribulova[1], Vladimir Sabik[2], Jozef Petrik[3], Peter Blasko[4], Peter Futas[5]*

Abstract: Cast iron castings represent more than 70% of the world's production of castings. Many factories influence their final quality. In the field of metallurgy, there are many factors influencing the final quality of cast iron. These are mainly charge materials, chemical composition, metallurgical preparation up to the final casting process. Even small deviations from metallurgical processing lead to fluctuations in melt quality and the occurrence of casting defects. Charge materials has a significant impact on the quality of cast iron, especially steel scrap, which is increasingly used from an economic and ecological point of view, especially when melting cast iron in electric furnaces. Cast iron produced from a higher content of steel scrap in the charge a higher hardness and tensile strength. On the other side, these cast irons has a higher tendency to chillout, brittleness, shrinkage, pearlitic microstructure, stresses and higher purity due to the difference in hardness at different wall thicknesses of the castings. It is the high hardness that is the problem in the final machining of castings. These negative properties are recorded mainly in heavy thick-walled castings with higher tensile strength and hardness. This negative effect is mainly due to the nitrogen content in the steel scrap, which is brought by the charge materials.

Based on these knowledges, operating melts were realized in the foundry's operating conditions. The influence of steel scrap in the charge and the possibility of eliminating its negative effects on the properties of cast iron were investigated. The metallurgical treatments suppressed the negative effects of the increased proportion of steel scrap in the charge.

Keywords: cast iron, charge materials, steel scrap, properties

1 Technical University of Košice, Slovakia.
* Corresponding author: peter.futas@tuke.sk

Do you have a spare PLAN?

Elena Krsljak[1*], Bosko Toljic[2], Danilo Arsenijevic[3], Zvezdana Kojic[4]

Abstract: The environmental pollution is affecting the living conditions; the raise of CO_2 levels, especially in indoor facilities is making a noticeable effect on the quality of life. IAQ (Indoor Air Quality) stands for the monitoring of different gas concentrations and it's direct impact on human health and secondary on the working performance. ASHARE ventilation Standard (1999) states that there should be 3 hourly air changes per room (ACH). THE AIM of this study was to examine the correlation between the O_2 and CO_2 concentrations (IAQ) and the subjective symptoms experienced by students with the artificial and low-rate ventilation. Materials and methods: 217 students involved, who answered the questionnaire while the temperature and O_2 and CO_2 concentration levels were being measured using the gas analyzer (MULTI RAE IR) within the rooms A and B. The measurements were made by the Hygiene Institute of Serbia. The study results have shown - Room A: temperature was 16.5 °C , CO_2 values (510 and 1240ppm), O_2 values (20.1% and 20.3%). 100% of questioned students stated that they felt cold, while 58% were unable to concentrate on the lectures. Room B: temperature (25.5 °C), CO_2 (1290-2670ppm) while the O_2 (19.8% to 20.29%). 94% of students found the air to be stuffy, 57% felt hot and 98% reported that they lacked fresh air. 96% gave a positive response when asked about the importance of a break during the lectures. 32% were not able to concentrate and 28% were only able to partially concentrate on the lectures. Conclusion: IAQ has shown that the ventilation rates within the rooms A and B were not adequate, which reflects on the students' ability to concentrate on lectures. Let's improve the

Keywords: O_2 and CO_2 concentration levels, spare plan.

1 School of Dental Medicine, Belgrade, Serbia.
* Corresponding author: elena.krsljak@stomf.bg.ac.rs

LSTM Networks in Prediction of the Demand for Compressed Air Depending on The Type of Production

Adam Galuszka[1*], Kamil Kasprzyk[2]

Abstract: Compressed air systems are widely used in industrial plants to generate the compressed air necessary for the daily operation of a facility. Since air compressors consume more electricity than any other type of facility equipment, an optimized and efficient air compressor system is essential for energy savings. There are usually many approaches to improving the performance of a compressed air system, including: miinimization of the energy losses during distribution, reduction of the system air losses such as air leaks and overpressure, pptimization of the demand side by minimizing the required optimal flow and pressure as well, choiceof the best energy-saving compressor. The worki s focused on application of the LSTM networks in prediction of the demand for compressed air depending on the type of production. The results indicate the possibility to apply online predictions to minimize the overall energy consumption by compressed air switch on-off strategy optimization.

Keywords: Artificial Intelligence, LSTM networks, Prediction, Compressed air

1 Silesian University of Technology, Gliwice, Poland.
* Corresponding author: adam.galuszka@polsl.pl

Influence of Steel Scrap in The Charge on Metallurgical Quality and Cast Iron Properties

Peter Futáš[1]*, Alena Pribulova[2], Jozef Petrik[3], Peter Blasko[4], Vladimir Sabik[5], Andrea Junakova[6]

Abstract: Cast iron castings represent more than 70% of the world's production of castings. Many factories influence their final quality. In the field of metallurgy, there are many factors influencing the final quality of cast iron. These are mainly charge materials, chemical composition, metallurgical preparation up to the final casting process. Even small deviations from metallurgical processing lead to fluctuations in melt quality and the occurrence of casting defects. Charge materials has a significant impact on the quality of cast iron, especially steel scrap, which is increasingly used from an economic and ecological point of view, especially when melting cast iron in electric furnaces. Cast iron produced from a higher content of steel scrap in the charge a higher hardness and tensile strength. On the other side, these cast irons has a higher tendency to chillout, brittleness, shrinkage, pearlitic microstructure, stresses and higher purity due to the difference in hardness at different wall thicknesses of the castings. It is the high hardness that is the problem in the final machining of castings. These negative properties are recorded mainly in heavy thick-walled castings with higher tensile strength and hardness. This negative effect is mainly due to the nitrogen content in the steel scrap, which is brought by the charge materials. Based on these knowledges, operating melts were realized in the foundry's operating conditions. The influence of steel scrap in the charge and the possibility of eliminating its negative effects on the properties of cast iron were investigated. The metallurgical treatments suppressed the negative effects of the increased proportion of steel scrap in the charge.

Keywords: cast iron, charge materials, steel scrap, properties.

1 Technical university of Kosice, Slovakia
* Corresponding author: peter.futas@tuke.sk

Influence of Cement on Hydraulic Properties of Metallurgical Slags

Alena Pribulova[1*], Peter Futas[2], Patrik Fedorko[3], Peter Blasko[4], Jozef Petrik[5]

Abstract: Slags are produced in a very large amount in pyrometallurgical processes. The global warming effect and natural resource saving are the general environmental topics nowadays. In addition, the landfilled with the waste materials has become a significant source of pollution of air, water and soil, and further adversely affects the human health, and the growth of plant and vegetation. Cement is very useful and popular binder in civil engineering. The production of one ton of cement emits approximately one ton of CO2. One possible alternative is a combination of metallurgical furnace slag and cement that is used as a binder. Blast furnace slag – granulated, blast furnace slag – gravel, cupola furnace slag – gravel, cupola furnace slag – granulated, slag from electric arc furnace were used in experiments. The mixing of slag and water was carried out by using mixer for 3 minutes to reach the best composition and homogeneity for samples production. For production of samples the mechanical press was used. The test was conducted on specimens of size Ø 50 x 50 mm. Pressed samples were tested on compressive strength immediately, then after 1 and 2 hours, then after 1, 2 and 7 days, and after 14, 21 and 28 days. Addition of cement to slag improves the compression strength of all slags. Utilization of slag only as a binder is not possible. In case of slags from electric arc furnace and slags from cupola furnace the compressive strength after seven days achieved maximum by composition 80% cement and 20% slag.

Keywords: Slag, Cement, Compressive strength, Hydraulicity.

1 Technical university in Kosice, Faculty of Materials, Metallurgy and recycling, Slovakia.
* Corresponding author: alena.pribulova@tuke.sk

Assessment of Geothermal Energy Based Combined Power and Ejector Refrigeration Cycle

Gamze Soytürk[1][*], Serpil Çelik Toker[2], Önder Kizilkan[3]

Abstract: Low temperature heat sources, such as solar energy, geothermal energy, and low temperature waste heat, exist in the world extensively. Most of them cannot be utilized by the conventional power machines efficiently. Recently, many combined power and refrigeration cycles have been proposed to make better use of them. In this paper, a new cooling and power system is presented regarding the important role of combined cooling and power systems in increasing the efficiency of power plants, as well as the ability of organic Rankine cycle (ORC) and ejector refrigeration cycle (ERC) systems to use low to medium grade energy sources. In addition, thermodynamic and parametric analyzes of the system using R600a as the working fluid are made.

Keywords: Organic Rankine Cycle, Ejector Refrigeration Cycle, Geothermal Energy, R600a

1 Isparta University of Applied Sciences, Isparta, Türkiye.
* Corresponding author: gamzeyildirim@isparta.edu.tr

An Assessment and Thermodynamic Performance Modelling of Partial Cooling CO2 Brayton Cycle Integrated with Solar Dish

Önder Kizilkan[1], Serpil Çelik Toker[2*], Gamze Soytürk[3]

Abstract: The aim of the present study is to investigate the energy and exergy analysis of solar dish collector driven partial cooling sCO2 (supercritical carbon-dioxide) Brayton cycle. EES software program is utilized to conduct the performance evaluation of the integrated system. Thermodynamic analysis results show that the energy and exergy efficiency of the solar energy driven Brayton cycle were calculated as 36.64% and 61.76%, respectively. On the other hand, parametric studies have been performed to examine the effect of solar radiation, ambient temperature, turbine inlet pressure and compressor inlet pressure on integrated cycle performance. The parametric results show that the net power produced in the Brayton cycle, the energy and exergy efficiencies of the cycle increase with the increase in solar radiation and ambient temperature. In addition, solar dish collector had the highest irreversibility rate with 87.7%, while the highest irreversibility rate was calculated in HTR with 47% for the remaining irreversibility rate.

Keywords: Partial cooling sCO2 Brayton cycle, solar dish collector, supercritical CO2, energy.

1 Isparta University of Applied Sciences, Isparta, Türkiye.
* Corresponding author: serpilcelik@isparta.edu.tr

The Impact of the Design Industry on the Economy: an empirical Study

Anisa Mekuli[1], Dea Mashkulli[2], Dina Bashota[3*]

Abstract: This paper aims to explore, analyze and discuss the impact of the design industry on the economy. The study utilizes reliance on an empirical approach by observing the measured financial performance of many global companies from the design industry. Performance measured by the productivity indicator is calculated as a statistical average of the output achievement of design companies expressed in monetary value. Our assumption is that the design industry has a high impact on the economy and this impact has increased steadily in the last decade. In this case, some of the factors that have played an important role in increasing the performance of design companies have been identified and elaborated. The focus of this study is on digital technologies and creativity (research and development) as key factors.

Keywords: Design industry, economy, productivity, performance, digital technologies, creativity.

1 University for Businesses and Technology, Kosovo.
* Corresponding author: db51814@ubt-uni.net

Prediction of Corrosion Level of Corroded Reinforced Concrete Columns from Crack Width

Yaşar Ayaz[1*]

Abstract: Cracking of the concrete and loss of adherence are the leading problems that occur with the formation of corrosion in reinforced concrete structural elements. The reason for the cracking of the concrete is the stresses that occur as a result of the volumetric expansion caused by the rust product formed as a result of corrosion. Corrosion affects the structural behavior of reinforced concrete structures, resulting in loss of life under the influence of a possible earthquake. Cracks occur in reinforced concrete elements due to corrosion. These cracks vary depending on the corrosion rate, concrete class and earthquake load. Reinforcement corrosion and cracks due to corrosion are considered as one of the most important factors that negatively affect the service life of reinforced concrete structures. In reinforced concrete columns, corrosion reduces the bearing capacity of the elements. The exact determination of corrosion is only possible with the stripping of the reinforcements. It is important to develop a practical model to detect corrosion levels of corroded reinforced concrete columns based on visual assessments in the field and to predict seismic performance levels. Many experimental and analytical studies have been carried out to predict the corrosion crack width of reinforced concrete members. In this study, data mining methods were used. In this study, it has been tried to estimate the section loss due to corrosion from the crack width by using data mining techniques and experimental study data obtained from the literature.

Keywords: Concrete, Column, Corrosion, Crack width, Data Mining

1 Inönü University, Malatya, Türkiye
* Corresponding author: yasar.ayaz@inonu.edu.tr

Renovation, Making the Most Efficient Use of Only Already Available Resources, Without Capital and Cash Flow

Gábor Fábián[1*]

Abstract: The restrictions, thanks to the low economic situation, give opportunities for executing low budget projects. With limited budget renovations, the decisions are based on the technically necessary interventions or on building in new functions. The technical contents and technical solutions need to be adjusted to the available resources. Treating a building as a whole, these changes can only be partial solutions. Finding the right intervention that the budget allow, highlighting the point is an essential task for both the architect and the client. To achieve this, every participant needs to change their point of view. Finding the right level and pace of an intervention during low budget project improves the ability of finding the right focus. Setting the content right is necessary during the execution of a limitedly financed project. During the renovation of the "Arkt Ellátó" we made certain changes on the building which were necessary for the shaping of its new function. We were looking for the technically necessary, but also satisfactory results when we defined our claims, and aesthetic desire which could be achievable with our limited finance. Keeping the possibilities in mind but stepping away from the conventions we didn't try to make it perfect. The project is permanently on the verge of achieving completion, compensating this with the quality of details and by giving unusual function to some components.

Keywords: renovation, available resources, transformation, low budget, sustainability.

1 Budapest University of Technology and Economics, Faculty of Architecture, Department of Explorative, Hungary
* Corresponding author: fabian.gabor@epk.bme.hu

Determination of Coal Quality for its Burning in the Thermal PowerPlant in Pljevlja

Biljana Zlaticanin[1*], Sandra Kovacevic[2]

Abstract: One of the largest power plants and thus largest producers of electricity in Montenegro is the thermal power plant in Pljevlja, which is coal-fired. The aim of this paper was to determine true quality of coal at the entry of the power plant. Also, the dependence between the coal and the ash content was determined.

Keywords: thermal power plant, coal

1 Faculty of Metallurgy and technology, Montenegro
* Corresponding author: biljana@ucg.ac.me

Experimental and Modeling Studies of the Al-Cu-Mg Phase Diagram

Biljana Zlaticanin[1*], Sandra Kovacevic[2]

Abstract: The article presents an experimental study of a phase diagram of a ternary Al-Cu-Mg system using differential scanning calorimetry (DSC), X-ray powder diffraction (XRD) analysis and quantitative microstructure analysis. The obtained experimental results were compared with the extrapolated phase diagram of the Al-Cu-Mg ternary system obtained by JMatPro's models based on the thermodynamic parameters available in literature. Reasonably close agreement between the experimental data and the calculated phase diagram was obtained.

Keywords: aluminium-copper-magnesium alloys, JMatPro, phase diagram

1 Faculty of Metallurgy and technology, Montenegro
* Corresponding author: biljana@ucg.ac.me

Automatic Analysis of Emotional States by Social Robots as Automated Planning Problem

Eryka Probierz[1], Anita Galuszka[2], Adam[3*]

Abstract: In this study, we propose the use of automatic planning in the presence of uncertainty systems to analyze the emotional state of a person and influence the state of diagnosis by a social robot. The purpose of the analysis of the emotional state was to create a database of characteristic facial expressions, the combination of which was used to define a given emotion. The emotions considered are: Sadness, Fear, Anger, Disgust, and Contempt. The scenarios considered include modeling uncertainty in detecting emotions. The result of the work is a set of two planning domains with illustrative examples. It is assumed that in the event of detecting negative emotions, the robot should react in a way that reduces them or does not escalate. In the implementation and extraction of solutions, the PDDL planning language, sensory planning and Allegro Common Lisp software were used.

Keywords: AI in simulation, AI planning, PDDL planning, social robotics, emotion recognition.

Silesian University of Technology, Poland
* Corresponding author: adam.galuszka@polsl.pl

VRP Problem with Constraints on the Capacity of Trucks and Suppliers' Requests on the Example of a Selected Distribution System in Poland

Adam Galuszka[1*], Eryka Probierz[2], Tomasz Grzejszczak[3], Marek Harasny[4], Marcin Wolak[5], Rafal Kern[6], Jaroslaw Smieja[7]

Abstract: Vehicle Routing Problems (VRP), consisting in determining the optimal routes for deliveries to a group of recipients, located at different points of location, are currently one of the most important classes of decision-making problems in logistics. In this paper we investigate the problem of determining optimal routes and loading of one type, assuming constraints imposed on the load capacity of the vehicle, declared customer needs and working time of drivers. As an input data we take PKN ORLEN stations with AdBlue available from the distributor located in Poland,

We are interested in the following scenario:

•every day, from a given location leaves a dozen or so vehicles (tank trucks) delivering goods (adblue noxy) to specific collection points,

•each vehicle visits several points along the way and drops a different amount of goods at each point,

•the points are located in different locations and have different opening hours,

•the task is to determine the optimal route for n vehicles, having m points to visit, assuming that at each point you should leave a certain amount of goods km,

•a vehicle does not have to take the maximum amount of goods if it is not able to drop everything on its route.

We adopted the simulating annealing algorithm (SA) developed in Matlab to the problem and present exemplary results. The results show that acceptable solutions can be determined in reasonable time for problem sizes based on real data. It should be note that part of objective function connected with working time of driver were simplified by assimung

Keywords: Logistics, AI-supported simulation, Simmulated annealing, real-data example

1 Silesian University of Technology, Poland
* Corresponding author: adam.galuszka@polsl.pl

Smart Waste Management: Waste Segregation using Machine Learning

Gayathri[1], Shola Usharani[2]*, Christie Vincent[3]

Abstract: In modern days, garbage collection plays an essential role as without which the complete environment will be messy and it makes the life tougher for all living beings. Hence proper garbage collection with automated procedures are open challenges. The existing systems focus on the adoption of drones in order to identify the location of wastes located across various places and co-ordination is carried out. But the major concept which need to be included is to have a proper garbage classification mechanism which need to have capability to detect multiple waste categories in a single point of time. The multi-object detection process to classify garbage are carried out using You Only Look Once (YOLO) algorithm. This algorithm is effective and achieves high accuracy of greater than 95% in exact classification. After classification, the location co-ordinates where the garbage remains unremoved along with its type is communicated to corresponding authorities for necessary action.

Keywords: Smart waste management; computer vision; image processing; multi-object detection; Cyber physical systems

1 VIT chennai campus, Chennai, India
* Corresponding author: sholausha.rani@vit.ac.in

Performance of Water Turbines and Generating Efficiency in Small HPPs

Vehebi Sofiu[1], Muhaxherin Sofiu[2], Sami Gashi[3*]

Abstract: In this paper, the description of the modern technology for small HPPs and the conventional approach when the amount of water is small is made, making a comparison with the türbine when the amount of water is optimal. The research has shown that the generating türbine with water flow with a small amount of $Qa = 0.67$ m3/s, where the rotation of the türbine rotor was 750 rpm, has generated electricity of 185 kW. The generating turbine, when the amount of water has increased by $Qa=10$ m3/s, electricity of 4.0 MW has been generated. The performance of the turbines depends on the flow of the amount of water, where the water level is 0.02 mm and the length of the pipes is 775 m. The purpose of this paper is the generating performance of the water turbines in HEC Orçusha with an installed power of 4.8MW for the two generators. The generating efficiency of the turbines depends on the rotation of the turbine wheel by adjusting the amount of water when it is a small amount and the approach of the operating period in the optimization of the nominal in the distribution system. The data measured for the generation of electricity at HEC Orçusha during the period of half of the year 2022, where there was a drought in the first three months, the generation of electricity was about 10% of the power capacity installed for the small turbine. Part of the second quarter, the average generating efficiency has increased to 82 %. The operation SCADA monitors the entire production process from the PC system and optimizes the nominal peak with the 35 kV distribution network and supply.

Keywords: power, cleaning up pollution, water turbine, exciter, generator performance

1 University for Businesses and Technology, Kosovo
* Corresponding author: sami.gashi@ubt-uni.net

Selection of Multimedia Data and Visualization of This Data for the Needs of Customer Service in the Tourism Industry

Tomasz Grzejszczak[1], Eryka Probierz[2], Adam Galuszka[3*]

Abstract: There is a noticeable trend in which tourists makes more and more photos during trips. In addition, managing these photos takes a long time. The aim of the research was to develop an algorithm for selecting the best photos that will be selected automatically by the user in order to maximize the individual preferences of a given user. Each photo is subject to a set of artificial intelligence algorithms that detects the set of attributes and assigns tags to images. Next, with the use of optimization methods and knowing user's preferences the set of images is chosen that maximizes the overall satisfaction function. The aim is to automatically create a travel memoir that can be exported as photobook. Depending on the cauterization function and Bayesian Rose Trees, the images are grouped into events that allows the presentation of trip in form of a graph. Depending on the satisfaction function, ascetics score and technical parameters, the images on each graph node are selected and presented in different position. The important functionality is the personalization of the user satisfaction function, providing different outcome for different users. Moreover, user can modify the parameters manually or those parameters are gathered and updated automatically with use of reinforcement learning methods basing on previous user choices.

Keywords: Artificial intelligence, Personalization, Optimalization, Image processing

---

1 Silesian University of Technology, Poland
* Corresponding author: adam.galuszka@polsl.pl

Bearing Capacity Estimation of Bridge Piles Footing- Cays Bridge Zallaq Istog

Muhamet Ahmeti[1], Hysen Ahmeti[2*]

Abstract: The purpose of this paper is to present the bearing capacity of foundation piles. There are various methods for calculating the bearing capacity and for the design of single columns including static formulas, dynamic formulas and a recently developed numerical method. The numerical method has been used to predict immediate pile movement under static load as well as ultimate pile load. The methods for design of pile groups that are presented are empirical in nature and include design against bearing capacity failure and design against excessive pile and soil settlement. The Zallqi Bridge that will be analyzed is located in the western part of Kosovo along the Istog river. For the foundations of the bridge over the Istog river were applied reinforced bored concrete piles. Bridge consists of two lateral spread footings on piles. Since the terrain where the bridge is supposed consist of layer of soft clay gray colour up to 15m depth, with variable characteristics. For this purpose were performed eight concrete pile length of 15m under foundations on both sides of the river. Piles are adopting the driven pile system Ø80mm. Based on the geotechnical soil parameters obtained from laboratory and field investigations, it is determined the load bearing capacity of two concrete driven piles and also were performed load-deformation charts for tests piles. Modulus of stiffness of clay layer is determined by field load test of pile. For this purpose, are used static penetration test. In order to compare the results, on the ground near the foundations of bridges are made two field pile load test, whereby are obtained results of bearing capacity for the field load test of piles. In many areas designers have pile-driving records from numerous projects, and may use a dynamic formula for

Keywords: Bridge abutment, pile, static penetration, bearing capacity, skin friction, field load test

1 University for Businesses and Technology, Kosovo
* Corresponding author: hysen.ahmeti@ubt-uni.net

Designing Business-Information Technology Alignment Continuity Management Framework

Habtamu Abune[1*], Million Meshesha[2]

Abstract: Maintaining continual business-information technology alignment (BITA) is crucial enabler of corporate success in today's changing business environment, technological innovation, and competitive business world. However, managing continuous BITA remains the main challenge in ethio telecom. One main reason is due to there is lack of framework which guides the company in this regard. Therefore, the main purpose of this study is to design a BITA continuity management framework that guides the company on how to maintain and manage continuous BITA. The study follows design science research methodology to design the proposed framework. The research entry point followed is problem-centered approach. Qualitative research approach was followed to collect and analyze the data. Primary data was collected using interviews and observation. Also, secondary data was collected using document analysis. Two chief officers, seven directors, and twelve managers were selected using purposive sampling from ethio telecoms business and information system divisionsmanagement. Thematic analysis techniques were used to analyze the collected data. The study proposed framework with five core components such as executive leadership support, change management, continuous BITA assessment, continuous alignment, and the creation of shared domain knowledge through building strong organizational culture. The proposed framework is demonstrated through an illustrative case study with an example by taking a telecom industry scenario and evaluating using the survey-based technique to 17 purposely selected experts from ethio telecom business and IS division management. Future research needs to consider applying the proposed framework in other organizations to further evaluate the acceptance of the framework.

Keywords: ethio telecom; Business IT Alignment; Continuous Business-IT Alignment; Alignment Continuity Management

1 Addis Ababa University, Ethiopia.
* Corresponding author: habtamu.abune@aau.edu.et

Deep Learning-Based Neuromuscular Disease Detection from the CWT Spectrum Using EMG Signals

Mehmet Ismail Gursoy[1*]

Abstract: Electromyography (EMG) is a common technique used to diagnose neuromuscular disorders by recording the electrical activity of muscles. Neuromuscular disorders refer to diseases that affect any part of the motor neuron, muscle tissue, nerve or muscle. Myopathy and neuropathy are two important types of neuromuscular diseases. The symptoms of these diseases can be very similar to each other. In this study, it is aimed to classify myopathy and neuropathic disease types using CWT and a deep learning algorithm. The EMG dataset used in this study was taken from the Physionet database. Data was obtained with the Medelec Synergy N2 EMG monitoring system by Oxford Instruments Medical (Old Working, United Kingdom). Normal data was obtained from a 44-year-old individual with no history of neuromuscular disease. Neuropathy data was obtained from a 62-year-old male patient with chronic low back pain and neuropathy due to right L5 radiculopathy. Myopathy data was obtained from a 57-year-old male patient with myopathy due to a longstanding history of polymyositis. The data was recorded at 50 kHz and reduced to a 4 kHz sampling frequency. During the recording process, 20 Hz and 5 kHz filters were used. In this study, EMG signals were analyzed using continuous wavelet transform (CWT) wavelet filter banks. In the CWT method, the Amor wavelet was chosen as the main wavelet. Normal, myopathy and neuropathy signals were separated into 125 ms (500 samples) windows and 100 scalogram images were obtained from each class. Then, scalogram images were classified with the AlexNet deep learning algorithm. The obtained classification performance was evaluated with parameters such as accuracy, precision, sensitivity and F1-score. According to the classification result, with the AlexNet deep learning a

Keywords: Neuropathy, Myopathy, CWT, Scalogram, Alexnet

1 Adıyaman University, Adıyaman, Türkiye.
* Corresponding author: mgursoy@adiyaman.edu.tr

Ultrafiltration Membranes With Improved Rejection of La3+

Alexandra Pulyalina[1*], Galina Polotskaya[2], Ilya Faikovi[3], Konstantin Grekov[4]

Abstract: The present investigation is devoted to development of new membrane materials for the recovery and recycling of rare earth metals from dilute solutions formed during the processing of electronic waste by hydrometallurgical methods. The focus was on isolation of lanthanum-alizarin complex, as the implementation of hydrometallurgical methods is currently performed with the formation of complex ions by introducing a specially selected complexing agent. To solve the task, the novel approach to formation of membranes based on copolyimide P84 was developed. Among commercially available materials, polyimides generally possess such properties as selectivity, good mechanical properties, thermal and chemical stability, which is due to the presence of rigid heterocyclic and aromatic rings in their chains. Ionic liquid (IL) 1-hexyl-3-methylimidazolium tetracyanoborate – [hmim][TCB] as environmentally friendly alternative to conventional polar aprotic amide solvents for P84 was firstly applied as co-solvent. The interaction of polyimide with solvent and ionic liquid affecting the morphology and transport properties was studied by quantum chemical calculations. The structure and physical parameters of the membranes were characterized by ATR-FTIR, TGA and SEM. Separation performance of membranes was investigated by complex ultrafiltration tests with pure water and an aqueous solution of bovine serum albumin as model mixtures for characterization of UF membranes, as well as lanthanum alizarin complex in an aqueous acetone solution. It was shown that the IL addition to the P84 casting solution increases the separation efficiency of the membranes.

Keywords: ultrafiltration, membranes, copolyimide, ionic liquids, La3+

1 Saint Petersburg State University, Russia.
* Corresponding author: alexandra.pulyalina@gmail.com

Full Scale Experiences with Wastewater Treatment Plants in the Tomato Industry

Joanna Boguniewicz-Zablocka[1*], Iwona Kłosok-Bazan[2], Mustafa Karaboyacı[3], Vincenzo Naddeo[4]

Abstract: This article discusses the various biological wastewater treatment methods used in agro-food industrial wastewaters. Diffrent type of reactors are compared considering operational challenges, treatment efficiency, technology assessment and recommendations for successful operation. In this work main emphasis is made to describe the operational experiences of tomato industries which undertake biological wastewater treatment, with particular emphasis on specific wastewater problems and their solutions. We studied treatment efficiency of the tomato wastewater treatment plant for 1 year. According to our analyses, the BOD and dCOD was reduced by 89% and 76%, respectively. Good results was achived for TP and TN removal. We also studied correlation between flow rates and removal efficiency

Keywords: tomato wastewater, BOD, COD, biological treatment

1 Silesian University of Technology, Poland
* Corresponding author: j.boguniewicz-zablocka@po.edu.pl

Presence of Disinfection Byproducts in the hot jacuzzi tube of Public Swimming Pool

Iwona Kłosok-Bazan[1*], Joanna Boguniewicz-Zablocka[2]

Abstract: The studies conducted in swimming pools areas have identified presence of many "resulting compounds", called disinfection byproducts. The way how disinfection byproducts are formed in swimming pool and hot jacuzzi tube waters is not fully explained. The formation of disinfection byproducts in water depends on many factors such as pH, chlorine dose, contact time, water temperature and the presence of various organic compounds, the so- called precursors. This article presents the results of a study carried out, admittedly in a large public swimming pool facility, for circulating water of hot jacuzzi tube. The analyses of selected disinfection byproducts were carried out in accordance with the test methods described in EN ISO 10301:1997 - Water quality - Determination of volatile halogenated hydrocarbon derivatives - Methods using gas chromatography. Agilent 7890B gas chromatograph equipped with an electron capture detector (GC-ECD) was used to determine trihalomethanes.

Despite the fact that maintaining the level of disinfection by-products determined as THM in facilities such as hot jacuzzi tubs is not a straightforward task, no exceedances of this parameter were recorded in any of the samples taken on six different times in the analysed facility. What is of concern is the level of chloroform, which was exceeded in more than 60% of the samples. As is well known, compounds identified as THMs are volatile substances, so aeration of the water affects their elimination from the liquid. These substances pass into the air causing an increase in THM concentrations in the air above the basin.

Keywords: disinfection byproducts, swimming pool, water treatment

* Corresponding author: klosok@poczta.onet.pl

Liquefaction Assessment Based on Shear Wave Analysis for the New Settlement Area in Erenler/Sakarya

Ali Silahtar[1*], Hasan Karaaslan[2]

Abstract:

This study aims to determine the liquefaction risk of the new settlement area in the Erenler district by shear wave analysis. This new settlement area is located on the alluvium of the Sakarya river with a shallow groundwater level distribution character. These alluvial soils were the origin of the damage distribution in the 1999 Izmit earthquake. Furthermore, many earthquakes with a magnitude of M>6.0 have occurred in the study area and its surrounding, both in historical and instrumental periods. In this context, shear wave velocity (Vs)-based liquefaction analysis was carried out to make a general preliminary assessment of the liquefaction potential of the study area. In this context, surface wave analysis measurement was carried out at 20 points to assemble a general liquefaction assessment for the study area. Liquefaction analysis was achieved thanks to the layer velocities obtained from the 1D depth-Vs sections for Kayen et al. (2013) liquefaction analysis approach. All these analyzes are constructed on the reoccurrence of the Mw: 7.4 1999 Izmit earthquake. In addition, the liquefaction potential index (LPI) distribution was generated from the liquefaction safety factor (SF) values calculated along the soil profile to examine the spatial liquefaction distribution. The liquefaction phenomenon is predicted in many layers along the soil profile at the data acquisition points in Kozluk, Alancuma, Kamışlı, and Bekirpaşa, located at the Sakarya river border and its close vicinity. LPI>15 values, defining the high class in LPI classification, were obtained due to low GF values near the surface in these locations. On the other hand, LPI values corresponding to very low-low class were calculated because the liquefiable layers are too deep or not in the vicinity of Kayalar and Yazılı in the south of the study area, and Nakışlı and Esence in the middle and northern part. In this context, it is predicted that there will not be any liquefaction risk in these areas. Furthermore, improving the results obtained from this study with geotechnical analyses and increasing the number of data acquisition points will allow the risk distribution in more detail.

Keywords: Liquefaction, shear wave velocity, Safety factor, Liquefaction potential index

[1] Sakarya University, Engineering Faculty, Department of Geophysics, Sakarya, Turkey
[2] Sakarya University, Engineering Faculty, Department of Geophysics, Sakarya, Turkey
* Corresponding author: asilahtar@sakarya.edu.tr

Implementation of Artificial Intelligence in CRM Systems in Industrial Companies

Raphael Olaniyi*[1]

Abstract: The dissertation thesis will investigate the needs and motivations for artificial intelligence (AI) integration into customer relationship management (CRM), companies´ readiness and it will determine purpose and areas of its use. It will examine real experiences of selected companies and perspective of their customers, reveal advantages and disadvantages and propose the framework for successful implementation that ensures balance between personalized customer interaction and respect to user's privacy.

Customer Relationship Management (CRM), that integrates people, processes, and technology to maximize relationships with all consumers, is a critical requirement for large and growing companies operating in a global competitive environment. Also new strategic directions, like Artificial intelligence (AI), become imperative for the success of innovative companies, nowadays. Considering the volume of data that has increased with recent modern technologies (like IoT etc.), and the necessity to manage information about customers more efficiently, companies need CRM software capable of extracting and analysing data in real-time so that they can make quick and fact-driven decisions. AI and CRM can assist organizations in predicting their customers' behaviour and expectations and help their employees to enhance customers' engagement and retention. Enhanced CRM will allow human touch via AI and will reduce treating customers as objects. A conceptual framework, which allows organizations to inspect if it is ready to adopt an AI-integrated CRM system, will be developed and the process of implementation will be proposed.

Keywords*: artificial intelligence (AI), customer relationship management (CRM), marketing, market, services, telecommunication, biotechnologies*

1. INTRODUCTION

Despite having origins rooted in myth and fiction, rapid technological advancements over a short time period have rendered A.I. anything but. The 21st century especially witnessed a huge influx of interest, investment, and development in Artificial Intelligence. The rise of superior computing power, advanced algorithms, and cost-effective data storage capabilities can all be attributed to this

* olaniyi@utb.cz
[1] Tomas Bata University, Zlin, Czech Republic.

A.I boom but perhaps one of its most significant drivers is big data. Artificial intelligence (AI) is a level of intelligence that includes machines that "think like a human" or otherwise think as though they are intelligent (Ertel, 2017). Artificial intelligence has attracted increased attention of varied disciplines making it one of the most exciting technologies. It has many sub-fields such as machine learning and natural language processing, and many of these fields are considered a crucial part of today's research related to computer science (Xue & Zhu, 2009).

AI has made its way into an increased volume of companies' infrastructures and solutions due to its revolutionizing data analytics power, increased efficiency and its proven capabilities providing an overall mostly positive impact on solutions it has been implemented to (Nayak & Dutta, 2017). Customer Relationship Management (CRM) is a system created to aid a user with relationship management and an overall sales and lead control. This research will explore the possibilities that AI offers to boost CRM's efficiency and usability. Customer Relationship Management is an area that attempts to increase sales, customer loyalty, and a piece of overall customer knowledge through data collection and analyses and simplified information output. AI's data collection and analysis capabilities make it a relevant technology to CRM thus creating an exciting opportunity which will be examined in this research.

Artificial Intelligence is when machines can simulate human intelligence and carry out tasks that require it without any human intervention. These include but are not limited to the perception of vision and speech, motion, learning, and reasoning to make decisions. From the beginning, CRM has used databases to achieve its goals in a simpler way. However, this information management has been focused mainly on collecting, storing and providing data at the request of clients, leaving aside the processes of extraction, analysis, and interpretation, which give real value to the information received. Coupled with the ever-increasing volumes of data that organizations must handle, it's easy to see why CRM needs the support of AI to adapt to the era of digital transformation.

A.I. surrounds us and we interact with it all the time, sometimes without even realizing it. On the internet, not only does it help us find the content we desire but also enables desirable content to find its way to us. It resides within our phones listening to our commands, deciphering our intentions and determining the answers to our queries. It makes our homes smarter, safer and more hospitable. AI is already transforming businesses and organizations, and change is accelerating. Billions in funding flood space, and companies use that money to pioneer AI-powered solutions that predict, personalize, and perform at scale. Artificial intelligence in customer relationship management will be one of the primary catalysts of intelligent CRM's growth over the next four years, supported by analytics, business intelligence and machine learning. Buyers will focus on the addition of emerging technologies that enable more compelling customer experiences.

At the stack level, there will be increasing use of AI for very specific purposes. Natural Language Processing (NLP) to friction reduction. This will be used at the very front end of the marketing process and the customer service process. Research related to this topic has increased in recent years making this thesis more relevant to conduct through still some specific areas are researched subtly. The use of AI in CRM has been studied more in individual areas of CRM or AI; thus, a

* olaniyi@utb.cz
[1] Tomas Bata University, Zlin, Czech Republic.

more general look into the topic is required. This thesis attempts to bring some of these areas together in creating a broader look into this revolutionizing phenomenon. Personal interest and recent talk of Salesforce and its technologies lead into an examination of Salesforce and its own integrated AI, Einstein. The main goal of this thesis is to examine current AI implementations in CRM and to give an overall look into benefits of AI technologies in CRM.

With the use of artificial intelligence customer relationship management (AI CRM), businesses can enhance customer engagement by analyzing their emotions and providing appropriate responses accordingly. A CRM system consolidates various customer information and stores it into a single database that can be easily accessed by all the employees of an organization. With the help of CRM, businesses can focus on not only their relationship with their customers, but also every individual related to an organization like employees, service providers, suppliers, and others. It can simply be put that CRM provides various benefits to businesses like improved client relationships, team collaboration, revenue, profitability, and much more. And, it is because of these benefits that CRM software market grow about 16% in 2018. But, if CRM is providing so many benefits to businesses, then what is the need to incorporate AI in it and create AI CRM? Well, that is because the best is not always perfect. Although CRM is very beneficial to organizations, AI CRM can further increase the efficiency of CRM.

H1: Although CRM is very beneficial to organizations, AI CRM can further increase the efficiency of CRM.

H2: AI in CRM will be one of the primary catalysts of intelligent CRM's growth over the next four years.

Literature review

A study by Iqbal and Khan (2021) argues that companies which have implemented AI in their Customer Relationship Management (CRM) and marketing as a whole, have reported significant impacts on company's growth in terms of customer loyalty and profitability. One way in which AI is transforming CRM is through sentiment analysis. According to Fatemi (2019), AI powered tools can analyze conversations and evaluate customers' emotional situations through the use of sentiment analysis. A research by Singh (2021) shows that an AI-powered CRM is can learn from past decisions and historical patterns to score the best leads for sales, predict future customer behavior, increases the scope of customer services, and leads to better and more effective marketing strategies.

Studies also reveal that AI in CRM helps in advancing data reliability. According to Dilmengani (2021) an AI integrated CRM system augments the role of decision making by identifying potential issues in the system, removing data duplicates and reporting errors. In addition, integrating AI with CRM systems enhances the system capacity to provide customized recommendation for salespersons and informs them the rationale behind certain recommended actions (Fatemi, 2019).

* olaniyi@utb.cz
[1] Tomas Bata University, Zlin, Czech Republic.

2. METHODOLOGY

The aim of the dissertation thesis will be to investigate the needs and motivations for artificial intelligence (AI) integration into customer relationship management (CRM), companies´ readiness and it will determine purpose and areas of its use. It will examine real experiences of selected companies and perspective of their customers, reveal advantages and disadvantages and propose the framework for successful implementation that ensures balance between personalized customer interaction and respect to user's privacy.

This research paper aims to answer the following questions. Still not limited to and expound more on AI and CRM in different fields, advantages and disadvantages and challenges of incorporating AI in CRM and business needs especially in decision-making.

1. What is AI and in business/organization, how can businesses use AI and CRM?
2. What is AI and the future of CRM? AI driven CRM, Big Data, and AI.
3. What is the relationship between AI and Sales, AI and Marketing, AI and Customer Service?
4. Will artificial intelligence substitute positions of employees?
5. What are the ethical concerns of AI business?
6. Will artificial intelligence make the employees work more in satisfying potential customers?

Considering the volume of data that has increased with recent modern technologies (like IoT etc.), companies need CRM software capable of extracting and analysing data in real-time to make quick and fact-driven decisions. AI can meet these needs. Furthermore, AI and CRM can also help organizations predict their customers' behaviour and expectations and help their employees to enhance customers' engagement and retention. The dissertation aims to answer the following more detailed questions on AI and CRM from different perspectives. For now the scope is settled rather broadly but it will be narrowed and specified later during the the work on the thesis.

1. What is the focus of CRM, and where does the need to combine it with Artificial intelligence come from? What will be the advantages and disadvantages of the integration of AI and CRM?
2. Via AI, CRM will allow "human touch" and reduce treating customers as objects. Customers will be demanding this. However, there are two double-edge swords: a) operational efficiency in conflict with exceptional customer experiences, b) customers expecting a company to know a lot about them in conflict with privacy concerns about knowing too much. Will customers view such a setting as a positive one or will they perceive it as a poor service experience?
3. Are CRM systems ready for AI integration? What is a framework of organizational readiness for effective AI and CM integration?
4. CRM provides various benefits to businesses like improved client relationships, team collaboration, revenue, profitability, and much more. It is because of these benefits that the

* olaniyi@utb.cz
[1] Tomas Bata University, Zlin, Czech Republic.

CRM software market grew about 25% in 2020. However, if CRM is providing so many benefits to businesses, what is the need to incorporate AI in it and create AI CRM then?

5. How hard will the robot make us work? In many call centres, warehouses, and other sectors, intelligent machines are managing humans. They are making work even more dangerous and gruelling Will this get better, will this make us work smarter, or will this reshape our thinking?

It is of great importance to define research from start to finish. As indicated by Denzin and Lincoln (2000a:371), research strategy, therefore, connects the researcher to accurate and specific methods and approaches for collecting and analyzing data. Research will be conducted in several steps in which the holistic approach will be applied:

(1) first, it will be necessary to review other relevant research studies and secondary data and elaborate literature review;

(2) second, to realize qualitative research in the form of case study on AT &T company to map perspectives of various relevant stakeholders (managers, employees, customers) that are related to AI and CRM (this will be realized via in-depth interviews);

(3) to realize quantitative research oriented especially on AT &T customer's perspective, investigating their awareness, experiences with artificial intelligence, expectations, perceptions and other aspects of the consumer behavior (this will be realized by administering questionnaires to customers)

(4) to compare all perspectives and propose the framework of successful implementation of AI in CRM of the company

Sampling techniques

The research participants will be selected through non-probability sampling techniques which involves non-random selection based on convenience. Convenience sampling technique will specifically be used in this research. According to Vehovar, Toepoel, and Steinmetz (2016) convenience sampling method is dependent on how easy it is for the researcher to access to subjects. The key data is expected to be collected from AT & T key stakeholders such as customers, employees, and managers. Significant sample will be selected based on availability and connectedness with the case company.

Data analysis

Qualitative data analysis: Interviews will be analyzed using thematic analysis technique

Quantitative data analysis: the questionnaire will be analyzed through quantitative methods

Triangulation: Triangulation of data will be conducted to compare quantitative findings to the qualitative results to develop a comprehensive understanding of study area and propose the framework of successful implementation of AI in CRM at AT&T Inc.

* olaniyi@utb.cz
[1] Tomas Bata University, Zlin, Czech Republic.

3. POTENTIAL CHALLENGES AND ETHICS

When proposing any project, it is essential to pre-empt any issues that may arise during the data collection and analysis phases to act in such matters and put solutions in place. Rarely can we find a technology that provides only a positive outcome for our society and lives. Artificial intelligence sure has its flaws and they scale from technical problems to deep ethical questions. This thesis focuses on AI's logical and infrastructural problems though it also explores more deeper concerns regarding topics such as warfare and ethicality.

☐   AI's infrastructural problems are vast, and they should be taken into a consideration when for instance a company is deciding on implementing an AI into their business or platform solutions. ☐ These problems include areas related to software, personnel, storage and security. Starting with software and algorithms, a company is required to finetune the AI solution for their use and this can prove problematic.

☐   Hand in hand with this problem follows personnel complication. Understanding AI is not quite as straightforward as one might think, and it calls for expertise on the topic. Lack of ability to adapt wanted AI into company's structure might have detrimental consequences rather than inherently positive results (Kiruthika & Khaddaj, 2017).

☐   AI proposes another problem, logic. Understanding human intelligence has proven difficult which means artificial intelligence is not different.AI can be un-predictable to the point where it can do decisions on its own that seem correct to it but are considered flawed by us.

☐   According to a research conducted by Lazanyi (2018), trust is considered a most important feature of AI. Also, over half of the respondents in the research answered that they are not at all ready to utilize AI. Mistrust is connected to resistance of change which is a major matter of controversy in general. Artificial intelligence in grand spectrum is considered unreliable and immensely unemotional which are values considered very important, not just in AI, but in general. ☐ Moving into another ominous topic, warfare. The sinister view we shall examine since the war is a constant on this planet. Opportunity that AI proposes to warfare might not be necessarily one of efficiency, which is intriguing to industrials, but one of survival. It is common sense that any authority given to an autonomous weapon might lead into an unsought outcome (White,1991). Lethal autonomous weapons systems (LAWS) are one example of extreme use of an AI in a weapon industry.

4. CONCLUSIONs AND RECOMMENDATIONs

Businesses today are leveraging big data to understand customer behavior and preferences in efforts to formulate improved strategies. However, presently less than 0.5% of all data is being analyzed and used (Forbes). This presents a huge opportunity to capitalize on this 'wasted' data by developing advanced analytical techniques based on artificial intelligence. This union of big data and A.I. is very likely going significantly impact the future by enabling businesses to derive more value from their data. By changing the nature of work and creating a new relationship between man and machine, A.I. could double annual economic growth rates in 2035 and boost labor productivity by 40% (Accenture). The rise of A.I and CRM presents businesses with a wide array of unique benefits and opportunities. It can empower them to provide better, more relevant

* olaniyi@utb.cz
[1] Tomas Bata University, Zlin, Czech Republic.

experiences to their customers and forge bonds with them in a way that was most not possible before. No wonder, artificial intelligence in business decision making plays a crucial role. With CRM and artificial intelligence, you can get all the data and predict customer behavior to have a proactive approach. As a conclusion about the topic, AI provides many benefits to many areas in our life and society, but the negative effects must not be overlooked. Opinions about the superintelligence and other extreme possibilities AI offers, roam the discussion widely and intensively. Superintelligence is a concept where an AI exceeds human intelligence thus providing even less control of an AI (Hurlburt, 2017). Present machines lack many human characteristics thus making them still more of an intelligent computer than of an intelligent human. This provides us, at least on a conceptual level, with enough control over an AI's doing. Problems are the one to be resolved, and research is conducted before integrating AI into everything in our lives.

REFERENCES

Vehovar, V., Toepoel, V., & Steinmetz, S. (2016). Non-probability sampling. *The Sage handbook of survey methods*, *1*, 329-45.

Kiruthika, J., & Khaddaj, S. (2017, October). Impact and challenges of using of virtual reality & artificial intelligence in businesses. In *2017 16th International Symposium on Distributed Computing and Applications to Business, Engineering and Science (DCABES)* (pp. 165168). IEEE.

Lazanyi, K. (2018, September). Readiness for Artificial Intelligence. In *2018 IEEE 16th International Symposium on Intelligent Systems and Informatics (SISY)* (pp. 000235000238). IEEE.

Hurlburt, G. (2017). Superintelligence: Myth or pressing reality?. *It Professional*, *19*(1), 6-11.

Ertel, W. 2017. Introduction to Artificial Intelligence. (2nd edition) Springer International Publishing.

Iqbal, T., & Khan, M. N. (2021). The Impact of Artificial Intelligence (AI) on CRM and Role of Marketing Managers.

Fatemi, F. (2019). 5 Ways Artificial Intelligence Is Transforming CRMs. *Forbes*

Dilmengani, C. (2021). AI-powered CRM Systems in 2021: In-Depth Guide. Retrieved from AI Multiple: https://research.aimultiple.com/crm-ai/

Singh, S. (2021). Adoption and Implementation of AI in Customer Relationship Management. (IMS Ghaziabad, India).

* olaniyi@utb.cz
[1] Tomas Bata University, Zlin, Czech Republic.

Recovering Industrial Heritage in the Small Towns. The Disused Gioppo Textile Factories in Montebelluna (Italy)

Enrico Pietrogrande[1*], Alessandro Dalla Caneva[1], Massimo Mucci[1]

Abstract: One of the most important issues in current urban regeneration policies is the recovering and transformation of the industrial heritage in small Italian towns. The city of Montebelluna in the province of Treviso, especially the hamlet named Biadene-Pederiva, is still today a significant example of the numerous disused industrial areas, which the local administration is planning to convert into new functions. The aim of this research is to investigate new design strategies for the urban regeneration of these areas, through the protection of their morphological, historical and social values from contemporary changing city. The method of " research by design" adopted here includes the tools of urban and morphological analysis and the use of contemporary architecture expressive resources; it leads to rethinking the relationship between memory conservation and the representation of new social and manufacturing needs through an innovative and sustainable way.

Moreover, some typical principles of sustainable architecture are applied in the design process, such as the reuse and recovery of existing areas and building materials, energy efficiency, the use of low environmental impact materials, and local identity preservation. The research was carried out as part of an agreement between the municipality of Montebelluna and the Department of Civil, Environmental and Architectural Engineering of the University of Padua; the results are a series of innovative urban and architectural transformation projects, capable of turning abandoned areas into something new. The case study presented here is the Filatura Gioppo textile factory, a typical industrial building from the 1930s, made of reinforced concrete and brick structure, including its own hydroelectric power plant for energy production and brick structure, including its own hydroelectric power plant for energy production. The proposal of transformation promotes the local tradition through the opening of a textile manufacturing museum, as well as tourist information centre, providing visitors with information on the area's attractions; other possibilities of functional conversion for commercial purposes were also explored, or for new educational activities aimed to preserve and revive traditional arts and crafts practices.

In conclusion, this design and research experience confirms that the recovering of industrial heritage, provided that it is carried out following an approach open to the contemporary interpretation of the morphological features of the area, can give new vitality as well as a new identity to small urban towns.

Keywords: urban regeneration; industrial Heritage; functional conversion; sustainable architecture

1 University of Padua, Department of Civil, Environmental and Architectural Engineering, Padua, Italy
* Corresponding author: enrico.pietrogrande@unipd.it

1. Introduction

Montebelluna is a town in the Veneto region of north-east Italy that underwent a phase of intense development between the mid-Nineteenth Century and the start of the Twentieth Century when manufacturing and marketing of the products were initially established (De Bortoli, 2006).
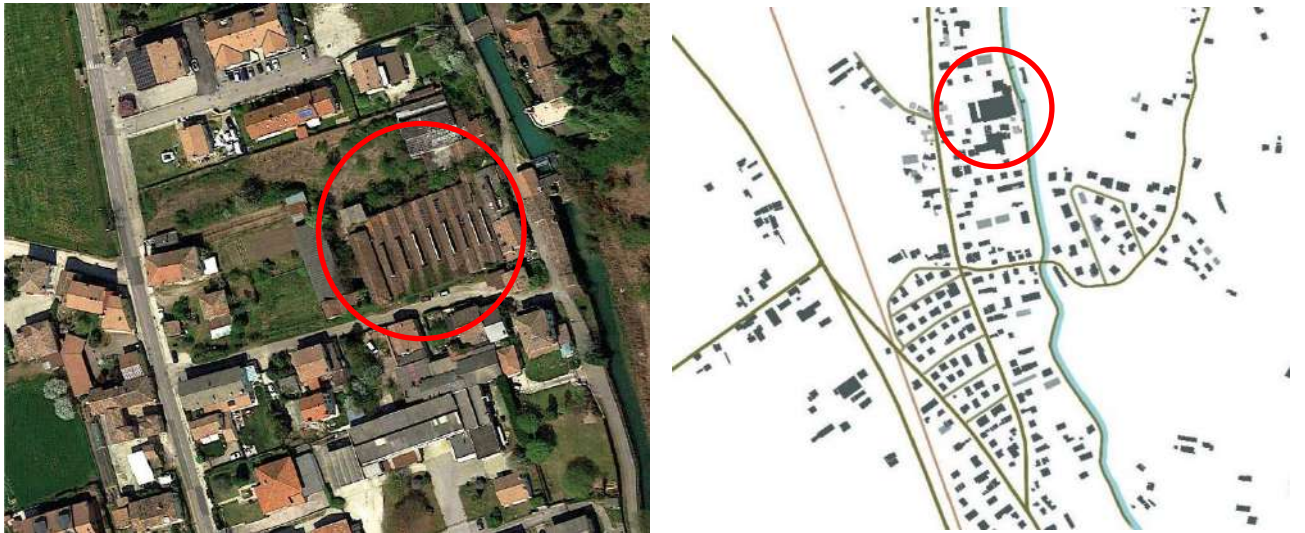
Figure 1. View from above of the former Gioppo Textile Factories at Montebelluna, in the hamlet of Biadene-Pederiva.
Figure 2. The former Gioppo Textile Factories and the building fabric in the area.

With the passing of time the first industrial cotton textile companies started operating in Montebelluna as well as pasta food processing and milling factories, plants producing superphosphates, and some timber processing yards. Great development of the footwear sector began (Binotto, 1984) whose influence on the territory can now be seen in the shoe and sports shoes museum in Montebelluna. (Durante, 1997). After this, other textile manufactures developed, and in particular the one named Gioppo that is the subject of these pages.

The former Gioppo Textile Factories are located in the north-west of the commune of Montebelluna near the hamlets of Pederiva and Biadene (figg. 1, 2). Mario Gioppo was already the owner of a textile factory in the city of Schio when he decided to take on a new industrial challenge in the area of Pederiva in 1938 and invested in a new activity of transforming textile fibres. Having obtained authorisation to use the waters of the Brentella Canal, he installed a new hydraulic turbine system used in spinning in May 1939. The original 1938 project for the building complex provided for a plant in three bodies. The first volume with a storey above ground was for production work having a pillar-beam construction in reinforced concrete, brick cladding, and a pointed, gabled roof with skylights corresponding with the central spans. The second volume of two storeys was for the gatehouse and accommodation for the caretaker. The third volume is in load-bearing perimeter brickwork with one storey above ground for offices, services, a metal working and mechanical workshop, and a carpentry workshop (fig. 3, 4).

Figure 3. Aerial **v**iew of the Gioppo plant between 1940 and 1950.
Figure 4. The former Gioppo plant viewed from inside the first building to the west.

Figure 5. Former Gioppo Textile Factories at Montebelluna, view of the façade of the first building to the west, current condition

Various extensions have been added through the years. Other two-storey buildings in load-bearing perimeter brickwork were constructed to the west of the original plant in 1948. In 1970 a new two-storey volume was added, and various other minor extensions were made in 1975. Disused for more than a decade, the former Gioppo Textile complex is in a condition of uniformly widespread advanced degradation (fig. 5). The buildings are reverting back to nature with vegetation out of control (fig. 6) so that the architecture is no longer visible on its southern side on Via dei Celato (fig. 7). Satellite images show that various parts of the roof have collapsed.

From the point of view of urbanism, the area is classified in the Commune's Transformations Plan as an industrial area to be redeveloped. The commune administration has required clean up and reconversion for some time now. Furthermore, the project site is subject to environmental landscape constraints in view of it being near the natural area of the hill of Montello and the watercourse called *Canale del Bosco*. The east façade of the former Gioppo plant also runs along the road called *Stradone del Bosco*, a cycle and pedestrian path with high landscape value that runs along the *Canale del Bosco* and the lower flanks of Montello hill.

The fragmentation of the building complex has facilitated selecting the volumes to preserve and to restore, conserving their historic architectural footprint for the purpose of integrating them with new other volumes in performing the proposed new functions.

Figure 6. The former Gioppo Textile Factories: view of the internal courtyards, current condition.
Figure 7. The former Gioppo Textile Factories: view of the south-facing façade on Via dei Celato.

2. Materials and Method

The "research by design" method with specific objectives was applied in two different phases (Van Ouwerkerk, M., Rosemann, J., 2001). The first phase in the planning process generally involves analysis of the context as a preliminary to choosing the best composition (figg. 8, 9). Here the context is considered to be pre-existing natural and artificial phenomena which are analysed using local historic sources and the urban morphology as well as the building typologies present in the urban fabric. Urban facts or structural elements characterising the territory may be identified in this part of the work and merit subsequent evaluation in the project. In fact, in being a traditional scientific research procedure, research as analysis already contains non-traditional aspects in the case presented in this paper: the criteria for the morphological analysis influence the type of knowledge in the project, and the analysis is carried out using spatial categories such as cartography, layouts, and digital techniques. Urban morphology is used in urbanism as an instrument to analyse the context and facilitates the development of the planning project, but at the same time the project is the instrument used to obtain the morphology. This circular relationship typical in "learning by doing" is caused by the project itself already belonging to the process of transformation analysed using the morphology (Kropf, 2020). Moreover, this guarantees that the learning by doing process functions by exchanging project and morphology in a teaching methodology course developed through time by continuously alternating the "looking" phase (analysis) with that of "making" (designing) in a circular way. It can be said that here the analysis intrinsically becomes "operational" in that it is aimed at instigating certain specific planning project actions.
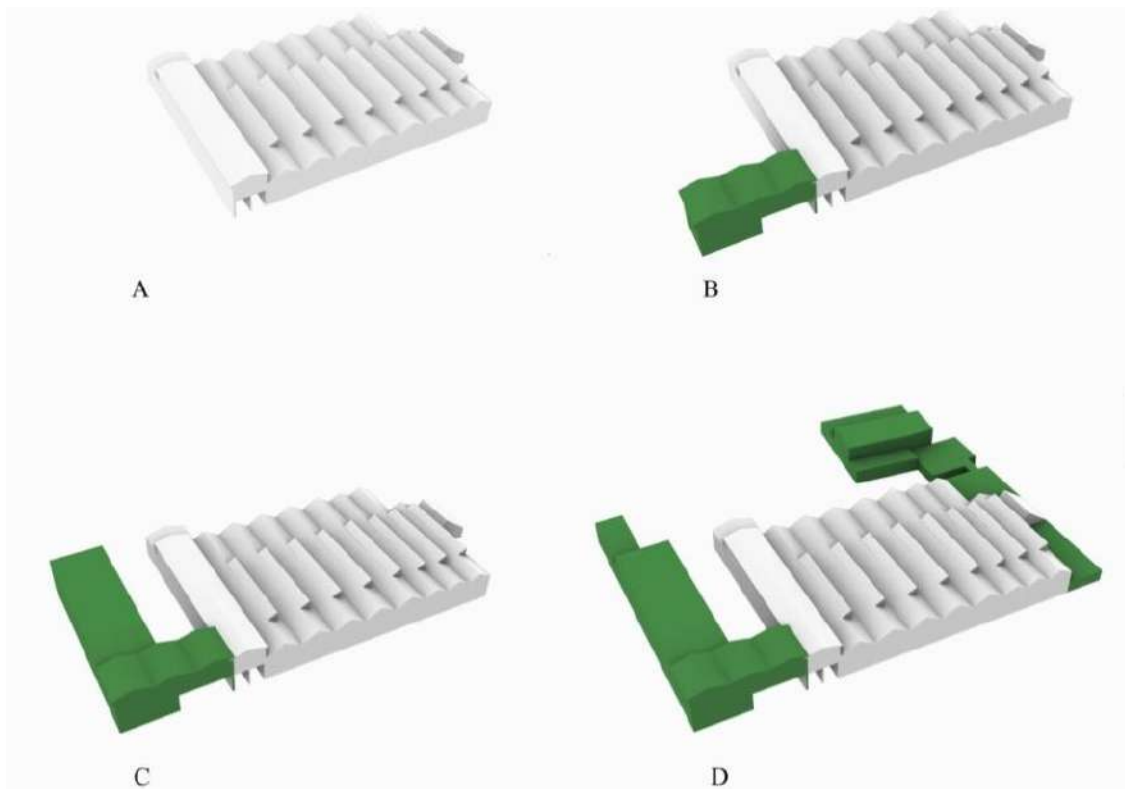
Figure 8. Analysis of the historical evolution of the plant: A) original 1938 construction; B) 1948 extension; C) 1970 extension; D) 1975 extension. From the work of the students Anna Faccioni, Sara Gaio, Marco Schiavo, Arianna Sergio.

Figure 9. Planivolumetric plan. From the work of Giacomo Bressan, Sofia Marigo, Sofia Ruzzon.

It is precisely from awareness of the current situation of fragmentation and incompleteness of the contemporary city that the need to establish urban re-composition arises while always within the process of reinterpreting what already exists (Schoonderbeek, 2017). In other words, the fragmentation is not accepted tout court as a representation of a "modern" way of life but is included in the project as an inevitable postmodern condition of recomposing by transformations that longs to fulfil an idea of not all-embracing unity. So the project phase carried out using the teaching methodology of "learning by doing" becomes research oriented in achieving a practical result and consequently comes under the field of applied research. Intervening in a concrete study area with several planning proposals means studying practical and achievable solutions to solve complex urban problems. The role of the professor in this phase is to be a critical guide who although he or she does not exclude plurality in approaches, helps the students to develop planning proposals coherent with the results of analysis achieved and with the aims of urban regeneration established. "Research by design" consequently becomes a collegial activity, no longer carried out by the individual (student or professor) but by a community of researchers, or better still, a "community of learners".

A third part of the study carried out at the same time as the other phases, but which contributes notably to the final outcome, is research into the designing references. The method in this case is the more traditional one of research "about" the project, generally applied in the field of history and criticism of architecture. Starting from analysis of the projects previously developed by selected reference authors, an understanding of the architectural characteristics and detailed redevelopment solutions adapted to the specific context can be gained. Therefore, here too the choice of models and on the basis of their reusable morpho-typological characteristics is research that becomes an integral part of the planning process.

3. Teaching experience in the study area

Some of the experiments in the urban regeneration projects for the abandoned Gioppo Textile plant in Biadene-Pederiva are summarised below. They were developed on the Architectural and Urban 2 Composition course at the Department of Civil, Environmental, and Architectural Engineering of the University of Padua taught by Professors Enrico Pietrogrande and Alessandro Dalla Caneva with the help of architect Massimo Mucci. The projects refer to the abandoned production area in the expectation of finding meaning and a role in the context. In general, the planning choices presented aim to enhance the quality of the spaces and pre-existing industrial crafts considered to trigger processes of redevelopment of the area socio-economically and environmentally.

Figure 10. Group consisting of Anna Faccioni, Sara Gaio, Marco Schiavo, Arianna Sergio. Project planivolumetric plan, south façade, perspective views.

Figure 11. Group consisting of Bressan Giacomo, Marigo Sofia, Ruzzon Sofia. Project planivolumetric plan, general plan, perspective view.

The project of the students Anna Faccioni, Sara Gaio, Marco Schiavo and Arianna Sergio (fig. 10) provide for the demolition of the existing volumes while keeping the main south-facing façade of the old spinning-mill intact. The façade constitutes the rule for arranging modular parts in an orderly manner, including staggering and organising them so as to define the series of main collective spaces. These constitute the place where the main volumes face each other in a functional unitary programme that provides for the constitution of a reception pole that includes a food and wine area to showcase local products, a service area for the sale and hire of bicycles, and a hostel. The latter is a crystal-clear glazed volume that rises to balance the choice to enhance the horizontality of the general arrangement of the volumes in the project. Porticoes, covered halls, and a greenhouse implement the functional programme of the project that provides for spaces offering a collective meeting-space. Flat public areas with evergreen trees enhance the union between nature and man.

The project by the students Giacomo Bressan, Sofia Marigo and Sofia Ruzzon (fig. 11) considers the maintenance of the pre-existing architecture absolutely necessary for enhancing the memory of the former spinning-mill. The idea provides for the constitution of a central courtyard around which the pre-existing spinning-mill buildings are arranged with two new volumes. The courtyard opens to the north to make a visual relationship with nature, the hills, and the Alps.

The idea of the courtyard has its origins in ancient times and its use is connected to the social value it possesses. With regard to the courtyard as the essential reason for the project, the words of Alvar Aalto come to mind when he described the planning competition for the municipality of Saynatsalo as follows: "I have used the closed courtyard as the main reason why it manages in some mysterious way to bring the instinct to be sociable to light. Since ancient times in Crete, Rome, and Greece, and through medieval times and the Renaissance, the meaning of the courtyard in government and municipal buildings has remained unchanged to the present day" (Reed, 1988).

To enhance the pre-existing building complex students propose a series of laboratories to promote and safeguard the craft of spinning and a museum about the history of textile crafts that mark the Montebelluna area. Promoting tourism and development of the communities of Paderiva and Biadene is one of the cardinal points in the redevelopment process. The new buildings include environments like a bar, a cinema-theatre, and a multipurpose room in addition to services for refreshments and for bike sharing, the latter combining with the cycle and pedestrian path that crosses Montello.
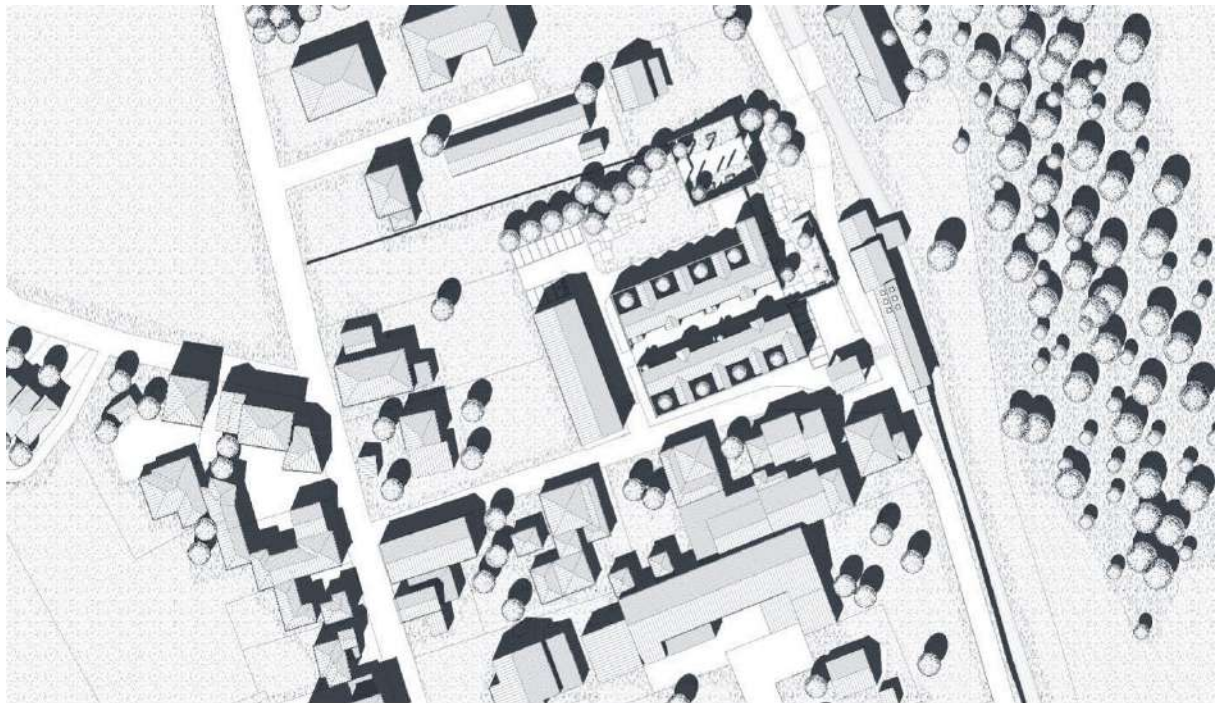
Figure 12. Group composed of Matteo Bottaro, Giacomo Maule, Vittorio Mazzon, Andrea Zamborlini. Project planivolumetric plan, perspective views.

Not unlike the first plan presented, the plan of the students Matteo Bottaro, Giacomo Maule, Vittorio Mazzon, and Andrea Zamborlini (fig. 12) also hypothesises keeping the main façade to the south, considered to be the only meaningful theme in the memory of the spinning-mill. Furthermore, the volume that closes the west side is also kept, arranged in opposition to the mill that closes the area to the east. Starting from this premise, the idea is composed of finding a series of relationships between the parts. In particular, the east-west axis, parallel with the main façade on the south side, unites the pre-existing building with the mill. The axis constitutes the tool for organising a series of modular volumes with reference to the rule imposed by the regular sequence of the gables of the main south-facing façade. Another north-south orthogonal axis is arranged along the original access in order to relate the project to the parking area and the green park to the north where the redevelopment of a degraded volume on the theme of the ruins is provided for.

The main theme is given by the volumes arranged along the east-west axis. This is the starting point for constructing an urban block of residential houses where the axis becomes the road along which the residences are aligned. The theme of the residences takes the form of the idea of the house with a courtyard. The former mill becomes a bar restaurant and is enhanced by a small urban piazza placed in continuity with the space of the urban road constituting the public meeting place of the residential community. Lastly, the pre-existing volume to the east houses shop spaces for the residents.

3. Results

It is considered that the project aspires to construct parts of a city in a dialectic relationship with the pre-existing (Molinari,1997). Nowadays the project tends to disperse the traditional experiences of space with the ideology of the clean slate so territories are considered to be fields open to free interpretations with the insertion of liquid architecture that tends to extraordinary spectacularity in a general process of aestheticization of the world. An alternative to this way of taking the urban project according to methods rooted in history is proposed in critical reasoning where renewal of the architecture is in continuity with the general characteristics of a culture of living and dwelling in the place.

4. Discussion and Conclusions

The urban planning project is not required to intervene with surprising effects by using muscular architectures that only value themselves and the personal ambition of the planner. Architecture is required to enter the context by discretely interpreting the settlement rules in it, the characteristics of the place, and its atmosphere (Pietrogrande, 2019). That is, constructing spatial sequences by arranging volumes in continuity with the pre-existing ones.

The dialogue the project establishes with the techniques of composing means continuity with the character of the place can be re-found. Above all from a spatial point of view, because architecture is principally the art of building the space. In the space, in fact, the values that define the environmental atmosphere rich in content and meaning the citizenry recognises as its own are collected together. Consequently, the project should be understood in the logic of development of spatial sequences related to other pre-existing ones already present.

References

Binotto, R., (1984). Montebelluna e il suo comprensorio, Montebelluna.

De Bortoli, L., (2006). Montebelluna e il mercato. Origini e costruzione di una città, Treviso.

Durante, A. (ed., 1997). Montebelluna fa giocare il mondo, Montebelluna.

Gasparini, D., (ed., 1992). Montebelluna. Storia di un territorio. Cartografia ed estimi tra Sei e Settecento, Venice.

Kropf, K., (2020). Using design as a tool to teach urban morphology. Urban Form and Design, 14, 2020, 10-13.

Molinari, L., (ed., 1997). Enesto Nathan Rogers. Esperienza dell'architettura, Milan.

Pietrogrande, E., (ed., 2019). Frammenti di città. Aree dismesse tra rinascita e cultura del progetto. Milan.

Reed, P., (ed., 1988). Alvar Aalto 1898-1976, Milan.

Schoonderbeek, M., (2017). A Theory of "Design by Research"; Mapping Experimentation in Architecture and Architectural Design. Ardeth, 1, 63-79. https://journals.openedition.org/ardeth/962 (date of access: 18.07.2022).

Van Ouwerkerk, M., Rosemann, J., (2001). Research by Design: International Conference Faculty of Architecture Delft University of Technology in co-operation with the EAAE/AEEA November 1-3 2000: Proceedings A. Delft University Press, Delft, Netherlands.

DynasticNet: Dynamic and Static Multi-Network

Bekir Eren Çaldıran[*], Tankut Acarman

Abstract: In this work, a deep learning model, a multitask network is proposed to localize dynamic traffic objects such as cars, motorcycles, bicycles, buses, trucks, static traffic objects such as color classified traffic lights and traffic signs, pedestrians, segment drivable area and detect lane lines. The network design has a unified architecture, one shared encoder for feature extraction and three decoders for three tasks. The multi-network proposed is trained and tested with BDD100K dataset. Evaluation results show that the proposed method is the fastest multi-network on the dataset with 47.62 FPS. Around multi-networks, proposed work has the second place on drivable area segmentation and lane line detection. Dynamic object localization performance of the network is state-of-theart with 40% performance increase compared to other models.

1. Introduction

Intelligent vehicle technologies require accurate and reliable perception to execute maneuvering tasks. Vehicles need to understand the driving environment to navigate safely. For an intelligent vehicle to detect multiclass objects including stationary and dynamic objects, drivable area and lane lines, a variety of technical features need to be engineered. To accomplish these tasks, humans use a combination of sensors, eyes and brain to process. Therefore, to drive like a human, neural networks as brains and various sensors as eyes are needed for autonomous vehicles. In this work to interpret the environment with camera sensor, multiple tasks need to be accomplished. Recently, multitask networks are proposed to handle different tasks altogether. With the right configurations and training, multi-task networks are capable of having better performance than single task networks on both accuracy and speed. We proposed our own deep learning model, a multitask network that is able to interpret driving environment by itself. Proposed model is able to localize dynamic traffic objects such as car, bike, motorcycle, bus and train, static traffic objects as traffic sign and color classified traffic light, pedestrians, drivable area and lane lines. We called this dynamic and static multi-network as "DynasticNet". We refer to it as so throughout the rest of the paper. To train and test DynasticNet, we used Berkeley Deep Drive 100K dataset (BDD100K)(Yu et al., 2018). To evaluate previous works, multiple subjects will be detailed seperately. Camera perception models of single and multi-task are reviewed. For camera models, in the open literature, most methods handle tasks

[1] Galatasaray University, Faculty of Engineering and Technology, Department of Computer Engineering, Istanbul, Turkey
[2] Galatasaray University, Faculty of Engineering and Technology, Department of Computer Engineering, Istanbul, Turkey
[*] Corresponding author: eren.caldiran@ozu.edu.tr

separately. Single task networks for lane detection, drivable area segmentation and traffic object detection are reviewed respectively. In following multi-task networks are detailed.

Lane line detection: Earlier methods for lane line detection used machine learning algorithms to detect lane lines. The methods used had a poor and slow performance. Then with the rising application of deep learning, network models specified for lane line detection tasks are proposed. To exemplify the single task lane line detection networks, some network models are given. Spatial Convolutional Neural Network (SCNN) in (Pan et al., 2018) makes use of convolutional layers to enable messages pass between pixels across rows and columns in a layer, but it is considered slow for a single task network due to slice-by-slice convolution. When a faster model is considered, in (Qin et al., 2020) a global feature is introduced by a row-based classification by locating lane lines on certain rows. In (Hou et al., 2019) SAD-ENet, a lightweight network that uses Self Attention Distillation (SAD) to allow model to learn from itself without additional supervision or labels are proposed. Examined models are used in the lane line detection performance comparisons. These single task models are specified for only lane line detection tasks.

Traffic object detection: Recently, the performance of object detection models is improved with great momentum. There have been different model proposals, one stage methods, two stage methods, detections with anchors, etc. On top of that as classification models used as backbones are also enhanced, with newer models such as, ResNet in (He et al., 2016), EfficientNet in (Tan & Le, 2019) and RegNet in (Radosavovic et al., 2020), object detectors gain a speed and performance boost. One stage methods such as SSD in (Liu et al., 2016) and YOLO in (Redmon et al., 2016) combine classification and localization. Based on these networks, there are also detection networks proposed on top of them. Two stage methods use region proposal to extract features and on top of the proposals, objects are localized and classified. Region based Convolutional Neural Network (R-CNN) in (Girshick et al., 2014) and Region-based Fully Convolutional Network (R-FCN) in (Dai et al., 2016) are representatives for two stage detectors. In comparison with respect to two-stage methods, one stage methods are suitable for intelligent vehicles since they have the potential to be executed on a real-time basis.

Traffic object segmentation: Segmentation methods try to estimate each pixel of the image to classify it correctly. Compared to an object detection model, segmentation models have much more classes to handle. When examples of segmentation methods capable of detecting dynamic and static traffic objects and pedestrians are examined, Pyramid Scene Parsing Network (PSPNet) in (Zhao et al., 2017) exploits the capability of global context information by different regionbased context aggregation through pyramid pooling module together with the proposed pyramid scene parsing network. Deeplabv3+ in (Chen et al., 2018) has a spatial pyramid pooling module and encode-decoder structure combined for the advantages from both methods. In (Yin et al., 2020), Disentangled Non-Local Neural Networks (DNLNet) uses a disentangled non-local block to decouple attention computation and visual clues of salient boundaries. These models mentioned are used in the performance evaluation of traffic object localization.

Drivable area segmentation: Drivable area is segmented under semantic segmentation tasks when deep learning methods are introduced. Under segmentation tasks, usually the road is segmented as a whole. The segmentation methods do not have the separation we have, which is to segment to road but also learn the drivable space on it, considering each lane, and upcoming traffic lane on a two-way drive road. When road segmentation via segmentation models is examined, in (Long et al., 2015) Fully Convolutional Networks (FCNs) have been proposed by making use of a Convolutional Neural Network (CNN) classifier by replacing fully connected

layers with 1x1 convolutions. Then, transposed convolutions are utilized to up-sample back to the original image size. Unet in (Ronneberg et al., 2015) uses the encoder-decoder architecture and skip connections to obtain high resolution outputs. These models mentioned are used in our model structure and the usage details are given in the upcoming section.

Multitask learning: Rather than focusing on single task networks of computer vision, multi-task models deployed for simultaneously handling different tasks together to be advantageous on both performance, resource usage and speed. We focus multi-task models that perform detection of drivable area, lane line and traffic objects tasks, which have attracted a lot attention recently. In (Qian et al., 2020), DLTNet capable of segmenting drivable area, lane line and detects traffic objects, has a common encoder and three decoder branches. Decoders in DLT-Net are connected with context tensors. Context tensors are based on the information from drivable area, and these tensors increase the performance by concatenating drivable area parameters with lane line and traffic object branch. The DLT-Net underlying methodology is based on the idea that all lane lines and some of the traffic objects (only vehicles in their case) are located on the drivable area. Our presented multinetwork, DynasticNet, detects traffic sign and lights that are above the drivable area. A context tensor is not obtained since we are also focused on traffic lights, pedestrians and traffic signs as well. MultiNet (Teichmann et al., 2016) has simultaneous street classification, road segmentation and traffic object detection for cars with one encoder and three separate decoders. Cell based method is used in detection branch of MultiNet which detects object based on anchors. YoloP in (Wu et al., 2021) detects lane lane, drivable area and traffic objects. YoloP is on a real-time basis, uses the BDD100K dataset, and reaches a high-level result in accuracy and speed. MultiNet is trained with the KITTI dataset. DLT-Net, YoloP and DynasticNet has been trained with the BDD100K dataset. While comparing the slight differences, KITTI dataset does not include lane line, and MultiNet does not have lane line detection task. Although DLTNet includes lane line detection task, lane line evaluation results have not been presented. In consequence, DynasticNet's lane line evaluation results, cannot be compared with these existing multi-task networks except YoloP. DLT-Net and MultiNet segments drivable area as a whole road. In DynasticNet, our presented approach separates lanes while segmenting drivable area. When drivable area is segmented, complete road is not segmented as drivable area, instead each lane in the drivable area is separated and detected. And the opposite direction of the road is detected as a non-drivable area, which is well presented for autonomous driving and lane keeping. DLT-Net and YoloP uses Feature Pyramid Network in their encoder design in (Lin et al., 2017). After shrinking the image to a certain level, before giving feature maps to separate decoder branches, both approaches make use of FPN to fuse different feature map results. After the fusion of neighbor layers, output layers are given to the decoder.

2. Material and Method

This chapter concerns the methodology for building the 2D camera multi-network DynasticNet. The process of creating a multi network with multiple output branches and multiple loss functions are explained in detail. DynasticNet is presented in Figure 1. Encoder branch of the network shrinks the image and gets feature maps with the help of pre-trained VGG-16 architecture, consisting of 3x3 convolutional and max pooling layers. The 3x3 convolutional layers learn to extract feature maps from input images, max-pooling layers use these feature maps to create smaller images with extracted features remaining. With the help of transfer learning, as VGG16 network is pre-trained with ImageNet (Russakovsky et al., 2015) dataset, which nearly has 1000 classes, using its already trained parameters to achieve feature extraction is advantageous and thanks to pre-trained parameters of VGG16. The last layer of the encoder

branch is given directly as an input to three decoders. For the first two up sampling operation inside each decoder branch, the corresponding layer from the encoder is fused. DynasticNet in Fig. 1 can jointly detect lane lines, drivable area and localize traffic objects as dynamic, static and pedestrians. If the static object is a traffic light, the color is also classified. In the decoder branches, the proposed method in FCN in (Long et al., 2015), increasing the size 8 times in the last layers (output layers with stride 8) is used to give results with details enhanced. To further enhance the resolution of our results and the performance, skip layers, which have been presented by Unet in (Ronneberg et al., 2015), are used as well.
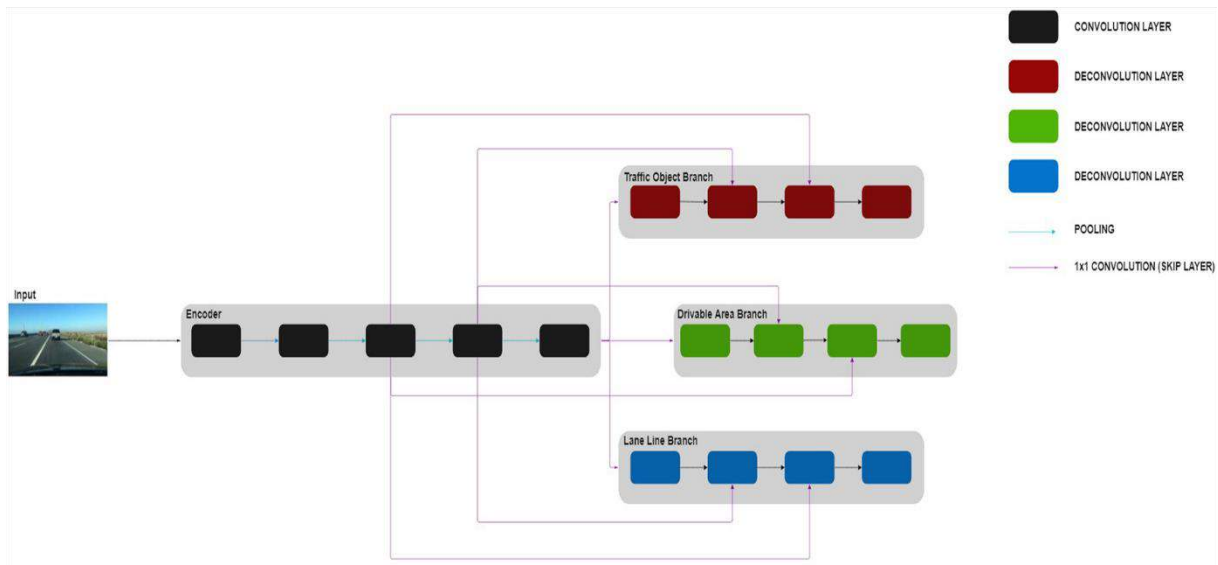
Figure 1. DynasticNet has one shared encoder for feature extraction and three decoders for three tasks. The last feature map is given as the input to decoders, the fusing operation is used in each decoder branch separately.

2.1. Encoder branch

A pre-trained network model, VGG16 in (Simonyan et al., 2014), is used as the feature extractor. Main advantage of using convolutional layers to extract features is to be able to extract high level features. Last fully connected layers of VGG are replaced with 1x1 convolutions to feed three decoders separately from single encoder output. Encoder output has the size of original image divided by 32.

2.2. Decoder branch

For all decoder branches, the same single output from encoder part is given as an input. Separate skip layers for each branch are used to fuse information from different layers. By fusing information with skip layers, high resolution outputs are achieved. In decoder branches, transposed convolutional layers are used instead of up sampling and then applying convolution. Last transpose convolution layers have a stride of 8. Branches are elaborated as follows:

Drivable area and lane line branch: All branches get an input of original image 32 times divided. With skip connections and transposed convolutional layers, input image is up sampled to the original image size. The output image of this branches has two channels, which represent the probability of each pixel for drivable area and background, and also the probability of each pixel for lane line and background.

Traffic object branch: In this branch, multiple outputs, each can be considered as different detection result are fused together under three classes, which are so-called dynamic traffic objects, static traffic objects and pedestrians. This is not as equal to semantic segmentation methods that calculate each class as a different object with their unique label shapes. Instead, localization is applied here based on the bounding box labels where inside it is filled with class labels.

Loss function and training: from three decoders, the network gives three different outputs. For drivable area branch, cross entropy loss is used. For lane line and traffic object branch, class imbalance is a problem. Lane lines constitute a very few of the image compared to background area samples. Considering traffic object case, the number of dynamic objects is higher in comparison with the number of static objects whereas static objects constitute a large number with respect to the number traffic light colors. To tackle these class imbalances, a special approach, focal loss in (Lin et al., 2017) is used. Focal loss focuses on miss classified examples. It aims to minimize the classification error between pixels and focuses on hard labels. Focal loss adds a modulating factor to cross entropy loss with tunable focusing parameter which helps the network to balance the weights, to not only focus on the most common class and to learn hard labels easier. Equation 1 and 2 gives binary cross entropy (CE) loss and focal loss (FL), respectively (Lin et al., 2017). In Equation 2, β indicates the weighting factor and μ indicates the tunable focusing parameter.

$$CE(p, y) = \begin{cases} -log(p) & \text{if } y = 1 \\ -log(1-p) & \text{otherwise.} \end{cases} \tag{1}$$

$$FL(p, y) = \begin{cases} -\beta(1-p)^{\mu} log(p) & \text{if } y = 1 \\ -(1-\beta) p^{\mu} log(1-p) & \text{otherwise.} \end{cases} \tag{2}$$

For all branches, each pixel in the image has a class. For drivable area and lane line branch, each pixel has either background or foreground value, either zero or one. For traffic object branch, each pixel has either background or one of the fifth foreground classes, either zero or a number between one and five. The multi-task loss is given in Equation 3. Total loss is the sum of three loses coming from the three branches. Lc is short for cross entropy loss and Lf is for focal loss. Drivable area branch uses cross entropy loss, traffic object and lane line branches use focal loss. For three branches ti, di, li indicates network prediction probability value for traffic object, drivable area and lane line branch respectively and ti*, di*, li* indicates the corresponding ground truth value. Since each pixel of the image has a loss value, the total loss of an image is calculated by the sum of all pixels, therefore W indicates the image width and H indicates the image height. α1, α2 and α3 are the loss weights of traffic object, drivable area and lane line branch respectively. Weight of the losses are chosen to avoid focusing on most common mask on the image during the training stage. In consequence, lane lines, compared to drivable area, are subject to a much higher weight as the ground truth masks covers a very few of the data content provided by the frame. These values are tuned to reach at the highest result

extracted from our network. Weights are chosen as 1, 1 and 10, respectively. While training, Adam is used as the optimizer and learning rate is set to 1e-4.

$$Loss = \alpha 1 \sum_k^{W*H/2} Lf(ti, t_i^*) + \alpha 2 \sum_k^{W*H} Lc(di, d_i^*) + \alpha 3 \sum_k^{W*H} Lf(li, l_i^*) \quad (3)$$

For training and evaluation purposes, images from the BDD100K dataset are resized from 1280x720x3 to 640x384x3 to use computing resources in an efficient and effective manner, to save memory and speed up the learning process. The used encoder VGG16 is trained with ImageNet in (Russakovsky et al., 2015), with images having the size of 224x224. Therefore, training our network with images resized by half (1280x720 to 640x384) has increased the level in accuracy and computational speed. To ease the learning process, preprocessing is used. The preprocessing method used in the training of VGG16, which zero centers the values with respect to ImageNet dataset, has been applied. In training and evaluation, Tesla P100 was the GPU used.

3. Results

DynasticNet is trained end to end with the BDD100K dataset. Since the label of the test set is not published, network is evaluated with the validation set. The experiments are separated and explained based on the output tasks. Starting with drivable area, results for lane lines and finally traffic objects are given in detail.

3.1 Drivable area results

Mean intersection over union (mIoU) is used to evaluate drivable area results. For drivable area, BDD100K separates drivable areas as alternative and direct lanes. In DynasticNet, we do not have that separation. We only separate background and drivable area with all lanes having the same category. In drivable area, each lane is same for us without considering if it is an alternative or direct lane. Throughout our evaluation study, the mIoU metric is performed on separating background and foreground (drivable area). In Table 1, drivable area segmentation results are compared with multi-task networks. There are other single-task segmentation methods retrained with BDD100K that have drivable area segmentation but separates lanes as direct and alternative then calculate IoU for both classes and average. Mean mIoU of these methods are in the interval 77% and 85% according to results published in official BDD100K model zoo. When segmentation of drivable area without the distinction of direct and alternative lanes are checked, DynasticNet has the second place among multi-networks using the BDD100K dataset. When all methods compared, while constructing YOLOP, they retrained PSPNet to compare its performance with their own work. Although official PSPNet drivable area segmentation mIoU result is 83.80, it is stated that YOLOP got mIoU result of 89.6, ranking the metric result of DynasticNet in the third place considering drivable area segmentation around all BDD100K models. DynasticNet outperforms MultiNet and DLTNet by 22.1% and 21.2%, respectively. In terms of speed, DynasticNet model is 5 times faster than these models and it has the first place in inference speed by exceeding YOLOP 16.15%. Visualization results of the drivable area segmentation are plotted between Figure 3 and Figure 5.

Table 1. Benchmarking results of drivable area segmentation

Networks	mIoU(%)	Speed (fps)
MultiNet	71.60	8.60
DLTNet	72.10	9.30
YOLOP	91.50	41.00
DynasticNet	87.39	47.62

Figure 3. Visualization of the drivable area segmentation result. In two-way road case, incoming lane is not segmented.

Figure 4. Visualization of the drivable area segmentation result. Each lane is separated in terms of drivable area.

Figure 5. Another visualization of the drivable area segmentation results that shows each lane is separated in terms of drivable area.

3.2 Lane line results

Lane lines are trained and evaluated based on the actual lane masks from BDD100K. For the evaluation of lane line detection, to only focus on foreground, Intersection over union (IoU) metric for lanes are used. Also, pixel accuracy is calculated for this task. In Table 2, results for

lane line detection are compared versus the existing models. For lane line detection, only multi-task network that has evaluation is YOLOP. For this task, comparison is with YOLOP and other single task state-of the art lane detection models. All other methods in this comparison use single line (usually center line) for a lane line representative. We use several lane classes and since we trained the network with official BDD100K masks, it is more challenging to learn. In terms of IoU for lanes, since we train with official masks, it is more complex for the network to represent a lane line with two lines. In terms of accuracy, a higher result is obtained. In SCNN, input size is 800 × 288 and pixel sizes for lane lines are 16 in training and 30 in evaluation. These changes make their evaluation very specific to lane lines. ENet-SAD and YOLOP uses images with size 640x384 and single center line with width set to 8 in training and 2 at evaluation. For us, pixel width is 2 in training and testing also the image size is same with ENet-SAD and YOLOP, which is 640x384. Around multi-networks, DynasticNet has the second place on lane line detection. Visualizations for lane line detection are given in Figure 6, Figure 7 and Figure 8.

Table 2. Benchmarking results of lane line detection

Networks	Accuracy (%)	IoU(%)
SCNN	35.79	15.84
ENet-SAD	36.56	16.02
YOLOP	70.50	26.20
DynasticNet	70.27	15.15

Figure 6. Visualization of the lane line detection result. Road curbs and lane lines are detected. These are the direct masks from predictions and are not post processed by any means of line fitting.

Figure 7. Visualization of the lane line detection result. Dashed lines are detected.

Figure 8. Another visualization of the lane line detection result.

3.3 Traffic object results

For traffic objecs, MultiNet, DLT-Net and YOLOP have a detection task and can only be evaluated by vehicle objects. Localization is used in our work and Intersection over union (IoU) scores for each class can be calculated based on the ground truth bounding box labels of the objects where the bounding box is filled with class labels like in semantic segmentation. In semantic segmentation, shapes of the labels are different for cars, people, bike etc., Here, all classes have box as the label shape. Using a common shape for labeling helps us bring multiple classes under the same category and learn all of them as one. Instead of creating an object detector, as our aim is to work with multiple tasks, this localization technique of objects as dynamic/static objects are useful and faster. To create a detector for these tasks, instead of grouping multiple classes under super categories, each class would be considered separately. Pedestrians and traffic signs would be two of the different classes. Also red light and green light would be classified beforehand.

To calculate the performance, Intersection over union (IoU) metric is used. Each corresponding ground truth and network output result for a class is mapped together to get their intersection and union. Then intersection of these results is divided by their union to achieve IoU. The performance is compared with single task semantic segmentation methods re-trained with the BDD100K dataset. The IoU metric results of specific objects given in BDD100K model zoo are used to get performance results of the segmentation methods. While calculating IoU for dynamic objects, the mean of other methods IoU results on car, bus, bicycle, motorcycle and truck are calculated. Since traffic lights are classified in this work but not in segmentation methods, separate categories used to calculate the performances. Considering dynamic objects' IoU, segmentation methods "motorcycle" and "truck" category results lower their mean. Since the data size of red light and pedestrians is lower compared to other categories in the training data, our results are lower on these categories as expected. Mean IoU (mIoU) is calculated according to the categories on Table 3.

As cars, bike, motorcycle, bus, truck are grouped and trained together under dynamic traffic objects, a performance boost is gained instead of focusing each of these objects separately. Although segmentation methods are one of the greatest models, they do not perform that great at BDD100K dataset due to its complexity. The presented approach performs better on green lights because of the imbalance between red and green light. There are lots of images in the dataset, captured at nighttime. Nighttime images make it complicated to seperate red lights from car's red stopping light, causing misclassification of a red traffic light. And secondly, depending on the state regulations, lights are not mounted in a unique manner, some lights are mounted with a metal pole holding the light and some are mounted with a cable above the road surface. Traffic object localization results in different road scenes are visualized in Figures between 9 and 11.

Table 3. Results for traffic object localization. Comparison results versus the state-of-the-art single task segmentation methods on BDD100K dataset.

Networks	Dynamic IoU (%)	Pedestrian IoU (%)	Sign IoU (%)	Light IoU (%)	Red Light IoU (%)	Green Light IoU (%)	mIoU (%)
DNLNet	53.12	53.92	49.23	40.60	-	-	49.22
PSPNet	52.66	55.08	48.98	41.52	-	-	49.56
DeepLab v3+	52.06	55.28	49.71	42.06	-	-	49.78
Dynastic Net	73.54	41.38	42.88	-	31.58	41.51	46.18
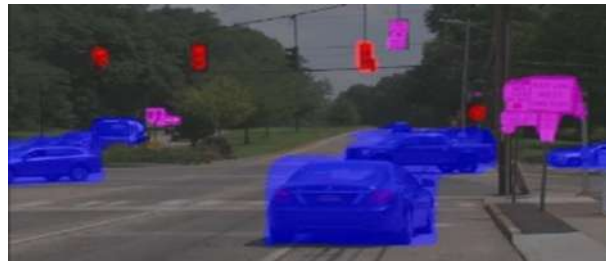
Figure 9. Visualization of the traffic object localization results. Red color indicates red light, dark purple indicates traffic signs and blue indicates dynamic objects.

Figure 10. Green indicates green light, dark purple indicates traffic signs and blue indicates dynamic objects.

Figure 11. Red indicates red light, dark purple indicates traffic signs, magenta indicates pedestrians and blue indicates dynamic objects.

4. Discussion and Conclusions

In this paper, a multi-network model, DynasticNet is proposed to handle different tasks simultaneously. Drivable area and lane line is detected while localizing dynamic objects, static objects, pedestrians and classified traffic light colors. DynasticNet has the second place on drivable area segmentation and lane line detection among multi-networks using the BDD100K dataset. In dynamic object localization, the presented multi-network model performs 40% better than the stateof-the art segmentation methods. By labeling different objects under the same class and training, classes with a smaller number of samples such as motorcycle, bike and truck are learnt in an efficient and effective manner. Around multi-networks, DynasticNet has the first place for inference speed by 16.15%. Within average 21ms latency of the network, pre-processing, inference by model and post-processing latencies are combined, total time it takes to input an image and acquiring the output is given. By referring to our average 21ms latency, with 47.62 FPS, DynasticNet can run in real-time on standard and embedded devices.

ACKNOWLEDGEMENT

References

Chen, L., Zhu, Y., Papandreou, G., Schroff, F. and Adam, H. (2018). Encoder-decoder with atrous separable convolution for semantic image segmentation., European conference on computer vision (ECCV), Springer, pp 801– 818.

Dai, J., Li, Y., He, K., and Sun, J. (2016). R-fcn: Object detection via region-based fully convolutional networks., Advances in neural information processing systems, 29, pp. 379-387.

Girshick, R., Donahue, J., Darrell, T. and Malik, J. (2014). Rich feature hierarchies for accurate object detection and semantic segmentation, Computer Vision and Pattern Recognition (CVPR), 2014 IEEE Conference on, IEEE, pp. 580-587.

He, K., Zhang, X., Ren, S. and Sun, J. (2016). Deep residual learning for image recognition. Computer Vision and Pattern Recognition (CVRP), 2016 IEEE Conference on, IEEE, pp. 770-778.

Hou, Y., Ma, Z., Liu, C. and Loy, C. C. (2019). Learning lightweight lane detection cnns by self attention distillation, International conference on computer vision (IEEE/CVF), pp. 1013-1021.

Lin, T., Goyal, P., Girshick, R., He, K. and Dollár, P. (2017a). Focal loss for dense object detection., Computer Vision and Pattern Recognition (CVPR), 2017 IEEE Conference on, IEEE, pp. 2980-2988.

Lin, T. Y., Dollár, P., Girshick, R., He, K., Hariharan, B. and Belongie, S. (2017b). Feature pyramid networks for object detection., Computer Vision and Pattern Recognition (CVPR), 2017 IEEE Conference on, IEEE, pp. 2117-2125.

Liu, W., Anguelov, D., Erhan, D., Szegedy, C., Reed, S., Fu, C. Y. and Berg, A. C. (2016). Ssd: Single shot multibox detector., European conference on computer vision, Springer, pp. 21-27.

Long, J., Shelhamer, E. and Darrell, T. (2015). Fully convolutional networks for semantic segmentation., Computer Vision and Pattern Recognition (CVPR), 2015 IEEE Conference on, IEEE, pp. 3431- 3440.

Pan, X., Shi, J., Luo, P., Wang, X. and Tang, X. (2018). Spatial as deep: Spatial cnn for traffic scene understanding., AAAI Conference on Artificial Intelligence, Vol. 32, No. 1.

Qian, Y., Dolan, J-M. and Yang, M. (2020). Dlt-net: Joint detection of drivable areas, lane lines, and traffic objects, IEEE Transactions on Intelligent Transportation Systems, pp. 4670–4679.

Qin, Z., Wang, H. and Li, X. (2020). Ultra-fast structure-aware deep lane detection, European Conference on Computer Vision, Springer, pp. 276-291.

Radosavovic, I., Kosaraju, R. P., Girshick, R., He, K. and Dollár, P. (2020). Designing network design spaces, Computer Vision and Pattern Recognition (CVPR), 2020 IEEE Conference on, IEEE, pp. 10428-10436.

Redmon, J., Divvala, S., Girshick, R. and Farhadi, A. (2016). You only look once: Unified, real-time object detection, Computer Vision and Pattern Recognition (CVPR), 2016 IEEE Conference on, IEEE, pp. 779-788.

Ronneberger, O., Fischer, P. and Brox, T. (2015). U-net: Convolutional networks for biomedical image segmentation, International Conference on Medical image computing and computer-assisted intervention, Springer, pp. 234-241.

Russakovsky, O., Deng, J., Su, H., Krause, J., Satheesh, S., Ma, S., Huang, Z., Karpathy, A., Khosla, A., Bernstein, M., Berg, A-C. and Fei-Fei, L. (2015). Imagenet large scale visual recognition challenge, International journal of computer vision, pp. 211-252.

Simonyan, K. and Zisserman, A. (2014). Very deep convolutional networks for large-scale image recognition, arXiv preprint arXiv:1409.1556.

Tan, M. and Le, Q. (2019). Efficientnet: Rethinking model scaling for convolutional neural networks, International conference on machine learning, PMLR, pp. 6105-6114.

Teichmann, M., Weber, M., Zoellner, M., Cipolla, R. and Urtasun, R. (2018). Multinet: Real-time joint semantic reasoning for autonomous driving, IEEE Intelligent Vehicles Symposium (IV), pp. 1013-1020.

Yin, M., Yao, Z., Cao, Y., Li, X., Zhang, Z., Lin, S. and Hu, H. (2020). Disentangled non-local neural networks, In European Conference on Computer Vision, Springer, pp. 191-207.

Yu, F., Chen, H., Wang, X., Xian, W., Chen, Y., Liu, F., Liao, M., Madhavan, V. and Darrell, T. (2020). Bdd100k: A diverse driving dataset for heterogeneous multitask learning, Computer Vision and Pattern Recognition (CVPR), 2020 IEEE Conference on, IEEE, pp. 2636-2645.

Zhao, H., Shi, J., Qi, X., Wang, X. and Jia, J. (2017). Pyramid scene parsing network. Computer Vision and Pattern Recognition (CVPR), 2017 IEEE Conference on, IEEE, pp. 2881-2890.

Blending Training of Students and Promotion of Space Technologies by Designing Satellite Communications

Viorel Bostan[1], Valentin Ilco[1], Vladimir Melnic[1], Alexei Martiniuc[1], Vladimir Vărzaru[1], Nicolae Secrieru[1]*

Abstract: The purpose of this paper is to promote satellite communications by creating a communication and control platform that simplifies the interaction between the operator and the communication algorithms. The communication platform represents the application level of the nanosatellite communication stack and allows to provide the user with a simple and explicit graphical interface on the one hand and on the other hand it must automate, as much as possible, the nanosatellite communication process. The platform must allow users to receive useful information received from the nanosatellite, information on the status of the satellite and its subsystems, and to send to the nanosatellite the appropriate commands to configure it, reset it or request useful data. The general communication architecture with the nanosatellite is obtained after the implementation of the communication platform and the monitoring of the nanosatellites. In order to make the training process more efficient, it is proposed to apply the blending elearning approach. There are online courses on the elearning moodle TUM platform that reflect both the theoretical and practical part of satellite communications, which are mandatory for students studying these disciplines, as well as accessible to other students who want to get acquainted with modern satellite technologies.

Keywords: satellite communication, educational nanosatellite, ground station, blending training

I. INTRODUCTION

The National Center for Space Technologies (NCST) of Technical University of Moldova (TUM) has been oriented towards a series of nanosatellites, according to the international standard CubeSat. In 2019, the NCST team participated in the fourth round of the KiboCUBE Program with the "TUMnanoSAT" nanosatellite project proposal and won this competition for free launch by JAXA. This project includes the student-initiative design and fabrication of critical components, including the payload and CubeSat modules. From the other hand the satellite communication is also very important. The reception of the satellite telemetry data and

payload data is achieved through a radio architecture. The functionality of a traditional radio architecture, within a satellite communication, is primarily based on hardware components, with minimal software configurability. Conventionally, they consist of: modulators, coders, amplifiers, filters, mixers, etc., dedicated to a certain mode of transmission. The software part is dedicated to the control of the interfaces with the communication network. Given that the hardware predominates in this model, a possible upgrade of the system would mean a total change of the model and a redesign of the system. SDR or Software Defined Radio solves this problem.

The discussed communication platform represents the application level of the nanosatellite communication stack and allows to provide the user with a simple and explicit graphical interface on the one hand and on the other hand it must automate, as much as possible, the nanosatellite communication process. The platform allows users to receive useful information received from the nanosatellite, information on the status of the satellite and its subsystems, and to send to the nanosatellite the appropriate commands to configure it, reset it or request useful data. Based on this communication platform, the students acquired experience with industrial level integration and testing procedures. Undergraduate teams working on TUMnanoSAT lead the design and fabrication of the payload, structure, and system integration, providing experience with systems engineering, technical writing, and various cross-disciplinary applications. Over fifty undergraduate students, several graduate students and faculty members from several departments were involved in this project in both the development and testing of the TUMnanoSAT nanosatellite subsystems to enhance understanding of the fundamentals of engineering.

In order to make the training process more efficient, it is proposed to apply the blending elearning approach. There are online courses on the elearning moodle TUM platform that reflect both the theoretical and practical part of satellite communications, which are mandatory for students studying these disciplines, as well as accessible to other students who want to get acquainted with modern satellite technologies.

II. RECEIVING STATIONS OF TUMNANOSAT

Successful missions require good communication with the ground segment. The satellite subsystem is based on the Endurosat UHF transceiver, based on the SI4463 integrated circuit from Silicon Labs. The basic features of the messages transmitted by TUMnanoSAT are:
- GMSK Modulation
- AX.25 protocol
- 9600 baud-rate
- NRZI and G3RUH Scrambled
- 1 W transmission power
- Beacon Frequency: 1/30 s
- Telemetry Frequency: On request

TUM Center of Space Technologies has 2 ground stations with the following architecture:

The ground stations are located at 200 km distance. Each station has two antennas assembly. The antennas, mounted on the mast, are connected with RF ecoflex cable to the LNAs (Low Noise Amplifiers). X-Quad 70cm and X-Quad 2m to LNA SP70 and LNA SP200 respectively. The next node connected from the LNAs consists of coaxial relays which split the signal for

feeding it into the ICOM IC-9100 and USRP B200/E310 to be further processed. Besides the main RF connections there is also a data line connection from the PC Ground station to the signal processing units (ICOM and USRP) and a control line connection to the rotator controller and relays.

Ground station have 2 possible variants of SDR configuration:
- The first choice is USRP B200 as a peripheral device and a PC as a processing device, connected through USB interface (preferably USB 3.0 for more bandwidth)
- The second choice is USRP E310 as both, peripheral device and processing device. USRP E310 uses its FPGA for digitizing the received data and its core for processing, working as a standalone device and mounted directly on antenna mast.

Regardless of the configuration of SDR that we choose, a software program is needed to process the data. The easiest way to create such software is to use GnuRadio Companion. In the figure 3 is presented flowgraph created in GNU Radio for communication with TUMnanoSAT, the telecommand part. ZMQ PULL Message Source is used as a socket for external application, then these messages are encoded in a AX.25 frame. Fixed Length Framer is modified digital block to create radio packet according to TUMnanoSAT Si4463 transceiver. Also Center of Space Technologies at Technical University of Moldova arranged a Mission Monitor and Control System where it is possible to see and control each antenna and get the information from a specific satellite. The software used for tracking is Gpredict. In Mission Monitor and Control System is integrated as well remote control of satellite communication ground stations [7] .

One of the biggest problems that face universities ground stations is their underutilization problem. Most of the time, ground stations sit unused due to short window of communication with satellite. The communications window for common CubeSats in the LEO is about 12 min per pass in the best-case scenario. In practice, however, the quality of a pass is very sensitive to the environmental factors as well as maximum elevation of the satellite as seen from the ground station. One of solution is, of course, utilization of networks that allow collaboration and collection of data between ground station operators. There are a lot of projects meant to make easier communication between stations [2].
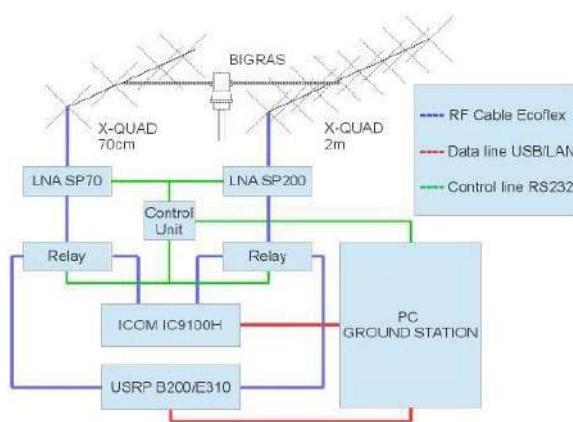
| **Figure 1.** TUMnanoSAT ground stations architecture | **Figure 2.** Antennas assembly at TUM NCST |

TUM Center of Space Technologies started to implement its own network of ground stations, during 2016-2018 under the project "Developing the Terrestrial Satellite Networks as a Platform for Cooperation with European Spatial Technology Partners" in partnership with the Space Sciences Institute (SSI) of Romanian Space Agency (ROSA). The idea of connecting ground stations through a virtual network of computers was developed within the project, which allows considerable extension of the radio visibility period of a satellite and, consequently, increasing the amount of data sent. Another opportunity is the simultaneous reception of data from a satellite via several ground stations, and storing them in the command center, where the data packages will merge. For the first stage were connected ground stations from TUM Center of Space Technologies and ground station from SSI of ROSA, Bucharest, Romania, based on which the interaction procedures were verified [5].

III. REMOTE CONTROL OF SATELLITE COMMUNICATION GROUND STATIONS

The TUM Center of Space Technologies network of ground stations is designed and constructed so as to ensure the communication among stations regionally / worldwide via the Internet. Ground stations can communicate via client applications with server components based on TCP / IP protocol. The architecture developed enables centralizing the data received from a satellite by different ground stations in the same database. Client applications can only communicate with the server, Server components having the administrative role. The Server component is the only link of the system which provides access to the database and is able to communicate with all client applications in the system. In order to implement the remote control of ground stations, the "client-server" classical architecture was taken as the basis consisting of three parts: a VPN server and a separate network device that interconnects the main server and the clients in a secure manner; the main high-performance server that manages the entire network and provides a web interface for end users; a number of clients PCs worldwide connected to the VPN network. Clients can be of two categories: the first category - only to access the web interface, and the second category - to connect the ground station to the network for its joint use [5-9].

Figure 3. Mission Monitor and Control System

Currently, the VPN server runs on the computer MikroTik Cloud Router with advanced performance - a high level of flexibility and a wide range of possibilities. The main server is running on the "blade" type server Sun Microsystems and Ubuntu Server LTS is used as operating system and provides a range of personalized services developed for the remote control of ground stations. For the purpose of redundancy, a second "blade" type server is installed, identical to the main one. The client computer can be any type of PC, from a medium performance SBC to a "high-end" desktop computer. The choice depends on the purpose of the end user, which may consist of access to the web interface and / or connection to the ground station. At the current stage of implementation, the client software for the connection to the ground station has been tested successfully on a Raspberry PC SBC module and a desktop PC, which is running an Ubuntu distribution, but it can run any other operating system: Microsoft Windows, Mac OS X, GNU / Linux and even on BSD derivatives.

Figure 4 Server components of remote control of the ground stations.
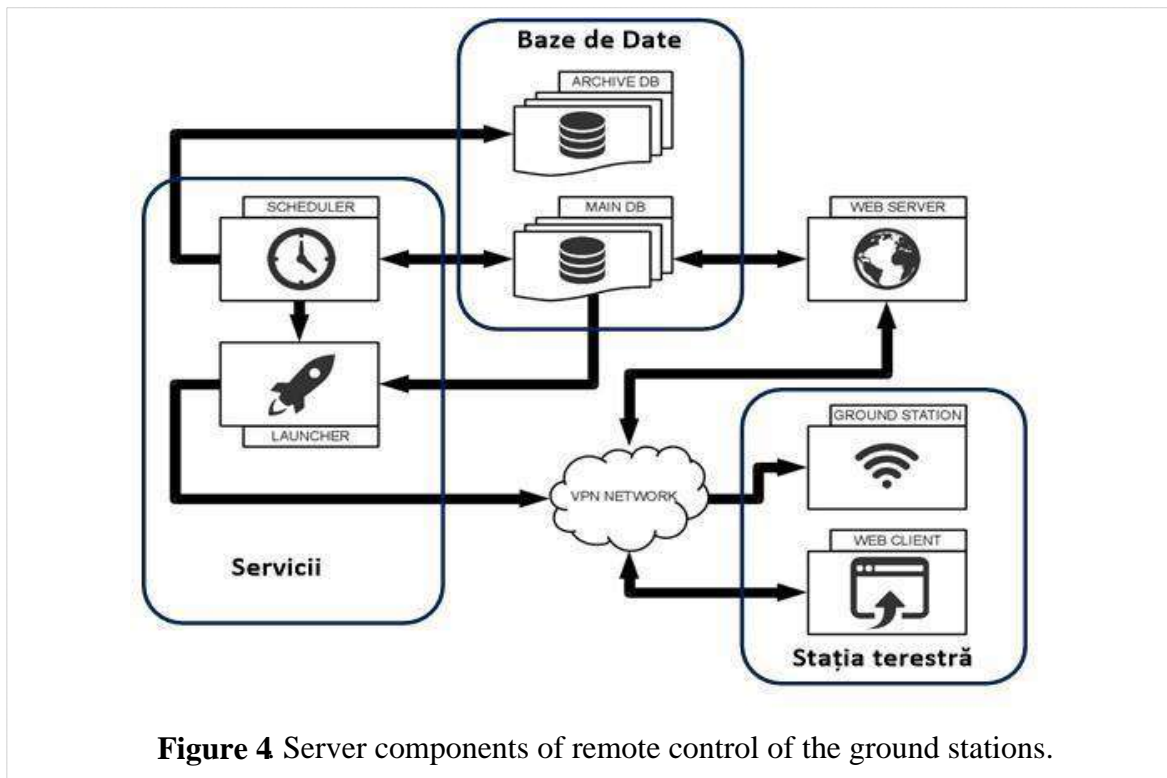
The Software "server-side" component was developed at NSTC that provides the following services and / or certain functional destinations [10-13]:

⬚ **Main DB** – the main database for storing data necessary for current operations (data stored for a short period of time);

⬚ **Scheduler** – monitors the main DB for current data, making decisions based on previously acquired data - appealing the **Launcher** or sending data to the **DB archive**; maintaining and updating TLEs and future observations based on updated information;

⬚ **DB archive** – database in which previous data is stored in the long term;

⬚ **Web Client** – GUI component, enables end users to interact with the system in order to schedule new observations or remove old ones, view information about the connected ground stations etc. (only accessed by clients of the VPN network);

⬚ **Web Server** – ensures the functionality of the Web Client component and access to databases;

⬚ **Launcher** – is the service that communicates with clients (those with the ground station connected), sending them commands required to fulfil specific tasks based on some parameters provided by Scheduler;

⬚ **Ground Station** – is the end point of the system that receives and executes the requested commands.

⬚ **VPN network** – client-server communication via secured VPN network tunnel; **Server Link** – the client receives all commands from the server-side component.

IV.   DATA MANAGEMENT FOR INFORMATION RETRIEVAL IN GROUND STATIONS NETWORKS

Monitoring ground stations are not built typically parallel because, on the one hand, the beam of radio waves from the satellite is relatively narrow and, on the other hand, the development

of several backup ground stations for a space agency can be very expensive. Networks of educational ground stations can share resources to ensure simultaneously the reception of the data stream from a single satellite. The reception from a "downlinks" satellite offers both opportunities and challenges. The opportunity is to get redundant data from ground stations, and the challenge lies in the need to develop a system that requires the use of appropriate methods of management and data synchronization.

Data management has evolved from the idea of combining multiple data streams from the same satellite, received at a number of geographically distributed ground stations. Theoretically, these data streams received in parallel by ground stations should be identical, but in reality they differ for several reasons. For example, the interaction time of each satellite and ground station differs depending on the route. When two routes overlap, the ground stations being geographically spaced apart, there is a small period of time during which only one of them will be in contact with the satellite. Thus, each station receives different sets of data frames. To solve this problem ground stations of the network must be synchronized between them, to command data frames received on a common time scale worldwide. This supposes both synchronizing computer clocks and timing of subsequent data streams.

V. BLENDING TRAINING OF STUDENTS TO PROMOTE SPACE TECHNOLOGIES

In the last time it is observed a slowing interest of pupils and students towards a research or engineering career. In the same time there was noticed an underperformance of current students in engineering and science. Analyzing the reasons for this poor performance, there were identified several key factors including the quality and incompleteness of academic programs, the existing gap in scientific knowledge among school teachers, the lack of information, motivation, environment and opportunities for children and students regarding the science and technology. Space endeavors and related technologies are a constant and strong catalyser for human scientific development and can be successfully used to attract the interest towards science and engineering of a larger number of people from four target groups at different education levels: children, high school students, students and master degree students, PhD students.

As a global approach project includes raising awareness about space field, generating relevant project ideas and their implementation, creating a favorable environment for personal scientific development among the target groups. The outreach activities are differentiated for each group taking into account their education levels and backgrounds. For the first group, it is intended to draw the attention towards the space science through movies and lectures held at the planned planetarium located in the observatory at NCST-TUM. Furthermore, for those interested there will be available online lectures and contest proposals placed on the planned website platform.

In order to initiate the 2-nd group in the space technology there were planned the online lectures on relevant science areas such as of physics, mathematics and programming, followed by the proposals to use the gained knowledge in practical activities related to aircraft flights and mechanics of celestial bodies, assembling simple Robo-KITs, aircraft and copters KITs and even classroom satellites (CubeSat format). To boost and maintain the motivation there are planned contests and summer schools. The general scope of activities

planned for this target group consists in increasing the number of high school students with an interest towards university education in the specialties related to space science and engineering.

For the current university students, the proposed activities include online and video lectures on advanced topics not covered by standard curriculum such as microcontrollers and electronics used in spacecraft and satellites, satellite design, attitude control and stabilization etc, generating project proposals (including license and Master Degree theses) related to space science and their implementation, summer schools and workshops with invited speakers from the consortium partners. The biggest motivation will be to have the opportunity to participate in the design and elaboration of SATUM. The partners involved in the project will compliment each other in creating and implementing the educational content, and sharing their expertise and knowledge.

Regarding the PhD students, it is necessary to prepare intriguing research topics, provide an adequate environment, equipment and assistance and offer the possibility of bringing their ideas to life. The partners also can be involved in co-advising joint Doctoral Degree theses. All information about recent developments of space science and technology, online and video lectures, contest conditions, assistance will be integrated on the to be developed website platform that will allow effectively and efficiently share resources, communicate with target groups, disseminate results and distribute the project information to the press and the public.

Figure 5. The scheme to promote the space technologies for the I level - pupils in schools and level II - students from universities.
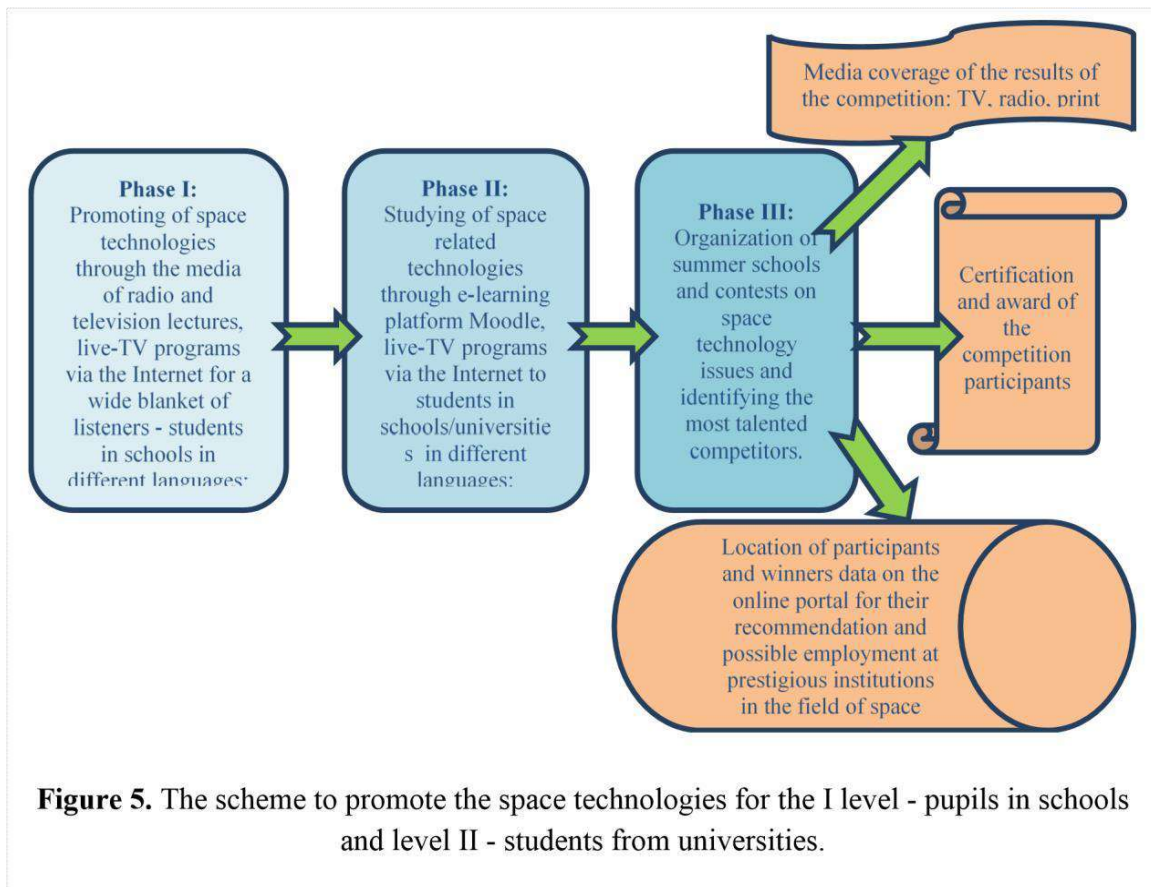
In order to achieve the main goal of this proposal - excluding the lack of scientists, engineers and technicians on the area of space research and development by dissemination of

experiences in the space domain and to contribute to building of long-term partnerships between peoples from different Europe countries there are planned activities that can act as catalyzers in motivating pupils and students at different ages and education levels: **Phase I:** Promoting of space technologies through the media of radio and television lectures, live-TV programs via the Internet for a wide blanket of listeners - students in schools in different languages: Romanian and English as possible. **Phase II:** Studying of space related technologies through e-learning platform Moodle, live-TV programs via the Internet to students in schools/universities in different languages: Romanian and English as possible [15-16]. **Phase III:** Organization of summer schools, workshops and contests on space technology issues and identifying the most talented competitors. Training cycle ends with a media coverage as party competition and awarding participants. An important point is to create a "database" of participants with recommendations for their admission at prestigious institutions and/or companies engaged in space research and technology development.

VI. CONCLUSION

TUM Center of Space Technologies developed a terrestrial infrastructure with a modern approach in the communication procedures with the microsatellites using Software Defined Radio technology for communication. SDR provides a new approach to designing a network of ground stations satellite, an approach that brings primarily significant reduction in design complexity and cost and offers a flexible environment, versatile radio architecture development. There were identified a several key factors including the quality and incompleteness of academic programs, the existing gap in scientific knowledge among school teachers, the lack of information, motivation, environment and opportunities for children and students regarding the science and technology. The implementation of project results will improve the quality of teaching by providing all study materials and imposing a study discipline as well as for parttime studies, continuing education and full-time studies.

Acknowledgements

REFERENCES

[1] C. Simpson, A. Burjek, W. Patton, E. G. Hackett Jr., C. O'Neill „Ground Station Infrastructure Development at the University of Alabama, Tuscaloosa" In: 70 th International Astronautical Congress (IAC), Washington D.C., 21-25 October, 2019

[2] "SDRF cognitive radio definitions working document, SDRF-06-R-0011-V1.0.0". [Online]. Available: http://groups.winnforum.org/d/do/1585.

[3] Bostan I., Secrieru N., Candraman S., Margarint A., Barbovschi A. "National space technologies center infrastructure connection to global educational network for satellite operation." - În: Meridian Ingineresc, nr. 2, 2015, Chișinău. Bostan I., Secrieru N., Candraman S., Margarint A., Barbovschi A. "Connecting the infrastructure of National Centre of Space

Technologies to Global Educational Network for Satellite Operations" - In: Proceeding of the 5th International Conference "Telecommunications, Electronics and Informatics", May 20-23, 2015, Chișinău, Vol. 1.

[4]   Margarint A., Barbovschi A. "Automation of satellite tracking for worldwide ground stations" - In: Proceeding of the 5th Int. Conf. "Telecommunications, Electronics and Informatics", May 20-23, 2015, Chișinău, Vol. 1, p. 421-422.

[5]   Levineț N., Ilco V., Secrieru N. "Satellite telemetry data reception an processing via soft ware defined radio" - In: Meridian Ingineresc Nr.2, 2015, Chișinău, p. 72-76.

[6]   Bostan I., Cantzer V., Secrieru N., Bodean G., Candraman S. Research, "Design and Manufacture of Functional Components of The Microsatellite "Republic of Moldova". - In: 2nd International Communication Colloquium, Aahen, 2014, p. 19-30.

[7]   Bostan I., Piso I.M., Bostan V., Badea A., Secrieru N., Manciu G. V. "Prospects for cooperation of the technical university of Moldova with Romanian space agency in the field of space technologies" - In: Meridian Ingineresc, 2016, Nr. 2, pp. 89 – 95.

[8]   Bostan I., Piso I.M., Bostan V.,Badea A., Secrieru N., Trusculescu M., Candraman S., Margarint A. "Architecture of the ground stations - satellites communication network" - In: Meridian Ingineresc, 2016, Nr. 2, pp. 96 – 103.

[9]   Bostan I., Dulgheru V., Secrieru N., Bostan V., Sochirean A., Candraman S., Gangan S., Margarint A., Grițcov S. "Dispozitive mecatronice, tehnologii industriale și satelitare" - În: Academos, nr. 1 (32), 2014, p. 21-25.

[10]   Ion Bostan,Ioan-Marius Piso,Viorel Bostan,Alexandru Badea,Nicolae Secrieru, Marius Trusculescu, Sergiu Candraman, Andrei Margarint, Vladimir Melnic. "Arhitectura rețelei stațiilor terestre de comunicații cu sateliți" - In: Akademos, nr. 2 (70), 2016, p. 70-75.

[11]   TUMnanoSAT proposal for CubeSAT Mission Application for the Fourth Round in the framework of United Nations/Japan Cooperation Programme on CubeSat Deployment from the International Space Staation (ISS) Japanese Experiment Module "KiboCube". – Technical University of Moldova. Chișinau, 2019. 63 p.

[12]   Bostan, Ion; Secrieru, Nicolae; Ilco, Valentin; Levineț, Nicolae; Bostan, Viorel; Candraman, Sergiu; Gîrşcan, Adrian; Margarint, Andrei. *"Educational space missions of TUMnanoSat family"* - . In: *Telecommunications, Electronics and Informatics. 24-27 mai 2018*, Chișinău. Tehnica UTM, 2018, pp. 295-302. ISBN 978-9975-45-540-4.

[13]   Secrieru, Nicolae; Candraman, Sergiu; Andronic, Serghei; *Younger generation inspiration and motivation through exposure to space technology* - In: Proceedings of the conference "Telecommunications, Electronics and Informatics", Chisinau, Moldova, May 20-23, 2015 [15] "*Mobile and satellite communications*" - lecture course and course project - http://moodle.utm.md/course/view.php?id=641

[16] "*Space technologies practics with a nanosatellite*" - Mobile and Satellite Communications practice and labs course - http://moodle.utm.md/course/view.php?id=494

Motivation for the Younger Generations Through Information and Communication Technology

Serghei Andronic[1], Nicolae Secrieru[1]*

Abstract: This paper deals with a challenge for the information and communication technologies (ICT). The main objective is to provide the target groups (children/young people, students, and PhD students) motivation, and opportunities to pursue careers in information and communication technology. Amongst specific objectives are: to enhance the promotion of research and technological achievements in this domain, among target groups; closing the gap in education programs used by schools and universities, related to information and communication science, by creating appropriate content (video lectures, on-line lectures) and implementation of information (competitions, summer schools, workshops); providing opportunities for pupil and student to develop their motivated ideas in science and information and communication technology; creation of courses on web platforms that integrate effectively promotion of research, achievements, results dissemination and efficient sharing of resources with online education target groups.

This paper presents how to teach, using the web, the components of an e-learning course website, and the structure of the instructional process. These learning environments will improve student performance in ICT courses offered at Technical University of Moldova ("TUM"). Our web-based instructional methodology focuses on teaching the systematic problem-solving skill. The development of courseware materials for student engineers in Republic of Moldova will have an increasing impact on the national scene of engineering education.

Keywords: computer-aided learning efficiency, information and communication technologies providing

1. Introduction

The open-source learning management systems ("LMS"), such as MOODLE, are platforms that allow users to build and offer online courses. It was built for traditional online classrooms, which attract a large number of students. Moodle is suited for organizations that want a full-featured, customizable LMS. The platform offers educational tools, analytics and SCORM compliance. The trade-off is that the platform is over 10 years old. The number of configuration options can be daunting, and system performance suffers with larger numbers of students. Our main objective is to provide the target groups (students and PhD students) motivation, and opportunities to pursue careers in information and communication technology. Amongst specific objectives are: to enhance the promotion of research and technological achievements in this domain, among target groups; closing the gap in education programs used by schools and universities, related to information and communication science, by creating appropriate content (video lectures, on-line lectures) and implementation of information (competitions,

[1] Technical University of Moldova, Space Technologies Center, Chisinau, Rep. of Moldova
* Corresponding author: nicolae.secrieru@cnts.utm.md

summer schools, workshops); providing opportunities for student to develop their motivated ideas in science and information and communication technology; creation of courses on web platforms that integrate effectively promotion of research, achievements, results dissemination and efficient sharing of resources with online education target groups. In order to make the training process more efficient, it is proposed to apply the blended e-learning approach. There are online courses on the TUM Moodle e-learning platform that reflect both the theoretical and practical part of communications, which are mandatory for students studying these disciplines. It is also accessible to other students who want to get acquainted with modern communication, including the satellite technologies.

2. Learning system structure on the TUM Moodle platform

A modular and hierarchical structure was incorporated in designing the organization of the learning system. Five levels were maintained to hierarchically structure the contents. The learning material was classified into modules at each level to ease the content and course management by providing flexibility for reuse. An example of such structure of the learning system is shown in Figure 1, based on the "Satellite communication" online course from TUM Moodle Platform [4, 6].

The structure resembles that of an academic curriculum. Each level can be compared to the levels in the traditional education system. The top level in the system structure was broadly divided into categories called "modules". This stage is similar to the different streams and majors in the academic curriculum that a student can take. As there may be different courses available in each stream that make them unique, the modules consist of
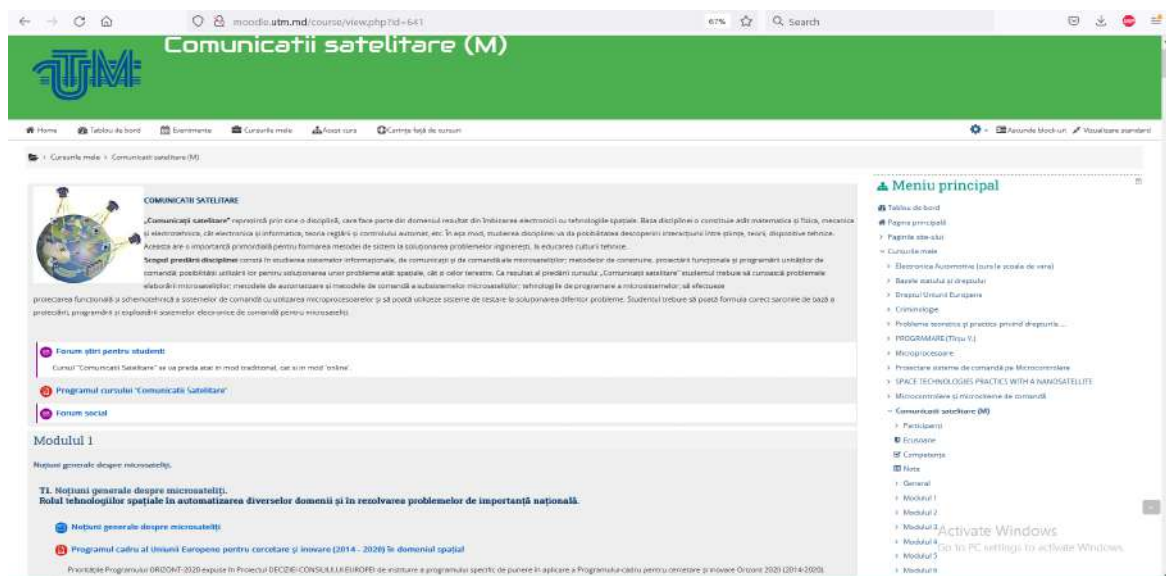
Figure 1. Learning System Structure

The lessons were further divided into "objectives" to provide a fundamental learning experience for the students, with explicit material focusing on specific topics. These objectives, which are the building blocks for the entire learning system, are comparable to the different chapters in a textbook used for a course. The last level in the learning system represents the content organization and presentation for each objective. The contents for the objective were displayed by segregating into frames. This level in the system is similar to the pages of each chapter in the textbook. As each chapter may vary in the number of pages, the objectives were

also designed to vary from 1 to 20 frames depending on the volume of content. Though each frame displayed specific content, they were made self-contained in a single environment for an objective. This was done to maintain continuity in learning and minimize waiting time to load each frame. This frame-based structure was designed to display small chunks of material and help the user to grasp concepts gradually before proceeding to the next one.

3. Mobile and Satellite Communication course organization

The course organization is based on Bloom's taxonomy of education objectives, applied to e-learning of Mobile and Satellite Communication [1, 4]. As engineering curricula and courses continue to be restructured due to emerging technologies and ideas, it has become difficult to decide what body of knowledge should be retained and what is to be left out, given that the length of time for undergraduate education is limited to four years.

The choice of using e-learning technologies should also include the commitment to assess the course content, the learning outcomes, and interaction needs. These are also known as the "Five I's" of effective e-learning: interaction, introspection, innovation, integration, and information. Interaction refers not only to the communication that should occur between the student and the teacher, or the student with other students, but also the interaction between the students and the content of the course. Thus, asynchronous, and synchronous communications as well as the presentation of print materials and links to the Internet form the technology needs of interaction. Introspection is the interpretation, revision, and demonstrated understanding of concepts. Discussion boards and graphics can be effective technologies to encourage introspection. Innovation refers to the ability of teachers to experiment with technologies in order to address various learning styles. Thus, combination of audio, video, and asynchronous discussion can provide various opportunities for students to learn. Integration reflects the integration of facts, concepts, theories, and practical application of knowledge. Using case studies, print exercises, and role-play can create a setting in which integration can occur. Information refers to the knowledge and understanding that is a prerequisite for students to move to the next level of learning [1,4].

The instructional objectives provide the basis for instructional activities in and outside of the classroom/laboratories. For each class, the students come in with different learning styles and capabilities. Variation in learning styles of the students can be addressed through course organization. Today, the course organization is generally at the prerogative of the teacher who teaches the course. However, there is a general consensus and effort is being mounted by all faculty members to adapt instructional techniques that enhance student learning in and out of the classroom. It is therefore the teacher who is required to take into consideration the different learning styles, in order to build the class presentations around a combination of pedagogical techniques, so as to accommodate all the students enrolled in the course.

Shown in Table 1 is a sample of course objective for mobile and satellite communication. It is obvious from the objectives that this is not a traditional first circuit course in a typical communication engineering program. Also noteworthy is that only the first two sets of objectives are written out in detail. As a rule, the objectives indicate things that the student must be able to do at the end of the course.

Table1: Sample Instructional of the mobile and satellite communication

Objectives	Contents of lessons
To know: - main definitions of communications satellite; - classification and	T4. Satellite communications. T4.1 Development of satellite systems. Types of orbits Space system components: space segment; the terrestrial segment; user segment. Modes of communication

generations subsystems of satellite communications. Be able to: - to know the structure hardware and software communication systems for satellites; - to determine the mode needed for solving concrete problems of communication; - to know the functions of various communication subsystems.	between segments of space systems. Recommendations for the implementation of the microsatellite communication subsystem (continuous use of "beacon", use of common modes for amateur radio, verification of the possibility of monitoring the satellite at the launch stage with other ground stations). T4.2 Digital communication techniques. Techniques that allow basic band signals to be transmitted remotely, to adapt the characteristics of the signals transmitted to the constraints imposed by communications through satellite channels: power and bandwidth. The ways in which these resources can be traded from one another. Ways to achieve an optimal compromise, giving it maximum capacity at minimum system costs. Typical functions implemented for transmitting digital signals: processing or formatting tape; modulation and digital demodulation; encoding and decoding. Bit error rate (BER) per bit energy ratio and spectral power density (Ec / N0), power bandwidth trade-off due to the encoded channel.

It is pertinent to call the student's attention to the entries in the instructional objective Table 1. The writing of instructional objectives or course objectives is an elaborate exercise that takes a lot of time. Generally, the instructional objectives are divided into weekly activities and entered into the course calendar.

Some helpful strategies for establishing education objectives for on-line courses are:

a) Establishing online threaded discussions that deal specifically with assignments and projects;

b) Establishing course projects that:

- require problem finding and problem solving, not only the raw memorization of facts and information; and
- challenge everyday thinking to address diverse perspectives on issues.

c) Establishing learning outcomes that translate to and have lasting benefit to real-world practice.

d) Create conditions for a knowledge sharing community to emerge and create as many opportunities as possible for others to learn your infrastructure for knowledge sharing.

Motivation and opportunities for students and masters to pursue a career in information and communication science, including space science, can be successfully achieved by promoting research and technology achievements in information science, communications, and space technology and by actively involving them in a real scientific project with great impact.

In order to increase interest in information research, communication, space and satellite technologies, which in turn will positively influence the overall scientific performance of future and current students, TUM has set up several laboratories for the development of communication systems, created a space technologies center with the long-term goal of development, manufacturing and launching nanosatellites. On the other hand, it has concluded collaboration agreements with companies and operators of mobile and satellite communications to involve students in their real projects.

4. The study of the quality of blending learning

In order to establish the general level of motivation and satisfaction of students regarding the quality of blended learning, an extensive survey was conducted, in which the following aspects were addressed: the degree of satisfaction with reference to the quality of organized distance learning; focus on distance learning; prompt response to requests from teachers and colleagues; the degree of correspondence of the knowledge obtained with the expectations; the efficiency of teaching the material; the degree of difficulty of learning through the form of distance learning; the degree of qualification of teachers for distance teaching; the degree of ease of learning through the proposed teaching materials; the quality of the theoretical courses and the practical activities carried out at a distance; the duration of the individual study and the availability of further follow-up of this form of training [2, 3].

The applied questionnaire includes 11 questions with answers and 2 open-ended topics for the presentation of opinions and suggestions. The survey was conducted online, through the platform My University - Student, (https://utm.md/universitatea-mea/) between 27.04 - 28.05 2020 and 27.02.- 27.04.2021. The survey was completed by 870 (20.2%) and 608 (13.26%) students, respectively. The survey was implemented in the following conditions for teaching activities: fully online in the spring semester, academic year 2019/2020, in blended format (theoretical activities and some practical online activities, face-to-face laboratory work) for the autumn semester and fully online for the spring semester in the academic year 2020/2021.

We will present some comparative results of the survey conducted in the two rounds, highlighting the aspects of improvement and those suggested for the development of the blended form of distance learning: two topics, which address issues related to student expectations and perceived effectiveness of online teaching (figure 2,3).
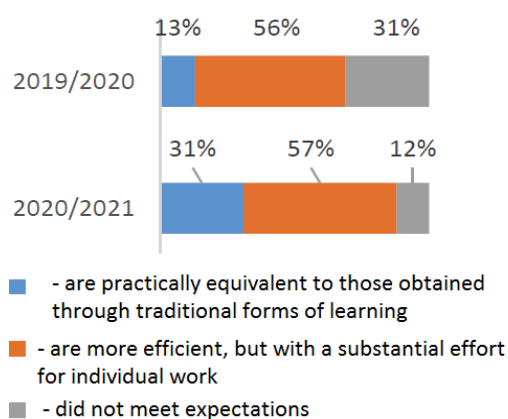
Figure 2. To what extent did the knowledge gained in the distance learning process met expectations?
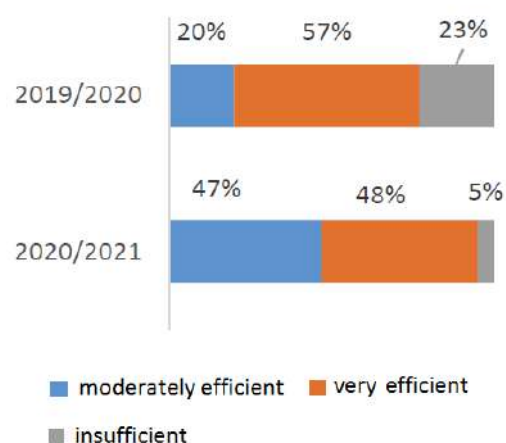
Figure 3. How effectively was the material taught through the form of blended learning?

Regarding the quality of the knowledge obtained in the academic year 2020/2021, 31% of the respondents mentioned that the knowledge obtained corresponded to the expectations, being registered a substantial increase of this quota of respondents (by 18%). The share of those dissatisfied with the knowledge obtained has decreased compared to a.u. 2019/2020 by 19%, and the number of partially satisfied remained relatively constant. In the same context, 47% of respondents believe that the material was taught efficiently, compared to 20% of the academic year 2019/2020, 48% consider that the learning material was taught moderately efficient, and 5% - not at all efficient, decreasing by 18% compared to academic year 2019/2020.

Conclusion

In order to motivate students for an effective acquisition of ICT material, it was proposed that the study activities be carried out in a mixed/blended way, through online courses, by applying pedagogical methods, but also methods and materials characteristic to traditional forms of teaching - face-to-face teaching and involvement of students in real projects.

For a real transition to the form of distance learning, but also the introduction of online training as a form of support for traditional forms of learning, the following directions of activity can also be summarized:

1. Selection of training strategies appropriate to the form of education, adapted to the general cycle and field of study and, of course, to the discipline taught.

2. Ensuring correct and effective learning for students. The form of online studies is focused on asynchronous activities, and this requires the reorganization of the informational content of the courses without affecting the scientific nature of the taught material.

3. Improving the scientific-teaching staff in the field of distance teaching methodology and designing teaching materials oriented towards this form of teaching. There were identified several key factors, including the quality and incompleteness of academic programs, the existing gap in scientific knowledge among schoolteachers, and the lack of information, motivation, environment, and opportunities for students regarding the science and technology. The implementation of the real project results will improve the quality of teaching by providing all study materials and imposing a study discipline for all forms of study, part-time studies, continuing education and full-time studies.

References

1. Adascaliţei Adrian , Secrieru Nicolae, Todos Petru. Running OER MOOC university courses by using moodle platform. - In: Procedeeng of Telecommunications, Electronics and Informatics, Chişinău, Moldova, 20-23 mai 2015

2. ANDRONIC, Serghei, BERNAZ, Luminiţa, TUTUNARU, Irina, BALAN Stela, MUNTEANU, Diana. The quality of distance learning during the Covid-19 pandemic in terms of student satisfaction (in Romanian). In: Journal of social science. ISSN 2587-3490/E-ISSN 2587-3504. Disponibil: https://jss.utm.md/wp-content/uploads/sites/21/2021/09/JSS-3-2021_10.52326jss.utm_.2021.43.04.pdf.

3. Institutional and didactic digital transformations for distance engineering education in the Republic of Moldova, (DIGIFORME) - Project code: 20.70086.23/COV (70105) https://www.asm.md/la-academia-de-stiinte-au-avut-loc-audierile-publice-ale-proiectelor-privind-combaterea-si.

4. Mobile and satellite communications - lecture course and course project - http://moodle.utm.md/course/view.php?id=641

5. Secrieru, Nicolae; Candraman, Sergiu; Andronic, Serghei; Younger generation inspiration and motivation through exposure to space technology - In: Proceedings of the conference "Telecommunications, Electronics and Informatics", Chisinau, Moldova, May 20-23, 2015

6. Space technologies practics with a nanosatellite - Mobile and Satellite Communications practice and labs course - http://moodle.utm.md/course/view.php?id=494

7. Todos, P., Secrieru, N., Guvir, S. Architecture of interuniversity's digital network in applied Science themes and economics in Moldova «CRUNT» - In: The 9th International Scientific Conference eLearning and software for Education, Bucharest, April 25-26, 2013, pag.333..338.

Investigation of Load Dependent Behavior of Boost Converter with Perturb and Observe Maximum Power Point Tracking for Thermoelectric Generators

Hayati Mamur[1*], Çiğdem Akyıldız[1], Mehmet Ali Üstüner[1]

Abstract: To obtain maximum power in thermoelectric generators (TEG), converters with maximum power point tracking (MPPT) algorithms are used. However, the maximum power point (MPP) cannot be achieved for each load value in these converters. In this study, the range of the load that can be connected to operate the TEG in the most efficient way with a non-isolated boost converter embedded in the Perturb&Observe (P&O) MPPT algorithm was investigated. For this purpose, a 50 W boost converter was calculated and connected to a 45.76 W TEG. Simulation studies of the TEG and the converter were carried out in MATLAB/Simulink environment. When the load value connected to the converter is smaller than the TEG internal resistance, it was observed that the P&O algorithm could not produce sufficient duty cycle rate and did not work actively. When the connected load value is equal to or greater than the TEG internal resistance, the P&O algorithm produced the duty cycle rate to follow the MPP value and reduced the load dependence of the TEG.

Keywords: Thermoelectric generator, MPPT, Boost converter, Load limit

1. Introduction

Thermoelectric generators (TEG) used to recover waste heat are semiconductor elements. Output power increases in direct proportion to the temperature difference between their surfaces **(Mamur and Üstüner, 2021)**. Since the efficiency of TEGs is low, it is important to obtain maximum power for improving their working performance and ensure that they work close to full capacity. To generate maximum power from the TEG, the total internal resistance of the TEG system and the external load resistance connected to the TEG system must be equal **(Bond et al., 2015)**. The circuit diagram of TEG and load connection is given in **Figure 1**. The load resistance in the circuit varies.

[1] Manisa Celal Bayar University, Engineering Faculty, Electrical and Electronics Engineering Department, Manisa, Türkiye
* Corresponding author: hayati.mamur@cbu.edu.tr
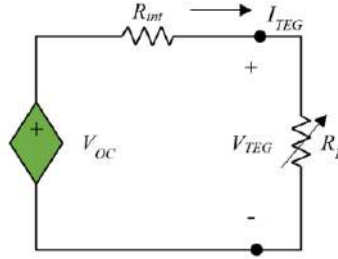
Figure 1. TEG load connection

The load in the TEG system is connected to obtain power from the TEG. Maximum power point (MPP) is reached when the load resistance and TEG internal resistance are equal **(Bhuiyan et al., 2022)**. This situation cannot always be achieved because the load is not always the same and the internal resistance of the TEG changes depending on the temperature **(Mamur and Çoban, 2020a)**. But this equality is always desired.

The maximum power from the TEG is explained by the following equation, depending on the open circuit voltage and internal resistance:

$$P_{TEG\_MAX} = \frac{V_{OC}^2}{4R_{int}} \qquad (1)$$

Where, P_{TEG_MAX} is the maximum power of TEG in (W), V_{OC} is the open circuit voltage of TEG in (V), and R_{int} represents the internal resistance of TEG in (Ω). TEG current and TEG voltage vary linearly with load. Since the DC-DC converter connected between the TEG and the load is the load of the TEG, making the TEG internal resistance and the DC-DC converter resistance equal is carried out by the MPPT program. Thus, both the highest efficiency from TEG is obtained and voltage regulation is ensured **(Tsai and Lin, 2010)**. When the converter is connected between TEG-load, now the load resistance of TEG is this DC-DC converter.

Ahmet et al. **(2022)** used a load resistor and a boost converter under different conditions to compare MPPT algorithms in photovoltaic (PV) systems. In the load resistance calculation and converter design, they did not specify the exact value of the resistance value in the PV system model. Dileep and Singh **(2017)** focused on the connection between converters and load resistors. They explained the relationship between the load resistors and the input impedance according to the converter type in their study. However, although many studies have been done using them, the relationship between selected load resistors, converter and input impedance has not been mentioned. Attar et al. **(2020)** conducted a study to find the optimum electrical load resistance in TEG systems without converters with MPPT.

2. Material and Method

Among MPPT methods, the most popular is the Perturb&Observe (P&O) algorithm **(Qasim et al., 2021)**. MPPT is required because when generated from TEGs, not only the change in load but also the change in temperature causes a difference in the MPP value. For this reason, in the study, a boost converter is used.

The boost converter is in the group of converters that increase the DC voltage level from low voltage to high voltage level. Using the boost converter equations, the following result is obtained:

$$\frac{V_{in}}{I_{in}} = \frac{V_o \times (1-D)}{I_o/(1-D)} = \frac{V_o \times (1-D)^2}{I_o} = R_L \times (1-D)^2 \qquad (2)$$

Where, V_o, V_{in}, D, I_{in}, I_o, and R_L are the output voltage in (V), the input voltage in (V), the duty cycle, the input current in (A), the output current in (A) and the load resistance in (Ω) of the converter, respectively. Hence, (2) shows that in boost converters, the load resistance can be increased up to an infinite resistance with the TEG internal resistance.

A TEG system was developed in the MATLAB/Simulink environment to carry out the study. In this TEG system, as many TEG modules as desired can be connected in series and parallel. The amount of power obtained varies according to the serial and parallel connection. A boost converter has been added to the TEG system. A gradually adjusted load is connected to the output of the boost converter. The internal resistance of the TEG system is 5.84 Ω. The values of the load resistor connected to the output of the converter were gradually changed to 1, 3, 5.84, 7, 9, 11, 15, 20, 30 and 45 Ω.

3. Results

In the simulation study performed in MATLAB/Simulink environment, the load values of the TEG system were changed gradually. It would be better to think of these modified values as values above and below the internal resistance of the TEG system. In the study carried out, these values below 5.84 Ω are these values below the internal resistance of the TEG system. These values 5.84 Ω and above are these values above the internal resistance of the TEG system. In addition, analysis was made for the case of $R_{int} = R_L$, where it is equal. The MPP value of the modeled TEG system is 45.76 W. The curves of change in current, voltage, and power in the TEG system under constant surface temperatures and variable loads of the TEG, performed in the MATLAB/Simulink simulation environment, are shown in **Figure 2**.
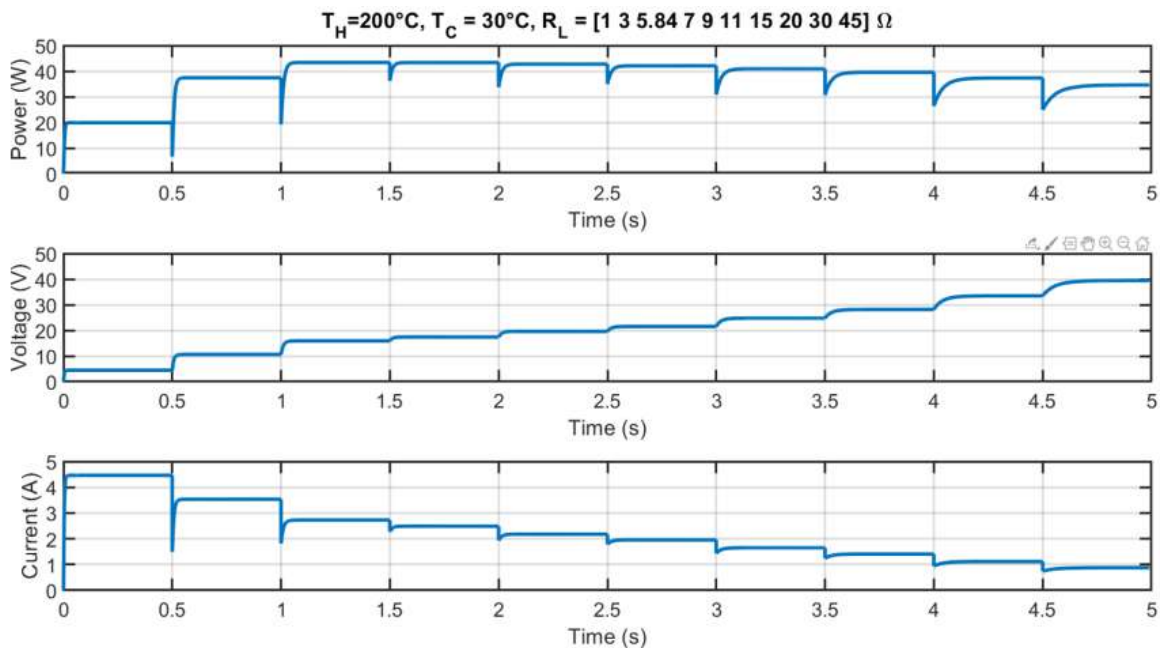
Figure 2. The curves in current, voltage and power of TEG system under variable loads

4. Discussion and Conclusions

At the load resistance values lower than the internal resistance of the TEG system, MPP cannot be followed due to the working principle of the boost converter. In the study, this situation is clearly seen in the first two resistance values of the MATLAB/Simulink simulation studies.

In cases where the load resistance values connected with the internal resistance of the TEG system are equal and large, the boost converter working with the *D* values produced by the P&O MPPT algorithm provides the MPP value by matching the impedance. However, approaching the full MPP value is difficult due to the losses in the boost converter. However, at high load values, the power value that drops considerably without using a boost converter with MPPT enables the follow-up of MPP when using a boost converter with P&O MPPT algorithm. However, when high load values are reached, the output voltage of the boost converter increases with increasing *D* values and the MPPT error percentage increases.

Acknowledgements

References

Ahmad, M. E., Numan, A. H., & Mahmood, D. Y. (2022). A comparative study of perturb and observe (P&O) and incremental conductance (INC) PV MPPT techniques at different radiation and temperature conditions. Engineering and Technology Journal, 40(02), 376-385.

Attar, A., Lee, H., & Snyder, G. J. (2020). Optimum load resistance for a thermoelectric generator system. Energy Conversion and Management, 226, 113490.

Bhuiyan, M. R. A., Mamur, H., Üstüner, M. A., & Dilmaç, Ö. F., (2022). Current and future trend opportunities of thermoelectric generator applications in waste heat recovery. Gazi University Journal of Science, 1-1.

Bond, M., & Park, J. D. (2015). Current-sensorless power estimation and MPPT implementation for thermoelectric generators. IEEE Transactions on Industrial Electronics, 62(9), 5539-5548.

Dileep, G., & Singh, S. N. (2017). Selection of non-isolated DC-DC converters for solar photovoltaic system. Renewable and Sustainable Energy Reviews, 76, 1230-1247.

Mamur, H., & Coban, Y. (2020a). Detailed modeling of a thermoelectric generator for maximum power point tracking. Turkish Journal of Electrical Engineering & Computer Sciences, 28(1), 124-139.

Mamur, H., & Üstüner, M. A. (2021) Improved perturb and observe maxımum power poınt trackıng method wıth thermoelectrıc generator model. International Scientific Conferance, Gabrova.

Tsai, H. L., & Lin, J. M. (2010). Model building and simulation of thermoelectric module

using Matlab/Simulink. Journal of Electronic Materials, 39(9), 2105.

Qasim, A. M., Alwan, T. N., PraveenKumar, S., Velkin, V. I., & Agyekum, E. B. (2021). A New maximum power point tracking technique for thermoelectric generator modules. Inventions, 6(4), 88.

An FDTD Modeling of GPR for Detecting and Mapping Archeological Sites

Muhammet Cihat Mumcu[1*], İzzet Yavuz[2], Ercan Aykut[3], Sena Taş[4]

Abstract: An ultra-wideband electromagnetic sensor called Ground-Penetrating Radar (GPR) is utilized to identify things that may be concealed behind or inserted into walls in addition to subsurface objects. These GPR applications are employed in both military and civilian operations, including mine detection, earthquake rescue missions, and archeological site investigation. Archaeologists can benefit from looking for designated targets that are concealed between the walls, like air pockets. Due to the ability to create more sophisticated and realistic models thanks to constantly growing computer power, numerical modeling techniques are more appealing. The dielectric characteristics of composite materials have recently been studied using a variety of numerical techniques, including finite element (FE), finite difference time domain (FDTD), method of moments (MOM), small perturbation method (SPM), and Monte Carlo (MC). Since it is efficient and adaptable to simulate the subsurface layers and numerous buried objects with various geometries and dielectric properties, the FDTD method is particularly well suited for GPR modeling among these numerical approaches. The groundpenetrating radar (GPR) simulation on dispersive and homogeneous soil is detailed in this study using a two-dimensional (2-D) time-domain numerical approach. The partial differential equations for time-stepping of the electromagnetic fields are discretized using the finitedifference time-domain (FDTD) approach. The Lorentz model is used to simulate soil dispersion. The dispersive soil parameters are obtained by fitting the model to the published experimental data. In order to imitate an open area, the perfectly matched layer (PML) is expanded to reach dispersive material and employed as an absorbing border condition.

Keywords: Ground-Penetrating Radar (GPR), Finite-Difference Time-Domain (FDTD), Perfectly Matched Layer (PML), Lorentz model, buried objects.

1. Introduction

Ground Penetrating Radar (GPR) is a research technique that is widely used in shallow geophysical applications. It is a radar system that sends electromagnetic (EM) waves to the ground through an antenna with appropriate features, receives the reflected wave by striking the target under the ground with another or the same antenna with appropriate characteristics, and transforms the detected signal into meaningful information by processing the objects beneath the ground. A transmitting antenna sends high-frequency and short-pulsed electromagnetic waves (between 10 MHz and 3 GHz) to the underground, and radar signals are sent to the ground, and the underground structures are examined in high-resolution with

1,2,3 Istanbul Gelişim University, Gelisim Vocational School, Department of Electric, Istanbul, Turkey
4 Istanbul Gelişim University, Gelisim Vocational School, Department of Electronics Technology, Istanbul, Turkey
* Corresponding author: mcmumcu@gelisim.edu.tr

radargrams created by using the time of their reflections in the ground. The underground waves are transmitted at a center frequency, and this frequency is critical in the wave penetration depth, scattering, and absorption phenomena in the medium. Furthermore, the dielectric permeability, electrical conductivity, and magnetic permeability values of underground materials significantly impact the propagation of wave fields underground. Analyzing and interpreting the environment can be difficult due to the heterogeneous parameters of the analyzed region and the complexity of the GPR system (Liu and Guo 2016).

The method has a wide range of applications and is used to solve almost all geophysical problems. Specifically shallow geological problems (stratigraphy, fault determinations, landslides, karstic cavity determinations, shallow groundwater aquifer surveys, etc.), examination of archaeological structures and living cultural heritage, engineering applications (pipeline research, examination of tunnel-highway and railway lines, building reinforcements, and investigation of problems inside the building, etc.), unexploded military material and mine detection, forensic medicine, and so on (Guo et al. 2011).

The natural situation in the underground, particularly in shallow environments with very complex features, the difficulties arising from the nature of the method, and the generally lossy, scattering, wave absorbing, and emitting properties of the environments all contribute to significant problems and misinterpretations in method interpretations. As a result, numerical modeling of the underground feature of the environment to be studied will be extremely beneficial in terms of strengthening the interpretation. In recent years, the rapid advancement of computer hardware and capabilities has resulted in the development of modeling techniques in the GPR method. Single frequency models, time domain models, ray tracing, transmissionreflection techniques, integral techniques (MOM-moments method), and discrete element methods are used in GPR modeling (Myroshnychenko and Brosseau 2005; Meles et all 2012).

Simple transmission-reflection techniques and basic ray tracing are based on models that geometrically describe objects by comparing the relative permittivity (ε) and conductivity (σ) of objects with sharp interfaces. The fundamental source wavelet is used to calculate the GPR responses modeled by these methods for each interface (mostly Ricker wavelet associated with the central antenna frequency). Thus, two-dimensional artificial radargrams of the associated underground models are created on geometric foundations, and the finite difference time domain (FDTD) modeling technique is used. With advanced modeling tools, FDTD is a popular method for modeling more complex environments. This technique produces better models than ray tracing, especially when modeling complex, lossy, and dispersive subsurface situations. It is a very realistic method for displaying subsurface structures in accurate three-dimensional geometry, especially when combined with the GPR antenna (Wang et al. 2011).

In this study, the numerical methods used with GPR were thoroughly examined, and a threedimensional environment modeling was created using the FDTD method. A perfectly matched layer, which is widely used in the FDTD calculation method and limits the simulation area by absorbing the oncoming waves without reflection, is designed to minimize erroneous interpretation in calculations and simulations. The simulation results were computed using the MATLAB program.

2. GPR Modelling

Ground Radar Technology, mainly named as Ground Penetrating Radar (GPR), can also be found in the literature under the names "Ground-probing Radar", "Sub-Surface Radar", or "Surface-Penetrating Radar (SPR)". The first ground radar was built by Sir Robert WatsonWatt in 1935. Detection of the buried objects under the ground without damage is achieved by GPR. The schematic representation of the underground radar system is given in Figure 1. (Grasmueck et al. 2005; Bianchini Ciampol 2019; Knigh 2001; Yalçıner 2009). This detection system operates with electromagnetic waves. First, electromagnetic waves are sent from GPR to the ground, then it hits the object and reflects back to the receiver. This trip of the wave is called double-way trip time. Finally, the type of object can be detected by means of the trip time (Yalçıner 2009; Fischer et al.1994; Belce et al. 2019; Kılıç et al. 2018; Annan 2009).
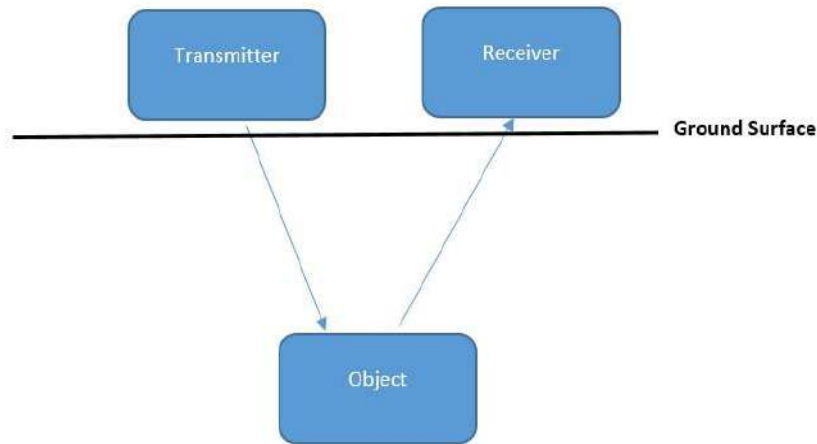
Figure 1. The schematic representation of the underground radar system (Belce et al. 2019).

Because the geometry of buried objects, such as air pockets and clay walls, is frequently thought of as being invariant in the third dimension, the modeling of electromagnetic wave scattering in GPR detection can be condensed into a 2-D problem. Fig. 1 displays a 2-D FDTD computational model for GPR detection. A transmitting source is positioned on the ground in the center of the soil's surface. The medium's 7 m horizontal and vertical dimensions. The two layers of the medium in this model are air in the upper layer, which has a thickness of 1 m, and soil in the lower layer, which has a thickness of 6 m. In the soil layer, which has air pockets at its interior clay walls, three rooms are buried at depths of 3 meters, 2 meters, and 4 meters. The PML boundary serves as the FDTD region's outermost limit (Mumcu and Bayar 2020).
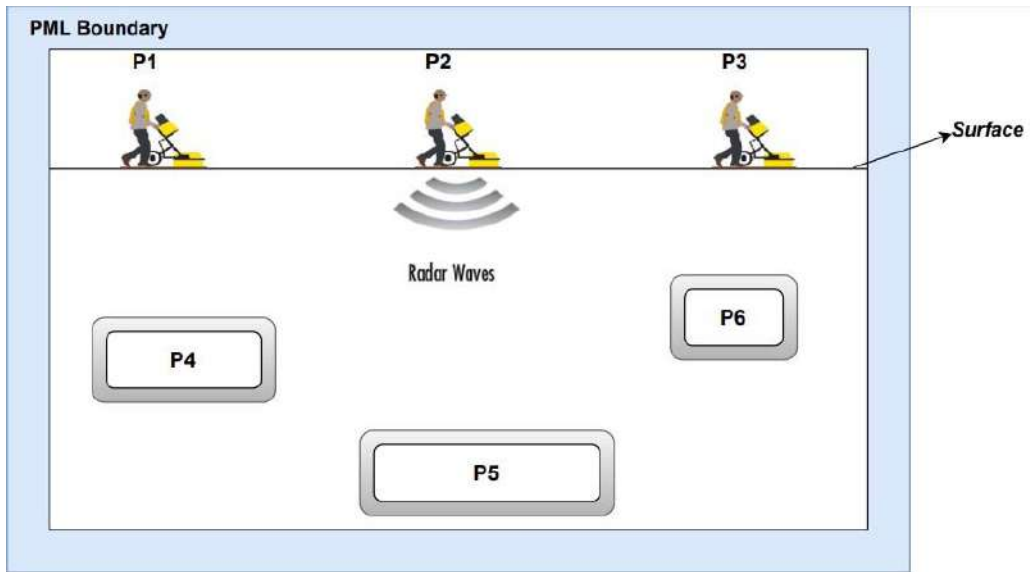
Figure 2. FDTD computational model for detecting buried objects and medium layers in GPR.

3. Numerical Approach

Cell phones, television, computers, laser and radar technologies, electric motors, and many other devices and systems that we use in our daily lives and whose application areas are expanding on a daily basis are all based on electromagnetic mechanisms in theory. Radar technologies, for example, are used in military applications such as missile tracking, missile guidance, airport traffic control or speed control tracking, and traffic safety applications. As a result, systems based on electromagnetic operating principles have a significant social impact.

The study of the relationships between electric charges at rest and in motion is known as electromagnetic field theory. Maxwell's equations, which are a system of unified partial differential equations, are used in this field to describe the interactions of electrical charges. With advancements in computer technology, faster and simpler calculation methods for solving equations of complex systems that may require large amounts of calculations come to the fore. Computational electromagnetics (CEM) is the study of electromagnetic system computational methods (Bondeson et al. 2012).

CEM is a relatively new field of study. CEM is becoming an important design tool in both industry and academic research. It is critical for shortening the process and effectively using it in electrical device design and analysis. CEM has a wide range of applications. It is used in microwave applications, microwave network design, and antenna analysis. Figure 2 depicts CEM methods based on various principles that are commonly used in the literature (Garg 2008). In this study, the FDTD method is used to analyze and calculate GPR systems.
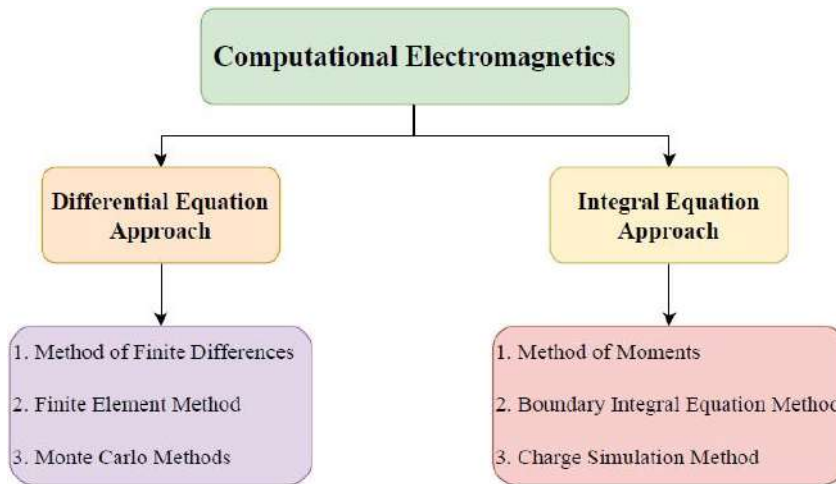
Figure 3. Classification of computational methods of electromagnetic fields.

3.2. Finite Difference Time Domain (FDTD)

The solution to an electromagnetic problem consists of solving Maxwell's equations under the given boundary and initial conditions. The finite-Differences in Time Domain (FDTD) method is widely used in the direct solution of electromagnetic problems. Since FDTD is a method that allows layered and heterogeneous modeling of the soil, the electromagnetic parameters of the soil layers can be changed according to simulation scenarios, and the use of broadband sources, it is frequently preferred in realistic GPR simulations.

In the solution of differential equations, continuous functions are discretized and a solution with a certain approximation is obtained by using the finite difference method over the related derivative. Starting with the most general form of dispersion, the Lorentzian form, the frequency domain polarization field can be written as

$$P(w) = b\frac{a}{\qquad} + jcw - dw_2 \qquad (1)$$

Inversion to the time domain via the inverse Fourier transform

$$bP(t) + cP'(t) + dP''(t) = aE(t) \qquad (2)$$

Approximating the time derivatives in (2) at time instant *n-1* is a critical step toward developing a consistent and general FDTD algorithm. As a result, the following update equation is obtained:

$$\frac{P_n - P_{n-2}}{\qquad} \quad \frac{P_n - 2P_{n-1} + P_{n-2}}{\qquad} \, bP_{n-1} + c \, 2\Delta t + d \quad \Delta t_2 \quad = aE_{n-1}$$

(3)

or

$$n = \underline{4d - 2b\Delta t_2} \, P^{n-1} + \underline{-2d - c\Delta t} \, P^{n-2} + \underline{2a\Delta t_2} \, E^{n-1} \qquad (4)$$

$$P$$

$$2d + c\Delta t \qquad\qquad 2d + c\Delta t \qquad\qquad 2d + c\Delta t$$

which can be expressed in the form

$$P^n = C_1 P^{n-1} + C_2 P^{n-2} + C_3 E^{n-1} \qquad (5)$$

For any type of dispersion relation, the constants C_1, C_2, C_3, and can be found (see Table I). In the case of multipole dispersion, the same relation is written for each pole, with the three constants set to the appropriate values.

TABLE I. Dispersion Relation Constants

Dispersion term in frequency domain	C_1	C_2	C_3
Lorentz Pole a $P(w) = \dfrac{a}{b + jcw - dw}{}_2\, E$	$\dfrac{4d - 2b\Delta t^2}{2d + c\Delta t}$	$\dfrac{-2d - c\Delta t}{2d + c\Delta t}$	$\dfrac{2a\Delta t^2}{2d + c\Delta t}$

The electric field intensity update equation is given by

$$E^n = \dfrac{D^n - \sum^N}{\varepsilon_0 \varepsilon_\infty} \quad_i P_{iN} \qquad (6)$$

where N is the number of poles and the updated value of the electric flux density D^n is obtained using the standard Yee's algorithm [Alsunaidi and Jabr 2009].

4. Simulation Results

First, the five pole Lorentz equation parameters for %40 moist soil are calculated using [Sato 2001]

$$_r(w) = {}_\infty + ({}_s - {}_\infty) \sum_{p=1}^{5} w\frac{G_p w_{p2}}{{}_p} {}_2 + j2\delta_p w - w_2 \qquad (7)$$

Where %40 moist soil parameters are

$$a = 0.2\, x_0\, x\, ({}_s - {}_\infty) x\, w_0{}^2 \qquad (8)$$
$$b = w_0{}^2 \qquad\qquad (9)$$
$$c = 2\, x\, \Delta \qquad\qquad (10)$$
$$d = 10^{-25} \qquad\qquad (11)$$

where $\infty = 13.7$, $s = 15$, $w_0 = 15$, $\Delta = 9 \times 10^{-7}$ for first pole,
$\infty = 13.7$, $s = 25$, $w_0 = 15$, $\Delta = 1 \times 10^{-7}$ for second pole,
$\infty = 13.7$, $s = 26$, $w_0 = 15$, $\Delta = 1 \times 10^{-7}$ for third pole,
$\infty = 13.7$, $s = 33$, $w_0 = 11$, $\Delta = 6 \times 10^{-9}$ for fourth pole and
$\infty = 13.7$, $s = 25$, $w_0 = 17$, $\Delta = 6 \times 10^{-9}$ for fifth pole coefficients.

The simulation results of five receivers in various locations are shown in Figure 4 (a)-(f).
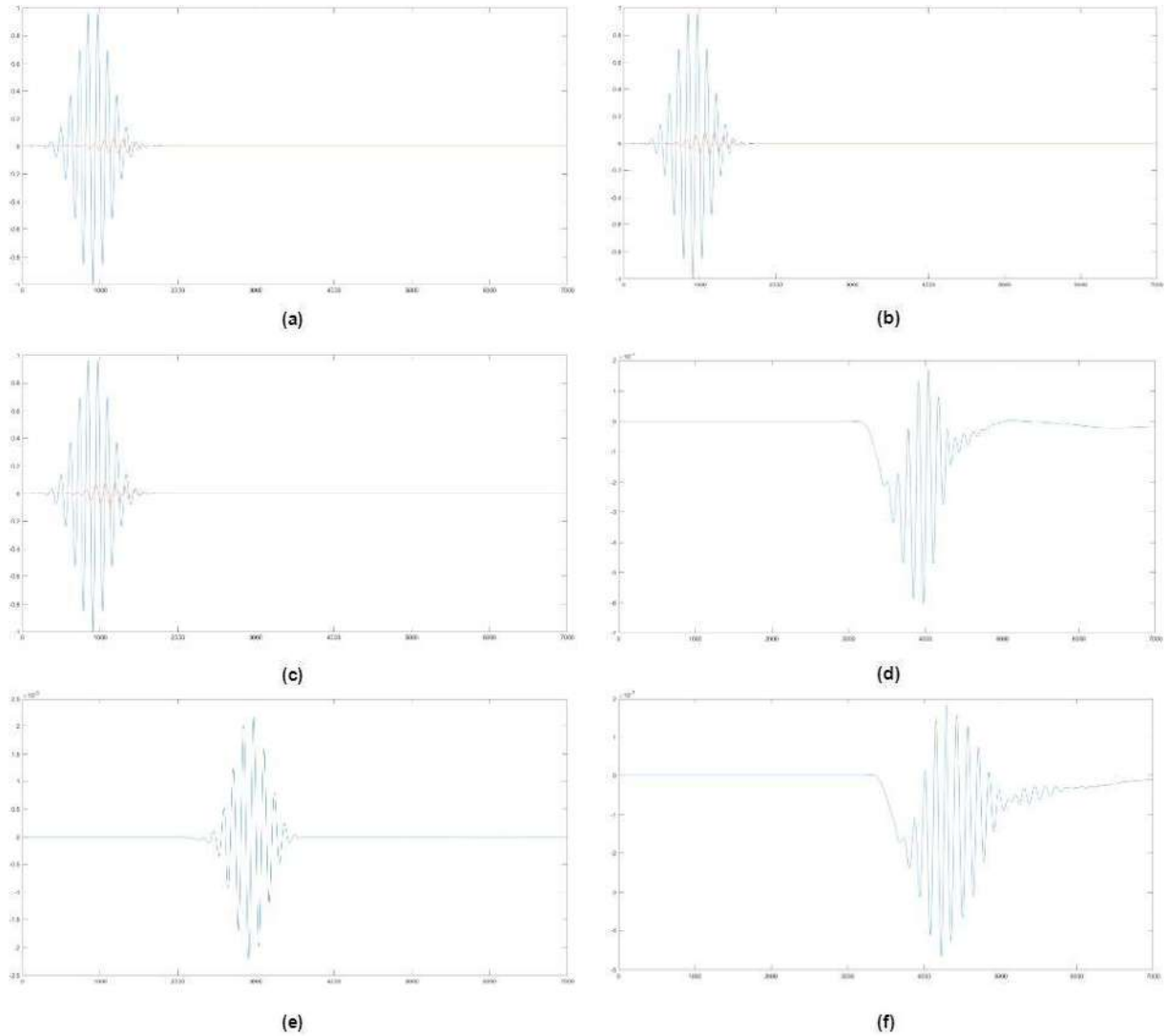
Figure 4. The magnitude graph of (a) P_{source}-P_1 probes, (b) P_{source}-P_2 probes, (c) P_{source}-P_3 probes, (d) P_4 probes, (e) P_5 probes, (f) P_6 probes,

4. Conclusion

An FDTD model was used in this study to simulate GPR detection of buried rooms. This simulation assists archaeologists in scanning ancient areas during excavations. Further research could concentrate on the interpretation, mapping, and imaging of the GPR response, as well as the extension of the 2-D FDTD simulating of GPR detection to the 3-D FDTD simulating.

References

Alsunaidi, M. A., & Al-Jabr, A. A. (2009). A general ADE-FDTD algorithm for the simulation of dispersive structures. *IEEE Photonics Technology Letters*, *21*(12), 817-819.

Annan, A. P. (2009). Electromagnetic principles of ground penetrating radar. Ground penetrating radar: theory and applications, 1, 1-37.

BELCE, E., BEKLER, T., KURBAN, Y. C., & YALÇINER, C. Ç. (2019). Ayasofya Müzesi Zemin Yüzey Deformasyonlarının Yeraltı Radarı (GPR) İle İncelenmesi. Academic PlatformJournal of Engineering and Science, 7(3), 362-366.

Bianchini Ciampoli, L., Tosti, F., Economou, N., & Benedetto, F. (2019). Signal processing of GPR data for road surveys. Geosciences, 9(2), 96.

Bondeson, A., Rylander, T., & Ingelström, P. (2012). *Computational electromagnetics*. Springer.

Fischer, S. C., Stewart, R. R., & Jol, H. M. (1994, June). Processing ground penetrating radar data. In Fifth International Conferention on Ground Penetrating Radar (pp. cp-300). European Association of Geoscientists & Engineers.

Garg, R. (2008). *Analytical and computational methods in electromagnetics*. Artech house

Grasmueck, M., Weger, R., & Horstmeyer, H. (2005). Full-resolution 3D GPR imaging. Geophysics, 70(1), K12-K19.

Guo, L. X., Liang, Y., Li, J., & Wu, Z. S. (2011). A high order integral SPM for the conducting rough surface scattering with the tapered wave incidence-TE case. *Progress In Electromagnetics Research*, *114*, 333-352.

Kılıç, G., Temel, A., & Torun, Y. (2018) Yeraltı Radarı Yardımıyla Kentsel Su/Atık Su Sistemlerinin ve Kaçak Su Yerlerinin Belirlenmesi.

Knight, R. (2001). Ground penetrating radar for environmental applications. Annual Review of Earth and Planetary Sciences, 29(1), 229-255.

Liu, Y., & Guo, L. X. (2016, July). FDTD investigation on GPR detecting of underground subsurface layers and buried objects. In *2016 IEEE MTT-S International Conference on Numerical Electromagnetic and Multiphysics Modeling and Optimization (NEMO)* (pp. 1-2). IEEE.

Meles, G. A., Greenhalgh, S. A., Green, A. G., Maurer, H., & Van der Kruk, J. (2011). GPR full-waveform sensitivity and resolution analysis using an FDTD adjoint method. *IEEE Transactions on Geoscience and Remote Sensing*, *50*(5), 1881-1896.

Mumcu, M. C., & Bayar, S. (2020). Parallel Implenetation of the GPR Techniques for Detecting and Mapping Ancient Buildings by Using CUDA. *Avrupa Bilim ve Teknoloji Dergisi*, 352-359.

Myroshnychenko, V., & Brosseau, C. (2005). Finite-element method for calculation of the effective permittivity of random inhomogeneous media. *Physical Review E*, *71*(1), 016701.

Sato, M. (2001). Gpr and its application to environmental study. *Center for Northeast Asia Studies (CNEAS), Tohoku University*.

Wang, A. Q., Guo, L. X., & Chai, C. (2011). Fast numerical method for electromagnetic scattering from an object above a large-scale layered rough surface at large incident angle: vertical polarization. *Applied optics*, *50*(4), 500-508.

Yalçıner, C. Ç. (2009). Gömülü Yapıların Yeraltı Radarı (GPR) Yöntemi ile Araştırılması: Büyük Menderes grabeni'nde Paleosismolojik ve Arkeosismolojik Uygulamalar (PhD thesis, Institute of Science).

Design and Implementation of a Bionic Hand Control with Mobile Software

Hayati Mamur[1*], Ceren Dölek[1], Mehmet Ali Üstüner[1]

Abstract: The aim of this study is to realize the design and application of bionic hand that can be controlled by mobile application for handicapped individuals. The aerobic designs necessary to solve this problem were made and a prototype was produced and controlled with Arduino Mega 2560 microcontroller. For the five fingers of the bionic hand designed with the work carried out, the independent movement of the five fingers from the fingertip to all the other joints has been successfully performed using five SG90 model mini servomotors. The movement of the servomotors is provided by the software developed with the MIT AI2 Companion program on the mobile phone. The software algorithm has been fulfilled separately for each finger and each joint. Microcontroller and mobile phone communication is done with HC-06 Bluetooth module. Servomotor fin connections are made with fishing line with the tip of each finger. The two joints of the thumb and three joints of the other four fingers are controlled by winding the fishing line, which is connected to the servomotor, according to the determined rotation angle. Thus, the control of the fingers on the hand was realized through the mobile application.

Keywords: Bionic hand, SG90 mini servomotor, microcontroller, mobile application, HC-06 Bluetooth module

1. Introduction

The ability of people without limbs to do their own work and to adapt to life can be solved with bionic hands. The bionic hand allows the individual to continue their daily lives like other healthy individuals by completing the missing hand limb. In order to solve this problem, necessary aerobic designs must be made, formulas must be drawn up, and a prototype must be produced and controlled by controllers. When a literature review is conducted, it is seen that various studies have been carried out on this subject from the past to the present. **Karaçizmeli et al. (2014)** carried out the control of the mechatronic-based robotic hand with the position information obtained from the human hand with the help of flexibility sensors mounted on the glove. They performed hand control with data from sensors connected to the glove in the other hand. However, they also stated that there is a disadvantage that hand control is not provided independently of the other hand. **Şenli (2011)** fulfilled a bioelectrical database of the activity of hand muscles and made interaction network and interface work between human and prosthetic hand using this database. In addition, he subjected the recorded bioelectrical signals to a series of preprocessing, established the relationships between the electromyogram (EMG)

---

[1] Manisa Celal Bayar University, Engineering Faculty, Electrical and Electronics Engineering Department, Manisa, Türkiye
* Corresponding author: hayati.mamur@cbu.edu.tr

signals and hand and finger movements, and provided the control of the bionic hand with a microcontroller. Lastly, **Andrecioli and Engeberg (2013)** developed an adaptive sliding mode prosthetic hand controller with a variable slope manifold. Considering all these studies, it can be predicted that bionic hand studies will continue without slowing down. In the presentation of this study, after a short introduction given above, "Materials and Methods" are expressed in the second part. After showing the "Results and Discussion" obtained in the third part, "Conclusions" is given at the end of the paper.

2. Material and Method

Arduino MEGA 2560 microcontroller is used to control the whole system. It is also preferred for power sharing with Arduino UNO. Among the reasons why this microcontroller finds many applications today; programming with an integrated development environment (IDE) and coding with commands similar to the C programming language. Arduino microcontrollers have at least one 5 V regulated integrated circuit (IC) and one 16 MHz crystal oscillator **(Hidayanti et al., 2020)**. An external programmer is not needed for programming Arduino microcontrollers, because a bootloader program is already written to the microcontroller. Arduino Mega 2560 can be powered by an external power supply in the range of 6-20 V. However, when a supply under 7 V is made, the 5 V pin may output less than its value, and therefore the board may start to work unstable. When the board is supplied with a voltage greater than 12 V, the regulator may overheat. This may cause damage to the card. Considering all these, it is recommended to limit the supply voltage of the recommended microcontroller to the range of 7-12 V **(Allahverdi et al., 2019)**. HC-06 Bluetooth module is used in the communication of the microcontroller used with the mobile device. The Bluetooth module has been developed for short distance communications, and this communication protocol uses the 2.4-2.48 GHz industrial, scientific and medical (ISM) band. Servomotors are closed-loop motors that can minimize position errors that may occur in the system, receive continuous feedback and are highly preferred in position control. They are divided into three according to their working angles; 120-140°, 0-180° and 0-360° servomotors. In the implemented system, RC (Radio Control) Tower Pro SG90 DC type mini servomotor, which provides position control at small powers, is used. In the study, two methods were applied to obtain and compare the determined angle values of each finger and knuckles. The first one is obtained by making the relationship between the arc length and the angle with the method of finding the central angle in the circle. The second method is obtained by measuring the rotation time of the servomotor, that is, by the relationship established between the position of the servomotor and the pulse width. The first method is related to the length of the servomotor fin and the length of the finger from the root to the knuckle. Therefore, the rotation angle of the servomotor blade was calculated based on the formula for calculating the center angle in the circle. The angle of rotation and the length of the arc of the circle are described as follows:

$$Q = S/r \tag{1}$$

$$|S| = (Q \times 2 \times \pi \times r)/360 \tag{2}$$

where, Q represents the rotation angle of the servomotor vane, r the servomotor vane length, and S the length from finger root to knuckle. The ratio of arc length to radius gives the angle of rotation. From here, the angle of rotation is again found in detail as follows:

$$Q = [(360/2) \times S]/(2 \times \pi \times r) \tag{3}$$

The fin length of the servomotors used in the realized bionic hand design is taken as $r = 1.5$ cm and the π value is taken as 3.14. Since the servomotor blade can provide a maximum of 180° rotation, the calculation was made over the semicircle and $360 / 2$ was written in the formula in (3). The second method is the measurement of the servomotor rotation time, that is, the relationship between the servomotor position and the pulse width. After the electronic circuit connections were made with the bionic hand prototype, the code written in the Arduino IDE program was uploaded to the microcontroller board and Bluetooth connection was provided in the mobile application. It was made in 3D printer for mechanical design and green polylactic acid (PLA) filament was used as material. The realized bionic hand design and electronic setup are presented in detail in **Figure 1**.

(a) (b)
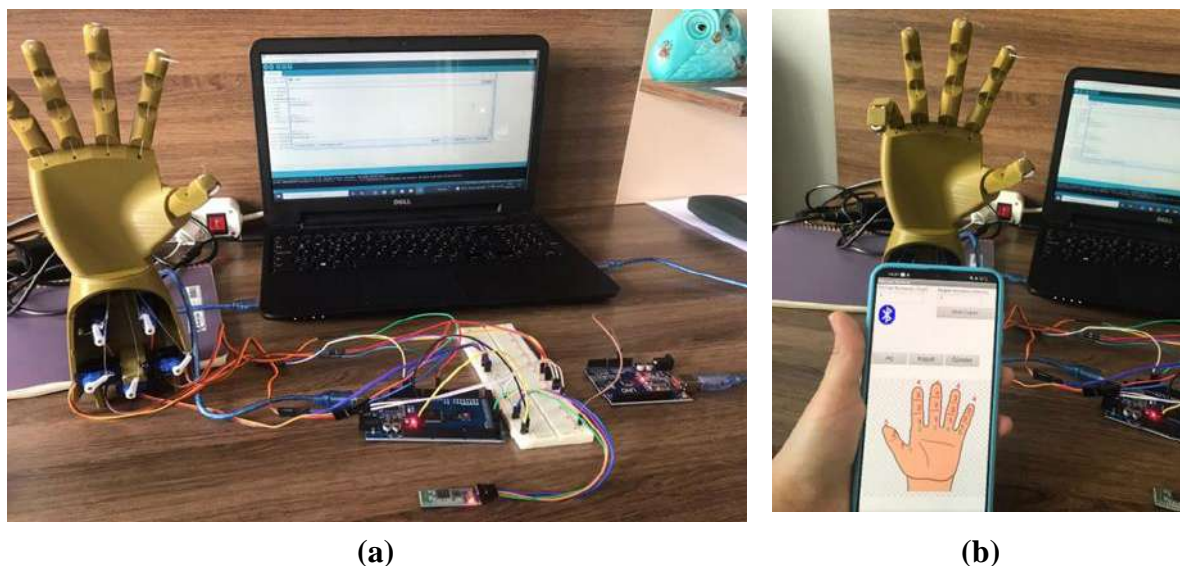
Figure 1. The performed bionic hand design and electronic setup

3. Results and Discussion

In the program calculated using these two methods, the servomotor blade rotation angles determined by the experimental practice-observation method are given in **Table 1**.

Table 1. Center angle calculation, rotation angle values found with PWM signal-servomotor position relationship and used in the program.

Finger name	Knuckle number	Length to finger knuckle, S (cm)	Servomotor blade length, r (cm)	Servomotor blade rotation angle found from equation (3) with center angle calculation, Q (°)	Full closing time of finger knuckle (ms)	Rotation angle of servomotor blade found with PWM signal and servomotor position relationship, Q (°)	Rotation angle values used in the program, Q (°)
Thumb	First knuckle	2	1.5	38.216	0.594	106	112
	Second knuckle	3	1.5	95.541	0.924	165	170
Index Finger	First knuckle	2	1.5	38.216	0.235	42	50
	Second knuckle	2.4	1.5	84.076	0.532	95	100
	Third knuckle	3	1.5	141.401	0.918	164	170
Middle finger	First knuckle	2	1.5	38.216	0.202	36	40
	Second knuckle	2.5	1.5	71.656	0.375	67	80
	Third knuckle	3.5	1.5	152.866	0.941	168	179
Ring Finger	First knuckle	2	1.5	38.216	0.336	60	63
	Second knuckle	2	1.5	76.433	0.610	109	115
	Third knuckle	3	1.5	133.758	0.969	173	179
Little finger	First knuckle	1.5	1.5	28.663	0.459	82	91
	Second knuckle	1.75	1.5	62.102	0.717	128	135
	Third knuckle	2.5	1.5	109.873	0.958	171	179

(3) is used in the first method for the servomotor blade rotation calculation. In the second method, the PWM signal-servomotor position relationship is considered. In the second method, when the PWM signal and servomotor position relationship is calculated using the ratio proportional method, since the time taken for a 90° rotation angle of the servomotor blade is 0.5 ms, the time taken for a 1° rotation angle is 0, It is calculated that $5/90 = 0.0056$ ms. The exact closure times of the knuckles of each finger were found by timing with a stopwatch. Servomotor blade rotation angles were calculated for each finger and knuckle using the found times rotation angle/rotation time ratio.

4. Conclusions

In this study, a bionic hand and its control were successfully carried out with the mobile application, which is the target of the project. The project was designed and implemented as closely as possible to the normal human hand size, based on joint control of the fingers attached to a hand body prototype. In the applications made, it has been observed that the PWM method, which adjusts the angle of the servomotor in the control of the servomotor blade rotation angles, gives more successful results. Achieving precise grip angles of the fingers has not been fully realized due to tolerances in mechanical designs. In order to adjust this sensitivity, the angle values were improved with the experimental apply observation method.

Acknowledgements

References

Allahverdi, Ç., Şahan, A., & Özdemir, M. Y. (2019, July). Mühendislik ve temel bilim projelerinde Arduino kullanımı. In International Congress on Human Computer Interaction, Optimization and Robotic Applications, (pp. 70–74).

Andrecioli, R., & Engeberg, E. D. (2013). Adaptive sliding manifold slope via grasped object stiffness detection with a prosthetic hand. Mechatronics, 23(8), 1171-1179.

Deng, H., Zhong, G., Li, X., & Nie, W. (2016). Slippage and deformation preventive control of bionic prosthetic hands. IEEE/ASME Transactions On Mechatronics, 22(2), 888-897.

Hidayanti, F., Rahmah, F., & Wiryawan, A. (2020). Design of motorcycle security system with fingerprint sensor using arduino uno microcontroller. International Journal of Advanced Science and Technology, 29(05), 4374-4391.

Karaçizmeli, C., Çakır, G., & Tükel, D. (2014, April). Robotic hand project. In 2014 22nd Signal Processing and Communications Applications Conference (SIU) (pp. 473-476). IEEE.

Şenli, K. (2011). EMG (Elektromiyografi) Kontrollü Protez Kol Tasarımı (Doctoral Dissertation, DEÜ Fen Bilimleri Enstitüsü).

Isolation and Identification of Bacteriocin Producer Enterococci from Traditional Turkish Cheeses

Geleneksel Türk Peynirlerinden Bakteriyosin Üreticisi Enterokokların İzolasyonu ve Tanımlanması

Didem Akpınar Kankaya

Abstract: In this study, a total of 12 presumptive bacteriocin-producing lactic acid bacteria were isolated from six of 40 different traditional Turkish cheeses. The activity spectrum of the isolates was tested against ten different indicator bacteria and it was determined that some of the isolates showed zones against the indicator bacteria that ranged from 2 to 35 mm. According to the activity spectrum results, isolates coded DP8.3, DP9.3, DP35.1, and DP35.2, which give sharp-edged zones and have a broad activity spectrum, were chosen as study material. Proteolytic enzyme treatment was performed to determine the protein nature of the antimicrobial substances produced by the isolates. As a result of the proteolytic enzyme treatments, it was determined that the antibacterial substances produced by DP8.3, DP9.3, and DP35.2 lost their activity with pepsin, trypsin, proteinase K, and α-chemotrypsin but were not affected by catalase. It was determined that the antibacterial substance produced by the DP35.1 isolate lost its activity with trypsin, proteinase K, and α-chemotrypsin but was not affected by catalase and pepsin. The isolates' genomic DNA was extracted, and these isolates were identified using specific primers for the *Enterococcus* genus and *Enterococcus* species. At the same time, the 16S rDNA region of the isolates was amplified by polymerase chain reaction (PCR). According to the results obtained by molecular methods, DP8.3, DP9.3 coded isolates were identified as *E. faecium* and DP35.1, and DP35.2 coded isolates as *E. mundtii*.

Keywords: Cheese, bacteriocin, *Enterococcus*, proteolytic enzymes

Özet: Bu çalışmada incelenen 40 farklı geleneksel Türk peyniri örneklerinin altı tanesinden 12 muhtemel bakteriyosin üreticisi laktik asit bakterisi izole edilmiştir. İzolatların aktivite spektrumu on farklı indikatör bakteriye karşı test edilmiş ve izolatlardan bazılarının indikatör bakterilere karşı 2 ile 35 mm arasında değişen zonlar verdiği tespit edilmiştir. Aktivite spektrumu sonuçlarına göre, keskin kenarlı zon veren ve geniş aktivite spektrumuna sahip DP8.3, DP9.3, DP35.1 ve DP35.2 kodlu izolatlar çalışma materyali olarak seçilmiştir. İzolatların ürettiği antimikrobiyel maddenin protein doğasını belirlemek için proteolitik enzim uygulaması yapılmıştır. Proteolitik anezim uygulaması sonucunda DP8.3, DP9.3 ve DP35.2 tarafından üretilen antibakteriyel maddelerin pepsin, tripsin, proteinaz K ve α-kemotripsin ile aktivitelerini kaybettikleri ancak katalazdan etkilenmedikleri belirlenmiştir. DP35.1 izolatının ürettiği antibakteriyel maddenin tripsin, proteinaz ve K α-kemotripsin ile aktivitesini

Isparta University of Applied Sciences, Gelendost Vocational School, Department of Food Technology, Isparta, Turkey
Corresponding author: didemkankaya@isparta.edu.tr

kaybettiği ancak katalaz ve pepsin enzimlerinden etkilenmediği tespit edilmişitir. İzolatların genomik DNA'sı izole edilmiş ve bu izolatlar *Enterococcus* cinsi ve *Enterococcus* türlerine ait spesifik primerler kullanılarak tanımlanmıştır. Aynı zamanda izolatların 16S rDNA bölgesi polimeraz zincir reaksiyonu (PZR) ile amplifiye edilmiştir. Moleküler yöntemlerle elde edilen sonuçlara göre DP8.3, DP9.3 kodlu izolatlar *E. faecium* ve DP35.1 ve DP35.2 kodlu izolatlar *E. mundtii* olarak tanımlanmıştır.

Anahtar kelimeler: Peynir, bakteriyosin, *Enterococcus*, proteolitik enzimler

---

1. Giriş

Gıda kaynaklı patojenler çeşitli hastalıklara, komplikasyonlara hatta gıdanın tüketilmesi ile ölüme sebep olabilmektedir (Heredia ve Garcia, 2018). Bu sebeple çiğ ve işlenmiş ürünlerde patojenlerin kontrolü büyük önem taşımaktadır. Bakterilerin kontrolü amacıyla fiziksel, kimyasal ve biyolojik yöntemler kullanılabilmektedir (Yi vd., 2020). Son yıllarda tüketicilerin sağlık kavramı hakkındaki düşüncelerinin değişmesi ve sağlıklı gıda talebindeki artışa bağlı olarak gıda endüstrisinde kimyasal katkı maddelerinin yerine doğal koruyucuların kullanılma olanaklarının araştırılması ön plana çıkmıştır. Bakteriyosinler gıda bozulmalarına ve patojen bakterilere karşı antimikrobiyel etkileri sebebiyle özellikle doğal gıda koruyucusu olarak dikkatleri çekmektedir (Kaškonienė vd., 2017). Bakteriyosinler bir bakteri tarafından ribozamal olarak sentezlenen, diğer bakteriler üzerinde dar veya geniş etki spektrumuna sahip antimikrobiyel peptitlerdir (Cotter vd., 2005). Bu antimikrobiyel peptitler bozulmaya sebep olan bakteriler ve gıda kaynaklı patojenler üzerinde inhibisyon etkisine sahiptirler (Graham, vd., 2020). Bakteriyosinlerin inhibisyon etkisi genel olarak hücre membranı üzerinde etkili mekanizmalar ile gen ekspresyonu ve protein sentezinde etkili mekanizmalar olarak sınıflandırılabilir (Negash ve Tsehai, 2020). Bu sayede bakteriyosinlerin veya bakteriyosin üreticisi laktik asit bakterileri (LAB)'nin doğal biyokoruyucular olarak kullanılma olanakları artmaktadır (Kaškonienė vd., 2017; O'Connor vd., 2020). Gıdaların muhafazasının yanı sıra geniş spektrumlu antibiyotiklerin aksine yakın ilişkili hedef patojenlere karşı toksisite ve dar bir öldürme spektrumunun olması bakteriyosinlerin aynı zamanda hayvan sağlığının korunması amaçlı kullanılma potansiyelini de ortaya çıkarmıştır (Kaškonienė vd., 2017). Bakteriyosinlerin tanımlanması, bakteri izolatlarının antibakteriyel aktivitesinin taranması, bakteriyosinlerin enstrümental veya moleküler yöntemlerle saflaştırılması ve tanımlanması prosedüerlerini kapsamaktadır (Kaškonienė vd., 2017). Bununla birlikte son yıllarda farklı kaynaklardan bakteriyosin üreticisi izolatların elde edilmesi ve gıda endüstrisinde potansiyel kullanımlarına yönelik çalışmalar bulunmaktadır (Felicio vd., 2015, Avcı ve Özden Tuncer, 2017; Kondrotiene vd., 2018; Gök Charyyev vd., 2019; Castilho vd., 2020). Bu çalışmada da Isparta ilindeki pazarlardan toplanan geleneksel yöntemlerle üretilmiş peynir örneklerinden bakteriyosin üreticisi LAB izole edilerek tür düzeyinde tanısı gerçekleştrilmiştir.

2. Materyal ve Yöntem

2.1. Materyal

Muhtemel bakteriyosin üreticisi LAB'nin izolasyonu için Isparta ilindeki pazarlardan toplanan 40 adet geleneksel yöntemlerle üretilmiş peynir örnekleri izolasyon materyali olarak kullanılmıştır.

2.2. Yöntem

2.2.1. Muhtemel bakteriyosin üreticisi suşların taranması

Muhtemel baktreriyosin üreticisi suşların taranması amacıyla toplanan peynir örneklerinden 10'ar gram tartılarak 90 mL steril fizyolojik tuzlu su (FTS) içerisinde homojen hale getirilmiş, seri dilüsyonları hazırlanarak de Man Rogosa and Sharpe Agar ve Enterococcosel Agar ortamlarına Drigalski spatülü ile yayılmıştır. Ekim yapılan Petri kutuları 37 °C'de 24-48 saat inkübasyona bırakılmıştır. İnkübasyon süresi sonunda koloni gelişimi gözlenen Petri yüzeylerine *Enterococcus faecium* ATCC 51559 veya *Listeria monocytogenes* ATCC 7644 inoküle edilen yumuşak agar ortamları homojen olarak yayılmıştır. Petriler 37 °C'de 24 saat inkübasyona tabi tutulmuş, inkübasyon süresi sonunda keskin kenarlı, net zon veren koloniler muhtemel bakteriyosin üreticisi olarak değerlendirilmiş ve Gram pozitif, katalaz negatif olduğu tespit edilen izolatlar izole edildiği besiyerinin sıvı formunda kültüre edilerek %20 (v/v) gliserol içeren ortamlarda -20 °C'de muhafaza edilmiştir.

2.2.2. İzolatların antibakteriyel aktivite spektrumunun belirlenmesi

İzolatların antibakteriyel aktivite spektrumlarının belirlenmesinde nokta ekim yöntemi kullanılmıştır (van Belkum vd., 1989). İndikatör bakteri olarak *L. monocytogenes* ATCC 7644, *L. innocua* LMG 2813, *Staphylococcus aureus* ATCC 25923, *S. aureus* ATCC 6538, *Lactococcus lactis* LMG 2910, *Pediococcus pentosaceus* LMG 2001, *E. faecium* ATCC 51559, *E. faecalis* ATCC 51299, *E. faecalis* ATCC 29212, *E. faecalis* LMG 2708 kullanılmıştır. Antibakteriyel aktivite spektrumu belirlenecek izolatlar MRS agar besiyerine öze ile sürülüp 37 °C'de 24 saat inkübasyona bırakılmıştır. Gelişen koloniler steril kürdan yardımıyla alınarak MRS agar ortamına nokta ekim yöntemiyle ekim yapılmış ve Petri kutuları 37 °C'de 24 saat inkübasyona bırakılmıştır. Süre sonunda gelişen koloniler üzerine her biri uygun besiyeri ortamında geliştirilen indikatör bakterilerden 100 µL inoküle edilmiş yumuşak agar besiyerleri üst tabaka olarak dökülmüştür. Üst tabaka dökülmüş Petri kutuları indikatör bakterilerin gelişmesi için uygun sıcaklıkta 24 saat inkübe edilmiş, inkübasyonu takiben izolatların indikatör bakterilere karşı verdiği zon çapları ölçülmüştür.

2.2.3. Proteolitik enzim uygulaması

İzolatlar tarafından üretilen antibakteriyel maddenin protein doğasının belirlenebilmesi için proteolitik enzim uygulaması yapılmıştır. Bu amaçla Eppendorf tüplerine alınan 1'er mL aktif kültür 10000 rpm'de 5 dakika süre ile santrifüjlenmiştir. Üst faz karıştırılmadan alınıp 0,45 µm por çaplı membran filtreden geçirilerek steril edilmiştir. Steril kültür üst sıvılarından 20 µL alınarak MRS agara damlatılmış damlaların yaklaşık 1 cm uzağına da konsantrasyonu 50 mg/mL olacak şekilde pepsin (pH 3.0), tripsin (pH 7.0), proteinaz K (pH 7.0), α-kemotripsin (pH 7.0) ve katalaz (pH 7.0) enzim solüsyonlarından 20 µL damlatılmıştır. Damlaların agara nüfuz etmesi sağlandıktan sonra Petrilerin üzerine 100 µL *E. faecalis* ATCC 51299 inoküle edilmiş yumuşak agar dökülmüştür. 37 °C'de 24 saatlik inkübasyonun ardından oluşan zon yapıları incelenmiştir (Ryan vd., 1996).

2.2.4. Bakteriyosin üreticisi izolatların tür düzeyinde tanısı

2.2.4.1. Genomik DNA izolasyonu

İzolatların genomik DNA'sı Cancilla vd. (1992) tarafından belirtilen yöntem ile izole edilerek, DNA örneklerinin elektroforezi % 0.7 (w/v) agaroz oranı ile hazırlanan jellerde gerçekleştirilmiştir. Elde edilen genomik DNA örnekleri -20 °C'de muhafaza edilmiştir.

2.2.4.2. İzolatların *Enterococcus* cinsine ve *Enterococcus* türlerine özgü primer çiftleri kullanılarak polimeraz zincir reaksiyonu (PZR) ile tanısı

İzolatların *Enterococcus* cinsine (Sahoo vd., 2015) ve *E. casseliflavus*, *E. durans*, *E. faecalis*, *E. faecium*, *E. gallinarum*, *E. hirae* ve *E. mundtii* türlerine özgü primer çiftleri kullanılarak PZR ile tanısı gerçekleştirilmiştir (Jackson vd., 2004). Çoğaltılan PZR fragmentlerinin elektroforezi % 2 agaroz oranı ile hazırlanan jellerde gerçekleştirilmiştir.

2.2.4.3. İzolatların 16S rDNA dizi analizi ile tür düzeyinde tanısı

İzolatların 16S rDNA bölgesinin PZR ile çoğaltılmasında Edwards vd. (1989) tarafından önerilen üniversal bakteri primerleri kullanılmıştır. Çoğaltılan 16S rDNA PZR fragmentlerinin elektroforezi %1 agaroz (w/v) oranı ile hazırlanan jellerde yapılmıştır. PZR ürünlerinin DNA dizi analizi BM Yazılım Danışmanlık ve Laboratuar Sistemleri Ltd. Şti'de (Ankara) yaptırılmıştır. Örneklerin 16S rDNA dizi benzerliği National Center for Biotechnology Information (NCBI) BLAST programı kullanılarak analiz edilmiştir.

3. Araştırma Bulguları

Çalışma kapsamında Isparta ilindeki pazarlardan toplanan 40 adet geleneksel peynir örnekleri muhtemel bakteriyosin üreticisi suşların taranması için izolasyon materyali olarak kullanılmıştır. Taranan örneklerin 6 adedinden (5 taze beyaz peynir, 1 tulum peyniri) 12 adet koloninin muhtemel bakteriyosin üreticisi olduğu düşünülerek çalışma materyali olarak seçilmiştir.

Muhtemel bakteriyosin üreticisi olarak seçilen 12 adet izolatın 10 farklı indikatör bakteriye karşı aktivite spektrumu nokta ekim yöntemi ile belirlenmiştir. İzolatlardan bazılarının kullanılan indikatör bakterilere karşı zon vermediği tespit edilirken, bazı izolatların incelenen indikatör bakterilere karşı 2 ile 35 mm arasında değişen çaplarda zon verdiği tespit edilmiştir. Geniş aktivite spektrumuna sahip, keskin kenarlı zon veren DP8.3, DP9.3, DP35.1 ve DP35.2 kodlu izolatlar ile diğer analizlere geçilmiştir.

DP8.3, DP9.3, DP35.1 ve DP35.2 kodlu izolatların ürettiği antimikrobiyel maddelerin protein doğası proteolitik enzim uygulaması ile incelenmiştir. DP8.3, DP9.3 ve DP35.2 kodlu izolatların ürettiği antimikrobiyel maddenin proteinaz K, tripsin, α-kemotripsin ve pepsin enzimleri ile aktivite kaybına uğradığı, katalaz enziminden ise etkilenmediği tespit edilmiştir. DP35.1 kodlu izolatın ürettiği antimikrobiyel maddenin ise proteinaz K, tripsin, α-kemotripsin enzim uygulamaları ile aktivite kaybına uğradığı ancak katalaz ve pepsin enzimlerinden etkilenmediği belirlenmiştir. Elde edilen sonuçlar neticesinde incelenen 4 adet izolat bakteriyosin üreticisi olarak tanımlanmıştır.

Bakteriyosin üreticisi olan 4 adet izolatın *Enterococcus* cinsine özgü primer çifti ile yapılan PZR çalışması sonucunda izolatların tamamının *Enterococcus* cinsi üyesi olduğu tespit edilmiştir *E. casseliflavus*, *E. durans*, *E. faecalis*, *E. faecium*, *E. gallinarum*, *E. hirae* ve *E. mundtii* türlerine özgü primer çiftleri kullanılarak yürütülen PZR çalışmaları sonucunda DP8.3 ve DP9.3 kodlu izolatların *E. faecium* türüne özgü 215 bç büyüklüğünde; DP35.1 ve DP35.2 kodlu izolatların ise *E. mundtii* türüne özgü 98 bç büyüklüğünde fragmentler verdiği tespit edilmiştir. İzolatların PZR ile çoğaltılan 16S rDNA bölgelerinin dizi benzerliği BLAST programı kullanılarak tespit edilmiştir. 16S rDNA dizi analizi sonuçlarına göre DP8.3 ve DP9.3 kodlu izolatlar *E. faecium*, DP35.1 ve DP35.2 kodlu izolatlar ise *E. mundtii* türü üyesi olarak tanımlanmıştır.

4. Tartışma ve Sonuç

Çalışma kapsamında keçi peyniri, koyun peyniri, olgunlaştırılmış beyaz peynir, taze beyaz peynir, çökelek, tulum peynir gibi farklı peynir örnekleri Isparta ilindeki pazarlardan toplanmış ve örneklerin 6 adedinden muhtemel bakteriyosin üreticisi izolat elde edilmiştir. Elde edilen verilere benzer şekilde yapılan farklı çalışmalar peynir başta olmak üzere süt ve süt ürünleri (Özden Tuncer vd., 2013; Goh ve Philip, 2015; Cavicchioli vd., 2016; Vimont vd., 2017; Avcı ve Özden Tuncer, 2017; Pei vd., 2018; Al-Madboly vd., 2020; Öztürk, 2022), et ve et ürünleri (Fontana vd., 2015; Casaburi vd., 2016; Altınkaynak ve Tuncer, 2020; Geniş, 2022), balık ve deniz ürünleri (Iseppi vd., 2019), boza (Gök Charyyev vd., 2019), turşu (Qiao vd., 2020; Yi vd., 2020) gibi farklı gıda kaynaklarından bakteriyosin üreticisi LAB'nin izole edildiğini göstermektedir.

Muhtemel bakteriyosin üreticisi olduğu düşünülen 12 izolatın *L. monocytogenes* ATCC 7644, *L. innocua* LMG 2813, *S. aureus* ATCC 25923, *S. aureus* ATCC 6538, *L. lactis* LMG 2910, *P. pentosaceus* LMG 2001, *E. faecium* ATCC 51559, *E. faecalis* ATCC 51299, *E. faecalis* ATCC 29212, *E. faecalis* LMG 2708 indikatör bakterilerine karşı aktivite spektrumunun incelendiği çalışmalarda izolatların LAB'nin yanı sıra *L. monocytogenes* ve *S. aureus* gibi gıda patojenlerine karşı da aktivite gösterdiği belirlenmiştir. İncelenen izolatların tamamının *L. monocytogenes* ATCC 7644, *L. innocua* LMG 2813, *S. aureus* ATCC 25923 ve *E. faecalis* ATCC 51299 indikatörlerine karşı değişen oranlarda aktivite gösterdiği tespit edilirken, izolatların aynı zamanda vankomisin dirençli *E. faecium* ATCC 51559 (DP8.1 hariç), *E. faecalis* ATCC 51299 indikatörlerine karşı da aktivite göstermesi dikkat çekicidir. Çalışmada elde edilen verilere benzer şekilde Avcı ve Özden Tuncer (2017) tarafından incelenen bazı peynir izolatlarının, aralarında *L. monocytogenes*, *S. aureus*, *E. faecalis* türlerine ait suşlara karşı antibakteriyel aktivite gösterdiği bildirilmiştir. Vimont vd. (2017) deve sütü izolatı olan 10 adet enterokok suşundan en geniş aktivite spektrumuna sahip LCW44 izolatının bazı LAB'nin yanı sıra *L. monocytogenes*, *L. innocua*, *S. aureus* ve *E. faecalis* türüne ait suşlara karşı da aktivite gösterdiğini tespit etmişlerdir. Altınkaynak ve Tuncer (2020) fermente sucuk izolatı olan *E. mundtii* YB6.30 izolatının *L. monocytogenes*, *L. innocua*, *S. aureus* gibi indikitör bakterilerin yanı sıra *E. faecium* ATCC 51559, *E. faecalis* ATCC 51299 indikatörlerine karşı da değişen çaplarda zon verdiğini bildirmişlerdir.

İzolatların antibakteriyel aktivite spektrumlarının incelenmesi sonucunda geniş aktivite spektrumuna sahip, özellikle vankomisin dirençli *E. faecalis* ATCC 51299 indikatörüne karşı yüksek aktivite gösteren DP8.3, DP9.3, DP35.1 ve DP35.2 kodlu izolatların ürettiği antimikrobiyel maddenin protein doğasının belirlenmesi için proteolitik enzim uygulaması yapılmıştır. İzolatların ürettiği antimikrobiyel maddenin proteinaz K, tripsin, α-kemotripsin ve pepsin (DP35.1 hariç) enzimleri ile aktivite kaybına uğradığının ancak katalaz enziminden ise etkilenmediğinin tespit edilmesi antimikrobiyel maddenin protein doğasında olduğunu kanıtlamaktadır. Bu sebeple DP8.3, DP9.3, DP35.1 ve DP35.2 kodlu izolatlar bakteriyosin üreticisi olarak tanımlanmıştır. Daha önce farklı araştırmacılar tarafından yapılan çalışmalarda bakteriyosinlerin protein doğasında olması sebebiyle kısmen veya tamamen proteolitik enzim uygulamalarından etkilendiği bildirilmiştir (Avcı ve Özden Tuncer, 2017; Gök Charyyev vd., 2019).

Bakteriyosin üreticisi olduğu tespit edilen DP8.3 ve DP9.3 kodlu izolatların moleküler yöntemlerle *E. faecium*, DP35.1 ve DP35.2 kodlu izolatların ise *E. mundtii* türü üyesi oldukları tespit edilmiştir. Enterokoklar yüksek sıcaklık, yüksek tuz ve asit konsantrasyonları gibi olumsuz koşullara karşı toleranslarından dolayı çoğu gıda ortamında karşımıza çıkmaktadır (Moreno vd., 2006). Bununla birlikte gıdalardan izole edilen bakteriyosin üreticisi suşların daha çok *E. faecium* ve *E. faecalis* türlerine ait olduğu (Avcı ve Özden Tuncer, 2017; Gök Charyyev vd., 2019; Qiao vd., 2020); ancak *E. mundtii* türüne ait suşların

da izole edildiği yapılan farklı çalışmalarda (Espeche vd., 2014; Iseppi vd., 2019; Altınkaynak ve Tuncer, 2020) rapor edilmiştir.

Bakteriyosin üreticisi izolatlar gıda endüstrisinde starter kültür veya yardımcı starter kültür kombinasyonlarında yer alabildikleri gibi ürettikleri bakteriyosinler de gıda muhafazasında kullanılabilmektedir. Bu sebeple bakteriyosin üreticisi suşların ve ürettikleri bakteriyosinin tanımlanması, suşların güvenlik değerlendirmesinin yapılması ve gıda endüstrisinde kullanım olanaklarının araştırılması önem taşımaktadır.

Kaynaklar

Al-Madboly, L.A., El-Deeb, N.M., Kabbash, A., Nael, M.A., Kenawy, A.M., Ragab, A.E., (2020). Purification, characterization, identification, and anticancer activity of a circular bacteriocin from *Enterococcus thailandicus*. Frontiers in Bioengineering and Biotechnology, 8, 450.

Altınkaynak, T., Tuncer, Y., (2020). Fermente sucuktan izole edilen antilisterial *Enterococcus mundtii* YB6.30 tarafından üretilen bakteriyosinin karakterizasyonu, Gıda, 45(5) 963-976.

Avcı, M., Özden Tuncer, B., (2017). Safety evaluation of enterocin producer *Enterococcus* sp. strains isolated from traditional Turkish Cheeses. Polish Journal of Microbiology, 66(2), 223-233.

Cancilla, M.R., Powell, I.B., Hillier, A.J., Davidson, B.E., (1992). Rapid genomic fingerprinting of *Lactococcus lactis* strains by arbitrarily primed polymerase chain reaction with 32P and fluorescent labels. Applied and Environmental Microbiology, 58(5), 1772-1775.

Casaburi, A., Martino, V.D.I., Ferranti, P., Picariello, L., Villani, F., (2016). Technological properties and bacteriocins production by *Lactobacillus curvatus* 54M16 and its use as starter culture for fermented sausage manufacture. Food Control, 59, 31-45.

Castilho, N.P.A., Todorov, S.D., Oliveira, L.L., Bersot, L.S., Nero, L.A., (2020). Inhibition of *Listeria monocytogenes* in fresh sausage by bacteriocinogenic *Lactobacillus curvatus* UFV-NPAC1 and its semi-purified bacteriocin. LWT-Food Science and Technology, 118, 108757.

Cavicchioli, V.Q., Camargo, A.C., Todorov, S.D., Nero, L.A. (2017). Novel bacteriocinogenic *Enterococcus hirae* and *Pediococcus pentosaceus* strains with antilisterial activity isolated from Brazilian artisanal cheese. Journal of Dairy Science, 100(4), 2526-2535.

Cotter, P.D., Hill. C., Ross, R.P., (2005) Bacteriocins: developing innate immunity for food. Nature Reviews Microbiology, 3, 777-788.

Edwards, U., Rogall, T., Blöcker, H., Emde, M., Böttger, E.C., (1989). Isolation and direct complete nucleotide determination of entire genes. Characterization of a gene coding for 16S ribosomal RNA. Nucleic Acids Research, 17(19), 7843-7853.

Espeche, M.C., Tomás, M.S.J., Wiese, B., Bru, E., Nader-Macías, M.E.F., (2014). Physicochemical factors differentially affect the biomass and bacteriocin production by bovine *Enterococcus mundtii* CRL1656. Journal of Dairy Science, 97(2), 789-797.

Felicio, B.A., Pinto, M.S., Oliveira, F.S., Lempk, M.W., Pires, A.C.S., Lelis, C.A., (2015). Effects of nisin on *Staphylococcus aureus* count and physicochemical properties of Minas Frescal cheese. Journal of Dairy Science, 98(7), 4364-4369.

Fontana, C., Cocconcelli, P.S., Vignolo, G., Saavedra, L., (2015). Occurrence of antilisterial structural bacteriocins genes in meat borne lactic acid bacteria. Food Control, 47, 53-59.

Geniş, B., (2022), Çiğ et ve Et Ürünlerinden Bakteriyosinojenik Koagülaz-Negatif Stafilokokların ve Laktik Asit Bakterilerinin İzolasyonu ve Starter Kültür Olarak Kullanım Potansiyellerinin Belirlenmesi. Süleyman Demirel Üniversitesi, Fen Bilimleri Enstitüsü, Gıda Mühendisliği Anabilim Dalı, Doktora Tezi, 167 sayfa,

Goh, H.F., Philip, K., (2015). Isolation and mode of action of bacteriocin BacC1 produced by nonpathogenic *Enterococcus faecium* C1. Journal of Dairy Science, 98(8), 5080-5090.

Gök Charyyev, M., Özden Tuncer, B., Akpınar Kankaya, D., Tuncer, Y., (2019). Bacteriocinogenic properties and safety evaluation of *Enterococcus faecium* YT52 isolated from boza, a traditional cereal based fermented beverage. Journal of Consumer Protection and Food Safety, 14, 41-53.

Graham, K., Stack, H., Rea, R., (2020). Safety, beneficial and technological properties of enterococci for use in functional food applications-a review. Critical Reviews in Food Science and Nutrition, 60(22), 3836-3861.

Heredia, N., Garcia, S., (2018). Animals as sources of food-borne pathogens: A review. Animal Nutrition, 4(3), 250-255.

Iseppi, R., Stefani, S., de Niederhausern, S., Bondi, M., Sabia, C., Messi, P., (2019). Characterization of anti‑*Listeria monocytogenes* properties of two bacteriocin‑producing *Enterococcus mundtii* isolated from fresh fish and seafood. Current Microbiology, 76, 1010-1019.

Jackson, C.R., Fedorka-Cray, P.J., Barrett, J.B., (2004). Use of a Genus- and species-specific multiplex PCR for identification of enterococci. Journal of Clinical Microbiology, 42(8), 3558-3565.

Kaškonienė, V., Stankevičius, M., Bimbiraitė-Survilienė, K., Naujokaitytė, G., Šernienė, L., Mulkytė, K., Malakauskas, M., Maruška, A., (2017). Current state of purification, isolation and analysis of bacteriocins produced by lactic acid bacteria. Applied Microbiology and Biotechnology, 101(4), 1323-1335.

Kondrotiene, K., Kasnauskyte, N., Serniene, L., Gölz, G., Alter, T., Kaskoniene, V., Maruska, A.S., Malakauskas, M., (2018). Characterization and application of newly isolated nisin producing *Lactococcus lactis* strains for control of *Listeria monocytogenes* growth in fresh cheese. LWT Food Science and Technology, 87, 507-514.

Moreno, M.F., Sarantinopoulos, P., Tsakalidou, E., De Vuyst, L., (2006). The role and application of enterococci in food and health. International Journal of Food Microbiology, 106(1), 1-24.

Negash, A.W., Tsehai, B.A., (2020). Current applications of bacteriocin. International Journal of Microbiology, 4374891.

O'Connor, P.M., Kuniyoshi, T.M., Oliveira, R.P., Hill, C., Ross, R.P., Cotter, P.D., (2020). Antimicrobials for food and feed; a bacteriocin perspective. Current Opinion in Biotechnology, 61, 160-167.

Özden Tuncer, B., Ay, Z., Tuncer, Y., (2013). Occurrence of enterocin genes, virulence factors, and antibiotic resistance in 3 bacteriocin-producer *Enterococcus faecium* strains isolated from Turkish Tulum Cheese. Turkish Journal of Biology, 37(4), 443-449.

Öztürk, H., (2022). Küçükbaş Hayvan Ağız Sütlerinden İzole Edilen Bakteriyosin Üreticisi Laktik Asit Bakterilerinin Fonksiyonel Özellikleri ve Güvenlik Değerlendirmesi. Süleyman Demirel Üniversitesi, Fen Bilimleri Enstitüsü, Gıda Mühendisliği Anabilim Dalı, Doktora Tezi, 219 sayfa.

Pei, J., Li, X., Han, H., Tao, Y., (2018). Purification and characterization of plantaricin SLG1, a novel bacteriocin produced by *Lb. plantarum* isolated from yak cheese. Food Control, 84, 111-117.

Qiao, X., Du, R., Wang, Y., Han, Y., Zhou, Z., (2020). Isolation, characterisation and fermentation optimisation of bacteriocin-producing *Enterococcus faecium*,Waste and Biomass Valorization, 11, 3173-3181.

Ryan, M.P., Rea, M.C., Hill, C., Ross, R.P., (1996). An application in Cheddar Cheese manufacture for a strain of *Lactococcus lactis* producing a novel broad-spectrum bacteriocin, lacticin 3147. Applied and Environmental Microbiology, 62(2), 612-619.

Sahoo, T.K., Jena, P.K., Nagar, N., Patel, A.K., Seshadri, S., (2015). In vitro evaluation of probiotic properties of lactic acid bacteria from the gut of labeo rohita and catla catla. Probiotics and Antimicrobial Proteins, 7(2), 126-136.

Van Belkum, M.J., Hayema, B.J., Geis, A., Kok, J., Venema, G., (1989). Cloning of two bacteriocin genes from a lactococcal bacteriocin plasmid. Applied and Environmental Microbiology, 55(5), 1187-1191.

Vimont, A., Fernandez, B., Hammami, R., Ababsa, A., Daba, H., Fliss, I., (2017). Bacteriocin-producing *Enterococcus faecium* LCW 44: A high potential probiotic candidate from raw camel milk. Frontiers in Microbiology, 8, 865.

Yi, L., Qi, T., Hong, Y., Deng, L., Zeng, K., (2020). Screening of bacteriocin-producing lactic acid bacteria in Chinese homemade pickle and dry-cured meat, and bacteriocin identification by genome sequencing, LWT - Food Science and Technology, 125, 109177.

Warehouse Location Selection for Possible Great Istanbul Earthquake

Asli Gul Yalcindag[1], Mehtap Dursun[1*], Nazli Goker[1]

Abstract: It is known that since the beginning of the humankind, millions of people and shelters have been destroyed by earthquakes. Just as there have been devastating earthquakes in Turkey in the past, it is expected to happen in the coming years as well. The aim of this article is to determine the optimum disaster logistics warehouse locations in order to deliver the emergency aid materials to the points of need as soon as possible and to meet the needs after the expected great Istanbul earthquake. The model was set up in two steps to determine the number of warehouses to be opened with the set covering problem in the first step, and to minimize the weighted distance with p-median in the second step. The established model was solved using The General Algebraic Modeling System (GAMS), and the optimum scenario was decided according to the results and the scenarios were mapped.

Keywords: Disaster logistics warehouse, earthquake, location selection, p-median, set covering problem

1. Introduction

Earthquake is the event of sudden vibrations that occur due to fractures in the earth's crust, spreading in waves and shaking the environments they pass through (AFAD, 2019). Earthquake is a natural event that cannot be prevented. It is known that since the beginning of the world, millions of people and shelters have been destroyed by earthquakes. Turkey is geographically located in a region with a high earthquake risk. In our country, devastating earthquakes have occurred in the past, and they are expected to happen in the coming years as well.

One of the earthquakes expected to occur is the "Great Istanbul Earthquake". If we examine the major earthquakes that have occurred for the last 1 century along the North Anatolian fault line, starting with the Erzincan earthquake with a magnitude of 7.9 in 1939, the next major earthquakes have always occurred further west on this line. This is because when an earthquake occurs on this fault line, the released energy is transferred to the west. The last time there was an earthquake in Izmit in 1999, great loss of life and property was experienced. The next stop of earthquakes on this fault line is Istanbul. Many studies by experts reveal that it is inevitable that a devastating earthquake will occur in Istanbul in the near future. Such an earthquake in Istanbul, Turkey's largest metropolis and economic center, will cause great losses throughout the country. In order to minimize these losses, this issue should be given great importance, and precautions should be taken to be prepared for earthquakes.

Various preparations are being made against the expected earthquake in Istanbul. One of them is disaster logistics warehouses. The centers where emergency aid materials are stored to be sent to the damaged areas in disasters and emergencies are defined as disaster logistics

[1] Galatasaray University, Industrial Engineering Department, Decision Analysis Research and Application Center, Ortakoy, Istanbul, Turkey
* Corresponding author: mdursun@gsu.edu.tr

warehouses (AFAD, 2014). Disaster logistics warehouses contain materials such as medical supplies, tents, beds, blankets, heaters and kitchen sets.

In this study, using mathematical programming methods, the focus will be on determining the optimum logistics warehouse locations in order to deliver the emergency aid materials to the points of need as soon as possible and to meet the needs in case of a possible major Istanbul earthquake. In the study, the article "Logistic Warehouse Location Selection Problem in Disaster Management: Maltepe District" by Aydın, Ayvaz and Küçükaşçı (2017) was taken as a starting point, and all districts of Istanbul were emphasized instead of Maltepe. Facility location optimization model established by Boonmee et al. (2017) in their study was also employed while creating the model. According to the outputs obtained from this study, it can be decided where the warehouses should be established, the suitability of the existing warehouse and facility locations can be discussed, and arrangements can be made to ensure that the citizens suffer as little damage as possible in a possible Istanbul earthquake.

2. Material and Method

In this study, a mathematical model will be established to determine the optimum disaster logistics warehouse locations for a possible major Istanbul earthquake. The problem under consideration is modeled in two steps. In the first step, different scenarios with different coverage distances will be established, and the minimum number of warehouses to be established with the set covering problem will be determined. In the second step, the results of the first step will be given as input to the p-median problem, and demand-weighted distance minimization and assignments will be made.

Indices
i: Index of the demand points (Districts)
j: Index of the facilities (Candidate logistics warehouses)
Parameters
n : Number of potential facilities
S : Coverage distance of the facilities planned to be opened (km)
a_{ij} : 1 if the distance between demand point i and facility j is less than or equal to S, 0 otherwise
w_i : Demand of the demand point i
d_{ij} : Minimum distance between demand point i and facility j
p : Number of facilities to serve
Decision variables
x_j : 1 if a facility is established at point j, 0 otherwise
y_j : 1 if a facility is opened at point j, 0 otherwise
g_{ij} : 1 if demand point i is assigned to facility j, 0 otherwise

Step 1:
Objective function
$$\min z = \sum_{j=1}^{n} x_j \tag{1}$$
Constraints
$$\sum_{j \in J} a_{ij} . x_j \geq 1 \qquad \forall i \ (i = 1, \dots, n) \tag{2}$$
$$x_j \in \{0,1\} \qquad \forall j \ (j = 1, \dots, n) \tag{3}$$

Step 2:
Objective function
$$\min z = \sum_{i=1}^{n} \sum_{j=1}^{n} w_i . d_{ij} . g_{ij} \tag{4}$$

Constraints

$$\sum_{j=1} g_{ij} = 1 \qquad \forall i \ (i = 1, \dots, n) \tag{5}$$

$$g_{ij} \leq y_j \qquad \forall i, j \tag{6}$$

$$\sum_{j=1}^{n} y_j = p \tag{7}$$

$$g_{ij}, y_j \in \{0,1\} \tag{8}$$

In Step 1, Eq. 1 indicates that we want to minimize the number of facilities placed. Eq. 2 means that each demand point must be serviced by at least one facility. In this model, more than one facility can serve a demand point because there is not only one demand point assignment to a facility. Eq. 3 is the constraint of the decision variable being 0-1 integer.

In Step 2, Eq. 4 minimizes the overall distance between demand points and candidate facilities. Eq. 5 ensures that each demand point receives service from only one facility. Eq. 6 ensures that no demand point is assigned to the facility that is not open. Eq. 7 allows p units to be opened. Eq. 8 is the constraint for decision variables to be 0-1 integers.

3. Case Study

For determining the locations of disaster logistics warehouses, the booklet of possible earthquake loss estimates in Istanbul by districts, prepared in 2020 by Istanbul Metropolitan Municipality (IMM) and Kandilli Observatory, is used. In the booklet, the number of households in very heavy, heavy and moderately damaged residential buildings is used to estimate the number of families that will need emergency shelter after a possible Istanbul earthquake. In accordance with this, number of households that will need temporary shelter were calculated for the Mw=7.5 earthquake scenario for each district. These values in the booklet are used as demands in the model. Districts are demand points. To determine the demand points, the coordinates of the district centers were used.

IMM established a disaster response facility in Halkalı in 2006. IMM then identified 40 potential locations to set up additional facilities and warehouses. Görmez (2008) obtained the coordinates of these locations from the Geographical Information System (GIS) used by IMM and shared these coordinates in her master's thesis. In this study, these coordinates given in Figure 1, are used as candidate logistics warehouse locations.

Figure 1. Map of the candidate logistics warehouses (Görmez, 2008)

In the study, the distances of each demand point (districts) to each facility (logistics warehouses) were calculated using the Euclidean distance formula (Eq. 9)

$$d(A,B) = \sqrt{(x_1 - x_2)^2 + (y_1 - y_2)^2}$$ (9)

These data were entered while running our model. In the first step, 7 different scenarios with 40, 45, 50, 55, 60, 65 and 70 km coverage distances were considered. For this, 7 different experiments were conducted by entering S as 40, 45, 50, 55, 60, 65 and 70. According to the test results, the number of warehouses to be opened for each scenario and which warehouses to be opened will be found. By using the results obtained at this step in the second step, it will be seen which warehouse will serve which districts and a decision will be made according to the results of the objective function that minimizes the total distance between the districts and the candidate warehouses. The GAMS program will be used to run the model.

4. Results and Discussions

The problem is coded in GAMS, the results in Table 1 for Step 1 and Table 2 for Step 2 are obtained. The name of the districts are provided in Table 3.

Table 1. Results of Step 1

Scenario	Coverage distance S (km)	Number of storages to open	Storage no
Scenario 1	40	2	7, 21
Scenario 2	45	2	32, 36
Scenario 3	50	2	25, 35
Scenario 4	55	2	12, 25
Scenario 5	60	1	11
Scenario 6	65	1	10
Scenario 7	70	1	3

Table 2. Results of Step 2

Scenario	S (km)	Objective function	Storage No.	Districts to be served
Scenario 1	40	10.862.805,98	7	2:6, 9:13, 17, 25:30, 34:37
			21	1, 7, 8, 14:16, 18:24, 31:33, 38, 39
Scenario 2	45	10.513.175,91	32	1, 8, 14, 16, 18, 19, 22:24, 31:33, 38, 39
			36	2:7, 9:13, 15, 17, 20, 21, 25:30, 34:37
Scenario 3	50	8.468.443,53	25	2:6, 10:13, 17, 25:30, 34:37
			35	1, 7:9, 14:16,18:24, 31:33, 38, 39
Scenario 4	55	9.615.695,88	12	1, 6:12, 14:16, 18:24, 30:33, 38, 39

			25	2:5, 13, 17, 25:29, 34:37
Scenario 5	60	13.290.759,13	11	All
Scenario 6	65	11.946.363,12	10	All
Scenario 7	70	16.690.656,53	3	All

Table 3. District no

1.	Adalar	11.	Fatih	21.	Şişli	31.	Sancaktepe
2.	Avcılar	12.	Gaziosmanpaşa	22.	Tuzla	32.	Ataşehir
3.	Bakırköy	13.	Güngören	23.	Ümraniye	33.	Çekmeköy
4.	Bağcılar	14.	Kadıköy	24.	Üsküdar	34.	Arnavutköy
5.	Bahçelievler	15.	Kağıthane	25.	Zeytinburnu	35.	Beylikdüzü
6.	Bayrampaşa	16.	Kartal	26.	Esenler	36.	Büyükçekmece
7.	Beşiktaş	17.	Küçükçekmece	27.	Silivri	37.	Esenyurt
8.	Beykoz	18.	Maltepe	28.	Çatalca	38.	Sultanbeyli
9.	Beyoğlu	19.	Pendik	29.	Başakşehir	39.	Şile
10.	Eyüp	20.	Sarıyer	30.	Sultangazi		

When we consider the objective functions, we see that the optimal scenario is Scenario 3 with a coverage distance of 50. According to this scenario, logistics warehouses should be established at location 25 in Kartaltepe, Küçükçekmece and at location 35 in Ümraniye, Fatih Sultan Mehmet. We mapped this scenario in Figure 2.

Figure 2. Map of Scenario 3

In real life, it can be decided that warehouses cannot be established in these locations for some reason, therefore the locations of the other 6 scenarios can be evaluated. For example, since congestion and damage may occur on the Bosphorus bridges after the earthquake, it may be decided to serve the districts on the side where each warehouse is located, so that Scenario 2 can be implemented. The maps of the other 6 scenarios are as in Figures 3-8.
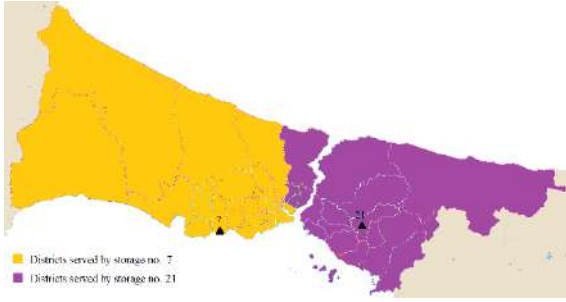
Figure 3. Map of Scenario 1
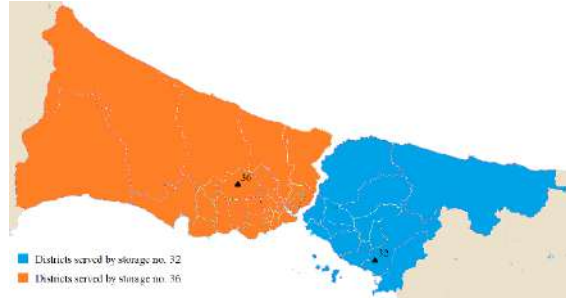
Figure 4. Map of Scenario 2
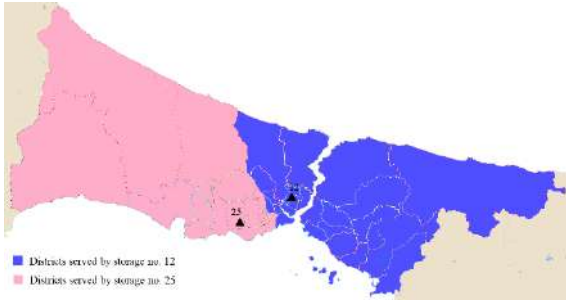
Figure 5. Map of Scenario 4
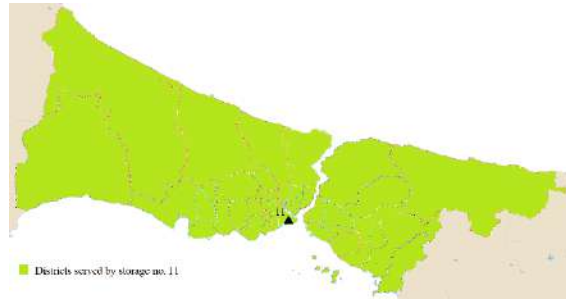
Figure 6. Map of Scenario 5
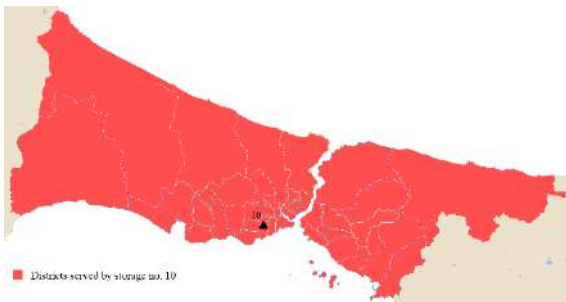
Figure 7. Map of Scenario 6

Figure 8. Map of Scenario 7

5. Conclusions

In order to prevent the chaos that may occur after the earthquake, it is very important to determine the locations of the warehouses where the aid materials will be stored with an accurate analysis, so that unnecessary traffic and lost time can be avoided. Having access to help as soon as possible after the earthquake is important not only for the health of the citizens affected by the earthquake, but also for their psychology. The sooner these earthquake victims get help, the sooner they can go on with their lives with less harm. To make the earthquake victims return to their normal lives also has a social significance. This is how the country's service and education systems can survive. We believe that the results of this project will contribute to these issues.

In this study, factors such as cost, highways and traffic conditions in Istanbul were not taken into account. In addition, estimates of the number of households that will need emergency shelter are considered deterministic, and it is assumed that there are no capacity limits. The study can be developed to be more realistic in the future, taking into account costs, highways, capacity and traffic. Scenarios can be developed for the number of households that will need

shelter and different possibilities can be evaluated. Scenarios can be developed regarding the magnitude of the earthquake as well.

Acknowledgements

References

AFAD, (2014). Açıklamalı Afet Yönetimi Terimleri Sözlüğü. [Online]. Available: https://aats.afad.gov.tr/

AFAD, (2019). Deprem Nedir? [Online]. Available: https://www.afad.gov.tr/deprem-nedir

Aydın, H., Ayvaz, B., Küçükaşçı, E.Ş., (2017). Afet Yönetiminde Lojistik Depo Seçimi Problemi: Maltepe İlçesi Örneği. Journal of Yasar University, 12, 1-13.

Boonmee C., Arimura M., Asada T., (2017). Facility location optimization model for emergency humanitarian logistics. International Journal of Disaster Risk Reduction, 24, 485-498.

Görmez, N., (2008). Disaster response and relief facility location for İstanbul. Orta Doğu Teknik Üniversitesi, Fen Bilimleri Enstitüsü, Endüstri Mühendisliği Bölümü, Yüksek Lisans Tezi.

İstanbul Büyükşehir Belediyesi, Kandilli Rasathanesi ve Deprem Araştırma Enstitüsü, (2020). İstanbul İli Olası Deprem Kayıp Tahminlerinin Güncellenmesi Projesi.

Cost Minimization by Liner Shipping Transport Integration into the Supply Chain and Supplier Selection in a New Production Facility

Ahmet Karakaya[1], Mehtap Dursun[1]*, Nazli Goker[1]

Abstract: As a result of liberalization and the globalization of international trade, factors of production and consumer products come from destinations around the world, and therefore the interdependence of supply chains between suppliers and wholesalers is increasing day by day. In this research, an optimization is carried out for the transportation in the supply chain, which aims to change route because of Russia and Ukraine war. The method is applied to the supply chain of a company that sells ready meals. This study aims to increase the competitive structure in the new market by reducing the cost of a fast food company that does not carry out maritime transport in its supply chain.

Keywords: Cost minimization, liner shipping, supplier selection, supply chain management

1. Introduction

As a result of liberalization and the globalization of international trade, factors of production and consumer products come from destinations around the world, and therefore the interdependence of Supply Chains between suppliers and wholesalers is increasing day by day. The effectiveness of Supply Chains has also become very important for proper competition in international markets that have emerged with the removal of trade barriers between countries (Apaiah & Hendrix, 2005). The analysis of the supply chain, which includes all its actors, must meet requirements such as meeting customer demands under constraints such as the delivery capacity of suppliers, the production capacity of factories, and the storage capacity of distribution centers. This requires complex processing of a large number of variables, which requires resorting to optimization to achieve optimal results, both to speed up the process and to ensure sufficient precision (Zhalechian et al., 2016).

Entering a market of large wholesalers and supermarket chains has increased competition at the expense of small farmers. About 30-35% of total food produced is wasted each year due to inadequate infrastructure and ineffective supply chains. Globalization has also led to a collapse in biodiversity and ecosystems, obesity and increased food poverty, and the impossibility of consumers knowing enough about food source and quality (Bortolini et al., 2016).

However, consumers today are increasingly aware of the negative impacts of a globalized food system and are eager to reconnect directly with farmers, support local communities, consume healthy food. In addition, global food demand is projected to increase by 50% by 2030, leading to increased demand for resources for production and transportation.

Planners, stakeholders and researchers wonder if they will have enough healthy food in the future, and at what cost. For this reason, companies, especially in food supply chains, need to

[1] Galatasaray University, Industrial Engineering Department, Decision Analysis Research and Application Center, Ortakoy, Istanbul, Turkey
* Corresponding author: mdursun@gsu.edu.tr

be faster, cheaper and more flexible than their competitors in order to meet customer expectations, as well as apply sustainable paradigms. When all these conditions are taken into consideration, both producers and farmers will benefit economically by purchasing the raw materials directly from the farmers and eliminating them from the intermediaries in the food supply chain. Thanks to the fresh and natural raw materials taken directly from the farmer, the harms of the products to human health will be reduced. By collecting back the used products from the end customer, the harm of wastes to the environment will be prevented and economic benefit will be provided by recycling the products.

In this research, an optimization has been carried out for the transporting in the supply chain, which aims to change route because of Russia and Ukraine war. The proposed model to define the optimal configuration allows decision making from raw material suppliers to possible distribution centers to the customer. This optimization was applied on the supply chain of a company selling ready-cooked food. Our study proposes to go further by interweaving for the several parameters which is possible suppliers and transportation costs.

2. Case Presentation and Problem

Nimo is an active and developing company that has been in the Ukrainian market since 1942. In the Food and Ready Meal sector, Nimo works with companies that it exports to 7 countries, raw material suppliers from 3 countries, and about 30 different store chains where its products are sold in the domestic market.

It processes raw materials it has supplied from its suppliers. The company has a large store for wholesale plasters, chains of Ukrainian stores selling its own products. It has a warehouse to store the products it produces in Ukraine, a processing in facility, raw material and semi-raw material warehouses. It supplies raw materials for its products mainly from Russia. It also imports 55% of the final product to Russia. The company wants to develop its market network since 2013. With the Russia-Ukraine crisis, the company wants to expand to Europe and plans to establish a production facility in Europe. The work contents planning a route and choosing a supplier with the data we receive from the company. Because Nimo will open a new production facility in Europa and distribution will be provided from there.

The company plans to establish a new production facility in Albania. For this reason, it has started to search for new suppliers and markets. It receives its products and supply raw materials by land transport. However, it wants to be competitive in the European market and to have a place in the market share with competitive prices with using sea transportation.

Interaction with counterparties in the supply network on behalf of the company is established as follows: A report is created on the success of the supplier in certain positions and based on this it is decided whether to reorder a particular product from a supplier. If a positive decision has been made, the purchasing department creates an order, which is then sent to the suppliers. According to the information they have given us, there is no problem regarding the possible suppliers and their countries in terms of quality and shelf life. For this reason, with the information and cost information given in this study, a choice will be made in terms of planning a route and supplier in sea transportation.

A study will be made for a container routing and empty container routing with the given cost coefficients. The suppliers used by the company with land transportation are as follows.
a)   Romania
b)   Ukraine
c)   Poland
The company related to the above suppliers has done a study and sent us the cost of 50.000 over the coefficients. If the result is less than 50,000 in our study, it has been reported that working with LS reduces the cost and a decision will be made in this direction. While calculating the

cost coefficients, they evaluated the raw material price and the data received from LS companies within the scope of confidentiality and gave them to us by establishing this numerical connection between them.

Our work will take place in the following 2 stages. Stages are;

a)   Testing possible supplier routes between containers loaded with raw materials and determining their costs (Row material)

b)   Determining cost of containers loaded with final products

3. Mathematical Model

Notations are presented in Table 1 to facilitate the presence of notation marks.

Table 1. Notations

Parameters	
c^s_{ij}	The cost of sending an empty container of type s over the service network from node i to node j (i,j)
c^k_{ij}	The cost of sending a unit of commodity k over the service network from node i to node j (i,j)
d^k	The demand quantity for commodity k
u_{ij}	The vessel capacity over the service network from node i to node j (i,j)
M	Sufficiently large non-negative number
N	Number of nodes in service network
Decision Variables	
Y^s_{ij}	Amount of empty container flow of type s over the service network from node i to node j (i,j)
ξ_k	Amount of artificial flow for commodity k
x^k_{ij}	Dual variable associated with constraints
Sets	
A	Set of service arcs in Graph G
N	Set of service nodes in Graph G
N^d	Set of destination nodes (Commodity or Empty container) in Graph G
N^o	Set of origin nodes (Commodity or Empty container) in Graph G
K	Set of commodities sent over the service network in Graph G
S	Set of empty container types i.e., foldable containers folded as s=1, s=2 or s=3 containers (Only empty containers
Miscellaneous	
i	A node of service network in Graph G
j	A node of service network in Graph G
k	A commodity
O^k	Origin node of commodity K
D^k	Destination node of commodity K
G = (N,A)	Graph representing the liner shipping network

The mathematical formulation of Laden and foldable Empty Container routing Problem

(LECP) can be given as follows.

$$z^* = \min \sum\sum c^k_{ij}x^k_{ij} + \sum\sum c^s_{ij}\delta^s_{ij} + \sum M\xi^k \qquad (1)$$

$$\text{s.t} \quad \sum x^k_{ij} - \sum x^k_{ji} + \xi^k = d^k \qquad \text{if } i = O^k; \forall k \in K \qquad (2)$$

$$\sum x^k_{ij} - \sum x^k_{ji} - \xi^k = -d^k \qquad \text{if } i=D^k; \forall k \in K \qquad (3)$$

$$\sum x^k_{ij} - \sum x^k_{ji} = 0 \qquad \forall i \in N \setminus \{O^k,D^k\}, \forall k \in K \qquad (4)$$

$$\sum x^k_{ij} + \sum \delta^s_{ij} \leq u_{ij} \qquad \forall (i,j) \in A \qquad (5)$$

$$\sum\sum s(\delta^s_{ji} - \delta^s_{ij}) - \sum\sum (x^k_{ij} - x^k_{ji}) \geq 0 \qquad \forall i \in N \qquad (6)$$

$$x^k_{ij} \geq 0 \; \forall (i,j) \in A, \qquad \forall k \in K \qquad (7)$$

$$\delta^s_{ij} \geq 0 \; \forall (i,j) \in A, \qquad \forall s \in S \qquad (8)$$

$$\xi^k \geq 0 \qquad \forall k \in K \qquad (9)$$

4. Application

There is no need for cold chain application for raw materials. For this reason, the containers we use can be used as laden and foldable containers. The model was used in the same form for supplier selection.
  1st possible 3 supplier countries are as follows;
  a)   Spain
  b)   Tunisia
  c)   Belgium
The information required for the model is shown in Tables 2-4.

Table 2. Arcs and cost coefficient for 1ˢᵗ scenario

Origin (Node i)	Destination (node j)	Cost Coefficient
Belgium	Spain	38
Spain	Tunisia	20
Tunisia	Albania	13
Belgium	Tunisia	45
Albania	Belgium	54

Table 3. Commodities origins and destinations 1ˢᵗ scenario

Commodity	Origin (node i)	Destination (node j)
Raw Material 1	Belgium	Albania
Raw Material 2	Spain	Albania
Raw Material 3	Tunisia	Albania

Table 4. Countries end container demands for 1ˢᵗ scenario

Country	Container Demands
Belgium	200
Spain	200
Tunisia	200
Albania	600

Using given information above, the optimal solution of objective function is 13.950.
2nd possible 3 supplier countries are as follows;
    a) Portugal
    b) Morocco
    c) Italy

The information required for the model is shown in tables 5-7.

Table 5. Arcs and cost coefficient for 2nd scenario

Origin (Node i)	Destination (node j)	Cost Coefficient
Portugal	Morocco	7
Morocco	Italy	24
Italy	Albania	5
Morocco	Albania	30
Albenia	Portugal	33

Table 6. Commodities origins and destinations 2nd scenario

Commodity	Origin (node i)	Destination (node j)
Raw Material 1	Portugal	Albania
Raw Material 2	Morocco	Albania
Raw Material 3	Italy	Albania

Table 7. Countries end container demands for 2nd scenario

Country	Container Demands
Portugal	200
Morocco	200
Italy	200
Albania	600

Using given information above, the optimal solution of objective function is 11.950.
3rd possible 3 supplier countries are as follows;
    a) Denmark
    b) Portugal
    c) Tunisia
The information required for the model is shown in Tables 8-10

Table 8. Arcs and cost coefficient for 3rd scenario

Origin (Node i)	Destination (node j)	Cost Coefficient
Denmark	Portugal	40
Portugal	Tunisia	23
Tunisia	Albania	13
Albania	Denmark	59

Table 9. Commodities origins and destinations 3rd scenario

Commodity	Origin (node i)	Destination (node j)
Raw Material 1	Denmark	Albania
Raw Material 2	Portugal	Albania
Raw Material 3	Tunisia	Albania

Table 10. Countries end container demands for 3rd scenario

Country	Container Demands
Denmark	200
Portugal	200
Tunisia	200
Albania	600

Using given information above, the optimal solution of objective function is 15.750. Based on the above optimizations, the lowest cost route is the route in scenario 2. Row material 1 supply from Portugal, row material 2 supply from Morocco, Row material 3 supply from Italy. This selection is give us 25% cost saving according to worst scenario.

5. Conclusions

Supply chain is the general expression of the system of producing and delivering a product or service from the very beginning of the procurement of raw materials to the final delivery of the product or service to the end consumers. The supply chain is a set of processes that encompasses all aspects of the manufacturing process, including the activities involved at each stage, the information transmitted, the natural resources converted into useful products, human resources, and other components that go into the finished product or service. Businesses have to optimize their supply chains in order to maintain their cost and market advantage by delivering quality products and services to the end consumer as soon as possible and at the desired time. The increase in global trade at this level has been an inevitable result of minimizing transportation costs in order to reduce the cost for exporting countries. Increasing fuel costs in the global have put great pressure on the cold chain. For this reason, maritime transportation has become the number one point for cost reduction. Containerization of frozen commodities is steadily progressing, while bulk reefers retain a significant market share, particularly for certain commodity flows. With the spread of containerization, the competition between frozen bulk and container becomes increasingly intense. More academicians are focusing on this area, while business leaders are looking for practical tools to help them with their daily operations and decision-making.

Increasing fuel prices in the world have caused a great cost increase in supply chains. For this reason, the use of more economical transportation lines has gradually increased. Along with rising fuel prices, the amount of fuel used is constantly harming our planet. In addition to cost optimization, this study was also carried out in terms of sustainable engineering and green engineering concepts. A green planet is the greatest gift we can give to future generations.

References

Apaiah, R. K., Hendrix, E. M. T. (2005). Design of a supply chain network for pea-based novel protein foods. Journal of Food Engineering, 70(3), 383-391.

Bortolini M., Faccio, M., Ferraria, E., Gamberi, M., Pilati, F. (2016). Fresh food sustainable distribution: cost, delivery time and carbon footprint three-objective optimization. Journal of Food Engineering, 174, 56-67.

Zhalechian, M., Tavakkoli-Moghaddam, R., Zahiri, B., Mohammadi, M. (2016). Sustainable design of a closed-loop location-routing-inventory supply chain network under mixed uncertainty. Transportation Research Part E: Logistics and Transportation Review, 89, 182-214.

Criteria Evaluation of Agile Outsourcing Provider Selection Problem: An Intuitionistic Fuzzy Mapping Approach

Nazli Goker[1*], Mehtap Dursun[2]

Abstract: In project management, agility has emerged to deal with the limitations of traditional methodologies that are linear and sequential. An agile project consists of both planned processes and iterations. In global competition, obtaining agile processes in outsourcing procedures allows the firms to keep up with the changes and dynamic issues. In this work, the factors that influence agile provider selection decision are evaluated, and their importance weights are determined. Intuitionistic fuzzy cognitive map is an appropriate technique due to the presence of interrelationships among evaluation criteria, fuzziness, vagueness, and hesitation in data. The application is illustrated through a case study, which is conducted in a white goods manufacturer that performs in Turkey.

Keywords: Intuitionistic fuzzy sets, intuitionistic fuzzy cognitive map, agile provider selection, project management.

1. Introduction

Agile project management notion is launched in 2001 to deal with ineffectiveness in describing customer needs, managing the changes of the project requirements, and cost saving. It has been emerged from unpredictable properties of customer requirements, technologic progresses, and unstability of business problems (Lei et al. 2017). At first, Waterfall project management methodology, which is linear and sequential, was used in managing the projects. Agile project management methodology has emerged to eliminate the shortcomings of Waterfall project management methodology. In an agile project, processes are planned and then managed in iterative manner. The outcomes achieved from an iteration lead to construct the following project stage (Totten, 2017).

In competitive global markets, agility concept has become more and more crucial in managerial processes. Correspondingly, agility in outsourcing processes has emerged in order to cope with changes and dynamic environment. Outsourcing process disintegrates the jobs by collaborating with a provider in lieu of insourcing an activity (Liu et al. 2008; Tsai et al. 2010). Recently, outsourcing has been a part of strategic management and operations management, although it was firstly employed in the early 1990s in information technologies (IT) to achieve cost savings and technical efficiency (Tjader et al. 2014).

In the last years, researchers have contributed to the "provider evaluation/selection" literature by developing several decision making frameworks. Ecer (2018) combined fuzzy AHP (analytic hierarchy process) and EDAS (evaluation based on distance from average solution)

---

[1] Galatasaray University, Istanbul, Türkiye
* Corresponding author: nagoker@gsu.edu.tr

for third party logistics (3PL) provider selection in marble industry. Ji et al. (2018) integrated MABAC (multi-attribute border approximation area comparison) and ELECTRE methods for outsourcing provider selection with neutrosophic fuzzy numbers. Sremac et al. (2018) used rough SWARA (step-wise weight assessment ratio analysis) and rough WASPAS (weighted aggregated sum product assessment) methodologies by combining rough Dombi aggregation operator into the 3PL provider selection framework. In a similar manner, Singh et al. (2018) proposed fuzzy AHP and fuzzy TOPSIS integrated framework for 3PL provider selection for a cold supply chain in food industry. Li et al. (2018) solved 3PRL provider selection using cumulative prospect theory and then provided a comparative analysis employing fuzzy TOPSIS technique for an electronics company.

Recently, Percin (2019) identified the best performing outsourcing provider in chemical industry combining fuzzy SWARA and fuzzy axiomatic design (AD) methodologies, and then provided a sensitivity analysis in order to compare the results with those of other decision making techniques namely fuzzy TOPSIS and fuzzy VIKOR. Govindan et al. (2019) proposed ELECTRE-based stochastic multi-criteria acceptability analysis for 3PRL provider selection for an Indian manufacturer. Ljubojevic et al. (2019) proposed two-stage decision framework for outsourcing provider selection in transportation sector. The hybrid two-stage method combines DEMATEL with a novel outranking methodology. In a similar manner, Zarbakhshnia et al. (2020) identified the best 3PRL provider that performs for car parts production company by integrating fuzzy AHP and grey multi-objective optimization by ratio analysis.

This work introduces an intuitionistic fuzzy cognitive map (IFCM) technique to determine the importance degrees of agile provider selection criteria. The presence of interrelationships among evaluation criteria, fuzziness, vagueness, and hesitation in data led us to employ IFCM methodology as an appropriate tool.

The remaining sections of the paper are organized as follows. Section 2 explains briefly intuitionistic fuzzy cognitive map methodology. The following section illustrates the application via a case study conducted in white goods industry. Final section delineates conclusions and future research directions.

2. Intuitionistic Fuzzy Cognitive Maps

Intuitionistic fuzzy cognitive map (IFCM) technique includes intuitionistic fuzzy numbers into cognitive maps in order to determine the power of cause-and-effect relationships (Dogu and Albayrak, 2018). First, concept nodes and power of causal links among them are defined by obtaining experts' opinions. Second, the power of causal links is represented by intuitionistic fuzzy numbers that are associated with intuitionistic fuzzy scale. Hence, membership, non-membership, and hesitation values are identified. Finally, N x N weight matrix is formed by employing the information collected from the experts.

The following iterative formulation of IFCM is run until the system will be stabilized, in other words, all factor weights will converge (Iakovidis and Papageorgiou, 2011). In this way, the concepts' values are computed.

$$A_i^{(k+1)} = f\left(A_i^{(k)} + \sum_{\substack{j \neq i \\ j=1}}^{N} A_j^{(k)} w_{ji}^{\mu} - A_j^{(k)} w_{ji}^{\pi} \right) \tag{1}$$

where $A_i^{(k)}$ is the value of concept C_i at k^{th} iteration, w_{ji} is the weight of the connection from C_j to C_i, w_{ji}^{μ} and w_{ji}^{π} denote the weight matrices that show membership values and hesitation values of causal links, respectively, and f is a threshold function, which is considered as sigmoid function for this work.

3. Case Study

This work presents an IFCM approach for evaluating agile provider selection criteria in Turkish white goods sector. The best performing provider alternative will provide an IT-based project to the case company. The case study is conducted through three experts' opinions. Initially, the evaluation criteria which are given in Table 1, are identified by interviewing the project managers of the case firm.

Table 1. Evaluation criteria

Label	Concept
C_1	Cost
C_2	Lead time
C_3	Customer participation
C_4	Communication
C_5	Ability to react to change
C_6	Self-organization
C_7	Responsiveness
C_8	Innovative skills

The experts provide their opinions by reaching a consensus and they used the linguistic scale shown in Table 2.

Table 2. Linguistic Scale

Linguistic term	Intuitionistic fuzzy number
VH	<0.95,0.05>
H	<0.70,0.25>
M	<0.50,0.40>
L	<0.25,0.70>
VL	<0.05,0.95>

The linguistic data, membership values, non-membership values, and hesitation values for causal relationships, are given in Tables 3, 4, 5, and 6, respectively.

Table 3. Linguistic Data for Causal Relationships

	C_1	C_2	C_3	C_4	C_5	C_6	C_7	C_8
C_1	-	-	-	-	-	-	-	-
C_2	-	-	-	-	-	-	-	-
C_3	-	M	-	-	VH	-	VH	-
C_4	-	H	-	-	L	-	-	VL
C_5	-	M	-	-	-	-	VH	-
C_6	-	M	-	-	M	-	M	-
C_7	-	-	H	-	H	-	-	-
C_8	-	-	-	-	-	-	-	-

Table 4. Membership values

	C_1	C_2	C_3	C_4	C_5	C_6	C_7	C_8
C_1	0	0	0	0	0	0	0	0
C_2	0	0	0	0	0	0	0	0
C_3	0	0.5	0	0	0.95	0	0.95	0
C_4	0	0.7	0	0	0.25	0	0	0.05
C_5	0	0.5	0	0	0	0	0.95	0
C_6	0	0.5	0	0	0.5	0	0.5	0
C_7	0	0	0.7	0	0.7	0	0	0
C_8	0	0	0	0	0	0	0	0

Table 5. Non-membership values

	C_1	C_2	C_3	C_4	C_5	C_6	C_7	C_8
C_1	0	0	0	0	0	0	0	0
C_2	0	0	0	0	0	0	0	0
C_3	0	0.4	0	0	0.05	0	0.05	0
C_4	0	0.25	0	0	0.7	0	0	0.95
C_5	0	0.4	0	0	0	0	0.05	0
C_6	0	0.4	0	0	0.4	0	0.4	0
C_7	0	0	0.25	0	0.25	0	0	0
C_8	0	0	0	0	0	0	0	0

Table 6. Hesitation values

	C_1	C_2	C_3	C_4	C_5	C_6	C_7	C_8
C_1	0	0	0	0	0	0	0	0
C_2	0	0	0	0	0	0	0	0
C_3	0	0.1	0	0	0	0	0	0
C_4	0	0.05	0	0	0.05	0	0	0
C_5	0	0.1	0	0	0	0	0	0
C_6	0	0.1	0	0	0.1	0	0.1	0

C₇	0	0	0.05	0	0.05	0	0	0
C₈	0	0	0	0	0	0	0	0

IFCM technique is employed and importance weights of agile provider selection factors are obtained by running the formulation (1) until it will be stabilized, and the values of concepts will remain same. FCMapper software is used for these operations. The concepts' values are given in Table 7.

Table 7. Importance weights of digital transformation factors

Label	Concept	Weight
C_1	Cost	0.6590
C_2	Lead time	0.9087
C_3	Customer participation	0.8054
C_4	Communication	0.6590
C_5	Ability to react to change	0.9378
C_6	Self-organization	0.6590
C_7	Responsiveness	0.9461
C_8	Innovative skills	0.6685

4. Discussion and Conclusions

To obtain the importance weights of agile provider selection criteria for an IT-based project conducted in white goods industry, evaluation factors are determined through expert opinions and then algorithm of the work is reported by considering IFCM technique. Importance weights of concepts are assigned by applying IFCM methodology, responsiveness is the most influential factor however cost, communication, and self-organization are the effective ones. Future research directions will focus on proposing group decision making approach for evaluating the criteria of agile provider evaluation in various sectors.

Acknowledgements

References

Dogu, E., & Albayrak, Y. E. (2018). Criteria evaluation for pricing decisions in strategic marketing management using an intuitionistic cognitive map approach. Soft Computing, 22, 4989-5005.

Ecer, F. (2018). Third-party logistics (3PLs) provider selection via fuzzy AHP and EDAS integrated model. Technological and Economic Development of Economy, 24(2), 615-634.

Iakovidis, D. K., and Papageorgiou, E. (2011). Intuitionistic fuzzy cognitive maps for medical decision making. IEEE Transactions on Information Technology in Biomedicine, 15, 100-

107.

Govindan, K., Kadzinski, M., Ehling, R., & Miebs, G. (2019). Selection of a sustainable third-party reverse logistics provider based on the robustness analysis of an outranking graph kernel conducted with ELECTRE I and SMAA. Omega, 85, 1-15.

Ji, P., Zhang, H., & Wang, J. (2018). Selecting an outsourcing provider based on the combined MABAC–ELECTRE method using single-valued neutrosophic linguistic sets. Computers&Industrial Engineering, 120, 429-441.

Lei, H., Ganjeizadeh, F., Jayachandran, P. K., & Ozcan, P. (2017). A statistical analysis of the effects of Scrum and Kanban on software development projects. Robotics and Computer-Integrated Manufacturing, 43, 59-67.

Li, Y. L., Ying, C. S., Chin, K. S., Yang, H. T., & Xu, J. (2018). Third-party reverse logistics provider selection approach based on hybrid-information MCDM and cumulative prospect theory. Journal of Cleaner Production, 195, 573-584.

Liu, L.B., Berger, P., Zeng, A., & Gerstenfeld, A. (2008). Applying the analytic hierarchy process to outsourcing location decision. Supply Chain Management: An International Journal, 13(6), 435-449.

Ljubojevic, S., Pamucar, D., Jovanovic, D., & Vesovic, V. (2019). Outsourcing transport service: a fuzzy multi-criteria methodology for provider selection based on comparison of the real and ideal parameters of providers. Operational Research: An International Journal, 19, 399-433.

Percin, S. (2019). An integrated fuzzy SWARA and fuzzy AD approach for outsourcing provider selection. Journal of Manufacturing Technology Management, 30(2), 531-552.

Singh, R., Gunasekaran, A., & Kumar, P. (2018). Third party logistics (3PL) selection for cold chain management: a fuzzy AHP and fuzzy TOPSIS approach. Annals of Operations Research, 267, 531-553.

Sremac, S., Stevic, Z., Pamucar, D., Arsic, M., & Matic, B. (2018). Evaluation of a third-party logistics (3PL) provider using a rough SWARA-WASPAS model based on a new rough Dombi aggregator. Symmetry, 10, 1-25.

Tjader, Y., May, J.H., Shang, J., Vargas, L.G., & Gao, N. (2014). Firm-level outsourcing decision making: A balanced scorecard-based analytic network process model. International Journal of Production Economics, 147, 614-623.

Totten, J. (2017). Critical success factors for agile project management in non-software related product development teams. Ph.D. thesis, Western Michigan University.

Tsai, W.H., Leu, J.D., Liu, J.Y., Lin, S.J., & Shaw, M.J. (2010). A MCDM approach for sourcing strategy mix decision in IT projects. Expert Systems with Applications, 37, 3870-3886.

Zarbakhshnia, N., Wu, Y., Govindan, K., & Soleimani, H. (2020). A novel hybrid multipleattribute decision-making approach for outsourcing sustainable reverse logistics. Journal of Cleaner Production, 242, 118-461.

A Survey: A novel hybrid automatic intrusion detection system using machine learning technique for anomalous detection based on traffic

Vınod D, Prasad M[*]

Abstract: The use of the internet has increased dramatically resulting in more sensitive data being transmitted and managed online. Security risks on the Internet have recently created a big challenge on a global scale. As a result in today's information technology era cyber security has emerged as a critical global issue which must be resolved. Intrusion Detection System (IDS) is one of the security monitoring system. Because of the ambiguity in the detecting process the number of false alarms has increased. This requires the design of a novel approach that would not only improve detection accuracy but also decrease false positives. The automated intrusion detection system (IDS) faces a significant problem in detecting intrusions early and effectively. As always, accurate intrusion detection with fewer false positives has evaded us. The vagueness in the perimeter between the normal and anomalous network traffic is one of the main reasons for the inaccuracies in the detection engine of the existing automated IDS. The effectiveness of the currently available IDS in detection of anomalous network connection lags in certain key performance aspects, namely limited accuracy in detection and high false positives. Most of the automated IDS proposed in literature have been implemented using one particular methodology and the detection engine in them is not optimized. The ambiguity during the detection process has also resulted in increase in the number of false alarms. This warrants the need for a novel methodology which would not only increase the detection accuracy but also reduce the false positives. This study proposes a hybrid methodology where new, improved, nature-inspired algorithms are used along with the classical detection methods to accurately detect intrusions. A novel hybrid approach to effectively and efficiently classify anomalous network traffic two hybridized approaches namely a.) Intrusion detection using hybrid Support Vector Machine and Dynamic Ant Colony Clustering (SDAC) b.) Fuzzified Ant System (FAS) have been proposed for detecting the intrusions. To enhance the effectiveness of the suggested hybridized classifiers an existing dimensionality reduction methodology Sequential Floating Selection (SFS) based Modified sequential Floating Forward Selection (MFFS) method has also been incorporated. The computer network benchmark dataset Network Security Laboratory Knowledge Discovery in Data Bases (NSL-KDD) has been used for the purpose of experimentation and validation of the proposed methodology.

[1] Vellore Institute of Technology Chennai Campus, Research Associate, SCOPE, Chennai, India
[2] Vellore Institute of Technology Chennai Campus, Assistant Professor, SCOPE, Chennai, India
  * Corresponding author: prasad.m@vit.ac.in

1. Introduction

Human beings protected and secured their property and privacy physically with fence, locks, signature, stringent government laws and life style since long time. With advent of networked electronic automation systems, hackers are provided with more chances to hack critical systems and cripple services for example intercept communications sent to aircrafts, freeze bank accounts, manipulate satellite data and shut down military control systems. In the modern, cyber-dependant world, security of computer systems has become one of the high priority global and societal issues that need to be addressed. The exponential growth of the Internet has paved way for the growth of the bespoken web based applications such as ecommerce, government and various other mission critical services. On the other hand, the networked computers have been exposed to external threats such as intrusions via the Internet. This scenario has greatly augmented the need for the security of networked computers and information systems. It has become mandatory to further strengthen the security of the networked information systems and services to safeguard it from adversaries. Intrusion Detection Systems (IDS) are required to identify intrusions aimed at disrupting the normal operation of information systems in production by malicious users. They work in tandem with the other attack prevention (firewalls, authentication and user roles) and attack avoidance (encryption and decryption) methods. This work uses Network Intrusion Detection System (NIDS), to detect the intrusions to the information systems through the network.

Intrusion refers to an attack on the networked computing facility with the intention of causing harm or to compromise Confidentiality, Integrity and Availability (CIA). Intrusions could be in different forms such as networked based attacks against vulnerable services, privilege escalation of users in hosts or launch of malware and so on. Intrusion detection is the process of detecting non-compliance usage of information systems or attacks on computing facility and networks. Intrusion Detection System (IDS) is an automated tool implemented in the hardware or in the software or combination of the both for the purpose of detecting intrusion. An IDS seems to be one of the most opted security technology solutions among the various other alternate mechanisms adopted to secure enterprise networks. The intrusion detection system is a handy tool which functions like a security camera or a burglar alarm. This intrusion dtection system can be configured to log events, which can be used for forensic evidence purposes to punish the adversary. However much of the intrusion detection system in trigger a higher rate of false alarms, which poses to be a hindrance.

An intrusion detection system provides visibility and control which are the two key aspects that aid in securing a network. Visibility makes the network traffic apparent helps in decision making thus influencing in security policy building directly. Control in turn is used to prohibit access to privileged areas in computer networks, which is otherwise used to impose compliance to the security policy. The placement of an intrusion detection system in a computer network, as shown in the Figure 1, it is normally located behind a firewall. It is designed meticulously to look for malicious network traffic and is in the second and final stage of protection in action.
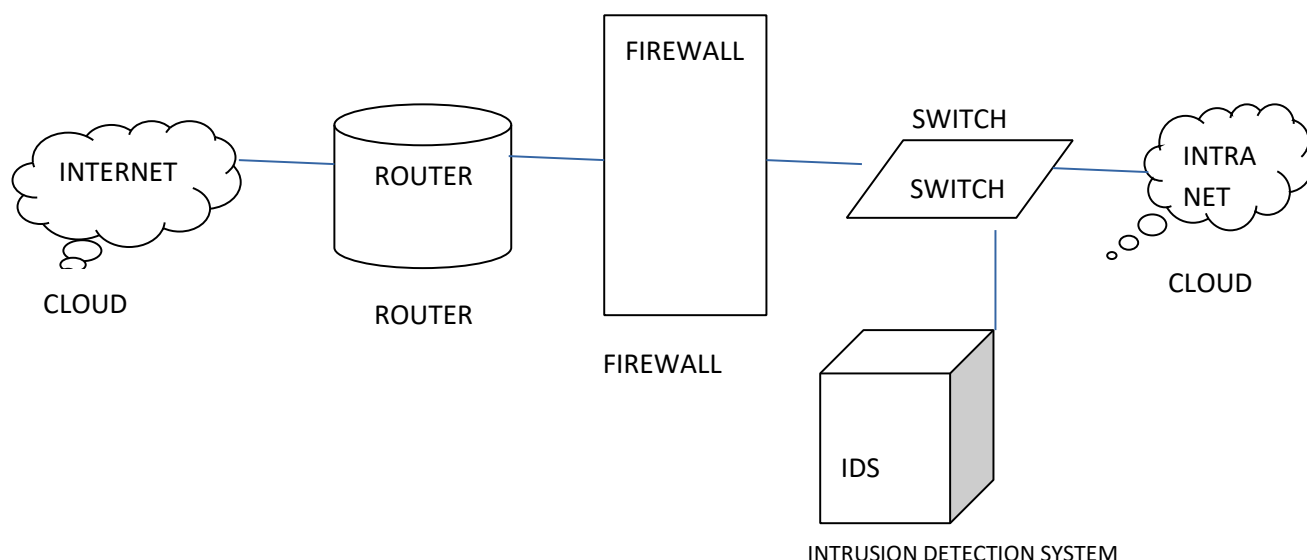
Figure 1: placement of an IDS in enterprise networks

The IDS works in tandem with the firewall and one cannot replace the other. The present study investigates and proposes a hybrid approach for developing automatic IDS, in which a nature inspired-technique is ensemble with one of the conventional classification techniques to effectively detect the anomalous network traffic that enter and exit a protected enterprise network.

Some of the more specific objectives of this study are as follows: 1. To extensively analyze and understand data in the existing benchmark dataset and use it to assess the effectiveness of an intrusion detection system. 2. To discover and extort optimal features of a network connection records that foster accuracy of detection using the proposed feature selection approach. 3. To adopt a hybrid paradigm by integrating nature-inspired technique with a classical classifier in order to improve the accuracy as against the existing conventional IDS. 4. To experiment, measure and analyze the effectiveness of the suggested methods with other prominent approaches that have already been proposed in literature.

To realize the hybrid paradigm, two different implementations combining nature inspired technique with popular classification techniques accompanied with a feature extraction process have been proposed. i. Ant Colony Clustering algorithm : It is used to generate precise data points to a) update the learning model developed by the classical Support Vector Machine (SVM) b) improve the learning process of the classifier c) make the learning process dynamic. ii. Ant Colony Optimization algorithm: It is used to mine optimal rules, which in turn is used by the fuzzy system for effective classification. This proposed approach has been evaluated using the benchmark dataset called the NSL KDD and real time data set. It is believed that the proposed approach will satisfy the unique security needs of the modern complex and high speed networks and would be the better-of-the-best IDS and also be a regular part of the multilayer defence and security implementation in the future.

2. Literature Survey:

Achmad Akbar Megantara et al. [1] suggested an intrusion detection system model for detecting and identifying any cyber attacks that intrudes on the network system. This research includes a hybrid machine learning model that combines feature selection using feature importance ranking from the decision tree algorithm with data reduction techniques using the local outlier factor to increase the performance of network intrusion detection systems. In the data reduction process hybrid machine learning model provide a method for computing the feature selection threshold value and identifying outlier data. The author suggests a hybrid machine learning model in this study which incorporates feature selection and reduction of data procedures. The importance value of each feature towards the dataset label is determined throughout the feature selection process. Remove zero valued features to identify low and high important characteristics then split the remaining data using median data to construct a threshold mechanism. The cutoff off factor for such an anomalous score will be determined using a gaussian distribution. The feature selection procedure combines extremely important data with label decisions and is classified into three techniques such as filter based, wrapper based and embedded based techniques. The embedded based technique is to merge filter method which is a pre-processing step in which relevant features are extracted based on the goodness‖ metric of the feature done by statistical methodology and wrapper method uses machine learning algorithms to each candidate feature subset to assess and then evaluate the subset in order to discover the potential subset that best represents the original data set.

Merve Ozkan-Okay et al. [2] suggested an intrusion detection system model that can help secure wireless local area network by identifying and stopping malicious activity. It is necessary to identify traffic attacks with extreme precision in order to protect a wireless local area network. Fast detection is required in addition to high accuracy detection. In this regard, an approach for efficiently and reliably detecting attacks is provided. The anomaly based intrusion detection system method hypothesizes that anomalous behavior is rare and differs uniquely from the normal behaviour. It also extracts patterns and develops a model based on normal behaviour. The anomaly based intrusion detection system detects anomaly in audit data if there is any deviation from the perceived model. The anomaly based techniques are used to determine behaviors and extract rules. The signature based intrusion detection system detects intrusions by matching the audit data with the pre- defined signature of security policy, vulnerabilities and attacks of the audit system available in the signature database. The signature based intrusion detection system also has the capability to detect well-known attacks with a high detection accuracy and low false alarm rate. The effectiveness of this method is highly dependent on the richness of the knowledge base. On the Knowledge Discovery and Data Mining 99 dataset the proposed approach and machine learning techniques were used for training and classification.

Mahmoud Said ElSayed et.al. [3] have proposed a hybrid intrusion detection system approach can increase the effectiveness and performance when compared to single intrusion detection system approach. The suggested model integrates machine learning algorithms with convolutional neural network architecture. The deep models of the data characteristics are

obtained using machine learning algorithms. The network based security incidents are in the form of suspicious network traffic which originate from the external or internal network hosts and are targeted to victim systems. The complexity and frequency of network based attacks launched by tactical attackers is also increasing with every passing day. The attack packets are disguised with typical network packets and go undetected by the packet header based filtering mechanism. Even though other studies have used deep learning to detect network intrusions the majority of these approaches neglect the impact of the over-fitting problem when deep learning algorithms are implemented. As a result deep learning may have an influence on the anomaly detection systems robustness resulting in poor simulation results for day zero attacks. Additionally when compared to single deep learning models, the proposed method outperforms them in all assessment criteria. To train and evaluate the performance of all strategies several datasets are employed including the In-software defined network the most recent dataset for software defined networks. A light weight hybrid network intrusion detection system has been proposed to meet the present high speed network security needs while also successfully detecting non-conforming network traffic.

Ahmed I. Salehet.al. [4] have proposed a hybrid intrusion detection system which might be used in real time basis and is well suited to the multi class classification challenge. Intrusion Detection System is a powerful security tool that analyses network traffic to assist prevent unauthorized access to network resources. The network based security incidents are in the form of suspicious network traffic which originate from the external or internal network hosts and are targeted to victim systems. A naive base feature selection method is employed in a hybrid intrusion detection system to minimize the dimensionality of sample data. Further the outlier rejection is a new feature of the hybrid intrusion detection system that other systems lack. Outliers are noisy input samples that when used in model training will result in a greater rate of misclassification. Outliers were rejected using a distance-based method that prioritized the much more useful training instances which were then utilized to train a optimized support vector machine. After that optimized support vector machine is used to exclude outliers. Finally using a prioritized K nearest neighbors classifier hybrid intrusion detection system can successfully detect attacks after outlier rejection. As a result the hybrid intrusion detection system is a three edged approach with Naive base feature selection for dimensionality reduction, optimized support vector machine and perform high detection rate specifically for the attacks.

Mokhtar Mohammadi et.al. [5] have proposed merging support vector machines with additional classifiers to deal with intrusions and security attacks. Each strategy has used a distinct approach to reduce the overhead of using several classifiers while also improving the accuracy and detection rate of intrusion detection. This method studies intrusion detection system schemes using decision trees, adaboost, K nearest neighbour and artificial neural networks in combination with the support vector machine. The proposed wrapper based approach namely the Modified Forward Floating Selection and multi class Support Vector Machine to generate an optimal set of features from the NSL KDD dataset for effective network intrusion detection. The detection rate is used as fitness and the support vector machine

parameters are encoded as bats. The knowledge discovery in databases cup dataset is employed to check this technique. The intrusion detection system methods that use a genetic algorithm in the intrusion detection system and support vector machines to produce a global model in each node which is responsible for detecting intrusions was also suggested by the authors. The principle component analysis space is searched using a genetic algorithm and a subset of principal components is selected. Then using a support vector machine this technique is trained and tested on the features chosen. In the fitness function of the genetic algorithm factors like precision and the quantity of features are employed to reduce the false alarm rate and increase the detection rate. The supervised approaches, in general, use a fully labeled dataset to train the support vector machines. Although this method is the most accurate at identifying intrusions it is difficult to locate a completely labeled dataset in real security applications. Unsupervised intrusion detection systems do not require access to a labeled dataset and use different clustering algorithms to arrange comparable data samples into clusters. Despite the fact that these methods do not require labeled datasets but they have a high false alarm rate problem. Support vector machine is one of the most opted and a popular supervised machine learning technique used to develop classifiers. This method constructs an optimal hyper plane which is used to separate the data in to two categories. The process for selecting the best feature is critical in assuring the detector's performance, speed, precision, and dependability. Filtering techniques, wrapper methods, and embedded methods are three different types of feature extraction methods that are used to solve this problem. The filtering techniques take into account the importance of the features determined by univariate statistics. Wrapper method uses machine learning algorithms to each candidate feature subset to assess and then evaluate the subset in order to discover the potential subset that best represents the original data set. Wrapper methods on the other end will be using a classifier to determine which features to use based on their performance. The optimal feature selection process is wrapped inside the classifier and the result is used as a metric to decide the optimal feature subset. The model of an intrusion detection system model must be analyzed using particularly unique intrusion detection system tools known as Snort after it has been created using the procedures stated above. Besides intrusion detection system techniques can be evaluated on the hosts under study in real world circumstances.

Dhruba Jyoti Kalita et.al. [6] proposed a method for dealing with the support vector machine design in a dynamic manner. Dynamism can happen in two forms during the training of a support vector machine parameter and during the optimization of the support vector machine's hyper parameters over a certain period of time. The suggested approach includes techniques to address both of the mentioned scenarios. To find the best solution in the first situation we may simply use quantized multiple particle swarm optimization with anti convergence theory. The second instance of dynamism during support vector machine classifier training on the other hand is more difficult to handle. In this scenario, data is delivered in batches, and as previously stated, the optimal solution changes owing to the nature of the data, affecting the classification accuracy rate of support vector machine classifiers. Until the next set of data arrives we must halt the optimization process. This must be done in order to make the most use of the available resources. When one start the optimization method each time new data is received and on the either hand the model will become ineffective in terms of processing time. To prevent this a continuous flow of information about the process of optimization must be used at various periods in time allowing optimization to begin based on that knowledge. The

proposed approach selects the optimal settings for the support vector machine hyper-parameters in a dynamic environment. A light weight intrusion detection system which removed redundant data, identified relevant features and accurately identified intrusions. It employed a neural ensemble decision tree to detect the network intrusions The amount of searching levels contained in the above proposed framework is one of its limits, even though it performs well for dynamic support vector machine model selection. Function searching at various levels takes a long time. Instead of using many layers of searching a single level of searching can be used. For anomaly based intrusion detection they used a Multiclass Support Vector Machine. In this approach the parameters of the Multiclass Support Vector Machine were optimized by particle swarm optimization to detect intrusions. Data finally arrives in batches in a dynamic context. As a result the classification model may degrade with time. There should be a mechanism that allows to re estimate the model's fitness online if we want it to keep its performance. In this approach the parameters of the Multi class Support Vector Machine were optimized by particle swarm optimization to detect intrusions. The proposed work's main goal is to develop a framework that uses support vector machines to classify samples in a dynamic context. The Knowledge discovery in databases Cup dataset was used to conduct the experiments and the experimental results obtained in this approach were compared with various methods such as K-Means and multi class support vector machine with parameters optimized by grid method.

Ansam Khraisat et al. [7] have proposed a classification of contemporary intrusion detection systems which offers a detailed analysis of important recent works as well as a list of often used datasets for evaluation. Thus it identifies future work in order to avoid such techniques and keep systems more secure through describing the evading techniques used among intruders to avoid detection. Cyber attacks are growing more sophisticated making reliable detection of intrusions more difficult. The security services credibility as well as data confidentiality, integrity and availability could be affected if attacks are not prevented. An alarm is raised once when an intrusion occurs. The effectiveness of the system depends on upto-date attack knowledge available in its knowledge base. A prediction engine was used to raise alarms whenever it had detected an intrusion. The signature intrusion detection system host logs are examined for patterns of instructions that have been earlier known as spyware. Intrusion detection system were found to enhance the signature patterns for normal and various attacks in the form of rules which in turn resulted in a better classification of intrusions. Expert systems were used to detect malicious activity thereafter. Intrusion detection expert system was known to be the first step towards the realization of a hybrid Intrusion detection system which is signature analysis and anomaly detection is to be implemented in critical and secure government information technology deployments. Intrusion detection systems can be classified using the same input data sources that are used to detect anomalous behaviour. A host based intrusion detection system can detect insider attacks which don't require network traffic. A network based intrusion detection system can check many computers which are connected to the network. Network intrusion detection system can detect external harmful behaviors that may be triggered by a potential attack at an early stage before the threats propagate to another computer system.

A network based intrusion detection system uses packet capture and Net Flow to monitor network traffic gathered from a single network. The proposed hybrid module takes care of classification of anomalous traffic. The outcome of the previous step which is a one dimensional distance based feature, was used to represent an input data sample for intrusion detection to be done by a k-nearest neighbour classifier. The authors conducted several experiments using the knowledge discovery in databases CUP'99 data set and the results obtained by the proposed approach showed an improvement in the detection rate and accuracy when compared to the individual methods. The authors also carried out experiments with their system using the knowledge discovery in databases – cup 99 dataset and found its performance either to be better than or similar to other classifiers such as k-nearest neighbour and support vector machine in terms of accuracy, detection rate and false alarms. The results of the proposed method showed that it outperformed other methods used for comparison and had a detection rate of 97.64 percent, false positive rate of percent and false negative rate of 2.45 percent.

Earum Mushtaq et al. [8] have proposed a hybrid framework for intrusion detection that mixes the benefits of an autoencoder and then utilizing long short term memory for categorization into normal and anomalous samples. When designing an efficient intrusion detection system the curse of dimensionality as well as experiments on the dataset shows that the model has small false alarm rate and greater recognition accuracy. The features are often extracted by rebuilding the network using an autoencoder and then training the intended residual network with the extracted features on the dataset network security laboratory Knowledge discovery in databases. In terms of accuracy true rate and false alarm rate the experimental results are better. On the network security laboratory Knowledge discovery in databases dataset an autoencoder and then utilizing long short term memory performance displays classification accuracy of 89 percent, detection rate of 89.84 percent and false alarm rate of 11 percent demonstrating the proposed model's superior performance to current state of the art methodologies. In order to improve the performance of intrusion detection method combining autoencoder and long short term memory this paper has comparison experiment of feature selection methods. By training in a hierarchical form deep learning techniques can extract input at a higher level of abstraction. A correlation based feature selection bat algorithm technique and an ensemble classifier are used to choose optimal features in an intrusion detection system. The most significant characteristics are chosen on the basis of the classification technique is proposed and followed by a voting mechanism for final classification. Experiments have been validated with the benchmark NSL KDD data set and their method had an accuracy of 87.37 percent and a detection rate of 87.4 percent. Sun proposed a deep feed neural network with relevant features extracted using an additional tree classifier which has an accuracy of 85.48 percent on the network intrusion dataset whereas Kasongo supports a deep learning technique based on wrapper based feature extraction. However their technique is computationally inefficient. Several researchers in the field of cyber security have recently published on deep learning with developing feature selection approaches. A network dataset is a collection of information related to network traffic and is created using tools used for capturing and analyzing network traffic. The UNSW-NB15 dataset was utilized which reached 92 percent accuracy but with a high far. The proposed model stability and effectiveness are guaranteed by statistical

analysis. Through the use of deep stacked autoencoder and shallow learning with the classification technique the proposed work successfully addresses these challenges. To make the best use of the proposed network intrusion detection method we want to hybridize the deep learning model to deal class imbalance problems with sophisticated generative adversarial networks in the near future. Utilizing the knowledge discovery and data mining Cup data set for testing it was discovered that the approach excelled previous algorithms of a same kind in terms of accuracy and false alarm rates.

M. R. Gauthama Raman et.al. [9] suggested a support vector machine based on the hyper clique enhanced gravitational search algorithm as an accurate and adaptable intrusion detection method to enhance the detection rate and false alarm rate of support vector machines. The Curse of Dimensionality as well as the trade-off between a high detection rate and a low false alarm rate makes designing a reliable and efficient intrusion detection system a difficult task. The author developed developed a one class classifier to classify one of the most vulnerable type of attack vectors. The one class classifier was implemented using the Support Vector Data Description. The half partition strategy of selecting and retaining nonsupport vectors of the current increment of classification named as Candidate Support Vectors which is likely to become the support vectors in the next iteration of classification. Many quality measures, stability tests and statistical tests are provided for the hyper clique enhanced gravitational search algorithm. Many network administrators and security experts are concerned about intrusion detection. To identify intrusions and safeguard networked systems from cyber attacks and authenticating mechanisms has also been implemented. Traditional security measures on the other hand are limited in scope and usually fail to safeguard networks against newer attacks and intrusion methods. Intrusion detection systems that observe, evaluate and detect anomalous network behavior provide adequate security against a wide range of current and emerging cyber threats that threaten the confidentiality, integrity, and availability of information systems. The method of attempting to get instances of network attacks by comparing current behavior to the expected activities of an intruder is called misuse detection. Anomaly detection systems can detect unknown attacks however they have a large false alarm rate. The classification relies on heuristics instead of signatures to identify any form of misuse that deviates from regular system operation. They also conducted various experiments to compare their results with the various forms of Incremental support vector machine. They also have proposed an optimized intrusion detection system using soft computing mechanism and Principle Component Analysis to transform the input sample into a new feature space. While the genetic algorithm as used for optimum principle components the Support Vector Machines was used as a classifier. The authors used the Knowledge discovery in databases Cup dataset for experimenting with the proposed system. Their approach of Principle Component Analysis, genetic algorithm and support vector machine had a detection accuracy of 99.6 percent when compared to a method of Principle Component Analysis and support vector machine which had a detection accuracy of 97.58 percent.

Yuyang Zhou et.al. [10] have proposed a new intrusion detection system based on feature selection and ensemble learning approaches. Ensemble based hybrid intrusion detection system is a novel method of modeling and implementing intrusion detection system is based on combining one or more machine learning algorithms. The ensemble was done to take advantage of the efficiency in each algorithm of the ensemble to build a competent classifier. This approach is highly beneficial where the problem can be divided into sub problems and solution to each such sub problem can be solved by the individual algorithm of the ensemble. The authors proposed a hybrid distributed intrusion detection system to combat the latest intrusions. The authors used two Adaboost based intrusion detection algorithms. While the researchers used the tradition Adaboost with decision stumps as weak classifiers in the first algorithm, online Adaboost with online Gaussian mixture models as weak classifiers were used in the second. A distributed framework approach where the local parameterized online Adaboost model constructed in each host is combined using the particle swarm optimization and support vector machines to produce a global model in each node which is responsible for detecting intrusions was also suggested by the authors. The results indicated that it outperformed other intrusion detection system in terms of false positives and detection. The authors suggested an approach which is a feature representation method known as Cluster Centre and Nearest Neighbour. In this approach two distances are measured and summed with the first based on the distance between each data sample and its cluster centre and the second between the data and its nearest neighbour in the same cluster. The outcome of the previous step which is a one-dimensional distance based feature, was used to represent an input data sample for intrusion detection to be done by a k-nearest neighbour classifier. The feature selection strategy which can be used as a preprocessing phase can reduce computational complexity aims to remove unnecessary features while maintaining or even improving the intrusion detection system's performance. Abdullah also proposed a framework for intrusion detection utilizing characteristics from the NSL-Knowledge discovery database dataset which is related to partitioning the incoming dataset into sub-sets then integrating with the information gain filter. Gaikwad and Thool developed a light weight intrusion detection system which removed redundant data identified relevant features and accurately identified intrusions. It employed a neural ensemble decision tree to detect the network intrusions. Several experiments were carried out using Knowledge discovery in databases Cup 1999 data set and found its performance both to be better than or similar to other classifiers such as K nearest neighbor and support vector machine in terms of accuracy, detection rate and false alarms.

Jiyuan Cui et.al. [11] have proposed a Gaussian mixture model. In this model the issues of data unbalance and a lack of uncommon attack samples can be successfully addressed. First the trained model detection rate for a few attack classes is low because of dimensional dataset which reduces overall recognition accuracy. Second the vast size and data unbalance affects the performance of intrusion detection classifier. These classifier are now facing issues in improving minority class detection accuracy, finding unknown threats and decreasing false alarm rates. The authors used Principal Component Analysis and Fisher's Discriminant Ratio for feature selection and noise removal. The authors used Probabilistic Self Organizing Map for modeling the feature space and for differentiating between anomalous and normal network connections. In order to acquire a more detailed representation of the data an extraction of features module based on stacked auto encoders is presented. Experiments were conducted using NSL-KDD data set and also compare the performance with other intrusion detection techniques. The ultimate objective in the development and implementation of automatic intrusion detection system is to accomplish the best levels of accuracy in detection and reduction in false positives. The auto encoder is made up of a three layer network. The feature extraction function, especially for minority class data, cannot match the requirements when the data dimension is high. As a result this research develops a sparse auto encoder based feature extraction module that reduces the dimensionality of data features and exploits deep representation. After the auto encoder has been trained the hidden layer's output features are used as the input for the next auto encoder. This purpose obviously tends to adopt a hybrid approach for intrusion detection system design and implementation. A hybrid classifier for intrusion detection was chosen to combine several techniques so that the system accuracy can be appreciably superior. This module is used to help training in minimizing data unbalance and increasing the model's identification skills when executing multi classification jobs. The shallow learning model can't analyze the feature representation well because it can't handle with high dimensional complicated data. A fuzzy logic based methodology has been proposed to generate classification rules and natureinspired methodology such as Ant Colony Optimization has been further used to generate precise rules used for effective classification. The network connections were matched with these intrusion patterns to detect network intrusions The experimental findings reveal that this Gaussian mixture model enhances overall and uncommon attack detection accuracy and provides better intrusion detection outcomes. According the authors, the results produced by the proposed system was comparatively better in terms of predictive accuracy and convergence.

Mozamel M. Saeed et.al. [12] have proposed to increase the effectiveness of classifiers that were trained to recognize unknown attack signatures. The following goals which are addressed in this paper are used to identify and investigate the most often used classifiers in intrusion detection system implementation, to assess the performance of the individual classifiers on an individual basis and to create a hybrid classifier using the strengths of both

classifiers. The original KDD 1999 datasets and the network security laboratory-knowledge discovery databases were employed in the study. The proposed approaches were evaluated in virtualized networked settings and traffic workloads in this paper. Cycle numbers were detected using a Support Vector Machine, while period detection was completed using coefficients and signal shifts. Since no one has presented a hybrid strategy for finding anomalies predicted events that did not occur and unexpected events can be found using a hybrid approach at various sampling frequencies. The detection of anomaly was done using the weighted k-means clustering algorithm to detect novel intrusions by clustering the network connections data to collect the most of intrusions together in one or more cluster. Anomaly detection is the activity of detecting occurrences that occur unexpectedly, as well as objects that vary significantly from the usual. Data scientists use it to find anomalies in unlabeled data in a method known as unsupervised detection of anomaly. Data anomalies is related about unexpected events such as phishing, financial fraud, structural defects, textual flaws, system failures and system malfunctions. Because the purpose of this article is to deal with attacks and an anomaly was examined in which no vector was detected in the database as typical traffic. The feature selection approaches were discussed, as well as their classification benefits and consequences for network outlier detection databases. The type of data to be handled with and the relevant feature selection method to be used are the determinants. Some of the characteristics in the directed example were minimal such as protocol type while the remaining were numerical ratio scales. When discussing a situation from a theoretical standpoint degradation in classifier performance is not taken into account. On the other hand irrelevant and noisy variables have a significant impact on k-nearest neighbour and support vector machine models. Moreover few linear models with least angle regression are particularly prone to noisy data and related factors. For evaluation three distinct classification examples were used as well as up to five classifications for assessment in order to reduce the bias caused by specific classifiers. When using this method for feature extraction, a least absolute shrinkage and selection operator least angle regression based classifier was also included. The results obtained by this method exhibit a higher detection rate and a lower false positive rate when compared to other neural network. They have utilized the KDD 99 data set for the evaluation purpose and found that their framework has produced better accuracy and lesser false positive.

3. Material vs Method

Anomaly based network intrusion detection in networks looks for patterns in network data traffic which show non-conformity when compared to normal network traffic. Network anomalies are further classified in to two types, namely (a) performance associated anomaly and (b) security associated anomaly. Security associated anomaly is further classified into (i) point, (ii) contextual and (iii) collective anomaly.

3.1. Anomaly Based Network Intrusion Detection System

A plethora of network security devices such as firewall, IDS, Data Leak Prevention System (DLP) and content filtering systems such as anti-spam, anti-virus are available. Due to the ubiquitous nature of the Internet, network based attacks (DNS spoofing, port scanning, ping of death, etc.) and intrusion is a very common menace.

The present day enterprise networks are posed with intrusions or attacks that are polymorphic and continuously evolving. These intrusions and attacks demand a specific device that is exclusively meant for the surveillance of the network in real time, the anomaly based network intrusion detection system is such a device, which can be an essential equipment of the enterprise security strategy and a handy tool for network security administrators and team members as well.

3.2 Prototype of A Generic Anamoly-Based Network Intrusion Detection System

The security based research community and commercial organizations have proposed and developed many NIDS. While the development of a prototype for an effective ABNIDS is still evolving, a prototype of a generic ABNIDS has been presented in the Figure2.

A.   Detector: Being the most sensitive part of IDS, it is used to sense the non-confirmed network flow. An algorithm to detect abnormality is implemented as a misuse detector or as an anomaly detector.

B.   Reference Information: This is a repository of known attack signature or patterns of normalcy. This information base should be efficiently organized in such a way that it can easily be updated and swiftly referred to.

C.   Configuration Information: The information contained in this database is crucial and is used to configure and fine-tune the operation of the detector. This information gives directions to the detector such as sensing audit data from the sensor and deciding on the type of actions to be carried out after detecting an anomaly, etc.

D.   Alarm Generator: This module accepts the output generated by the detector. The output of this module is either an active response to make a immediate corrective action in the monitored environment or an alert due to an suspicious event to the security personnel of the monitored environment. The alert is in the form of an email, a pop-up in the console or an audible signal.

E.   Security Authority: On the reception of alert or alarm, the security personnel take response action based on the severity of the nonconformance. The existing reference information is updated as and when new intrusion patterns are evident.

Figure2: Architecture of a generic Network Intrusion Detection System (NIDS)

F.   Sensor: This block monitors each packet of a network flow that enters and exits the network and is implemented to operate either on online or offline mode.

G.   Audit data storage and pre-processing: IDS store audit data on a permanent or temporary basis for future reference during processing. In order to conserve the storage space and speed up the detection process, the dimensionality of the data is reduced by pre-processing.

H.   Intermediate repository: This space is used by the detector engine to store and retrieve intermediate data and incomplete signatures and patterns.

Passive response (Security officer response)
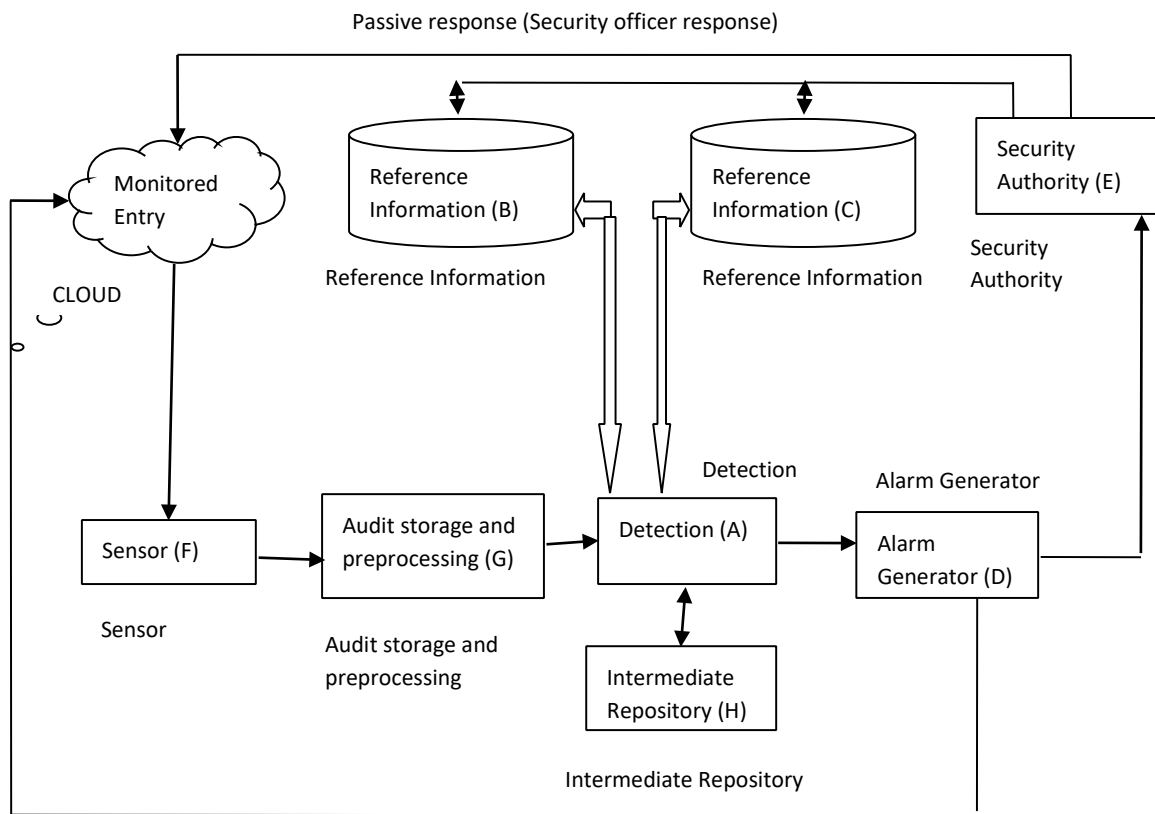
Active response

3.3 Design Of Hybrid Automatic Intrusion Detection System

The following are some of the major steps involved in the implementation of the proposed SDAC are:

☐ Preprocess the training datasets

☐ Select optimal features using the Modified sequential Floating Forward Selection (MFFS).

☐ Modify the supervised Support Vector Machine (SVM) learning algorithm

☐ Modify the unsupervised Ant Colony Clustering (ACC) algorithm Generate

☐ a hybrid NIDS by combining SVM and ACC

Most of the existing single and hybrid classifiers rarely meet the ever-growing, fast and hostile networks. Therefore, it is important to hybridize machine learning techniques are applied to build network intrusion detection system models to provide security to enterprise networks. The proposed methodology leverages the advantages of support vector machine and Ant Colony algorithm to generate an adaptable model which is capable of dynamically updating knowledge whenever new information is made available. This hybridized approach is known as the SVM based Dynamic Ant Clustering (SDAC). The classical SVM is modified to make it capable of learning new information online. The modified SVM is known as Online SVM (OSVM). The new information to be learnt is provided by the modified Dynamic Ant Colony Clustering (DAC) algorithm. These two algorithms work in tandem to generate a model to detect intrusions.

A record in the dataset is attributed with several features. It is represented as a data point for SVM during the training phase for classification purpose. In case of ant colony clustering algorithm, the network connections are represented as objects. Clustering of objects by the ants

is based on the swarm similarity of the neighbour. During the training phase the traditional support vector machine is generated using complete training dataset which is a time consuming process that makes it unsuitable for online implementations. SVM offers higher accuracy even when irrelevant data points except support vectors are removed from the training dataset. The proposed Online SVM (OSVM) is iteratively trained with a randomly selected data points from the training dataset until the required level of detection accuracy is attained. Figure 3 represents the schematic view of the online SVM. It consists of classifier C which is trained by the selected dataset K. A selector S iteratively selects new data points from T which is the entire training dataset for the consecutive learning process.
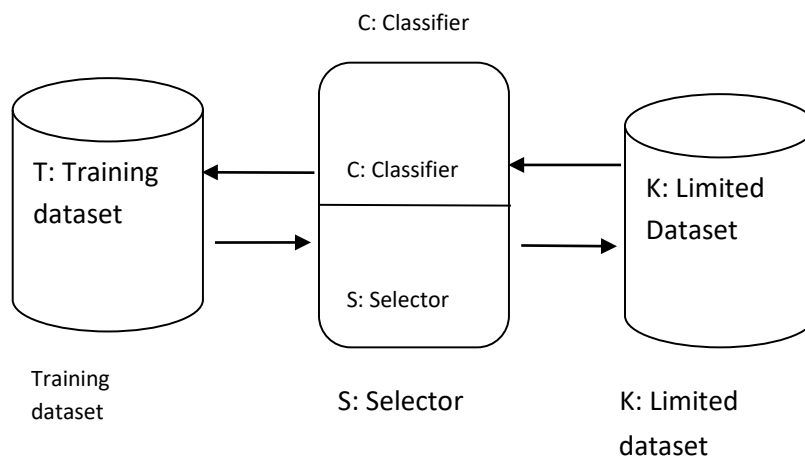
Figure3: schematic view of online SVM

The selection of data points from the training dataset is highly influenced by the operation of the modified ant colony clustering algorithm known as the Dynamic Ant Colony Clustering (DAC). This algorithm receives the support vectors as input from the OSVM in order to cluster the objects in the search space. The clustered objects are further given as input to the OSVM for the next iteration of the learning process. The detection process is a hybrid approach by combining OSVM and DAC.. The OSVM and DAC work in tandem to classify the audit data. The DAC further classifies the attack class to particular type of the attack. The classification of the audit record into either one of the five classes is the output.

4. Results
A review of the best known IDS from literature has helped us identify the high priority issues that are to be addressed. Proactive and accurate detection of intrusion in real time enterprise computer network continues to be a big challenge for automatic IDS. The operation and uptime of the network is affected when there is an improper operation of the IDS, when certain attacks go undetected. Such security incidents results in heavy losses both to the enterprises and to the nation at large. The performance of the IDS has not been effective due to ambiguity that prevails in detecting anomalous network traffic. It is very difficult to predict the difference or to clearly identify the difference between normal and anomalous network traffic. The most important

show stoppers in the performance of automatic IDS are as follows: i Classification of the mistrustful packets

Classification refers to the detection of intrusive network traffic. Network traffic is bursty and most times, the hostile packets are camouflaged with the benign packets.

ii Ambiguity Management

Due to a certain degree of vagueness that exists in the periphery between normal and anomalous network traffic, it is very difficult to classify the network packets in a reliable manner. Therefore, optimally classifying intrusions in a network flow continues to be a challenging task.

iii Robustness of Inference Engine

An inference engine is to be trained with precise and latest knowledge in order to handle and classify the audit data in a robust manner in high speed production networks.

Intrusion Detection (ID) is a continuous process involved in detecting inapt, wrong or anomalous action attempted by intruders or legitimate users of the ICT facility. An Intrusion Detection System (IDS) is a software tool installed in a dedicated, special purpose hardware device used to monitor the network or system activity under vigil and subsequently to generate reports to a management station or console.
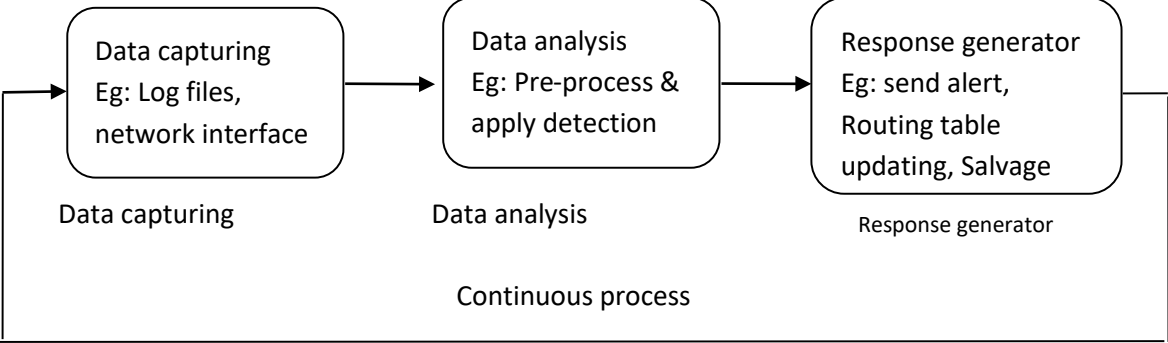
Figure 4: Three essential steps of Intrusion Detection

The major challenge of ID is its size and streaming nature of the audit data. This requires that the ID technique is computationally efficient in processing voluminous streaming data in online mode. This situation at time also leads to generation of considerable number false alarms. Machine learning techniques have proved their strength in key areas of applications like fraud detection, prediction of equipment failures pattern and image detection, email spam filtering and etc. With the availability of high-performance computers augmented with huge storage capacity, an ensemble of machine learning technique and swarm intelligence used to build a efficient hybrid IDS in this thesis. Though machine learning techniques have high performance testimonials, they need a heavy cognitive load. This issue can be resolved by adopting one of the dimensionality reduction algorithms to precisely reduce the vastness of the data used in the training process. It is believed that the generation of precise data set and fine tuning of the performance of the inference engine or the classification rules generated would help in meeting the challenges identified in ID.

5. Discussion and Conclusions

A review of the best known IDS from literature has helped us identify the high priority issues that are to be addressed. Proactive and accurate detection of intrusion in real time enterprise computer network continues to be a big challenge for automatic IDS. The operation and uptime of the network is affected when there is an improper operation of the IDS, when certain attacks go undetected. Such security incidents results in heavy losses both to the enterprises and to the nation at large. The performance of the IDS has not been effective due to ambiguity that prevails in detecting anomalous network traffic. It is very difficult to predict the difference or to clearly identify the difference between normal and anomalous network traffic. The most important show stoppers in the performance of automatic IDS are as follows: Classification of the mistrustful packets

Classification refers to the detection of intrusive network traffic. Network traffic is bursty and most times, the hostile packets are camouflaged with the benign packets.

Ambiguity Management

Due to a certain degree of vagueness that exists in the periphery between normal and anomalous network traffic, it is very difficult to classify the network packets in a reliable manner. Therefore, optimally classifying intrusions in a network flow continues to be a challenging task.

Robustness of Inference Engine

An inference engine is to be trained with precise and latest knowledge in order to handle and classify the audit data in a robust manner in high speed production networks.

This section discusses the proposed wrapper-based approach namely the Modified Forward Floating Selection (MFFS) and multiclass Support Vector Machine (SVM) to generate an optimal set of features from the NSL KDD dataset for effective network intrusion detection. The wrapper method outperforms the filter method. The proposed MFFS feature selection method is a modified version of the renowned feature selection algorithm Sequential Forward Feature Selection (SFFS), which is one among the best feature selection algorithms and effective in certain problems. It has also given better results when compared to the other sequential approaches. Multiclass SVM is a Machine Learning (ML) algorithm, which is known for its effectiveness in classification. The efficiency of the chosen feature subset is evaluated using decision tree classifiers such as C4.5 classification algorithm, Random Forest and Naive Bayes Tree. The precision, detection rate and false positive rate was used to analyze the prediction quality of the suggested approach. The Network Security Laboratory Knowledge Discovery in Data Bases dataset used by the research community in the testing and training phases of IDS models. It is evident from the results that the optimal feature set shows a considerable improvement in the detecting accuracy and minimizing training and testing time. The various steps of the proposed feature selection methodology are such as preprocessing, normalization and feature selection.

5.1 Preprocessing of the dataset

Pre-processing of dataset is an essential step in both feature selection and classification process. In the NIDS domain, pre-processing of the dataset converts the network traffic in to observations and each such observation corresponds to a feature vector, which is classified as normal or anomalous. Most classification algorithms are capable of handling only numeric values. Therefore, pre-processing the dataset to contain values that could be easily handled by the learners and classifiers is very important.

5.2 Feature normalization

The Network security laboratory knowledge discovery databases dataset contains 41 features which includes 7 discrete and 34 continuous attributes with a wide assorted range of values. This is an extra pre-processing step, which involves data transformation known as normalization. The attributes with high range values influence the low range value during the classification stage of the IDS model. The 34 continuous attributes hold values ranging from 0 to 6291668.

5.3 Modified Forward Floating Selection (MFFS)

A wrapper technique has been developed to choose the optimal features from the audit dataset. This a modular approach and it consists of three modules:

1. A search Function (Exponential, Sequential, Randomized – Determines the subset of features) 2. Evaluation Function (Objective – Maximize detection accuracy)

3. Predictor Function (A black box – any classification method)

The Figure 5 illustrates various processes involved in the proposed MFFS wrapper based feature selection approach
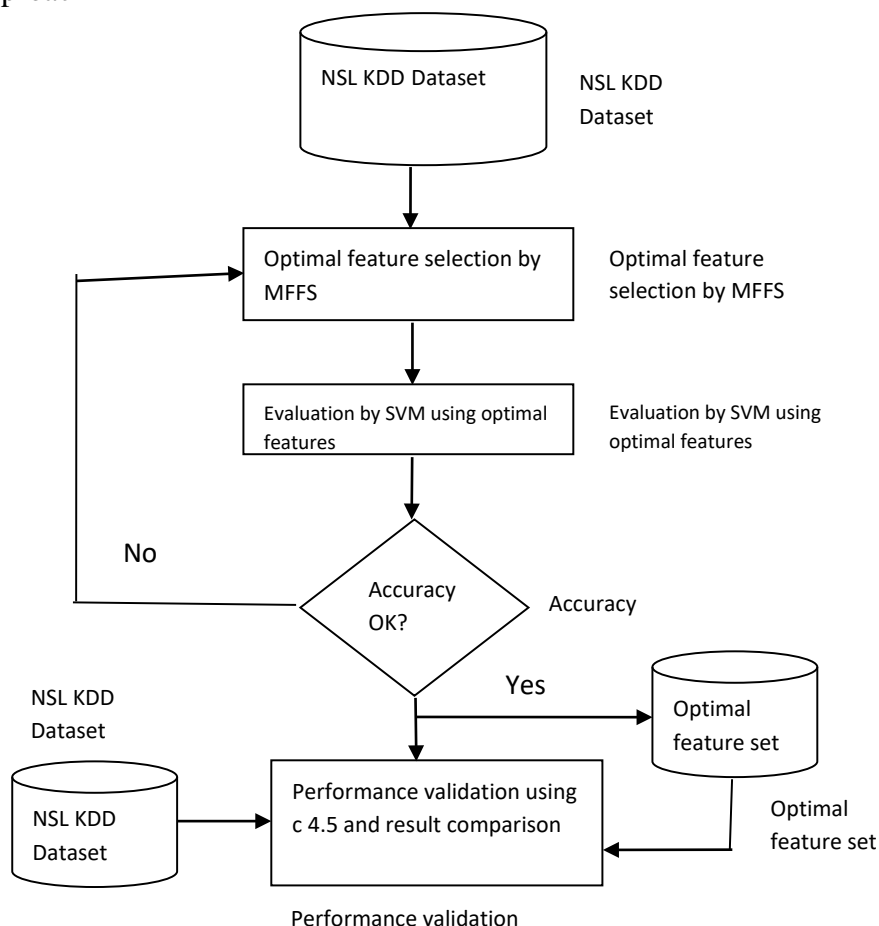
Figure 5 Steps involved in the proposed MFFS

Many attribute selection algorithms have been proposed in the literature survey by the research community. A search process is used to find the best feature selection in which f is an optimal set of features selected from large data set A, where C is a criterion function - detection rate is used to evaluate the selected sub set. The proposed feature selection algorithm, namely the

Modified Forward Floating Selection (MFFS) is an enhanced version of the flagship Sequential Forward Floating Search (SFFS) algorithm.

6. Acknowledgements

Contributions of the research work are as follows:

Novel and improved method known as MFFS for selection of optimal features from the audit dataset is implemented.

Hybridization of modified Ant Colony Clustering algorithm and Support Vector Machine namely SDAC is done to optimally detect intrusions in networks is implemented.

Hybridization of Enhanced Ant Colony Optimization algorithm and Fuzzy Logic namely FAS to detect intrusions in networks by adversaries is implemented.

Validation of MFFS, SDAC and FAS is done by conducting various experiments with NSL KDD and real time audit dataset.

To highlight, FAS proved to outperform other intrusion detection system with an increase in detection accuracy of 99.42% and a reduced false positive rate of 0.58%.

7. References

[1]   Achmad Akbar Megantara and Tohari Ahmad, "A hybrid machine learning method for increasing the performance of network intrusion detection systems", Journal of Big data-Springer, 8, Article number: 142 (2021)

[2]   Merve Ozkan-Okay, Omer Aslan, Recep Eryigit and Refik Sameta, "SABADT: Hybrid Intrusion Detection Approach for Cyber Attacks Identification in WLAN," IEEE Access 9, 157639-157653 Nov 2021.

[3]   Mahmoud Said ElSayed, Nhien-An Le-Khac, Marwan Ali Albahar and Anca Jurcut, "A novel hybrid model for intrusion detection systems in SDNs based on CNN and a new regularization technique", Journal of Network and Computer Applications-Elsevier Volume 191, 1 October 2021, 103160.

[4]   Ahmed I. Saleh, Fatma M. Talaat and Labib M. Labib, "A hybrid intrusion detection system (HIDS) based on prioritized k-nearest neighbors and optimized SVM classifiers," Artificial Intelligence Review volume 51, pages403–443 (2019).

[5]   Mokhtar Mohammadi a and Tarik A. Rashid, "A comprehensive survey and taxonomy of the SVM-based intrusion detection systems", Journal of Network and Computer ApplicationsElsevier Volume 178, 15 March 2021, 102983.

[6]   Dhruba Jyoti Kalita and Shailendra Singh, "SVM Hyper-parameters optimization using quantized multi-PSO in dynamic environment" Springer, Soft Computing volume 24, pages 1225–1241 (2020).

[7]   Ansam Khraisat, Iqbal Gondal, Peter Vamplew and Joarder Kamruzzaman," Survey of intrusion detection systems: techniques, datasets and challenges" Springer Open Cyber security volume 2, Article number: 20 (2019).

[8]   Earum Mushtaq, Aneela Zameer, Muhammad Umer, Asima Akber Abbasi," A two-stage intrusion detection system with auto-encoder and LSTMs" Applied Soft Computing-Elsevier Volume 121, May 2022, 108768.

[9]   M. R. Gauthama Raman, Nivethitha Somu and Sahruday Jagarapu," An efficient intrusion detection technique based on support vector machine and improved binary gravitational search algorithm" Springer Artificial Intelligence Review volume 53, pages3255–3286 (2020).

[10]   Zhou, Guang Cheng, Shanqing Jiang and Mian Dai," Building an efficient intrusion detection system based on feature selection and ensemble classifier" Elsevier Computer Networks Volume 174, 19 June 2020, 107247.

[11]   Jiyuan Cui, Liansong Zong, Jianhua Xie & Mingwei Tang. "A novel multi-module integrated intrusion detection system for high-dimensional imbalanced data" Springer Applied Intelligence April 2022.

[12]   Mozamel M. Saeed, "A real-time adaptive network intrusion detection for streaming data: a hybrid approach" Neural Computing and Applications volume 34 pages 6227–6240 (2022)

[13]   Tavallaee M, Bagheri E, Lu W, Ghorbani AA. A detailed analysis of the KDD CUP 99 data set in Computational Intelligence for Security and Defense Applications. In: Computational Intelligence for Security and Defense Applications CISDA, pp. 1–6. 2009. [14] Amiri F, Rezaei Yousefi M, Lucas C, Shakery A, Yazdani N. Mutual information-based feature selection for intrusion detection systems. Journal of Network and Computer Applications, 2011; 34(4):1184–99.

[15]   Mohammed MN, Ahmed MM. Data preparation and reduction technique in intrusion detection systems: ANOVA-PCA, International Journal of Computer Science and Security (IJCSS) 2019; 13(5):167–82.

[16]   Almasoudy FH, Al-Yaseen WL, Idrees AK. Differential evolution wrapper feature selection for intrusion detection system. Procedia Computer Science. 2020; 167(2019):1230–9.

[17]   Zhou Y, Cheng G, Jiang S, Dai M. Building an efficient intrusion detection system based on feature selection and ensemble classifier. Computer Networks. 2020; 174:107247. [18] Aljawarneh S, Aldwairi M, Yassein MB. Anomaly-based intrusion detection system through feature selection analysis and building hybrid efficient model. Journal of Computational Science, 2018;25:152–60.

[19]   Nkiama H, Zainudeen S, Saidu M. A subset feature elimination mechanism for intrusion detection system, International Journal of Advanced Computer Science and Applications 2016; 7(4):148–57.

[20]   Iman AN, Ahmad T. Data reduction for optimizing feature selection in modeling intrusion detection system. International Journal of Intelligent Engineering and Systems 2020; 13(6):199–207.

Sustainable Production Approach: Evaluation of Leather Wastes in Woven Surfaces

Nilüfer Bayraktar[1], Meruyert Kaygusuz[2,*], Şebnem Temir Gökçeli[3]

Abstract: As in all areas of production today, sustainable development guides the design field and gives direction to designers. The concept of design is evaluated not only for its aesthetic and technical aspects, but also for its sustainability. Leather, which is one of the indispensable raw materials of many industrial areas, is a sustainable material as it is organic, does not harm human health and long-lasting. However, various wastes can be generated at the end of leather items production processes which create a pollution load on the environment and ecosystem. For this reason, it is thought that the reuse of "waste materials" such as leather pieces from garment enterprises in different designs will both contribute to the solution of the pollution problem and be beneficial in the development of value-added products with material savings. In our study, small pieces of unused leather remaining from the garment production enterprises were cut in certain sizes and the surface was created by weaving with the classical Turkish knot technique (gördes knot) and rug technique on the carpet loom, and two products, women's shoes and handbag, were designed by using surfaces created with a sustainable approach.

Keywords: Sustainability, Ecology, Leather wastes, Weaving, Design

Sürdürülebilir Üretim Anlayışı: Deri Atıklarının Dokuma Yüzeylerinde Değerlendirilmesi

Özet: Günümüzde sürdürülebilir kalkınma; üretimin her alanında olduğu gibi tasarım alanına da rehberlik etmekte ve tasarımcıya yön vermektedir. Tasarım kavramı yalnızca estetik ve teknik yönü ile değil, aynı zamanda sürdürülebilir olması açısından da değerlendirilmektedir. Birçok endüstriyel alanın vazgeçilmez hammaddelerinden biri olan deri, organik bir malzeme olması, insan sağlığına zarar vermemesi ve uzun ömürlü olması ile sürdürülebilir bir malzemedir. Ancak deri ürünleri üretim süreçleri sonunda ortaya çıkan çeşitli atıklar, çevreye ve ekosisteme kirlilik yükü oluşturmaktadır. Bu nedenle konfeksiyon işletmelerinden çıkan deri parçaları gibi "atık malzemelerin" farklı tasarımlarda yeniden kullanılmasının, hem kirlilik sorunun çözümüne katkı sağlayacağı, hem de malzeme tasarrufu ile katma değerli ürünlerin geliştirilmesinde de faydalı olacağı düşünülmektedir. Çalışmamızda konfeksiyon üretim atölyelerinden kalan kullanım dışı küçük deri parçaları belli ölçülerde kesilerek halı tezgâhında klasik Türk dügüm tekniği (gördes düğümü) ve kilim tekniğiyle dokunarak yüzey oluşturulmuş

[1]Uşak Üniversitesi, Lisansüstü Enstitüsü, Tasarım Çalışmaları ABD, Uşak, Türkiye
[2]Isparta Uygulamalı Bilimler Üniversitesi, Teknik Bilimler Meslek Yüksekokulu, Tekstil, Giyim, Ayakkabı ve Deri Bölümü, Isparta, Türkiye
[3]Uşak Üniversitesi, Güzel Sanatlar Fakültesi, Moda Tasarımı Bölümü, Uşak, Türkiye
*meruyert_k@hotmail.com

ve sürdürülebilir bir yaklaşımla oluşturulan yüzeyler kullanılarak kadın ayakkabı ve el çantası olmak üzere iki adet ürün tasarlanmıştır.

Anahtar Kelimeler: Sürdürülebilirlik, Ekoloji, Deri atıkları, Dokuma, Tasarım.

1. Giriş

Doğanın sınırlı kaynaklarına rağmen; sanayileşme, nüfus artışı, teknolojik gelişmeler, küreselleşme ve çeşitli üretim yaklaşımları sonucunda ortaya çıkan hızlı tüketim kültürü ekosistem üzerinde olumsuz etkilere neden olmaktadır. Bu gelişmelerin sonucunda tüm dünyanın ana gündem maddeleri arasında "sürdürülebilir yaklaşımlar" yer almaktadır. Sürdürülebilirlik, yaşam kalitesini düşürmeden tüketim toplumu olmaktan sıyrılarak, çevre, toplumsal sorumluluk ve ekonomik çözümler ile ilgili değişimleri desteklemektedir (Gürcüm ve Tanyer, 2021).

Günümüz tüketicisinin sürdürülebilir farkındalığı gün geçtikçe artmakta; satın alacakları ürünün yalnızca tasarımını değil aynı zamanda var oluş hikayesini de öğrenmek istemektedirler. Bu nedenle üreticilerin, üretimin aşamasında ürünlerinin sürdürülebilirliği konusunda daha hassas olmaları gerekmektedir. Son zamanlarda doğal kaynaklar konusunda yapılan çalışmalar daha az su ve enerji tüketilerek üretilen çevre dostu ürünleri gündeme getirmiştir.

Ancak deri sektörü, üretim prosesi gereği su ayak izi ve karbon ayak izi değerleri benzer sektörlere kıyasla yüksek olduğu belirtilmektedir (Düzgün, 2020). Ayrıca üretim esnasında kullanılan kimyasal maddeler, makine parkuru kullanımından kaynaklı enerji tüketimi ve lojistik unsurlar nedeni ile çevresel etkileri oldukça yüksektir. Son yıllarda deri üretiminde kullanılan kimyasalların çevreye verdiği zararın önüne geçilebilmek için ekolojik deri üretimine ağırlık verilmeye başlamıştır.

Deri doğanın bize sunduğu en şık ve en kullanışlı materyallerinden biridir. Doğal bir biyo kumaş özelliğine sahip olup, deriden yapılan ürünler, çevresel etkilerden korurken (kar, yağmur, rüzgâr vs.) derinin gözenekleri hava geçirgenliği sağlar. Deri, yumuşak, esnek, dayanıklı ve kolay deforme olmayan, yüzeyindeki gözenekleri sayesinde hava ve su buharı geçirgenliği veya "nefes alma" özelliğine sahip, her türlü ürün tasarımına elverişli bir materyaldir. Kullanıldığı ürüne asalet, şıklık ve lüks bir görünüm verir. Gerçek deri doğal bir malzeme olduğu için doğada çözünür/bozunur ve bu açıdan da çevre dostudur. Derinin yapısal özellikleri onu tasarım açısından çekici hale getirmekte ve başta hazır giyim olmak üzere ayakkabı, çanta ve aksesuar, iç mekân dekorları, mobilya vb. alanlarda tercih edilmesine neden olmaktadır (Kaygusuz, 2020).

Pek çok endüstri alanın vazgeçilmez hammaddelerinden biri olan derinin, organik bir malzeme olup, insan sağlığına zarar vermemesi ve kullanım ömrünün uzun olması onun sürdürülebilir olarak nitelendirilmesini sağlamaktadır. Ancak deri üretim süreçleri sonunda ortaya çıkan atıklar, ekosistem içinde güvenli bir şekilde depolanamayacağı için genellikle gömülmekte veya yakılmaktadır (Chen ve Chen, 2020). Böyle bir durum sadece deri malzeme israfı olmayıp, yaşanılan çevrenin kirlenmesine de neden olmaktadır.

Yeşil üretim teknolojilerini teşvik eden geleneksel (Azalt, Yeniden Kullan ve Geri Dönüştür) 3R (Reduce, Reuse and Recycle) konsepti, sürdürülebilir üretimin temelini oluşturan daha yeni 6R (Reduce, Reuse, Recover, Redesign, Remanufacture, Recycle) konsepti (Azalt, Yeniden Kullan, Geri Kazan, Yeniden Tasarla, Yeniden Üret, Geri Dönüştür) tarafından aşılmıştır. Moda

üretiminde sürdürülebilirliği artırmak için geri dönüşüm kolayca uygulanabilir. Geri dönüşüm, diğer bir deyişle çöp olarak atılacak olan malzemelerin toplanıp işlenerek yeni ürünlere dönüştürülmesi sürecidir. Moda söz konusu olduğunda, depolanan kullanılmamış kumaşlar, deri ve diğer malzemeler, bu metodoloji ile yeni ürünler elde edilerek geri kazanılabilen atıklardır (Cimatti et al., 2017).

Deri artıkları, yaratıcı tasarımlarla farklı ürünlerde süslemeler şeklinde veya temel ögeleri yapmak için kullanılabilir (Dhingra ve Muthusamy, 2017). Özellikle sürdürülebilir üretimin önem kazandığı son yıllarda, tasarımcılar ve firmalar çevreye duyarlı ürünlere yönelmişlerdir. Sürdürülebilir tasarım kavramının ortaya çıkmasından beri tasarımcılar, artık ürünleri tek bir estetik yönden değil, kaynak ve çevresel faktörleri de entegre ederek sürdürülebilir kalkınmaya rehberlik etme perspektifinden ürün sürdürülebilirliğine odaklanmaktadırlar. Böylece, çok fazla kirliliğin olduğu günümüzde, mevcut "atık materyalin" yeniden tasarlanıp tekrar kullanılmasının sadece kirlilik sorununu çözmekte kalmayıp, aynı zamanda pratik ve uygulanabilir bir yol olan malzeme tasarrufu amacına da ulaşılabileceği düşünülmektedir (Chen ve Chen, 2020).

Dünya genelinde sürdürülebilirlik pek çok tasarımcı markaya ilham kaynağı olmuş ve sosyal sorumluluk bilinci ile çalışmalarına yön vermişlerdir. Örneğin, 2017 yılında lüks marka Burberry, deri parçalarını çanta ve diğer aksesuarlara dönüştürmek için lüks marka Elvis & Kresse ile ortaklık kurmuştur. Aynısı lüks marka Hermes ve diğer şirketler de gerçekleştirmişler (Anonim, 2020). Bunun yanı sıra, Yeni Zelanda'da bulunan 'Eco-Demo' Deri Yüzey Üretim Fabrikası, geri dönüşümlü deri sınıfında, kullanılan deri kemerlerden kapılar, yatak başlıkları ve benzeri mobilyalar tasarlamaktadır. Ünlü ayakkabı tasarımcısı Andrea Verdura ayakkabı üretiminden kalan derileri geri dönüştürülmüş materyaller tasarımlarında buluşturarak çevreci, dayanıklı ve şık ayakkabılar tasarlamaktadır. İngiliz ayakkabı şirketi "Terra Plana", çevresel açıdan sürdürülebilir geri dönüşüm malzemeler ve bitkisel tabaklanmış atık derilerden tasarlanmış ilginç ayakkabıları ile çevre dostu konseptine kendi benzersiz damgasını vurmaktadır (Gürler et al., 2017).

Bu çalışmada, deri konfeksiyon atölyelerinde kesimden kalan kullanım dışı küçük parçalar halı tezgâhında karışık teknikle dokunarak dokuma yüzeyi oluşturulmuş ve sürdürülebilir ürün odaklı yaklaşımla bu yüzeyleri kullanarak etnik tarzda ürün tasarımları yapılmıştır.

2. Malzeme ve Yöntem

Atık finisajlı ve süet deri parçalar deri konfeksiyon atölyelerinden temin edilmiştir. Daha sonra bu atık parçalar renklerine ve cinslerine göre ayrılmıştır. Halı tezgâhında deriyle bütünlük sağlaması amacı ile çözgü ipi olarak mumlu ip kullanılmıştır. Önceden belirlenen tasarıma göre halı ve kilim olmak üzere iki farklı teknik kullanılarak doku yüzeyi oluşturulmuştur. Kullanılacak renk ve cinslerine göre ayıklanmış deri parçaları belli bir en ve boy ölçüsünde ayarlanarak klasik halı tezgâhında dokuma yüzeyi Türk düğüm (Gördes düğümü) tekniği ile dokunmuştur. Çalışmada kullanılan malzemeler (mumlu ip ile atık deri parçaları) ve dokuma tezgâhı görselleri Şekil 1'de yer almaktadır.

**Şekil 1.** Kullanılan malzemeler ve dokuma tezgâhı (URL 1-3)

3. Deneysel Sonuçlar ve Tartışma

Dokuma

<u>Çözgü</u>: Halı tezgâhının alt ve üst leventlerinin arasına halı boyunca yatay olarak zemine dik ve birbirlerine paralel olarak çaprazlama belli bir sistemde geçirilen iplerdir (Şekil 2'de bordo iplik ile gösterilmektedir).

<u>Atkı</u>: İlme sıralarının arasına ve dokunacak halının enine paralel olarak elle geçirilen farklı türde ipliklerdir (Şekil 2'de mavi iplik ile gösterilmektedir).

<u>Türk Düğümü (Gördes Düğümü)</u>: Gördes düğümünde ilme iki çözgü telinin etrafından dolanarak çözgü tellerinin arasından çıkarılma yöntemi ile bağlanır ve kesilir (Şekil 2). Tarihte bilinen ilk düğümlü halı olan 'Pazırık Halısı' bu teknik ile dokunmuştur.
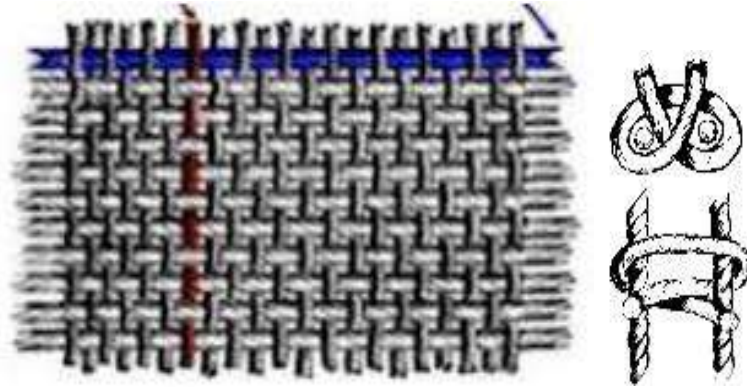
Şekil 2. Çözgü, atkı ve düğüm görselleri (URL 4, 5)

Halı dokuma tekniği

Dokuma için öncelikle mumlu ipler alt ve üst leventlerden geçirilerek çözgü oluşturulmuştur. Çözgü iplerinin üzerine tasarlanan desen çizilmiş ve hangi teknikle hangi bölgeler dokunacak tespit edilmiştir. Başlangıç dokuması olarak çözgüde mumlu ip kullanılmış ve atkı atılmıştır. Bu işlem beş sıra tekrar edilmiştir. Belli bir ölçüde hazırlanan ve renklerine göre ayrılan deri ve süet parçaları Türk düğümü (Gördes düğüm) tekniği ile dokunarak havlı olan halı yüzey dokuması oluşturulmuştur. Havlı dokumanın her sıra sonunda bir sıra mumlu ip ile atkı atılmıştır. Böylece dokuma yüzeyinin daha sıkı ve dik kalması sağlanmıştır.

Kilim dokuma tekniği

Kilim, yere yayılan havsız yaygıların tümüne verilen isimdir. Çözgü ve atkı ile dokunan iki iplikli dokumadır (Soysaldı, 1999). Bu çalışmada tasarlanan desenin kilim kısımlarında belli uzunlukta kesilen deri parçaları atkı olarak kullanılmıştır. Dokuma yüzeyi bezayağı tekniği ile atkının bir alttan bir üsten geçirilmesi ile oluşturulmuştur (Şekil 3).
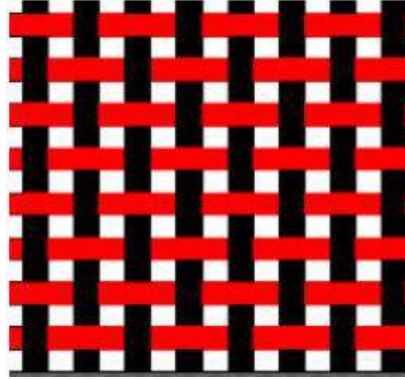
Şekil 3. Bezayağı tekniğinin uygulama görseli (URL-6)

Klasik Türk düğüm tekniği kullanarak atık deri parçaları ile dokunulan yüzey aşağıda verilen görselde sunulmaktadır (Şekil 4). Görselden de görüldüğü gibi, deri şeritleri dokumaya özgünlük katmış ve dokuma iplikleri ile renk uyumu sergilemiştir. Ayrıca deri parçalarının dokumada havlı bir şekilde kullanılması dokuma yüzeyine dolgunluk ve zengin bir görüntü sağlamıştır.
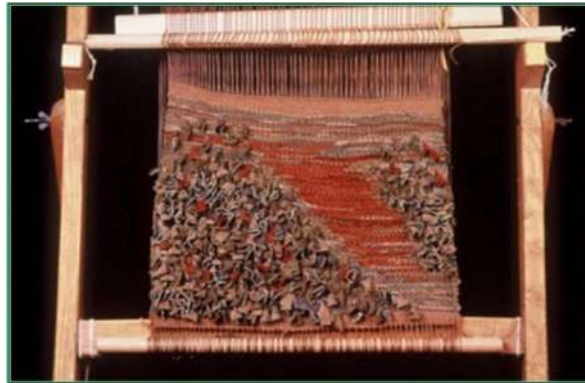
Şekil 4. Atık deri ile yapılan dokuma yüzeyinin halı tezgâhındaki görüntüsü

Atık deri parçaları ile elde edilen dokuma yüzeyinden 37 numara kadın topuklu ayakkabısı tasarlanmıştır (Şekil 5). Dijital ortamda tasarlanan ayakkabının prototipi yapılmıştır. Tasarlanan ayakkabı örneğinde, ayakkabının burun/uç kısmında dokuma yüzeyi kullanılmış, ayakkabının üst kısmı süet deriden tokalı kemer kombini ile tamamlanmıştır. Süet derinin rengi, dokuma yüzeyinde kullanılan deri renkleri ile uyum göstermesine dikkat edilerek kiremit renginde seçilmiştir. Topuk yüksekliği 9 cm olarak ayarlanmıştır.

Şekil 5. Dokuma yüzeyinden tasarlanan ayakkabı örneği

Atık deri parçaları ile elde edilen dokuma yüzeyinden diğer bir ürün olarak tasarlanan ayakkabı ile uyumlu kadın el çantası tasarlanmıştır (Şekil 6). Çanta 20 cm yüksekliğinde olup, genişliği 40 ve eni 15 cm'dir. Çantanın gövdesi atık derilerle karışık teknik kullanarak dokunmuş yüzeyi temel alarak tasarlanmıştır. Çanta sapları kilim tekniği ile dokunulmuş yüzeyden oluşturulmuştur. Etnik bir tarzın hâkim olduğu çantanın dijital ortamda prototipi hazırlanmıştır. Her kadının rahatça kullanılabileceği tasarımda seçilen toprak tonlarının sonbahar kış mevsimine uyumlu olacağı düşünülmektedir. Tasarlanan çanta aslında kot (jean), kadife veya başka kombinler ile her mevsimde kullanıma uygundur.

Şekil 6. Dokuma yüzeyinden tasarlanan çanta örneği

Atık deri parçaları kullanarak oluşturulan dokuma yüzeyler ile tasarlanan aksesuarların renk ve yapı açısından benzersiz ve ayrıcalıklı ürünler olduğu, bunları kullanacak her kadının şık ve özgün görünmelerine katkı sağlayacaktır. Araştırmanın sonuçlarına göre, yapılan tasarımların deri katı atıkların değerlendirilmesi açısından çevre dostu/ekolojik ürünler olmanın yanı sıra tarzı ile farklı bir cazibeye sahip oluğu, modaya katkı sağlayacağı öngörülmektedir. Ayrıca bu yöntemle yapılan ürünlerde geleneksel dokuma yöntemi geliştirilerek moda akımına etnik bir bakış açısı getireceği şüphesizdir. Geleneksel halı ve kilim tekniği kullanılarak sürdürülebilir bir yaklaşımla oluşturulan yüzeyde; atık deriler değerlendirilirken dokuma sanatına da farklı bir bakış açısı sağlanmıştır. Üstelik oluşturulan dokuma yüzeylerin, ev dekorasyonunda kullanılacak yastık, ranır (runner), farklı amaçlı dekoratif örtüler, lambader, paravan vb. ürünlerin yapımı için de uygulanabilir. Bu yöntemle tasarlanan ürünlerin özgün ve benzersiz olması nedeniyle tüketiciler için daha çekici olabileceği kanaatindeyiz.

4. Sonuçlar ve Öneriler

Değişen iklim ve çevre koşullarının yanı sıra deri üretiminde kullanılan su ve kimyasallar da çevreye ciddi şekilde zarar vermektedir. Git gide artan dünya nüfusu ile birlikte tüketim hızı da artmakta ve bu durum ekolojik dengeyi olumsuz etkilemektedir. Çevreye verilen zararları

önlemek ve gelecek nesillere daha yaşanılır bir dünya bırakmak, ancak üretim ve tüketim alanında sürdürülebilir bir yaklaşımla mümkündür. Bu bilinç son yıllarda birçok sektörde olduğu gibi deri sektöründe de önem kazanmış ve firmalar tasarımlarında bu konuyu dikkate almaya başlamışlardır. Bu çalışmada deri konfeksiyon atölyelerinden kalan kullanım dışı küçük deri parçalarından halı tezgâhında klasik halı ve kilim tekniğiyle dokuma yüzeyi oluşturulmuş ve sürdürülebilir bir yaklaşımla oluşturulan yüzeyler kullanılarak kadın ayakkabı ve el çantası olmak üzere iki adet ürün tasarlanmış ev dekorasyon alanında gerekli teknik yapı oluşturularak hazırlanan prototip tasarımlarda paravan, lambader vs. gibi uygulanabilirliği görülmüştür. Sürdürülebilir yaklaşımla atık deriler kullanılarak tasarlanan bu ürünlerle toplumun bu konuda bilincinin ve farkındalığının artırmasına katkı sağlamaya çalışılmıştır. Atık parçaların değerlendirilmesi uzun vadede sadece çevre açısından değil, doğal kaynakların kullanımı açısından da yarar sağlayacak, atık parçalardan üretilen katma değeri yüksek yeni ürünler ülke ekonomisine de katkı sağlayacaktır. Günümüzde atıklar toplumların üzerinde ekonomik ve sosyal açıdan yük oluşturmaktadır. Her ne kadar tekstil, deri, gıda vs. atıkları teknolojik olarak çözümlenmeye çalışılsa da sorun büyüklüğü karşısında yetersiz kalmaktadır. Benzer bir çalışma atık kot (jean) parçaları ile de düşünülmüş ve ön denemeleri oluşturulmaktadır. Her geçen gün biraz daha kirletilen dünyamızda sürdürülebilirlik gelecek nesillerin devamlılığı için kaçınılmazdır.

Kaynaklar

Anonim, (2020). "The State of Fashion", McKinsey & Company. https://www.mckinsey.com/~/media/McKinsey/Industries/Retail/Our%20Insights/State%20of%20fashion /2021/The-State-of-Fashion-2021-vF.pdf. (Erişim tarihi 10.03.2022)

Chen, A., Chen Y. (2020). Study on Redesign of Scrap in Leather Design. International Conference on Energy, Natural Resources and Electric Power IOP Conf. Series: Earth and Environmental Science 598, 012009, 1-4.

Cimatti, B., Campana, G., Carluccio, L. (2017). Eco Design and Sustainable Manufacturing in Fashion: a CaseStudy in the Luxury Personal Accessories Industry. Procedia Manufacturing 8, 393 – 400.

Dhingra, H., Muthusamy, A. (2017). Surface Design Techniques and Embellishments for Sustainable Leather Products. IULTCS XXXIV Congress, Chennai, India.

Düzgün Ç. (2020). "Sürdürülebilir Tasarım Malzemesi Olarak "Deri'. Lisansüstü Öğrencileri Sanat ve Tasarım Sempozyumu Bildiri Kitabı ve Sergi Kataloğu, İstanbul Aydın Üniversitesi Yayınları, İstanbul.

Gürcüm, B. H., Tanyer, S. (2021). "Moda Tasarımında Sürdürülebilirlik İle Yeniden Doğuş". İdil, 80, 549–562.

Gürler, D., Kılıç, E., Güllü, S. (2017). Sustainable Product Design and Examples of Leather Material Recycling, Annals of The University of Oradea: Fascicle of Textiles, Leatherwork, vol. XVIII, (2), 141-144.

Kaygusuz M., (2020). "Deri, Kürk ve Suni Deri". Tekstil Malzeme Bilgisi kitabında, Ed. Prof. Dr. H. B. Gürcüm, Atatürk Üniversitesi, Açık öğretim Fakültesi, Moda Tasarımı Programı öğrencileri için ders kitabı, Erzurum, Türkiye.

Soysaldı, A. (1999). "Türk Kilimlerinde Dokuma Teknikleri ve Boyama Özellikleri". Erdem, 30, 599-613.

Görsel kaynakları

URL-1. https://www.ayakkabimalzemesi.com/urun/sim-mumlu-ip-1-2-mm-500mt-leathercraft Erişim tarihi 12.03.2022

URL-2. https://www.sondakika.com/haber/haber-artik-deri-parcalarindan-canta-uretiyor-12921350/ Erişim tarihi 12.03.2022

URL-3. https://www.izatolye.com.tr/urun/hali-kilim-dokuma-tezgahi-80x120cm/ Erişim tarihi 12.03.2022

URL-4. https://asyamakine.com.tr/atki-temizleme-strecleme-makinasi.asp Erişim tarihi 12.03.2022

URL-5. https://www.eracarpets.com/yayinlar/hali-dokuyucusu/index.htm Erişim tarihi 12.03.2022

URL-6. https://tekstilsayfasi.blogspot.com/2013/01/dokuma-kumasta-orgu-cesitleri.html

A Probabilistic Approach to the Modelling of the Corrosive Wear Percentage of Bulkhead Panels for Bulk Ships

Špiro Ivošević [1*], Nataša Kovač[2],

Abstract: This paper gives an approach to the probabilistic approach to the corrosion percentage estimation model for transversal bulkhead plating, as a structural part of fuel oil tanks located in the double bottom of ageing bulk carriers. By using the huge thickness measurements data from regular Special Survey after 10, 15, 20 and 25 years of explanation, in this paper we analyse data of the percentage of diminution of as build thickness for transfers bulkhead plating's of fuel oil tanks on 25 ageing bulk carriers. The related best fitted linear two-parameter distribution model for the corrosion wastage is obtained as a function of the ship's age assuming that the coating life can be 15 years. Considering 25 ageing vessels, 71 fuel oil tanks hull structure thickness collected during 38 special ships surveys, a total of 660 measuring data expressed in percentage of steal diminution well considered. In developing a linear probabilistic model, two-parameter distributions were considered for two separate water-tight areas. In that way, the cumulative density function for the corrosion percentage involved in the mentioned linear model is considered here as a continuous random variable. The obtained statistical, numerical and graphical results show that the normal and logistic distribution would be appropriate for the probabilistic corrosion percentage estimation model for considered watertight bulkhead thickness plating of bulk carrier's fuel oil tanks.

Keywords: bulk carrier; fuel oil tanks; transverse bulkhead plates; corrosion; probabilistic corrosion rate estimation model;

1. Introduction

Even collision, grounding, and fire can cause catastrophic damage and total loss of vessels, in many published articles, authors identify corrosion, fatigue cracking and local dent as the most influenced mechanisms of age-related deterioration (Paik et al. 2006).
There is a lot of different definition of corrosion, but corrosion can be defined as the destructive attack on material by a reaction with its environment (Popolola et al. 2013; Melchers et al. 2004, 2005, and 2008). As a result of the corrosion process in different environments, the basic materials lose weight or thickness as well as mechanical properties of the structure (strength, ductility and impact strength) and change the chemical composition of the metal. The impact of corrosion depends on the industry, and the World Corrosion Organization (WCO) estimates that the annual cost of corrosion worldwide is around $US2.4 trillion (3% of the world's GDP) (Valasqueyz et al. 2014).
Considering up-to-date research, a lot of shipwrecks resulted in more than 2000 human casualties (Roberts and Marlow 2002; IMO 2007) and 47% of incidents involved ships aged over 25 years (INTERCARGO 2010).

[1] University of Montenegro, Faculty of Maritime Studies Kotor, Kotor, Montenegro
[2] University of Donja Gorica, Faculty of Applied Sciences, Mathematical Department, Podgorica, Montenegro
* Corresponding author: spiroi@ucg.ac.me

The ageing of vessels, environmental influences and regular ship operations are the dominant influence on ship exploitation. The corrosive damage of steel hull structures is influenced by numerous factors such as marine environment (submerged, atmospheric or closed), chemical characteristics of seawater, cargo, and air, as well as various operational factors (e.g., transport routes, maintenance systems, surface protection systems, the frequency of cleaning, sludge collection, water content, use of heaters and inert gas system in tankers, etc.). Different types of vessels, maintenance and operations together with the above-mentioned factors, can lead to the different forms of corrosion as they are uniform, intergranular, galvanic, crevice, pitting, hydrogen damage, stress-corrosion, corrosion fatigue, hydrogen-induced cracking, cavitation, erosion and fretting corrosion, (Chaturvedi 2009).

In previous research, a lot of authors were motivated to investigate corrosion degradation of some structural members such as transversal bulkhead of bulk carriers (Yamamoto et al. 1998) or deck plating of tankers (Guo et al. 2008; Garbatov et al. 2005; Jurišič et al. 2017), cargo holds and ballast tanks (Paik et al. 2004; Yamamoto et al. 1998; Norhazilan et al. 2007), or all structural members (Paik et al. 1998, 2003 and 2004).

Fuel tanks that store heavy fuel can be located in different internal ship's hull spaces. Topside, double bottom or deep tanks are often heated to the temperature of 60-70 ^{0}C. The heating affects the surface of tanks and steel plates of adjacent areas as they are water ballast tanks, cargo space, dry space, etc. Researching corrosion of fuel oil tanks of ageing bulk carriers, the authors of this article investigated inner bottom plating and longitudinal girder of fuel oil tanks (Ivošević et al. 2017, 2019, and 2020).

This paper is organized as follows. Section 2 considers the related database and probabilistic corrosion rate estimation model related to the ship hull structure. The third section gives results and four give concluding remarks.

2. Materials and Methodology

The purpose of this research work is to examine the behaviour corrosion process on different structural plates of fuel oil tanks of ageing bulk carriers. A large database has been provided by the Thickness measurement Reports which were collected through numerous standardized and very detailed measurements performed during the regular Special Survey, which was done after every 5 years of exploitation. In that sense, only bulk carriers' fuel tanks' structural plating time-dependent deteriorations caused by the general corrosion have been analysed.

The research in this paper is a continuation of previous research on fuel oil tanks which is dealing with inner bottom plating and longitudinal watertight girders (Bauk et al. 2011; Ivošević et al. 2017, 2019, and 2020). The transverse bulkheads of fuel oil tanks affected by general corrosion were the subject of this paper. Cracks, damages and other types of deformation which are not deal with the corrosion process are not considered in this research.

The corrosion process on the marine structure is an electrochemical process between the steel structure and the surrounding environment. The environment of fuel oil tanks from the outside should be seawater, cargo, ballast tanks or any other open or close space conditions, while from the inside is fuel oil. Due to the intensive corrosion process loss of thickness can be expressed in mm diminution or percentage of loss of as build thickness can be considered (Ivošević et al. 2017, 2019, and 2020). In this article percentage of diminution of original as build thickness is well considered.

2.1. Input data set brief description

In this article, only fuel tanks placed in double bottom areas were considered. Usually, depending on the length and projected design, these oil tanks are spatially positioned along the

main axis of the bulk carrier, but they can be placed perpendicularly from side to side of a vessel. A total of 25 ageing bulk carriers ranging from 5 to 25 years of age and corresponding fuel oil tanks were investigated. All bulk carriers were measured between 2005 and 2017, during the regular special surveys which were done after 5, 10, 15, 20 or 25 years of the exploitation life cycle. Some of the bulk carriers were monitored two or three times during the time of monitoring and a total of 38 different special surveys and 71 different fuel oil tanks were collected.

As a continuation of previous research into the ten structural areas of fuel tanks in this article were analysed only forward transversal bullheads were noted as areas A9 and A10 (Figure 1). As the fuel tanks are arranged in a row, each fuel tank has after and forward watertight bulkhead plates. As the bulkheads of adjacent fuel tanks are exposed to fuel on both sides, only the bulkheads separating the fuel and ballast tanks were considered. Since the areas of the partitions in the double-ducts are exposed to different influences from the upper and lower sides of the tank, these are the two areas taken into consideration. These are the upper and lower areas of the transverse bulkheads.

Legend:
A_1 – Bottom plate
A_2 – Inner bottom plate
A_3 – Inside girder (watertight), lower
A_4 – Inside girder (watertight), upper
A_5 – Side (watertight) girder, lower
A_6 – Side (watertight) girder, upper
A_7 – Floor after (watertight), lower
A_8 – Floor after (watertight), upper
A_9 – Floor fore (watertight), lower
A_{10} – Floor fore (watertight), upper
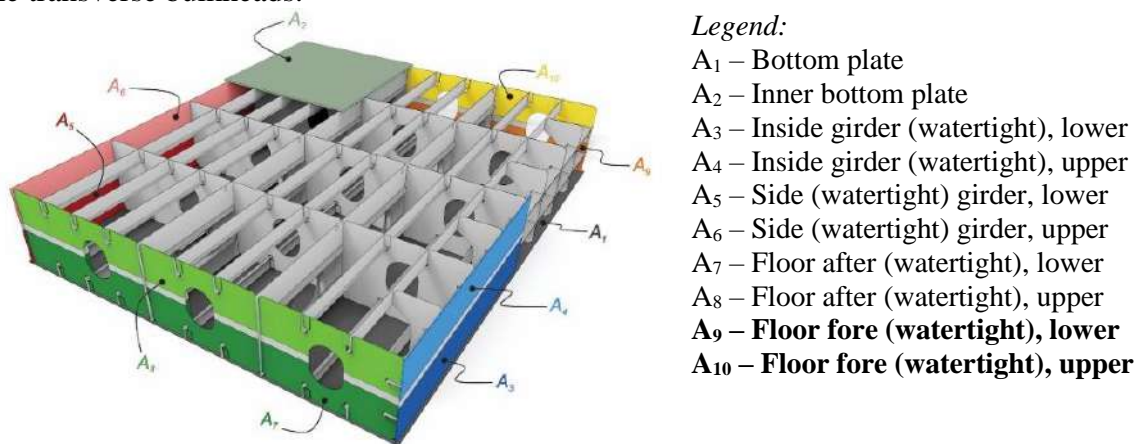
Figure 1. Basic structural scheme of considered fuel tank areas (A1 - A10) (Ivošević et al. 2017)

This paper gives an approach to the probabilistic corrosion rate estimation model for transversal bulkheads expressed in percentage (%) of diminution of as build thickness of bulkhead plate. Due to the gauging process can be considered that diminution of less than 2,5 % or 0,3 mm of original thickness can be a variation in gauging, only gauging which diminution of more than 2,5% was considered in this research. In that case, a total of 660 gauging were analysed, 342 measurements in the lower part and 314 measurements on the upper parts of bulkheads as it is presented in Table 1.

As all structural parts were protected by paint during the building process, protecting paint exists depending on a lot of different factors such as is quality of paint, use of sacrifice anodes, maintenance of tanks, frequency of ballast operations, etc. Regarding collected measuring data, and assuming that corrosion start when diminution of gauging is above 2,5% in this article we assume that the corrosion process starts after 15 years of exploitation.

Table 1 Averages of plate thickness due to corrosion, $d(t)$ (depth of corrosion in the percentage of diminution), for Lower and Upper parts of transversal bulkheads

A_9 – The lower part of bulkheads					
Years	5	10	15	20	25
% of diminution	0.5	0.5	1.2	4.9	12.5
No. of measurements	22	40	52	100	128

A$_{10}$ – The upper part of bulkheads					
Years	5	10	15	20	25
% of diminution	0.3	0.8	1.1	5.2	15.4
No. of measurements	22	32	44	96	120

As can be seen from Figure 1, all tanks have two different transversal bulkheads, after and forward. After bulkheads are usually in the engine room located but the forward bulkhead is directed to ballast tanks or following fuel tanks. Only forward fuel tanks have a transversal bulkhead which is connected with a ballast tank. In that case, in this paper, we analyse only forward transversal bulkhead plates. Considering historical data, it can be concluded that this area was under the different influence of the environment.

High bulkheads vary from vessel to vessel. Sometimes, these tanks are inside ballast tanks and sometimes are wide to the shell of the vessel (Ivošević et al. 2017). Bulkhead plate is from the back side directed to fuel oil tanks and from the front side to condition in water ballast tanks. The upper part of the bulkhead connected to the inner bottom plating is directed to Cargo Hold and different types of cargo, cargo operation and exchangeable environment conditions are in Cargo Hold. The lower part is connected to bottom plating and the influence of seawater. Considering the above, the upper part is under more stress operations and different environmental conditions. Also, the water ballast tanks, usually not full with water, in the upper part can be considered a more wet and dry cycle depending on the lower part of the bulkheads. From state previously, thickness measurement data may vary and they show a different distribution in the upper and lower part of bulkheads while we separately analyse in this paper the upper and lower part of bulkheads.

2.2. Methodology

In the scientific literature dealing with the study of metal corrosion processes, the destructive processes are usually modelled analytically or in the form of probabilistic models (Qin and Cui 2003). In contrast to the usual approach in which the corrosion depth $d(t)$ (at time t) is observed as a function of the exploitation time of the metal product (Qin and Cui 2003; Paik and Thayamballi 2002) and is usually modelled by the expression

$$d(t) = c_1(t - T_{cl})^{c_2}. \tag{1}$$

In formula (1), $d(t)$ is the corrosive wear, t is the elapsed metal exploitation time, and T_{cl} is the duration of the protective, anti-corrosive layer. Parameters c_1 and c_2 are usually the subject of research and are determined in the process of modelling corrosive processes. There are some common values for the parameter c_2 that have been proposed in the scientific literature (Qin and Cui 2003; Paik et al. 1998), however, the actual value that adequately describes the empirical data may vary from these proposed values (Ivošević et al. 2019a).

Following the suggestions from the leading scientific literature (Paik and Thayamballi 2002) in this article, the assumption is that the parameter $c_2 = 1$. However, the model represented by expression (1) is modified so that instead of corrosion rate (parameter c_1), the corrosion process is viewed as a percentage of wear concerning the original thickness of the metal plate, which was measured before the start of metal exploitation. Also, in this work, the corrosive process is viewed as a stochastic variable, which describes the corrosive process more realistically, because it is known that corrosion is influenced by a large number of external factors that have uncertainty characteristics.

Assuming that $c_2 = 1$ and that the average initial thickness of the metal plate for the observed ship structure is $\overline{d_0}$, model (1) is transformed into a new model by simple division by $\overline{d_0}$ as follows:

$$p(t) = \frac{d(t)}{d_0} = \frac{c_1}{d_0}(t - T_{cl}) = p_0(t - T_{cl}) \text{ (with } t > T_{cl}) \qquad (2)$$

where p_0 represents the annual corrosion percentage. Given that the corrosion processes in the two observed ship structures develop rather slowly, in further statistical analyses it is assumed that $T_{cl} = 15$ years.

By modelling the corrosive process in the manner shown in formula (2), it is possible to view the values of $p(t)$ as a continuous random variable. As a result, it is possible to apply the statistical procedure of fitting continuous distributions to the empirical data obtained in this way. In other words, it is possible to characterize the percentage of corrosive wear through adequate probability density functions (PDF) and cumulative density functions (CDF). The quality of fitted continuous distributions was checked using the Kolmogorov-Smirnov test, by taking the standard value of the alpha parameter and calculating the value of the test statistic. Details are shown in the next section.

3. Results

This section describes a statistical approach to approximate the cumulative distribution function of the percentage of annual corrosion p_0 defined in the previous section which is further considered as a continuous random variable.

From the empirical database, at the beginning of statistical analyses, all percentage values that are less than 2.5% were eliminated, which is equivalent to the elimination of corrosive wear of less than 0.3mm. In this way, only data for percentages related to measurements after 15 years of ship exploitation remained in the new database. This fact supported the assumption that it is sufficient to set T_{cl} to a value of 15 years.

In this paper, the analyses are limited to standard two-parameter distributions only. More precisely, to describe the annual percentage wear of the lower and upper part of bulkheads, some standard two-parameter distributions such as Erlang, Normal, Logistic, Weibull, etc., were considered.
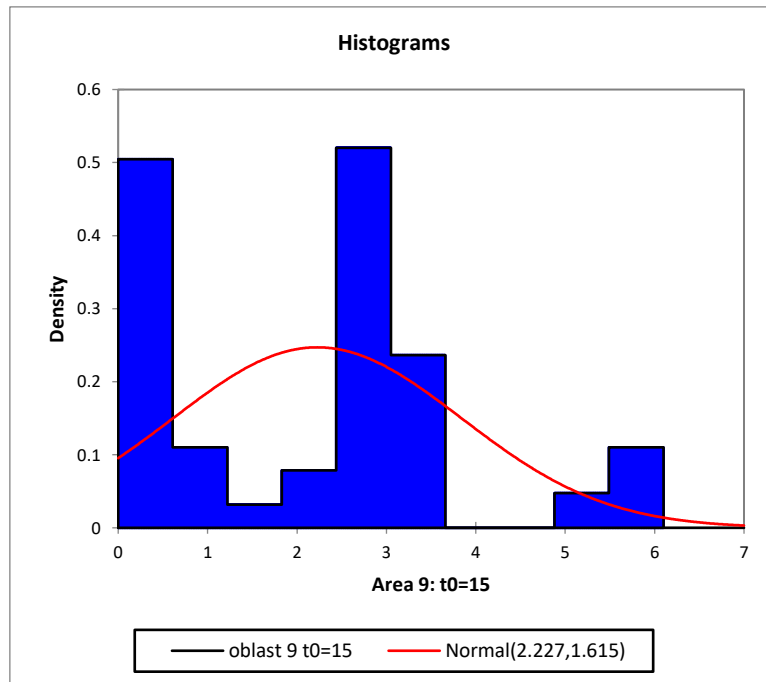
Figure 2. The empirical PDF and the PDF of the best fitted Normal distribution for the lower part of bulkheads

To check the quality of the fitted theoretical distribution, the Kolmogorov-Smirnov test was used, in which the value of 0.01 was taken as the α parameter. The null hypothesis was that the empirical data follow the observed two-parameter continuous distribution, while the alternative hypothesis supported the position that the empirical data do not follow the theoretical distribution.

In the case of the lower part of the bulkhead structure, the best results are obtained by the Normal distribution with parameters $\mu = 2.227$ and $\sigma = 1.615$. Figure 2 shows a graphical representation of the histogram of empirical data and the PDF for the fitted Normal distribution, while Figure 3 shows the corresponding empirical and theoretical CDFs.
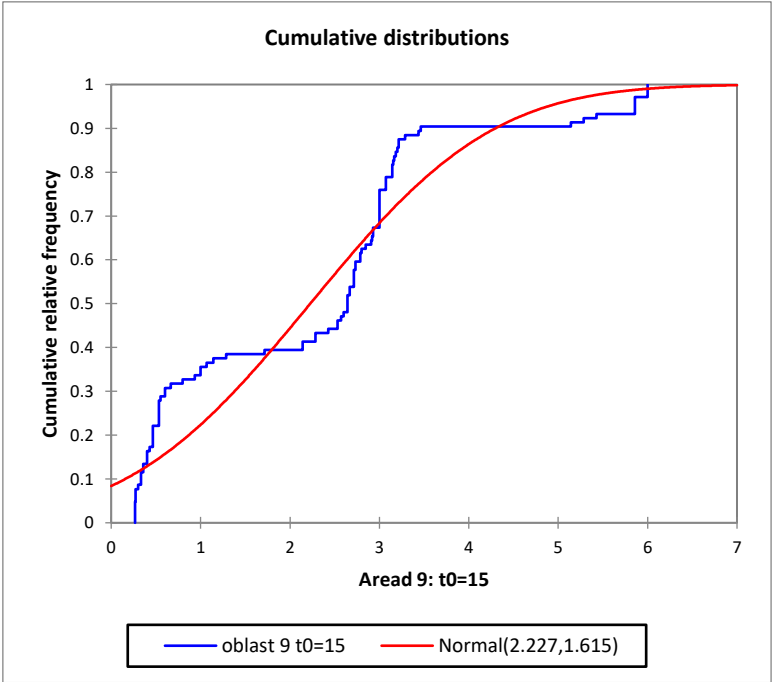
Figure 3. The empirical CDF and the CDF of the best fitted Normal distribution for the lower part of bulkheads

After applying the Kolmogorov-Smirnov test, the values of the test statistic $D = 0.151$ and $p-value = 0.016$ ($P(x \leq 0.151) = 0.984$) were obtained. As the computed p-value is greater than the significance level $\alpha = 0.01$, one cannot reject the null hypothesis H0, i.e., the sample follows a Normal distribution. It means that the chance of type I error, rejecting a correct H0, is too high: 0.016 (i.e., 1.6%).

The Logistic distribution best describes the empirical data related to the upper part of the bulkhead. The values for location parameter $\mu = 2.272$ and scale parameter $s = 0.973$ were obtained as the best parameters for Logistic distribution. Figure 4 shows a set of empirical data related to the upper part of the bulkhead in the form of a histogram. Figure 4 additionally shows the PDF of the previously characterized Logistic distribution, while Figure 5 shows the graph of empirical and Logistic CDF.
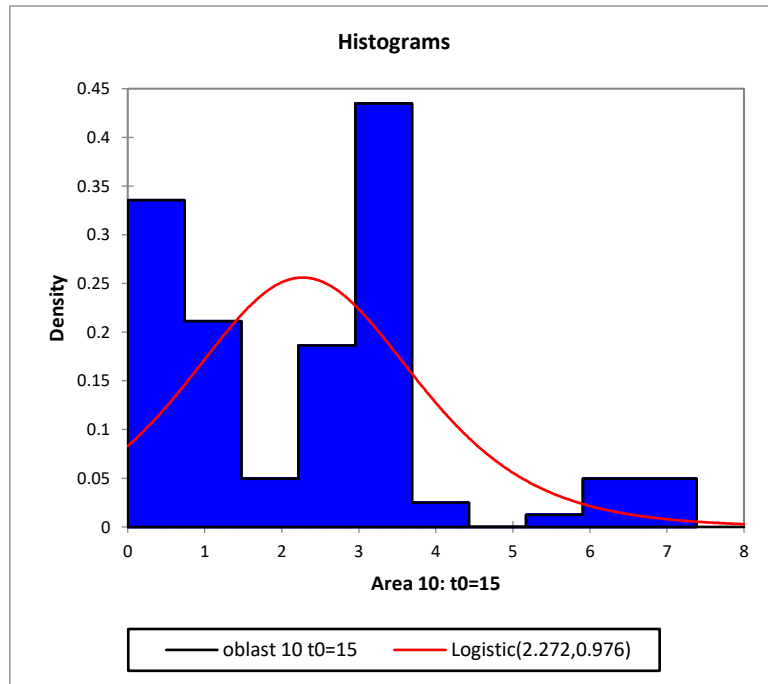
Figure 4. The empirical PDF and the PDF of the best fitted Logistic distribution for the upper part of bulkheads
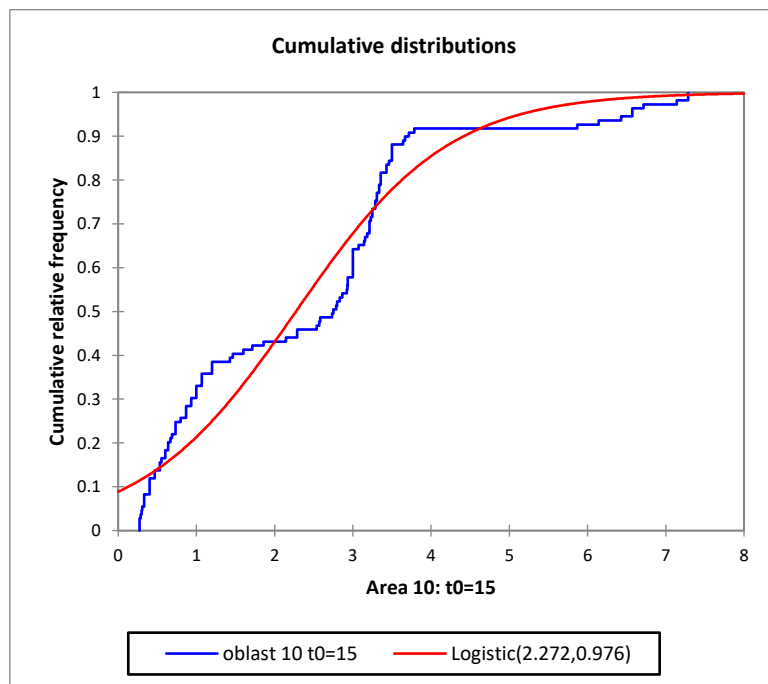
Figure 5. The empirical CDF and the CDF of the best fitted Logistic distribution for the upper part of bulkheads

The Kolmogorov-Smirnov test showed that the null hypothesis cannot be rejected. In other words, the difference between the data sample and the Logistic distribution is not big enough to be statistically significant, because the calculated values are the test statistics $D = 0.135$ and $p - value = 0.034$. The test statistic D equals 0.135, which is in the 99% region of acceptance: $[-\infty, 0.340]$.

Based on the conducted statistical analysis and the basis of the results of the Kolmogorov-Smirnov test, it is possible to observe the percentage of corrosive wear as a continuous random variable, which in the case of the lower part of the bullhead is best described by the Normal distribution, while in the case of the upper part of the bullhead, the Logistic distribution shows the best results.

4. Discussion and Conclusions

Based on the observed empirical data and with the proposed statistical data analysis methodology, the following can be concluded:
- corrosion of the upper segments is somewhat more intense compared to the lower areas of the bulkheads,
- for both ship structures, two-parameter theoretical distributions are obtained that adequately describe the corrosion process with statistically significant results, under the assumption that $\alpha = 0.01$ and that the Kolmogorov-Smirnov test is applied.
- for the lower part, the best characteristics are shown by the Normal distribution, and for the upper area, the best is the Logistic distribution.

As can be seen in Figures 2-5, the theoretical distributions do not perfectly fit the empirical data. The images show occasional "wavy" deviations of empirical data set from the theoretical distributions. As a result, for example, increasing the α value in the Kolmogorov-Smirnov test would lead to the rejection of the null hypothesis. In addition, the observed effect size D is large (0.151 and 0.135). This indicates that the magnitudes of the difference between the sample distribution and the Normal distribution and Logistic distribution are large.

To obtain better fits of theoretical distributions compared to empirical data of observed ship structures, further studies should be directed towards a larger empirical database, elimination of potential outliers, consideration of multi-parameter continuous distributions, and application of more complicated corrosion models.

Acknowledgements

References

Bauk, S., Aleksić, M., Ivošević, Š. (2011). Scanning the fuel tanks' Corrosion Wastage of Some Aged Bulk Carriers Due to Security Reasons, PROMET – Traffic & Transportation, 23 (6), 459–470.

Chaturvedi TP. (2009). An overview of the corrosion aspect of dental implants (titanium and its alloys). Indian Journal Dental Res, 20: 91–98.

Garbatov, Y., Guedes Soares, C., Wang, G. (2005). Non-linear time dependent corrosion wastage of deck plates of ballast and cargo tanks of tankers, 22nd International Conference on Offshore Mechanics and Arctic Engineering, OMAE 2005–67579, Halkidiki, Greece.

Guo, J., Wang, G., Ivanov, L., Perakis, A.N. (2008). Time-varying ultimate strength of aging tanker deck plate considering corrosion effect, Marine Structures, 21(4), 402–419.

IMO, 2007. MSC 83/INF.6, Bulk carrier casualty report.

Intercargo, 2010. Casualty report 2010.

Ivošević, Š., Mestrovic, R., Kovač, N. (2017). An Approach to the Probabilistic Corrosion Rate Estimation Model for Inner Bottom Plates of Bulk Carrier, Shipbuilding: Theory and Practice of Naval Architecture, 68 (4), 57-70.

Ivošević, Š., Meštrović, R., Kovač, N. (2019). Probabilistic estimates of corrosion rate of fuel tank structures of aging bulk carriers. International Journal of Naval Architect and Ocean Engineering, 11, 165–177.

Ivošević, Š., Meštrović, R., Kovač, N. (2019a). A comparison of some multi-parameter distributions related to estimation of corrosion rate of aging bulk carriers, In proceedings of 7th International Conference on Marine Structures, CRC Press, Taylor & Francis Group, Dubrovnik, 403-410.

Ivošević, Š., Meštrović, R., Kovač, N. (2020). A Probabilistic Method for Estimating the Percentage of Corrosion Depth on the Inner Bottom Plates of Aging Bulk Carriers. Journal of Marine Science and Engineering, 8, 442.

Jurišić, P., Parunov, J., Garbatov, Y. (2017). Aging effects on Ship Structural integrity, Brodogradnja, 68 (2),15-28.

Melchers, R. (2004). Pitting corrosion of mild steel in marine immersion environment – Part 2: variability of maximum pit depth. Corrosion 60, 937-944.

Melchers, R. (2005). Statistical characterization of pitting corrosion – part 1: data analyses. Corrosion, 61, 655-664.

Melchers, R., Jeffrey, R. (2008). The critical involvement of anaerobic bacterial activity in modeling the corrosion behavior of mild steel in marine environments. Electrochimica Acta, 54, 80-85.

Norhazilan, M.N., Smith, G.H., Yahaya N. (2007). The Weibull time-dependent growth model of marine corrosion in seawater ballast tank, Malaysian Journal of Civil Engineering, 19 (2), 142–155.

Paik J.K. (2004). Corrosion Analysis of Seawater Ballast Tank Structures, International Journal of Maritime Engineering, 146 (A1), 1-12.

Paik, J.F., Brennan, F., Carlsen, C.A., Daley, C., Garbatov, Y., Ivanov, L., Rizzo, C., Simonsen, B.C, Yamamoto, N., Zhuang H. Z. (2006). Report of Committee V.6 Condition Assessment of

Aging Ships, 16th International Ship and Offshore Structures Congress, Southampton, UK.

Paik, J.K., Kim, S.K., Lee, S.K. (1998). A probabilistic corrosion rate estimation model for longitudinal strength members of bulk carriers, Ocean Engineering, 25 (10), 837–860.

Paik, J.K., Lee, J.M., Park, Y.I., Hwang J.S., Kim, C.W. (2003). Time–variant ultimate longitudinal strength of corroded bulk carriers, Marine Structures, 16, 567–600.

Paik, J.K., Thayamballi, A.K. (2002), Ultimate strength of aging ships, Journal of Engineering for the Maritime Environment, 1 (1), 57-77.

Popolola, L.T., Grema, A.S., Latinwo, G.K., Gutti, B., Balogun, A.S. (2013). Corrosion problems during oil and gas production and its mitigation. International Journal of Industrial Chemistry 4, 35.

Qin, S., Cui, W. (2003). Effect of corrosion models on the time-dependent reliability of steel plated elements, Marine Structures, 16, 15-34.

Roberts, S.E., Marlow, P.B. (2002). Casualties in dry bulk shipping (1963–1996), Marine Policy, 26, 437–450.

Valasquez, J., Van Der Weide, J., Hernandez, E., Hernandez, H.H. (2014). Statistical modeling of pitting corrosion: extrapolation of the maximum pit depth-growth. International Journal Electrochemical Science, 9, 4129-4143.

Yamamoto, N., Ikagaki, K. (1998). A Study on the Degradation of Coating and Corrosion on Ship´s Hull Based on the Probabilistic Approach, Journal of Offshore Mechanics and Arctic Engineering, 120, 121-128.

Prioritization of Success Factors in E-commerce

Nazli Goker[1*], Mehtap Dursun[1]

Abstract: Internet, which emerged towards the end of the twentieth century, caused changes in many areas. It also affected the field of trade and brought great innovations. With the development of the e-commerce system, businesses are not limited to their local regions and have the opportunity to address the global market. As in physical business channels, customer satisfaction is very important in e-commerce. Businesses need to keep customer satisfaction at the maximum level in e-commerce. This study examines current e-commerce business models and customer satisfaction research. The factors that affect the success and efficiency of e-commerce business model are evaluated, and their importance weights are determined. Decision Making Trial and Evaluation Laboratory (DEMATEL) method is employed for the evaluation.

Keywords: DEMATEL, e-commerce business model, multiple criteria decision making.

1. Introduction

The main reason for the increase in the use of e-commerce can be exemplified by the Internet, but it cannot be said that e-commerce is so popular only because of the increase on the Internet. Being in the e-commerce system has many advantages for businesses. It is a system that can provide 24/7 service as it is not based on human power. In this way, companies can always serve their customers. Since there is no need to operate a real store during online sales, businesses have the flexibility to sell without having to pay fees such as office space fees and staff costs. With the development of the e-commerce system, businesses are not limited to their local regions and have opportunity to address the global market. Moreover, due to the online trading system, inventory tracking has become easier and more traceable supply chain networks have been formed. The e-commerce system also offers many advantages for customers. Online shopping eliminates the need for customers to spend time shopping. Thanks to online shopping, prices have become clear and comparable. E-commerce is completely independent of time and place. In this way, he was not affected by the pandemic process induced by the corona virus, on the contrary, he became stronger. Also, there are many e-commerce benefits similar to these benefits.

Although the online shopping system seems to pose a threat to physical merchandising, physical sales channels from online shopping are not expected to completely disappear. Contrary to this idea, with a good e-commerce service, brands can offer customers a unique customer experience and gain customer loyalty. The customer loyalty thus created will also contribute positively to purchases in physical stores. It is a necessity for businesses to exist in the e-commerce system, which has such advantages and has many users. Failure to be included in the

[1] Galatasaray University, Industrial Engineering Department, Decision Analysis Research and Application Center, Ortakoy, Istanbul, Turkey
* Corresponding author: nagoker@gsu.edu.tr

online system can be considered strong enough to spell the end of a business, given the ever-increasing competitive environment.

Many companies are involved in this advantageous e-commerce system. Thousands of companies have recently been and continue to be involved in this beneficial ecosystem. This has led to an increasingly competitive environment in online commerce. With the competitive environment, many e-commerce models have been formed to improve the system. These models differ by product variety, opportunity structure, price structure, or operational structure. Businesses should enter the e-commerce market with good market research for their products and the most appropriate e-commerce business model for their product or service. In this study, the evaluation of e-commerce business model success factors in terms of customer satisfaction will be discussed. The factors that affect the success and efficiency of e-commerce business model are evaluated, and their importance weights are determined. Decision Making Trial and Evaluation Laboratory (DEMATEL) method is employed for the evaluation. The rest of the study is organized as follows. DEMATEL method is explained in Section 2. Case study is illustrated in Section 3, and finally, conclusions are provided in the last section.

2. DEMATEL Method

The DEMATEL methodology developed by the Science and Human Affairs Program of the Battelle Memorial Institute of Geneva between 1972 and 1976 (Fontela and Gobus, 1976; Tzeng et al., 2010). Based on the graph theory, the DEMATEL method can divide multiple factors into a cause-effect group, and it enables the decision maker to visualize influences between criteria with a network relationship map (Yang and Tzeng, 2011).

The method begins by generating the initial direct influence matrix A. The elements a_{ij} of the matrix A represent the direct influence of each factor i exerts on each factor j, evaluated by a decision maker. The matrix A is normalized by using (1) and it is named as the matrix D (Hsu et al., 2012).

$$D = s.A, \tag{1}$$

where

$$s = \min\left[\frac{1}{\max_{1 \le i \le n} \sum_{j=1}^{n} |a_{ij}|}, \frac{1}{\max_{1 \le i \le n} \sum_{i=1}^{n} |a_{ij}|} \right] \tag{2}$$

The total relation matrix T is defined as $T = D(I - D)^{-1}$ where I is the identity matrix.

Define r and c be n x 1 and 1 x n vectors representing the sum of rows and sum of columns of the total relation matrix T, respectively. Suppose r_i be the sum of ith row in matrix T, then r_i shows both direct and indirect effects given by factor i to the other factors. If c_j denotes the sum of jth column in matrix T, then c_j shows both direct and indirect effects by factor j from the other factors (Yang and Tzeng, 2011).

When solving a decision making problem, the use of DEMATEL method enables also the decision maker to obtain the importance weights of the criteria, in addition to its ability to visualize the interactions between them.

The degree of importance for a factor i is considered as equals to the sum $(r_i + c_j)$ when $j= i$. A

network relationship map which explains the structural relations among factors can be obtained by setting up a threshold value which is determined by the decision makers. Additionally, the difference $(r_i - c_j)$ represents the net effect that factor i contributes to the system. A factor i is a net causer if $(r_i - c_j)$ is positive, and when $(r_i - c_j)$ is negative, factor i is a net receiver (Yang and Tzeng, 2011).

3. Case Study

DEMATEL method is employed to evaluate the e-commerce business model success factors. First, success factors, which are given in Table 1, are identified by reviewing the literature as well as by collecting experts' opinions.

Table 1. E-commerce business model success factors

F_1	Reliability
F_2	Accessibility
F_3	Performance
F_4	Design
F_5	Delivery
F_6	Product
F_7	After sale service

In order to apply DEMATEL method, a team of three experts indicates the influence of each criterion i exerts on each factor j of the others, using an integer scale which is generally going from "0" (no influence) to "4" (very high influence) represented in Table 2.

Table 2. Influence degrees

No influence	0
Very low influence	1
Low influence	2
High influence	3
Very high influence	4

The obtained initial direct influence matrix is shown in Table 3.

Table 3. Initial direct influence matrix

	Reliability	Accessibility	Performance	Design	Delivery	Product	After sale service
Reliability	0	0	3	0	2	0	0
Accessibility	1	0	2	0	3	0	2
Performance	2	2	0	0	3	1	1
Design	0	0	2	0	0	4	0
Delivery	2	3	1	0	0	0	0
Product	2	0	2	3	0	0	0
After sale service	3	0	1	0	0	0	0

The weights of the the e-commerce business model success factors are calculated as in Table 4.

Table 4. Weights of the e-commerce business model success factors

Factor	Weight
Reliability	0.15672065
Accessibility	0.15794493
Performance	0.20770585
Design	0.09996587
Delivery	0.1737553
Product	0.12333765
After sale service	0.08056975

4. Conclusions

To obtain the importance weights of success factors of e-commerce business model, evaluation criteria that influence success are determined through expert opinions and then algorithm of the work is reported by considering DEMATEL method. Performance and delivery are the most important factors however design and after sale service are the least important criteria. Future research will focus on proposing group decision making approaches for determining the most appropriate e-commerce business model.

Acknowledgements

References

Fontela, E., Gobus, A. (1976). The DEMATEL observer. Battelle Geneva Research Center.

Hsu, C.-H., Wang, F.-K., Tzeng, G.-H. (2012). The best vendor selection for conducting the recycled material based on a hybrid MCDM model combining DANP with VIKOR. Resources, Conservation and Recycling, 66, 95-111.

Tzeng, G.-H., Chen, W.-H., Yu, R., Shih, M.-L. (2010). Fuzzy decision maps: a generalization of the DEMATEL methods. Soft Computing, 14, 1141-1150.

Yang, J. L., Tzeng, G.-H. (2011). An integrated MCDM technique combined with DEMATEL for a novel cluster-weighted with ANP method. Expert Systems with Applications, 38, 1417-1424.

Bonding D2 Tool Steel with Different Curve Surfaces and Investigation of The Mechanical

Mahir Uzun[1*], Bahar Akçadağ[2]

Abstract: In the process from the past to the present, different methods have been used to bring the materials together. These traditionally known methods are; joining methods such as rivets, soldering, bolting and welding. There are methods that are more commonly used than these methods. This method, called adhesive, is more convenient and more practical. In this study, cycloid, epicycloid, involute and 45 degree curves with different curved surface geometries were modeled in Solidworks program with the help of mathematical formulas. After the curved surface models created were pasted in the Solidworks program, meshing was applied for the models with curved surface geometry in the ANSYS analysis program. After this process, three point bending finite element analysis was performed on the test samples. During the analyses, St52 structural steel was taken as the test sample and DP 8405 adhesive belonging to the 3M brand was taken as the adhesive type and the properties of the materials were defined. The damage load of the piece with a curved surface of 45 degrees was found and then this damage load was applied to the other pieces with curved surfaces, respectively. During the three point bending analyses, the number of finite element points was obtained as 77.191 and the number of elements as 16,836 and the adhesive thickness was taken as 0.2 mm. As a result of the finite element analysis, it has been determined that the curved surface with maximum three-point bending strength is a 45 degree curved surface.

Keywords: Adhesive, Structural Steel, Three Point Bend Analysis, Damage Load, Finite Element Analysis.

Introduction

The bonding process has many advantages compared to other joining methods. It has advantages such as being easy to apply, not causing a difference in the crystal structure, and not creating stress concentration. There are studies on adhesives in the literature. In a study, the torsional and mechanical behavior of ring-section transmission shafts, which are interlocked with two types of adhesives with different properties, were investigated. According to the results obtained, the graphs of the data were prepared, evaluated and

[1] Inonu University, Engineering Faculty, Mechanical Engineering, Malatya, Turkey
* Corresponding author: mahir.uzun@inonu.edu.tr
[2] Inonu University, Engineering Faculty, Mechanical Engineering, Malatya, Turkey
* Corresponding author: akcadagbahar533@gamil.com

compared. It has been determined that ring-section rods bonded with DP410 adhesive perform better than rods prepared with DP490 adhesive (İmak &Turgut,2020). A double pin joint was applied and bonded with different types of adhesive and stress analyzes were investigated in the laminated plate at different orientation angles. ANSYS program was used in analysis, modeling and solution processes. A tensile load was applied to the material, and stresses between the models were determined with different adhesive types in the material and hole regions, and at different orientation angles in the laminated composite plate (Benli & Erzincanlı, 2021). The effects of surface preparation with adhesion mechanisms, surface energy, surface morphology and surface roughness on adhesion were investigated. For this purpose, adhesives and their properties, mechanical tests applied to adhesive bonds, adhesion mechanisms, defects in adhesive bonds and the factors affecting a good bonding with adhesion theories were discussed, and the effect of surface energy and surface roughness and morphology on the joint was investigated (Gürsel & Yıldız, 2021). Stress analysis of the composite parts, which were bonded together with an embedded single acting patch, which was subjected to tensile load, was carried out using the three-dimensional finite element method. Composite parts produced using epoxy/carbon with different orientation angles and DP410 as adhesive type were used in the analysis. As a result, it has been shown that orientation angles and patch length are effective in joining using adhesive (Sülü, 2018). It has been understood that the design parameters in the lap pipe bonding joints are the pipe wall thickness, the overlap length and the adhesive thickness are the important design parameters in the pipe bonding joints (Saraç, 2021). The effect of the nanoparticle ratio in the bonding joints obtained by adding carbon nanoparticles into the epoxy adhesives on the adhesion strength on rough surfaces was investigated. As a result of the study, it has been shown that nanoparticles positively affect the adhesion strength up to a certain extent, then the effects decrease (Aydın, 2019).

In this study, unlike other studies, plates with cycloid, epicycloid, involute and 45-degree curved surfaces were designed in Solidworks package program and bonding simulations were carried out. After bonding, the three-point bending strength from the mechanical properties of the plates with curved surfaces was determined and compared using the finite element method using the ANSYS analysis program.

Material and Method

In this study, primarily cycloid, epicycloid, involute and 45 degree curves were modeled in Solidworks program using mathematical relations.

Cycloid curve equation;

$$x = r(t - sint) \tag{1}$$

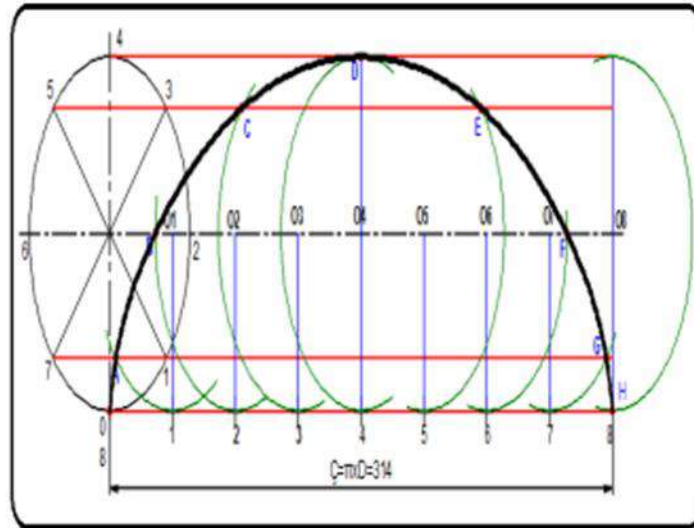A sample model with a cycloid curved surface was created in the Solidworks program using the equation (Figure 1).

Figure 1: Cycloid curve geometry (Uzun & Çetin, 2020)

Epicycloid curve equation;

$$x = r\,(k+1)cost - \; rcos(k+1)t \tag{2}$$

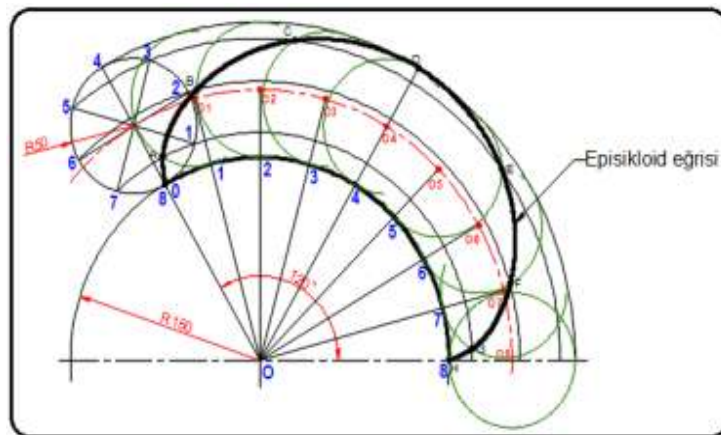A sample model with epicycloid curved surface was created in the Solidworks program using the equation (Figure 2).

Figure 2: Epicycloid curve geometry (Uzun & Çetin, 2020)

Involute curve equation ;

$$x = r(cost + (t-a)sint) \tag{3}$$

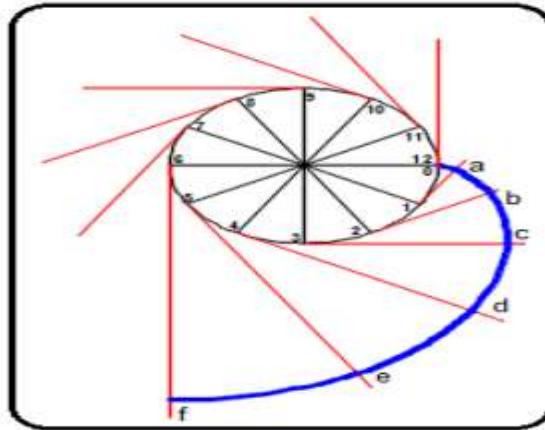Equation of the involute curved surface sample model was created in Solidworks program (Figure 3).

Figure 3: Involute curve geometry (Uzun & Çetin, 2020)

The sample model with a 45 degree curved surface was created in the Solidworks program in Figure 4d.

Depending on the condition *x* used in equations 1, 2 and 3, *x* in the *x* coordinate abscissa (mm), *r* the radius value, *t* the angular value of the moving point (degrees) $0 \leq t \leq 2\pi$, $k = 1$, *a* is the origin (0,0) stands for distance.

The length of the modeled samples was taken as 150 mm, the thickness as 10 mm, and the width as 25 mm.

By using Equations 1, 2 and 3, cycloid, epicycloid and involute curves were created in Solidworks program, respectively, and then these curves were created as adhesive model (Figure 5) and jointing simulations were performed (Figure 4). The analysis piece with a 45 degree curved surface is simulated in Figure 4d.
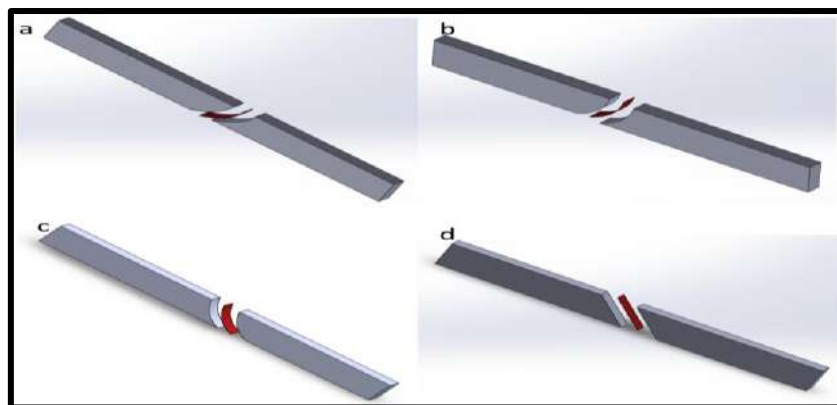
Figure 4: Part simulations modeled in Solidworks (Uzun &Akçadağ,2022)

Adhesive side lower edge length was taken as 35.36 mm and lower horizontal edge length was taken as 10 mm (Figure 5).
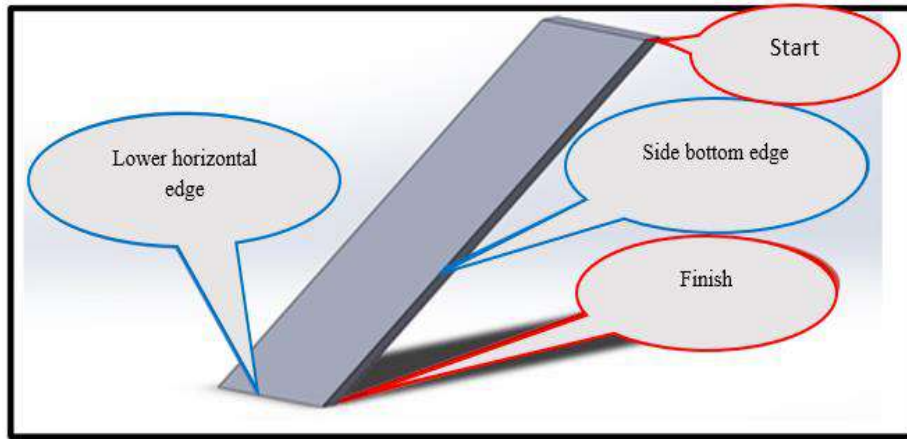
Figure 5: Modeled adhesive interlayer (Uzun &Akçadağ,2022)

The ANSYS program was used to perform finite element analysis of the samples whose models were created in the Solidworks package program and glued simulations were made. In order to be able to analyze in the ANSYS program, firstly, the mesh process was performed. While performing the mesh process, different mesh techniques were tried and the mesh that was suitable for mesh quality was determined. As a criterion, the optimum value of mesh quality close to 1 was selected and considering this value, it was determined that the most suitable mesh was edge sizing (Figure 6). During the analyses, St52 structural steel (Table 1) was used as test samples, and DP8405 numbered acrylic adhesive of 3M brand was used as adhesive type (Table 2).

Table 1: Mechanical Properties of St 52 Structural Steel (Akçadağ, 2022)

Denstiy (kg / m³)	**7.850**
Young's Modulus (MPa)	2E +5
Poisson Ratio	0.3
Bulk Module (MPa)	16.667E + 5
Shear Module (MPa)	76.923E+4

Table 2: Mechanical Properties of DP 8405 Adhesive (Akçadağ, 2022)

Adhesive Type	Acrylic
Viscosity	No Sagging
Product Color	Green
Opening Time (minute)	6-10
Working time (minute)	4-6
Full Curing (hour)	24
Physical Form	Fluid Liquid
Denstiy (kg / m³)	1.030
Young's Modulus (MPa)	62E+05
Poisson Ratio	0.3
Bulk Module (MPa)	51.667E+02
Shear Module (MPa)	23.846E+02

In models with cycloid, epicycloid, involute and 45 degree curved surfaces, the mesh numbers are respectively; 78.504, 89.008, 89.008, 77.191. The number of elements are respectively; 17.136, 19.536. 19.536 was determined as 16.836.

For three-point bending analysis, models with cycloid (Figure 6a), epicycloid (Figure 6b), involute (Figure 6c) and 45 degree (Figure 6d) curved surfaces were meshed. Then, the boundary conditions required for the analysis were defined one by one, and the analysis force was entered as a step. The adhesive yield stress is 16.5 MPa. In order for the samples to be damaged, the value of 16.5 MPa is accepted as the limit, and in order to exceed this value, 2.000 N, 3.000 N, 2.000 N and 2.000 N step forces were applied to the cycloid, epicycloid, involute and 45 degree curved surfaces, respectively (Figure 7).
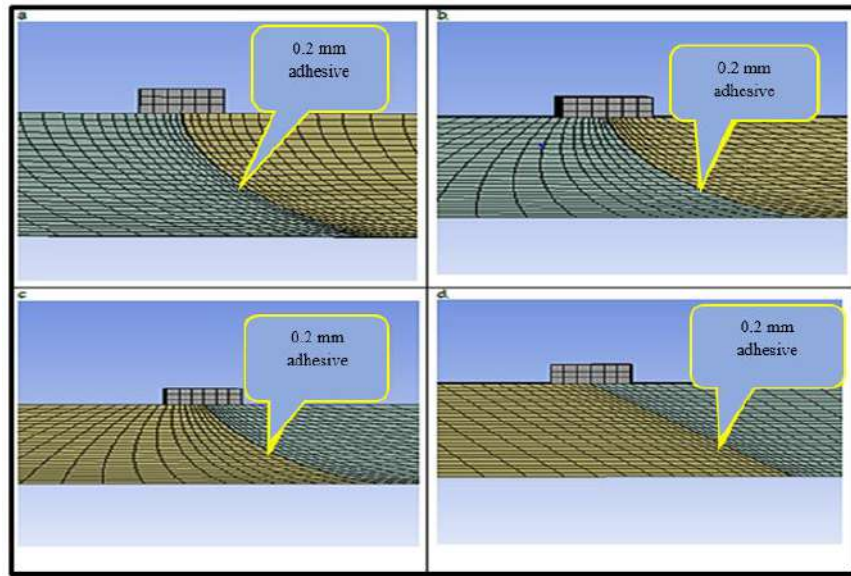
Figure 6: Part mesh models with curved surfaces (Uzun &Akçadağ,2022)
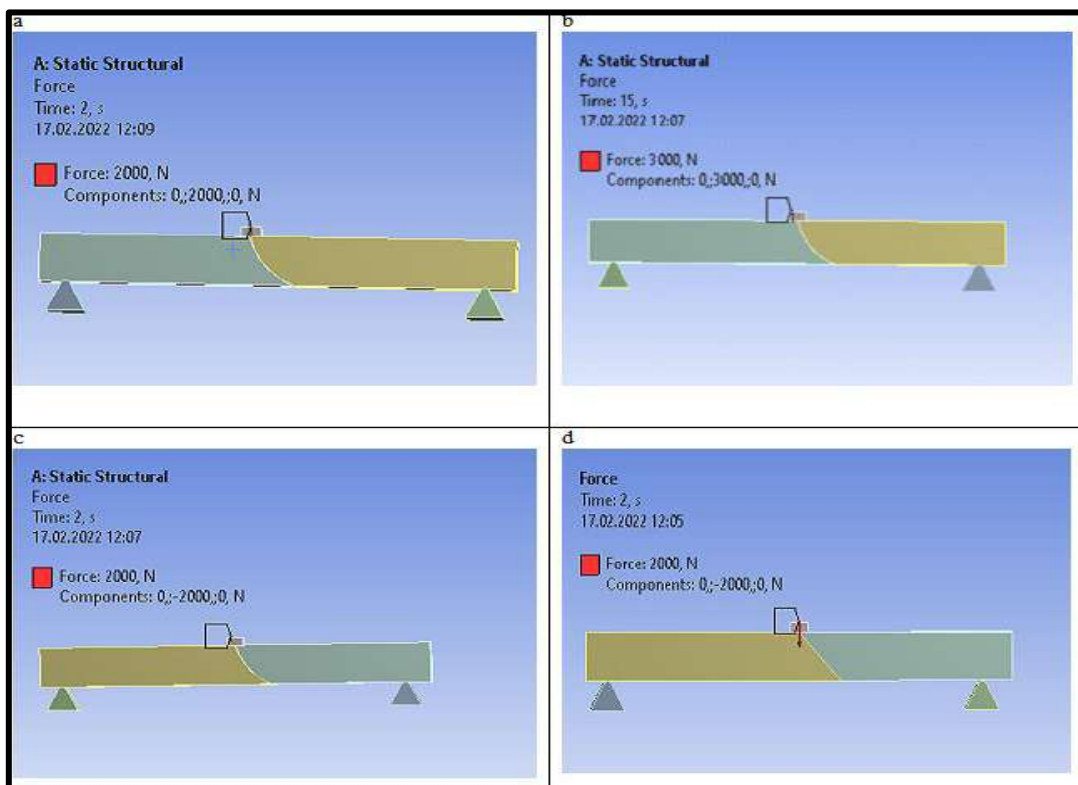
Figure 7: Applying force to curved surface specimens (Uzun &Akçadağ,2022).

Three point bending analysis was applied to the samples with curved surfaces after meshing in ANSYS. As a result of the analysis, it was determined that the maximum von Mises stress on the adhesive surface occurred at the lower part of the back surface, and at 45 degrees, it was formed at the bottom part. Considering the yield criterion, the maximum strengths of the

cycloid (Figure 8a), epicycloid (Figure 8b), involute (Figure 8c), and 45 degree (Figure 8d) surfaces are respectively; It was determined as 1.266 N, 1.180, 1.233 and 2.000 N (Figure 8).
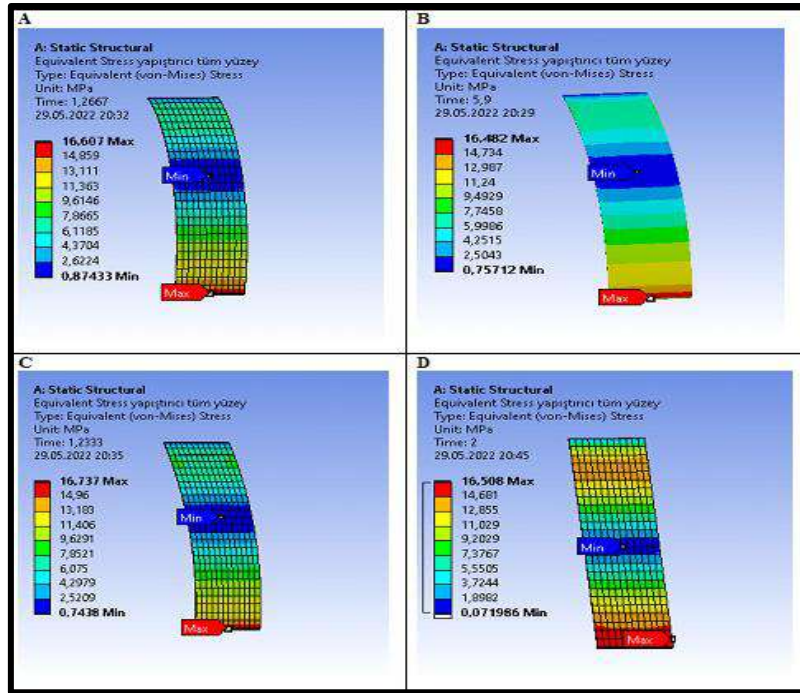
Figure 8: Adhesive whole surface von mises stress analysis (Akçadağ, 2022)

The von Mises stresses were compared under the applied force along the y-axis for the adhesive lower horizontal edge. It was observed that the stresses did not change along the edge on cycloid, epicycloid and involute surfaces, first remained constant on the 45 degree surface, then rose again and reached the initial value. It was determined that the maximum stresses occurred at the 45 degree surface (Figure 9).
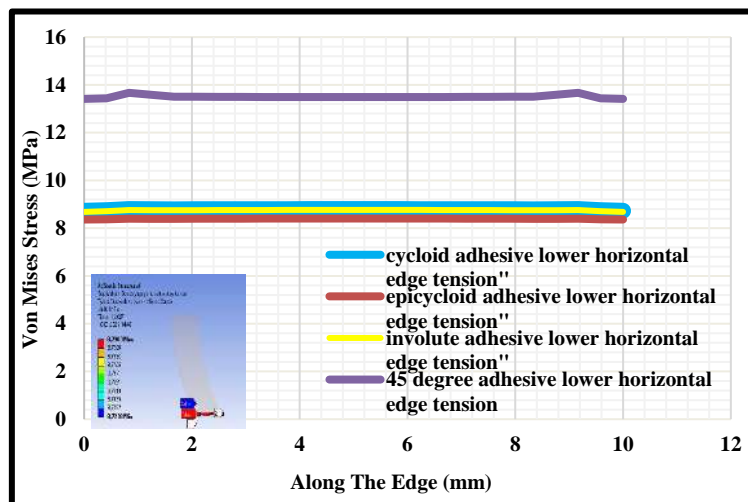
Figure 9: Von Mises stress plot along the adhesive lower horizontal edge (Akçadağ, 2022)

Results

In this study, three point bending analyzes were applied to the models in order to determine the durability of the models with different curvilinear surfaces. As a result of the study;

- As a result of the three-point bending analysis for the cycloid whole surface, the maximum strength strength was 1.266 N and the adhesive was determined at the bottom of the back surface.

- As a result of the three-point bending analysis for the epicycloid whole surface, the maximum strength force was found to be 1.180 N on the lower part of the adhesive back surface.

- As a result of three-point bending analysis for the entire surface of involute, the maximum strength force was 1.233 N, and the adhesive was formed on the lower part of the back surface.

- As a result of the three-point bending analysis for the entire surface of 45 degrees, the maximum strength force was 2.000 N, and the adhesive was formed at the bottom of the back surface.

As a result of the analysis, it was determined that the maximum stresses occurred on the adhesive back surface. The surface with a maximum three-point bending strength was determined to be a curved surface of 2.000 N and 45 degrees.

Thanks

References

Akçadağ, B., (2022). Eğrisel Geometrili Yüzeylerin Yapıştırılması ve Mekanik Özelliklerinin Araştırılması (Yüksek Lisans Tezi). İnönü Üniversitesi, Malatya.

Aydın, S., (2019). Karbon Nanopartiküllerin Epoksi Yapıştırıcılarda Etkilerinin İncelenmesi, Çukurova Üniversitesi Mühendislik Mimarlık Fakültesi Dergisi, 34(3), ss. 143-154.

Benli, S., Erzincanlı, İ., (2021). Çift Pimli ve Yapıştırmalı Kompozit Plakalarda Farklı Yapıştırıcı Türleriyle Gerilme Analizi, Iğdır Üniversitesi Fen Bilimleri Enstitüsü Dergisi, 11(1): 575-589.

Gürsel, A., Yıldız, S., (2021). Yapıştırıcı Birleştirmelerde Bağlantı Mukavemetini Etkileyen Faktörler: Yüzey Morfolojisi ve Yüzey Enerjisi, Düzce Üniversitesi Bilim ve Teknoloji Dergisi, 9 (2021), 987-996.

İmak, A., Turgut, A., (2020). Farklı Yapıştırıcılarla Birleştirilen Halka Kesitli Transmisyon Çeliklerinin Mekanik Davranışlarının Araştırılması, International Journal of Innovative Engineering Applications, vol: 4, issuse: 1.

Saraç, İ., (2021). Boru Yapıştırma Bağlantılarında Farklı Tasarım Parametrelerinin Yapıştırıcı Tabakasında Gerilme Dağılımına Etkisinin Sayısal olarak Araştırılması, Uludağ Üniversitesi Mühendislik Fakültesi Dergisi, Cilt: 26, Sayı: 1.

Sülü, İ. Y., (2018). Çekme Yükü Altında Gömülü Tek Tesirli Yama ile Yapıştırılarak Birleştirilmiş Kompozit Parçaların Gerilme Analizi, BEÜ Fen Bilimleri Dergisi, 7(2) 284-295.

Uzun, M., Akçadağ, B., (2022). Sikloid, Episikloid, Evolvent, 45° Eğri Yüzeylerin Yapıştırılması ve Mekanik Özeliklerinin Sonlu Elemanlar Yöntemi ile Araştırılması, Iğdır Üniversitesi Fen Bilimleri Enstitüsü Dergisi, 12(2):990-1002.

Flexural Strength Behavior of Aged Glass-Carbon/Epoxy Hybrid Composites in Seawater, Engine Oil and Diesel Fuel Degradation Environments

Ahmet Saylık[1*], Şemsettin Temiz[2]

Abstract: In this study, glass/epoxy (GFRP), carbon/epoxy (CFRP) and glass-carbon epoxy hybrid (GCFRP) eight-layer composites manufactured by the vacuum assisted resin transfer molding method were subjected to aging in an artificial seawater, engine oil and diesel fuel environment for 30, 60 and 90 days, after which the effect of aging on the degradation and flexural performances of the composite specimens was examined. When the mean flexural strengths of the composites whose flexural performances were reviewed at the end of each month were analyzed, it appeared that the flexural modulus and flexural strengths of CFRP and GCFRP composites decreased more in the artificial seawater environment than the engine oil and diesel fuel environments as a result of aging. When the flexural performances of CFRP composites were examined, it was concluded that the environment that reduced the flexural modulus and flexural stress the most was the engine oil environment. It was calculated that the flexural stress strengths of GFRP composites at room conditions decreased by 16.58% with aging in artificial seawater environment, by 5.95% in engine oil, and by 5.83% in diesel fuel environment. And the flexural stress strengths of CFRP composites at room conditions decreased by 14.01% with aging in artificial seawater environment, by 16.86% in engine oil, and by 12.20% in diesel fuel environment. It was concluded that the three-point bending performances of hybrid GCFRP composites formed by stacking glass-carbon fibers together showed flexural strength values close to GFRP composites.

Keywords: Fiber reinforced composite, environmental degradation, flexural strength hybrid composites, aging process.

1. Introduction (Times New Roman 12pt)

Fiber Reinforced Plastics (FRPs) are widely used in constantly developing fields such as aerospace, defense and medical industries due to their high specific strength, stiffness and lightness. Fiber-reinforced plastics such as carbon fiber-reinforced plastics (CFRPs) and glass fiber-reinforced plastics (GFRPs) are considered ideal materials, especially in the aerospace industries where high strength-to-weight ratios are more suitable. Exposure of polymer composites to harsh weather conditions often results in structural deterioration, also known as degradation. This can be caused by humidity, seawater or distilled water, hot steam, ultraviolet radiation, and exposure to low or high temperatures (Felipe et al. 2019). A number of researchers investigated the effects on the mechanical proper-ties of fiber-reinforced polymer matrix composites exposed to different environmental conditions (Kumar, Singh, and

[1] Mus Alparslan University, Faculty of Architecture and Engineering, Mechanical Engineering, Mus, Turkey
[2] Inonu University, Engineering Faculty, Mechanical Engineering, Malatya, Turkey
* Corresponding author: a.saylik@alparslan.edu.tr

Nakamura 2002; Shin, Kim, and Hong 2003; Shokrieh and Bayat 2007; Peterson et al. 2008). When the flexural behavior of flax and hemp-based hybrid composites exposed to cryogenic environment was examined, it was determined that the flexural stress values of the composites left in the cryogenic environment for 45 minutes decreased by 3.78% (G et al. 2022). Many studies have been conducted under various environ-mental conditions to examine the mechanical durability of polymer matrix composites formed through hybridization of carbon and glass fiber with other fiber types. For example, the effect of nanoparticle reinforcement on carbon fiber-reinforced composites was investigated (Zeltmann, Poveda, and Gupta 2015; Chiang, Chou, and Shen 2020) , and nanoparticle reinforcement was used on glass fiber-reinforced composites to strengthen laminates under environmental aging (Nayak et al. 2020). Determining the durability of marine vessels designed with rein-forced polymer matrix composites in sea water, salt water and similar liquid environments is an important field of study. Composites have been developed and optimized for use in off-shore industries (Kootsookos and Mouritz 2004; Mula et al. 2005). When the carbon/flax fiber hybrid composites were aged by applying the high temperature water immersion process, it was determined that the composites with carbon fiber layers on the surface had higher flexural stress and modulus than the composites with flax fiber on the surface (Cheng et al. 2020). By looking at the behavior of water diffusion in car-bon/epoxy composites under static tensile stress, it became clear how the coupling effects between water and mechanical loading of the composites affect the damage development (Humeau, Davies, and Jacquemin 2018) . C-glass woven fiber composites were tested by soaking in a 10 wt.% aqueous H_2SO_4 (1.89 mol/L) concentration environment at different temperatures and for different durations. As a result, it was concluded that C-glass fibers had more durability in acidic environments than E-glass and carbon fibers (Tanks, Arao, and Kubouchi 2018). Hybrid rods manufactured with unidirectional carbon/glass (core/shell) pultrusion technology with a diameter of 19 mm were manufactured and immersed in water at different temperatures (Kafodya, Xian, and Li 2015), and in oil wells (Li et al. 2020), and the relations be-tween shear strength and interface shear strength and degradation times of the rods were examined. When the 3-point bending stress behaviors of glass/carbon/epoxy and 7-layer ply layered composites were studied under different thermal bending loads, it was found that the magnitude of the CTE mismatch between carbon and epoxy was higher than that of glass and epoxy, and the rate of strength and modulus deterioration of composites with more CE layers increased as the test temperature increased (Rathore et al. 2017). GFRP and CFRP epoxy composites were aged in artificial sea water for 45 days, and it was concluded that the flexural strength of glass/epoxy laminates decreased by about 3.1%, while the flexural strength of carbon/epoxy laminates de-creased by 7.7% (Ghabezi and Harrison 2020) . In testing the flexural performance of carbon/glass hybrid FRP composite laminates was investigated, G_2C_4G2 was placed symmetrically on the stress and compression sides. It was concluded that composites with G2C4G2 array with such two glass layers had approximately 18.3% higher flexural stress than composites with C2G4C2 array (Chen et al. 2019).

In this study, after aging of carbon/epoxy, glass/epoxy and glass-carbon hybrid epoxy composite laminates in artificial seawater, engine oil and diesel fuel environment for 30, 60 and 90 days, the three-point bending stress behavior and degradation conditions of composite laminates were compared. The flexural strength effect of the aging effect was analyzed and interpreted.

2. Materials and Methods

In this section, the production of composite samples, the creation of aging environments and the three-point bending test are explained.

2.1. Materials – reinforcement, resin and composite laminate manufacture

In order to manufacture the composites, 300 gr/m2 woven type E-glass (twill) fiber and 200 gr/m2 woven type carbon (plain) fibers were used as reinforcement element as shown in Figure 1. EPIKOTE epoxy system was used as matrix in composite production (German Lloyd); RIM 135 was used as resin, and RIMH 137 was used as hardener. The mixing ratio of epoxy and hardener was 100:30. Three types of homogeneous layered composites were manufactured by reinforcing epoxy matrix composites with carbon, glass and glass-carbon fibers. For the manufactured composites, fiber fabrics were prepared in 8 layers of 300 x 300 mm2 sized pieces. The mechanical proper-ties of the glass and carbon fibers used in the study are shown in Table 1.

Table 1. Mechanical and physical properties of used materials as component in composite structure.

Material properties	Carbon fiber (twill woven)	Glass fiber (plain wowen)	Resin (RIM 135, RIMH137)
Young's modulus (GPa)	240	81.50	105
Density (g/cm^3)	1,79	2,58	1,19
Tensile Strength (MPa)	3800	2306	70
Tensile strain (%)	1.6	2.97	12

As shown in Figure 1, GFRP composites consisting of 8 layers of glass fiber, CFRP consisting of 8 layers of carbon fiber, and glass-carbon fiber reinforced hybrid composites (GCFRP) comprised of 2 layers of glass fiber in the top and bottom layers, and 4 layers of carbon in the middle, 8 layers in total, were used.
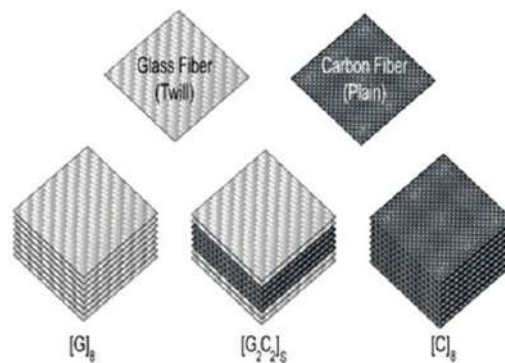
Figure 1. Laminate codes and labeling system of stacking order.

Composite specimens were manufactured using the vacuum assisted resin transfer molding method (VARTM) as shown in Figure 2. All of the composites left in the vacuum environment were manufactured by being kept at room temperature at 25 °C for one day. The fiber volume ratio of glass/epoxy composites (GFRP) was 50.91%, the fiber volume ratio of carbon epoxy composites (CFRP) was 56.06%, and the fiber volume ratio of glass-carbon epoxy hybrid (GCFRP) composites was 54.2%. The thickness of the manufactured glass/epoxy composite sheets (GFRP) was 1.90±0.1 mm, the thickness of the car-bon/epoxy composite sheets (CFRP)

was 1.85±0.1mm, and the thickness of the glass-carbon epoxy (GCFRP) hybrid epoxy composites was 1.87±0.1 mm.
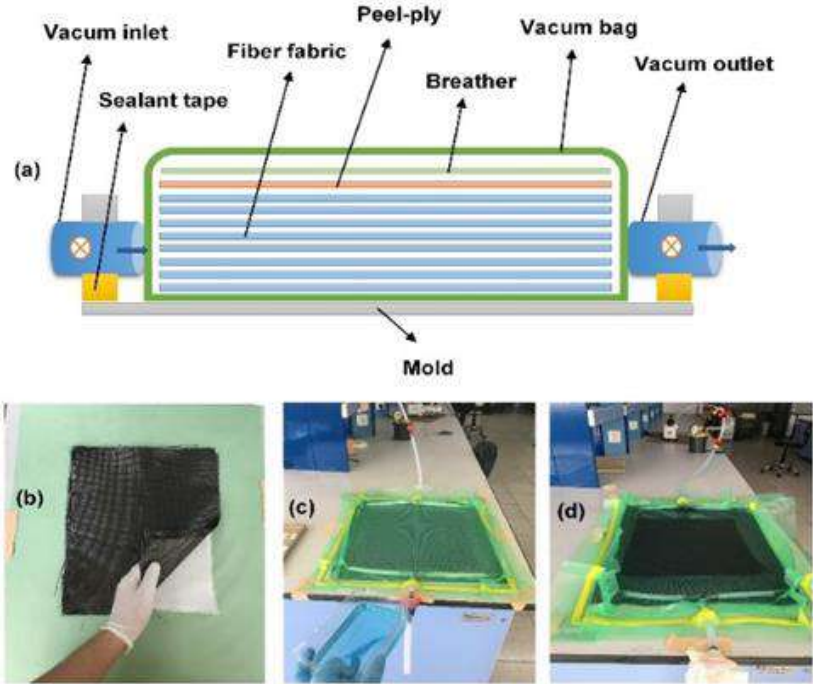

Figure 2. Preparation of composites: (a) VARTM method scheme, (b) stacking of fibers, (c) transferring the resin to the vacuum environment, (d) vacuum environment.

2.2. Aging of composites

For three point bending tests GFRP, CFRP and GCFRP composite specimens were aged for 30, 60 and 90 days in artificial seawater, engine oil and diesel fuel environments shown in Figure 3. Artificial seawater environment; In the laboratory, 35 g of salt was added to a beaker and then tap water was added until the total mass was 1000 g, by mixing until the salt was completely dissolved in the water, an artificial seawater environment was prepared. *Shell Helix HX7 10W-40* engine oil was used for the engine oil environment, and *Shell V Power* diesel fuel was used for the diesel fuel environment. GFRP, CFRP and GCFRP samples were aged in the environments shown in Figure 3 for 30, 60 and 90 days, respectively, and bending test samples were taken at the end of each period. The surfaces of the three point bending samples taken from the environment were cleaned with a dry cloth.

Figure 3. The process of placing composites into degradation environments.

2.3 Three-point bending test

The composite plates manufactured with the above-mentioned VARTM technology were cut mechanically with a high-speed computer numerical control (CNC) milling ma-chine, and rectangular bending test specimens of 150 mm (length) x 25 mm (width) dimensions were prepared. Following the aging process, the test specimens were taken from the environment, cleaned, wiped and made ready for experimentation. As shown in Figure 4, five specimens for each compo-site were tested on the 10 kN capacity Shimadzu AGS- X brand test device for the experiments, and their mean values were reported. The bending test with a span-to-thickness ratio of 32:1 was performed at a constant speed of 1 mm/min at room temperature according to ASTM D7264 [43]. The flexural strength (σ_F), modulus (E_F) and strain to rupture (ε_F) are determined by the following expressions:

$$\sigma_F = \frac{3P_{max}L}{2wt^2} \tag{1}$$

$$\varepsilon_F = \frac{6dt}{L^2} \tag{2}$$

$$E_F = \frac{mL^3}{4wt^3} \tag{3}$$

Here, L is the length of the distance between the spans, w is the width of the test specimen and t is the thickness of the test specimen. P_{max} is the maximum load before fracture, m is the slope of the first segment of the load/displacement curve, and d represents the maximum bending before fracture.
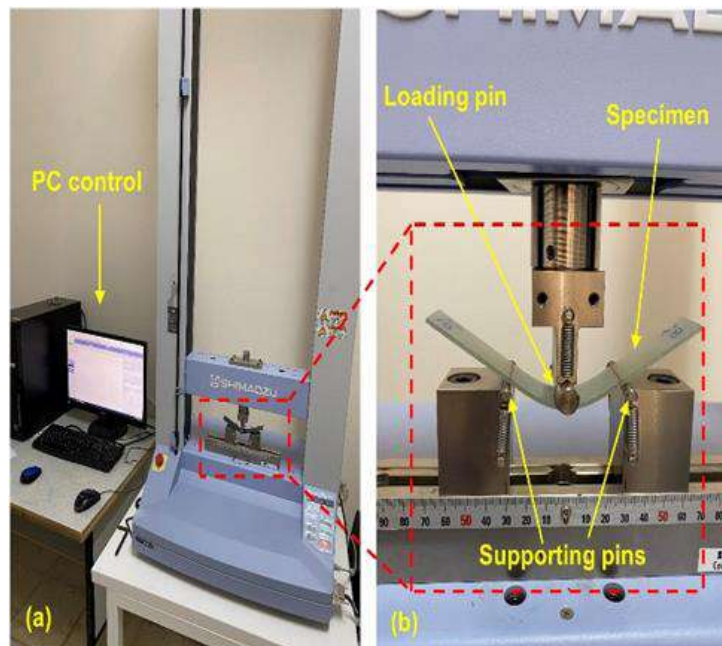
Figure 4. Bending test setup: (a) Shimadzu AGS- X tester, (b) There-point bending test.

3. Results

In the present study, GFRP, CFRP and GCFRP composites were aged in three different environments for three different time periods, and the changes in flexural performance of the composites at room conditions were examined and compared. The flexural stress performances of GFRP composites aged in artificial seawater environment, engine oil environment, and diesel fuel environment are shown in Figure 5a, Figure 5b, and Figure 5c, respectively. The flexural stress performances of CFRP composites aged in artificial seawater environment, engine oil environment, and diesel fuel environment are shown in Figure 6a, Figure 6b and Figure 6c, respectively. The flexural stress performances of GCFRP composites aged in artificial seawater environment, engine oil environment, and diesel fuel environment are shown in Figure 7a, Figure 7b, and Figure 7c, respectively.
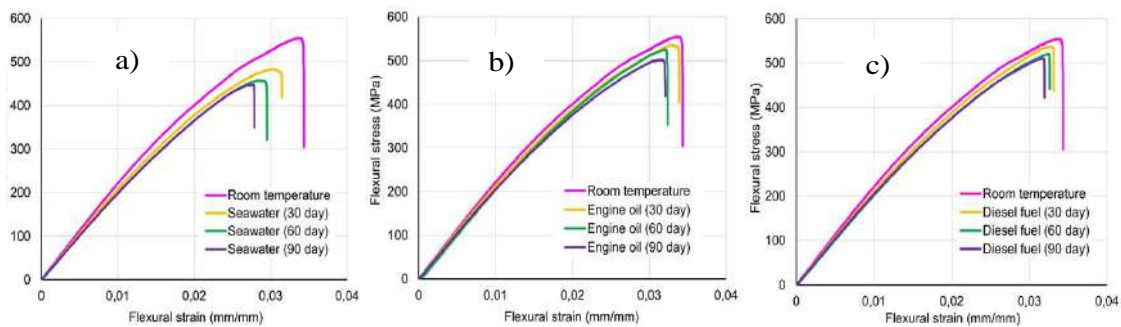
Figure 5. Flexural stress-strain graph of GFRP composites a) artificial seawater, b)engine oil, c) diesel fuel environment.
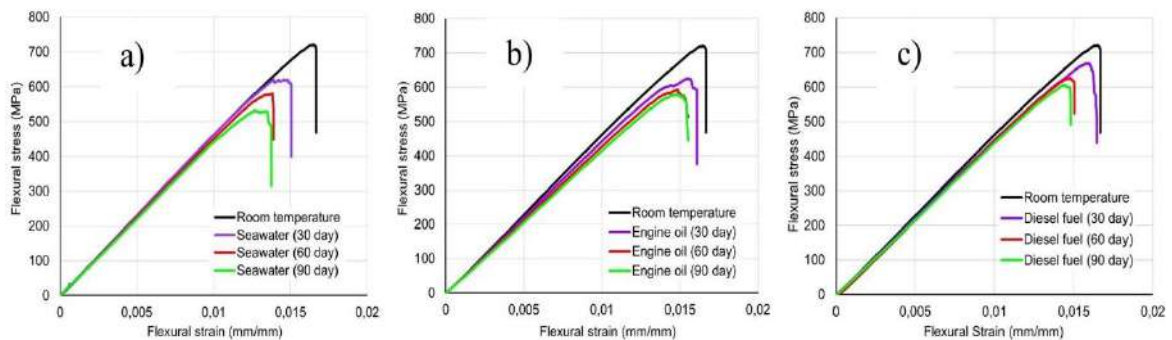
Figure 6. Flexural stress-strain graph of CFRP composites a) artificial seawater, b) engine oil, c) diesel fuel environment.
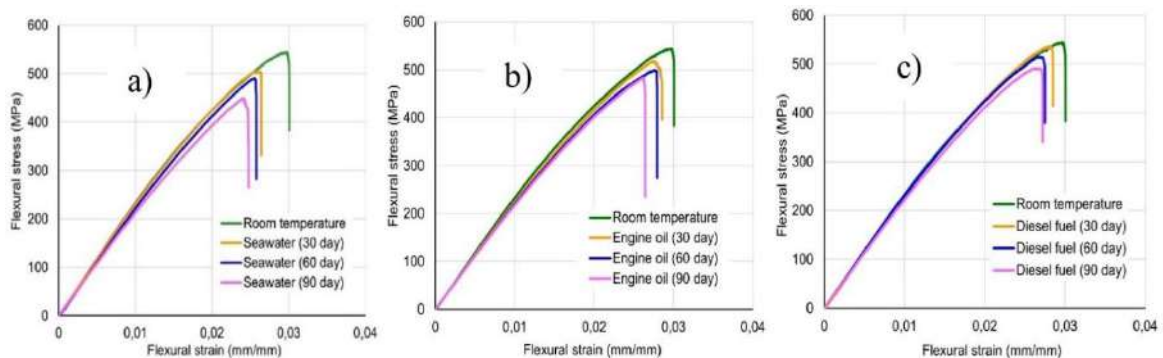
Figure 7. Flexural stress-strain graph of GCFRP composites a) artificial seawater, b)engine oil, c) diesel fuel environment.

When the effect of aging of GFRP composites for different time periods and in different environmental conditions on the flexural behavior was examined, it was seen that as the aging time increased in artificial seawater environment as shown in Figure 5a, and the gap between the stress-strain curves decreased significantly compared to the engine oil environment (Figure 5b) and diesel fuel environment (Figure 5c) flexural stress-strain curves. When the effect of aging of CFRP composites for different time periods and in different environmental conditions on the flexural behavior was examined, it was clearly seen in Figure 6b that the gap between the stress-strain curves with the increase of the aging time in the oil environment was higher compared to the aging in the artificial seawater environment (Figure 6a) and diesel fuel environment (Figure 6c). When the effect of aging of GCFRP hybrid composites for different time periods and in different environmental conditions on the flexural behavior was examined, it was determined that the gap between the curves of the flexural stress-strain curve in the artificial seawater environment shown in Figure 7a was more pronounced than the engine oil aging (Figure 7b) and diesel fuel environment (Figure 7c).
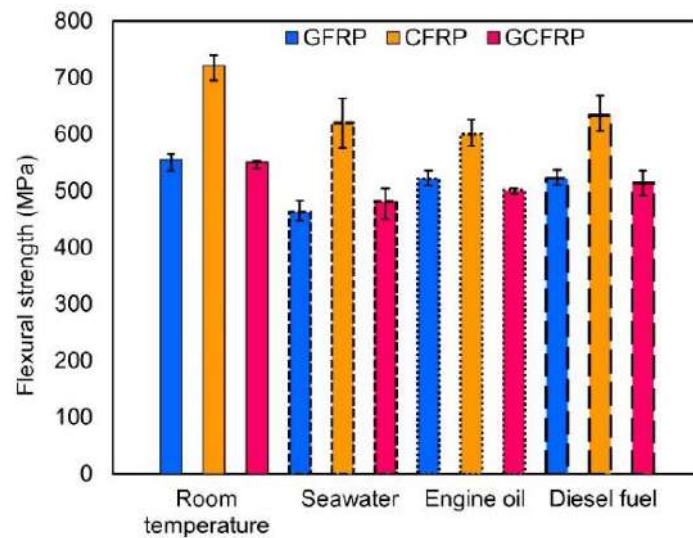

Figure 8. Comparison of the mean flexural strengths of CFRP, GFRP and GCFRP composites aged for 90 days.
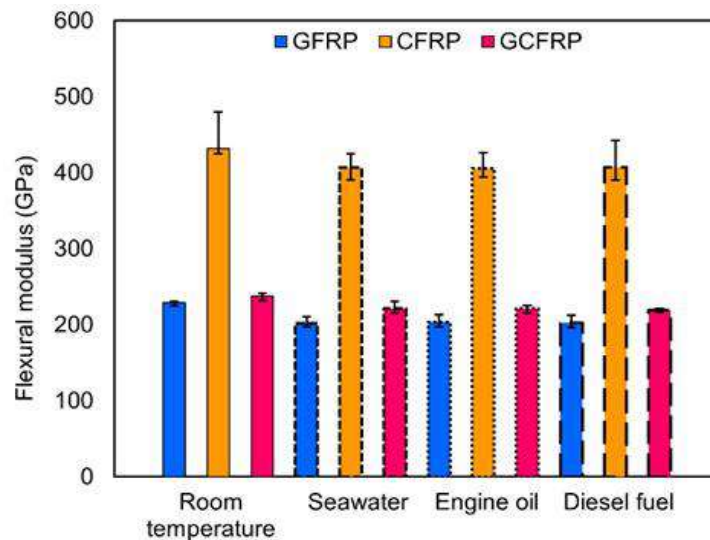
Figure 9. Comparison of the mean flexural modulus of CFRP, GFRP and GCFRP composites aged for 90 days.

The mean flexural strengths of the data obtained from the stress-strain curves of the composites aged for 90 days in different environments are shown in Figure 8, and their flexural modulus are shown in Figure 9. The mean flexural stress strength was determined by calculating the stress values of the composite specimens aged for 30, 60 and 90 days, respectively, in three different environments (Figure 8). It was calculated that the flexural stress strengths of GFRP compo-sites at room conditions decreased by 16.58% with aging in artificial seawater environment, by 5.95% in engine oil, and by 5.83% in diesel fuel environment. And the flexural stress strengths of CFRP composites at room conditions decreased by 14.01% with aging in artificial seawater environment, by 16.86% in engine oil, and by 12.20% in diesel fuel environment. The flexural stress strengths of GCFRP hybrid compo-sites at room conditions decreased by 12.59% with aging in artificial seawater environment, by 9.12% in engine oil, and by 6.62% in diesel fuel environment. Figure 10 shows the damages that occurred on the composites after the three-point bending test. The specimens started to fracture after bending along the loading pin. Fiber fracture and delamination occurred depending of the region where bending damage occurred.
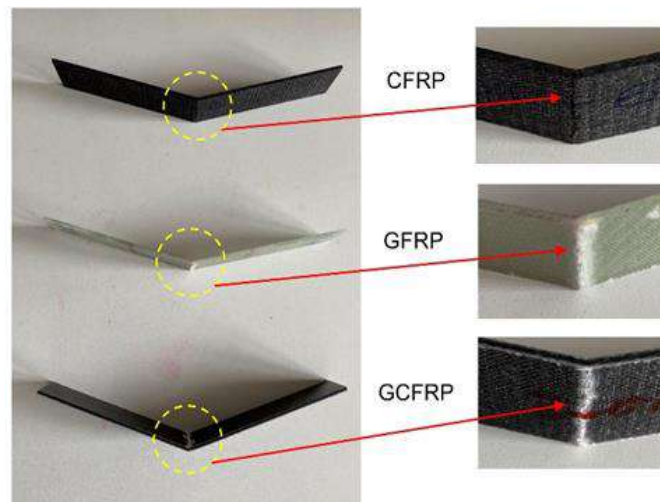
Figure 10. Fracture damage after bending test in CFRP, GFRP and GCFRP composites.

4. Discussion and Conclusions

The flexural strengths of GFRP, CFRP and GCFRP composites aged for 30, 60 and 90 days in different degradation environments were compared and evaluated. The evaluations obtained as a result of this study can be listed as follows:

- As a result of aging of CFRP and GCFRP composites in an artificial seawater environment, it was observed that flexural modulus and flexural strengths decreased more than they did in engine oil and diesel fuel environments.

- When the flexural performances of CFRP composites were examined, it was determined that the environment that changed the flexural modulus and flexural stress the most was the engine oil environment. When the flexural performance of the glass-carbon hybrid composites was examined, it was concluded that the flexural strengths and flexural modulus values were close to those of GFRP composites.

- In the present study, a scientific approach was presented about the effects of degradation and mechanical changes to marine vessels with a composite structure, composite engine piston applications, and to oil tank designers through seawater environment, engine oil environment, and diesel fuel environment, respectively.

- Designers can improve strength in different environmental conditions by changing the glass/carbon arrays for layered composite design and modelling.

Acknowledgements

References

Chen, Dongdong, Guangyong Sun, Maozhou Meng, Xihong Jin, and Qing Li. 2019. "Flexural Performance and Cost Efficiency of Carbon/Basalt/Glass Hybrid FRP Composite Laminates." *Thin-Walled Structures* 142 (March): 516–31.

Cheng, Mingyang, Yucheng Zhong, Umeyr Kureemun, Dongfeng Cao, Haixiao Hu, Heow Pueh Lee, and Shuxin Li. 2020. "Environmental Durability of Carbon/Flax Fiber Hybrid Composites." *Composite Structures* 234 (November 2019): 111719.

Chiang, Chin Lung, Hsin Yin Chou, and Ming Yuan Shen. 2020. "Effect of Environmental Aging on Mechanical Properties of Graphene Nanoplatelet/Nanocarbon Aerogel Hybrid-Reinforced Epoxy/Carbon Fiber Composite Laminates." *Composites Part A: Applied Science and Manufacturing* 130 (November 2019): 105718.

Felipe, R. C.T.S., R. N.B. Felipe, A. C.M.C. Batista, and E. M.F. Aquino. 2019. "Influence of Environmental Aging in Two Polymer-Reinforced Composites Using Different Hybridization Methods: Glass/Kevlar Fiber Hybrid Strands and in the Weft and Warp Alternating Kevlar and Glass Fiber Strands." *Composites Part B: Engineering* 174 (October).

G, Velmurugan, Shaafi T, Bhagavathi M.S, and Siva Shankar V. 2022. "Evaluate the Tensile, Flexural and Impact Strength of Hemp and Flax Based Hybrid Composites under Cryogenic Environment." *Materials Today: Proceedings* 50: 1326–32.

Ghabezi, Pouyan, and Noel Harrison. 2020. "Mechanical Behavior and Long-Term Life Prediction of Carbon/Epoxy and Glass/Epoxy Composite Laminates under Artificial Seawater Environment." *Materials Letters* 261: 127091.

Humeau, Corentin, Peter Davies, and Frédéric Jacquemin. 2018. "An Experimental Study of Water Diffusion in Carbon/Epoxy Composites under Static Tensile Stress." *Composites Part A: Applied Science and Manufacturing* 107: 94–104.

Kafodya, Innocent, Guijun Xian, and Hui Li. 2015. "Durability Study of Pultruded CFRP Plates Immersed in Water and Seawater under Sustained Bending: Water Uptake and Effects on the Mechanical Properties." *Composites Part B: Engineering* 70 (March): 138–48.

Kootsookos, A., and A. P. Mouritz. 2004. "Seawater Durability of Glass- and Carbon-Polymer Composites." *Composites Science and Technology* 64 (10–11): 1503–11.

Kumar, Bhavesh G., Raman P. Singh, and Toshio Nakamura. 2002. "Degradation of Carbon Fiber-Reinforced Epoxy Composites by Ultraviolet Radiation and Condensation." *Journal of Composite Materials* 36 (24): 2713–33.

Li, Chenggao, Xiaoli Yin, Yancong Liu, Rui Guo, and Guijun Xian. 2020. "Long-Term Service Evaluation of a Pultruded Carbon/Glass Hybrid Rod Exposed to Elevated Temperature, Hydraulic Pressure and Fatigue Load Coupling." *International Journal of Fatigue* 134 (January): 105480.

Mula, S., T. Bera, P. K. Ray, and B. C. Ray. 2005. "Effects of Hydrothermal Aging on Mechanical Behavior of Sub-Zero Weathered GFRP Composites:" 25 (6): 673–80.

Nayak, B. Arnimesh, Shubham, Rajesh Kumar Prusty, and Bankim Chandra Ray. 2020. "Effect of Nanosilica and Nanoclay Reinforcement on Flexural and Thermal Properties of Glass Fiber/Epoxy Composites." *Materials Today: Proceedings* 33: 5098–5102.

Peterson, Edward C., Ranjit R. Patil, Alan R. Kallmeyer, and Kenneth G. Kellogg. 2008. "A Micromechanical Damage Model for Carbon Fiber Composites at Reduced Temperatures:"

Rathore, Dinesh Kumar, Rajesh Kumar Prusty, Sarat Chandra Mohanty, Bhanu Pratap Singh, and Bankim Chandra Ray. 2017. "In-Situ Elevated Temperature Flexural and Creep Response of Inter-Ply Glass/Carbon Hybrid FRP Composites." *Mechanics of Materials* 105: 99–111.

Shin, Kwang Bok, Chun Gon Kim, and Chang Sun Hong. 2003. "Correlation of Accelerated Aging Test to Natural Aging Test on Graphite-Epoxy Composite Materials." *Journal of Reinforced Plastics and Composites* 22 (9): 849–61.

Shokrieh, Mahmood M., and Alireza Bayat. 2007. "Effects of Ultraviolet Radiation on Mechanical Properties of Glass/Polyester Composites." *Journal of Composite Materials* 41 (20): 2443–55.

Tanks, Jonathon D., Yoshihiko Arao, and Masatoshi Kubouchi. 2018. "Diffusion Kinetics, Swelling, and Degradation of Corrosion-Resistant C-Glass/Epoxy Woven Composites in Harsh Environments." *Composite Structures* 202 (March): 686–94.

Zeltmann, Steven Eric, Ronald L. Poveda, and Nikhil Gupta. 2015. "Accelerated Environmental Degradation and Residual Flexural Analysis of Carbon Nanofiber Reinforced Composites." *Polymer Degradation and Stability* 121: 348–58.

Some Considerations on Correlation Between Port Equipment Maintenance and Environmental Aspects

Deda Đelović[1*]

Abstract: Results of researches which can be found in available literature sources, confirm that some environmental aspects (emissions in air, water pollution, etc.) in the seaports are caused by factors directly related to the port equipment (port equipment technological adequacy degree, port equipment downtime, etc.). If the role which maintenance has in preventing and eliminating port equipment downtimes is taken into account, than correlation between the port equipment maintenance and environmental aspects becomes clear.

After a general overview on the sea port`s sustainable development and some elements of theoretical analyses of top 10 environmental priorities of the port sector and their evolution over the years (according to European Sea Port Organization Environmental Report 2021), key environmental aspects in the handling process with dry bulk cargoes are identified. In the next phase of made considerations, port equipment downtime in the cargo handling process is defined as one of principal reasons for environmental aspects appearance. Through the final phase of considerations, some elements which determine role of the port equipment maintenance in the environmental aspects optimization are analyzed. Concrete results presented in this paper are related to the environmental management system and port equipment maintenance system in the Port of Bar (Montenegro).

Keywords: environmental aspects, port equipment maintenance.

1. Introduction

Ports form a vital link in the overall trading chain (Esmer, 2008). Seaports play a role of utmost importance and acts as an incentive to the development of marine economy in particular and national economy in general (http://m.tapchiqptd.vn). The importance of seaports for countries cannot be underestimated. Benefits to the National Economy - maritime ports work to employ manpower and reduce the size of unemployment in the country, as well as to increase imports to the country itself and work to revive the countries that have ports (https://tijaratuna.com).

[1] Port of Bar, Obala 13.jula 2, 85 000 Bar, Montenegro

Correspoding author: djelovic.deda@gmail.com

Ports constitute an important economic activity in coastal areas. The higher the throughput of goods and passengers year-on-year, the more infrastructure and associated services are required (www.vliz.be). Ports are no longer the maritime services providers of the past. They are multimodal transport and logistics centres, focal points of leisure and tourism, and, increasingly also, hubs for sustainable industry and clean energy (ESPOa, 2021). Ports serve as important transportation hubs that facilitate goods movement to businesses in local communities and worldwide markets (www.epa.gov).

All transport modes need to become more sustainable, with green alternatives widely available and the right incentives put in place to drive the transition (https://transport.ec.europa.eu).

Sustainble development of ports has to be based on reliable bases, officially adopted and widely recognized. In that sense, here are systematized some of the principal elements of strategic documents at the European Union level, as well as at National level (in Montenegro) where port sustainable development goals and directions can be recognized/are defined.

Sustainable and Smart Mobility Strategy – putting European transport on track for the future (European Commission, 2020)**:** - Mobility and transport matters to us all. From daily commuting to work, visiting family and friends, tourism, to the proper functioning of global supply chains for the goods; - the most serious challenge facing the transport sector is to significantly reduce its emissions and become more sustainable; - ports should become multimodal mobility and transport hubs, linking all the relevant modes. This will improve air quality locally thereby contributing to improved health of nearby residents. Inland and sea ports have a great potential to become new clean energy hubs for integrated electricity systems, hydrogen and other low-carbon fuels, and testbeds for waste reuse and the circular economy;

The European Green Deal (European Commission, 2019)**: -** The European Green Deal calls for a 90% reduction in greenhouse gas emissions from transport, in order for the EU to become a climate-neutral economy by 2050, while also working towards a zero-pollution ambition. To achieve this systemic change, it is needed to (European Commission, 2020): (1) make all transport modes more sustainable, (2) make sustainable alternatives widely available in a multimodal transport system and (3) put in place the right incentives to drive the transition. These are the three pillars of our future actions; - The European Green Deal calls for a substantial part of the 75% of inland freight carried today by road to shift to rail and inland waterways. Short-sea shipping and efficient zero-emission vehicles can also contribute to greening freight transport in Europe (European Commission, 2020).

The 2030 Agenda for Sustainable Development (https://sdgs.un.org/goals) - adopted by all United Nations Member States in 2015, provides a shared blueprint for peace and prosperity for people and the planet, now and into the future. At its center are the 17 Sustainable Development Goals (SDGs), which are an urgent call for action by all countries - developed and developing - in a global partnership. The 17 SDGs are integrated—they recognize that action in one area will affect outcomes in others, and that development must balance social, economic and environmental sustainability (www.undp.org). Following SDGs are directly connected with reducing environmental impact of the port area (www.epa.gov): SDG3- good health and wellbeing, SDG7 – affordable and clean energy, SDG8 – decent work and economic growth, SDG9 – industry, innovation and infrastructure, SDG11 – sustainable cities and

communities, SDG12 – responsible consumption and production, SDG13 – climate action, SDG14 – life below water, SDG15 – life on land, SDG17 – partnership for the goal;

National Strategy of Sustainble Development - 2030 (NSSD) (Ministry of sustainble development and tourism, 2016)**: -** within the strategic goal of the NSSD related to mitigating the impact of climate change are defined measures to reduce the level of greenhouse gas emissions by 2030 by 30%, compared to 1990; - the key sectors for increasing resource efficiency are: energetic sector, construction, agriculture, transport, and the service sector, i.e. tourism;
- in the case of transport, it is important to promote modes of transport that are more favorable for the environment, to define and apply incentive measures in this sense, as well as to apply instruments to minimize the negative impact of transport on the environment

Development Strategy of Transport System in Montenegro – 2019 - 2035 (Ministry of traffic and maritime affairs, 2019)**: -** specific goal 1.4. - improve the connectivity of the Port of Bar - port infrastructure and services should be improved in order to support intermodal activities and potentially attract additional flows of passenger and cargo traffic; - specific goal 2.3. - revitalization and/or reconstruction of the maritime transport infrastructure; - Port of Bar operates significantly below its capacity. The main barriers for using the port's opportunities from regional markets are: lack of adequate infrastructure, etc.

Development Strategy of Maritime Economy in Montenegro – 2020 - 2030 (Ministry of traffic and maritime affairs, 2020)**: -** strategic goals of the integrated maritime policy - 5. the growth of the maritime economy is based on the principles of the green economy; - operational objective: 5.1 to create appropriate conditions in the public and private maritime sector for economic growth based on the principles of the green economy.

Evolution of the environmental priorities in the European Union ports is shown with the next table (Table 1.).

Table 1. Evolution of the environmental priorities in the European Union ports

Priority	2017	2018	2018/ 2017	2019	2019/ 2018	2020	2020/ 2019	2021	2021/ 2020	2021/2017	**Average rank**	
AQ-Air Quality	1	1	const.	1	const.	1	const.	1	const.	const.	**1**	**1**
EE-Energy Consumption	2	2	const.	2	const.	3*	-1	3	const.	-1	**2,4**	**2**
NO-Noise	3	3	const.	4	-1	4	const.	4	const.	-1	**3,6**	**3**
WQ-Water quality	4	8	- 4	10	-2	7	+3	6	+1	-2	**7**	**7**
DO-Dredging operations	5	9	- 4	9	const.	9	const.	8	+1	-3	**8**	**8**
PW-Garbage/Port waste	6	10	- 4	7	+3	8	-1	10	-2	-4	**8,2**	**10**
PD-Port development (land related)	7	6	+1	8	-2	10	-2	9	+1	-2	**8**	**8**
LC-Relationships with the local community	8	4	+4	5	-1	5	const.	5	const.	+3	**5,4**	**5**

SW-Ship waste	9	5	+4	6	-1	6	const.	7	-1	+2	**6,6**	**6**
CC-Climate changes	10	7	+3	3	+4	2	+1	2	const.	+8	**4,8**	**4**

(source: an analysis done based on (ESPO b, 2021))

*)From the year 2020, priority "Energy Consumtion" is renamed to "Energy Efficiency".

In the Table 1. are presented changes of the environmental priorities in the European Union ports in the period from 2017 to 2021. If the whole period is considered, than following principal conclusions are clear: - Air quality (AQ) was constantly the first priority;
- the biggest advancement (+8) is related to priority Climate changes (CC), from the rank "10" in 2017 to the rank "2" in 2021; - priority Garbage/Port waste fall from the rank "6" in the 2017 to the rank "10" in 2021.

2. Identification of Environmental Aspects in the Handling Process with Dry Bulk Cargoes

An **e**nvironmental aspect is defined in ISO 14001:2015 as an element of an organization's *activities*, *products* or *services* that may impact, or does impact, the environment. An environmental impact is a result of an environmental aspect
(https://14000store.com).

There are six categories of Environmental Aspects (https://14000store.com): Emissions to Air, Releases to Water, Waste Management, Contamination of Land, Consumption of Natural Resources and Raw Materials, Other Environmental Issues (noise, odors, etc.).

Another way to classify environmental aspects is to break them down to areas in organization of where they could arise (https://14000store.com): Within the office, During Manufacturing Processes, Transportation, Boilers or other machinery.

Classifications will help to understand and determine what control an organization have over environmental aspects and prioritize any that may need to be controlled. These categories are (https://14000store.com): Controlled, Influenced, Significant, Nonsignificant, Positive.

Environmental risk is particularly difficult to define except in terms of specific items such as spills. Some of the problems with the measurement of environmental risk are (Eni SpA, 2019): some environmental discharges are continuous but have indeterminate effects; some environmental hazards are short term in duration but have long term effects changing over time; some environmental hazards may have quite different effects on, for example, air quality, water quality and ecology, making a global measure of environmental risk difficult to define.

In assessing environmental risk, one should pay attention to separate risks from impacts. Risks refers to acute phenomena, impacts normally refers to chronic effects (that may be negative but also positive) (Eni SpA, 2019).

The risk assessment of environmental pollution is reduced to the calculation of product of two factors, as follows: - Frequency factor (probability of aspect occurrence); - Factor of seriousness

of environmental consequences, which that aspect has caused (Milosavljevic, 2003; Staletovic et al., 2012; Kokic Arsic et al., 2006).

Risk of environmental pollution (R) is calculated as the product of the probability of occurrence the frequency of a particular aspect of the environment (VU) and the seriousness of consequences for the quality of primary environmental factors (air, water, land, etc.) (TP) as follows: R=VU x TP (Staletovic et al., 2012).

2.1 Object of research

Object of research is cargo handling process with dry bulk cargoes in the Port of Bar (Montenegro), as this class of cargoes dominated in the overall throughput for the period from 2017 to 2021 (as shown with the Table 2.) as well as environmental management system and port equipment maintenance system in the Port of Bar (Montenegro).

Table 2. Throughput structure in the Port of Bar (Montenegro)
for the period from 2017 to 2021

Year	Overall throughput (t)	Dry bulk cargoes		Ro-Ro and general cargoes		Liquid bulk cargoes	
		quantity (t)	share (%)	quantity (t)	share (%)	quantity (t)	share (%)
2016	1,209,186.70	833,924.23	68.97%	121,589.99	10.06%	253,672.47	20.98%
2017	1,700,204.86	1,349,415.40	79.37%	83,181.86	4.89%	267,607.59	15.74%
2018	1,382,563.42	1,035,112.00	74.87%	67,280.94	4.87%	280,170.48	20.26%
2019	1,562,003.91	1,223,176.54	78.31%	69,688.55	4.46%	269,138.82	17.23%
2020	1,645,542.36	1,380,555.21	83.90%	40,834.98	2.48%	224,152.18	13.62%
2021	1,457,244.89	1,142,953.56	78.43%	49,692.87	3.41%	264,598.46	18.16%

(source: Port of Bar, 2022)

2.2 Objective of research

Objective of reasearch has following components: - identification of environmental aspects in the cargo handling process with dry bulk cargoes; - identification of factors which causing environmental aspects; - defining interconnections between environmental aspects and port equipment maintenance; - defining environmental priorities based on identified environmental aspects.

2.3 Hypothesis of reasearch

H: An environmental priority in a port depends on port equipment maintenance, too.

2.4 Research methodology

Elements of methodology used for conducting this research is shown with the Table 3. Raws of the Table 3. reffered to methodology phase whose resuslts are presented in this paper (in total or partially) are shadowed.

Table 3. Elements of methodology

PHASE (F_i)	DOCUMENTARY BASE/FORM OF DATA SYSTEMATIZATION	PLANNED RESULT (PR_j)
FZ_1: Throughput structure analysis (yearly)	**Documentary base** Report on throughput structure per year (Port Information System) **Form of data systematizaton**	PR_1: Share (%) of cargo group in overall throughput

Year	Throughput	Dry bulk		Ro-Ro/ general		Liquid	
	(t)	quantity (t)	share (%)	quantity (t)	share (%)	quantity (t)	share (%)

Table 3. - continuation
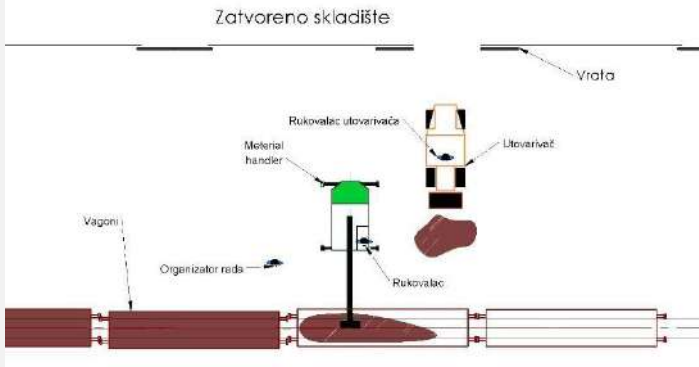
FZ$_2$: An analysis of cargo handling technology, per cargo types, c$_i$, and operations, o$_j$	Documentary base Cargo Handling Technology (per cargo type and operations with that type of cargo)	PR$_2$: Identified types of port equipment, E$_{jm}$, used in realization of handling operation with concrete type of dry bulk cargo

Documentary base
Cargo Handling Technology
(per cargo type and operations with that type of cargo)

TEHNOLOGIJA RADA

RASUTI TERETI – R011: KONCENTRAT BAKRA

Form of data systematizaton

Cargo type, c$_i$	Operation, o$_j$	Description of operation per phases, PH$_{jk}$	Used resources per operation – all phases, Rjl	Port equipment – all pahses, E$_{jm}$	
...					

Operation: Vagon – Closed warehouse – used resources
(given as an exapmple)

FZ$_3$: Identification of environmental aspects, EA$_{jk}$, per dry bulk cargo types and operations (excluding dangerous goods)	Documentary base	PR$_3$: Environmental aspects per dry bulk cargo types and operations, EA$_{jk}$: Emissions to Air (E-A), Releases to Water (R-W), Waste Management (WM), Contamination of Land (C-L), Consumption of Natural Resources and Raw Materials (C-R), Other Environmental Issues – noise (O-N) – odors (O-O).

Documentary base

- documentation related to cargo handling process planning, realization and control;
- literature sources,
- standard – general international and specific for port operations.

Form of data systematizaton

Cargo type, c$_i$	Operation, o$_j$	Operation phases, PH$_{jk}$	Environmental aspects per operation phase, EA$_{jk}$
...			

Table 3. - continuation

FZ$_4$: Defining level of risk of environmental pollution, R$_{jk}$, related to environmental aspects, EA$_{jk}$	Documentary base - documentation related to cargo handling process planning, realization and control; - literature sources, - standard – general international and specific for port operations. Form of data systematization 	Environmental aspects, EA$_{jk}$	Risks, R$_{jk}$
			PR$_4$: Defined level of risks of envirinmental pollution, R$_{jk}$, related to environmental aspects, EA$_{jk}$
---	---	---

FZ$_5$: Generalization of environmental aspects per operations with dry bulk cargo (excluding dangerous goods)	Documentary base - documentation related to cargo handling process planning, realization and control; - literature sources, - standard – general international and specific for port operations. Form of data systematization 	Operation, O	Environmental aspects per operation – all, E
			PR$_5$: Environmental aspects per operations with dry bulk cargoes - summary
---	---	---
FZ$_6$: Identifying classes of factors which generate environmental aspects, EA$_{jk}$, per operations and dry bulk cargo types	Documentary base - documentation related to cargo handling process planning, realization and control; - literature sources, - standard – general international and specific for port operations. Form of data systematization 	Cargo type, c$_i$	Operation, o$_j$	Environmental aspects, EA$_{jk}$	Classes of factors, F$_{jk}$, which are generating environmental aspects, EA$_{jk}$
---	---	---	---
...					PR$_6$: Classes of factors, F$_{jk}$, which generate environmental aspects, EA$_{jk}$, per operations and dry bulk cargo types
FZ$_7$: An analysis of class of factors related to port equipment used in the handling operations with dry bulk cargo	Documentary base - documentation related to cargo handling process planning, realization and control; - literature sources, - standard – general international and specific for port operations.	PR$_7$: Elements of class of factors related to port equipment

Table 3. - continuation

| FZ$_8$: Establishing data base for defining correlations between environmental aspects, EA$_{jk}$, and parameters which characterize port equipment maintenance, EM$_{jm}$ | Documentary base

- documentation related to cargo handling process planning, realization and control;
- literature sources,
- standard – general international and specific for port operations.

Form of data systematization

A) Identification environmental aspects (EA$_{jk}$) directly caused by factors related to port equipment, E$_{jm}$ (defining data series)
<table><tr><td>No.</td><td>Date</td><td>Shift</td><td>Time</td><td>EA$_{jk}$</td><td>Description</td><td>Quantification</td><td>Port equipment, E$_{jm}$</td></tr><tr><td>...</td><td></td><td></td><td></td><td></td><td></td><td></td><td></td></tr></table>
B) Identification of parameters related to port equipment maintenance, EM$_{jm}$, causing environmental asepcts (defining data series)
<table><tr><td>No.</td><td>EA$_{jk}$</td><td>Port equipment, E$_{jm}$</td><td>Parameters related to maintenance, EM$_{jm}$</td></tr><tr><td></td><td></td><td></td><td></td></tr></table> | PR$_8$: Established data series for defining correlations between environmental aspects, EA$_{jk}$, and parameters which characterize port equipment maintenance, EM$_{jm}$ |
| FZ$_9$: An analysis of role and importance of the port machinery in context of identified elements of class of factors related to port equipment | Documentary base

- documentation related to cargo handling process planning, realization and control;
- literature sources,
- standard – general international and specific for port operations. | PR$_9$: Identified role and importance of maintenance of port equipment maintenance |

Remark: "FZ" – phase of the methodology: "PR" – planned result of methodology phase;

3. Results of Research
3.1 Result: Identified types of port equipment used in the handling operations with dry bulk cargoes

Based on the defined cargo handling technoologies with dry bulk cargoes (Port of Bar, 2022), in the Table 4. are presented results of analyses of port equipment classes used in the handling operations with dry bulk cargoes.

Table 3. - continuation

FZ_{10}: Establishing mathematical correlations between parameters characteristic for environmental aspects, EA_{jk} (quantiy of spilled cargo, intensity of emissions in air, ...) and parameters related to port equipment maintenance, E_{jm}	Documentary base	PR_{10}: Mathematical correlations between parameters characteristic for environmental aspects, EA_{jk} (quantiy of spilled cargo, intensity of emissions in air, ...) and parameters related to port equipment maintenance, E_{jm}
	- documentation related to cargo handling process planning, realization and control; - literature sources, - standard – general international and specific for port operations, - data series formed through the previous phases of methodology implementation .	

Table 4. Port equipment per cargo handling operations

Cargo	Operations	Port equipment (moveable)									
		GC	MHC	MH	SL	MC	WL	FL	TR	grab	spreader
DBC - Dry bulk	DBC_1 - wagon – open storage area (and vice versa)	*					*			*	
	DBC_2 -wagon – closed warehouse (and vice versa)			*			*			*	
	DBC_3 -Truck – open storage area (and vice versa)						*				
	DBC_4 -Truck – closed warehouse (and vice versa)						*				
	DBC_5 - Container – closed warehouse (tipping)						*		*		
	DBC_6 -Stuffing containers						*				
	DBC_7 -Ship - open storage area (and vice versa)		*							*	

Table 4.

	Operations	GC	MHC	MH	SL	MC	WL	FL	TR
	DBC_8 -Ship – closed warehouse (and vice versa)		*				*	*	
	DBC_9 -Ship – silo	*						*	
	DBC_{10} – Silo – ship			*					
	DBC_{11} - Wagon – silo (and vice versa)				*				
	DBC_{12} -Truck – silo (and vice versa)								

Remark: GC – gantry crane; MHC – mobile harbour crane; MH – material handler; SL – ship loader; MC – mobile crane; WL – wheel loader; FL – fork lift; TR – truck;

3.2 Result: Generalization of environmental aspects per operations with dry bulk cargoes

In the Table 5. are identified environmental aspects per cargo handling operations with dry bulk cargoes (general case related to dry bulk cargoes as a class): Emissions to Air (E-A), Releases to Water (R-W), Waste Management (W-M), Contamination of Land (C-L), Consumption of Natural Resources and Raw Materials (C-R), Other Environmental Issues - noise (O-N), odors (O-O).

Table 5. Environmental aspects in the handling operations with dry bulk cargoes

Cargo	Operations	Environmental Aspects (top five)						
		E-A	R-W	W-M	C-L	C-R	O-N	O-O
DBC - Dry bulk	DBC_1 - wagon – open storage area (and vice versa)	*	*	*		*	*	
	DBC_2 -wagon – closed warehouse (and vice versa)	*	*	*		*	*	
	DBC_3 -Truck – open storage area (and vice versa)	*	*	*		*	*	
	DBC_4 -Truck – closed warehouse (and vice versa)	*	*	*		*	*	
	DBC_5 -Container – closed warehouse (tipping)	*	*	*		*	*	
	DBC_6 -Stuffing containers	*	*	*		*	*	
	DBC_7 -Ship - open storage area (and vice versa)	*	*	*		*	*	
	DBC_8 -Ship – closed warehouse (and vice versa)	*	*	*		*	*	
	DBC_9 -Ship – silo	*	*	*		*	*	
	DBC_{10} –Silo-ship	*	*	*		*	*	
	DBC_{11} -Wagon – silo (and vice versa)	*	*	*		*	*	

DBC$_{12}$ -Truck – silo (and vice versa)	*	*	*		*	*	
Number of appearances	12	12	12	12		12	12

3.3 Result: Classes of factors which generate environmental aspects - general

Based on the results of analyses shown with tables 4. and 5., per each operation with dry bulk cargo can be defined relations between environmental aspects and port equipment used in operations in a form of matrix (as examples are given: Table 6. – a matrix related to operation DBC$_1$ – wagon to open storage area (and vice versa); Table 7. – a matrix related to operation DBC$_2$ – wagon to closed warehouse (and vice versa).

Table 6. Matrix related to operation DBC$_1$ – wagon to open storage area (and vice versa)

Port equipment	Environmental Aspects (top five)						
	E-A	R-W	W-M	C-L	C-R	O-N	O-O
Gantry crane	*	*	*		*	*	
Wheel loader	*	*	*		*	*	
Grab	*	*	*			*	

Table 7. Matrix related to operation DBC$_2$ – wagon to closed warehouse (and vice versa)

Port equipment	Environmental Aspects (top five)						
	E-A	R-W	W-M	C-L	C-R	O-N	O-O
Material handler	*	*	*		*	*	
Wheel loader	*	*	*		*	*	
Grab	*	*	*			*	

Principal classes of factors which generate environmental aspects are, F$_{jk}$:
- F$_{1k}$ - Human factors (improper operating, opening grab at the bigger heights than recommended, ...);
- F$_{2k}$ – Factors related to port infrastructure (problems with power supply, ...);
- F$_{3k}$ – Factors related to port equipment: technical and exploitation performances of port equipment (energy consumption per hour, etc.); port equipment technological adequacy; port equipment downtime frequency; port equipment life cycle phase; etc.;
- F$_{4k}$ – Cargo characteristics;
- F$_{5k}$ – Factors related to port warehouses (open and closed); -   F$_{6k}$ – Factors related to system of dust reduction/elimination;
- F$_{7k}$ – Factors related to system of surface waters treatment; etc.

3.4 Result: Role and importance of port equipment maintenance

Resepcting two groups of previously presented results – established correlation between environmental aspects and port equipment per cargo handling operation and recognized group of factors related to port equipment as one of environmental aspects generators, than role and

importance of the port equipment maintenance and its correlation with environmental aspects can be clearly recognized.

Like other industries with the need for consistent turnaround rates, the shipping industry depends on port equipment and trained operators to maximize uptime. Improper maintenance can significantly decrease the productivity rates projected during an operational assessment (https://blog.sennebogen-na.com). General inter-connections between cargo handling system and port equipment maintenance system in a seaport are very complex (Delovic a, 2005).

Previous analyses have established that one of the basic patterns of the appearance of environmental aspects is downtime in the exploitation of port equipment.
The negative consequences of environmental aspects (their character, volume and intensity) are determined by the parameters that determine downtime (type of downtime, its manifestation, ...)

Previously mentioned represent a key basis for identifying the role of maintenance in the optimization of environmental aspects in the handing process with dry bulk cargoes. The role of maintenance is minimization of both: the number of occurrences and the duration of downtime, respecting the adopted management criteria

Introducing the effects of maintenance activities (in the optimization of environmental aspects during cargo handling operations) into the optimal area implies adequately modeled and appropriately implemented actions on:
• establishment of the optimal maintenance organizational model;
• choosing the optimal maintenance concept;
• optimal use of maintenance resources (maintenance personnel; maintenance materials; spare parts; machines; tools; equipment; maintenance workshop); etc.

At the same time, all elements of the maintenance system should be constantly improved.

3.5 Result: Elements of correlation between the port equipment costs and costs related to environmental aspects

The necessity of optimal implementation of maintenance activities in order to minimize the number of occurrences and the duration of the state of "out of order" (downtime) of port equipment can be illustrated from the aspect of costs that are a consequence of its downtime in the cargo handling process. The costs, C_u, that occur during this can be mathematically interpreted as follows (on the basis of (Delovic b, 2005):

$$C_u = \sum_{i=1}^{n} c_i \qquad (1)$$

where: c_i – costs components (i = 1, 2, ..., n);

Respecting the objective of the subject research, the following two components of costs are considered in particular:

- c_1 – costs of interrupting the cargo handling process;
- c_2 – costs of environmental aspects;

Components c_1 and c_2 are of complex structures.

$$c_1 = \sum_{j=1}^{m} c_{1j} \qquad (2)$$

where: c_{1j} – components of costs of interrupting the cargo handling process (j = 1, 2, ..., m);

The most significant (with the largest share) components of costs c_1 are: c_{11} – costs that are a consequence of reducing labor productivity; c_{12} – costs that are a consequence of "pausing" in the time allowed for the execution of the service; c_{13} – costs incurred due to the reduction of the labor force utilization ratio; c_{14} – costs incurred due to the reduction of the coefficient of utilization of port equipment; c_{15} – costs of reducing the trust of service users towards the port; ...

$$c_2 = \sum_{k=1}^{p} c_{2k} \qquad (3)$$

where: c_{2k} – components of costs related to environmental aspects (k = 1, 2, ..., p);

From the set of c_{2k} cost components, the following are specifically mentioned:

c_{21} – costs of prevention and removal of consequences of air emissions; c_{22} – costs of prevention and removal of consequences of releases to water; c_{23} – waste management costs; c_{24} – costs related to the consumption of energy and natural resources; c_{25} – costs of prevention and elimination of noise consequences; ...

By defining the above mentioned (and other) cost components in a certain time interval, the basis for quantifying the role of maintenance in the process of optimizing (reducing to absolute minimum) the negative effects of environmental aspects during cargo handling is established.

4. Discussion and Conclusions

Results of the research shown in this paper confirm following top five environmental aspects in the handling operations with dry bulk cargoes in the Port of Bar (Montenegro): emissions to air, releases to water, waste management, consumption of natural resources and raw materials and noise.

Based on the identified priority environmental aspects, environmental priorities for the Port of Bar can be defined: Air Quality, Water Quality, Port Waste, Ship Waste, Energy Efficiency (Energy Consumption), Noise, Local Community.

By the results of research, its starting hypothesis is confirmed: based on identified correlations between environmental aspects in the handling operations with dry bulk cargo and port equipment maintenance, and clear links among environmental aspects and environmental priorities, conlusion is that an environmental priority in the port depends on port equipment maintenance, too.

All defined objectives of the research are achieved: environmental aspects in the cargo handling process with dry bulk cargoes (per operations) are identified; - factors which causing environmental aspects are identified; - interconnections between environmental aspects and port equipment maintenance are defined; - environmental priorities based on identified environmental aspects are defined, too.

Author plans to continue researches in this field in accordance with defined methodology, trying to define relations which adequately describe interconnections between parameters wich characterize environmental aspects and parameters which characterize port equipment maintenance.

References

Delovic, D., (2005). Some Aspects of Correlation Between Cargo Handing System and Port Machinery Maintenance System, International Journal "Total Quality Management and Excellence", 4 (33).

Delovic, D., (2005). Elementi korelacije održavanje – aspekti životne sredine u procesu pretovara generalnih tereta, Zbornik radova sa Konferencije održavanja "KOD 2005", Bar.

Economic importance of ports. https://www.vliz.be/projects/sail/fiches/10.pdf (date of approach: 19.04.2022).

Eni SpA, (2019). HSE Risk Management and Reporting, Professional Operating Instruction, Procedure "Opi sg hse 001 ups r03", Milan.

Esmer, S., (2008). Performance Measurements of Container Terminal Operations, Dokuz Eylul Universitesi. http://www.sbe.deu.edu.tr/dergi/cilt10.say%C4%B11/10.1 %20esmer.pdf (date of approach: 07.04.2022).

ESPO Green Guide 2021 - A Manual for European Ports Towards a Green Future (2021). https://www.espo.be/media/ESPO%20Green%20Guide%202021%20-%20FINAL.pdf, p.2 (date of approach: 22.06.2022).

ESPO Environmental Report 2021-EcoPortsinSights (2021). https://www.espo.be/media/ESP-2844%20(Sustainability%20Report%202021)_WEB.pdf (date of approach: 18.05.2022).

European Commission, (2020). COM/2020/789 final Sustainable and Smart Mobility Strategy. https://eur-lex.europa.eu/legal-content/EN/TXT/?uri=CELEX:52020DC0789 (date of approach: 25.06.2022).

European Commission, (2019). COM/2019/640 final European Green Deal. https://ec.europa.eu/info/strategy/priorities-2019-2024/european-green-deal/transport-andgreen-deal_en (date of approach: 02.07.2022).

https://tijaratuna.com/en/importance-of-seaports/ (date of approach: 18.04.2022).

https://www.epa.gov/community-port-collaboration/ports-primer-21-role-ports#:~:text=Ports%20serve%20as%20important%20transportation,local%20communities%20and%20worldwide%20markets (date of approach: 24.06.2022).

https://transport.ec.europa.eu/transport-themes/mobility-strategy_en (date of approach: 24.06.2022).

https://www.undp.org/sustainable-development-goals (date of approach: 16.05.2022).

https://14000store.com/articles/what-is-an-environmental-aspect/ (date of approach: 19.05.2022).

https://blog.sennebogen-na.com/how-to-maintain-port-equipment (date of approach: 20.06.2022).

Kokic Arsic, A., Milivojevic, J., Kanjevac Milovanovic, K., (2006). Vrednovanje znacaja uticaja aspekata zivotne sredine na primeru firme "Banja Komerc, Zbornik radova sa Festivala kvaliteta 2006, Kragujevac, B36-B39.

Milosavljevic, D., Milovanov, B., (2003). Unapredjenje sistema upravljanja yastitom zivotne sredine po standardima ISO 14000, Journal of Applied Engineering Science, Belgrade, 1 (1), 41-48

Ministry of sustainble development and tourism, (2016). National Strategy of Sustainble Development 2030. Podgorica.

Ministry of traffic and maritime affairs, (2019). Development Strategy of Transport System in Montenegro – 2019 – 2035. Podgorica.

Ministry of traffic and maritime affairs, (2020). Development Strategy of Maritime Economy in Montenegro – 2020 – 2030. Podgorica.

Port of Bar, (2022). Cargo handling technologies with dry bulk cargoes.

Staletovic, S., Kovacevic, S., Kovacevic, M., (2012). Methodological Approach to the Identification and Environmental Impact Assessment for the Project "Magniesite Minning in the Deposit Cavlovac – Masnica". Journal "Mining Engineering"", No.3, 183-194.

Sustainable Development Goals. https://sdgs.un.org/goals (date of approach: 15.05.2022).

The importance of seaports to the country's economy. http://m.tapchiqptd.vn/en/research-and-discussion/the-importance-of-seaports-to-thecountrys-economy-16048.html (date of approach: 17.04.2022).

Ultrasound-assisted extraction of the industrial apple pomace: the effect of solvent and sonication time on antioxidant and antimicrobial activities

Faraja Gonelimali[1,2*], Beatrix Szabó-Nótin[1], Mónika Máté[1]

Abstract: Byproducts from agro-industrial processing of fruits contain an enormous amount of bioactive compounds most of which are useful in food additives. Proper extraction and processing of these compounds are still challenging for their use in food, medicine and cosmetics. In this study, the effects of solvent type and sonication time on antioxidant and antimicrobial activities of the industrial apple pomace were investigated. Food-grade solvents; water, ethanol and acetone were used to obtain extracts from the dried pomace by sonicating for 0, 10, 35 and 60 minutes at 40 kHz. Total phenolic content (TPC), antioxidant and antimicrobial activities were determined by the Folin ciocalteu, Ferric reducing ability of plasma (FRAP) and Agar well diffusion methods respectively. Results indicated that acetone was the best solvent for extracting the apple pomace. It resulted in significantly highest TPC (1.64 - 2.08 mg GAE/g DW) and antioxidant (0.97 - 1.19 mg AAE/g DW) compared to ethanol, TPC (0.95 - 1.35 mg GAE/g DW) antioxidant (0.59 - 0.61 mg AAE/g DW) as well as water TPC (0.48 - 0.63 mg GAE/g DW) antioxidant (0.25 - 0.42 mg AAE/g DW). Moreover, acetone was the only solvent that produced extracts exhibiting antimicrobial activity (Diameter of inhibition zone = 9.33 - 11.00 mm). Sonicating the acetonic pomace for 10 minutes yielded extracts with the best TPC, antioxidant and antimicrobial activity. Acetone should be regarded as the best solvent in producing food additives rich in antioxidants and antimicrobials from the apple pomace as far as ultrasound-assisted extraction is concerned.

Keywords: Apple pomace, Ultrasound-assisted extraction, Antioxidant, Antimicrobial, Food additives

1. Introduction

Agro-industrial waste from fruit processing industries contains an enormous quantity of bioactive compounds, particularly polyphenols. For a long time, there has been an interest in exploiting the use of these compounds in food additives, cosmetics and pharmaceuticals (Peschel et al. 2006; Carunchia et al. 2015; Lizcano et al. 2019; Fernandes et al. 2021). The Polyphenol group is comprised of phenolic acids, anthocyanins and flavonoids. These compounds make fruits an important and healthy foods thanks to their contribution on flavor, color and antioxidant activities (Carvalho and Conte-Junior, 2021). During fruit processing to

[1] Hungarian University of Agriculture and Life Sciences, Institute of Food Science and Technology, Department of Fruit and Vegetable Processing Technology, Budapest, Hungary

[2] University of Dar es Salaam, College of Agricultural Sciences and Food Technology, Department of Food Science and Technology, Dar es Salaam, Tanzania

* Corresponding author: fgonelimali@gmail.com

produce juices, huge quantities of these compounds are left in the byproducts called pomace. Pomace is the solid byproducts of fruit processing obtained after pressing fruits to squeeze out the juice.

Apples (*Malus domestica*) are important agro-industrial fruits that are processed to produce juice, wine and cider. Processing of the apples results in the production of enormous amounts of apple pomace that are richer in polyphenols than the obtained juices (van der Sluis et al. 2005; Persic et al. 2017). Polyphenols are the major chemical compounds present in the apple pomace and some of the specific compounds include chlorogenic acid, catechin, epicatechin and hydrocinamic acid (Fernandes et al. 2019b; Li et al. 2020). These compounds play an important role in the health properties of the apples (Koutsos and Lovegrove, 2015; Rana and Bhushan, 2016), complimenting a famous phrase "*An apple a day keeps the doctor away*". Other constituents of the apple pomace that has found wide application in food products include pectin and dietary fibers (Paraman et al. 2015; Naqash et al. 2017). Generally, compounds found in the apple pomace make the pomace a potential source of raw materials for food additives.

Apple pomace can be regarded as an important source of food additives thanks to their antioxidant properties and antimicrobial activity among others, of their polyphenol compounds. Aqueous and organic solvents extracts of the apple pomace exhibit an interesting gargantuan antioxidant property (Benvenutti et al. 2019; Carpes et al. 2021; Manzoor et al. 2022). The antioxidant is of paramount importance in the food industry as it is a cornerstone of healthy foods. It slows oxidation, a naturally occurring phenomenon in our bodies that results in the formation of free radicals which cause aging, inflammation and chronic diseases including cancer (Shahidi and Ambigaipalan, 2015). Moreover, extracts from apple pomace display antimicrobial activity against a wide range of microorganisms (Carpes et al. 2021; Hammad et al. 2021). These properties can be studied further and exploited for developing natural food additives to replace commonly used synthetic preservatives and antioxidants most of which are increasingly becoming concerned regarding their effect on consumers' healthy.

Therefore, this study aimed at investigating the effect of solvent selection and sonication time on antioxidant and antimicrobial properties of the apple pomace extracts by ultrasound-assisted extraction.

2. Material and Method

2.1 Sample preparation

Apple pomace samples (2020/2021 harvest season) were collected from a juice processing factory (Agrana Juice ltd, Hungary). The pomaces were dried at 60°C in a circulating air oven (LP 232/1, Hungary) for 3 hours to a moisture content of about 10% followed by further drying at a vacuum oven (60°C, 65 mbar) for another 3 hours to reach a final moisture content of about 4%. The dried apple pomace was ground into powder using a multi chopper grinder (PRINCESS) for 20 seconds followed vacuum package and stored in the glass desiccator jar until the day of the extraction.

2.2 Extraction

Extraction was done using the ultrasound-assisted extraction method as described by Riaz et al. (2018) with some modifications. Briefly, 10 g of apple pomace powder were mixed with 200 mL water, acetone (80%) and ethanol (80%) in flasks. The flasks were then placed in a water bath ultrasonic device (HBM 16 liter, Netherlands). Samples were sonicated at 40 kHz, and 240 watts at 20°C for 0, 10, 35 and 60 minutes. After sonication, the pomace was allowed to stay in

contact with the solvent overnight (15 hours) at room temperature followed by centrifugation and then filtration on filter paper under a vacuum. The solvent was removed to about one-third under rotary evaporation (IKA, RV10) followed by further drying at 60°C circulating air oven for complete drying. The amounts of obtained residues were determined and the extraction recovery was deduced using the equation given below. The residues were then dissolved in water to obtain a final concentration of 400 mg/mL and stored at -20°C.

$$Extraction\ recovery\ (\%) = (Weight\ of\ extract \div weight\ of\ the\ pomace) \times 100$$

Where weight of extract is the weight of residues obtained after removal of extraction solvent (g) and weight of the pomace is the initial apple pomace weight mixed with a solvent (10g)

2.3 Total phenolic content

Total phenolic content (TPC) was determined by the Folin ciocalteu method (Singleton and Rossi, 1965). Briefly, 1250µL of the Folin reagent (10% v/v) was pipetted into a test tube followed by 50µL of methanol (80%). Then, 200 µL of the prepared extracts (Dilution 100×) were added and the mixture was allowed to stand for 3 minutes followed by the addition of 1000µLm of the Na_2CO_3 solution (74.2 g/L). The mixture was well shaken and incubated in a water bath at 50°C for 5 minutes followed by reading the absorbance at 760 nm on a spectrophotometer (HITACHI 2900). Gallic acid was used to prepare the calibration curve (R^2 = 0.99) and the results were expressed as mg gallic acid equivalent/g dry weight (mg GAE/g DW) apple pomace.

2.4 Antioxidant activity

Antioxidant activity was determined by the Ferric Reducing Ability of Plasma (FRAP) method (Benzie and Strain, 1996). Briefly, the FRAP reagent was prepared by mixing 3.6 mM Sodium acetate buffer, 20 mM $FeCl_3.6H_2O$ and TPTZ (10 mM TPTZ: 40 mM HCL) in a ratio of 10:1:1. 1500µL of the prepared FRAP reagent was pipetted in the test tube followed by 20µL of the extracts (Dilution 10×) and 30µL of the distilled water. The mixture was then well shaken and allowed to stand for 5 minutes at room temperature followed by measuring the absorbance at 530nm using a spectrophotometer (HITACHI 2900). Ascorbic acid was used to prepare the calibration curve (R^2 = 0.99) and the results were expressed as mg ascorbic acid equivalent/g dry weight (mg AAE/g DW) apple pomace.

2.5 Antimicrobial activity

Antimicrobial activity on the microorganism of food interest, *Listeria innocua* CCM9030, was determined using the agar well diffusion method as described by Balouiri et al., (2016) and Morgan et al., (2022) with some modifications. Briefly, bacteria cells were grown overnight on a Trypticase soy agar (TSA) slant to obtain fresh bacteria cells. Fresh colonies from the TSA slants were then suspended in peptone water (8.5g/L NaCl; 1g/L peptone) and the concentration of cells was adjusted to 0.5 McFarland standard (1.5×10^8 cells /mL) using McFarland Densitometer (DEN-1B, BioSan) followed by dilution (10×) in peptone. 100µL of the prepared bacteria cells (1.5×10^6 cells/mL) was mixed with 25 mL of molten TSA medium in a sterile petri dish. Upon solidification, small wells (6 mm) were made using a sterile tip followed by the addition of 100µL of the apple pomace extracts (400mg/mL) in the respective wells. Water (a solvent used for dissolving the extracts) was added to the respective wells as a negative control. The plates were then left in the biosafety cabinet for 30 minutes to allow the extracts to diffuse into the media. Thereafter, the plates were incubated at 37°C for 24 hours. The

presence of clear zones of inhibition around wells was observed under the light and the diameter was measured using a ruler.

2.6 Statistical analysis

All experiments were done in triplicate or more. There were two investigated factors; Type of solvent which had three levels (Acetone, water and ethanol) and Sonication time which had four levels (0, 10, 35 and 60 Minutes). Normal distribution and homogeneity of variance assumptions were checked by Kolmogorov -Sminorv and Levene's tests respectively. Two-factor complete randomized ANOVA was used for analysis. A Posthoc test using Turkey was conducted for the factors that had shown significant effect at 95% confidence. The evaluation was done using the statistical software IBM SPSS version 20.

3. Results

Extraction recovery of apple pomace was highly influenced by the solvent type F (2, 24) = 20.78, p<0.001 with water resulting in a significantly high amount of the extracts compared to acetone and ethanol. Sonication time alone didn't influence the extraction recovery F (3, 24) = 1.49, p = 0.24, however, the factor had an influence when interacted with the solvent type F (6, 24) = 4.72, p<0.01. The effect of sonication time was observed on acetone and water only (Table 1).

Both solvent type and sonication time had a significant effect on the total phenolic content (TPC) of the apple pomace extract, F (2, 24) = 272.17, p<0.001 and F (3, 24) = 3.84, p<0.05 respectively. Moreover, Interaction between solvent type and sonication time had a significant effect on TPC yield F (6, 24) = 3.68, p<0.01 (Table 2).

The solvent type had a strong influence on the antioxidant activity of the apple pomace extracts F (2, 57) = 330.54, p<0.001. Contrary, Sonication time didn't have effect on the antioxidant activity F (3, 57) = 2.48, p=0.07. The influence of sonicating time was significant only on interacting with the solvent type F (6,57) = 4.78, p<0.001 (Table 3).

Antimicrobial activity of the apple pomace extracts was strongly influenced by solvent type F (2,55) = 6251.33, P<0.001, Sonication time F (3, 55) = 8.47, p<0.001 and the interaction of the two factors F (6,55) = 8.19, p<0.001. Both ethanol and water resulted in extracts that couldn't manifest antimicrobial activity against the tested strain (Table 4).

Table 1. Effect of solvent and sonication time on extraction recovery from apple pomace.

Sonication time (Minutes)	Extraction recovery (%)		
	Acetone	Ethanol	Water
0	27.89 ± 4.22^{aA}	30.20 ± 1.85^{aA}	37.10 ± 0.87^{bB}
10	31.80 ± 0.36^{aB}	29.73 ± 0.46^{aA}	35.20 ± 3.27^{bAB}
35	29.30 ± 2.16^{aAB}	30.80 ± 1.56^{aA}	33.23 ± 0.25^{bAB}
60	29.97 ± 0.57^{aAB}	31.37 ± 1.23^{aA}	30.57 ± 3.22^{aA}

Data represent means of triplicate measurements ± Standard deviation. Superscript small letters indicate the presence/absence of significant differences along the row. Superscript capital letters indicate the presence/absence of significant differences along the column.

Table 2. Effect of solvent type and sonication time on Total phenolic content of the apple pomace

Sonication time (Minutes)	Total phenolic content (mg GAEg^{-1} DW)		
	Acetone	Ethanol	Water
0	2.05 ± 0.12^{cAB}	1.22 ± 0.10^{bAB}	0.48 ± 0.06^{aA}
10	2.08 ± 0.19^{cB}	0.95 ± 0.08^{bA}	0.63 ± 0.04^{aA}
35	1.64 ± 0.20^{cA}	0.99 ± 0.05^{bAB}	0.55 ± 0.20^{aA}
60	1.95 ± 0.12^{cAB}	1.35 ± 0.27^{bB}	0.50 ± 0.15^{aA}

Data represent means of triplicate measurements ± Standard deviation. Superscript small letters indicate the presence/absence of significant differences along the row. Superscript capital letters indicate the presence/absence of significant differences along the column.

Table 3. Effect of solvent type and sonication time on antioxidant activity of the apple pomace.

Sonication time (Minutes)	Ferric reducing ability of plasma (mg AAEg^{-1} DW)		
	Acetone	Ethanol	Water
0	0.92 ± 0.16^{cA}	0.61 ± 0.07^{bA}	0.42 ± 0.05^{aB}
10	1.19 ± 0.19^{cB}	0.59 ± 0.04^{bA}	0.30 ± 0.07^{aA}
35	1.07 ± 0.13^{cAB}	0.58 ± 0.06^{bA}	0.29 ± 0.05^{aA}
60	0.97 ± 0.10^{cAB}	0.59 ± 0.04^{bA}	0.25 ± 0.05^{aA}

Data represent means of triplicate measurements ± Standard deviation. Superscript small letters indicate the presence/absence of significant differences along the row. Superscript capital letters indicate the presence/absence of significant differences along the column.

Table 4. Effect of solvent type and sonication time of apple pomace extracts on inhibition zones of the bacterium *Listeria innocua*.

Sonication time (Minutes)	Diameter of the inhibition zone (mm)		
	Acetone	Ethanol	Water
0	11.00 ± 1.00^{B}	NA	NA
10	10.00 ± 0.00^{AB}	NA	NA
35	10.50 ± 0.58^{B}	NA	NA
60	9.33 ± 0.52^{A}	NA	NA

Data represent means of triplicate measurements ± Standard deviation. Superscript capital letters indicate the presence/absence of significant differences along the column. NA means the inhibition zones were not observed thus statistical analysis was not done

4. Discussion and Conclusions

Sonicating the pomace in acetone for 10 minutes resulted in a significantly higher quantity of extracts compared to that without sonication, however, further sonication resulted in a decrease of the extracts to levels similar to the one without sonication (Table 1). Similar results on aqueous extracts were observed by (Grigoras et al. 2013) who reported the extraction recovery of 27 – 42% for apple pomace from various cultivars. However, for ethanolic extracts, they observed a recovery of 9 – 14% which was much lower than ours. Observation of significant high values of extraction recovery of water extracts could be due to the polarity index of water where it is highly polar than the two solvents thus dissolving a wide range of compounds such as polysaccharides and free sugars (Fernandes et al. 2019a) while acetone and ethanol

selectively dissolve nonpolar compounds. This is evidenced by the fact that although the recovery of the extracts using acetone and ethanol were the least, their biological activities; Total phenolic content (Table 2) and antioxidant activity (Table 3) were significantly much higher than that of water extracts.

The solvent type showed the strongest influence on TPC compared to sonication time. Furthermore, the interaction between solvent type and sonication time had a higher influence on the yield of TPC compared to sonication time (Table 2). The highest amounts of TPC (1.95 – 2.08 mg GAE/g DW) were obtained when acetone was used as extraction solvent and at all sonication times, the amounts of TPC were significantly higher in acetone than in the rest of the solvents. In ethanol, TPC ranged from 0.95 – 1.22 mg GAE/g DW while in water it ranged from 0.48 – 0.63 mg GAE/g DW. Similarly, Rana et al., (2015) obtained the highest amount of TPC 3.31 mg GAE/g DW pomace when 50% acetone was used as extraction solvent compared to ethanol (2.17 mg GAE/g DW). Renard et al., (2001) observed that there is an interaction between the cell walls of the apple pomace and the polyphenols and the interaction affects the extractability of the polyphenols. Their research reiterates that acetone being chaotropic, tends to lower the interaction of the polyphenols with the cell wall matrices and thus efficiency in extracting polyphenols from the apple matrices. The presence of a high amount amounts of TPC in acetone and subsequently lower in ethanol and water is also based on the fact that the polarity of acetone is lower than that of ethanol and the polarity of ethanol is lower than that of water. Thus, much of the polyphenol compounds were extractable in the least polar compound decreasing with an increase in the polarity of the solvent. These results suggest that acetone, a food-grade solvent, can be a reliable solvent in obtaining apple pomace extracts with a high amount of TPC.

Similar to total phenolic content (TPC), at all extraction times, the antioxidant activity was significantly highest in acetone extracts, followed by ethanol and least in water extracts. As postulated in the TPC, high antioxidant activity in acetone extracts is attributed to the properties of the solvent where acetone has the least polarity followed by ethanol and the highest in water. Similar results were reported by Gharedaghi et al., (2020) where the acetonic extracts of apple pomace showed the highest antioxidant than ethanol and water. However contrary to our results, in their research, water extracts displayed higher antioxidants than ethanol. The results indicate that phenolic compounds present in the apple pomace are effectively extractable when a solvent with low polarity is used and thus as displayed by acetone and ethanol complementing a famous phrase in chemistry "*like dissolves like*". In acetone, extracts without sonication (Time = 0) had a significantly low FRAP value compared to that sonicated for 10 minutes. However, the FRAP values dropped to values statistically similar to that without sonication as sonication time kept increasing to 60 minutes (Table 3). Similarly, Mieszczakowska-Frąc et al., (2016) observed that sonicating apple matrices for a longer time reduced the amount of polyphenols in water extracts. This can be due to the destructive effect of polyphenols on prolonged exposure to sonication (Grönroos et al. 2004; Wang et al. 2020). As far as ultrasound-assisted extraction is concerned, acetone is the best extraction solvent for apple pomace extracts with high antioxidant activity compared to ethanol and water.

Similar to Total phenolic content (TPC) and Ferric Reducing Ability of Plasma (FRAP), antimicrobial activity was manifested on acetone, while it was neither observed on ethanol nor water extracts (Table 4). Zhang et al., (2016) also reported that acetone is capable of producing extracts with antimicrobial activity (*E. coli* and *S. aureus)* from ultrasound-assisted extraction of the apple pomace. Similarly, Zardo et al., (2021) observed that acetone resulted in apple pomace extract with the highest antimicrobial activity against *S. enterica, S. aureus* and *E. coli* compared to ethanol as well as methanol. Failure of the ethanol and water to produce extracts

with antimicrobial activity complements the observations made on TPC and FRAP values where the two properties were very weak compared to acetone. Interestingly and contrary to our expectations, within acetone extracts, it was observed that antimicrobial activity decreased to a significant lowest amount when the pomace was sonicated for the longest time (60 minutes). A similar trend was observed on TPC as well as on FRAP. This suggests that sonication time is an important factor in the extraction of the apple pomace when using acetone. Sonicating the pomace longer reduces the amount of phenolic content as well as the biological activity of the pomace.

Conclusively, The industrial application of bioactive compounds from agro-industrial waste products of fruit origin in food, cosmetics and pharmaceutical is hampered by the inefficiency in extracting and processing the compounds into a fine usable state. The effects of solvent selection and sonicating time on antioxidant and antimicrobial activities of the apple pomace were investigated. It was observed that the two factors highly impact the recovery of extracts from the pomace, the amount of polyphenol compounds, antioxidant and antimicrobial activity. Ten minutes was found to be the best sonication time to produce acetonic extracts with the best biological activity. The use of the apple pomace as a source of food additives for antioxidant and antimicrobial properties is promising. Acetone, a food-grade solvent has shown great reliability in extracting useful compounds from the pomace when using the ultrasound-assisted extraction method however, further studies such as optimization of the extraction process using the solvent and purification of the extracts are recommended.

Acknowledgements

References

Balouiri, M., Sadiki, M., Ibnsouda, S.K., (2016). Methods for in vitro evaluating antimicrobial activity: A review. Journal of Pharmaceutical Analysis, 6(2), 71–79. Available at: https://doi.org/10.1016/j.jpha.2015.11.005.

Benvenutti, L., Bortolini, D. G., Nogueira, A., Zielinski, A. A. F., Alberti, A., (2019). Effect of addition of phenolic compounds recovered from apple pomace on cider quality. LWT, 100, 348–354. Available at: https://doi.org/10.1016/J.LWT.2018.10.087.

Benzie, I.F.F., Strain, J.J., (1996). The Ferric Reducing Ability of Plasma (FRAP) as a Measure of 'Antioxidant Power': The FRAP Assay. Analytical Biochemistry, 239(1), 70–76. Available at: https://doi.org/10.1006/ABIO.1996.0292.

Carpes, S. T., Bertotto, C., Bilck, A. P., Yamashita, F., Anjos, O., Bakar Siddique, M. A., Harrison, S. M., Brunton, N. P., (2021). Bio-based films prepared with apple pomace: Volatiles compound composition and mechanical, antioxidant and antibacterial properties. LWT, 144, 111241. Available at: https://doi.org/10.1016/J.LWT.2021.111241.

Carunchia, M., Wang, L., Han, J.H., (2015). The use of antioxidants in the preservation of snack foods. Handbook of Antioxidants for Food Preservation. Woodhead Publishing, 447–474. Available at: https://doi.org/10.1016/B978-1-78242-089-7.00019-1.

Carvalho, A.P.A., Conte-Junior, C.A., (2021). Health benefits of phytochemicals from Brazilian native foods and plants: Antioxidant, antimicrobial, anti-cancer, and risk factors of metabolic/endocrine disorders control. Trends in Food Science & Technology, 111, 534–548. Available at: https://doi.org/10.1016/J.TIFS.2021.03.006.

Fernandes, I. de A.A., Maciel, G.M., Ribeiro, V.R., Rossetto, R., Pedro, A.C., Haminiuk, C.W.I., (2021). The role of bacterial cellulose loaded with plant phenolics in prevention of UV-induced skin damage. Carbohydrate Polymer Technologies and Applications, 2, 100122. Available at: https://doi.org/10.1016/J.CARPTA.2021.100122.

Fernandes, P.A.R., Ferreira, S.S., Bastos, R., Ferreira,I., Cruz, M.T., Pinto, A., Coelho, E., Passos, C.P., Coimbra, M.A., Cardoso, S.M., Wessel, D.F., (2019a). Apple pomace extract as a sustainable food ingredient. Antioxidants, 8(6), 189. Available at: https://doi.org/10.3390/antiox8060189.

Fernandes, P.A.R., le Bourvellec, C., Renard, C.M.G.C., Nunes, F.M., Bastos, R., Coelho, E., Wessel, D.F., Coimbra, M.A., Cardoso, S.M., (2019b). Revisiting the chemistry of apple pomace polyphenols. Food Chemistry, 294, 9–18. Available at: https://doi.org/10.1016/J.FOODCHEM.2019.05.006.

Gharedaghi, J., Aliakbarlu, J., Tajik, H., (2020). Antioxidant potential of apple pomace extract and its efficacy in alginate coating on chemical stability of rainbow trout fillet. Journal of Food Measurement and Characterization, 14, 135–141. Available at: https://doi.org/10.1007/s11694-019-00275-5.

Grigoras, C.G., Destandau, E., Fougère, L., Elfakir, C., (2013). Evaluation of apple pomace extracts as a source of bioactive compounds. Industrial Crops and Products, 49, 794–804. Available at: https://doi.org/10.1016/j.indcrop.2013.06.026.

Grönroos, A., Pirkonen, P., Ruppert, O., (2004). Ultrasonic depolymerization of aqueous carboxymethylcellulose. Ultrasonics Sonochemistry. Elsevier, 9–12. Available at: https://doi.org/10.1016/S1350-4177(03)00129-9.

Hammad, K.S.M., Elsayed, N., Elkashef, H., (2021). Development of a whey protein concentrate/apple pomace extract edible coating for shelf life extension of fresh-cut apple. International Food Research Journal, 28(2), 377–385. Available at: https://doi.org/10.47836/ifrj.28.2.19.

Koutsos, A., Lovegrove, J.A., (2015). An Apple a Day Keeps the Doctor Away – Inter-Relationship Between Apple Consumption, the Gut Microbiota and Cardiometabolic Disease Risk Reduction. Diet-Microbe Interactions in the Gut. Elsevier, 173–194. Available at: https://doi.org/10.1016/B978-0-12-407825-3.00012-5.

Li, W., Yang, R., Ying, D., Yu, J., Sanguansri, L., Augustin, M.A., (2020). Analysis of polyphenols in apple pomace: A comparative study of different extraction and hydrolysis procedures. Industrial Crops and Products, 147. Available at: https://doi.org/10.1016/j.indcrop.2020.112250.

Lizcano, S.C., Dávila, J.A., Hernández, V., (2019). Fruit Agroindustrial Wastes for Preparing Beverages for Medicinal Purposes by Supercritical Fluid Extraction Technology: Andes Berry (Rubus glaucus benth) Case, Production and Management of Beverages. Grumezescu, A.M., Holban, A.M (Eds.) Elsevier. Available at: https://doi.org/10.1016/B978-0-12-815260-7.00005-5.

Manzoor, S., Masoodi, F.A., Rashid, R., Dar, M.M., (2022). Effect of apple pomace-based antioxidants on the stability of mustard oil during deep frying of French fries. LWT - Food Science and Technology, 163, 113576. Available at: https://doi.org/10.1016/j.lwt.2022.113576.

Mieszczakowska-Frąc, M., Dyki, B., Konopacka, D., (2016). Effects of Ultrasound on Polyphenol Retention in Apples After the Application of Predrying Treatments in Liquid Medium. Food and Bioprocess Technology, 9(3), 543–552. Available at: https://doi.org/10.1007/s11947-015-1648-z.

Morgan, A., Darby, D., Bruce, T., Romero, A., Cooksey, K., (2022). Development of an antimicrobial coating containing nisin and pectin for deli meat turkey bologna. LWT - Food Science and Technology, 159, 113210. Available at: https://doi.org/10.1016/j.lwt.2022.113210.

Naqash, F., Masoodi, F.A., Rather, S.A., Wani, S.M., Gani, A., (2017). Emerging concepts in the nutraceutical and functional properties of pectin—A Review. Carbohydrate Polymers. Elsevier. Available at: https://doi.org/10.1016/J.CARBPOL.2017.03.058.

Paraman, I., Sharif, M.K., Supriyadi, S., Rizvi, S.S.H., (2015). Agro-food industry byproducts into value-added extruded foods. Food and Bioproducts Processing, 96, 78–85. Available at: https://doi.org/10.1016/j.fbp.2015.07.003.

Persic, M., Mikulic-Petkovsek, M., Slatnar, A., Veberic, R., (2017). Chemical composition of apple fruit, juice and pomace and the correlation between phenolic content, enzymatic activity and browning. LWT - Food Science and Technology, 82, 23–31. Available at: https://doi.org/10.1016/J.LWT.2017.04.017.

Peschel, W., Sánchez-Rabaneda, F., Diekmann, W., Plescher, A., Gartzía, I., Jiménez, D., Lamuela-Raventós, R., Buxaderas, S., Codina, C., (2006). An industrial approach in the search of natural antioxidants from vegetable and fruit wastes. Food Chemistry, 97, 137–150. Available at: https://doi.org/10.1016/j.foodchem.2005.03.033.

Rana, S., Gupta, S., Rana, A., Bhushan, S., (2015). Functional properties, phenolic constituents and antioxidant potential of industrial apple pomace for utilization as active food ingredient. Food Science and Human Wellness, 4, 180–187. Available at: https://doi.org/10.1016/j.fshw.2015.10.001.

Rana, S., Bhushan, S., (2016). Apple phenolics as nutraceuticals: assessment, analysis and application. Journal of Food Science and Technology, 53(4), 1727–1738. Available at: https://doi.org/10.1007/s13197-015-2093-8.

Renard, C.M.G.C., Baron, A., Guyot, S., Drilleau, J.F., (2001). Interactions between apple cell walls and native apple polyphenols: quantification and some consequences. International Journal of Biological Macromolecules, 29(2), 115–125. Available at: https://doi.org/10.1016/S0141-8130(01)00155-6.

Riaz, A., Lei, S., Akhtar, H.M.S., Wan, P., Chen, D., Jabbar, S., Abid, M., Hashim, M.M., Zeng, X., (2018). Preparation and characterization of chitosan-based antimicrobial active food packaging film incorporated with apple peel polyphenols. International Journal of Biological Macromolecules, 114, 547–555. Available at: https://doi.org/10.1016/j.ijbiomac.2018.03.126.

Shahidi, F., Ambigaipalan, P., (2015). Phenolics and polyphenolics in foods, beverages and spices: Antioxidant activity and health effects - A review. Journal of Functional Foods, 18, 820–897. Available at: https://doi.org/10.1016/j.jff.2015.06.018.

Singleton, V.L., Rossi, J.A., (1965). Colorimetry of Total Phenolics with Phosphomolybdic-Phosphotungstic Acid Reagents. American Journal of Enology and Viticulture, 16(3), 144–158. Available at: http://www.ajevonline.org/content/16/3/144.abstract.

van der Sluis, A.A., Dekker, M., van Boekel, M.A.J.S., (2005) Activity and Concentration of Polyphenolic Antioxidants in Apple Juice Stability during Storage. Journal of Agricultural and Food Chemistry, 53(4), 1073–1080. Available at: https://doi.org/10.1021/jf040270r.

Wang, P., Cheng, C., Ma, Y., Jia, M., (2020). Degradation behavior of polyphenols in model aqueous extraction system based on mechanical and sonochemical effects induced by ultrasound. Separation and Purification Technology, 247, 116967. Available at: https://doi.org/10.1016/j.seppur.2020.116967.

Zardo, D.M., Alberti, A., Zielinski, A.A.F., Prestes, A.A., Esmerino, L.A., Nogueira, A., (2021). Influence of solvents in the extraction of phenolic compounds with antibacterial activity from apple pomace. Separation Science and Technology, 56(5), 903–911. Available at: https://doi.org/10.1080/01496395.2020.1744652.

Zhang, T., Wei, X., Miao, Z., Hassan, H., Song, Y., Fan, M., (2016). Screening for antioxidant and antibacterial activities of phenolics from Golden Delicious apple pomace. *Chemistry Central Journal*, 10, 47. Available at: https://doi.org/10.1186/s13065-016-0195-7.

Effect of Silica Fume on The Mechanical Properties of Slag Based Geopolymer Concretes

**Mehmet Burhan Karakoç[1]*, Mehmet Akif Sağır[1], Enes Ekinci[1],
Ahmet Özcan[2], Abdurrahman Yolcu[1]**

Abstract: In this study, the fire resistance of slag based geopolymer concretes was investigated and the effect of silica fume (SF) on this resistance was determined. In slag based geopolymer concretes activated using 12M NaOH solution, 0, 5 and 10% by weight SF was substituted for slag. After the samples that completed their curing period were exposed to temperatures of 250, 500 and 750 ºC for 1 hour, the mechanical (compressive and flexural strengths) properties of the samples were examined. As the SF substitution increased, the mechanical properties of the samples increased. While the SF substitution had a positive effect on the fire resistance of the samples.

Keywords: Slag, geopolymer concrete, fire resistance, silica fume

1. Introduction

Advantages such as superior durability and mechanical properties, ease of production and application made concrete the most preferred material in the construction sector. In the production process of cement, which is an indispensable component of concrete, both excessive consumption of natural resources and CO_2 gas emissions pose a great threat to a sustainable environment [1]. On the other hand, ordinary Portland cement (OPC) production also releases other harmful gases, including nitrogen oxide (NO_x) and sulfur trioxide (SO_3), which further accelerates global warming and contributes to acid rains [2].

Geopolymer binders can be mentioned as the most environmentally friendly alternative to OPC, which has a very negative impact on the environment. Geopolymers formed as a result of activating aluminosilicate precursors obtained in the form of natural or industrial waste with alkali activators have many advantages compared to OPC. Examples of these advantages are performances such as superior mechanical properties, low permeability, good resistance to acid, sulfate and freeze-thaw effects [3], [4], [5], [6]. In addition to these advantages, the fact that geopolymer can take approximately 90% of its final strength in the first three days offers an advantageous use potential in critical applications [7].

This study investigated the effect of SF addition on fire performance in slag-based geopolymer concretes. In the solid part, 0%, 5%, and 10% of silica fume was substituted into the slag and alkaline activation was achieved with a 12 M NaOH solution. The geopolymer concrete samples produced in this way were exposed to temperatures of 250, 500 and 750°C at the end of the

[1] Inonu University, Faculty of Engineering, Civil Engineering, Malatya, Turkey
[2] Dumlupınar University, Faculty of Engineering, Civil Engineering, Kütahya, Turkey
* Corresponding author: mehmet.karakoc@inonu.edu.tr

28th day. The compressive and flexural strengths of geopolymer concretes, which were kept for 1 hour at the specified temperature values, were investigated. Experimental findings clearly demonstrated that substitution of SF had a positive effect on fire performance of geopolymer concrete samples.

2. Material and Method

In this study, slag was used as the binder material. In the mixtures, 0, 5 and 10 % SF was substituted for slag. Additionally, the specific gravity and specific surface areas of slag and SF were determined as 2.86 and 2.25 g/cm^3, 3996 and 17980 cm^2/g, respectively. Table 1 presents the chemical compositions of slag and SF. Alkali activation of geopolymer concrete samples was obtained with 12 M NaOH solution prepared 24 hours before casting. In addition, river aggregates were preferred as fine (0-4 mm) and coarse aggregates (4-8 mm).

Table 1. Chemical composition of slag and SF

Component (%)	SiO$_2$	Al$_2$O$_3$	Fe$_2$O$_3$	CaO	MgO	SO$_3$	S^{-2}	Na$_2$O	K$_2$O	TiO$_2$	Mn$_2$O$_3$	LOI
Slag	32.47	9.94	1.25	32.45	9.31	0.82	0.33	0.31	0.85	1.16	3.51	3.6
SF	83.40	1.20	0.60	0.40	8.80	0.60	-	1.00	1.40	-	-	5.80

The high temperature (250°C, 500°C and 750°C) performances of the geopolymer concretes, whose production phase was completed in this way, were investigated after 28 days of curing. The geopolymer samples, which were exposed to the specified temperature values for 1 hour, were left to cool in the air. Then, compressive strength and flexural strength tests were performed on geopolymer concretes. The compressive strength test was carried out in accordance with the ASTM C109/C109M-20b [8] and the flexural strength test was carried out in accordance with the ASTM C78-02 [9].

3. Results

3.1. Compressive strength of geopolymer concrete samples

Fig. 1 shows the effect of SF substituted in different ratios on geopolymer concrete samples on high temperature performance. For the laboratory cured samples, the maximum compressive strength values were observed from geopolymer concrete samples consisted of 10% SF. Similar to the samples cured in the laboratory, 10% SF substitution resulted in the highest compressive strength values in all geopolymer concrete samples exposed to high temperatures. This situation demonstrated that the increase in the SF substitution rate significantly increases the compressive strength values. This was thought to be due to the fine structure of SF leading to a denser microstructure. Moreover, while the maximum compressive strength values of geopolymer concrete samples were observed at 250°C, minimum maximum compressive strength values were observed at 750°C.
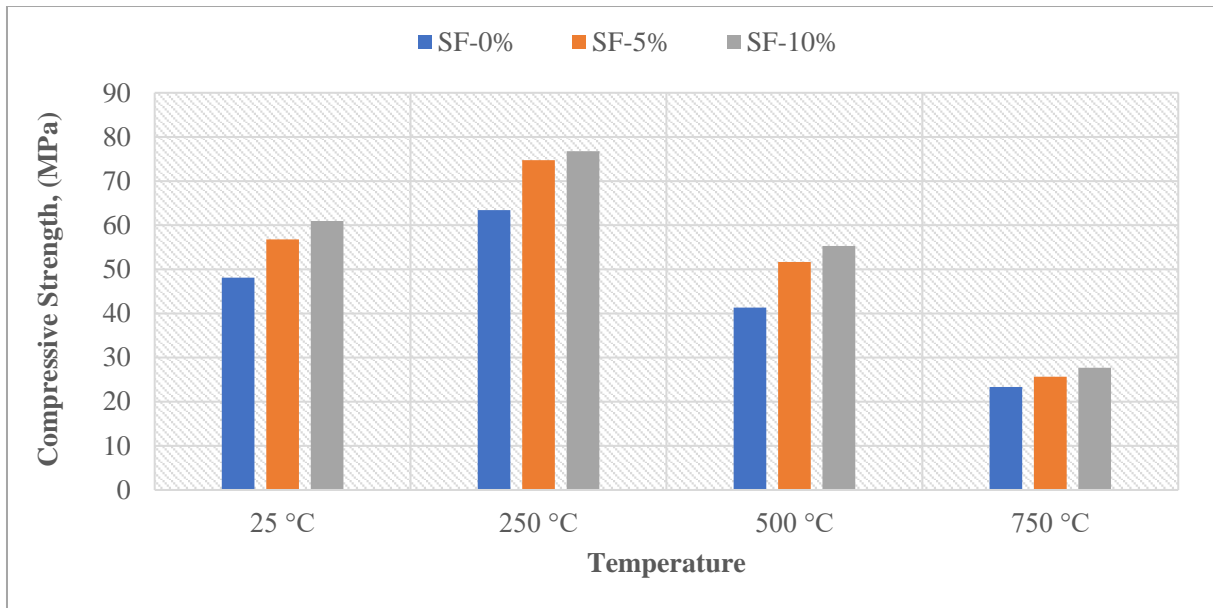
Fig. 1. Compressive strength values of geopolymer concrete samples

3.2. Flexural strength of geopolymer concrete samples

The flexural strengths of the 28-day samples are given in Fig. 2. As can be seen in Fig. 2, with the increase of substitution of SF, flexural strength of geopolymer concrete samples increased dramatically. Increasing the SF substitution ratio from 0% to 5% increased the flexural strength values by about 3%, while the use of 10% of SF caused an increase of about 10% in the flexural strength values. With the addition of fine SF, the (-Si-O-Si-O-) bridge chains, which are facilitated to form, cause the particles to be tightly bound, resulting in a denser and more compact matrix structure. Here, this dense and compact matrix causes increases in compressive strength and flexural strength values [10].

4. Discussion and Conclusions

This paper investigated the effect of usage of SF at the different ratios on the mechanical properties of geopolymer concrete samples exposed to high temperatures. The obtained findings clearly demonstrated that with the increase of usage ratio of SF led to superior mechanical properties at all different temperature values.

Acknowledgements
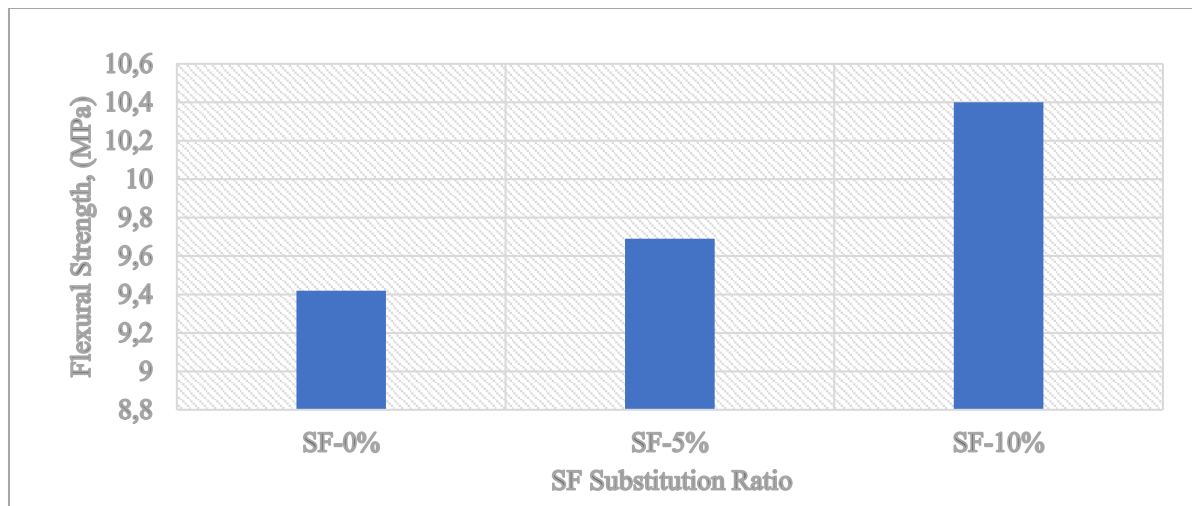
Fig. 2. Flexural strength values of geopolymer concrete samples

References

[1] Elzeadani, M., Bompa, D. V., & Elghazouli, A. Y. (2021). Preparation and properties of rubberised geopolymer concrete: A review. *Construction and Building Materials*, *313*, 125504.

[2] Rajendran, M., & Akasi, M. (2020). Performance of crumb rubber and nano fly ash based ferro-geopolymer panels under impact load. *KSCE Journal of Civil Engineering*, *24*(6), 1810-1820.

[3] Gao, K., Lin, K. L., Wang, D., Hwang, C. L., Tuan, B. L. A., Shiu, H. S., & Cheng, T. W. (2013). Effect of nano-SiO2 on the alkali-activated characteristics of metakaolin-based geopolymers. *Construction and Building Materials*, *48*, 441-447.

[4] Deb, P. S., Sarker, P. K., & Barbhuiya, S. (2016). Sorptivity and acid resistance of ambient-cured geopolymer mortars containing nano-silica. *Cement and Concrete Composites*, *72*, 235-245.

[5] Van Jaarsveld, J. G. S., Van Deventer, J. S. J., & Lorenzen, L. (1997). The potential use of geopolymeric materials to immobilise toxic metals: Part I. Theory and applications. *Minerals Engineering*, *10*(7), 659-669.

[6] Luhar, S., Chaudhary, S., & Luhar, I. (2019). Development of rubberized geopolymer concrete: Strength and durability studies. *Construction and Building Materials*, *204*, 740-753.

[7] Rosenberger, R. (2018). Behaviour of Reinforced Crumb Rubber Ordinary Portland Cement and Geopolymer Concrete Beams. *The UNSW Canberra at ADFA Journal of Undergraduate Engineering Research*, *11*(2).

[8] ASTM C109/C109M-20b, (2020). Standard test method for compressive strength of hydraulic cement mortars (using 2-in. or 50 mm] cube specimens). ASTM International, West Conshohocken, PA. https://doi.org/10.1520/C0109_C0109M-20B.

[9] ASTM C78-02, (2002). Standard test method for flexural strength of concrete (using simple beam with third-point loading). ASTM International, West Conshohocken, PA. https://doi.org/10.1520/C0078-02.

[10] Yang, Z.X., Ha, N.R., Jang, M.S., Hwang, K.H., Lee, J.K. (2009). The effect of SiO_2 on the performance of inorganic sludge-based structural concretes. Journal of Ceramic Processing Research, 10(3), 266-268.

Variable Round Robin based Shortest Job First (VRS): A Novel Hybrid Task Scheduling Algorithm for IoT networks

Jayasudha M[1], Vijayalakshmi C[2]

Abstract: At the advent of the 21st century and the era of Industry 4.0, the use of cloud computing has enormously risen across various sectors that includes, healthcare, home automation and agriculture. The field of cloud computing has evolved into a new paradigm namely edge computing in which Internet of Things (IoT) devices are used to make the applications more feasible. But, the processes in edge computing are more time sensitive and resource allocations are elastic in nature. In order to cope up with these requirements, scheduling of processes across the IoT network plays a paramount role to achieve the necessary performance requirement. In order to strive for this performance, the master node in every IoT network schedules the processes by the Central Processing Unit (CPU) to achieve the maximum utilization. In this paper we seek to come up with an improved scheduling algorithm for uniprocessor systems. Our proposed algorithm is called Variable Round Robin based Shortest Job First (VRS) Algorithm. A detailed result analysis after taking several scenarios, showed the proposed algorithm giving better results than traditional RR using same static time quantum and sometimes even better than SJF algorithm which is stated in the paper.

Keywords: Internet of Things, CPU Scheduling, Round robin Scheduling, Shortest Job First Scheduling.

Introduction

At present a lot of real-world solutions are based on IoT technology along with cloud computing. In contrast to the traditional computing model, cloud computing gives the benefit of flexible resource usage, on demand consumption with dynamic allocation and pay-as-you-go feature which makes it convenient for implementing applications based the IoT architecture. Cloud Computing gives a heterogeneous environment to connect various IoT based devices to achieve a solution to real world problems. Most of the IoT application uses the concept of edge computing in which the storage and processing are brought closer to the peripheral devices on the network. Influence of Web 3.0 on the field of cloud computing has engendered a decentralized and distributed version of computing known as fog computing. All of these are possible because of Virtual Machines (VM) which are used widely used today. One common thing that hasn't changed with all these advancements is the need of task scheduling algorithms. This is due to the fact that resource

1School of Computer Science and Engineering, Vellore Institute of Technology, Chennai India
2School of Computer Science and Engineering, Crescent Engineering College, Chennai India
1bhavani7rs@gmail.com,2vijic.edu@gmail.com

utilization, efficient energy usage and acquisition delay are some of the primary parameters of these highly advanced real-time systems.

Similar to scheduling of tasks in IoT, many complex hybrid algorithms are used by different operating systems for scheduling different processes. Windows Operating System has a Round Robin scheduling algorithm at its core, but the scheduling algorithm may change to First Come First Serve (FCFS) or Shortest Job First (SJF) according to specific scenarios to achieve maximum efficiency. Macintosh OS used non-pre-emptive scheduling prior to Macintosh Operating System X (OSX), and preemptive since then. OSX supports both multiple feedback queue scheduling and RR scheduling algorithms. The multilevel feedback queue algorithm partitions the ready queue into several different queues, allowing a process to move between queues. Each run queue in this algorithm has various priorities that are handled in different ways.

Linus scheduler uses a complex scheme as its scheduling algorithm. It is a combination of preemptive priority and biased time slicing. The algorithm assigns longer/larger time quantum to higher priority tasks and shorter/smaller time quantum to lower priority tasks. For the past couple of years, many authors have introduced different variants of CPU scheduling to improve system performance. Most of them are achieved by coupling the base algorithm that is known to us like Priority, the shortest job first, and round-robin. The main problem that can occur while coming up with an efficient algorithm is starvation of processes [1].

In IoT, designing an optimal scheduling algorithm should maximize the CPU utilization and throughput and minimize the latency and power consumption. Some researchers have proposed to increase the time quantum of RR after the first cycle and decrease it again in the next thus forming an alternate pattern that might lead to a reduction in turnaround time (TAT) for given burst time (BT) of processes [2]. SJF is an efficient algorithm that gives the shortest waiting time (WT) but the disadvantage of it is that it needs to have prior knowledge of the execution time of processes. Thus, it is best suited for only batch processes [3]. One of the best advancements to SJF is the highest response ratio (HRRN) [4]. It uses a task priority, which is calculated according to the equation

$$Priority = 1 + \frac{WT}{BT} \tag{1}$$

A longer waiting process will get priority by this method which reduces the overall WT [4].

Another approach that was proposed is the blend of need-based planning calculation and RR that evaluates the priority-based RR CPU Scheduling. It has the benefit of effective CPU utilization along with the merit of a RR in reducing starvation [5]. A new RR-based scheduling algorithm for OS - dynamic quantum using the mean average [6] introduces a novel idea to estimate the average BT of the processes that are in the ready queue which is assigned as dynamic time quantum, after every CPU cycle. The shortest burst time priority and user priority is used as the basis of importance for scheduling the processes in the fair priority RR with dynamic time quantum.

In this paper, we introduce a hybrid approach for CPU scheduling by combining the two famous base algorithms - Shortest Job First and Round Robin. To add some heuristic into it we add two parameters alpha and variable time quantum (VTQ), which is explained in the latter part of this paper. We have compared our VRS algorithm with the scenarios presented in the other research papers. We conclude by discussing the results obtained with the help of a comparison table and give some ideas for future work.

Proposed Work

In our proposed RR algorithm, a priority queue is used in place of the regular case as in the case of the traditional RR algorithm. Next process after the current time quantum cycle is finished is chosen from the priority queue, this process has the shortest burst time and is not the current process. However, there is no pre-emption if the remaining burst time of current process is within the range –

$$0.5 * TQ - 1.5 * TQ \tag{2}$$

 in this case the current process continues for another cycle of Time quantum. We have also introduced variable time quantum in our algorithm as opposed to the static time quantum used in traditional algorithm. As soon as 1 process completes its execution, Variable Time Quantum (VTQ) is made using the formula –

$$alpha * BT \left[current\ process\right] + (1 - alpha) * VTQ \tag{3}$$

where alpha is a variable which can be changed in accordance to the user's choice. The time quantum finally changes to VTQ when the CPU completes 5 CPU cycles. The visual representation of the algorithm can be seen in flowchart presented in Figure 1.
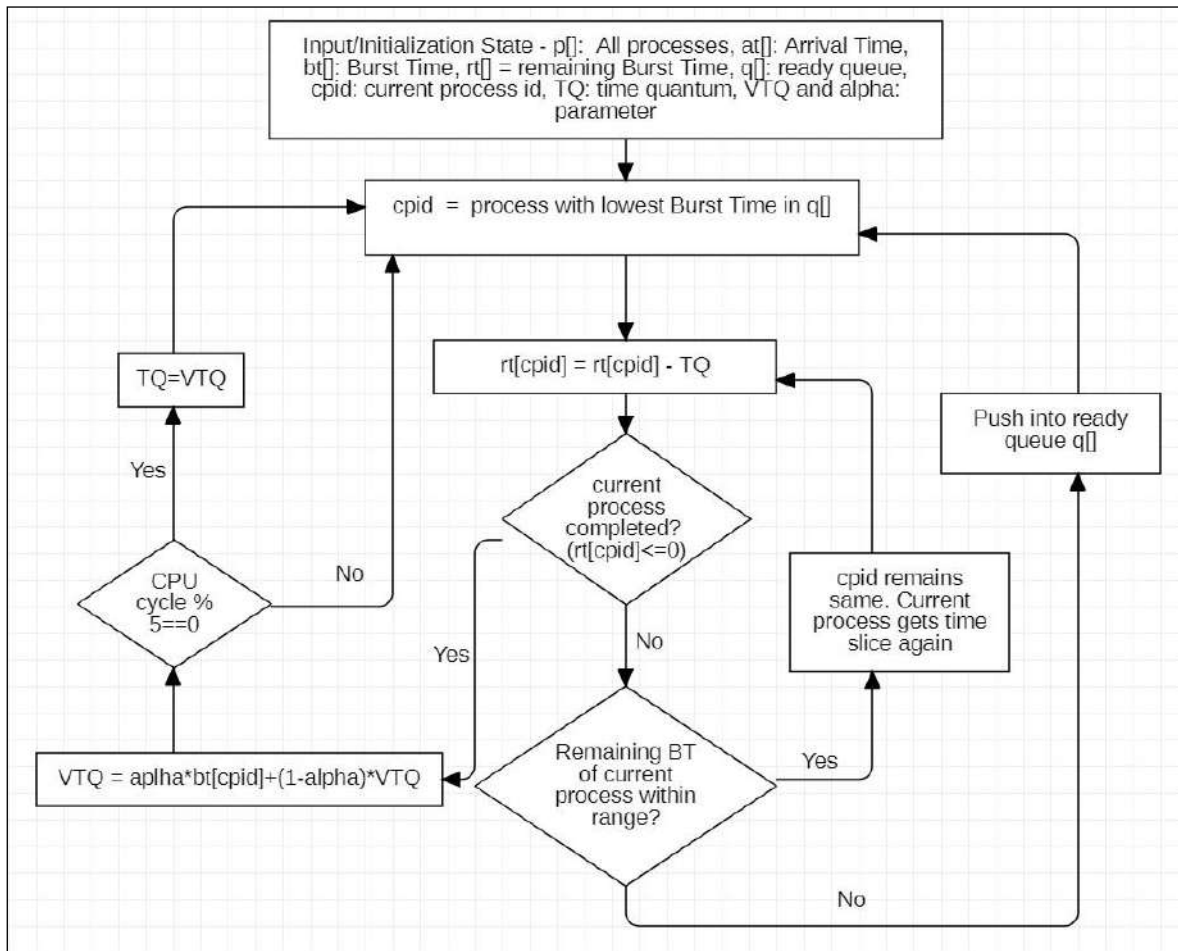
Figure 1: Flowchart of VRS algorithm

The steps for the algorithm are given below-

1. Priority queue is used in place of the regular queue.
2. Current process which needs to be given the time slice is selected based on the burst time of all the processes present in the ready queue.
3. Process with the shortest burst time is selected.
4. If the process has BT remaining after giving the time slice, it is pushed again in the ready queue.
5. If the remaining BT is within the range of Eq.2, it is selected again as the current process.
6. If the process completes after giving it the time slice, value of variable time quantum is changed according to the Eq.3, where alpha is variable for every case.
7. The time quantum is changed to variable time quantum (rounded to nearest whole number), after every period of 5 CPU cycles.
8. Steps for 2 to 7 are repeated until all the processes have completed.

Results and Discussions

 In this section we have discussed the outcome of the VRS algorithm on various scenarios. Firstly, a case study is done using a custom scenario to test the VRS algorithm and compare it with basic scheduling algorithm (Section 3.1). Then a comparative study is done between VRS and other existing algorithms using the scenarios presented in four different research papers (Section 3.2). All the time values are measures in unit time.

3.1 Case Study – VRS

In the following scenario presented in Table 1, there are four processes with their process id (PID), arrival time (AT) and burst time (BT). For VRS algorithm to work, we need to decide the initial time quantum (TQ) and alpha value. In this scenario the value for TQ is 2 and alpha is 0.3. The Figure 2 showcases the scheduling done with VRS algorithm using Gantt Chart representation. We can see that VTQ value is updated whenever the remaining BT of process becomes 0. TQ value is changed to VTQ after every 5 cycles.

Table 1 The sample scenario of four processes

PID	AT	BT
P1	0	8
P2	2	2
P3	6	3
P4	9	1

	P1	P2	P1	P3	P3	P4	P1	P1
0 2		4	6	8	9	10	12	14
Remaining BT	6	0	4	1	0	0	2	0
Updating parameters		VTQ=0.6+1.4	TQ=VTQ		VTQ=0.9+1.4	TQ=VTQ		

Figure 2: Gantt Chart representation for the given scenario VRS algorithm

Table 2 shows the result of VRS program that was run on the given scenario. The table contains the details of arrival time (AT), burst time (BT), completion time (CT), turnaround time (TAT) and waiting time (WT) of all the processes. The total execution time for scheduling these 4 processes is 14. The average TAT comes out to be 5 and average WT is 1.5. The throughput is 0.285714.

Table 2 The outcome of the VRS algorithm on the 4 processes

PID	AT	BT	CT	TAT	WT
P1	0	8	14	14	6
P2	2	2	4	2	0
P3	6	3	9	3	0
P4	9	1	10	1	0

The comparison of VRS with RR, SJF and Shortest Time Remaining First (STRF) is presented in Table 3. It can be inferred from the table that VRS algorithm does a better job than both RR and SJF algorithms. VRS combines the best of both SJF and RR which makes it suitable for this scenario. This analysis is done on the basis of average turnaround time (Avg TAT) and average waiting time (Avg WT). It can be seen in this scenario, the result of STRF and VRS comes out to be same with respect to Avg TAT and Avg WT. This is not true for all scenarios but sometimes VRS can give the exact same result of base scheduling algorithms.

Table 3 Comparison Table of VRS algorithm with other basic algorithms

Algorithm	Avg TAT	Avg WT
RR with TQ=2	6	2.5
SJF	6.5	3
STRF	**5**	**1.5**
VRS Algorithm TQ=2 Alpha =0.3	**5**	**1.5**

3.2 Comparison of results with other research papers

In this section, we have compared the results obtained from the VRS algorithm with the ones stated in different research papers using the exact same scenarios used in them. The four papers taken for this comparative study are: An Optimized SJF for CPU scheduling (Muhammad et al [7]), A novel hybrid of SJF and RR with dynamic variable quantum time task scheduling technique (Samir Elmougy et al [8]), A Modified Priority Preemptive Algorithm for CPU Scheduling (Kunal Chandiramani et al [9]) and Equitable Shortest Job First: A Preemptive Scheduling Algorithm for Soft Real-Time Systems (Mario Jean Rene et al [11]). All the comparison is done on the basis of Avg TAT and Avg WT.

Article 1: Muhammad et al [7] has taken a scenario in which there are 5 processes. All the processes come at different arrival time. It can be seen from Table 4 that VRS algorithm performs better than their proposed algorithm with margin of 0.4 units. The Average TAT and WT for VRS algorithm comes out to be 13 and 6.4 respectively.

Table 4 Comparison Table of VRS algorithm with other algorithms presented in the paper

Algorithm	Avg TAT	Avg WT
RR with TQ=5	18	11.4
SJF	13.2	6.6
Muhammad et al [7]	13.4	6.8
VRS Algorithm TQ=3 Alpha=0.3	**13**	**6.4**

Article 2: Samir Elmougy et al [8] has taken a scenario in which there are 6 processes. All the processes come at different arrival time with some processes having a longer BT. It can be seen from Table 5 that the SJF algorithm performs the best in this scenario. Nevertheless, the VRS algorithm works better than the SRSQ of the comparing paper by a significant margin.

Table 5 Comparison Table of VRS algorithm with other algorithms presented in the paper

Algorithm	Avg TAT	Avg WT
RR with TQ=8	67.83	51.5
SJF	**42.83**	**26.5**
SRSQ [8]	58.09	41.806
VRS Algorithm TQ=8 Alpha=0.3	44.833	28.5

Article 3: Kunal Chandiramani et al [9] has taken two scenarios in their paper. The authors have compared their algorithm with a simple priority pre-emptive algorithm in their paper, so they have given each process some priority value. All the processes arrive at the same time. In VRS algorithm, no priority is used for the processes hence the algorithm will treat each process with equal priority.

In the first scenario, there are 3 processes with their burst time and priority. VRS algorithm gives a better avg TAT and WT values as compared to other algorithms, which can be seen in Table 6. Since no priority is used in the VRS algorithm, it comes up with a better CPU scheduling than others.

Table 6 Comparison Table of VRS algorithm using Scenario 1

Algorithm	Avg	Avg
	TAT	WT
Priority pre-emptive	14.00	8.33
Modified Priority Preemptive TQ=2 [9]	11.33	5.667
VRS Algorithm TQ=2 Alpha =0.3 (All processes have equal priority)	**8.67**	**3**

In the second scenario, there are 5 processes with their burst time and priority. In Table 7 also we can observe that the VRS algorithm performs better as compared to others in the second scenario which was presented in the paper.

Table 7 Comparison Table of VRS algorithm using the Scenario 2

Algorithm	Avg TAT	Avg WT
Priority pre-emptive	22.20	16.40
Modified Priority Preemptive TQ=2 [9]	15.60	9.80
VRS Algorithm TQ=2 Alpha =0.3 And all processes at same priority	**12.8**	**7.00**

Article 4: Mario Jean Rene et al [11] have taken a scenario in which there are 5 processes which arrive at the same time but has huge variation in the BT of different processes. The authors of this paper have not given the average TAT value and so the comparison is only done on the basis on average WT for this paper.

It can be inferred from the Table 8 that the VRS algorithm performs as good as SJF and is better than the proposed algorithm which is presented in the research paper used for the comparison.

Table 8 Comparison Table of VRS algorithm with other algorithms presented in the paper

Algorithm	Avg TAT	Avg WT
FCFS	-	25.6
SJF	-	**13.8**
Enhanced SJF [11]	-	14.8
VRS Algorithm TQ=3 Alpha =0.3	24.8	**13.8**

Table 9 Final Performance Comparison

Ref No	Avg TAT		Avg WT	
	Previous work	**VRS**	**Previous work**	**VRS**
[7]	13.4	**13.0**	6.8	**6.4**
[8]	58.09	**44.833**	41.806	**28.5**
[9] Scenario 1	11.33	**8.67**	5.667	**3**
[9] Scenario 2	15.60	**12.8**	9.8	**7.0**
[11]	-	**24.8**	14.8	**13.8**

In all the considered articles, it is evident that VRS algorithm performs better with respect to Avg TAT and Avg WT.

Conclusion and Future Work

 At the end, we came up with an improved, efficient approach for IoT applications. Our algorithm outperformed most of the algorithms proposed in other papers as both discussed and showcased above. It proved to be better than all the traditional scheduling algorithms and fell short only to the Preemptive Shortest Job first algorithm by only a small margin. This report compares the best scheduling algorithms using the same scenarios from four different research papers in both tabular and graphical formats.

In our proposed algorithm we have not taken the waiting time of the process into consideration and thus there is a possibility of starvation as the priority of doing Round Robin is given to the smallest remaining burst time. The VRS algorithm can be extended to systems with multiple cores and a priority function can also be introduced to tackle the problem caused by starvation in future works.

References

1. Silberschatz, A., Galvin P. B., & Gagne G. (2004). Operating System Concepts, (7th ed.), Wiley

2. Raman, Dr.Pradeep Kumar Mittal, "An Efficient Dynamic Round Robin CPU Scheduling Algorithm (EDRR)", International Journal of Advanced Research in Computer Science and Software Engineering, 4(5), pp. 907-910, May 2014.

3. P.Surendra Varma, "A Finest Time Quantum for Improving Shortest Remaining Burst Round Robin (SRBRR) Algorithm", Journal of Global Research in Computer Science, 4 (3), pp. 10- 15, March 2013

4. Tanenbaum, A. S. (2007). Modern Operating Systems, (3rd ed.), Prentice Hall.

5. Rajput I. S., and Gupta D. (2012) A priority based round robin CPU scheduling algorithm for real time systems International Journal of Innovations in Engineering and Technology 1(3) 1-11

6. Abbas Noon, Ali Kalakech, and Seifedine Kadry, (2011) "A New Round Robin based Scheduling

Algorithm for Operating Systems: Dynamic Quantum Using the Mean Average", International Journal of Computer Science Issues, Vol. 8, Issue 3, No. 1, pp 224-229.

7. Muhammad Akhtar, Bushra Hamid, Inayat ur-Rehman, Mamoona Humayun, Maryam Hamayun

and Hira Khurshid "An Optimized Shortest job first Scheduling Algorithm for CPU Scheduling". ISSN: 2090-4274

Journal of Applied Environmental and Biological Sciences 2015.

8. Samir Elmougy, Shahenda Sarhan and Manar Joundy "A novel hybrid of Shortes job first and round robin with dynamic variable quantum time task scheduling technique" Journal of Cloud Computing:Advances, Systems and Applications 2017.

9. Kunal Chandiramani, Rishabh Verma, Sivagami M Vellore Institute of Technology, Vandalur Kelambakkam Road, Chennai, 600127, India. "A Modified Priority Preemptive Algorithm for CPU Scheduling". International Conference on Recent Rrends in Advanced Computing, 2019 ICRTAC 2019.

10. Muhammad A. Mustapha Department of Mathematics, Ahmadu Bello University, Zaria, Nigeria Saleh E. Abdullahi Department of Computer Science, Nigerian Turkish Nile University, Abuja, Nigeria Sahalu B. Junaidu Iya Abubakar Computer Center, Ahmadu Bello University, Zaria,

Nigeria. "Optimization of Priority based CPU Scheduling Algorithms to Minimize Starvation of

Processes using an Efficiency Factor". International Journal of Computer Applications (0975 – 8887) Volume 132 – No.11, December2015

11. Rene, Mario J. and Kagaris, Dimitri. "Equitable Shortest Job First: A Preemptive Scheduling Algorithm for Soft Real-Time Systems."

INTERNATIONAL JOURNAL OF ENGINEERING RESEARCH AND INNOVATION 6, No.

1 (Jan 2014): 15-22.

12.   Robin Verma. Kiran Siwach, Sonia Rana, "An improve SJF Scheduling algorithm to Reduce Starvation under Multiprocessor Environment". International Journal of Innovations in engineering and Technology(IJIET).

13.   Basit Shazad, Muhammad Tanvir Afzal "OPTIMIZED SOLUTION TO SHORTEST JOB FIRST BY ELIMINATING STARVATION". ResearchGate, Conference Paper- November 2005.

14.   Ma, X., Gao, H., Xu, H. et al. An IoT-based task scheduling optimization scheme considering the deadline and cost-aware scientific workflow for cloud computing. J Wireless Com Network 2019, 249 (2019). https://doi.org/10.1186/s13638-019-1557-3

Landslide Susceptibility Assessment of Besni-Tut (Adıyaman) Region with Remote Sensing and GIS Technologies

Berna Tanrıverdi[1*], Osman Orhan[2], Senem Tekin[3]

Abstract: In this study, landslide susceptibility assessment was carried out with Analytical Hierarchy Process (AHP) and Artificial Neural Network (ANN) in a 1200 km² area of Tut (Adıyaman) vicinity. For this purpose, as a first step, the parameters required in the analyzes were prepared in the Geographical Information Systems (GIS) environment. The landslide inventory map of the region was updated with field studies. In the second stage, the parameters that are effective in the development of landslides in the region were scored between 1 and 9 by conducting surveys with experts in the field in order to make analyzes with the AHP method. By taking the average of the survey results, consistency analyzes of each parameter were performed and weighting ratios were calculated. According to the landslide susceptibility map; 23.53% of the study area and 71.55% of the landslides are located in high and very high susceptible areas. other susceptibility assessment with AHP, landslide susceptibility assessment was made with ANN. The data set generated from the study area was divided into three as 80% analysis, 10% test and 10% verification data by random selection method. The resulting landslide susceptibility map was evaluated in 5 classes as very low, low, medium, high and very high. According to the result susceptibility map; 30% of the study area and 78.4% of the existing landslides are located in high and very susceptible areas. The accuracy of the resulting landslide susceptibility maps was evaluated with the receiver operating characteristic curve and the area under the curve, and the accuracy of the landslide susceptibility map made with AHP was calculated as 0.820. As a result of the evaluations, it is observed that the accuracy of both models has a high value.

Keywords: AHP, ANN, Landslide, Landslide Susceptibility, Tut (Adıyaman).

1. Introduction

From past to present, natural disasters are one of the causes of loss of life and property of human beings. Damages caused by natural disasters are increasing all over the world over the years. The reasons for the increase in the number of natural disasters such as earthquakes, floods, and landslides are, in addition to natural causes, the development of unplanned settlements, especially in the last 10 years, in regions with a high potential for natural disasters (URL-1; URL-2). Landslides, which are among the natural disasters in question, are one of the disaster types that cause the most loss of life and property, but they show their effect even more due to the rapidly increasing irregular settlements. Landslide susceptibility and risk studies are of great importance in minimizing the number of damage caused by landslides (Nsengiyumva et al. 2018; Chawla et al. 2018; Min and Yoon, 2021; Xie et al. 2021; Tekin, 2021). In this sense, the use of statistical methods, Geographical Information Systems (GIS) and Remote

[1] Adıyaman Municipality, Directorate of Development and Urbanization, 2040, Center/Adıyaman, Turkey
[2] Mersin University, Department of Remote Sensing and GIS, Institute of Science and Technology, 33343 Mersin/Turkey
[2] Mining and Mineral Extraction Department, School of Technical Sciences, Adıyaman University, 02040, Adıyaman, Turkey
* Corresponding author: bernatnrvrd@gmail.com

Sensing (RS) have become the basic elements of the studies and have increased the accuracy and quality of these studies. In order to evaluate landslides, as in all types of natural disasters, information such as where landslides occurred in the past, under which factors they developed, and which triggering factors were affected, should be well known. In the evaluation of disaster data, inventory maps, archive, historical or event inventory maps should be considered as a whole in the regions where disasters occur. Susceptibility maps showing where landslides can occur spatially constitute one of the important stages of regional-scale planning and landslide mitigation studies (Tekin and Çan,2015; Tekin and Çan,2018; Abanco et al. 2016; Nsengiyumva et al., 2018; Chawla et al., 2018; Ietto et al., 2018; Silva et al., 2018; Achour et al., 2018; Chen et al., 2016). Preparation of landslide susceptibility maps; It depends on many factors such as the type and distribution of landslides and the reliability of the inventory map, as well as taking into account the appropriate environmental variables that predispose the landslides (Çan et al., 2013). Landslide susceptibility assessments consist of studies obtained by evaluating together the existing landslide inventory and environmental variables that cause landslides in regional studies. It consists of two methods, quantitative and qualitative, and both methods are evaluated in their own sub-headings. Within the scope of this study, analyzes were carried out with the AHP method, which is dependent on expert opinion, and the ANN method, which is one of the data-driven methods. In the study, landslide susceptibility analyzes were carried out around Tut district of Adıyaman. As the first stage of the study, national and international scientific studies on landslide susceptibility, in which the spatial likelihood parameter of landslides are determined, were examined, and studies on the method that would form the basis of the thesis study were explained. The landslide inventory map of the region was checked and updated together with the field studies, aerial photography and the data in the archive, and the data updated in the computer environment were digitized. There are many variables in the literature, among the environmental variables that cause landslides, and the parameters of geology (lithology), numerical elevation model (DEM) and derivative maps, which are considered to be the most effective in the thesis field and which are the most used in the literature, slope slope, roughness, topographic humidity index parameters were prepared in GIS environment. In order to create a landslide susceptibility map, two different susceptibility analyzes were performed and the results were compared. The reliability of the landslide susceptibility map was evaluated with the landslide inventory, success-prediction and receiver operating characteristic curves.

2. Material ve Method

2.1.Material

In this study, landslide susceptibility assessment was carried out using AHP and ANN method in an area of approximately 1200 km^2 around Tut district of Adıyaman province in the Southeastern Anatolia Region of Turkey. The study area is located within the M39a3, M39b4, M39b3, M40a4, M40a3, M40b4, M39d2, M39c1, M39c2, M40d1, M40d2 and M40c1 sheets on the 1/25000 scale map, and the study area map is shown in Figure 1.
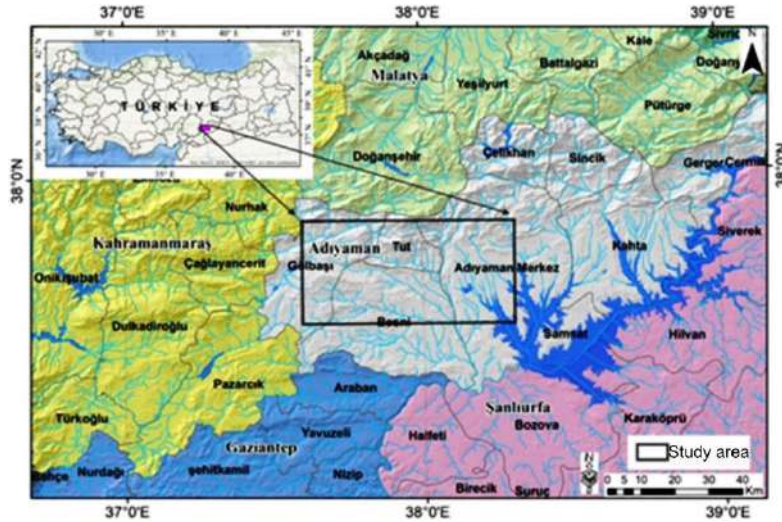
Figure 1. Study area location map.

The lithology map of the study area was compared with the landslide inventory map. Geologically, the units in the study area located south of the fault zone are tectonically overlain by the upper alloctane series (Akbaş et al. 2011). In the Upper Cretaceous-Miocene time, different nappes developed in the region with the merging of different tectonic units in the north of the Arabian continent. These nappes collided with the Arabian platform as the ocean receded at the end of the Eocene period. Depending on the deformations accumulated in the region as a result of the tensions between the nappes and the Arabian platform, the fault zone consisting of east-west reverse fault and thrust slices has developed (Akbaş et al. 2011). The study area and its surroundings are basically the Koçali Complex. Autochthonous units unconformably overlie the unit. The Jurassic-Lower Cretaceous Koçali complex includes the Koçali ophiolite and the volcano-sedimentary Koçali mélange (Yıldırım et al., 2012). As autochthonous units; It consists of Katel, Antak, Besni, Arpalık, Germav, Midyat, Hoya, Zeytin formations, Yavuzeli basalt and alluvium (Figure 2).
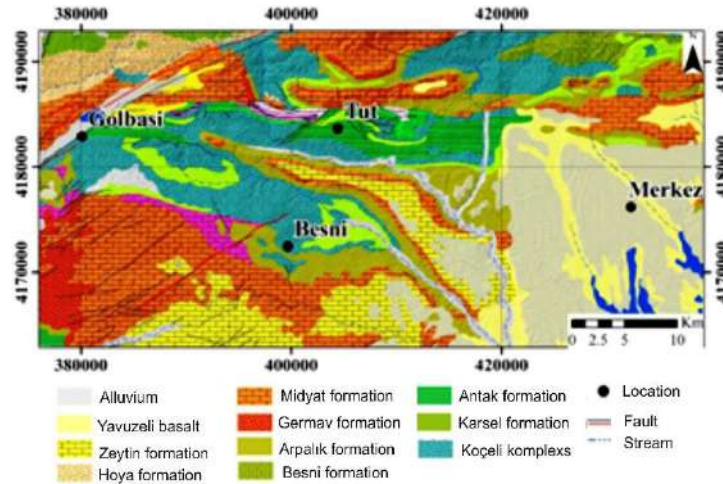
Figure 2. Geological map of the study area (Akbaş et al., 2011).

Within the scope of this study, first of all, a landslide inventory map was created. Satellite images and orthophoto images were examined as a first step for the created landslide inventory map. In addition to the images, the landslides in the AFAD and MTA archives were examined and field studies of the region were carried out. Satellite images were evaluated by comparing the field studies and archive records obtained with each other. The landslide inventory maps obtained as a result of the study are shown in Figure 3. According to these data, the landslide

with the smallest areal size of 175 landslides is 0.065 km^2, while the largest landslide is 10.36 km^2.
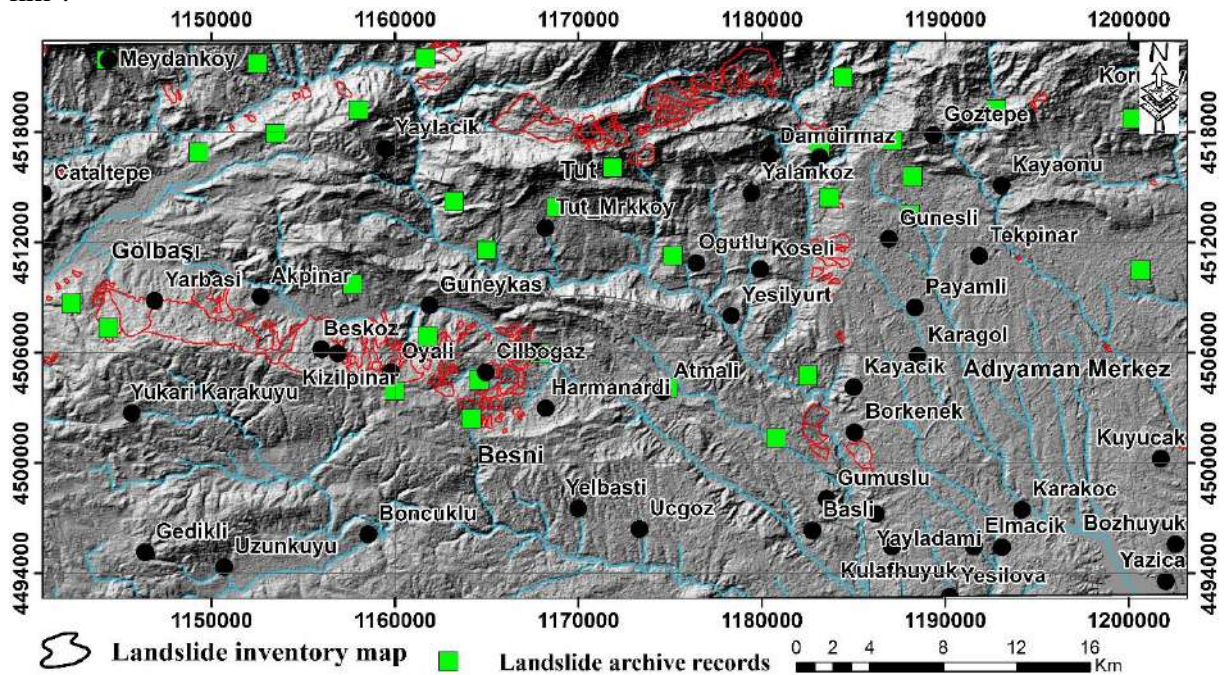
Figure 3. Landslide inventory map and archive records of the study area.

In line with the literature study for the evaluation of landslides, frequently used parameters were determined. Within the scope of the study, as environmental variables that prepare landslides, mainly geology, digital elevation model, roughness index, slope, curvature, topographic wetness index parameters were prepared in ArcGIS environment. Slope curvature, topographic wetness index (TWI) and roughness index parameters produced using the digital elevation model were used in the study with a raster-based 30 meters spatial resolution. Digital elevation model Global Digital Elevation Model GDEM (ASTER GDEM) V003 was used as ASTER Digital Elevation model (SYM). SYM was converted to WGS84 Zone 37 projection system. It is seen that the upper parts of the study area reach 2500 m heights. The slope parameter was used in almost all of the studies examined in the literature review. Slope map was created by using the "Slope" command under "3D Analyst" in ArcGIS software. The result obtained is that the slope of the study area on the map is between 0-63.27° degrees (Figure 4). The curvature derivative map produced for the study area was produced with the "Curvature" module in ArcGIS "3D Analyst" (Figure 4). In the curvature map, a negative value represents a concave, a positive value a convex, and a zero value a valley. It is observed that landslides are concentrated on concave slopes. Topographic wetness index (TWI) is the parameter obtained by considering the basin area and slope in order to determine the water holding capacity of the region in the absence of groundwater data. The roughness index shows the degree of irregularities on the surface, and the roughness values increase on the valley slopes where landslides are intensely observed in the study area. DEM and derivative maps of the study area are shown in Figure 4.
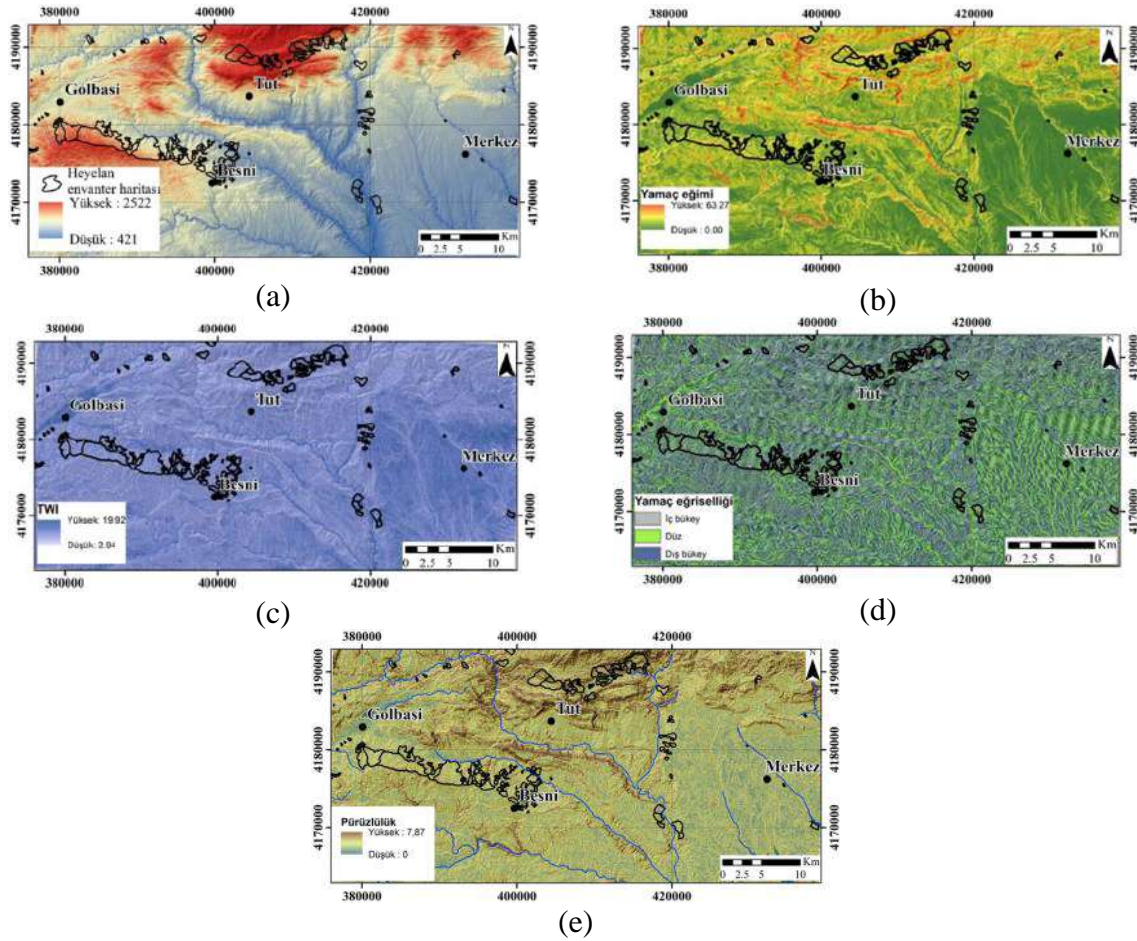
Figure 4. DEM (a), slope slope (b), TWI (c), slope curvature (d), roughness (e) parameters of the study area.

2.1. Method

2.1.1. AHP

AHP is a set of processes that compares each criterion with a set of options or alternatives. Within the scope of this study, as a first step, the parameters affecting the landslide in the region were determined by surveys conducted with experts. The predisposing factors for landslides for the susceptibility assessment are carried out by using a weighting method in which the relative value of the parameters determines the weight (Table 1). In this study, each parameter was weighted by taking the average value of the survey results conducted with the experts. The scores given are based on reasonable prioritization of the active factor in landslide susceptibility assessment (Saaty, 2008).

Table 1. Binary comparison in AHP 9-point rating

NUMERICAL VALUES	DEFINITION
1	Equivalent
3	low severity
5	high importance
7	Importance is too high
9	Extremely important (Absolute superiority)
2,4,6,8,9	Intermediate status

Then, binary variable matrices were created showing that one component dominates the other. The consistency ratio was calculated to find the continuity of the weights of the Binary compared factors. The advantage of the AHP method is that it provides CR as a relationship between consistency and degree of inconsistency. The appropriate value of CR is 0.1 for all large matrices, i.e. n>5. Therefore, a CR of 0.1 or less is of reliable significance. If the CR value is greater than 0.1 after the evaluations, the variables should be changed or the weights should be revised. In Table 2, the pairwise comparison matrices of the criteria are given, and the weights of the factors according to the Binary comparison matrix are shown in Table 3. According to the pairwise comparison matrix, the CI value is 0.09; A CR value of 0.076 indicates the accuracy of the evaluation.

Table 2. Binary comparison matrix.

Variables	Roughness	Curvature	TWI	DEM	Slope	Geology
Roughness	1.00	0.20	0.50	0.33	0.25	0.11
Curvature	5.00	1.00	0.50	0.33	0.33	0.25
TWI	2.00	2.00	1.00	0.16	0.33	0.20
DEM	3.00	3.00	6.00	1.00	1	0.50
Slope	4.00	3.00	3.00	1.00	1.00	0.50
Geology	9.00	4.00	5.00	2.00	2.00	1.00
TOTAL	24.00	13.20	16.00	4.83	4.92	2.36

Table 3. Weights and ranking of factors

Factors	Factors	Factor Ranking
Geology	0.367	1
DEM	0.222	2
slope	0.198	3
Curvature	0.092	4
TWI	0.080	5
Roughness	0.042	6

Factors were divided into classes in the AHP process, and their weights were calculated by making a pairwise comparison matrix within the classes. Studies showing similar characteristics with landslide susceptibility studies were taken into account while making the classification. The order and weights of the 6 factors are as follows (Table 4).

Table 4. Weights and ranking of sub-factors

Factors/ Subgroups		1	2	3	4	5	6	7	8	9	Bottom Weight
DEM		1	2	3	4	5	6	7	8	9	**(CR 0.06)**
(421)-(841.2)	1	1									0.060
(841.2)-(1261.4)	2	2	1								0.090
(1261.4)-(1681.6)	3	3	2	1							0.154
(1681.6) -(2101.8)	4	4	3	2	1						0.222
(2101.8) -(2522)	5	5	5	3	4	1					0.474
Slope		1	2	3	4	5	6	7	8	9	**(CR 0.05)**
(0)-(14.05)	1	1									0.053
(14.05)-(28.09)	2	2	1								0.078
(28.09)-(42.14)	3	3	3	1							0.152
(42.14) -(56.18)	4	5	4	2	1						0.245
(56.18) -(70.23)	5	6	5	4	3	1					0.473

Roughness		1	2	3	4	5	6	7	8	9	(CR 0.02)
(0)-(1.28)	1	1									0.053
(1.28) -(2.55)	2	2	1								0.095
(2.55) -(3.82)	3	3	2	1							0.167
(3.82) – (5.10)	4	4	3	2	1						0.266
(5.10) – (6.38)	5	6	5	4	2	1					0.420
TWI		1	2	3	4	5	6	7	8	9	**(CR 0.008)**
(2.41) -(5.46)	1	1									0.444
(5.46) -(6.73)	2	1/2	1								0.262
(6.73) -(8.32)	3	1/3	1/2	1							0.153
(8.32) -(10.51)	4	1/5	1/3	1/2	1						0.089
(10.51) -(19.35)	5	1/7	1/5	1/3	1/2	1					0.053
Slope Curvature		1	2	3	4	5	6	7	8	9	**(CR 0.005)**
Convex	1	1									0.243
Straight	2	1/3	1								0.088
Concave	3	3	7	1							0.669
lithology		1	2	3	4	5	6	7	8	9	**(CR 0.05)**
Koçeli	1	1									0.348
Midyat	2	1/2	1								0.236
Arpalık	3	1/3	1/2	1							0.158
Antak	4	1/4	1/3	1/2	1						0.104
Zeytin	5	1/5	1/4	1/3	1/2	1					0.069
Kastel	6	1/6	1/5	1/4	1/3	1/2	1				0.055
Others	7	1/7	1/6	1/5	1/4	1/3	1/4	1			0.030

A landslide susceptibility map was obtained with the ArcGIS software tool by using the landslide triggering 6 Factor and sub-factor weights and pixel values. The result values obtained were normalized and the result values were rearranged to be between (0)-(1). After the AHP analyzes were performed, a landslide susceptibility map of the region was obtained by using the raster calculator tool-in in Arcgis program with the weight coefficients of each variable and the overlapping analysis was performed (Figure 5).
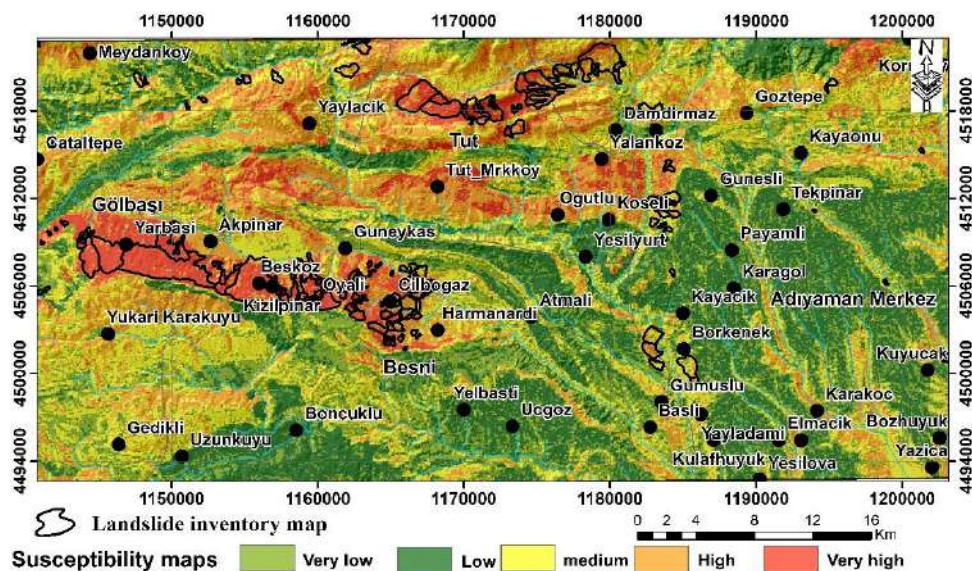
Figure 5. Landslide susceptibility map of the study area.

The performance evaluation of the obtained landslide susceptibility map was evaluated with the success prediction curve, the receiver operating characteristic curve and the area under the

curve. According to the success estimation curve, it is seen that the study area has 32.06 (very low), 27.10 (low), 17.32 (medium), 12.91 (high) and 10.62 (very high) susceptible areas (Figure 6). It has been calculated that all landslides in the study area are 4.57% (very low), 8.33% (low), 15.54% (moderate), 26.24% (high) and 45.31% (very high) susceptible areas. The accuracy evaluation of the model created for the landslide susceptibility map was performed with the receiver operating characteristic curve, and the value under the curve was calculated as 0.820 (Figure 6). This value shows that the accuracy of the established model has a high-very high prediction capacity.
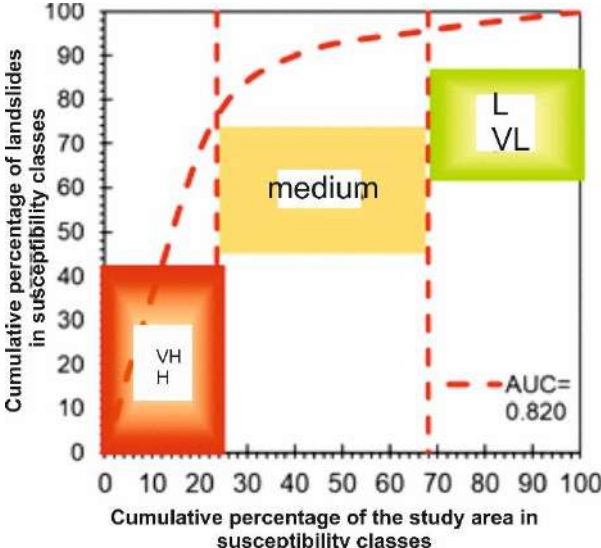
Figure 6. Success-prediction curve and receiver operating characteristic curves.

2.1.1. ANN

ANN is a set of mathematical modeling methods that interact with many elements similar to each other (Kohonen, 1982). Back propagation training algorithm in artificial neural network is also used in this study because it is the most widely used neural network method in the literature. There are two phases to using neural networks: the first phase is the training phase where the internal weights are calculated and the second phase is the classification phase. Typically, the back propagation algorithm trains the network until a targeted minimum error is achieved between the desired and actual output values of the network. After the training is complete, the network is used as a feed-forward structure to generate a classification for all data. Figure 7 shows the Artificial Neural Network structure.
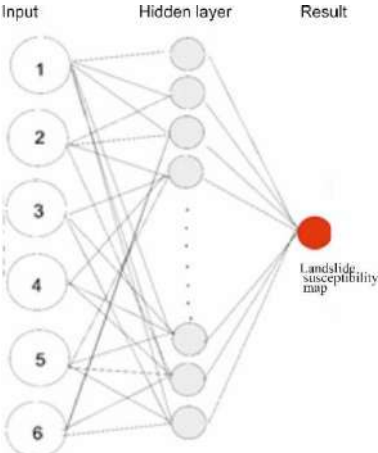
Figure 7. Artificial Neural Network structure.

Within the scope of this study, 6 variables were prepared according to 30 m spatial resolution. The number of hidden layers, ranging from two-thirds to two times the number of input layers suggested by Karsoliya (2012), was tried and the best result obtained was a susceptibility map using 15 hidden layers. The data set of the study area was divided into three as 80% analysis, 10% test and 10% validation data by random selection method. The landslide susceptibility map was evaluated in five equally spaced classes as very low, low, medium, high and very high. According to the susceptibility map obtained; Approximately 30% of the study area and 78.4% of the landslides are located in high and very high s susceptible areas. It is seen that the study area has 42.52 (very low), 28.30 (low), 15.42 (medium), 10.54 (high) and 3.22 (very high) susceptible areas (Figure 8). It has been calculated that all landslides in the study area are 3.72% (very low), 6.47% (low), 16.54% (moderate), 28.36% (high) and 44.91% (very high) sensitive areas (Figure 8).
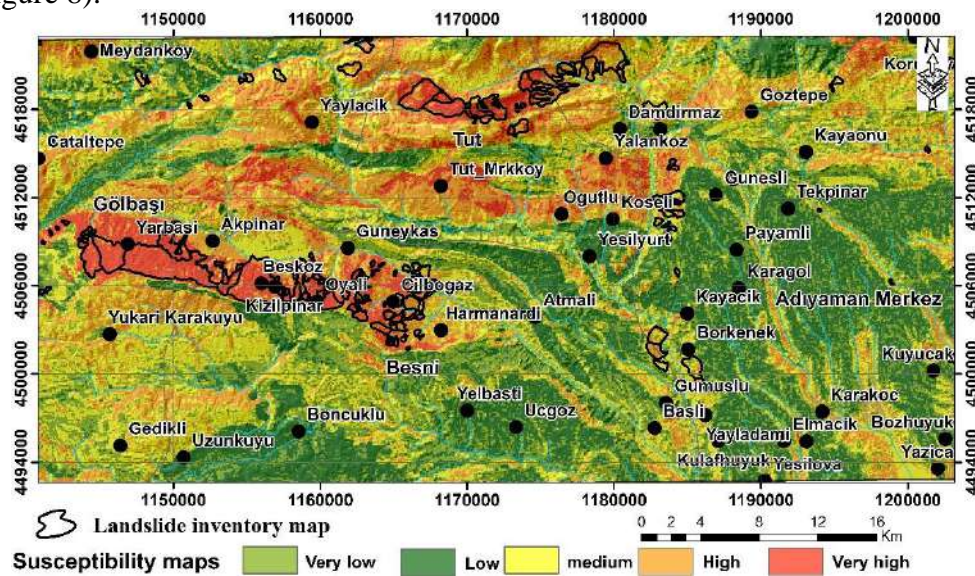
Figure 8. Landslide susceptibility map of the study area.

The accuracy of the resulting landslide susceptibility map was evaluated with the receiver operating characteristic curve and the area under the curve, and it was calculated as 0.84 for the entire study area, 0.82 for all landslides, and 0.83 for verification and test landslides (Figure 9).
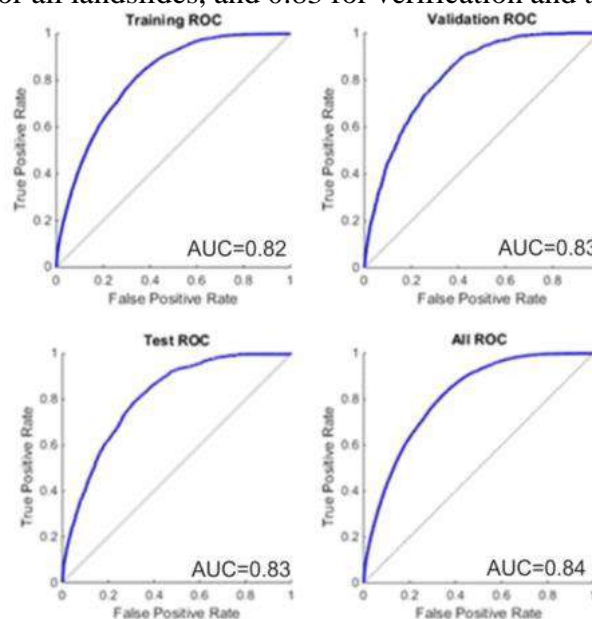
Figure 9. The receiver operating characteristic curve and the area under the curve

3. Results

In this study, landslide susceptibility maps were prepared by using Analytical Hierarchy Process Method and Artificial Neural Networks, one of the multivariate statistical analysis methods. Within the scope of this study, firstly the landslide archive records of the MTA were examined and then the historical landslide inventory map prepared by the General Directorate of MTA was evaluated. In addition to these, multi-time landslide inventory maps of the region were created with the analysis of aerial photographs taken on different dates and detailed field studies to be carried out in the region. The landslide susceptibility map obtained by the AHP method is used with equal intervals and the probability values are 0.00-0.20 (very low), 0.20-0.40 (low), 0.40-0.60 (moderate), 0.60-0.80 (high) and 0.80-1.00 (very high). The performance evaluation of the obtained landslide susceptibility map was evaluated with the success predction rate, the receiver operating characteristic curve and the area under the curve. According to the success prediction curve, it is seen that the study area has 32.06 (very low), 27.10 (low), 17.32 (medium), 12.91 (high) and 10.62 (very high) susceptible areas. It has been calculated that the landslide inventory database is located in 4.57% (very low), 8.33% (low), 15.54% (moderate), 26.24% (high) and 45.31% (very high) susceptible areas. The accuracy evaluation of the model created for the landslide susceptibility map was performed with the receiver operating characteristic curve, and the value under the curve was calculated as 0.820. For the susceptibility maps obtained with the Artificial Neural Network, the data set obtained from the study area was divided into three as 80% analysis, 10% test and 10% verification data by random selection method. By using the susceptibility map at equal intervals, probability values were evaluated in 5 classes as 0.00-0.20 (very low), 0.20-0.40 (low), 0.40-0.60 (medium), 0.60-0.80 (high) and 0.80-1.00) (very high). According to the obtained landslide susceptibility map; Approximately 30% of the study area and 78.4% of the existing landslides are located in high and very high sensitive areas. The accuracy of the obtained landslide susceptibility map was evaluated with the receiver operating characteristic curve and the area under the curve, and it was calculated as 0.84. It is seen that the study area has 42.52 (very low), 28.30 (low), 15.42 (medium), 10.54 (high) and 3.22 (very high) sensitive areas. It was calculated that all landslides in the study area were located in susceptible areas of 3.72% (very low), 6.47% (low), 16.54% (moderate), 28.36% (high) and 44.91% (very high). When the spatial distribution of the landslide susceptibility obtained by both methods in the entire study area and the percentages of all landslides occurred according to the susceptibility map are examined, 71.55% of the landslides in the susceptibility map obtained by AHP and 78.4% of the landslides in the susceptibility map obtained by AHP are high and very susceptible located in the fields. These values show that the susceptibility maps obtained by both methods are consistent with each other. In addition, the accuracy of the susceptibility map obtained with AHP was 0.82; the susceptibility map obtained with AHP was 0.84; It shows that the analyzes made with ANN give more reliable results than the analyzes obtained with AHP. However, the values obtained from both methods show that the accuracy of the confirmed model has a high-very high prediction capacity. As a result, it is thought that the data to be obtained in this study will contribute to the studies conducted to reduce the damages caused by landslides, as well as to determine the environmental factors that control landslides in the study area and the areas where landslides will occur spatially.

References

Abancó, C., Hürlimann, M., Moya, J., & Berenguer, M. (2016). Critical rainfall conditions for the initiation of torrential flows. Results from the Rebaixader catchment (Central Pyrenees). Journal of hydrology, 541, 218-229.

Achour, Y., Boumezbeur, A., Hadji, R., Chouabbi, A., Cavaleiro, V., & Bendaoud, E. A. (2017). Landslide susceptibility mapping using analytic hierarchy process and information value methods along a highway road section in Constantine, Algeria. Arabian Journal of Geosciences, 10(8), 194.

Akbaş, B., Akdeniz, N., Aksay, A., Altun, İ.E., Balcı, V., Bilginer, E., Bilgiç, T., Duru, M., Ercan, T., Gedik, İ., Günay, Y., Güven, İ.H., Hakyemez, H.Y., Konak, N., Papak, İ., Pehlivan, Ş., Sevin, M., Şenel, M., Tarhan, N., Turhan, N., Türkecan, A., Ulu, Ü., Uğuz, M.F., Yurtsever, A. ve diğerleri, (2011), 1:1.250.000 ölçekli Türkiye Jeoloji Haritası. Maden Tetkik ve Arama Genel Müdürlüğü Yayını, Ankara-Türkiye.

Chawla, A., Chawla, S., Pasupuleti, S., Rao, A. C. S., Sarkar, K., and Dwivedi, R. (2018). Landslide Susceptibility Mapping in Darjeeling Himalayas, India. Advances in Civil Engineering, doi: 2 10.1155/2018/6416492.

Chen, W., Chai, H., Zhao, Z., Wang, Q., & Hong, H. (2016). Landslide susceptibility mapping based on GIS and support vector machine models for the Qianyang County, China. Environmental Earth Sciences, 75(6), 474.

Çan, T., Duman, T. Y., Olgun, Ş., Çörekçioğlu, Ş., Karakaya Gülmez, F., Elmacı, H., Hamzaçebi, S., Emre, Ö., (2013), "Türkiye Heyelan Veri Tabanı", s. 1-6, TMMOB Coğrafi Bilgi Sistemleri Kongresi, 2013 11-13 Kasım 2013, TMMOB, Ankara.

Jacinth Jennifer, J., & Saravanan, S. (2021). Artificial neural network and sensitivity analysis in the landslide susceptibility mapping of Idukki district, India. Geocarto International, 1-23.

Karsoliya S., (2012), Approximating Number of Hidden layer neurons in Multiple Hidden Layer BPNN Architecture, Int. J. Eng. Trends Technol., 3(6), 714–717.

Kohonen T., (1982), Self-organized formation of topologically correct feature maps, Biol. Cybern., 43(1), 59–69.].

Lee, D. H., Kim, Y. T., & Lee, S. R. (2020). Shallow landslide susceptibility models based on artificial neural networks considering the factor selection method and various non-linear activation functions. Remote Sensing, 12(7), 1194.

Min, DH., Yoon, HK., (2021). Suggestion for a new deterministic model coupled with machine learning techniques for landslide susceptibility mapping. Sci Rep 11, 6594. https://doi.org/10.1038/s41598-021-86137-x.

Moragues, S., Lenzano, M.G., (2021). Lanfri, M. et al. Analytic hierarchy process applied to landslide susceptibility mapping of the North Branch of Argentino Lake, Argentina. Nat Hazards 105, 915–941. https://doi.org/10.1007/s11069-020-04343-8.

Nsengiyumva, J.B.; Luo, G.; Nahayo, L.; Huang, X.; Cai, P., (2018). Landslide Susceptibility Assessment Using Spatial Multi-Criteria Evaluation Model in Rwanda. Int. J. Environ. Res. Public Health, 15, 243. https://doi.org/10.3390/ijerph15020243.

Ozdemir, A. (2020). A Comparative Study of the Frequency Ratio, Analytical Hierarchy Process, Artificial Neural Networks and Fuzzy Logic Methods for Landslide Susceptibility Mapping: Taşkent (Konya), Turkey. Geotechnical and Geological Engineering, 1-29.

Silva, R. F., Marques, R., Gaspar, J. L. (2018). Implications of Landslide Typology and Predisposing Factor Combinations for Probabilistic Landslide Susceptibility Models: A Case Study in Lajedo Parish (Flores Island, Azores-Portugal). Geosciences, 8(5), doi:UNSP 153 10.3390/geosciences8050153.

Tekin S., ve Çan T., (2018). Maksimum Entropi Yöntemi ile Mut (Mersin) - Taşkent (Konya) Arası Kaya Düşme Kaynak Alanlarının Belirlenmesi, 71. Türkiye Jeoloji Kurultayı, Ankara, Türkiye, 23-27 Nisan 2018, ss.1003- 1004.

Tekin, S. (2021). Mantıksal Regresyon Yöntemi ile Adıyaman İli Heyelan Duyarlılık Değerlendirmesi. Bilge International Journal of Science and Technology Research , 5 (1) , 34-41 . DOI: 10.30516/bilgesci.883519.

URL-1: https://www.emdat.be/emdat_atlas/sub_html_pages/sub_html_TUR.html.

URL-2: https:// www, desinventar.net/.

Yildirim N., Parlak O., ve Robertson A., (2012), Geochemistry and tectonic significance of the Koçali ophiolite and the related Koçali melange, Adiyaman region, SE Turkey, 65th Geological Congress of Turkey, ss. 82-83.

Ophiolite melange mapping and Chromite prospecting using Landsat-8 OLI and ASTER data in Aladağ region (Turkey)

MamadouTraore[1]*, Tolga Çan[2], Senem Tekin[3]

Abstract: During the last 20 years, image-processing using the different techniques of Remote Sensing have become a directing and hopeful tool for lithological investigation and mineral mapping. Discrimination of chromite bearing mineralized zones associated with ophiolite complex has been successfully carried out in recent years. In the Adana region, ophiolitic rocks constitute an essential part of the Aladağ tectonic unit and include an important reserve of chromium in Turkey. The most complete studies about ophiolites in the area were studied the using traditional method in minerals exploration. The main aim of this study is to test the potential Sentinel-2, Landsat-8 OLI and Advanced Spaceborne Thermal Emission and Reflection Radiometer (ASTER) satellite data in order to discriminate and detect the potential chromite bearing mineralized zonesin Adadag region. Band Ratio (BR), Principal Component Analysis (PCA), Minimum Noise Fraction (MNF), Decorrelated Stretching (DS) Methods and Supervised classification were using to discriminate the ophiolite rocks. The results shows that, The Suppor Vector Machine (SVM), Spectral Information Divergence (SID) and the Spectral Angle Mapper (SAM) techniques were integrated in the GIS environment was applied on Sentinel-2 A data image to update the geological map Aladağ. The results of the methods show a correlation with the techniques used previously. Ophiolite complex rocks has been well mapped using the three methods. The techniques used in this research are suitable to detect or identify the high-potential chromite bearing areas in the ophiolite complex rocks using Sentinel-2 Landsat-8 OLI and ASTER data.

Keywords: Ophiolite mélange, Remote sensing, Supervised classification, mineral exploration

1. Introduction

Detailed information about the earth's surface can be obtained in different scales, synoptically and temporally using remote sensing technologies. In recent years, remote sensing techniques have been increasingly used in a wide variety of disciplines to obtained geoscientific data for both regional and site-specific investigations.

Exploration of Ophiolites complexes plays important role in geological and remote sensing studies (Pournamdari and Hashim, 2014). Many studies show that ultrabasic rocks contain significant metal deposits or mineralization that contain the element platinum group (PGE) and sulphides of Fe, Ni, Cr, Co Au, Cu, as well as useful minerals, called magnesioferrite, magnetite and awaruite which probably found in rocks as serpentinization minerals sequence (Rajendran and Nasir, 2014a).

[1] OYAK & Cimpor global holding, Department of Production (Raw material), Akoupé, Abidjan (Côte d'Ivoire) [2] Department of Geological Engineering, Çukurova University, TR-01330 Sarıçam, Adana, Turkey
[3] Mining and Mineral Extraction Department, School of Technical Sciences, Adıyaman University, 02040, Adıyaman, Turkey
* Corresponding author: matraba77@gmail.com

Recently, the exploration and mapping of ophiolitic rocks are one of the most essential research topics studied by geologists around the world, because they contain economically exploitable minerals such as chromium, copper, manganese, nickel.

Turkey's chromitic mineralization can be observed on ultramafic formations from cumulative and structural sectors of ophiolites rocks and they can be associated according to the structural stratigraphic aspects (Engin et al., 1985) (Fig.1). Ophiolite complexes often contains minerals such as chromites, magnesite, as best gold, nickel, massive sulfide, which provides very significant economic benefits (Ünlü, 2019). Recently, the ophiolitic complex rocks map are one of the most essential research topics around the world due to economically exploitable minerals such as chromium, copper, manganese, nickel. Turkish chromitite deposits have been identified as "Alpine type" deposits and can be observed on ultramafic formations from cumulative and structural in Aladağ region (Engin et al., 1985).
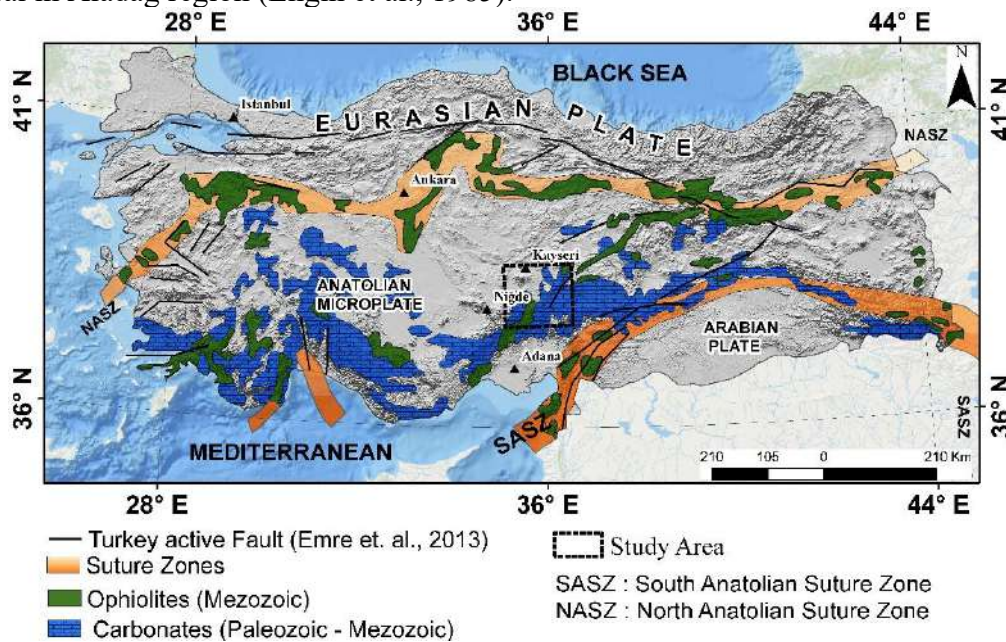
Figure 1. Distribution of ophiolites and related chromitites maps in Turkey (Modified After Okay and Tüysüz 1999) (Modified after MTA 2002).

In Adana, ophiolite formations constitute a significant section of the tectonic block of Aladağ region, forming a zone to the southeast of Pozantı (Fig.2). These lithological formations prolong to the northern border of the state, spanning about 30 km on the same strike in Kayseri region. The most comprehensive ophiolite study in the region was carried out by Tekeli et al., (1984). While the chromite occurrences first reported by the MTA in the region are poor quality, they constitute one of the most important regions of chromite mineralization in the world, at least in terms of mineral resources. Landsat series and ASTER remote sensing data have been used to mapping differents rocks formations and ore deposits in Ophiolites complex recently. Many researchers have used many remote sensing images to discriminate different rocks formation and ophiolites minerals associeted (Pour and Has him, 2011; Van Der Meer et al., 2012; Rajendran et al., 2012; Pour et al., 2014; Pour and Hashim 2015a, Tayabi et al., 2014; Pournamdari and Hashim, 2014; Pournamdari et al., 2014a, b; Rajendran and Nasir, 2014a, b; Ozkan et al., 2017; Abdelaziz et al., 2018). Landsat-8 OLI and ASTER remote sensing data were used in this part of research in order to mapping Ophiolites complex and differents rocks.
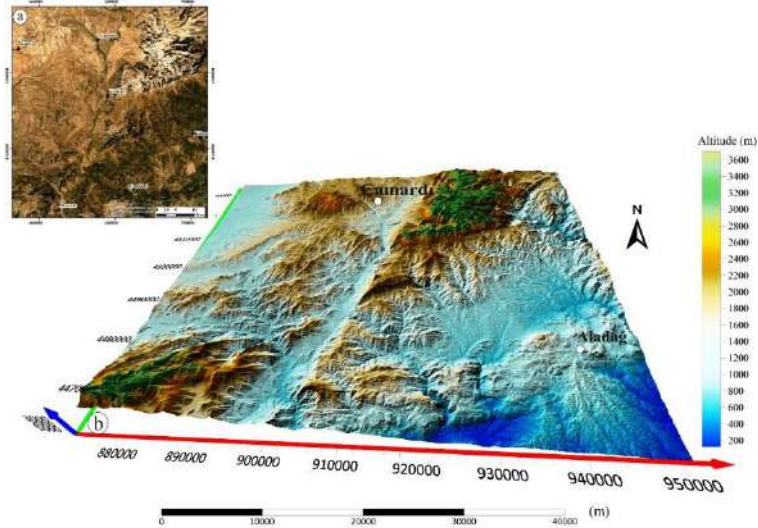
Figure 2. Localization (a) and 3D screen (b) of study area.

1.1. Geological Setting of Aladağ Region

The geology of the Pozanti-Aladağ region is dominated by ophiolites. These ophiolites formed part of a mass series distributed towards E-W in the Anatolide –Tauride belt (Parlak et al. 2009). The Pozanti ophiolitic formations- Karsanti commonly referred to as Aladağ ophiolite, is one of the biggest terrane of the Late Cretaceous ocean lithosphere in the Eastern Taurid belt. They cover an area of about 1300 km2 (Parlak et al. 2002). The ophiolitic complex is displace from ophiolite of Mersin to Ecemis fault. It's delimited by Oligocene and Neogene deposits around this fault to Neogene sediments in south and to carbonate units (Paleozoic Taurid) in north (Polat and Casey, 1995) (fig.3). Research on these ophiolitic Aladağ formations shows that, they consist mainly basic-ultrabasic, peridotites and isotropic gabbros. Ultrabasic accumulations come as a vast massif of dunite and wehrlite with minor layers of dunite and clinopyroxenite (Parlak et al., 2000, 2002).
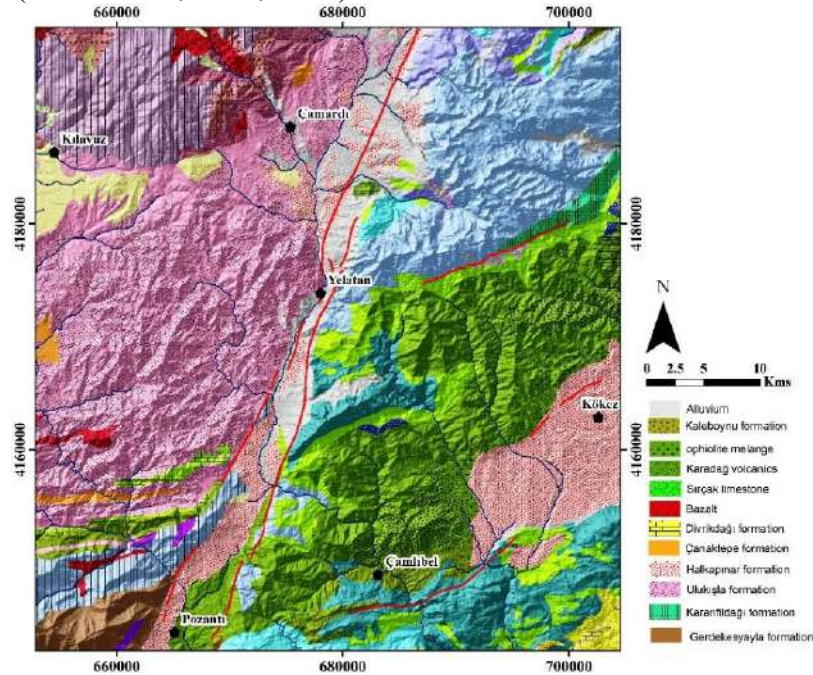
Figure **Hata! Belgede belirtilen stilde metne rastlanmadı.**. Geological maps of study area (Akbaş et al., 2002).

254

1.2. Chromitite Deposits in Study Area

Chromitite deposits are generally associated with ultramafic rocks (Fig.4). According to the original, geological order, minerals, texture and chemical properties, three main types are used in classification (Thayer, 1960 Jac and Thayer, 1972). Generally, in ultrabasic or basic intrusions of continental zone, they are usually large reserves and have a Cr / Fe and a rich erratic ratio. In Cr / Fe. One the best example is Bushveld complexes in South Africa; Chromitite (and magnetite) deposits have concentrated in side and are connected to ultrabasic or basic rocks formations. This class of chromite ore is not commercially exploitable. The most typical examples exist in Alaska and are known as Alaska and are also known as Alaskan-type intrusions; Deposits of alpine chromite (podiform). They are lenses or chromitite masses of irregular shape, with restricted continuity in direction and dip. These deposits have a very variable Cr content. The ratios of Cr / Fe are generally high. Reserves generally do not to exceed a hundred thousand tons. The chromite Cr / Fe ratios are usually high. The best examples in the world are generally observed in regions located on the Alpine mountain belt like Turkey, Greece, Cyprus, Iran and Pakistan etc.

Aladağ Ophiolite has a series of nappe containing metamorphic rocks at the basic - ultrabasic rocks. It is divided into two units, based on the rock association. The first is named as "tectonite" and is an ultrabasic record with a metamorphic design, originating from the upper mantle. Another unit is a cumulative type of assemblage, characterized by ultrabasic for mafic rocks.
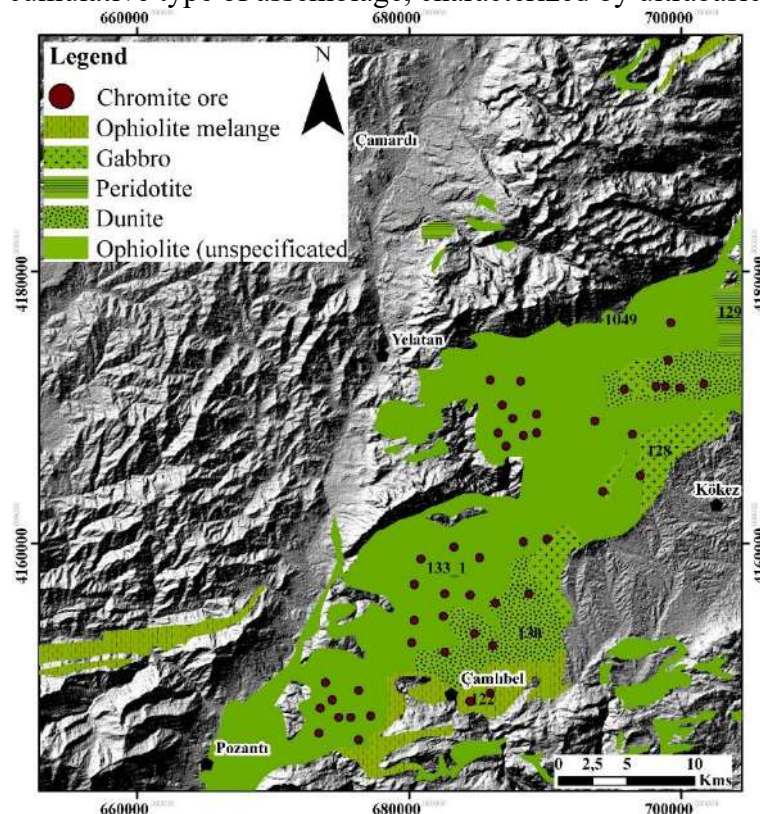
Figure 4. Chromitite occurrences and ophiolite complex rocks of Aladağ (Adana) region.

2. Material and Methods

The ASTER L1T (AST_L1T_00307192007083306_20150520160314_45593) data acquired on July 19, 2007 and Landsat-8 OLI were used in this research. The image has been already pre-georeferenced to UTM zone 36 North projection by using WGS-84 datum. Multispectral

images used in this thesis were obtained from in the U.S. Geological Survey Earth Resources Observation and Science Center (EROS) (http://earthexplorer.usgs.gov).

Cross-talk correction does not apply in this research because the ASTER L1T SWIR bands had already been processed. The atmospheric correction using Fast Line-of-sight Atmospheric Analysis of Spectral Hypercubes (FLAASH) algorithm was performed in the VNIR and SWIR bands of ASTER image. This correction is a basic exact atmospheric correction approach for satellite data which admit that reflectance from noise objects incorporates a generous component of atmospheric dissipation. The six SWIR bands and 3 VNIR bands of ASTER images were re-sampled to 30 m spatial resolution. For Landsat-8 OLI, the dark object subtraction atmospheric correction method was applied. This method is the best and easy atmospheric correction method apply in satellite image for lithological mapping because the image does not require in situ field or laboratory spectral measurements (Özkan et al.,2018). However, the Atmospheric correction (TOA) was used for Sentinel-2A. Band ratios techniques have been used by several authors for lithological mapping specially for ophiolitic formations (Hewson et al., 2001; Abdeen et al., 2001; Mars and Rowan, 2006; Gad and Kusky, 2007; Amer et al., 2010; Gabr et al., 2010; Rajendran et al., 2011, 2013). One of the popular band ratio using ASTER image for ophiolite rocks discrimination in Egypt is the Abdeen et al., (2001) (4/7, 4/1, 2/3 4/3) and (4/7, 3/4, 2/1). The band ratio ((2 + 4)/3, (5+ 7)/6, (7 + 9)/8) in RGB was used by Amer et al., (2010) to discriminate the ophiolite complex in Fawakhir. The previous band ratio applied in another area will be test in the case of this study. Nine bands (VNIR and SWIR) of ASTER image and 7 bands (VNIR-SWIR) of Landsat-8 OLI were used in PCA and MNF methods. In recent years, Decorrelation stretching has been used widely in remote sensing research to map geological formations (Abrams et al.,1988). This technic was used to delineate ophiolite rocks from other lithological formations in the region.

Finaly, based on the above results and of the spectral band lithological rocks, two supervised classifications as if Spectral Angle Mapper and Support Vector Machine were performed.

3. Results and Discussion

3.1.Processing and Results of the ophiolite complex rocks

3.1.1. False color composite (FCC)

The band ratio is one of the best methods suing in remote sensing for geological mapping and mineral exploration. In this research several previous band ratios performed for ophiolite mapping in arid and semi-arid region were tested in this research. In addition, the new band ratio was also evaluating to map ophiolite map in our study are. Many previous band ratios such as (6/4, 6/2, 7/6), (7/6, 6/ 5, 4/2), (6/7, 6/2, 6/5 ×5/4) for Landsat-8 OLI image, and ((4/7, 4/1, (2/3) *(4/3)), ((2+4) / 3, (5+7) / 6, (7+9) / 8) and (4/1, 4/5, and 4/7) for ASTER data in RGB were used in this study. It should be noted that these band ratios are very effective in the lithological discrimination of the ophiolite rock units. The new band ratios of Landsat-8 OLI (5/7, 4/2,5/4) for ASTER image were tested in this study. The band ratios (5/3, 5/1, 7/5) and (7/5, 5/4, 3/1)) and (5/7, 5/1, 5/4 × 4/3) pf Landsat TM equivalent to Landsat-8 OLI band ratio (6/4, 6/2, 7/6) and (7/6, 6/ 5, 4/2) and (6/7, 6/2, 6/5 ×5/4) were applied in the research (Fig.6).
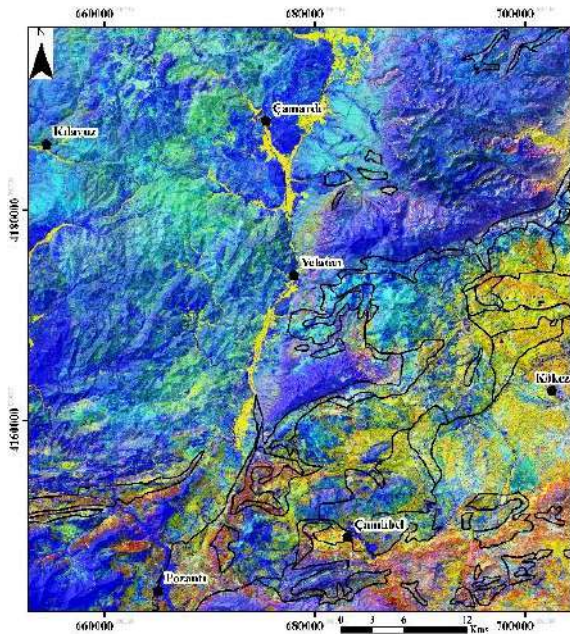
(a)
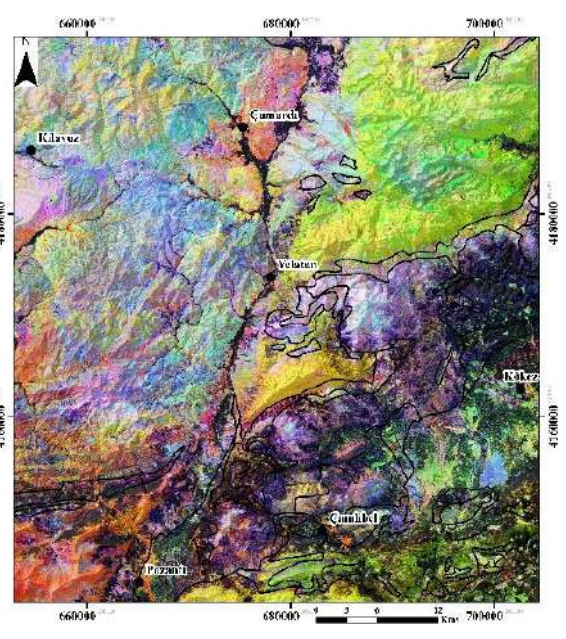
(b)

(c)
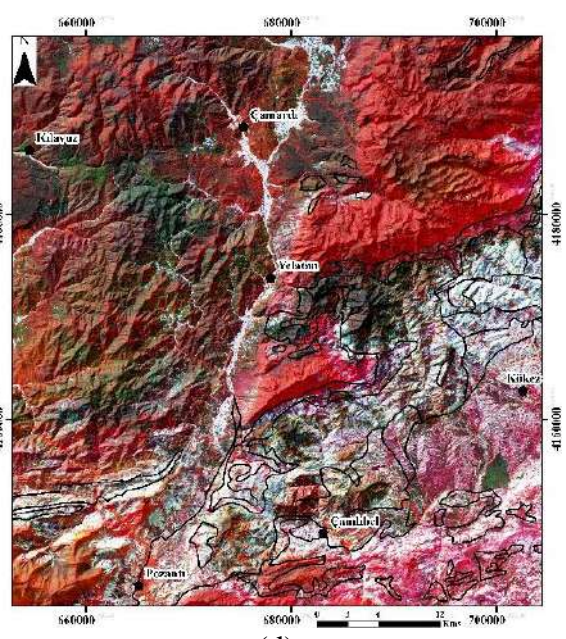
(d)

Figure 6. Landsat-8 OLI RGB band ratio image (a) (6/4, 6/2, 7/6), (b) (7/6, 6/ 5, 4/2) Gad and Kusky (2006), (c) (6/7, 6/2, 6/5 ×5/4) for Sultan, 1986 and (d) (5/7, 4/2,5/4) using in this study.

The band ratio ((4/7, 4/1, (2/3) *(4/3)) show the ophiolite formation in red- blue color. In the band ratio image (4/1, 4/5, and 4/7), the ophiolites are appearing in mangeta color. Whereas in the band ratio image (4/1, 4/5, and 4/7) the ophiolite appears in blue –mangeta (Fig.7).
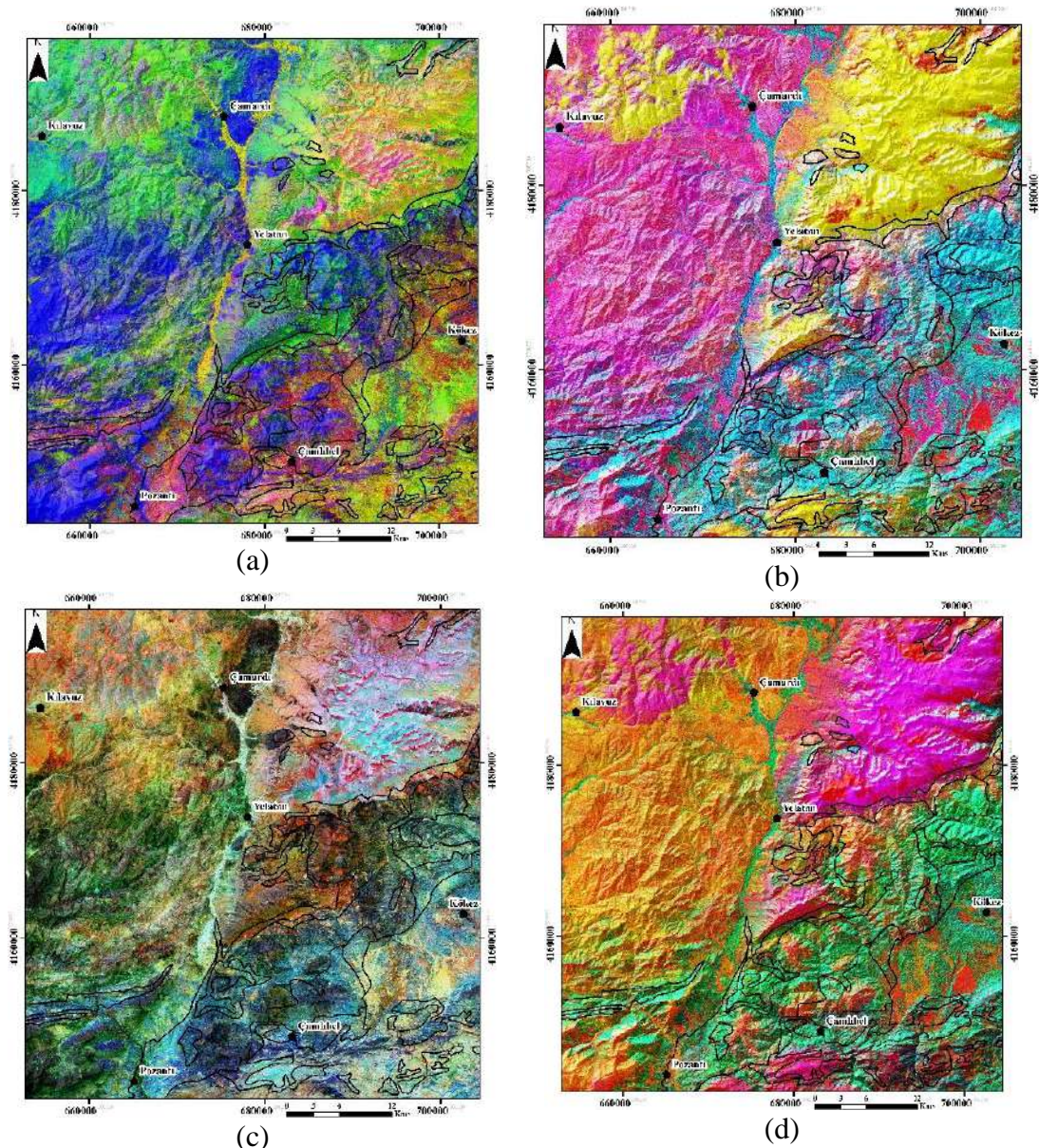
Figure 7. ASTER RGB band ratio image (a) (4/7, 4/1, (2/3) *(4/3) by Abdeen et al., (2001), (b) ((2+4) / 3, (5+7) / 6, (7+9) / 8) Amer et al., (2010), (c) (4/1, 4/5, 4/7) by Pour et al., (2013), and (d) (5/7, 4/2,5/4) used in this study.

Finally, in the new band ratio (5/7, 4/2, 5/4) image of ASTER, the ophiolite rocks are shown in green color. When the band ratios used in this research was compared, it is noted that, the old band ratios and the two new tests in this study show a good result in Landsat-8 OLI and ASTER image. Furthermore, this makes it possible to distinguish the different lithological formations from the region.

3.1.2. Principal Component Analysis (PCA) and Minimum Noise Fraction (MNF)

The Principal Component Analysis (PCA) method is used in this study to produce uncorrelated output bands, to segregate noise components, and to reduce the dimensionality of data sets. It was found that, the first PCA band contains more information in the data variance data and so on; In the part of the study. Nine bands of (VNIR and SWIR) ASTER image and seven bands of Landsat-8 OLI (VNIR and SWIR) were used. According to result of the PCA. Three bands (PC5, PC3, and PC1) ofLandsat-8 OLI and (PC3, PC2, and PC1) of ASTER displayed in RGB

were selected for better discrimination between ophiolitic rocks (serpentinites, gabbros, and basalt), and other rocks in the study area (carbonate, granite) (Fig. 8). The image interpretations according to geological map of PC5, PC3, and PC1 in RGB show that ophiolite complex is identified by green and dark color. And the result of PC3, PC2, and PC1in RGB for ASTER show that, the yellow and purple color was caraterzed by ophiolite rocks. As in the case of the PCA, VNIR and SWIR bands of Aster and Landsat image were chosen to map the ophiolitic formations of our study area. The MNF components, MNF5, MNF4, and MNF2 for Landsat-8 OLI and MNF1, MNF3, and MNF5 for ASTER were used to produce the RGB color composite in the study area. The result of MNF5, MNF4, and MNF2 in RGB for Landsat-8 OLI showed that, the ophiolite rocks as red green to maron color. The MNF1, MNF3, and MNF5 in RGB were also examined for lithological discriminations. In this case, the ophiolite rocks as appear in puple to dark green color (Fig.9).

(a)

(b)
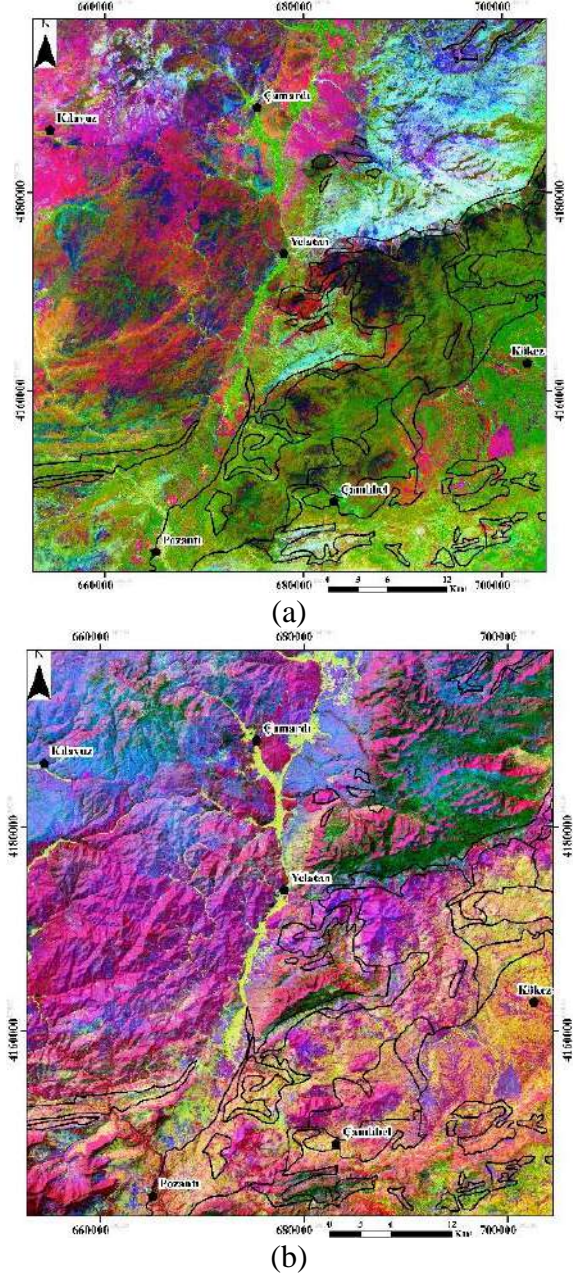
Figure 9. Minimun Noise Fraction (c) (MNF5, MNF4, and MNF2) for Landsat-8 OLI and (d) (MNF1, MNF3, and MNF5) for ASTER RGB image showing lithological units in the study area.

3.1.3. Decorrelated Stretch

The three band in color composite of Aster image and Landsat-8 OLI were selected to performed the decorrelated image. The band 2, 5 and 8 for ASTER and band 7, 5 and 2 for Landsat-8 OLI was using due to spectral characterize of rock units in this area. The band 2 for ASTER and band 5 for Lansat-8 contains and they are relating to the presence of iron. The band 5 for ASTER correspond to band 7 for Landsat-8 give us more information about hydroxyl-bearing. The band 8 for aster image contain more information about carbonate and serpentinite minerals (Rajendran et al., 2012). The selected decorrelated image shows almost all ophiolite rock types which are discriminated and separable in distinct colors comparable to previous the geology map in the study area (Fig.10).

| (a) | (b) |
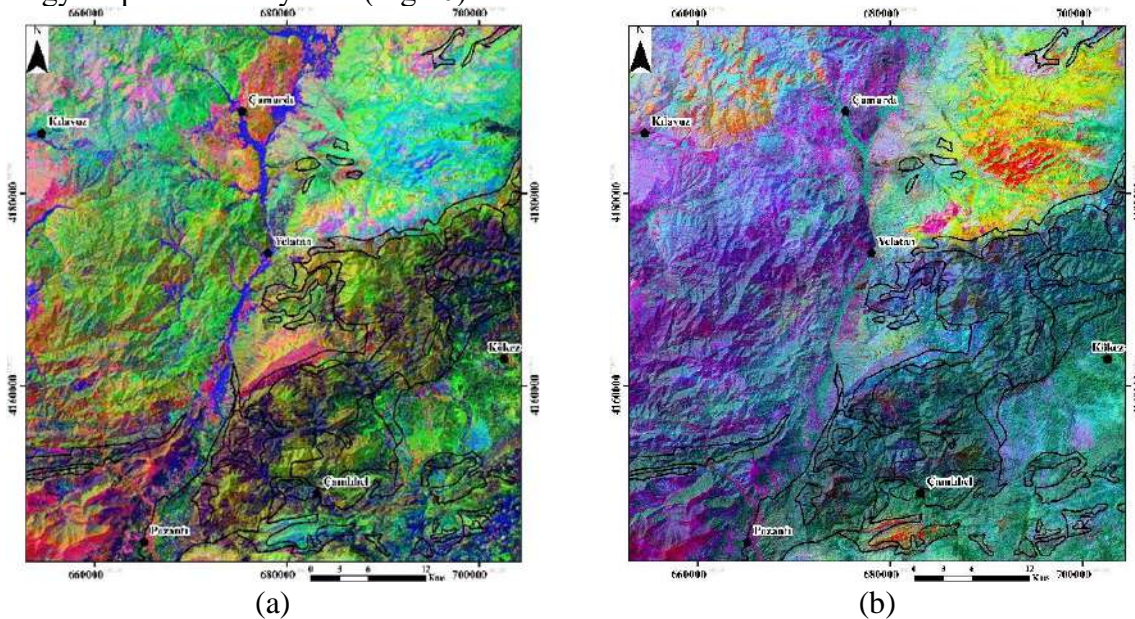
Figure 10. (a) Landsat-8 OLI RGB (7, 6, 5 bands) and (b)ASTER (2, 5, 8 bands) decorrelated image showing lithological units in the study area.

To associate the limits of ophiolitic formation of the previous geological map on the results obtained from differents methods applied on satellite images of the study area, the a good spatial correlation between these two data (previous geological map and ASTER image) were carried out and a clear discrimination between the different rocks of the region. The band ratio image shows better discrimination between ophiolite rocks more than the PCA and MNF image (Fig.10).

3.1.4. Supervised Classification SVM, SID and SAM

FCC, PCA, MNF technics were applies on mulspectral image to delinineate the boundary of the geological formation of the study area. Consequently, acceptable result was obtained from these methods. But for generating updated geology map and have a good accuracy of the study, it is necessary to make a supervision. In the case of this research, the Suppor vector Machine (SVM), Spectral Information Divergence (SID) and the Spectral Angle Mapper (SAM) technics were integrated in the GIS environment to update the geological map of Tufanbeyli and Aladağ area using Sentinel-2A data. The analysis of the map indicates that more differences exist between the used methods. The result of these methods shows a correlation with the techniques used previously. Ophiolite complex rocks has been well mapped using the three methods. However, the 1069 formations were not delimited in SVM (Fig.11 a), other were less visible with SID (Fig.11 b), and finally, some were very well discriminated by SAM (Fig.11 c). It

should be noted that the ophiolitic formations were very well delimited using the three algorithms. The statistical results derived from virtual verification, the previous geological map and geological formations in the field show that the overall accuracy and Kappa Coefficient are 64.70% and 0.69, 71.6% and 0.73 and 82.51% and 0.86 for SVM, SID and SAM respectively (Table 1). For this reason, the virtual verification of samples collected emphasizes that the detected Cr mineralization zones are accurate and can be considered for future systematic Cr exploration research (Fig.12 a, b, c and d).

(a)

(b)

(c)
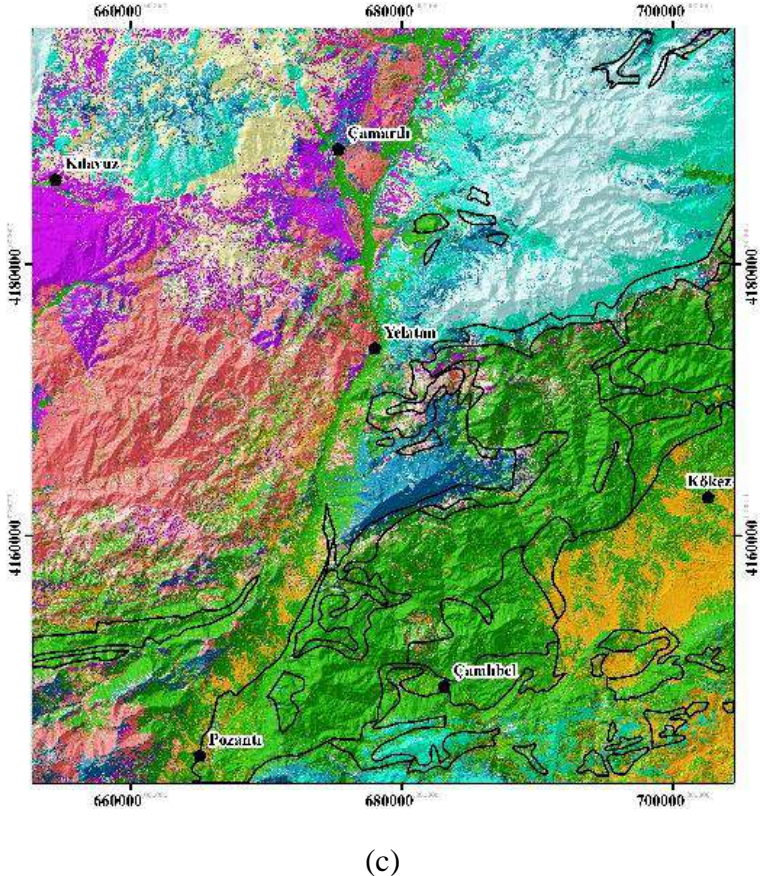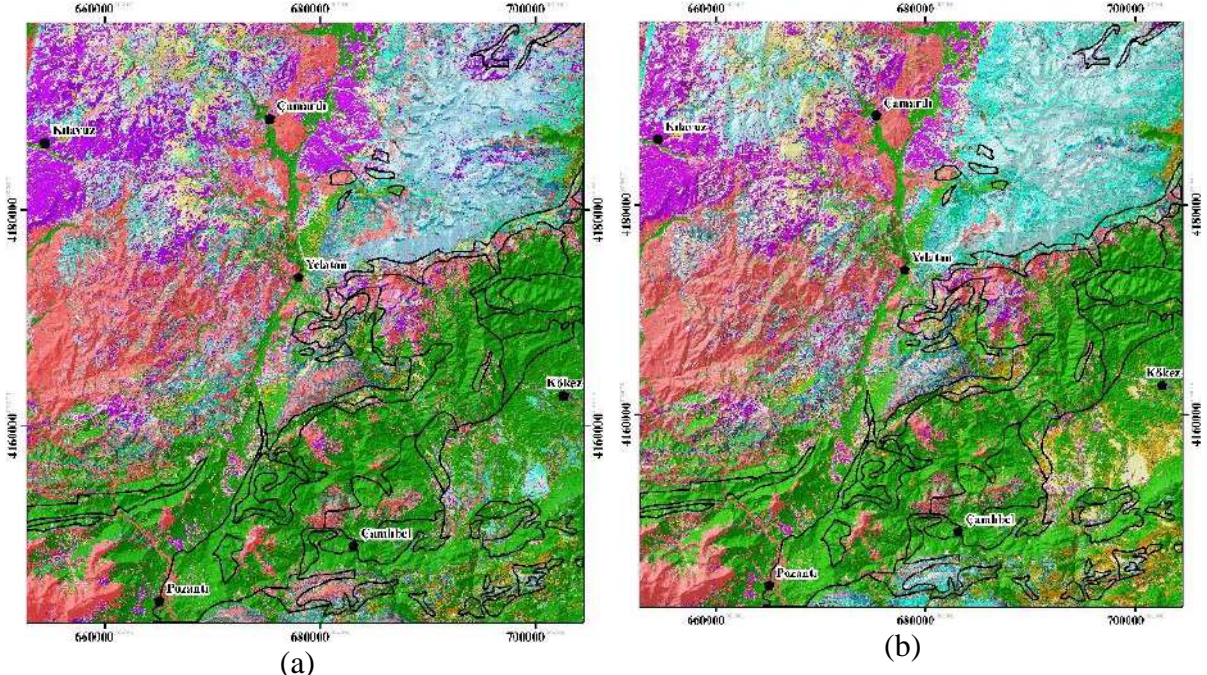
Figure 11. Supervised classification image-map (a) SVM, (b) SID and (c) SAM classification and for the Aladağ area.

Figure 12. Field photographs in the Aladağ area. (a) and (b) ophiolite melange, (c) Chromite mining and (d) contact between ophiolite rock and carbonate formation.

4.   Conclusion

In this research, a potential to identify ore deposits zones and to carried out lithological mapping of Anatolid-Taurid and CCAR scale ASTER, Landsat-8 OLI and Sentinel-2 A data image was tested. The differents methods and process that have been used in work highlight the success of Multispectral data using in this study for future applications in ore mineral exploration and Lithological mapping.

In Adana region, ophiolitic complexe form a biggest zone of Aladağ tectonic blok and contain a very big reserve of chromite mineral. The mainly researches about the ophiolitic complexe in this zone were carried out using traditional method.

The multispectral data imagery (ASTER, Landsat-8 OLI and Sentinel-2A) was using to discriminate the ophiolite rocks by applying BR, PCA, MNN, DS in this area.

The Suppor Vector Machine (SVM), Spectral Information Divergence (SID) and the Spectral Angle Mapper (SAM) techniques were integrated in the GIS environment was applied on Sentinel-2 A data image to update the geological map Aladağ. The result of these methods shows a correlation with the techniques used previously. Ophiolite complex rocks has been well mapped using the three methods.

However, the statistical results derived from virtual verification, the previous geological map and geological formations in the field show that the overall accuracy and Kappa Coefficient are 64.70 % and 0.69, 71.6 % and 0.73 and 82.51 % and 0.86 for SVM, SID and SAM respectively. For this reason, the virtual verification of samples collected emphasizes that the detected Cr mineralization zones are accurate and can be considered for future systematic Cr exploration research.

Field research, laboratory analysis and microscopy observation had been carried out to confirm the availability of alteration and potential zones of Cr mineralization in this research.

Regarding chromium, the samples were taken only in the region of Aladağ, after the analyses we detected three zones which present a concentration in ppm which is AD2(1525 ppm), AD3(2820 ppm) and AD 4(995 ppm).

The result of this research effectively confirms the results obtained from remote sensing techniques and shows that certain areas can be considered as potential for mineral exploration
The result of this research effectively confirms the results obtained from remote sensing techniques and shows that certain areas can be considered as potential for mineral exploration

References

Abdeen, M.M., Allison, T.K., Abdelsalam, M.G., Stern, R.J., 2001. Application of ASTER band ratio images for geologicalmapping in arid regions; the Neoproterozoic Allaqi Suture, Egypt. Geol. Soc. Am. Abstr. Programs 3 (3), 289.

Abdelaziz, R., El-Rahman, Y. A., & Wilhelm, S., 2018. Landsat-8 data for chromites prospecting in the Logar Massif, Afghanistan. Heliyon, 4(2), e00542.

Abrams, M.J., Rothery, D.A., Pontual, A., 1988. Mapping in the oman ophiolite using enhanced landsat thematic mapper images. Tectonophysics 151, 387–401.

AkbaĢ, B., Akdeniz, N., et. all., 2002. Turkey Geology Map General Directorate of Mineral Reserach and Exploration Publications. Ankara Turkey.

Amer, R., Kusky, T., Ghulam, A., 2010. Lithological mapping in the central eastern desert of Egypt using ASTER data. J. Afr. Earth Sci. 56, 75–82.

Engin, T., Özkan, Y.Z., Balcı, M., 1985. Türkiye Krom Yatakları ve MTA'nın Krom Aramacılığındaki Yeri [Chromite ore deposits of Turkey and the role of the MTA in chromite exploration]. 50th Year Symposium Abstracts Ankara, MTA

Gabr, S., Ghulam, A., Kusky, T., 2010. Detecting areas of high-potential gold mineralizations using ASTER data. Ore Geol. Rev. 38, 59–69. Gad, S., Kusky, T.M., 2007. ASTER spectral ratioing for lithological mapping in the Arabian– Nubian shield, the NeoproterozoicWadi Kid area, Sinai, Egypt. Gondwana Res. 11 (3), 326–335.

Gad, S., & Kusky, T., 2007. ASTER spectral ratioing for lithological mapping in the Arabian–Nubian shield, the Neoproterozoic Wadi Kid area, Sinai, Egypt. Gondwana Research, 11(3), 326-335.

Hewson, R.D., Cudahy, T.J., Mizuhiko, S., Ueda, K., Mauger, A.J., 2005. Seamless geological map generation using ASTER in the Broken Hill-Curnamona province of Australia. Remote Sensing of Environment 99, 159–172.

Mars, J.C., Rowan, L.C., 2006. Regional mapping of phyllic- and argillic-altered rocks in the Zagros magmatic arc, Iran, using Advanced Spaceborne Thermal Emission and Reflection Radiometer (ASTER) data and logical operator algorithms. Geosphere 2, 161 –186.

Okay, A., Tüysüz, O., 1999. Tethyan sutures of northern Turkey. Geol Soc London Spec Publ 156:475–515.

Özkan, M., Çelik, Ö. F., & Özyavaş, A. (2018). Lithological discrimination of accretionary complex (Sivas, northern Turkey) using novel hybrid color composites and field data. Journal of African Earth Sciences, 138, 75-85.

Özkan, M., Çelik, Ö. F., ÖzyavaĢ, A., 2018. Lithological discrimination of accretionary complex (Sivas, northern Turkey) using novel hybrid color composites and field data. Journal of African Earth Sciences, 138, 75-85.

Parlak, O., Höck, V., & Delaloye, M. (2002). The supra-subduction zone Pozanti–Karsanti ophiolite, southern Turkey: evidence for high-pressure crystal fractionation of ultramafic cumulates. Lithos, 65(1-2), 205-224.

Parlak, O., Rızaoğlu, T., Bağcı, U., Karaoğlan, F., & Höck, V. (2009). Tectonic significance of the geochemistry and petrology of ophiolites in southeast Anatolia, Turkey. Tectonophysics, 473(1-2), 173-187.

Pour, A.B., Hashim , M., 2015. Hydrothermal alteration mapping from Landsat-8 data, Sar Cheshmeh copper mining district, south-eastern Islamic Republic of Iran, Journal of Taibah University for Science, 9:2, 155-166, DOI: 10.1016/ j.jtusci.2014.11.008

Pour, B.A., Hashim, M., 2014. Structural geology mapping using PALSAR data in the Bau gold mining district, Sarawak, Malaysia. Adv. Space Res 54 (4), 644–654.

Pour, B.A., Hashim, M., Marghany, M., 2011. Using spectral mapping techniques on short wave infrared bands of ASTER remote sensing data for alteration mineral mapping in SE Iran. Int. J. Phys. Sci. 6 (4), 917– 929.

Pournamdari, M., Hashim, M., and Pour, A.B., 2014 a. Spectral transformation of ASTER and Landsat TM bands for lithological mapping of Soghan ophiolite complex, South Iran.Advances in Space Research,54, 694–709.

Pournamdari, M., Hashim, M., and Pour, A.B., 2014 b. Application of ASTER and Landsat TM data for geological mapping of Esfandagheh ophiolite complex, southern Iran. Resource Geology, 64, 233–246.

Rajendran, S., and Nasir, S., 2014 a. Hydrothermal altered serpentinized zone and a study of Ni-magnesioferrite-magnetite awaruite occurrences in Wadi Hibi, Northern Oman Mountain: Discrimination through ASTER mapping. Ore Geology Reviews, 62, 211–226.

Rajendran, S., and Nasir, S., 2014 b. ASTER mapping of limestone formations and study of caves, springs and depressions in parts of Sultanate of Oman. Environmental Earth Sciences, 71, 133–146.

Rajendran, S., Hersi, O.S., Al-Harthy, A.R., Al-Wardi, M., Elghali, M., Al-Abri, A.H., 2011 Capability of Advanced Spaceborne Thermal Emission and Reflection Radiometer (ASTER) on discrimination of carbonates and associated rocks and mineral identification of eastern mountain region (Saih HatatWindow) of Sultanate of Oman. Carbonates Evaporites 26, 351 – 364.

Rajendran, S., Nasir, S., Kusky, T.M., Ghulam, A., Gabr, S., El Ghali, M., 2013. Detection of hydrothermal mineralized zones associated with Listwaenites rocks in the Central Oman using ASTER data. Ore Geol. Rev. 53, 470–488.

Tekeli, O., Örgün, B.M., IĞık, A., 1984. Geology of the Aladağ Mountains. In: Tekeli O, Göncüoğlu CM (eds) International symposium on the geology of the Taurus Belt, 1983. MTA, Ankara, pp 143–158.

Ünlü, T., Dumanlılar, Ö., Tosun, L., Akıska, S., and Tiringa, D., 2019. Chapter 5 Turkish Iron Deposits. Springer Nature Switzerland AG 2019. Mineral Resources of Turkey, Modern Approaches in Solid Earth Sciences 16, https://doi.org/10.1007/978-3-030-02950-0_5.

Van der Meer, F.D.; van der Werff, H.M.A.; van Ruitenbeek, F.J.A.; Hecker, C.A.; Bakker, W.H.; Noomen, M.F.; van der Meijde, M.; Carranza, E.J.M.; De Smeth, J.B.; Woldai, T. 2012., Multi- and hyperspectral geologic remote sensing: A review. Int. J. Appl. Earth Obs. Geoinf. 2012, 14, 112–128.

Plachie vis-à-vis Sütlaç – Dishes in Which History Was Intertwined

Tabunşcic Olga[1*], Cazac Viorica[2], Coralia Babcenco[3]

Abstract: The traditional food of the natives of the Republic of Moldova over the centuries has gone hand in hand with the main and secondary occupations, the natural environment and climatic conditions, religion and socio-historical conditions. Geographically found at the confluence of many peoples, the evolution of Moldovan cuisine denotes many influences, including oriental ones due to historical imperatives. The impact of Turkish gastronomic culture is distinguished by several aspects such as: the combined preparation of meat with fruits, the tendency to use sheep meat and sheep products, etc. Many of the Turkish dishes were brought and introduced into the circuit using authentic terms. A specific preparation of Moldovan cuisine of Turkish origin is *Plachia* (sweet rice with milk, standing up) which we consider to have at its origins the Turkish dessert *Sütlaç*. The work presents the analysis of the technology of preparation and serving of plywood and sütlaç, highlighting the similarities and specific peculiarities.

Keywords: traditional cuisine, Plachie, Sütlaç, rice, gastronomic traditions.

1. Introduction

The gastronomic traditions and traditional cuisine specific to each country characterize a nation as well as traditional history, language and art. The Republic of Moldova is located geographically, in the meeting area between Central and South-Eastern Europe. From the food point of view, this positioning is characterized by the synthesis made in this space between the Balkan, "ottoman" or "byzantine" cuisine and the central one - European, German and Hungarian. From the south into the Moldovan cuisine entered the dishes made of vegetables, which include tomatoes, eggplants, peppers, onions, but also fruits, such as plums, quince, etc. Constantinescu, I. (1997). As an example, serve the dishes, such as: pot, moussaka, pilaf, various assortments of broths, lamb drob, saralia, etc. A general analysis of the diet of Moldovans of the XIX century and the beginning of the XX century, proves that society opts for a kitchen based on simplicity. The diversity of ingredients was small, and dishes made according to complex recipes were very rarely present on the daily table. The peasants saw food only as the main source of energy, without attributing to it the value of a generator of satisfaction and fulfillment. In this respect, the peasant preparation *Plachia*, prepared from the simplest ingredients, is also included.

The old documents talk a little about this dish, and the information brought in is very vague. The objectives of the study are related to: the identification of turkish influences on the name and technology of obtaining the culinary preparation sweet rice *Plachia* and its revitalization within the State Program 20.8009.0807.17 REVICULT.

[1] Academy of Economic Studies of Moldova, Department, Trade, Tourism and Catering, Chisinau, Republic of Moldova
[2] Technical University of Moldova, Faculty of Design, Industrial Design, Chisinau, Republic of Moldova
[3] National College of Commerce at AES, Chisinau, Republic of Moldova
* Corresponding author: viorica.cazac@dttp.utm.md

2. Material ve Method

Bibliographic research, field observation, interviewing and comparative analysis - are the methods applied for the collection, systematization and verification of information, with reference to the names, meanings, technologies, similarities and differences of preparation and serving of two culinary preparations, one considered traditional Moldovan *Plachia* and one of Turkish origin *Sütlaç*.

3. Names and meanings

The traditional Moldovan preparation *Plachia* also carries other names, such as "rice with milk /orez cu lapte" or " standing up (sculatoare)". In the Moldavian Linguistic Atlas, we quote: standing up (sculătoare) f -Plachie (the last kind of dishes served at the wedding). The last name is due to the fact that it is served at the end of various dinners (celebrating the birth of children, weddings, funeral dinners), foretelling that the event is over. According to the source DEX '09 (2009), we quote: PLACHÍE, plachii, s. f. 1.Fish food prepared with a lot of onions and a lot of oil, browned in the oven. 2. (Reg.) A kind of pilaf prepared from rice or grazing, with meat, with fish, with mushrooms or only with fat. – From ngr. plaki. In the Orthographic Dictionary of the Romanian Language, we quote: plachíe, plachíi, s.f. (inv.) metal vessel in which the food is cooked. Another source MDA2 (2010) presents another explanation of this term, namely: 3 (Reg) Food prepared from sweet milk thickened with groats or rice. In Republic of Moldova, *Plachia* is a food made from sweetened boiled milk in which rice groats are introduced and boiled until thickened. We can hypothetically assume that the name of this *Plachie* dish comes either from the name of the pilaf dish, which also consists of rice, or from the name of the metal dish intended for cooking food, which bears the same name *Plachíe*.

We can say that this dish has been prepared by the Romanians for hundreds of years, thus in the work of Burada (1882), we quote *"the most common foods that are made at the funeral dinners are: bird borscht, dumplings, cabbage rolls, Plachie (rice pilaf) and various steaks or other dishes that the late man liked being alive"*. The same thing is affirmed in Lucian's work – Lefter, V. (2013).

The on-site investigations have allowed the finding that this preparation is also being prepared in several localities in Gagauzia, under the name of *Sutliyash.* According to the Live Journal (available 1.08.2022) this dessert bears the identical name of *Sutliyash* in Serbia and Macedonia; in Bosnia this dish is called *Sutliya*; in Croatia - *Rija na mlecu* (in translation - rice with milk); in Montenegro - *Oriz na vareniky* and in Kosovo - *Tameloriz.*

The *Sutliyash* dessert according to Live Journal (available 1.08.2022), which has become in several countries as a local dish, is native to Turkey, where it is known as *Sütlaç.*

Among the most famous Turkish sweets, such as - künefe, dondumra, lokma, locum, baklava, helva is also found the *Sütlaç*. This is a dessert prepared on milk with the addition of rice that has a simple preparation technology. This tasty dish appeared in the simple way of eating the Ottoman peasant since ancient times. The name of the classic Turkish dessert *Sütlaç* comes from "süt", which in translation means "something from milk". The *Sütlaç* preparation falls into the group of sweet dishes (dessert), which we cannot say about *Plachie,* which depending on the technology of obtaining can be both dessert and basic preparation.

3. Results. Analysis of the technologies for the preparation of *Plachie* and *Sütlaç*

The field documentation, on the entire territory of the Republic of Moldova, allowed the finding of the preparation of Plywood through several preparation techniques, from which its variations

derive: *Plachie from fasting rice*, *Plachie from baked rice* and *Sweet plachie with milk*. The preparation technique depends on the event at which it is to be served, because the daily *Plachia* is rarely prepared by the moldovans, being found only in the list of dishes prepared on certain occasions: celebrating the birth of children, weddings, funeral dinners. In some localities of the Republic of Moldova (Orhei (Susleni), Calarasi (Petuşca, Ţânţăreni (Telenesti) only sweet *Plachia* is prepared on milk; in Chisinau, Nisporeni and in UT Gagauzia are prepared so much as dessert (celebrating the birth of children and weddings), but also as a main dish, without milk, with onions hardened on a lot of oil, prunes, which is currently served only at memorial tables, more often in the fasting periods of the year. In Orhei district (Susleni) it is prepared with the addition of raisins. Another source in the field allows us to report that in the past this preparation was prepared not only at ceremonies, we quote *"and how not to love pie, if it reminds you of childhood, of the parental home, of the aroma spread throughout the yard, when the mother "uncloged" the oven. At that time my mother used to do it only with plums and apples, but I added raisins and vanillin to them"*. The findings from the field lead us to the thought that even this delight of the Moldovans, loved by another time, tends to remain in the shadow of history and only the fact that Plachia (Figure 1.) is found in the menu of a restaurant in Balti sity, even if not in the classic version of preparation, with some modifications (instead of milk is used canned fruit juice that are part of the recipe) offers the hope of supervising this traditional preparation.

The raw materials used in the preparation of sweet *Plachia* with rice are: round grain rice, milk, eggs, sugar, butter, optional vanilla, raisins, nuts, fruits (apples, pears, plums). The technological process involves going through the following steps:

1. Beating eggs with sugar, adding vanilla and mixing them well.

2. Boiling the water, adding the rice to the boiling water and mixing them well so that the grains do not stick. Let the rice boil for only a minute, then turn off the fire and leave in water for 3-5 minutes until it swells a little.

3. Passing the rice through the strainers and rinsing with cold water to remove the excess starch.

4. Adding rice to the cauldron, milk, mixing with eggs beaten with sugar, melted butter and fruit peeled and cut into cubes or slices;

5. Mixing the composition, covering the pot with a lid and placing in the preheated preliminary oven at 180 ° C. After 20 minutes, the cauldron is uncovered, making it possible to evaporate the accumulated liquid from the fruit. The ready-made *Plachia* is left in the cauldron for a little while to congeal.

6. Warm serving as dessert.

Figure 1. Plachie

The technology of preparing the Turkish dessert *Sütlaç* involves the use of the following ingredients: milk, round grain rice, sugar, vanilla, corn starch, egg (yolks) by going through the following steps:

1. Boiling the rice in water according to the boiling time indicated for the type of rice. When the water has been absorbed completely, the fire stops and allowed to stand covered with a lid.

2. Separation of the egg whites from the yolks in a dish, addition of the sugar and the vanilla or vanilla sugar. Mixing and adding 2/3 of milk.

3. Putting the composition on the fire and stirring gently until the milk is heated.

4. Mixing the remaining milk with the starch and pouring it into the hot liquid. Adding the rice and stirring until the composition thickens a little;

5. Filling a pan with water up to half, and putting heat-resistant vessels in which the composition of milk with rice is poured;

6. Placing the pan in the preheated oven at 180 ° C and baking for 20 minutes until the rumen crust is made on the surface;

7. Remove it from the oven and let it cool.

8. Serving when the preparation is well cooled or can be served and warm. If served cold decorate with nuts or fruit.

Analyzing the ingredients in the composition of the recipe and the technological process of obtaining these two preparations, it is found that the traditional Moldovan sweet *Plachie* with rice has the same ingredients in its composition and the preparation method is the same as for the Turkish dessert *Sütlaç*. We only note that due to the fact that the recipe of the Turkish dessert *Sütlaç* contains starch, it has a finer and fluffier composition, while the recipe of sweet *Plachia* with rice includes various fruits, which attribute to the composition another structure. The analysis of the serving method shows the finding that the differences consist only in the fact that the Turkish dessert *Sütlaç* is prepared most often portioned directly into the dishes from which it is served.

4. Discussion and Conclusions

- For the Republic of Moldova, *Plachia* is not a specific preparation of a locality, it is prepared both in the center and in the south and north of the republic;
- The *Plachia* also bears other names, such as "rice with milk (orez cu lapte)" or "standing up" ("sculătoarea"). The last name is due to the fact that it is served at the end of various festive dinners (the birth of children, weddings, funeral events), signifying that the event is on the end;
- It can be prepared both sweet and salty;
- It is prepared on milk frequently, only during the period of fasting the milk is replaced by water;
- It can be served both hot and cold;
- The method of heat treatment can be slow boiling or baking;
- The sweet rice *Plachia* has in its composition the same ingredients as the Turkish dessert *Sütlac*, with only some small differences.

References

Constantinescu, I. (1997). O lume într-o carte de bucate: manuscris din epoca brâncovenească. Ed. Fundației Culturale Române, ISBN 9735770903.

DEX '09 (2009). Explanatory dictionary.

MDA2 (2010). Explanatory dictionary of the Romanian language.

Burada, T (1882). Datinele of the Romanian people at funerals. National Printing House, Iasi, Romania, pag. 45.

Lefter, V (2013). The funeral event in Moldova. Historical testimonies and ethnology, edited in the Scientific Bulletin of the National Museum of Ethnography and Natural History of Moldova, vol. 13 (26).

Live Journal (available 1.08.2022). The *Sutliyash.* https://voljena.livejournal.com/12763.html (01.08.2022).

Structural Features of Metamorphic Rocks Around Budağan Mountain (Emet/Kütahya)

Furkan Öztürk[1], Ali Kamil Yüksel[2*]

Abstract: Western Anatolia, comprises Menderes massif, Lycian nappes, Afyon and Tavşanlı zones, experienced regional high pressure/low temperature metamorphism by the contractional and extensional deformations of Alpine orogeny. The studied area, located 13 km NE of the Emet (Kütahya), is in Afyon Zone. Middle-Upper Triassic İkibaşlı Formation which consists of metaclastics and carbonate lenses, forms the lower part of the study area. Jurassic Budağan limestone, composed of dolomitic carbonates, conformably overlies the İkibaşlı Formation. These two formations are overlain tectonically and metamorphosed by an ophiolitic nappe of the Dağardı Melange. The direction of the nappe transportation which caused the metamorphism, can be determined with kinematic studies along this tectonic contact zone.

At the tectonic contact, Mesoscopic and microscobic structures which are used in kinematic studies, show that two different deformation phases, while the initial deformation phase (D1) is in ductile (Alpine), the last phase (D2) is brittle (Neotectonic). Neotectonic brittle high angle normal and oblique faulting (D2) overprint the ductile deformation phase (D1) in the study area. The measured linear structures in the metamorphic rocks of İkibaşlı Formation trend in NW−SE direction. Asymmetric sigmoids in the outcrops and rotated clasts in the oriented thin sections are used for determining the sense of movement of the tectonic slices and indicate top-to-the-NW sense of shear.

This research which was prepared within the scope of the master's thesis, has been supported by Balıkesir University Scientific Research Projects.

Keywords: Ophiolite emplacement, Kinematic indicators, Afyon Zone

1. Introduction

Western Turkey, separated by the İzmir-Ankara suture, is commanly divided into the Pontides in the north and Anatolide–Tauride Block in the south (Ketin, 1966; Şengör and Yılmaz, 1981; Okay et al. 1996) (Figure 1). The northern edge of the Anatolide-Tauride continent experienced regional HP/LT (high pressure/low temperature) metamorphism during the Alpine orogeny (Candan et al. 2005). The HP/LT Anatolides are generally subdivided into Tavşanlı Zone and Afyon Zone in the north and Menderes Massif and Lycian Nappes further

[1]Balıkesir University, Institute of Science and Technology, 10145, Çağış Campus, Balıkesir, TURKEY
[2]Balıkesir University, Faculty of Engineering, 10145, Çağış Campus, Balıkesir, TURKEY
*Corresponding author: akyuksel@balikesir.edu.tr

south by the type and age of the metamorphism (Okay and Tüysüz, 1999). Metamorphism of these tectonic units of the Anatolide-Tauride block in western Turkey is suggested by the transportation of nappes during Alpine evolution times (Şengör and Yılmaz, 1981; Şengör et. al. 1984). The emplacement direction of this nappe packages are in debate. Despite the debate about direction and age of the emplacement of the nappes, there are many structural analysis about Menderes Massif and Lycian Nappes (Bozkurt and Park, 1999; Güngör and Erdoğan, 2001) but there has not sufficient kinematic study in the Afyon Zone.

The studied area, composed of metamorphic rocks, carbonates, ophiolitic rocks and Neogen aged sedimentary rocks, located in Afyon Zone (Figure 1). Afyon Zone is made up of pre-Mesozoic basement and unconformably overlying Mesozoic cover series. Metamorphic rocks of this zone, which are unconformably overlain by Upper Palaeocene–Lower Eocene sedimentary rocks, indicate a Paleocene age for the regional HP/LT metamorphism related to northward subduction of the Anatolide–Tauride platform beneath the Sakarya Zone (Candan et. al. 2005). The burial depth of this zone was approximately 35 km and it experienced HP/LT metamorphism under blueschist facies depending on mineral paragenesis including Fe-Mg carpholites and estimated P/T conditions for this zone rocks give 350 ^{0}C and 6–9 kbar (Candan et. al. 2005). In this paper the features and sense of movement of the Afyon Zone rocks are described.
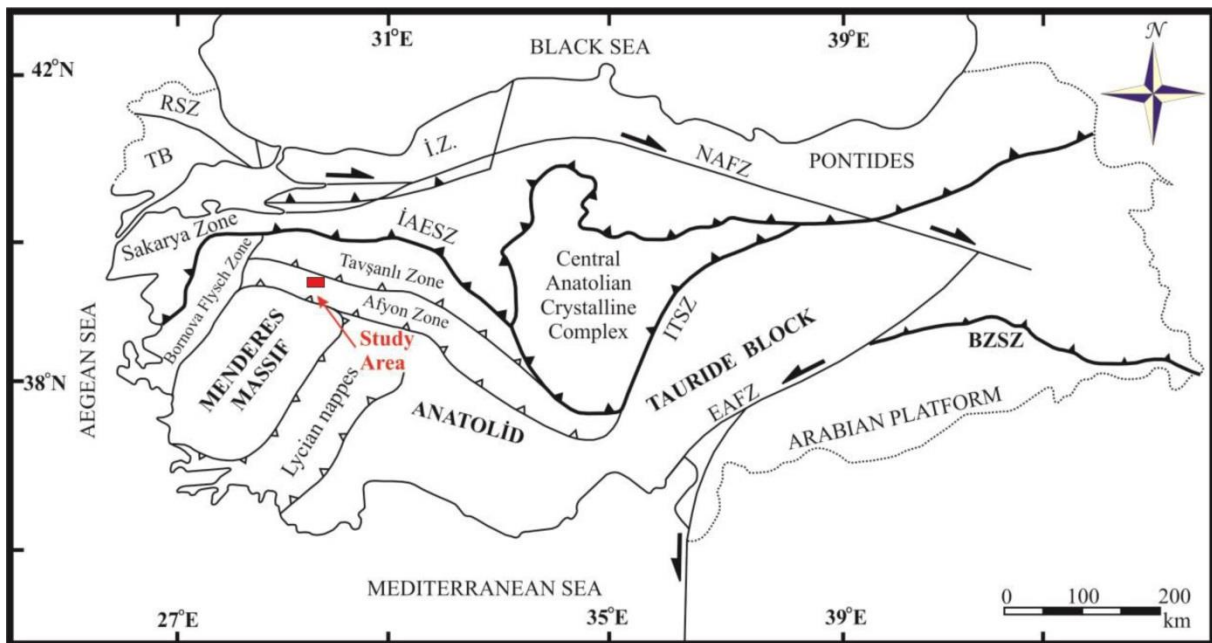
Figure 1: Simplified map shows the main tectonostratigraphic units and zones of Turkey and location of the study area (modified from Şengör and Yılmaz, 1981; Okay et al., 1996) (RSZ: Rhodope-Strandja Zone; TB: Thrace Basin; İ.Z.: İstanbul Zone; İAESZ: İzmir-Ankara Erzincan Suture Zone; BZSZ: Bitlis-Zagros Suture Zone; ITSZ: Inner Tauride Suture Zone; NAFZ: North Anatolian Fault Zone; EAFZ: East Anatolian Fault Zone)

2. Material and Method

2.1. Stratigraphy

Candan et. al. (2005) defined the stratigraphy of the Afyon Zone as a Pan-African basement and unconformably overlying Mesozoic cover rocks. In the Emet (Kütahya) region, Akay et. al. (2011) defined the only upper part of the Afyon Zone and distinguished the zone into İkibaşlı Formation and Budağan limestone. In this study, in the Budağan mount region (Emet/Kütahya), only the Mesozoic upper part of the Afyon Zone exposes also. There are not any outcrops of the Pan-African basement of the Afyon Zone in the study area. The stratigraphy of the study area starts at the base with Middle-Upper Triassic İkibaşlı Formation (Figure 2). Jurasic Budağan limestone, comprises dolomitic carbonates, overlies the İkibaşlı Formation conformably. These two formations are overlain tectonically by an ophiolitic nappe with a low angle.

İkibaşlı Formation consists of metaconglomerates, schists and marble interclations. The metaconglomeratic rocks, extending between the exit of the Işıklar Village and Saraycık road, forms the lowermost of the formation. The upper part of the formation passes to light-dark gray and light brown sericite-quartz schist, chlorite-sericite schist, biotite-sericite-quartz schist and chloritoid schist. In the metaclastics, there are white-gray-light blue coloured, thin recrystallized limestones and rarely dolomitic limestone lenses. The metaclastic rocks of the formation pass upward conformably to the Budağan limestone. The fossil contents of the formation indicate Triassic-Liassic age for the transition between the İkibaşlı and Budağan limestone (Akay et. al. 2011). In the Emet region, metaclastics and platform carbonates of the Afyon Zone are tectonically overlain along a low angle fault by Dağardı Melange of the İzmir-Ankara Suture Zone. Ultramafics which are composed of generally peridotites and serpentinized peridotites, are the most dominant rock type of Dağardı Melange in the study area. And also sub-ophiolitic metamorphic rocks were defined in this melange by Yüksel et. al. (2014) at Mount Murat region. The hornblende from these sub-ophiolitic metamorphic rocks yielded 100.7±1.3 Ma (Albian) (Yüksel et. al. 2014). The Baklan Granite and Eğrigöz pluton intruded into Mesozoic rocks after the emplacement of the ophiolitic nappe. The Baklan Granite was dated at 17,8±0,7–19,4±0,9 Ma by K/Ar method (Aydoğan et. al. 2008). In the study area, all units are unconformably overlain by Neogene units which bears borate minerals.
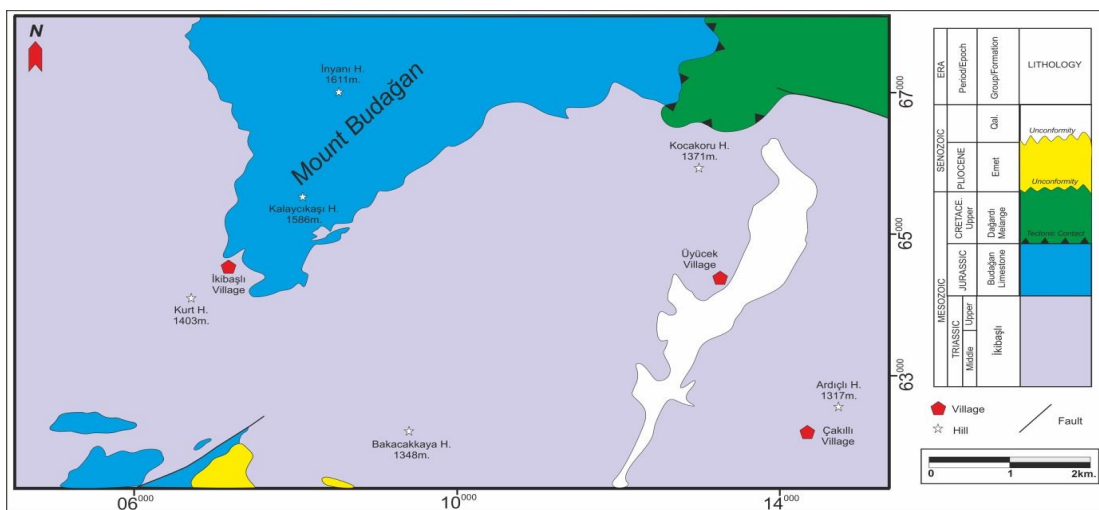
Figure 2: Geological map of the study area (modified from Akdeniz and Konak, 1979)

2.2. Kinematic studies

Kinematic studies from the contact zone between the Dağardı Melange and the underlying İkibaşlı Formation give information about the original position of these tectonic slices. Accordingly, we attached importance to mesoscopic and microscopic structures along the contact zone between these units. The methodology comprises systematic definitions and measurements of the mesoscopic shear criteria in outcrops oriented normal to the foliation and parallel to the associated stretching lineation and examinations of microscopic structures in oriented thin sections. Kinematic data gathered from mesoscopic and microscobic structures preserved in the metaclastics along the boundary between İkibaşlı Formation and Dağardı melange suggest two deformation phases (D1 and D2) and associated foliation and lineation (S1 and L1). The initial deformation phase (D1) is in ductile character and the last phase (D2) is in brittle character.

The L_1 mineral elongation/stretching lineation in the metaclastics is often contained within the S_1 foliation and is defined mostly by the preferred parallel alignment of mostly micas and quartz (Figure 3a). Trending of these lineations have been used to define the tectonic transport direction. Linear structures measured in the metaclastics are shown in the Schmidt diagram and generally lineations are NW−SE-trending (Figure 3b).
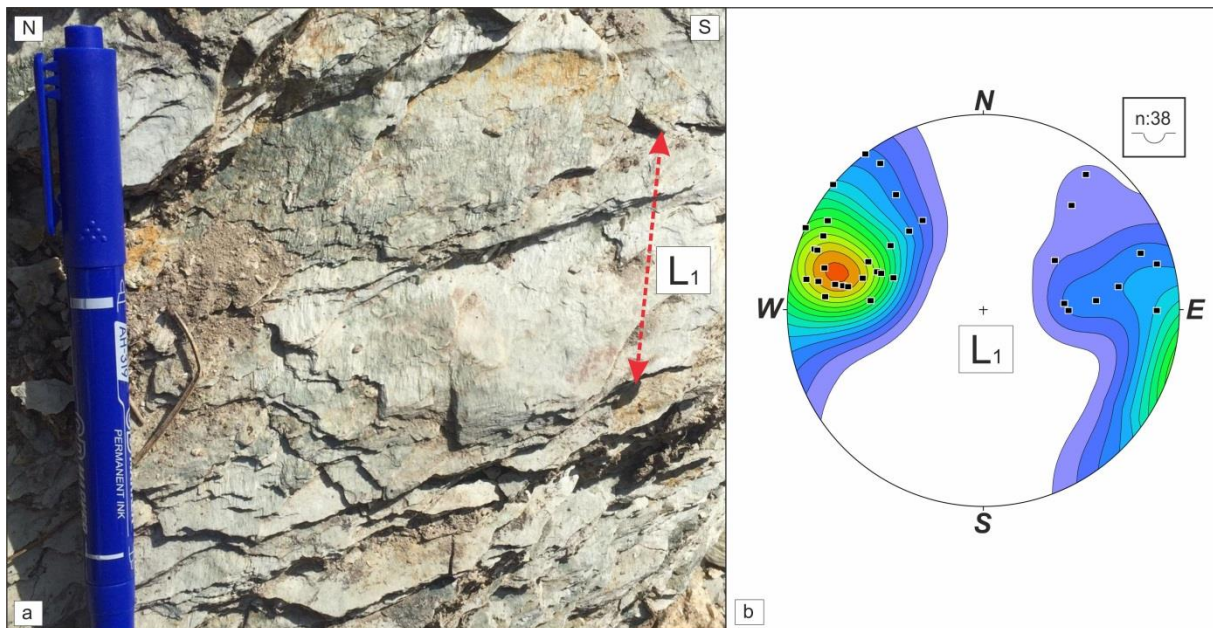
Figure 3: (a) The L1 mineral elongation/stretching lineation in the metaclastics of the İkibaşlı Formation (b) Contour diagram shows attitude of the linear fabric in the İkibaşlı Formation.

Asymmetric sigmoids in the outcrops and in the oriented thin sections and also rotated clasts are used for determining the sense of movement of the tectonic slices. Close to the tectonic contact, these sigmoids are asymmetric in sections normal to the foliation and parallel to the stretching lineation and indicate top-to-the-NW sense of shear (Figure 4a,b,c).
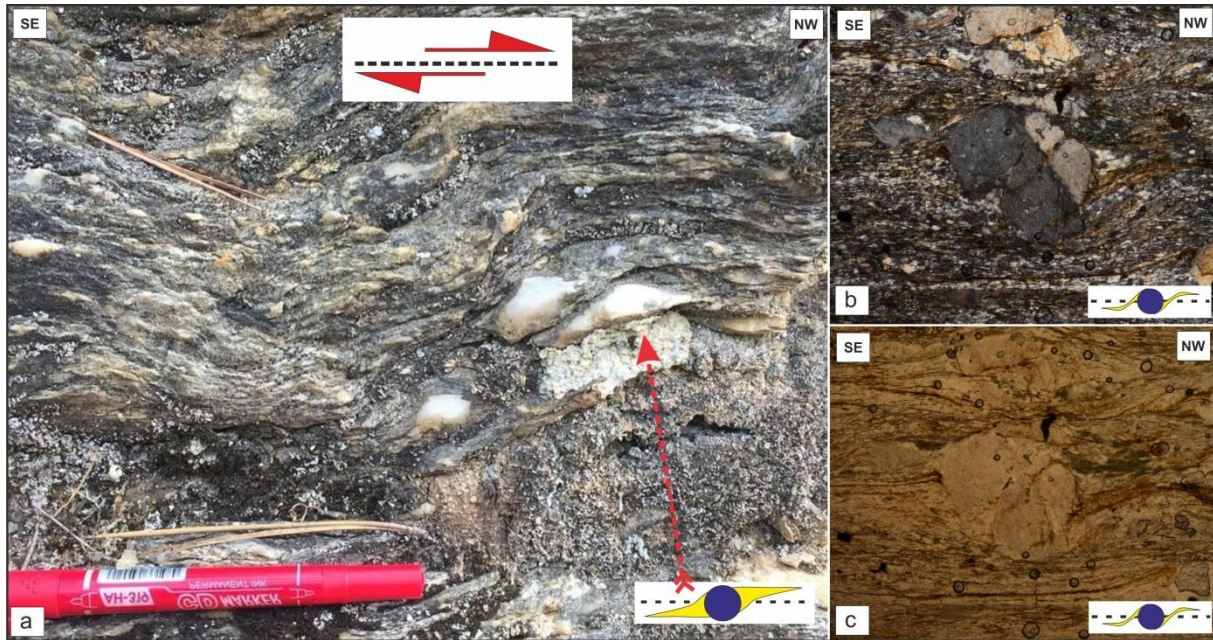
Figure 4: (a) Photograph shows asymmetrically deformed quartz pebble in the İkibaşlı Formation. (b) and (c) Rotated clast in the oriented thin section point to a top-to-the-northwest tectonic transport direction (Width of view is 2 mm)

The second deformation phase (D2) affected the study area and also the western Anatolia is the neotectonic brittle high angle normal and oblique faulting. These recent faults are the youngest structures in the study area and cut the well-developed S1 foliations in the İkibaşlı Formation and rocks of the ophiolitic nappe.

3. Results

Kinematic data gathered from mesoscopic and microscobic structures preserved in the metaclastics along the boundary between the İkibaşlı Formation and Dağardı melange, suggest two deformation phases (D1 and D2) and associated foliation and lineation (S1 and L1). The initial deformation phase (D1) is in ductile character and the last phase (D2) is in brittle character. A penetrative NW-trending strecthing lineation (L1) associated with thrusting was produced during the first deformation phase (D1). The kinematic indicators, the asymmetrical sigmoids, which observed both in the field and in the oriented thin sections, indicate top-to-the NW sense of shear at the tectonic contact between the İkibaşlı Formation and ophiolitic nappe. Neotectonic brittle high angle normal and oblique faulting (D2) overprint the ductile deformation phase (D1).

4. Discussion and Conclusions

Structural analysis in the study area (Afyon Zone) indicate top-to-the NW movement. This shear sense is inconsistent with previous studies of the metamorphism of the northern edge of the Anatolid-Tauride. Similarly, but in the Menderes Massif, Bozkurt and Park (1999) have adressed same incompatibility and proposed that top-to-the N-NNE sense of shear may have been related to the north-directed back-thrusting and internal imbrication of the Menderes Massif. Same top-to-the N-NNE fabrics of the Alpine contractional and extensional deformation phases have been determined in the submassives of the Menderes Massif (Verge, 1995; Işık and Tekeli, 2001; Lips et al. 2001; Hetzel et al. 1998). This study in the Afyon

zone was carried out in a narrow area within the scope of the master's thesis. More comprehensive studies are needed to better understand the tectonics of the region.

Acknowledgements

References

Akay, E., Işıntek, İ., Erdoğan, B., Hasözbek, A., (2011). Stratigraphy of the Afyon Zone aroun Emet (Kütahya, NW Anatolia) and geochemical characteristics of the Triassic volcanism along the northern Menderes Massif. Neues Jahrbuch für Mineralogie-Abhandlungen Band, 188 Heft 3, p. 297-316

Akdeniz, N. and Konak, N., (1979). Simav-Emet Tavşanlı-Dursunbey-Demirci yörelerinin jeolojisi. MTA Derleme No: 6547, 108 p. (Unpublished).

Aydoğan, M.S., Çoban, H., Bozcu, M., Akıncı, Ö., (2008). Geochemical and mantle-like isotopic (Nd, Sr) composition of the Baklan Granite from the Muratdağı Region (Banaz, Uşak), western Turkey: Implications for input of juvenile magmas in the source domains of western Anatolia Eocene–Miocene granites. Journal of Asian Earth Sciences, 33, 155–176.

Bozkurt, E. and Park, R.G., (1999). The structure of the Palaeozoic schists in the Southern Menderes Massif, western Turkey: a new approach to the origin of the main Menderes Metamorphism and its relation to the Lycian nappes. Geodin. Acta 12, 25–42.

Candan, O., Çetinkaplan, M., Oberhansli, R., Rimmele, G., Akal, C., (2005). Alpine high-P/low-T metamorphism of the Afyon Zone and implications for the metamorphic evolution of Western Anatolia, Turkey. Lithos, 84, 102-124.

Güngör, T. and Erdoğan, B., (2001). Emplacement age and direction of the Lycian nappes in the Söke-Selçuk region, western Turkey. Int. J. Earth Sci. 89, 874–882.

Hetzel, R., Romer, R.L., Candan, O., Passchier, C.W., (1998). Geology of the Bozdag area, central Menderes massif, SW Turkey: Pan-African basement and Alpine deformation. Geol. Rundsch. 87, 394–406.

Işık, V. and Tekeli, O., (2001). Late orogenic crustal extension in the northern Menderes massif (western Turkey): Evidences for metamorphic core complex formation. International Journal of Earth Sciences 89, 757-765.

Ketin, İ., (1966). Anadolu'nun Tektonik Birlikleri. MTA Dergisi. 66, 20-34 (In Turkish).

Lips, A.L.W., Cassard, D., Sözbilir, H., Yılmaz, H., Wijbrans, J., (2001). Multistage exhumation of the Menderes Massif, western Anatolia (Turkey). Int. J. Earth Sci. 89, 781–792.

Okay, A.I., Satır, M., Maluski, H., Siyako, M., Monie, P., Metzger, R., Akyüz S., (1996). Paleo- and Neo-Tethyan events in northwest Turkey: geological and geochronological constraints.in Tectonics of Asia (ed. A. Yin & M. Harrison), Cambridge University Press, 420-441.

Okay, A.İ., and Tüysüz, O., (1999). Tethyan sutures of northern Turkey, In: Durand, B., Jolivet, L., Horvath, D., Serrane, M. (eds), The Mediterranean Basins: Tertiary Extension within the Alpine Orogen, Geological Society, London, Special Publications, 156, 475-515.

Şengör, A.M.C. and Yılmaz, Y., (1981). Tethyan evolution of Turkey: a plate tectonic approach. Tectonophysics 75, 181–241.

Şengör, A.M.C., Yılmaz, Y., Sungurlu, O., (1984). Tectonics of the Mediterranean Cimmerides: nature and evolution of the western termination of palaeo-Tethys. In: Dixon, J.E., Robertson A.H.F. (Eds.), The Geological Evolution of the Eastern Mediterranean. Geological Society, Special Publication, London, 17, pp. 119–181.

Verge NJ., (1995). Oligo-Miocene extensional exhumition of the Menderes Massif, western Anatolia. Terra Abstracts 7:117.

Yüksel, A.K., Güngör, T., Kılıç, A.M., (2013). New Findings From Sub-Ophiolite Metamorphic Rocks in Northwestern Anatolia (Gediz-Kütahya). Geological Bulletin of Turkey, Volume 57, Number 2, 19-34 (In Turkish with English extended summary).

Determination of Total Antioxidant Capacity and Total Phenolic Content of Lagerstroemia Indica L. Leaves

Ümit Erdoğan[*1], Mustafa Karaboyacı[2]

Abstract: In the current study, we aimed to determine the total phenolic content (TPC) and total antioxidant capacity (TAC) of the ethanolic extracts of the ultrasonic - assisted *Lagerstroemia indica* L. leaves. In fall, *Lagerstroemia indica* L. leaves were collected from Isparta province of Turkey. Powdered *Lagerstroemia indica* L. leaves were subjected to ultrasonic extraction in 96% ethanol medium. The collected extracts were filtered from the residue and dried by evaporating the solvents with a rotary evaporator (IKA RV 10 digital, IKA, Germany) at 50 ºC under vacuum. we determined the TAC of extracts according to Ferriccyanide (Fe^{3+}) Reducing Antioxidant Power (FRAP) assay. On the other hand, TPC of the extracts was calculated according to the Folin-Ciocalteau method. FRAP value of extracts was calculated as 3.44 ± 0.27 mmol Trolox / g – extract. The total phenolics content of extracts were determined by the Folin-Ciocalteu procedure and 465.71 ± 5.64 mg gallic acid equivalent (GAE) of phenols was detected in 1 g extract. The data revealed that TAC of the *Lagerstroemia indica* L. leaves was quite strong. Morover, the results showed that TPC of the extracts was quite high.

Keywords: *Lagerstroemia indica* L. leaves, total phenolic content, total antioxidant capacity, FRAP assay, ultrasonic – assisted extraction

1. Introduction

The crape myrtle is a *Lagerstroemia indica* species from the *Lythraceae* familial, a tall shrub that sheds its leaves in winter, or a small tree with a rounded crown that can grow up to 6-7 m. The body bark is thin, smooth and unusually silver gray and brown in color. The flowers of crape myrtle are very showy. It blooms in summer in the form of clusters of 5-20 cm in length and can be in pink, white, lilac color. Its short-stemmed leaves take on very pleasant colors such as yellow, orangish and reddish brown in autumn. This pleasant appearance makes it a unique landscape plant.

The homeland of L. indica is China. The cultivars of the plant widespread in the regions like Bangladesh, Bhutan, Cambodia, India, Indonesia, Japan, Laos, Malaysia, Nepal, Pakistan, Philippines, Singapore, Sri Lanka, Thailand and Vietnam (Öztürk et al. 2018).

[1] Isparta University of Applied Sciences, Rose and Aromatic Plants Application and Research Center, Isparta, Turkey
[2] Süleyman Demirel University, Engineering Faculty Chemical Eng. Departmen, Isparta, Turkey
* Corresponding author: umiterdogan@sdu.edu.tr

The leaves of L. indica are used in traditional folk medicine. It is believed colloquially the leaves have, anticancer, antibacterial, antiviral, anti-obesity, antioxidant and blood sugar levels control properties. These features attract the attention of researchers on the leaves of the plant. Labib et al. (2013) reported that, aqueous methanol leaf extracts of Lagerstroemia indica L showed significant activities like anti- inflammatory, antipyretic, analgesic, antihyperglycemic, antioxidant and hepatoprotective. Ajaib et al. 2016, In their study, antimicrobial potential showed that extracts of L. indica were more effective than standard antimicrobial drugs and aqueous extract of leaves has highest TEAC value. Elsawi et al. (2018) in their study in which they investigated the effects of Lagerstroemia indica leaves on Alzheimer's, they stated that 80% ethanolic extract of L. indica showed a promising effect as an Alzheimer's agent.

In this study, the antioxidant content of the Lagerstroemia indica leaves grown in the Isparta region was investigated, during the defoliation season. The reason for choosing the defoliation season is to determine the antioxidant potential of the fallen leaves and to convert them into new products and evaluate them.

2. Materials and Methods

2.1. Chemicals

Ethanol (96%) was purchased from ISOLAB Laborgeräte GmbH (Eschau, GERMANY). Potassium hexacyanoferrate(III) ($K_3[Fe(CN)_6]$), di-Sodium hydrogen phosphate dihydrate ($Na_2HPO_4 \cdot 2H_2O$), Sodium dihydrogen phosphate dihydrate ($NaH_2PO_4 \cdot 2H_2O$), Iron(III) chloride hexahydrate ($FeCl_3 \cdot 6H_2O$), Gallic acid, trichloroacetic acid (TCA), were purchased from Merck (Darmstadt, Germany). All other chemicals used were analytical grade and obtained from either Sigma–Aldrich or Merck.

2.2. Plant Material

In fall, *Lagerstroemia indica* L. leaves were collected from, Isparta province of Turkey. Samples were also identified by Prof. Sabri Erbaş and deposited at the herbarium of Faculty of Agriculture, Isparta University of Applied Sciences, with voucher specimen numbers Lİ32-2022.

2.3. Preparation of solutions

The FRAP reagents were prepared as follows: To prepare 0.2 M phosphate buffer at pH 6.6, 7.80 g of $NaH_2PO_4 \cdot 2H_2O$ was dissolved in water and diluted to 250 mL with H_2O such that its final concn. would be 0.2 M; 8.90 g of $Na_2HPO_4 \cdot 2H_2O$ was dissolved in water and diluted to 250 mL such that its final concn. would be 0.2 M. To prepare 0.2 M phosphate pH 6.6 buffer, 62.5 mL of $NaH_2PO_4 \cdot 2H_2O$ solution was mixed with 37.5 mL of $Na_2HPO_4 \cdot 2H_2O$ and diluted to a total of 200 mL with H_2O (Stoll & Blanchard, 2009). Potassium ferricyanide solution (1%, w/v) was prepared daily by dissolving 1 g $K_3Fe(CN)_6$ in 1 mL of 1 M HCl and some water and diluting to 100 mL with water. Ferric chloride solution (0.1%, w/v) was prepared daily by dissolving 0.1 g of $FeCl_3 \cdot 6H_2O$ in 1 mL of 1 M HCl and some water and diluting to 100 mL with water. Trichloroacetic acid (TCA) solution (10%, w/v) was prepared by dissolving 10 g of TCA in water and diluting it to 100 mL with H_2O.

2.4. Ultrasound-assisted extraction

L. indica leaves were prepared prior to extraction by then grinding with a coffee grinder (Sinbo SCM 2934-Turkey). 5 g of ground *L. indica* leaves was immersed in 50 mL of 96% ethanol in a sealed bottle. Ultrasonic bath system (Power sonic 180, 40 kHz frequency and maximum 150 W, internal size: 300 mm × 150 mm × 100 mm) was used for extraction. Ultrasound extraction was performed under the following experimental conditions: temperature; 50 $^\circ$C, time; 45 min, solid/solvent ratio; 1:10 (w/v), and maximum ultrasound power (40 kHz and 150 W power). The collected supernatants were filtered from the residue and dried by evaporating the solvents with a rotary evaporator (IKA RV 10 digital, IKA, Germany) at 50 ^{o}C under vacuum.

2.5. Total phenolic content by the Folin-Ciocalteu method

The amount of total phenolic content of *L. indica* leaves extract was calculated with the Folin-Ciocalteu reagent as indicated by the Slinkard and Singleton method (1977). Folin-Ciocalteu is a procedure used for the estimation of total phenolic compounds. Gallic acid was used as a standard phenolic compound. Briefly, 40 µl sample (1 mL of extract solution contains 1 mg extracts), a gallic acid calibration standard, or blank (deionized or distilled water) was put into a 15 mL falcon tube. Then, 3.16 mL water, followed by 200 µL FC reagent was added and mixed thoroughly by pipetting or inverting and incubate 1 to 8 min. After 5 min, 600 µL of Na_2CO_3 (20%) was added and afterward the mix was permitted to represent 2 h with discontinuous shaking. The absorbance was measured at 760 nm in a spectrophotometer (SHIMMADZU UV-1280 UV-Vis Spectrophotometer). A calibration curve was made by getting ready 40 µL aliquots of 25, 50, 100, 200 and 400 µg mL^{-1} arrangements of Gallic acid and the outcomes were stated as gallic acid equivalents in milligram per gram [mg GAE/g] of the sample. Absorbance = 0.0012 x Total phenols [Gallic Acid Equivalent (mg)] +0.0099 (R^2: 0.9994). The assessment was performed in triplicate. The measure of phenolic content in extracts was determined by the accompanying equation:
T = C_1 x V/M
Where, T = Total phenolic content mg g^{-1} of extracts in GAE [Gallic acid equivalent]; C_1 = The Concentration of Gallic acid established from the calibration curve µg mL^{-1}; V = The Volume of extract solution [mL] M = The Weight of the extract [g].

2.6. The ferric reducing antioxidant power assay

The antioxidant activities of *L. indica* leaves extract were measured by the FRAP assay, performed essentially as described by Beerker et al. (2007). Briefly, to *x* mLof antioxidant solution were added (1−*x*) mL of EtOH (96%), 2.5mL of 0.2M phosphate buffer (pH 6.6) and 2.5mL of $K_3Fe(CN)_6$ solution (1%); the mixture was incubated at 50 ^{o}C on a water bath for 20 min. The incubated mixture was let to cool to room temperature, and 2.5mL of TCA (10%) was added. The solution was thoroughly mixed, an aliquot of 2.5mL was withdrawn, and 2.5mL water followed by 0.5mL of $FeCl_3 \cdot 6H_2O$ solution (0.1%) was added so that the final volume was 5.5 mL. The absorbance of the resulting Prussian blue solution at 700 nm (A_{700}) was measured after 2 min against a reagent blank.

3. Results and Discussion

3.1. Total phenolic content results

Total phenolic content was determined according to the Folin method. According to this analysis; high phenolic content indicates high antioxidant activity. According to the test used to measure the total amount of phenolic substances, the total amount of all water-soluble phenolic and polyphenolic substances was determined, since the Folin reagent forms a colored complex with all phenolic compounds such as phenolic acids, flavonoids, flavanols, anthocyanins. The content of phenolic compounds (mg/g) in *L. indica* leaves extract calculated using regression equation of calibration curve (y: 0.0012x + 0.009, r^2: 0.9994) (Figure 1) and expressed in gallic acid equivalents (GAE) was calculated to be 465.71 ± 5.64 mg/g (GAE/g-extract). However, different results have been reported in the literatüre. The total phenolic contents (TPC) of *L. indica* was assessed by using Folin-ciocalteu reagent and was found within the range 5.482 ± 0.08 to 40.333 ± 0.23 µg/mL of GAE with the maximum contents reported by petroleum ether bark extract and minimum contents by chloroform extract of leaves (Ajaib et al.,2016). In another study, total Phenolics identified in the 80% ethanolic extract of Lagerstromia indica were determined as 64.75 mg/g dry weight (Al-Snafi, 2019). The data presented in the current study revealed a higher total phenolic content when comparing previously reported findings. This is because the intensity of the ultrasound power generates extra vibration in the sample molecules and facilitates the recovery of target compounds from solid to liquid solvent phase (Samaram et al., 2015).
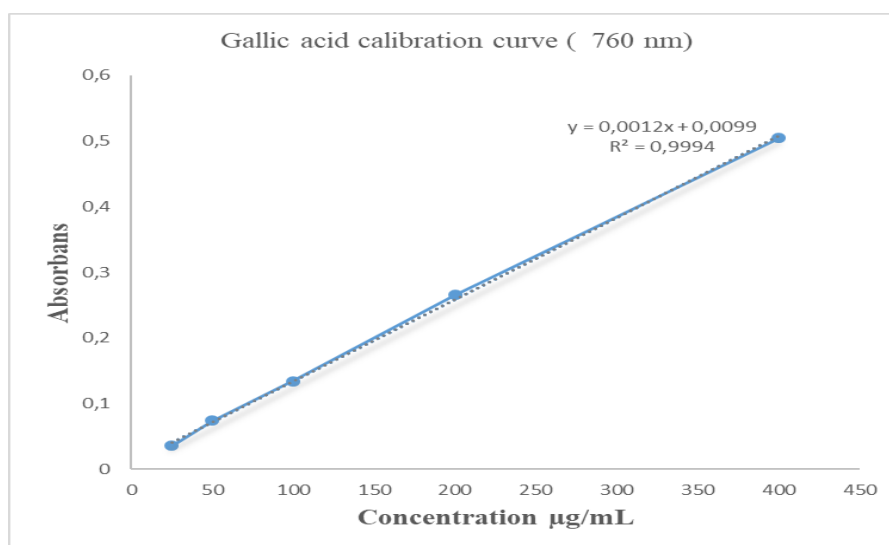
Figure 1. Gradient of absorbance vs. concentration graph for gallic acid calibration

3.2. Total antioxidant capacity results

We determined the TAC of extracts according to Ferriccyanide (Fe^{3+}) Reducing Antioxidant Power (FRAP) assay. In the FRAP method, the reducing capacity of extract was accomplished using Fe^{3+} to Fe^{2+} reduction assay. In this analysis, the yellow color of the FRAP test solution changed to shades of green and Prussian blue depending on the concentration of the reducing agent. The presence of reducing agents acting as antioxidants in the samples causes the Fe^{3+}/ferricyanide complex to be reduced to the ferric form. Thus, Fe^{2+} can be tracked by measuring the formation of Prussian blue of Perl at 700 nm (Gülçin et al., 2006). FRAP value

of extracts was calculated as 3.44 ± 0.27 mmol Trolox / g – extract (Table 1). In the literature, the ferric reducing antioxidant power of *L.indica* leaves was determined as 2.665 mmol Tr/g-extract (Xiang-mi et al., 2015).

Table 1. Total phenolic content and total antioxidant capacity of *L.indica* leaves

Sample	FRAP assay total antioxidant capacity (mmolTR/g- extract)	Total phenolic content (mg/g-extract)
L.indica leaves extract	3.44 ± 0.27	465.71 ± 5.64

4. Conclusions

The data revealed that TAC of the *Lagerstroemia indica* L. leaves was quite strong. Morover, the results showed that TPC of the extracts was quite high. More studies are needed to determine in detail the individual phenolic compounds of *Lagerstroemia indica* L. leaves and to evaluate their antioxidant activity according to different in vitro antioxidant methods.

References

Ajaib, M., Arooj, T., Khan, K.M., Farid, S., Ishtiaq, M., Perveen, S., & Shah, S., (2016). Phytochemical, Antimicrobial and Antioxidant Screening of Fruits, Bark and leaves of Lagerstroemia indica. Journal of the Chemical Society of Pakistan, 38(3).

Al-Snafi, A.E., (2019). A review on Lagerstroemia indica: A potential medicinal plant. IOSR Journal of Pharmacy, 9(6), 36-42.

Berker, K.I., Güçlü, K., Tor, I., & Apak, R., (2007). Comparative evaluation of Fe (III) reducing power-based antioxidant capacity assays in the presence of phenanthroline, batho-phenanthroline, tripyridyltriazine (FRAP), and ferricyanide reagents. Talanta, 72(3), 1157-1165.

Elsawi, S. A., Aly, H. F., Elbatanony, M. M., Maamoun, A. A., & Mowawad, D. M. (2018). Phytochemical evaluation of Lagerstroemia indica (L.) Pers leaves as anti-Alzheimer's. J Mater Environ Sci, 9(9), 2575-2586.

Gülçin, İ., Elias, R., Gepdiremen, A., & Boyer, L., (2006). Antioxidant activity of lignans from fringe tree (Chionanthus virginicus L.). European Food Research and Technology, 223(6), 759-767.

Labib, R. M., Ayoub, N. A., Singab, A. B., Al-Azizi, M. M., & Sleem, A. (2013). Chemical constituents and pharmacological studies of Lagerstroemia indica. Phytopharmacology, 4(2), 373-389.

Öztürk, N., Yüksel, B., Gedikli, H. (2018). New ınvasive species on Lagerstromia indica from Düzce and their management. Journal of Forestry Vol.14, Issue.1, p. 21-29

Samaram, S., Mirhosseini, H., Tan, C.P., Ghazali, H.M., Bordbar, S., & Serjouie, A., (2015). Optimisation of ultrasound-assisted extraction of oil from papaya seed by response

surface methodology: Oil recovery, radical scavenging antioxidant activity, and oxidation stability. Food Chemistry, 172, 7-17.

Slinkard, K., & Singleton, V. L., (1977). Total phenol analysis: automation and comparison with manual methods. American journal of enology and viticulture, 28(1), 49-55.

Stoll, V.S., & Blanchard, J.S., (2009). Chapter 6. Buffers. Principles and Practice1. https://doi.org/10.1016/S0076-6879(09)63006-8

Xiang-mi, K.O.N.G., Xue-jing, C.U.I., Mei-fang, C.H.A.N.G., & Wen-yi, K.A.N.G., (2015). Antioxidant activity of Lagerstroemia indica flower. Natural Product Research and Development, 27(2), 264.

Determination of Optimum Pyrolysis Temperature and Time in the Production of Activated Carbon from Lavender Pulp

Yaren Cömert[1*], Mustafa Karaboyacı[1]

Abstract: The cultivation of lavender, which is among the medicinal aromatic plants, is quite common in Turkey. According to TUIK 2021 database on lavender cultivation area and production, lavender production is 6,108 tons. In Isparta, on the other hand, lavender agriculture has a high production rate of 38 %. In this context, it has been observed that the waste after distillation is not evaluated in enterprises producing lavender. When the literature is examined, it is seen that the lavender straws left after distillation have not been used in the production of activated carbon until today. This creates a serious waste. In this study, aimed to recycle lavender straws, which is an agricultural waste, into the raw material supply chain. Considering that natural resources are gradually decreasing and the waste storage limits of the earth are fulfilled, it is important to transform a waste material into a commercial product and to realize new designs for the use of this product. In this context, since the product to be recycled is the waste of a raw material used in the cosmetics industry, natural soap and natural toothpaste will be designed from the extracts and activated carbon obtained and tested by producing samples from them.

Keywords: Essential oils, Lavandin waste, Activated carbon.

1. Introduction

Environmental problems are at the forefront of the problems that endanger the lives of all living things in the world. Considering that natural resources are gradually decreasing and waste storage limits are being fulfilled, a lot of work has been done on waste disposal recently. However, while the waste is being disposed of, it also brings with it bigger problems. Therefore, industry, agriculture, etc. Reducing the increasing costs by converting other recyclable wastes into new products increases the variety of new products, a new market emerges from the products destroyed as waste, thus contributing to the country's economy.

Essential oils have been commonly used in cosmetics for their pleasing aromas in products such as moisturizers, sunscreen, lotions, shampoos, bath and body products, soaps and perfumes, for centuries. (Cavanagh and Wilkinson, 2002).

Lavender (Lavandula spp.) is a very valuable essential oil plant from the Lamiaceae family. (Guenther, 1952).

[1] Suleyman Demirel University, Faculty of Engineering, Department of Chemical Engineering, Isparta, Turkiye
* Corresponding author: yaren.comert@ercetin.com

There are three important lavender species with high commercial value in world. These species are lavender (Lavandula angustifolia Mill.=L. officinalis L.=L. vera DC), lavandin (Lavandula intermedia Emeric ex Loisel.=L. hybrida L.) and spike lavender (Lavandula spica=L. latifolia Medik.). (Kara and Baydar, 2012).

Lavandin (Lavandula intermedia Emeric ex Loisel) is a sterile hybrid of Lavandula angustifolia P.Mill. × Lavandula latifolia (L.f.) Medikus. The plant is native from the Mediterranean area and is widely cultivated for essential oil production which is used for perfumes, cosmetics, food processing and soap production. . Lavander and lavandin distilled straws, the by-products of oil extraction, were traditionally used for soil replenishment or converted to a fuel source. They are mineral and carbon-rich plant residues and, therfore, a cheap, readily available source of valuable substances of industrial interest, especially aroma and antioxidants (e.g. terpenoids, lactones and phenolic compounds including coumarin, herniarin, α-bisabolol, rosmarinic and chlorogenic acids) (Lesage-Meessen et al., 2015).

Laura et al. (Torras-Claveria et al., 2007), they investigated the phenolic content of lavandin waste to find an alternative use for this material. Different antioxidant activity fractions as well as total phenolic contents were evaluated by different methods. Twenty-three phenolic compounds were combined to ion spray mass spectrometry and identified by liquid chromatography (LC/MS/MS). They suggested some structure-activity relationships by associating the type of cleaning activity of different fractions with the identified phenolic compounds. The contents of representative phenolic acids (chlorogenic and rosmarinic) of Lamiaceae were evaluated by high performance liquid chromatography-diode array detection (HPLC-DAD) and compared with those of other plant species.

Christophe et al. (Tiliacos et al., 2008), they extracted the waste belonging to the Grosso type of Lavandin with cyclohexane. The main components found as a result of GC-MS analysis of the extracts were lactones; coumarin and herniarin sesquiterpenes.

1.1. Activated Carbon

Activated carbon is a structure with high porosity and large surface area, which contains a high amount of carbon.

There are multiple methods to obtain activated carbon. Generally, raw materials are first carbonized under high temperature and inert atmosphere conditions to obtain high yields, and then activated carbon is produced by performing various activation processes (Abdullah et al. 2011).

1.2. Activated Carbon Production

There is a wide range of substances that can be used in the production of activated carbon. Among the substances that can be carbon, there are vegetable origin (wood, agricultural wastes, nut shells, fruit seeds, etc.), mineral origin (coal, lignite, peat, petroleum) or polymeric materials (plastics, worn tires) (Yeganeh et al., 2006).

Agricultural wastes and by-products, are fascinating as they fulfill most of the required properties as they are endowed with high carbon content, low inorganic, and are renewable materials generated in huge amounts every year (Girgis et al., 2007).

The properties of activated carbons may vary depending on the raw material used and the production method (Yeganeh et al., 2006). The selection of the raw material and activation conditions to be used in production offers the opportunity to design different activated

carbons for different applications. The activated carbon industry has been using some agricultural and industrial product residues or by-products as raw materials for evaluation in the last decade (Nabais et al., 2011).

1.3. Activated Carbon Activation

The main purpose of the activation process is to increase the pore volume and expand the surface area.

Activation is divided into two as physical and chemical activation.

1.4. Physical Activation

The physical activation method takes place in two stages: carbonization and activation.

First, the raw material is carbonized at high temperature. Then, the carbonaceous structure is activated at high temperatures with gases such as carbon dioxide (CO_2), oxygen (O_2), water vapor or a mixture of carbon dioxide and water vapor, and related reactions are carried out. Since the oxidizing gases used in the physical activation method bind the functional groups to themselves and remove these groups from the carbonaceous structure, the surface area and pore volume of the carbonaceous structure increase (Alan, 2019).

1.5. Chemical Activation

The chemical activation method is the type of activation that occurs with the use of certain chemicals.

Raw material, chemicals, carbonization temperature, impregnation rate directly affect the chemical activation method. Chemical substances facilitate the formation of microporous structures in activated carbon (Alan, 2019). In the chemical activation process, many chemicals such as boric acid, calcium hydroxide, calcium chloride, phosphoric acid, sulfuric acid, zinc chloride, iron (III) chloride, potassium carbonate, potassium hydroxide, manganese (II) chloride, nitric acid, sodium chloride, sodium sulfate chemicals can be used (Gerhartz, 1986; Wigmans, 1989).

In this study, activated carbon was obtained from lavandin straws, which is an agricultural waste after steam distillation of the lavandin plant.

2. Materials and Methods

2.1. Plant Material

Lavandin cv. Super (Lavandula × intermedia Emeric ex Loiseleur, Lamiaceae) collected during the flowering period in Isparta province. After distillation, the remaining material was air-dried at a temperature below 40 °C. Then were ground into powder with the help of a grinder and stored at 4 °C. Powder state is shown in figure1.

Figure 1. Powder of lavandin straws

2.2. Samples Preperation and Extraction

The extraction were performed with two organic solvents of increasing polarity: Ethyl acetate and n-hexane. For each solvent, 100 g of dry powder were extracted with 1000 mL of solvent by maceration for 48 h at room temperature. The mixture was filtered and evaporated using rotary evaporator to obtain the crude extract.

The obtained extracts were determined by GC-MS device for the amounts of essential oil components in their content.

2.3. Activated Carbon Preperation

After the extraction process, the lavandin straws separated from the filter and the optimum temperature and time were determined by conducting experiments in the N_2 atmosphere in the (GEMO PC107) muffle furnace to obtain activated carbon. The muffle furnace used in the production of activated carbon is shown in figure 2. Pyrolyzed activated carbons are shown in figure 3.

Figure 2. Muffle furnace used in the production of activated carbon

Figure 3. Pyrolyzed activated carbons

3. Results

After determining the appropriate temperature and time interval for the activated carbon, the values in graphics 1 and 2 are seen as determined. It has been determined that the optimum conditions for the production of activated carbon are 800 °C and 10 minutes.
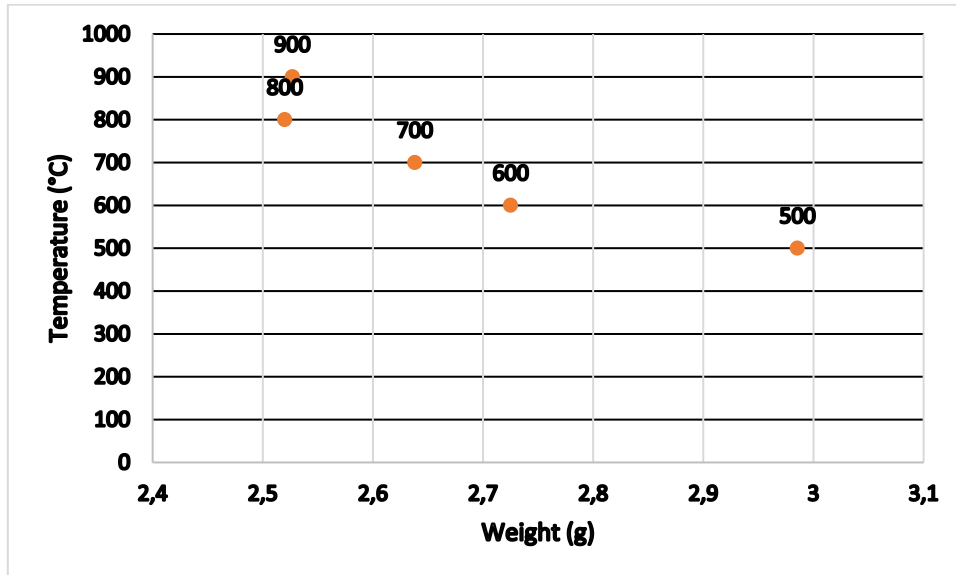
Graphic 1. Determining of optimum temperature
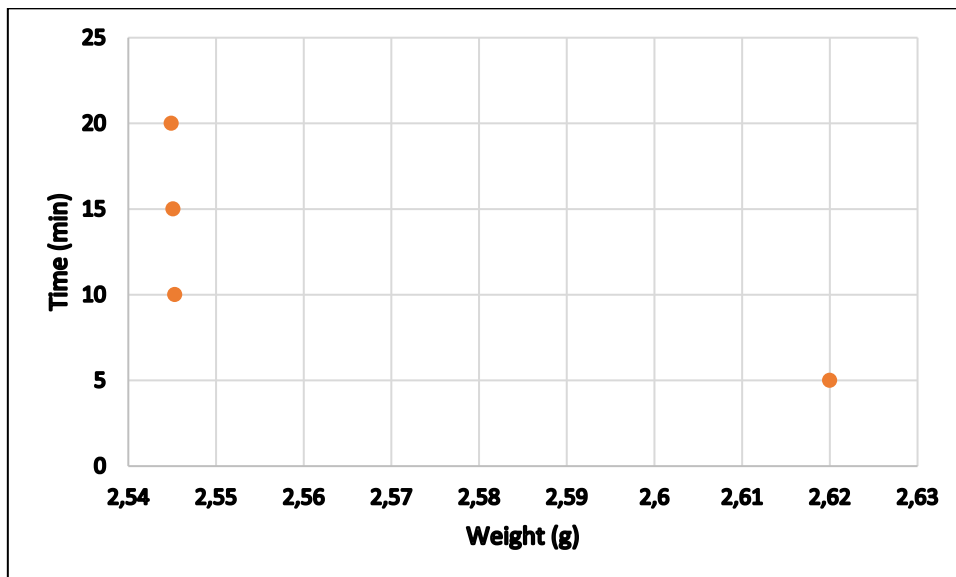
Graphic 2. Determining of optimum time

4. Discussion and Conclusions

In this study, the optimum pyrolysis time and optimum pyrolysis temperature required for the production of activated carbon from lavender pulp were determined. Accordingly, all pyrolysis is completed at 800 degrees and no further reduction in mass occurs. The time required for this was found to be 10 minutes. Since there is no study on the production of

activated carbon from lavender pulp in the literature, the results obtained will guide future studies.

Acknowledgements

References

Abdullah, M. O., Tan, I. A. W., & Lim, L. S. (2011). Automobile adsorption air-conditioning system using oil palm biomass-based activated carbon: A review. Renewable and Sustainable Energy Reviews, 15(4), 2061-2072.

Alan, S. (2019). Şeftali çekirdeği kabuğundan üretilen karbon destek maddesinin özellikleri üzerine farklı karbonizasyon şartlarının etkisi (Master's thesis, İnönü Üniversitesi Fen Bilimleri Enstitüsü).

Cavanagh, H. M. A., & Wilkinson, J. M. (2002). Biological activities of lavender essential oil. Phytotherapy research, 16(4), 301-308.

Gerhartz, W. (Ed.), 1986. Ullmann's: Encyclopedia Of Industrial Chemistry, Germany, A5, 124–140.

Girgis, B. S., Attia, A. A., & Fathy, N. A. (2007). Modification in adsorption characteristics of activated carbon produced by H3PO4 under flowing gases. Colloids and Surfaces A: Physicochemical and Engineering Aspects, 299(1-3), 79-87.

Guenther, E. 1952. The Essential Oils, R.E. Krieger Pub. Co. 5: 3-38.

Kara, N., & Baydar, H. A. S. A. N. (2012). Essential oil contents and composition of lavenders and lavandins cultivated in Turkey. Research on Crops, 13(2), 675-681.

Lesage-Meessen, L., Bou, M., Sigoillot, J. C., Faulds, C. B., & Lomascolo, A. (2015). Essential oils and distilled straws of lavender and lavandin: a review of current use and potential application in white biotechnology. Applied microbiology and biotechnology, 99(8), 3375-3385.

Nabais, J. M., Laginhas, C. E., Carrott, P., & Carrott, M. R. (2011). Production Of Activated Carbons From Almond Shell. Fuel Processing Technology(92), 234-240.

Tiliacos, C., Gaydou, E. M., Bessière, J. M., & Agnel, R. (2008). Distilled lavandin (Lavandula intermedia Emeric ex Loisel) wastes: a rich source of coumarin and herniarin. Journal of Essential Oil Research, 20(5), 412-413.

Torras-Claveria, L., Jauregui, O., Bastida, J., Codina, C., & Viladomat, F. (2007). Antioxidant activity and phenolic composition of lavandin (Lavandula x intermedia Emeric ex Loiseleur) waste. Journal of agricultural and food chemistry, 55(21), 8436-8443.

Wigmans, T., 1989. Industrial Aspects Of The Production And Use Of Activated Carbons. Carbon, 27, 13–22.

Yeganeh, M., Kaghazchi, T. And Soleimani, M. 2006. Effect Of Raw Materials On Properties Of Activated Carbons. Chemical Engineering & Technology, 29(10), 1247-1251.

Investigation of Encapsulation Efficiency of Olive Leaf Extract with Alpha and Beta Cyclodextrin

Şerife Çevik[1*], Mustafa Karaboyacı[2], Gülcan Özkan[3]

Abstract: In this study, it was aimed to investigate the extraction of phenolic substances from dried olive tree leaves and encapsulation techniques to convert this obtained extract into a storable form. Alpha and beta cyclodextrin were used as encapsulation material. The appropriate cyclodextrin dose and type were determined by providing the re-release of phenolic substances encapsulated in both cyclodextrins. Phenolic compounds were extracted by methanol extraction of olive leaves and total phenolic substance amounts were determined as mg GAE/g dry matter by Folin-Cialculate method. Extractions were carried out from olive leaves by methanol different dry matter/solvent ratio (5g/15mL, 5g/25 mL and 5g/35 mL) and determined highest total polyphenol content. Results shows that highest total polyphenol content is 42.58 – 49.59 mg GAE/g dry matter. According to the results obtained, alpha cyclodectrin is much more efficient than beta in calculating the encapsulation efficiency using water.Although the results are very close in the method using methanol, the efficiency of alpha cyclodesktrin is still higher than beta.

Keywords: Olive leaf, phenolic, encapsulation, alpha and beta cyclodextrin

1. Introduction

Olive (Olea europaea L.) leaves contain important phenolic compounds and therefore have been used in folk medicine for a long time. Olive leaves, which are generally seen as waste material after olive harvest, contain many phenolic compounds and the leaves containing this phenolic substance have antibacterial, antifungal and antioxidant properties. Due to the natural phenolic content and antioxidant properties of the olive leaf, it has commercial importance as it can be used directly as food. Olive leaves are rich in phenolic compounds with biological effects, one of the by-products of olive harvest.

Olive trees are among the longest-lived trees in the world. The main reason for this is that they produce a substance called "oleuropein", which gives the tree resistance against diseases and pests. Oleuropein belongs to a very specific group of coumarin-like compounds, called secoiridoids, which are abundant in Oleaceas, Gentianales, Cornales and many other plants. Iridoids and secoiridoids are compounds, usually glycosidically bound, produced from the secondary metabolism of terpenes as precursors of various indole alkaloids (Soler et al 2000). Oleuropein has been reported to have antioxidant, anticancer, anti-inflammatory, cardioprotective, neuroprotective, and hepatoprotective effects (Shamshoum et al 2017)

[1] Isparta University of Applied Sciences, Gelendost Vocational School, Dept of Food Proces., Isparta, Turkiye
[2] Suleyman Demirel University, Faculty of Engineering, Department of Chemical Engineering, Isparta, Turkiye
[3] Suleyman Demirel University, Faculty of Engineering, Department of Food Engineering, Isparta, Turkeye
* Corresponding author: serifecevik@isparta.edu.tr

Olives and olive leaves both contain oleuropein. It was first isolated from olive leaves erly 1900s (Barrett, 2015).
Talhiu et al. (2105) stated in their studies that 25 kg of by-products are obtained from the olive tree as a result of pruning every year. They stated that 25% by weight of this amount is formed by leaves, 25% by thick branches and the remaining 50% by thin branches.

That is, only at the end of pruning, 6.25 kg of leaves are obtained. If the leaves that can be collected after fruit harvest are added to this amount, it can be said that there is a great potential as a natural antioxidant source. Altıok et al. (2008) associated the use of olive tree leaves as a medicine in traditional medicine with the fact that the leaves are rich in polyphenols such as oleuropein, rutin, verbacoside, apigenin-7-glucoside and luteolin-7-glucoside.

In this study, olive tree leaves collected after harvest were macerated in different amounts of solvent and phenolic components were extracted by solid-liquid extraction. The optimum solvent/leaf ratio was determined from the results obtained. The obtained phenolic compounds were then encapsulated using alpha and beta cyclodextrin. The encapsulation efficiencies were analyzed and the appropriate cyclodextrin type was determined.

2. Materials and Methods

Olive leaves were picked from Antalya Province, Manavgat county by hand last year in October. Olive leaves were separated from the stem and left to dry at room at room temperature an than it was storage in vacuum packaging until the analysis. Methanol was purchase from Sigma- Aldrich, alpha and beta Cyclodextrin purchased from Ashland Global chemicals company.

2.1. Phenolic extraction

Olive leaves were ground with a Waring blender. 15 mL (1 to 3), 25 mL (1 to 5) and 35 mL (1 to 7) methanol were added to 5 g of ground olive leaves and kept in the dark at room temperature for 24 hours. After that samples filtered and stored in dark bottles until analysis. The total phenolic content of the extracts was determined by the Folin-Ciocalteu spectrophotometric method and the dry matter/solvent ratio in the extraction was determined. The highest total phenolic content was determined in the extraction performed with the addition of 15 mL of methanol on 5 g sample.

2.2. Determination of the total amount of phenolic substances

The total amount of phenolic compounds extracted from olive leaf by methanol was measured by using the Folin-Ciocalteu spectrophotometric method at a wavelength of 765 nm, and the result was calculated as mg gallic acid equivalent (GAE)/g leaf (Singleton ve Rossi, 1965).

2.3. Encapsulation of olive leaf extract with alpha and beta cyclodextrin

Alpha and beta cyclodextrin were used as coating material for the encapsulation process. The encapsulation was carried out by homogenizing the alpha and beta cyclodextrin, which is the coating material in different molar ratios of the extract. Powder alpha and beta cyclodextrins to be used in the encapsulation process were added to the 10 mL olive leaf extract with the

ratios of 0.0025 mol, 0.0010 mol and 0.0005 mol, and homogenized with Ultra Turrax (Ika, Staufen, Germany) for 7 minutes at 2500 rpm. The homogenized solution was transferred to glass petri dishes and dried in a vacuum dryer at 0.5 bar pressure at 40°C. The capsules obtained after drying were crushed and ground in a porcelain mortar. The ground powder capsules were sealed in the bottles in an airtight manner and stored at room conditions until analysis.

2.4. Encapsulation efficiency

The encapsulation efficiency (%EE) was calculated using Equation 1 by dividing the total phenolic substance encapsulated into the powder capsules to the total phenolic substance amount in the leaf extracts. There is no reference method for the effectiveness of the capsules. In this context, a preliminary study was carried out. In this context, a preliminary study was carried out. 10 mL of methanol was added to 1 g powder capsule and ultrasound assisted extraction was applied for 5 minutes at 100% power. The same process was carried out by adding water to the capsule. After the extraction process, the prepared solutions were centrifuged at 4000 rpm for 5 minutes. The polyphenol content of the capsule solution was determined using the Folin & Ciocalteau method (Najafi-Soulari et al., 2016).

$$EE \% = (We / Wt) \times 100 \qquad\qquad\qquad Eq.1$$

We: Total polyphenol content of the encapsulated samples
Wt: Total polyphenol content of the extract

3. Results

Extraction carried out from olive leaves by methanol different dry matter/solvent ratio (5g/15mL, 5g/25 mL and 5g/ 35 mL) and determined highest total polyphenol content. The total phenolic contents determined for all three trials are given in the table 1.

Table 1. Total total phenolic contents (mgGAE/g sample)

Trial 1	Trial 2	Trial 3
(5g leaf /15 mL methanol)	(5g leaf /25 mL methanol)	(5g leaf /35 mL methanol)
49.59± 0.43 mg GAE/g leaf	45.33± 0.86mg GAE/g leaf	42.58± 0.91mg GAE/g leaf

The total amount of phenolic content of the leafs was determined as gallic acid equivalent (GAE). It was determined as 42.58 – 49.59 mg GAE /g dry matter. As can be seen from the table, trial 1 has the highest total phenolic content. For this reason, in the continuation of the study, extraction was performed over this ratio (1 to 3).

Table 2. Quantities of α and β cyclodextrin used for 10 ml extract in encapsulation

α-Cyclodextrin	α-Cyclodextrin (g/10mL extract)	β-Cyclodextrin	β-Cyclodextrin (g/10mL extract)
0.0025 mol	2.43 g	0.0025 mol	2.84 g
0.0010 mol	0.97 g	0.0010 mol	1.14 g
0.0005 mol	0.49 g	0.0005 mol	0.57 g

Olive leaf extract (10 mL) was encapsulated with α and β cyclodextrin according to the mole ratio given in the table 2. As can be seen from the table 3, the amount of encapsulated

phenolic substance decreases depending on the increasing amount of cyclodextrin. For this reason, studies were continued with the highest yield ratio (0.0005 mol/10 mL) in the trials.

Table 3. Encapsule total phenolic content (mg GAE/g dry matter)

Mole	α-Cyclodextrin		β-Cyclodextrin	
	Methanol	Water	Methanol	Water
0.0025 mol	23.69±0.17	21.82±0.05	25.85±0.10	18.50±0.52
0.0010 mol	40.21±0.85	35.25±0.06	41.53±1.21	29.71±0.26
0.0005 mol	42.12±0.36	37.35±0.59	36.84±0.29	20.90±0.35

Table 4. Encapsule Efficiency (%)

Mole	α-Cyclodextrin		β-Cyclodextrin	
	Methanol	Water	Methanol	Water
0.0025 mol	47.76±0.74	44.00±0.09	52.12±0.14	37.31±1.04
0.0010 mol	81.08±1.71	71.08±0.11	74.29±0.42	42.14±0.70
0.0005 mol	84.93±0.73	75.32±1.19	83.75±1.73	59.92±0.52

The total polyphenol content of the capsule release solution was determined using the Folin & Ciocalteau method. Encapsulation efficiency of capsules dissolved with methanol was found to be higher than those dissolved with water. However, in the study with alpha cyclodextrin, the release of encapsulated phenolic substances back into the water was also quite high. This can be interpreted as beta cyclodextrin forms stronger inclusion complexes with phenolic substances and is not willing to re-release.

4. Discussion and Conclusions

According to the results obtained, the encapsulation efficiency of alpha cyclodextrine is higher than a very small amount of beta cyclodectrin in methanol solution. However, an important difference is that it has 20-40% higher efficiency in the re-release tests with water. In 2019, Jaski et al tried different methods to complex olive leaf extracts with β-cyclodextrin (β-CD) and to confirm how the extracts act as antioxidants in olive oil in free form and as inclusion complex. They obtainded extracts by pressurized liquid extraction at 343 K and 104 kPa with ethanol and determined total phenols by Folin-Ciocalteu was 0.12 kg GAE kg^{-1}. In our study, 50 mg/g was obtained by using 1:3 methanol at room conditions. Kaltsa et al., in their study in 2020, stated that the total polyphenol content of olive leaves can vary between 20.9 and 144.2 mg GAE/g, depending on the extraction method used.

References

Altıok, E., Bayçın, D., Bayraktar, O., Ülkü, S. (2008). Isolation of polyphenols from the extracts of olive leaves (Olea europaea L.) by adsorption on silk fibroin. Separation and Purification Technology, 62(2), 342-348.

Barrett, L. (2015). Olive Leaf Extract: The Mediterranean Healing Herb. Healthy Living Publications.

Jaski, J. M., Barão, C. E., Liao, L. M., Pinto, V. S., Zanoelo, E. F., & Cardozo-Filho, L. (2019). β-Cyclodextrin complexation of extracts of olive leaves obtained by pressurized liquid extraction. Industrial Crops and Products, 129, 662-672.

Kaltsa, O., Grigorakis, S., Lakka, A., Bozinou, E., Lalas, S., & Makris, D. P. (2020). Green valorization of olive leaves to produce polyphenol-enriched extracts using an environmentally benign deep eutectic solvent. AgriEngineering, 2(2), 226-239.

Najafi-Soulari, S., Shekarchizadeh, H., & Kadivar, M. (2016). Encapsulation Optimization of Lemon Balm Antioxidants in Calcium Alginate Hydrogels. Journal of Biomaterials Science, Polymer Edition, 27(16), 1631–1644.

Singleton, V.L., Rossi, J.A., 1965. Colorimetry of total phenolics with phosphomolybdic-phosphotungstic acid reagents. American journal of Enology and Viticulture, 16(3), 144-158.

Soler-Rivas, C., Espín, J. C., Wichers, H. J. (2000). Oleuropein and related compounds. Journal of the Science of Food and Agriculture, 80(7), 1013-1023.

Shamshoum, H., Vlavcheski, F., & Tsiani, E. (2017). Anticancer effects of oleuropein. Biofactors, 43(4), 517-528.

Talhaoui, N., Taamalli, A., Gómez-Caravaca, A. M., Fernández-Gutiérrez, A., Segura-Carretero, A. (2015). Phenolic compounds in olive leaves: Analytical determination, biotic and abiotic influence, and health benefits. Food Research International, 77, 92-108.

Determination of Cellulosic Content of Waste Lavender Stems

Özlem Karaboyacı[1*], Semra Kılıç[2]

Abstract: In this study, it was aimed to determine the chemical composition of lavender pulp, which became garbage after essential oil extraction. The cellulose content of waste lavender flowers was determined with Kurschner and Hoffer method, the chlorite method developed by Wise and Karl was used to determine the amount of holocellulose and lignin content was determined with TAPPI T 222 om-88 method. As a result of the study, it was determined that it contains 32 % cellulose. Cellulose obtained from waste can be used as raw material resource.

Keywords: Lavender waste, cellulose, lignin, chemical composition

1. Introduction

Lavender is the common name of plant species of Mediterranean origin that make up the genus Lavandula from the Lamiaceae family. It is a lavender genus, shrub-like plant with clustered spike-shaped blue, purplish or red flowers that grows in a wide area extending from the islands of the Atlantic Ocean to the countries around the Mediterranean and to India.

Lavandula genus has 48 species that naturally spread in different parts of the world. These species have hundreds of genotypes that differ in the chemical composition and developmental forms of their essential oils (Katar et al. 2020). There are three main types of lavender with high commercial value in the world. English lavender Lavander (Lavandula angustifolia Mill. = L. officinalis L. = L. vera DC) and Spike lavander (Lavandula spica = L. latifolia Medik.) have higher essential oil quality, while the hybrid named Lavandin (Lavandula) intermedia Emeric ex Loisel. = L. hybrida L.) has a higher essential oil yield (Karakaş and İzci 2021)

Lavender is a plant that is not picky in terms of soil. It grows very well in dry and calcareous soils with high permeability to lime and pH of 5.8-8.3. It is highly resistant to drought, heat and cold. However, sometimes cold damage is seen in regions with very harsh winters (Aslancan, and Sarıbaşi 2011). Our country is mostly under the influence of the Mediterranean climate. Therefore, lavender cultivation is very common in Antalya and Aegean regions in our country. It needs a mountainous area at an altitude of 600-2000 meters above sea level to grow. Since it likes sloping, barren and not very irrigated soil, there are several gardens in our country where mass production is made.

1 Süleyman Demirel University, Engineering Faculty, Bioengineering Department, Isparta, Turkey
2 Süleyman Demirel University, Science and Literature Faculty, Biology Department, Isparta, Turkey
* Corresponding author: ozlemkaraboyaci@gmail.com

The lavender oil obtained from the lavender flower can be easily used in meals and salads. At the same time, when used as a massage oil, it removes bad odors from the body. It is also good for headaches, stress and muscle aches.

The economy of lavender, which draws attention with its eye-catching color and scent, is developing rapidly every year. It can be used in many areas in the cosmetics, food, medicine, cleaning and health sectors, both with its visual contribution to ecotourism and its usage areas. This plant, which is unsuitable for irrigation and suitable for growing in barren places, is also in high demand by farmers. Lavenders, which have been preferred by producers in recent years for their contribution to tourism as well as their economic input, attract people with their beautiful appearance and smell. So much so that the producers have turned their fields into natural studio space. Especially photographers bride, groom, engaged couples take lots of photos among the lavenders. Domestic and foreign tourists spend their time wandering around the fragrant gardens.

1.1. Essential oil obtaining methods from lavender

1.1.1 Distillation

The distillation method was developed in Spain and France in the early 1300s to obtain essential oil. When it comes to years, new techniques have started to be implemented in order to meet the needs of different branches such as pharmacology (Kılıç , 2008).

There are various distillation and extraction methods to obtain essential oil. These are:

1.1.2. Distillation Methods

. Hydrodistillation

. Steam Distillation

. Vacuum Distillation

1.1.3. Extraction Methods

. Solvent Extraction

. Supercritical Fluid Extraction

. Microwave-Assisted Extraction

. Pressurized Solvent- Extraction

. Solid Phase Micro extraction

1.1.4. Simultaneous distillation and extraction

. Pressing

Samar Mansouria and his friends have got investigated the chemical composition of the Tunisian vine stems waste. The obtained data show that the stems are characterized by relatively high amounts of lignin (28.1%), holocellulose (65.4%) and extractives, especially in ethanol–toluene mixture (11.3%). In contrast, the □-cellulose content is low (35%). It has been concluded that ıt is suitable for paper raw material making, because the strings contain sufficient quantity of holocelülose (Mansouri, 2012).

In the study of Cömert and Karaboyacı, It is seen that there are 35 different components after distillation in the lavender stalks that are discarded as garbage.

The main component of this content is trans squalene, which constitutes one quarter of the total volatile content. Other main components are alphaBisabolol with 7.73%, Nonacosane with 10.74% and Tetratetracontan with 11.52% (Cömert, 2022).

In the study of Saldana et al.,They characterized coffee pulp (Coffea arabica)and green tea (Camellia sinensis) residues for use as a substrate for solid state fermentation for cellulase production. In 2017, world coffee production amounted to just over 9.2 million tons. Brazil was the world's largest producer (2.6 million tons), followed by Vietnam (1.5 million tons). It is estimated that 50% of the production is commercial. 4.6 million tons of green coffee is discarded as coffee pulp. As a result of the study, green tea residues emerge as a suitable material for the production of cellulase by solid fermentation (Saldana, 2021).

In the study of Chilev and her team in 2022, The global essential oils market demand was estimated at 247.08 kilotons in 2020 and is expected to grow at a compound annual growth rate of 7.5% from 2020 to 2027. These essential oils have gained importance in terms of therapeutic, cosmetic, aromatic, fragrance and spiritual uses. Their production produces enormous amounts of residual biomass. These waste residues contain natural antioxidants. It has attracted attention due to its benefits to human health (Chilev, 2022).

On the other hand, Karaboyacı and Uğur obtained dyestuff from waste lavender pulp in their study. After oil extraction, natural dyes were obtained from the pulp of lavender and Spartium junceum flowers and the pulp of Dimrit grape red wine. The dyeing of wool yarns with these compounds as natural dyestuffs was investigated and ecological wool dyeing was obtained by using non-toxic and ecological mordants. As a conclusion, it was demonstrated that pulps could create environmental pollution can be used as natural dye source for the ecological dyeing of textile woollen materials (Karaboyacı, 2014).

When the lavender flower production amounts in our country are examined, it is seen that 292 tons of lavender flowers were produced in Isparta and 108 tons of lavender flowers were produced in Afyonkarahisar. In 2019, 668 tons of production was made in Isparta and 279 tons in Afyonkarahisar. (TUIK,2020).

2. Materials and Methods

2.1. Cellulose Extraction

The cellulose extraction of waste lavender flowers was made by the Kurschner and Hoffer method (1931). Approximately 2 g of sample was treated with 100 mL of 1:4 (V/V mixture of nitric acid and ethanol and allowed to boil under reflux for 1 hour. After boiling for 1 hour, the sample was filtered and this process was repeated 3 times. After cooling, the remaining cellulose was filtered off and washed with distilled water until the filtrate was neutralized.

2.2. Holocellulose Extraction

Holocellulose is the carbohydrate complex that remains after the lignin substance of the plant has been removed. In the study, the chlorite method developed by Wise and Karl (1962) was used to determine the amount of holocellulose.

80 mL of distilled water was added to 2.5 g of waste lavender flower pulp. By adding 0.3 mL of acetic acid and 0.75 g of sodium chloride, the reaction was carried out at $80\,^{\circ}C$ for 1 hour under reflux. Afterwards, 0.3 mL of acetic acid and 0.75 g of sodium chloride were added again and waited for 1 hour. This process was repeated 3 times in total. After 3 hours, the mixture was filtered. The drying process was carried out by washing with distilled water and acetone.

2.3.Lignin Extraction

100 mL of 72% H_2SO_4 solvent was added to 2 g of waste lavender flower pulp. It was allowed to rest for 2 hours, stirring every 10 minutes. Then 300 mL of distilled water was added and boiled for 15 minutes. The drying process was carried out by washing with distilled water.

3. Results

The chemical composition of lavender obtained as a result of the analyzes are summarized in the table below. According to the results obtained, although the plant is not a perennial plant, it has a relatively high cellulose content. Although the stems have been previously distilled and degreased, they still contain 4 percent extractive material. therefore, waste straws can be re-evaluated both as a source of cellulose and as a source of extractive material.

Table 1. Chemical Composition of Spartium Lavender Flowers

Material	%
Cellulose	32
Holocellulose	64
Lignin	32
Extractive substances	4

Yan-xing et al., (2011) in their study named "Analysis of Chemical Components and Morphology of the Stem Fiber of Lavandula Pinnata L", have reported that, lavender stems benzene-alcohol extract content was 8.25%, total lignin content was 32.04%, and nitric-

ethanol cellulose content was 27.62%. The cellulose and lignin content obtained in this study is consistent with our study.

4. Discussion and Conclusions

The increase in the use of wood and the decrease in forest resources in the forest products industry led the paper industry to different alternative raw materials. One of them is the use of annual plants and their wastes in pulp and paper production. In this context, many studies have been carried out and are continuing. Fatma et al.studys in 2019 rose wastes includes %36 cellulose and high enough to be used in pulp production. Cömert et al. 2022 it is seen that there are 35 different components in the lavender stalks that are discarded as garbage after distillation. The main component in the content is trans squalane and constitutes one quarter of the total volatile content. In the study conducted by Sabathier et al. in 2017, they obtained 33.7% cellulose, 13.9% hemicelluloses and 14.7% lignin from lavender powders.

References

Aslancan, H., Sarıbaş, R. (2011). Lavanta yetiştiriciliği. Meyvecilik Araştırma İstasyonu Müdürlüğü, Yayın, 41.

Bekdaş, F., & Karaboyacı, M. (2019). Production of paper from rose wastes. Turkish Journal of Forestry, 20(3), 250-253.

Chilev, C., Simeonov, E., Dimitrova, B., Yonkova, V., Pietsch, S., Heinrich, S., & Peshev, D. (2022). Valorization of waste lavender residue from the essential oil industry for production of rosmarinic acid–a study on the solid-liquid extraction. Journal of chemical technology and metallurgy, 57(3), 522-532.

Cömert, Y. & Karaboyacı, M. (2022). Determination of Volatile Components of Waste Lavender Stalks and Isolation of Tributyl Acetylcitrate. M. Karaboyacı & A. Demirçalı (Eds.), Versatile Multidisciplinary Engineering Research (p. 205-220). Lithuania: SRA Academic Publishing.

Karaboyacı, M., & Uğur, Ş. S. (2014). Ecological wool dyeing with pulps of lavender, broom, and red wine. The Journal of The Textile Institute, 105(8), 821-827.

Karakaş, İ., İzci, B. (2021). Effects of Three Different Rooting Media on Some Rooting Parameters of Cuttings Belonging to Lavandula angustifolia and Lavandula intermedia Species. Acta Nat. Sci, 2(1), 68-75.

Katar, D., Can M ., Katar, N. (2020). Farklı lokasyonların lavandin (Lavandula× intermedia Emeric ex Loisel.)'de uçucu yağ oranı ve kimyasal kompozisyonu üzerine etkisi. Uluslararası Tarım ve Yaban Hayatı Bilimleri Dergisi, 6(3), 546-553.

Kılıç, A. (2008). Uçucu yağ elde etme yöntemleri. Bartın Orman Fakültesi Dergisi, 10(13), 37-45.

Mansouri, S., Khiari, R., Bendouissa, N., Saadallah, S., Mhenni, F., & Mauret, E. (2012).

Chemical composition and pulp characterization of Tunisian vine stems. Industrial Crops and Products, 36(1), 22-27.

Saldaña-Mendoza, SA, Ascacio-Valdés, JA, Palacios-Ponce, AS, Contreras-Esquivel, JC, Rodríguez-Herrera, R., Ruiz, HA, ... & Aguilar, CN (2021). Hindistan'ın Batı Ghats'ından izole edilen mantarları kullanarak selüloz üretimi için çay ve kahve endüstrilerinden gelen atıkların kullanılması. Sistem Mikrobiyolojisi ve Biyo-imalat , 1 (1), 33-41.

Sabathier, V., Louvel, S., Correa, G., Magniont, C., Evon, P., & Labonne, L. (2017). Incidence of the water-soluble compounds contained into lavender and sunflower bioaggregates on the hardening process of mineral binders. Academic Journal of Civil Engineering, 35(2), 62-68.

TUİK, 2020. Türkiye İstatistik Kurumu. https://www.tuik.gov.tr/ (Accessed March 10, 2022).

Zhang Y., Jun Y., Jian X., Sheng-long W., Hong W., (2011). Analysis of Chemical Components and Morphology of the Stem Fiber of Lavandula Pinnata L. Paper Science & Technology 4, 34-37

Otomobil Yüzü Tasarım Trendleri ve Tüketici Üzerindeki Etkileri / Automobile Face Design Trends and Their Impact on Consumers

Ümit Bayırlı*[1]

Abstract: The appearance of the products gives them a character and influences the consumer perception and purchasing decisions. The automobiles that are associated with the characters they have among the existing products in the market and marketed in this direction, and their faces, as they are perceived together with the radiator grilles and headlights, constitute the scope of this study. The study was carried out with 102 participants by questionnaire method and aimed to measure the perceptions of the participants on automobile faces. The participants evaluated 27 automobile faces using predetermined adjectives. With the collected data, the car face design trends that have changed since the 2000s and the effects of car faces on the consumers have been determined. In the light of the data obtained, it has been determined that the automobile faces that are being designed today are perceived by consumers as more and more aggressive, sporty, modern, robust, fast and attractive than the ones in 2000's and 2010's.

Keywords: Automobile face, consumer perception, product characteristics, industrial design

1. Giriş

Ürünler dış görünüşleri sebebi ile tüketiciler tarafından bir karaktere, kişiliğe büründürülürler. Nasıl ki insanlar tanımadıkları birinin yüz hatlarından yola çıkarak o kişi hakkında sempatik, ciddi, sert gibi sıfatları kullanarak çıkarımlar yapıyorsa, aynı şekilde ürünler hakkında da çıkarımlar yapar (Janlert & Stolterman, 1997). Bu çıkarımlar yapılırken ürünlerin fonksiyonları bir kenara bırakılıp sadece dış görünüşlerinden yola çıkılır. Bu bağlamda, otomobiller de insanlar tarafından sıkça bir karakter ile bağdaştırılarak öne çıkmaktadır. Otomobil üreticileri ve tasarımcılar da bu konu üzerinde pazarlama stratejileri geliştirmekte ve tüketicileri kendi ürünlerine çekmeye çalışmaktadır. Otomobillerin ön yüzleri bir karakterle bağdaştırılmaları hususunda önemli rol oynar. Farların gözlerle, radyatör ızgarasının da ağızla ilişkilendirildiği otomobil yüzleri, genellikle hayvan yüzleri ile benzeştirilir (Burgess & King, 2004; Sano, 2010). Bu çalışma kapsamında 2000'li yıllardan günümüze kadar tasarlananmış belirli otomobillerin yüzleri incelenmiş, tasarım trendleri belirlenmiş ve bu otomobil yüzlerinin tüketici üzerinde yarattığı etki tespit edilmiştir.

2. Ürün Tasarımlarının Tüketici Üzerinde Etkileri

İnsanlar ürünlerin şeklinden, renginden, kalitesinden, malzemesinden, işlevinden vs. etkilenerek satın alma kararları verirler. Yapılan çalışmalar bu satın alma kararlarının %80'inin görme eylemi sonucunda verildiğini ortaya koyar (Schmitt, Köhler, Dura & Diaz-Pineda,

Pamukkale University, Faculty of Architecture and Design, Department of Industrial Design, Denizli, Türkiye
* Corresponding author: ubayirli@pau.edu.tr

2013). Dolayısıyla ürünlerin dış görünüşü tüketicilerin algıları, yorumlamaları, duyguları, kararları ve eylemleri üzerinde büyük etkiye sahiptir (Bi, Li, Wagner & Reid, 2017; Bloch, 1995). Bu bilgi ışığında, firmalar ve tasarımcıları da tasarladıkları ürünlerin dış görünümlerine büyük önem verirler. Crilly, Moultrie ve Clarkson'a göre (2009) tasarımcılar, tasarladıkları ürünler vasıtası ile tüketicide sekiz farklı davranış biçimi ortaya çıkarmayı amaçlar: dikkatlerini çekmek, ürünü fark etmelerini sağlamak, ürünü ilgi çekici bulmalarını sağlamak, ürünün fonksiyonunu idrak etmelerini sağlamak, tasarım sürecinde amaçlanan nitelikleri kavramalarını sağlamak, kimliklerini olumlu bir şekilde ifade etmelerini sağlamak, duygularını ortaya çıkarmak ve eyleme teşvik etmek. Belirtilen davranış biçimlerinden çoğu ürünün dış görünüşü ve o dış görünüşün tüketici duyguları, kararları ve eylemleri üzerindeki etkileri ile yakından ilişkilidir.

Damasio'nun (1994) çalışmalarının sonuçları yaygın inanışın aksine insanların karar verme süreçlerinin mantıksal düşünce sonucu ortaya çıkmadığını savunmaktadır. Çalışmasında, beyin hasarları sonucu zarar görmüş duygusal sistemlerinin haricinde son derece sağlıklı olan insanların satın alma kararları veremedikleri görülmüştür. Bu nedenle duygusal sistemin satın alma kararlarında insanlar için büyük öneme sahip olduğu öne sürülebilir.
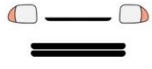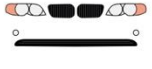
Tüketicilerin dikkatini çekmek ve satın alma kararlarını etkilemek hususunda tüketicileri tanımak da büyük öneme sahiptir. Bu bağlamda, kullanıcı ihtiyaç ve tercihlerinin belirlenmesi ve tasarımcıların tasarladıkları tasarım stratejileri ile tüketicilerin algıları arasındaki ilişkilerin ürün semantiği açısından incelenmesi oldukça önemlidir (Hsu, Chuang & Chang, 2000; Krippendorf, 1995). Firmalar ve tasarımcılar, tüketici araştırmaları yaparak, tüketicilerin ürünün görsel görünümünü nasıl yorumladıklarını tespit edebilir, istenen tepkiyi uyandıran kavramsal modelleri belirleyebilir, tüketici tarafından neyin çekici ve zevkli olarak algılandığını anlayabilir ve böylece gelecekteki tasarımlarını geliştirebilirler (Chang & Wu, 2007; Crilly, Moultrie & Clarkson, 2009; Jagtap, 2018). Bu bağlamda, bu çalışma, tüketicilerin otomobil yüzlerine ilişkin algılarını belirleyerek farların ve radyatör ızgaralarının görsel formuna nasıl tepki verildiğini anlamayı, bu tepkileri etkileyen stilistik kuralları ve form karakterlerini belirlemeyi ve tasarım sürecinde faydalanılmak üzere otomobil tasarımcıları bir rehber sunmayı amaçlamaktadır.

3. Yöntem

Tüketicilerin otomobil yüzleri üzerindeki algılarını belirlemek amacı ile, farklı yıllarda, farklı segmentlerde ve farklı üreticiler tarafından üretilmiş 27 adet otomobil belirlenmiştir (Şekil 1). Bu otomobilleri 2000'li, 2010'lu ve 2020'li yıllarda, Avrupa, Amerika ve Uzak Doğu menşeili üreticiler tarafından üretilmiş dokuz adet b, dokuz adet c ve 9 adet d segmenti otomobil oluşturmaktadır. Bir ürünün algılanması karmaşık bir süreç olduğundan ve biçim, renk, malzeme gibi birçok değişken birlikte çalıştığından dolayı (Hsu, Chuang & Chang, 2000; Mono, 1997) otomobil fotoğraflarını kullanmak yerine seçilen otomobillerin yüzlerinin siluetleri Adobe Illustrator programı kullanılarak oluşturulmuştur. Bu sayede marka, dış form, boyut gibi çalışmanın sonuçlarını etkileyebilecek değişkenlerin sayısını en aza indirgemek amaçlanmıştır.

Tüketicilerin algılarını ölçmek için, Kansei mühendisliği (Nagamachi, 1995), anlamsal diferansiyel yöntem (Osgood, Suci & Tannenbaum, 1957) ve görsel ürün deneyimi (Warell, 2008) gibi çeşitli yaklaşımlar yaygın olarak kullanılmaktadır. Bu yaklaşımlar sıfatlar, bu sıfatların sınıflandırılması ve bir değerlendirme aracı gerektirir. Bu çalışmada Likert ölçeklerini kullanan semantik diferansiyel yöntemi kullanılmış ve analizi izlenebilir kılmak ve katılımcıların harcadıkları zamanı azaltmak için zıt anlamlı sıfatlar tercih edilmiştir. Çalışma için gerekli olan sıfatlar, literatürden ve otomobil üreticilerinin web sitelerinden derlenmiştir.

Toplanan sıfatlar değerlendirilmiş, benzerleri elenmiş ve zıt anlamlılarıyla birlikte en çok kullanılan altı adet sıfat çalışma için seçilmiştir: ağırbaşlı – sportif, sempatik – agresif, kırılgan – sağlam, geleneksel – modern, itici – çekici ve yavaş – hızlı. Katılımcıların yanıtları çevrimiçi bir anket aracılığıyla toplanmıştır. Ankette katılımcılardan 27 adet otomobilin yüzlerini 7'li Likert ölçeği (bir tarafta bir sıfat, ortada nötr, diğer tarafta sıfatın zıt anlamlısı) üzerinden değerlendirmeleri istenmiştir. Katılımcılardan otomobili tanınmaları durumunda, resimlerde verilen otomobil yüzlerine odaklanmaları ve motor gücü, boyut, dayanıklılık, malzeme kalitesi gibi diğer özelliklerini göz ardı etmeleri istenmiştir.

Şekil 1. Çalışma kapsamında incelenen otomobil yüzleri

4. Bulgular

Çalışmaya çeşitli yaş gruplarında 102 katılımcı (31 kadın, 71 erkek) katılmıştır (Tablo 1). Sonuçlar SPSS kullanılarak analiz edilmiş ve her otomobilin 7'li Likert ölçeğinde aldıkları puanlar tespit edilmiştir.

Tablo 1. Katılımcı bilgileri

|	18-25	25-35	35-45	45-55	55 ve fazlası	Toplam
Kadın	9	4	8	5	5	31
Erkek	8	17	13	19	14	71
Toplam	17	21	21	24	19	102

Elde edilen bulgular ışığında Şekil 2, 3 ve 4'teki saçılım diyagramları oluşturulmuştur. Bu diyagramlarda otomobil modelinden sonra yazılan 1 rakamı o modelin 2000'lerde; 2 rakamı o modelin 2010'larda; 3 rakamı ise 2020'lerde tasarlandığını ve üretildiğini belirtmektedir.
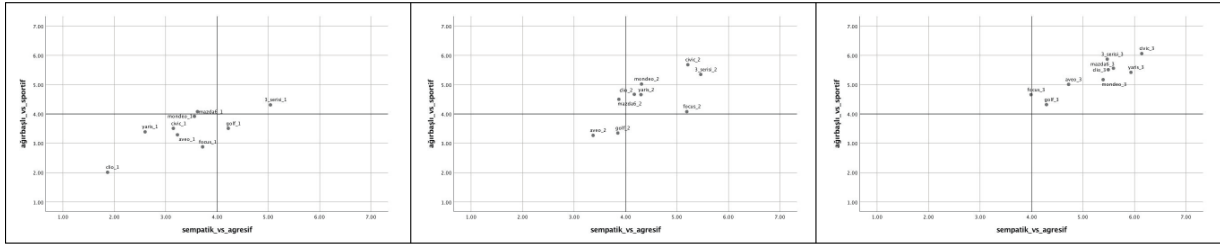
Şekil 2. Otomobil yüzlerinin ağırbaşlılık – sportiflik ve sempatiklik – agresiflik sıfatları kapsamında aldıkları ortalama puanlar (soldaki diyagram 2000'leri, ortadaki 2010'ları, sağdaki 2020'leri göstermektedir)
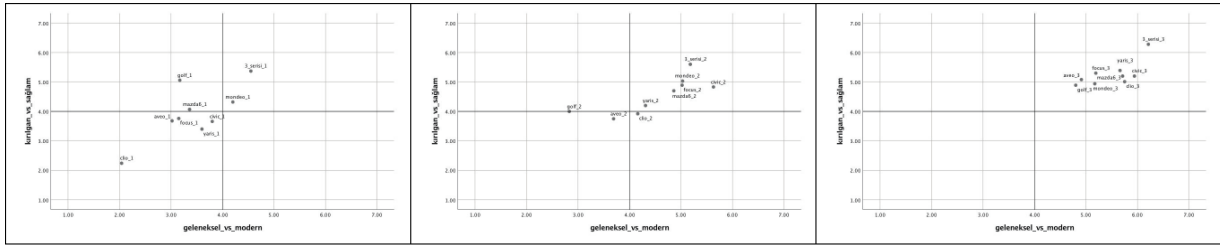
Şekil 3. Otomobil yüzlerinin kırılganlık – sağlamlık ve geleneksellik – modernlik sıfatları kapsamında aldıkları ortalama puanlar (soldaki diyagram 2000'leri, ortadaki 2010'ları, sağdaki 2020'leri göstermektedir)
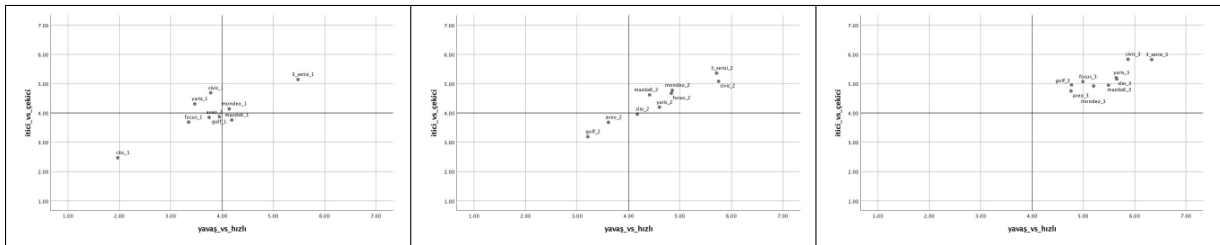
Şekil 4. Otomobil yüzlerinin iticilik – çekicilik ve yavaşlık – hızlılık sıfatları kapsamında aldıkları ortalama puanlar (soldaki diyagram 2000'leri, ortadaki 2010'ları, sağdaki 2020'leri göstermektedir)

Diyagramlar incelendiğinde 2000'li ve 2020'li yıllar arasında otomobil yüzlerinin kullanıcılar tarafından gitgide daha sportif, agresif, sağlam, modern, çekici ve hızlı olarak algılandığı belirtilebilir. Belirtilen yıllardaki otomobil yüzlerindeki değişim incelendiğinde ise giderek daha keskin hatlı farların ve büyük radyatör ızgaralarının tercih edildiğini söylemek mümkün. Bu hususta daha keskin çizgilerin ve hacimli formların kullanıcıda sportiflik, agresiflik, sağlamlık, modernlik, çekicilik ve hızlılık algısı yarattığı söylenebilir.

5. Sonuç

Tüketicide istenen algıları ve tepkileri uyandırmak için bir ürünün parçalarının görsel öğelerini ve özelliklerini ve tüm ürünün karakterini anlamak ve yeniden tasarlamak, endüstriyel tasarımda önemli bir husustur. Mevcut çalışmalar, araba yüzlerinin insan ve hayvan yüzleriyle

ilişkilendirilebileceğini öne sürmektedir (Burgess & King, 2004; Sano, 2010). Ancak, tüketicilerin bu yüz unsurlarının özelliklerini nasıl algıladıklarını belirlemekte yetersiz kalmışlardır. Bu anlamda bu çalışma, farların ve radyatör ızgaralarının özelliklerini ve tüketici üzerindeki etkilerini ortaya koymaktadır. Çalışmada yer alan otomobil yüzlerindeki tasarım unsurlarının yıllar içerisindeki değişimi yazarın çıkarımlarından oluşmaktadır. Ayrıca sonuçlar sadece Türk halkının algılarını yansıtmaktadır. Bu nedenle sonuçların genellenebilmesi için farklı kültürlerde farklı araba yüzlerini araştıran benzer araştırmalar yapılmalıdır. Ayrıca Janlert ve Stolterman'ın (1997) belirttiği gibi karakter, çeşitli özelliklerin bir kombinasyonudur ve karakterlerin genelini yansıtması için özelliklerin birbiriyle tutarlı olması gerekir. Bir tüketici, renk, boyutlar, gövde stili, malzemeler, güvenlik vb. gibi çeşitli yönleri göz önünde bulundurarak bir otomobille ilgili genel algısını sentezler. Bu nedenle, tasarım sürecinde üreticilere ve otomobil tasarımcılarına rehberlik etmesi için otomobil yüzlerinin yanı sıra diğer faktörler ve bunların karşılıklı ilişkileri de incelenmelidir.

Kaynaklar

Bi, Y., S. Li, D. Wagner, and T. Reid. (2017). "The Impact of Vehicle Silhouettes on Perceptions of Car Environmental Friendliness and Safety in 2009 and 2016: A Comparative Study." Design Science 3 (23): 1-33. doi: 10.1017/dsj.2017.22.

Burgess, S. C., and A. M. King. (2004). "The Application of Animal Forms in Automotive Styling." The Design Journal 7 (3): 41-52. doi: 10.2752/146069204789338389.

Chang, W., and T. Wu. (2007). Exploring Types and Characteristics of Product Forms. International Journal of Design 1 (1): 3-14.

Crilly, N., J. Moultrie, and P. J. Clarkson. (2009). "Shaping Things: Intended Consumer Response and the Other Determinants of Product Form." Design Studies 10 (3): 224-254. doi: 10.1016/j.destud.2008.08.001.

Damasio, A. R. (1994). Descartes' Error. New York: Putnam.

Hsu, S. H., M. C. Chuang, and C. C Chang. (2000). "A Semantic Differential Study of Designers' and Users' Product Form Perception." International Journal of Industrial Ergonomics 25 (4): 375-391. doi: 10.1016/S0169-8141(99)00026-8.

Jagtap, S. (2018). Intentions and Inspiration in Shaping Visual Appearance of Products: The Practice of Professional Industrial Designers in India. The Design Journal 21 (1): 85-107. doi: 10.1080/14606925.2018.1396075.

Janlert, L., and E. Stolterman. (1997). "The Character of Things." Design Studies 18 (3): 297-314. doi: 10.1016/S0142-694X(97)00004-5.

Krippendorf, K. (1995). "On the Essential Contexts of Artifacts or on the Proposition That Design Is Making Sense (Of Things)." In The Idea of Design, edited by Margolin, V. and Buchanan, R., 156-184. London: The MIT Press.

Mono, R. (1997). Design for Product Understanding. Stockholm: Liber AB.

Nagamachi, M. 1995. "Kansei Engineering: A New Ergonomic Consumer-Oriented Technology for Product Development." International Journal of Industrial Ergonomics 15 (1): 3-11. doi: 10.1016/0169-8141(94)00052-5.

Osgood, C. E., C. J. Suci, and P. H. Tannenbaum. (1957). The Measurement of Meaning. Urbana: University of Illinois Press.

Sano, S. (2010). "Facial Expressions in Car Design." Paper presented at the 7th International Conference on Design and Emotion, Chicago, October, 4-7.

Schmitt, R., M. Köhler, J. V. Dura, and J. Diaz-Pineda. (2013). "Objectifying User Attention and Emotion Evoked by Relevant Perceived Product Components." Journal of Sensors and Sensor Systems 3 (2): 315-324. doi: 10.5194/jsss-3-315-2014.

Warell, A. (2008). "Multi-Modal Visual Experience of Brand-Specific Automobile Design." TQM Journal 20 (4): 356-371. doi: 10.1108/17542730810881348.

Thermodynamic Analysis of Hydrogen Production from Seawater

Mehmet Altinkaynak [1*] ,Murat Ozturk[2]

Abstract: Today, the increasing population and this situation have caused an increase in the demand for energy. The use of renewable energy systems is becoming increasingly important due to the concerns arising from the decrease in fossil fuels and the environmental damage it causes. The offered system composes the freshwater production plant (FWPP), second part hydrogen production plant (HPP), third part hydrogen compression plant (HCP). The novelty of this paper is to design and analyze sea water driven integrated cycle for multigeneration with power and hydrogen production. The outputs of this study show that the energy and exergy efficiencies of the whole system are 68.04% and 58.92%, respectively. In addition, the fresh water and hydrogen productions produced in the system were calculated as 26.43 and 0.291 kg/s.

Keywords: Distillation; Energy; Exergy; Hydrogen production.

1.   Introduction

The increase in the human population also plays an important role among the reasons for the rapid increase in energy demands in the world. So how is the human population a factor at this point? The most important factor in the first place is the improvement of comfort conditions. Because as comfort conditions improve, the demands of human beings and, accordingly, the development of technology act together. The biggest input in providing comfort conditions is energy. There is a need for energy both in terms of technology and industry. Although there is energy production from fossil fuels today, the decrease in these resources, carbon dioxide emissions, global warming, etc. For such reasons, an inevitable search begins. Due to the environmental and sustainable nature of renewable energy sources, a rapid transition to this direction has begun. Rather than power generation from renewable energy sources, the rapid consumption of water resources is at alarming levels for now. It is a well-known fact that the world's water resources are concentrated in the seas. However, considering the impact of saltwater use on living conditions, these resources should be converted to fresh water with the help of chemical processes. Delpisheh et al. (2021) investigated the thermodynamic performance of a solar-assisted system to produce hydrogen from seawater. As a result of the parametric analysis, the authors found the hydrogen production rates to be 4.33 g/s, 2.62 g/s, and 3.54 g/s, respectively, according to the solar radiation values. Yilmaz et al. 2021 developed a novel system based on the gas turbine. The modeled system consists of the Brayton cycle,

[1] Isparta University of Applied Sciences, Faculty of Technology, Faculty, Department of Mechanical Engineering, Isparta, Turkey.
[2] Isparta University of Applied Sciences, Faculty of Technology, Faculty, Department of Mechatronic Engineering, Isparta, Turkey.
* Corresponding author: mehmetaltinkaynak@isparta.edu.tr

reheat Rankine cycle, ORC, thermal distillation and PEM. As a result of their analysis, they found that the energy and exergy efficiencies of the system were 0.6076 and 0.5671, respectively. In addition, the authors found that the hydrogen production rate was 0.001742 kg^{-1} and the clean water production 0.7647 kg^{-1}. Safari and Dincer offered a novel multigeneration model which are consist of the Brayton cycle, ORC, and multi-effect desalination unit useful products. Authors designed and conducted an integrated system so as to produce hydrogen, heat, and power. According to analyzes the energy and exergy efficiencies of proposed cycle were calculated as 63.6% and 40%, respectively. Further, the production rates power, freshwater, hydrogen, and hot water are acquired as 1102 kW, 0.94 kg/s, 0.347 kg/h, and 1.82 kg/s, respectively. In this study, the production of fresh water from sea water and, accordingly, the production and storage of hydrogen are considered.

2. Material Method

2.1. System Description

The design in which electrical energy production, hydrogen production, freshwater production, and hydrogen compression-storage systems using sea water are made is given in Figure 1.

The system consisting of these four parts has been examined separately. In the first part, freshwater production from sea water and electric energy were provided. During this process, seawater is filtered and chemically treated. Fresh water coming into the mixing chamber by applying the reverse osmosis method has a temperature of 44 °C. From here it is sent to the freshwater tank. Water heated up to 80 °C in the preheater of the PEM electrolyzer is sent to the PEM electrolysis. Before this stage, the energy of sea water discharged from reverse osmosis produces electrical energy with the help of a Pelton turbine. The generated electrical energy was sent to the PEM in the second part as input. The hydrogen obtained here was compressed and stored with the help of compressors.
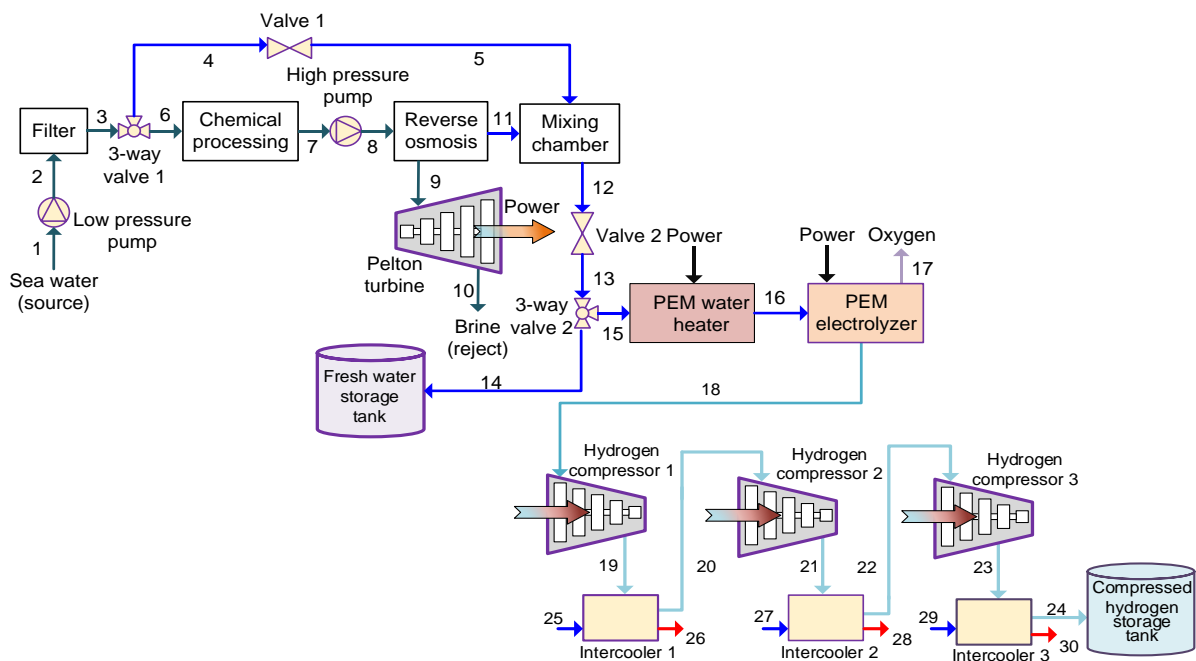

Figure 1. Seawater based hydrogen production and storage plant

2.2. Thermodynamics analysis

In the modeled, we examined the energy and exergy performances of the sea-water based hydrogen production and storage plant integrated usage system. Engineering Equation Solver (EES) package program is used in calculations. In this context, considering the first and second laws of thermodynamics, four fundamental equations of mass, energy, entropy and exergy equilibrium can be given as follows (Dincer and Rosen 2020).

$$\sum \dot{m}_i = \sum \dot{m}_o \tag{1}$$

$$\dot{Q}_i + \dot{W}_i + \sum \dot{m}_i \, h_i = \dot{Q}_o + \dot{W}_o + \sum \dot{m}_o \, h_o \tag{2}$$

$$\sum \dot{m}_i \, s_i + \sum \frac{\dot{Q}_k}{\dot{T}_k} + \dot{S}_{gen} = \sum \dot{m}_o \, s_o \tag{3}$$

$$\dot{E}x_{Q,i} + \dot{W}_i + \sum \dot{m}_i \, ex_i = \dot{E}x_{Q,o} + \dot{W}_o + \sum \dot{m}_o \, ex_o + \dot{E}x_d \tag{4}$$

Here, the subscripts i and e describe the streams inlet and exit the components. Also, h and s explain the enthalpy and entropy terms, respectively. The heat and work exergy rates can be defined as:

$$\dot{E}x_Q = \left(1 - \frac{T_0}{T}\right) * \dot{Q} \tag{5}$$

$$\dot{E}x_d = T_0 * \dot{S}_{gen} \tag{6}$$

After writing the general balance equation, the specific exergy term can be written as:
$$ex = (h - h_0) - T_0(s - s_0) \tag{7}$$

3. Results

Detailed performance analysis of the new design model, whose schematic representation is given above, is handled by determining the exergy destruction rates together with the energy and exergy efficiencies. Before moving on to these calculations, the assumptions presented in Table 1 in the system are made and the kinetic and potential energy changes of the whole system are neglected. The reference temperature and pressure are taken as 25 °C and 101.3 kPa, respectively. Besides, the whole plant and components are modeled as a steady-state flow. The results of this parametric study carried out with a package program called EES (Klein, 2021) are illustrated in Table 1 below.

Table 1. Thermodynamical properties of state points

Flow number	T (°C)	P (kPa)	$\dot{m}$ (kg/s)	h (kJ/kg)	s (kJ/kgK)	ex (kJ/kg)
1	44.5	101.3	48.45	177.8	0.6034	2.407
2	44.6	652	48.45	178.7	0.6047	2.973
3	44.6	652	48.45	178.7	0.6047	2.973
4	44.6	629	0.08325	187.3	0.633	3.11
5	44.66	320	0.08325	187.3	0.634	2.818
6	44.6	629	48.39	178.7	0.6047	2.951
7	44.6	610	48.39	178.7	0.6047	2.932
8	46.2	6002	48.39	190.4	0.6248	8.653
9	46.2	610	19.35	185.1	0.6248	3.344
10	41	101.3	19.35	163.7	0.559	1.619
11	46.2	320	29.03	193.7	0.6541	3.229
12	45.7	320	29.11	191.6	0.6476	3.092
13	45.75	101.3	29.11	191.6	0.6483	2.886
14	45.75	101.3	26.43	191.6	0.6483	2.886
15	45.75	101.3	2.682	191.6	0.6483	2.886
16	80	101.3	2.682	335	1.075	18.94
17	80	101.3	2.391	50.5	0.1556	127.2
18	80	101.3	0.291	4723	55.81	85.63
19	266.3	500	0.291	7426	55.36	2901
20	25	500	0.291	3933	46.79	1966
21	266.3	2500	0.291	7441	48.72	4896
22	25	2500	0.291	3942	40.13	3960
23	697	75000	0.291	14395	43.36	13449
24	25	75000	0.291	4419	25.83	8702
25	26	300	8.38	109.2	0.3809	0.2063
26	55	300	8.38	230.5	0.7678	6.117
27	26	300	8.394	109.2	0.3809	0.2063
28	55	300	8.394	230.5	0.7678	6.117
29	26	300	14.16	109.2	0.3809	0.2063
30	75	300	14.16	314.2	1.015	16

In addition, the generated/consumed power values and useful outputs obtained in the system are shown in Table 2.

Table 2. Production/consumption values and useful outputs

Component	Power production (kW)
Pelton turbine	414.2
Components	**Power consumption (kW)**
Low pressure pump	43.6
High pressure pump	566.2
PEM water heater	384.6
PEM electrolyzer	835.3
Hydrogen compressor 1	786.6
Hydrogen compressor 2	1021
Hydrogen compressor 3	3042
Useful outputs	
Hydrogen	0.291 kg/s
Fresh water	26.43 kg/s

The energy and exergy efficiencies of the sub-cycles that make up the system are given in Table 3. Also, the exergy destruction of the cycles is also given in Table 3.

Table 3. Efficiencies results of sub-cycles based on the energy and exergy perspective

Sub-plants and integrated plant	Energy efficiency	Exergy efficiency	Exergy destruction rate (kW)
Fresh water production plant	0.7017	0.6328	1943
Hydrogen production plant	0.7329	0.6605	2391
Hydrogen compression plant	0.5291	0.4169	4078
Overall plant	0.6804	0.5892	8412

Figure 2 shows effect of reference temperature on the energy efficiencies of integrated plant and its sub-plants. The effect of changing the reference temperature between 0 °C and 50 °C on the energy efficiency of the overall system (OS) ranged from 65.9% to 70.6%.
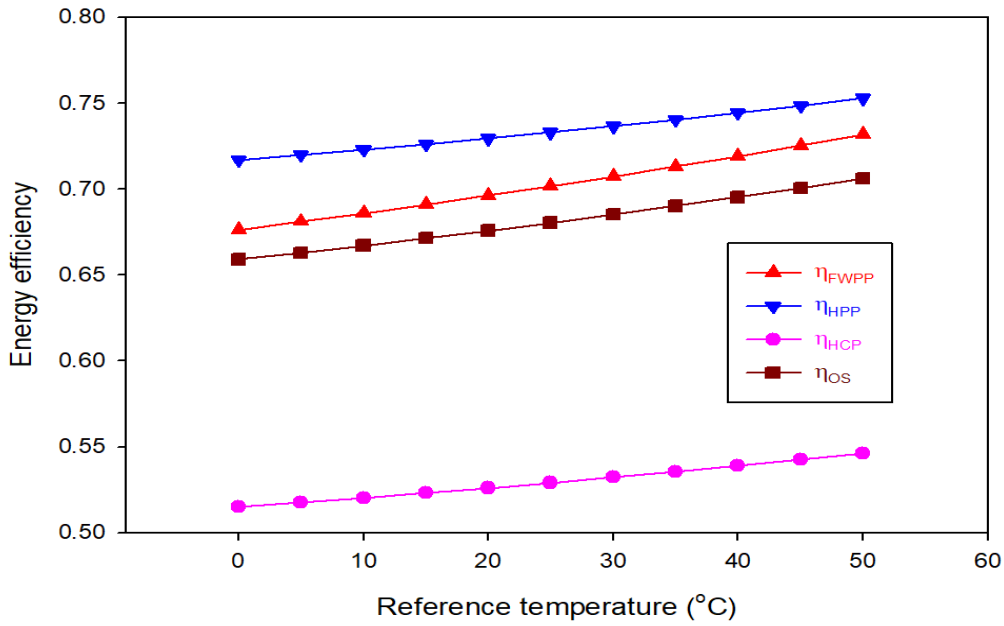
Figure 2. Effect of reference temperature on energy efficiency for overall system and its sub-plants

Figure. 3, shows the effect of reference temperature on the exergy efficiencies of the integrated plant and its sub-plants. The effect of changing the reference temperature between 0°C and 50°C on the exergy efficiency of the overall system (OS) ranged from 56.8% to 61.4%.
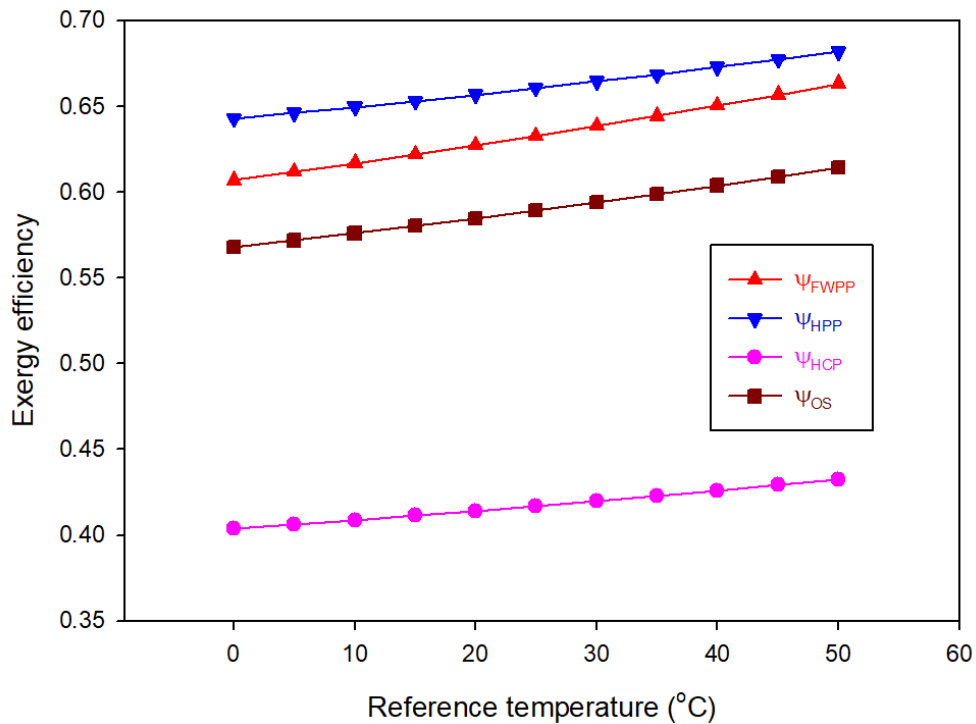
Figure 3. Effect of reference temperature on exergy efficiency for overall system and its sub-plants

Figure 4 shows the effect of reference temperature on power consumption and exergy destruction rate of integrated system. In terms of power consumption, it is seen that the net power consumption decreased from 6716 kW to 5565 kW by decreasing the reference temperature between 0 °C and 50 °C. When we look at the exergy destruction rate of the system, it is seen that the exergy discharge rate of the system decreases from 9471 kW to 7117 kW by decreasing the reference temperature between 0 °C and 50 °C.
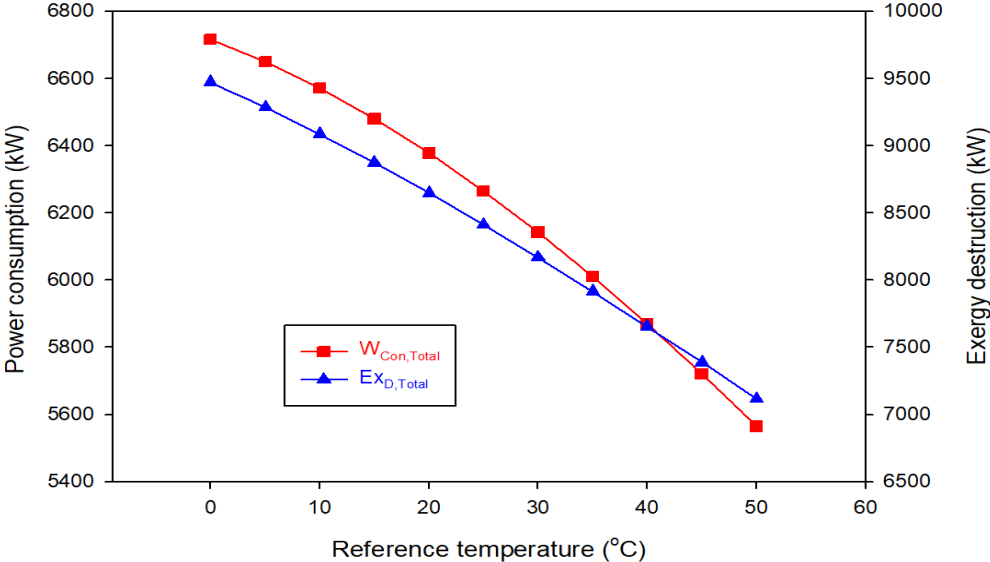
Figure 4. Effect of reference temperature on total power consumption and exergy destruction rate.

Figure 5 shows the effect of reference temperature on hydrogen production and freshwater production of integrated system. In terms of hydrogen production, it is seen that the hydrogen production increased from 0.2715 kg/s to 0.3276 kg/s by increasing the reference temperature between 0 °C and 50 °C. When we look at the fresh water production, it is seen that the fresh water production increased from 23.48 kg/s to 31.24 kg/s by increasing the reference temperature between0 °C and 50 °C.
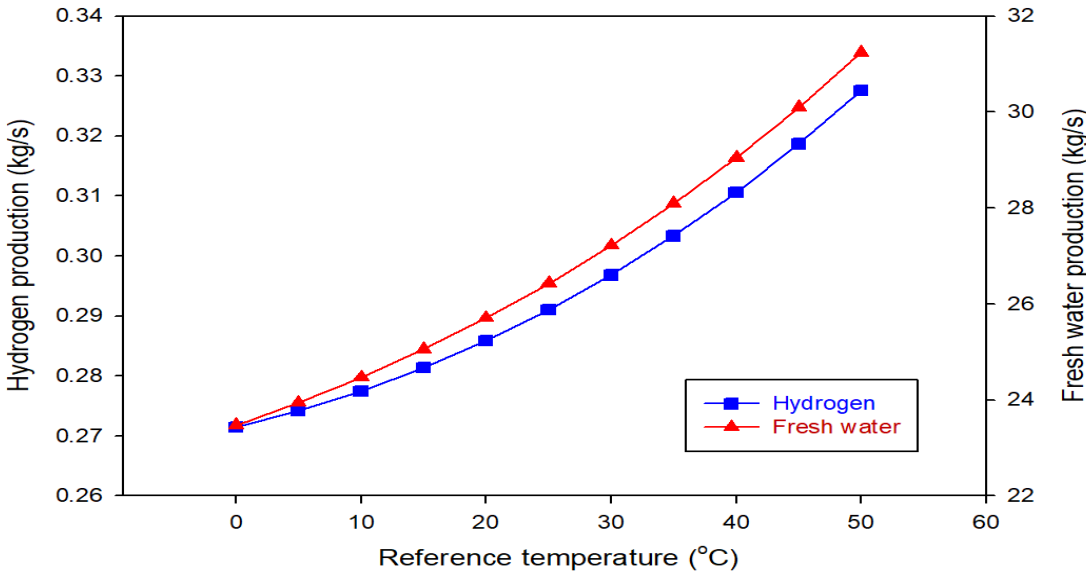
Figure. 5. Effect of reference temperature on hydrogen and fresh water production.

4. Conclusions

In this paper, energy and exergy analyzes of the Seawater based hydrogen production and storage plant integrated usage system. The system consisting of these four parts has been examined separately. The first part freshwater production plant (FWPP), the second part hydrogen production plant (HPP), the third part hydrogen compression plant (HCP), and the last part overall system (OS).

- In terms of energy efficiency, FWPP, HPP, HCP, and OS are 70.17%, 73.29%, 52.91%, and 68.04%, respectively.
- In terms of exergy efficiency, FWPP, HPP, HCP, and OS are 63.28%, 66.05%, 41.69%, and 58.92%, respectively.
- In terms of exergy destruction rate, FWPP, HPP, HCP, and OS are 1943 kW, 2391 kW, 4078 kW, and 8412 kW respectively.
- Hydrogen generation capacity is 0.291 kg/s and fresh water production capacity is 26.43 kg/s.

References

Delpisheh, M., Haghghi, M. A., Athari, H., & Mehrpooya, M. (2021). Desalinated water and hydrogen generation from seawater via a desalination unit and a low temperature electrolysis using a novel solar-based setup. International Journal of hydrogen energy, 46(10), 7211-7229.

Yilmaz, F., Ozturk, M., & Selbas, R. (2021). Development and performance examination of an integrated plant with desalination process for multigeneration purposes. Energy Conversion and Management, 240, 114275.

Safari, F., & Dincer, I. (2019). Development and analysis of a novel biomass-based integrated system for multigeneration with hydrogen production. International Journal of Hydrogen Energy, 44(7), 3511-3526.

Dincer, I., Rosen, MA., (2020) Exergy: Energy, Environment and Sustainable Development, Elsevier Science, Third Press, New York USA.

Klein, S. (2021). Engineering equation solver (EES), AcademicCommercial, V11.199. F- chart software. Madison, USA.

Solar Tower Supported Supercritical CO₂ Power Cycle and CU-CI Hydrogen Production

Mehmet Altinkaynak [1*] , Dogancan Celik[2], Murat Ozturk[3]

Abstract: Nowadays, because of the increasing population and the decrease in fossil fuels, governments have had to search for a clean and sustainable energy source. Solar energy is one of the most effective ways to solve problems. Power generation plants relied on renewable energy sources have considerable potential not only to overcome environmental issues but also to minimize global warming potential in the world. The proposed system consists of solar tower, sCO_2 cycle, tCO_2 cycle and thermo-chemical cycle. The principal object of this work is to design and analyze the study, solar driven integrated cycle for multigeneration with power and hydrogen production. The result of parametric analyzes of the study illustrated that at 25°C which are reference temperature the overall energy and exergy efficiencies 41.37% and 38.14% and net power, and the hydrogen production rates are 12483 kW, 0.1036 kgs^{-1}. For 800W/m^2 solar radiation, the overall energy and exergy efficiency of the system was found to be 41.82% and 39.07%. Moreover, net power, and hydrogen production rates are 13064 kW, 0.1093 kgs^{-1}.

Keywords: Solar energy; Solar tower; Cu-Cl cycle; Energy; Exergy; Hydrogen production.

1. Introduction

The energy demand, which emerged due to the rapid increase in population and economic developments, has become a major problem for the whole world. Although fossil fuels are still seen as primary energy sources today, the reserves of these resources are gradually decreasing. The use of solar energy is the best alternative way to avoid many threats (depletion of the ozone layer, climate and environmental changes, etc.) emerging from the use of fossil fuels. It is a clean, renewable, and sustainable type of energy that does not create pollution, which has an abundant source of solar energy. There are several studies about solar tower assisted sCO_2/tCO_2 power cycle in the literature.

AlZahrani and Dincer (2018) presented a novel system absorption refrigeration system supported reheat tCO_2 power cycle for CSP (concentration solar power) applications. Based on the proposed system, the energy and exergy efficiencies of the tCO_2 power cycle reached 34% and 82%, respectively. The authors have also computed the energy and exergy efficiencies of

[1] Isparta University of Applied Sciences, Faculty of Technology, Faculty, Department of Mechanical Engineering, Isparta, Turkey.
[2] Isparta University of Applied Sciences, Faculty of Technology, Faculty, Department of Energy System Engineering, Isparta, Turkey.
[3]Isparta University of Applied Sciences, Faculty of Technology, Faculty, Department of Mechatronic Engineering, Isparta, Turkey.
* Corresponding author: mehmetaltinkaynak@isparta.edu.tr

the integrated CSP system (solar to electricity) and were to be approximately 20% and 55%, respectively. Moreover, they stated that the integrated system is promising for CSP applications. Zhang et al (2022) proposed a novel cogeneration system. Their system is composed of sCO_2 (recompression Brayton cycle with intercooling and heating), steam Rankine and absorption cooling system. They calculated the energy and exergy efficiencies of the proposed system as 0.4304, 0.0915, 0.0234 and 0.4464, 0.0174, 0.0024, respectively, in terms of electricity, heating, and cooling capacity. Al-Sulaiman and Atif (2015) compared five different sCO_2 cycles (simple, regenerative, recompression, pre-compression, and split expansion) layouts in terms of their thermodynamic performance for the solar tower. They picked three days chosen 16th of March, the 11th of June, and the 10th of December to compare the net power and thermal efficiencies of sCO_2 cycles. They observed that the highest thermal and highest net power was the recompression sCO_2 cycle among all cycles, at June noontime. maximum thermal efficiency of this cycle alone was 52%, while the thermal efficiency of integrated system was found to be 40%. Corumlu and Ozturk (2021) suggested a novel multigeneration system assisted solar energy. Their parametric results indicate energy and exergy performances of suggested system were 22.21% and 14.02% respectively. Authors also found that hydrogen production rate was 0.002514 kg/s. Khan and Mishra (2021) investigated thermodynamical assessment of solar tower integrated with sCO_2 (pre-compression) and ORC cycle to recover energy from waste heat. They selected working fluid isopentane, R245fa, R236fa, isobutane and R227ea for ORC cycle. In their analysis, R227ea and isobutane working fluids were observed as the best and worst fluids. They calculated that net power and thermal efficiency of proposed system as 278.5 kW and 51.83%. Moreover, outcomes of study showed thermal efficiency and net power output of suggested system was increased 4.52% and 4.51%, utilizing ORC cycle. Khan and Mishra (2022) proposed a cascade sCO_2-ORC power cycle for the solar tower system. As a result of their analysis, they found the maximum exergy efficiency and thermal efficiency of the proposed system as 51.93% and 48.3%, respectively. They also observed that the best fluid for the ORC cycle is R1224yd(Z). Binotti et al. (2017) compared thermodynamical performance of three different sCO2 cycle (recompression, partial cooling, recompression with main compression intercooling) in terms of solar-to-electric efficiency in solar tower. The authors found that the best performing cycle among the three cycles was sCO_2 (recompression with main compression intercooling), and calculated the efficiency as 24.5%.

The principal object of this work is to design and analyze the study, the solar driven integrated cycle for multigeneration with power and hydrogen production.

2. Material and Method

2.1. System Description

In this work, solar energy is chosen as power supply of suggested multigeneration to beneficial outputs which are solar to power generation and hydrogen production. The proposed multigeneration system is demonstrated in Figure 1. As could be seen in this Figure 1, the suggested system composes of four subsystems that are solar cycle (SC) supercritical CO_2 cycle (sCO_2), transcritical CO_2 (tCO_2) cycle and thermo-chemical cycle (TC) for hydrogen production unit. A solar tower collector was used because of its high operating temperature and high concentration. The thermal energy collected from the heliostat field is transferred to the central receiver. The thermal energy collected in the central receiver supplies whole energy requirement of the system. The fluid at high temperature from the solar receiver at point 3 enters the sCO_2 turbine and as a result of the expansion in the turbine, electricity is generated. The gas with decreasing pressure and temperature from sCO_2 turbine at point 4 enters HEX-I for use in

Cu-Cl and tCO$_2$ cycles. The fluid whose temperature and pressure are still usable is transferred from the HEX-I to the HEX-II. In this work, thermo-chemical Cu-Cl cycle with four stages is utilized with the four stage to produce clean hydrogen. The Cu-Cl thermo-chemical cycle is a hybrid process that come off both heat and electricity, and hydrogen is generated just by diverse reactions tCO$_2$ sub-plant consists of the HEX-II, pump, condenser, and turbine. The tCO$_2$ liquid in saturated liquid phase at point 6 is sent to the tCO$_2$ pump to be pressurized. The fluid coming out of the tCO$_2$ pump is transferred to the HEX-II to become superheated steam. As a result of the heat transfer in HEX-II at point 8 enters tCO$_2$ turbine then electric power is generated. The fluid whose pressure drops in the HEX-II is sent to the sCO$_2$ compressor to pressurize and transferred to the solar receiver to complete the cycle.
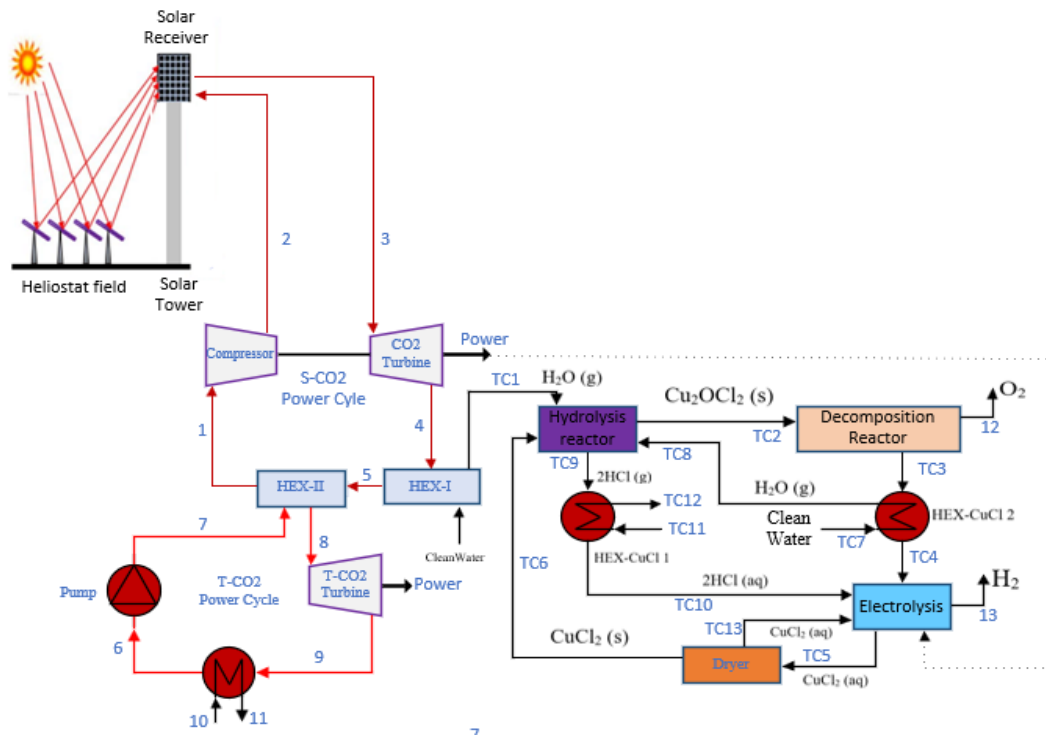
Figure 1. Schematic plan of the modeled integrated cycle

2.2. Thermodynamics Analysis

To analyze the thermodynamics of the presented integrated system, the temperatures, pressures, enthalpies, entropies, and exergies of all flows in the system are determined. For each part of the integrated plant, the exergy destruction rate is defined to determine the location of the irreversible plant losses. Engineering equation solver (EES) software was utilized to calculate the performance of integrated system.

System analysis and assumptions
- The integrated plant operates in the steady state working.
- Ambient temperature (T_0) and pressure (P_0) are chosen as 25 °C and 101.3 kPa.
- Pressure drops in the pipelines and parts are disregarded.
- Compressors, pumps, and turbines work at specified isentropic performances.
- Energetic and exergetic values for kinetic and potential energies are neglected.

In this part, the mass, energy, entropy, and exergy balance equations of the proposed system based on the first and second laws of thermodynamics are given below (Dincer and Rosen 2020).

Mass balance is defined as;

$$\sum \dot{m}_i = \sum \dot{m}_o \tag{1}$$

The subscript i and o represent inlet and outlet flow. Energy balance is written as;

$$\dot{Q}_i + \dot{W}_i + \sum \dot{m}_i h_i = \dot{Q}_o + \dot{W}_o + \sum \dot{m}_o h_o \tag{2}$$

$\dot{Q}$ and $\dot{W}$ indicate the heat transfer and work rate, respectively.

Entropy balance is described as;
$$\sum \dot{m}_i s_i + \sum \frac{\dot{Q}_k}{T_k} + \dot{S}_{gen} = \sum \dot{m}_o s_o \tag{3}$$
$\dot{S}_{gen}$ and s denote entropy generation and specific entropy, respectively.

Exergy balance is defined as;

$$\dot{Ex}_{Q,i} + \dot{W}_i + \sum \dot{m}_i ex_i = \dot{Ex}_{Q,o} + \dot{W}_o + \sum \dot{m}_o ex_o + \dot{Ex}_d \tag{4}$$

$\dot{Ex}_Q$ defines the exergy transfer rate of heat transfer throughout system boundaries.

$$\dot{Ex}_Q = \left(1 - \frac{T_0}{T}\right) \dot{Q} \tag{5}$$

Also, the exergy destruction rate can be expressed as;

$$\dot{Ex}_d = T_0 \dot{S}_{gen} \tag{6}$$

2.2.1. Cu-Cl Thermochemical Cycle

In this section of the study, the energy and exergetic equilibrium equations of the four-step Cu-Cl thermochemical process, which was presented in Table 1 for hydrogen production, and balance equations for multigeneration plant, are defined below for each component in Table 2.

Table 1. Chemical reactions of Cu-Cl cycle (Onder et al. 2020)

Stages	Reactions
Stage I (Electrolysis)	$2CuCl(aq)+2HCl(aq)\rightarrow H_2(g)+2CuCl_2(aq)$
Stage II (Dryer)	$CuCl_2(aq) \rightarrow CuCl_2(s)$
Stage III (Hydrolysis reactor)	$CuCl_2(s)+H_2O(g) \rightarrow Cu_2OCl_2(s)+2HCl(g)$
Stage IV (Decomposition reactor)	$Cu_2OCl_2(s) \rightarrow 0.5O_2(g)+2CuCl(l)$

Energy and exergy equations for hydrolysis reactor are defined below;

Hydrolsis reactor:

$$\dot{m}_{TC1}h_{TC1} + \dot{m}_{TC6}h_{TC6} + \dot{m}_{TC8}h_{TC8} = \dot{m}_{TC2}h_{TC2} + \dot{m}_{TC9}h_{TC9}$$

$$\dot{m}_{TC1}ex_{TC1} + \dot{m}_{TC6}ex_{TC6} + \dot{m}_{TC8}ex_{TC8} = \dot{m}_{TC2}ex_{TC2} + \dot{m}_{TC9}ex_{TC9} + \dot{E}x_{D,Hr}$$

Energy and exergy equations for decomposition reactor can be expressed as;

Decomposition reactor:

$$\dot{m}_{TC2}h_{TC2} = \dot{m}_{TC3}h_{TC3} + \dot{m}_{12}h_{12}$$

$$\dot{m}_{TC2}ex_{TC2} = \dot{m}_{TC3}ex_{TC3} + \dot{m}_{12}ex_{12} + \dot{E}x_{D,DC}$$

Energy and exergy equations for HEX-CuCl 1 can be written as;

HEX-CuCl 1:

$$\dot{m}_{TC9}h_{TC9} + \dot{m}_{TC11}h_{TC11} = \dot{m}_{TC10}h_{TC10} + \dot{m}_{TC12}h_{TC12}$$

$$\dot{m}_{TC9}ex_{TC9} + \dot{m}_{TC11}ex_{TC11} = \dot{m}_{TC10}ex_{TC10} + \dot{m}_{TC12}ex_{TC12} + \dot{E}x_{D,HEX-CuCl1}$$

Energy and exergy equations for HEX-CuCl 2are described as below;

HEX-CuCl 2:

$$\dot{m}_{TC3}h_{TC3} + \dot{m}_{TC7}h_{TC7} = \dot{m}_{TC4}h_{TC4} + \dot{m}_{TC8}h_{TC8}$$

$$\dot{m}_{TC3}ex_{TC3} + \dot{m}_{TC7}ex_{TC7} = \dot{m}_{TC4}ex_{TC4} + \dot{m}_{TC8}ex_{TC8} + \dot{E}x_{D,HEX-CuCl2}$$

Energy and exergy equations for electrolysis are defined as below;

Electrolysis:

$$\dot{m}_{TC4}h_{TC4} + \dot{m}_{TC10}h_{TC10} + \dot{m}_{TC13}h_{TC13} + \dot{W}_{SCO2,tur} = \dot{m}_{TC5}h_{TC5} + \dot{m}_{13}h_{13}$$

$$\dot{m}_{TC4}ex_{TC4} + \dot{m}_{TC10}ex_{TC10} + \dot{m}_{TC13}ex_{TC13} + \dot{E}x^{D}_{S-CO2,tur} = \dot{m}_{TC5}ex_{TC5} + \dot{m}_{13}ex_{13} + \dot{E}x^{D}_{elec}$$

Energy and exergy equations for dryer can be expressed as below;

Dryer:

$$\dot{m}_{TC5}h_{TC5} = \dot{m}_{TC13}h_{TC13} + \dot{m}_{TC6}h_{TC6}$$

$$\dot{m}_{TC5}ex_{TC5} = \dot{m}_{TC13}ex_{TC13} + \dot{m}_{TC6}ex_{TC6} + \dot{E}x^{D}_{Dry}$$

Table 2. Balance equations for multigeneration plant

Component	Mass Balance	Energy Balance	Entropy Balance	Exergy Balance
Solar Tower	$\dot{m}_2 = \dot{m}_3$	$\dot{m}_2 h_2 + \dot{Q}_{solar} = \dot{m}_3 h_3$	$\dot{m}_2 s_2 + \dfrac{\dot{Q}_{solar}}{T_{solar}} + \dot{S}_{gen,solar} = \dot{m}_3 s_3$	$\dot{m}_2 ex_2 + \dot{E}x^Q_{solar} = \dot{m}_3 ex_3 + \dot{E}x_{D,solar}$
sCO2 Turbine	$\dot{m}_3 = \dot{m}_4$	$\dot{m}_3 h_3 = \dot{m}_4 h_4 + \dot{W}_{SCO2,Turb}$	$\dot{m}_3 s_3 + \dot{S}_{gen,SCO2,Turb} = \dot{m}_4 s_4$	$\dot{m}_3 ex_3 = \dot{m}_4 ex_4 + \dot{W}_{SCO2,Turb} + \dot{E}x_{D,SCO2,Turb}$
sCO2 Compressor	$\dot{m}_1 = \dot{m}_2$	$\dot{m}_1 h_1 + \dot{W}_{SCO2,Cmp} = \dot{m}_2 h_2$	$\dot{m}_1 s_1 + \dot{S}_{gen,cmp} = \dot{m}_2 s_2$	$\dot{m}_1 ex_1 + \dot{W}_{SCO2,Cmp} = \dot{m}_2 ex_2 + + \dot{E}x_{D,SCO2,Cmp}$
tCO2 Turbine	$\dot{m}_8 = \dot{m}_9$	$\dot{m}_8 h_8 = \dot{m}_9 h_9 + \dot{W}_{TCO2,Turb}$	$\dot{m}_8 s_8 + \dot{S}_{gen,Turb} = \dot{m}_9 s_9$	$\dot{m}_8 ex_8 = \dot{m}_9 ex_9 + \dot{W}_{TCO2,Turb} + \dot{E}x_{D,TCO2,Turb}$
Condenser	$\dot{m}_9 = \dot{m}_6$ $\dot{m}_{10} = \dot{m}_{11}$	$\dot{m}_9 h_9 + \dot{m}_{10} h_{10} = \dot{m}_6 h_6 + \dot{m}_{11} h_{11}$	$\dot{m}_9 s_9 + \dot{m}_{10} s_{10} + \dot{S}_{gen,con} = \dot{m}_6 s_6 + \dot{m}_{11} s_{11}$	$\dot{m}_9 ex_9 + \dot{m}_{10} ex_{10} = \dot{m}_6 ex_6 + \dot{m}_{11} ex_{11} + \dot{E}x_{D,cond}$
tCO2 Pump	$\dot{m}_6 = \dot{m}_7$	$\dot{m}_6 h_6 + \dot{W}_{TCO2,Pump} = \dot{m}_7 h_7$	$\dot{m}_6 s_6 + \dot{S}_{gen,Pump} = \dot{m}_7 s_7$	$\dot{m}_6 ex_6 + \dot{W}_{TCO2,Pump} = \dot{m}_7 ex_7 + + \dot{E}x_{D,TCO2,Pump}$
HEX I	$\dot{m}_4 = \dot{m}_5$ $\dot{m}_{cl} = \dot{m}_{TCL1}$	$\dot{m}_4 h_4 + \dot{m}_{cl} h_{cl} = \dot{m}_5 h_5 + \dot{m}_{TCL1} h_{TCL1}$	$\dot{m}_4 s_4 + \dot{m}_{cl} s_{cl} + \dot{S}_{gen,HEX-I} = \dot{m}_5 s_5 + \dot{m}_{TCL1} s_{TCL1}$	$\dot{m}_4 ex_4 + \dot{m}_{cl} ex_{cl} = \dot{m}_5 ex_5 + \dot{m}_{TCL1} ex_{TCL1} + \dot{E}x_{D,HEX-I}$
HEX II	$\dot{m}_5 = \dot{m}_1$ $\dot{m}_7 = \dot{m}_8$	$\dot{m}_5 h_5 + \dot{m}_7 h_7 = \dot{m}_1 h_1 + \dot{m}_8 h_8$	$\dot{m}_5 s_5 + \dot{m}_7 s_7 + \dot{S}_{gen,HEX-II} = \dot{m}_1 s_1 + \dot{m}_8 s_8$	$\dot{m}_5 ex_5 + \dot{m}_7 ex_7 = \dot{m}_1 ex_1 + \dot{m}_8 ex_8 + \dot{E}x_{D,HEX-II}$

3. Results

This work suggested a novel solar energy-driven integrated system and performed detailed thermodynamic assessment and analyses of this integrated system. EES software package (Klein 2021) was used to acquire the requisite thermodynamic properties for each stream in the system. As seen in Figure 2, it was observed that the energy efficiency of the proposed subsystems and the overall system increased because of the reference temperature increasing from 0°C to 50°C. When the rates of increase in energy efficiency in subsystems were compared, it was seen that solar cycle had the highest increase and sCO₂ had the lowest increase. In this increased range, the energy efficiency of the overall system increased from approximately 39.98% to 42.40%.
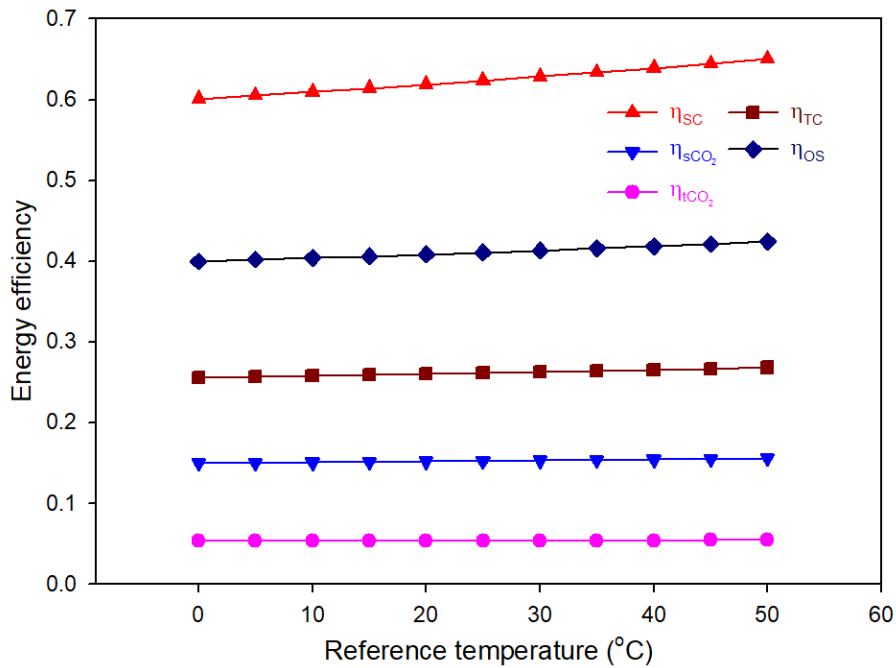

Figure. 2. Effect of reference temperature on energy efficiency

The effect of the change in reference temperature on the exergy efficiency of the system is given in figure 3. It was observed that the highest exergy efficiency performance was in the solar cycle and the lowest exergy performance was the thermo-chemical cycle. This reference temperature change between 0-50°C increases the exergy efficiency of the overall system from 36.94% to 39.57%.
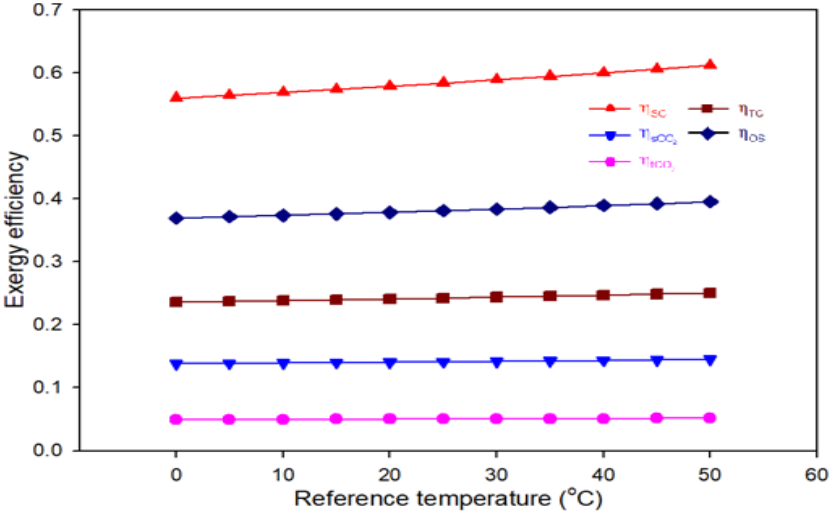

Figure. 3. Effect of reference temperature on exergy efficiency

Fig. 4 demonstrates the beneficial productions of suggested multigeneration plant that are power generation and hydrogen production Figure 4 shows that as the reference temperature increases, both the power generation and hydrogen generation rate increase. At 0°C of reference temperature, the overall power production is 12115kW and hydrogen production rate is 0.0986 kg/s. When the reference temperature attains 50°C the power production goes up to 13514 kW and the hydrogen generation rate rises to 0.1144 kg/s.
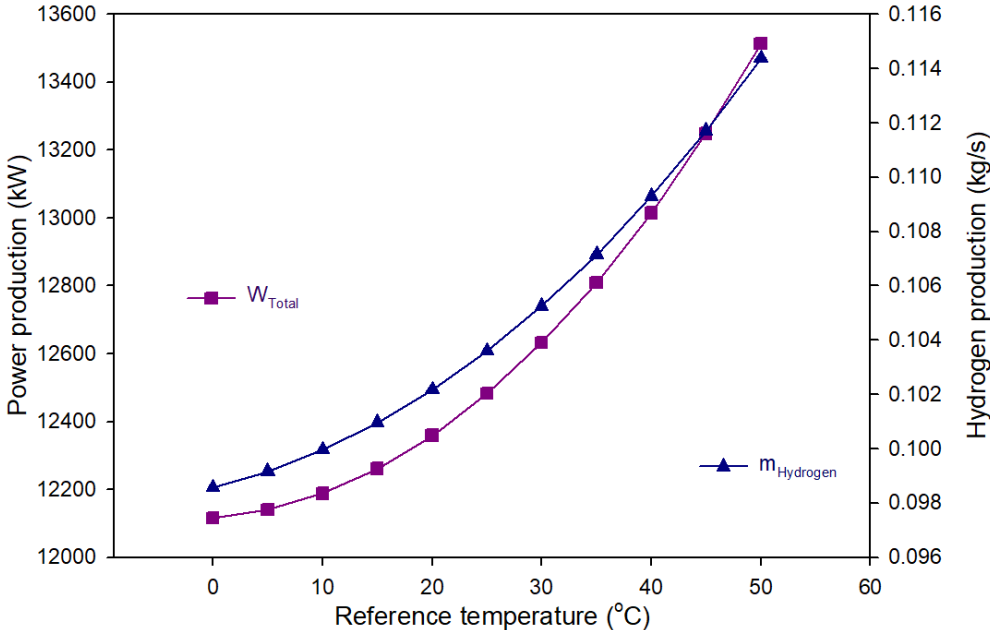
Figure. 4. Effect of reference temperature on power and hydrogen production

Figure 5 indicates the effect of variations in solar radiation on the energy efficiency of the system. As seen in Figure 5, the energy efficiency increase rate of sCO₂ and tCO₂ systems is lower than other systems. Although the lowest exergy performance was the thermo-chemical cycle highest energy efficiency performance was in the solar cycle. Moreover, the overall energy efficiency of the system increased from 39.15% to 43.47%
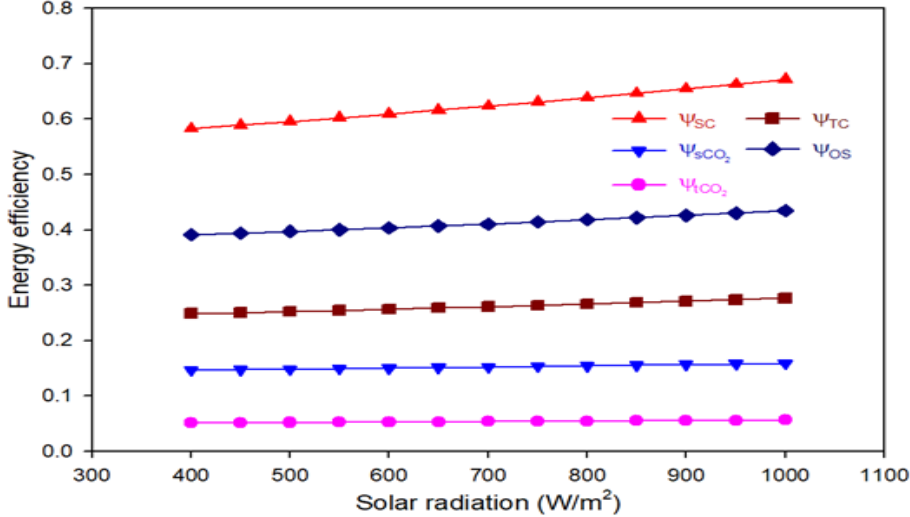

Figure. 5. Effect of solar radiation flux on energy efficiency

An increased curve similar to figure 5 is seen in Figure 6. The effect on the exergy efficiency of the system with the increase of solar radiation from 400W/m² to 1000W/m² is shown in figure 6. While this change did not seem to have much effect on exergy efficiency in sCO₂ and tCO₂ cycles, it was clearly seen that there was an increase in TC and SC cycles. Furthermore, the exergy efficiency of the solar cycle increased from 0.5365 to 0.6407, and the exergetic effectiveness of the overall system rose from 35.63% to 41.09%.
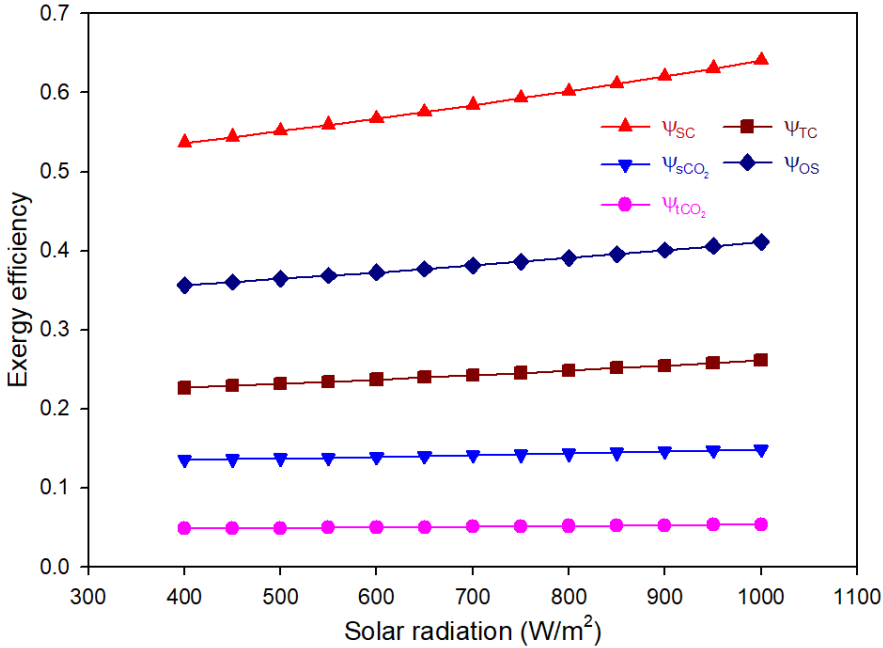
Figure. 6. Effect of solar radiation flux on exergy efficiency

Finally, Figure 7 indicates the production rate of the beneficial products of the cogeneration system depending on solar radiation. As a result of the change in solar radiation from 400 W/m^2 to 1000 W/m^2, the power produced in the system increased from 11417 kW to 14646 kW, and hydrogen production reached from 0.0976 kg/s to 0.1244 kg/s.
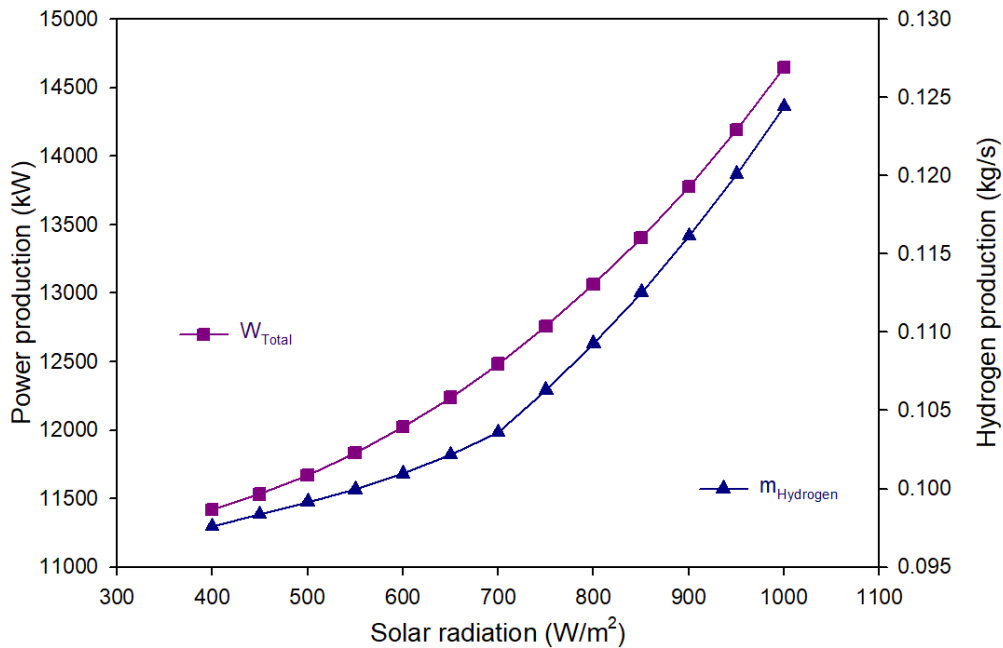

Figure. 7. Effect of solar radiation flux on power and hydrogen production

4. Discussion and Conclusions

The proposed system composes of the solar tower, sCO$_2$ cycle, tCO$_2$ cycle, and thermo-chemical cycle. The principal object of this work is to design and analyze the study, solar driven integrated cycle for multigeneration with power and hydrogen production. Moreover, some of the prominent outputs acquired from this offered work can be outlined as;

- The results of the thermodynamic analysis at the reference temperature are the overall energy and exergy efficiencies of 41.37% and %38.14. Also, the energy efficiency of the solar tower, sCO$_2$, tCO$_2$, and thermo-chemical cycle which are sub-cycles, is computed as 62.36%, 15.24%, 5.36%, 26.13% respectively. Moreover, the exergy efficiency of the solar tower, sCO$_2$, tCO$_2$ and thermo-chemical cycle were found to be 58.42%, 14.13%, 5.05% and 24.26% respectively. Further net power, and hydrogen production rates are 12483 kW, 0.1036 kgs^{-1}.

- Another parametric study for the modeled integrated system is solar radiation, which is the most important input of the system. For 800 W/m^2 solar radiation, the overall energy and exergy efficiency of the system was found to be 41.82% and 39.07%. Also, the energy efficiency of the solar tower, sCO$_2$, tCO$_2$ and the thermo-chemical cycle is calculated as 63.38%, 15.46%, 5.45%, and 26.61% respectively. Moreover, the exergy efficiency of solar tower, sCO$_2$, tCO$_2$ and thermo-chemical cycle is determined as 60.20%, 14.36%, 5.14%, 24.85% respectively. Further net power, and hydrogen production rates are 13064 kW, 0.1093 kgs^{-1}.

In addition, usable energy can be provided by transferring the waste heat from the heat exchangers and condensers used in this system to heating and cooling.

References

AlZahrani, AA., Dincer, I., (2018). Thermodynamic analysis of an integrated transcritical carbon dioxide power cycle for concentrated solar power systems. Solar Energy, 170, 557-567.

Al-Sulaiman, F. A., Atif, M., (2015). Performance comparison of different supercritical carbon dioxide Brayton cycles integrated with a solar power tower. Energy, 82, 61-71.

Binotti, M., Astolfi, M., Campanari, S., Manzolini, G., & Silva, P. (2017). Preliminary assessment of sCO2 cycles for power generation in CSP solar tower plants. Applied energy, 204, 1007-1017.

Corumlu, V., Ozturk, M., (2021). Thermodynamic assessment of a new solar power-based multigeneration energy plant with thermochemical cycle. International Journal of Exergy, 34(1), 76-102.

Dincer, I., Rosen, MA., (2020) Exergy: Energy, Environment and Sustainable Development, Elsevier Science, Third Press, New York USA.

Khan, Y., Mishra, RS., (2021). Performance evaluation of solar based combined pre-compression supercritical CO2 cycle and organic Rankine cycle. International Journal of Green Energy, 18(2), 172-186.

Khan, Y., Mishra, RS., (2022). Performance investigation of the solar power tower driven combined cascade supercritical CO2 cycle and organic Rankine cycle using HFO fluids. Australian Journal of Mechanical Engineering, 1-15.

Klein, S. (2021). Engineering equation solver (EES), AcademicCommercial, V11.199. F- chart software. Madison, USA.

Onder, G., Yilmaz, F., Ozturk, M., (2020). Thermodynamic performance analysis of a copper–chlorine thermochemical cycle and biomass based combined plant for multigeneration. International Journal of Energy Research, 44(9), 7548-7567.

Zhang, Z., Zhang, N., Yuan, Y., Jiao, W., Phelan, PE., (2022). Thermal and economic performance evaluation of a novel sCO2 recompression Brayton–steam Rankine–absorption cooling system based on solar energy. Journal of Thermal Analysis and Calorimetry, 1-16.

An Assessment and Thermodynamic Performance Modelling of Partial Cooling CO₂ Brayton Cycle Integrated with Solar Dish Collector

Serpil Çelik Toker[1*], Gamze Soytürk, Önder Kizilkan[2]

Abstract: The aim of the present study is to investigate the energy and exergy analysis of solar dish collector driven partial cooling sCO_2 (supercritical carbon-dioxide) Brayton cycle. EES software program is utilized to conduct the performance evaluation of the integrated system. Thermodynamic analysis results show that the energy and exergy efficiency of the solar energy driven Brayton cycle were calculated as 36.64% and 61.76%, respectively. On the other hand, parametric studies have been performed to examine the effect of solar radiation, ambient temperature, turbine inlet pressure and compressor inlet pressure on integrated cycle performance. The parametric results show that the net power produced in the Brayton cycle, the energy and exergy efficiencies of the cycle increase with the increase in solar radiation and ambient temperature. In addition, solar dish collector had the highest irreversibility rate with 87.7%, while the highest irreversibility rate was calculated in HTR with 47% for the remaining irreversibility rate.

Keywords: Partial cooling sCO_2 Brayton cycle, solar dish collector, supercritical CO_2, energy

1. Introduction

To meet the objective outlined in the Paris Agreement, green and low-carbon development has become as a critical topic for sustainable improving globally. According to the agreement, it is needed to keep the average global temperature increment down 2 °C (Unfcc, 2015). In this context, the use of renewable energy sources for low-carbon electricity generation is increasing rapidly recently. One of the most promising sources of renewable energy has been considered solar energy. Radiation from the sun is captured by solar collectors and converted into useful energy (Bellos et al. 2016). Concentrator solar collectors are more preferred as they provide grid flexibility and have long system lifetimes. It involves many various technologies such as concentrating solar collectors, solar power tower (Du et al. 2016), parabolic trough collector (Li et al. 2017), parabolic dish collector (Fuqiang et al. 2016) and linear Fresnel reflector (Qiu et al. 2017). The solar dish collector system has a higher conversion efficiency from solar radiation to heat, thanks to its higher concentration ratio (Reddy et al. 2016). Solar dish collectors can be used in many applications such as power generation, desalination (Alrobaian, 2022; Prado et al. 2016). In addition, these collectors can be integrated into gas turbines

[1] Isparta University of Applied Sciences, Technology Faculty, Department of Mechanical Engineering, Isparta, Turkey
[2] Isparta University of Applied Sciences, Technology Faculty, Department of Mechanical Engineering, Isparta, Turkey
* Corresponding author: serpilcelik@isparta.edu.tr

(Gavagnin et al. 2017), Rankine (Abid et al. 2016) and organic Rankine cycles (Loni et al. 2016), supercritical Brayton cycle (Khan et al. 2016). Considering the thermodynamic conversion of the solar energy source, the supercritical Brayton cycle, which uses carbon dioxide as the working fluid, has recently received a great deal of attention from industry and academics due to its advantages such as high performance, compact turbomachinery, less plant footprint and environmental development from greenhouse gas reduction (Dostal et al. 2002). It has also been confirmed by many scientists that the thermodynamic performance of the sCO_2 Brayton cycle is better than the conventional steam Rankine cycle at high operating temperatures (Angelino, 1968). Also, the flexible heat removal is another interesting feature of the sCO_2 Brayton cycle. CO_2 has almost ambient critical temperature (30.98 ˚C), which enables the incorporation of dry cooling technology, making it particularly suitable for utilization in arid areas with plentiful solar sources and water scarcity (Dostal et al. 2004). Normally, sCO_2 Brayton cycles are divided into single-flow and split-flow configurations. Single-flow layout consists of recuperation (Chen et al. 2019), intercooling (Uusitalo et al. 2019), reheating (Yang et al. 2020), inter-recuperation (Li et al. 2017), pre-compression (Luo and Huang, 2020), and split expansion (Al-Sulaiman and Atif, 2015) are employed. The recuperation configuration can effectively use the waste heat at the turbine outlet to advance thermal efficiency. Intercooling can decrease the inlet power of the compressor. Reheating can rise the expansion work of turbines. Split-flow sCO_2 cycles comprise recompression (Atif and Al-Sulaiman, 2017), pre-compression (Cao et al. 2022), preheat (Kim et al. 2021), partial cooling (Saeed and Kim, 2022), turbine split-flow I, turbine split-flow II, turbine split-flow III cycles. Combined sCO_2 Brayton cycles are formed by combining single-flow and split-flow Brayton cycles. Recently, many scientists have analyzed and compared sCO_2 Brayton cycles in different configurations in the literature for solar energy applications. Turchi et al. examined and compared the performances of different sCO_2 Brayton cycles (including simple regeneration cycle, recompression cycle, partial cooling cycle, and intercooling cycle) for solar tower application. Their results showed that the efficiency of partial cooling sCO_2 Brayton cycle with reheating and that of intercooling sCO_2 Brayton cycle with reheating could be 50%. Yang et al. were analyzed and compared the performance of four typical sCO_2 Brayton cycles including simple recuperator cycle, reheat cycle, recompression cycle and intercooling cycle under part load conditions. Their results show that the reheat cycle achieves higher efficiency than the simple recuperator cycle, and the recompression cycle and the intercooling cycle outperform the reheat cycle under part load conditions. Wang et al. compared the performance of six sCO_2 Brayton cycle schemes integrated into the solar tower system. In their results, they stated that the intercooling cycle generally reached the highest efficiency, followed by the partial cooling cycle and the recompression cycle. Chen et al. studied the performance of six 10 MW sCO_2 Brayton cycles, namely solar simple regeneration, recompression, precompression, intercooling, partial cooling, and split expansion. They stated that under the design conditions, the intercooling cycle operates with the highest efficiency, followed by the recompression cycle. Zhu et al. performed thermodynamic analyzes of different direct heated sCO_2 Brayton cycles (simple, pre-compression, compression, partial cooling, and intercooling) integrated into the solar tower. They also developed a mathematical model to compare Brayton cycles. In their results, they said that the turbine inlet temperature has an effect on the performance of the cycles. They noted that the intercooled sCO_2 cycle provides the highest overall efficiency, followed by recompression, partial cooling, and precompression cycles.

The literature review shows that there was limited research on the thermodynamic analysis of the partial cooling sCO_2 Brayton cycle with solar dish collector. The partial cooling sCO_2 Brayton cycle was usually integrated into the solar tower. In this study, thermodynamic analysis of the partial cooling sCO_2 Brayton cycle with solar dish collector was carried out. In addition,

the changes in the energy and exergy efficiencies of the cycle according to various parametric values such as solar radiation, ambient temperature, compressor inlet pressure and turbine inlet pressure were investigated.

2. System Description

Figure 1 shows the partial cooling sCO_2 Brayton cycle with solar dish collector. Integrated system consists of gas cooler, compressor, turbine, solar dish collector, low temperature recuperator (LTR), high temperature recuperator (HTR) and heat exchanger (HEX). Solar radiation is the main power supply for the system, and solar radiation is collected by using the solar dish. Therminol VPI salt solution, the heat transfer fluid used in the solar collector, absorbs the solar energy and transfers its heat to the CO_2 fluid used in the HEX of the Brayton cycle.
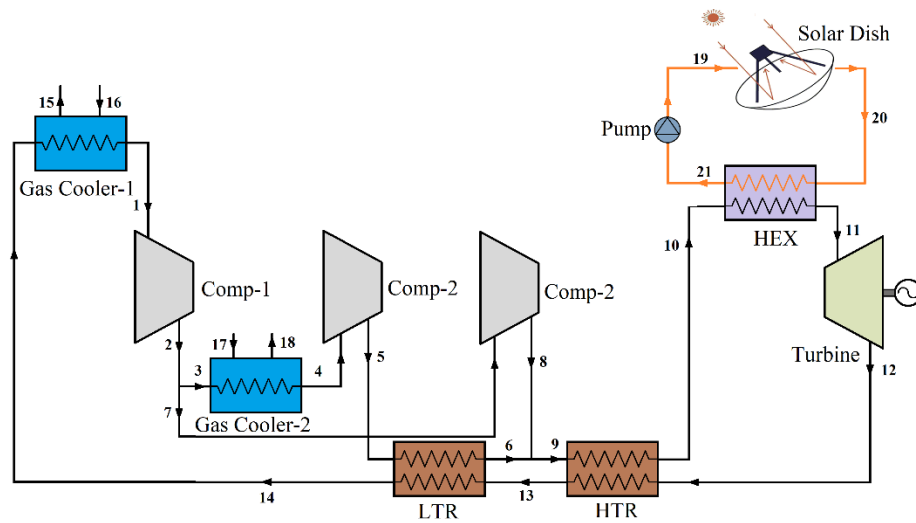
Figure 1. Partial cooling sCO_2 Brayton cycle with solar dish collector

3. Methodology

Energy and exergy analyses are performed using the EES (Engineering Equation Solver) program for the performance evaluation of the system. In this paper, the thermodynamic analysis is made under the following assumptions:
- The steady-state and steady-flow conditions are chosen for all system elements.
- The energetic and exergetic changes for kinetic and potential energies are neglected.
- The heat losses from pump, turbine and compressors are neglected.
- The pressure drops through the pipelines and heat exchangers are neglected.

The design considerations of the solar dish collector given here are mainly based on the reference (Ngo, 2013). The useful collected solar energy is defined as below:

$$\dot{Q}_u = F_R[S\,A_a - A_r U_L(T_{in} - T_a)] \tag{1}$$

here F_R is collector heat removal factor, S is the solar radiation, A_a is the aperture of the collector, A_r is the receiver area, U_L is the overall heat loss coefficient of solar collector between ambient and absorber tube, Tin is the inlet temperature of heat transfer fluid and T_a is the atmospheric temperature. F_R is determined from the following equation:

$$F_R = \frac{\dot{m}c_p}{A_r U_L}\left[1 - \exp\left(-\frac{U_L F' A_r}{\dot{m}c_p}\right)\right] \tag{2}$$

here c_p is the specific heat, $\dot{m}$ is the mass flow rate of liquid flowing in the absorber tube and F' is collector efficiency factor which is defined as below:

$$F' = \frac{U_0}{U_L} \tag{3}$$

here U_0 is the overall heat loss coefficient between surrounding and fluid flowing through the absorber tube. Further, the useful heat gain can also be calculated from another formula which is given by:

$$\dot{Q}_u = \dot{m}c_p(T_{out} - T_{in}) \tag{4}$$

here T_{out} is the outlet temperature of heat transfer fluid.

For the performance assessment of the solar-driven system the first and second laws of thermodynamics and the principles of conservation of mass are applied to each system element. The mass and energy balance equations for steady-state and steady-flow processes are written as (Cengel and Boles, 2015):

$$\sum \dot{m}_{in} = \sum \dot{m}_{out} \tag{5}$$

Here, $\dot{m}$ is the mass flow rate, subscripts "in" and "out" are the input and output states. Energy balance equality in a general method is written as (Bejan and Moran, 1996):

$$\sum \dot{m}_{in}\left(h + \frac{v^2}{2} + gz\right)_{in} + \sum \dot{Q}_{in} + \sum \dot{W}_{in} = \sum \dot{m}_{out}\left(h + \frac{v^2}{2} + gz\right)_{out} + \sum \dot{Q}_{out} + \sum \dot{W}_{out} \tag{6}$$

Here, $\dot{Q}$ is the heat energy transfer rate, $\dot{W}$ is the power transfer rate, h is the specific enthalpy, v is the velocity, z is the elevation, and g is the gravitational acceleration. Entropy balance equality is given as:

$$\sum \dot{m}_{in}s_{in} + \sum \frac{\dot{Q}}{T} + \dot{S}_{gen} = \sum \dot{m}_{out}s_{out} \tag{7}$$

Here, s is the specific entropy, and $\dot{S}_{gen}$ stands for entropy generation rate. An exergy balance equality of any system can be described as (Dincer and Rosen, 2013):

$$\sum \dot{m}_{in}\dot{ex}_{flow} + \sum \dot{Ex}^Q_{in} + \sum \dot{Ex}^W_{in} = \sum \dot{m}_{out}\dot{ex}_{flow} + \sum \dot{Ex}^Q_{out} + \sum \dot{Ex}^W_{out} + \dot{Ex}_{dest} \tag{8}$$

Where $\dot{ex}_{flow}$ is the flow exergy, $\dot{Ex}^Q_{in}$ is the exergy associated with heat flow across the control volume of the process, $\dot{Ex}^W_{in}$ is the exergy associated with work and $\dot{Ex}_{dest}$ is the exergy destruction. In the above equation, each term is defined as follows:

$$\dot{ex}_{flow} = (h - h_0) - T_0(s - s_0) \tag{9}$$

$$\dot{Ex}^Q = \dot{Q}\left(\frac{T - T_0}{T}\right) \tag{10}$$

$$\dot{Ex}^W = \dot{W} \tag{11}$$

$$\dot{Ex}_{dest} = T_0 \dot{S}_{gen} \tag{12}$$

The energy and exergy efficiency equations for the partial cooling sCO$_2$ Brayton cycle can be written as follows:

$$\eta_{en} = \frac{\dot{W}_{net}}{\dot{Q}_{in}} \tag{13}$$

$$\eta_{ex} = \frac{\dot{W}_{net}}{\dot{Ex}_{\dot{Q}_{in}}} \tag{14}$$

4. Results

In this study, the thermodynamic performance of the solar energy driven sCO$_2$ Brayton cycle is investigated. At the same time, parametric studies were carried out to examine the effects of solar radiation, ambient temperature, turbine inlet pressure and compressor inlet pressure on cycle performance. Therminol VPI is used as the heat transfer fluid in the solar collector system, and CO$_2$ natural working fluid is used in the Brayton cycle. Thermophysical properties such as temperature, pressure, enthalpy, and entropy of each point in the cycle are given in Table 1.

Table 1. Thermodynamic property data of partial cooling sCO$_2$ Brayton cycle with solar dish collector

State	T [°C]	P [kPa]	ṁ [kg/s]	h [kJ/kg]	s [kJ/kgK]	e [kJ/kg]	Ėx [kW]
1	32.00	8000	1.0	-210.4	-1.426	215.2	215.2
2	46.33	14142	1.0	-200.3	-1.423	224.2	224.2
3	46.33	14142	0.6	-200.3	-1.423	224.2	134.5
4	32.00	14142	0.6	-240.3	-1.551	222.4	133.4
5	43.95	25000	0.6	-225.9	-1.546	235.3	141.2
6	113.2	25000	0.6	-74.09	-1.113	258.1	154.8
7	46.33	14142	0.4	-200.3	-1.423	224.2	89.69
8	63.56	25000	0.4	-183.9	-1.418	239.0	95.60
9	92.95	25000	1.0	-118.0	-1.230	249.0	249.0
10	230.7	25000	1.0	119.7	-0.671	320.0	320.0
11	460.0	25000	1.0	412.5	-0.191	469.6	469.6
12	329.9	8000	1.0	280.0	-0.174	332.1	332.1
13	122.7	8000	1.0	42.24	-0.658	238.7	238.7
14	59.90	8000	1.0	-48.86	-0.910	222.8	222.8
15	24.89	101.3	3.86	104.4	0.366	0.00009	0.0004
16	34.89	101.3	3.86	146.2	0.504	0.6702	2.59
17	24.89	101.3	0.57	104.4	0.364	0.00009	0.0001
18	34.89	101.3	0.57	146.2	0.504	0.670	0.385
19	76.85	200	0.6	105.1	0.331	6.823	4.094
20	480.0	200	0.6	1011	2.002	414.5	248.7
21	286.2	200	0.6	523.1	1.256	148.9	89.35

Figure 2 shows the variation of cycle energy efficiency with solar radiation, while Figure 3 shows the variation of work produced from a partial cooling sCO$_2$ Brayton cycle with solar radiation. As the solar radiation value increased from 500 W/m^2 to 950 W/m^2, the energy efficiency of the cycle increased by 40%. Likewise, the amount of net power produced from the cycle increases with the increase in solar radiation. The reason for the increase in both the cycle energy efficiency and the net power produced from the cycle is that the temperature of

the fluid leaving the solar collector increases with the increase of solar radiation, and therefore the fluid temperature entering the turbine increases.
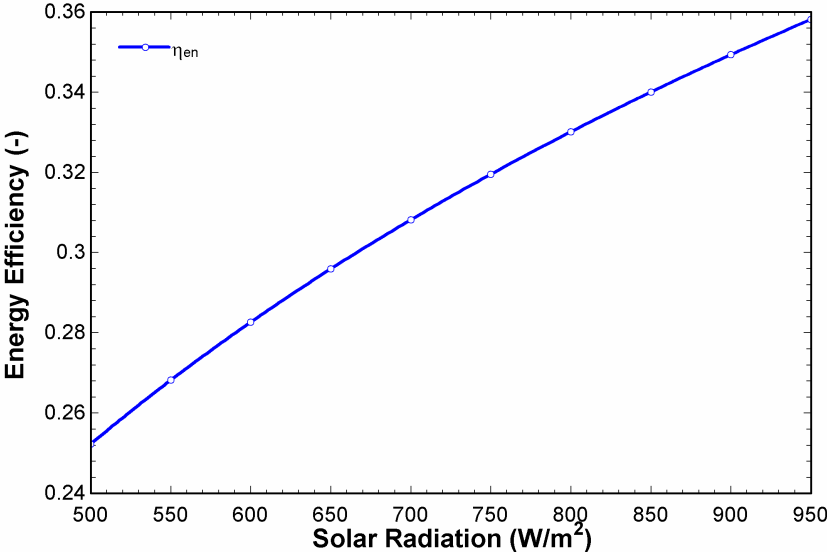

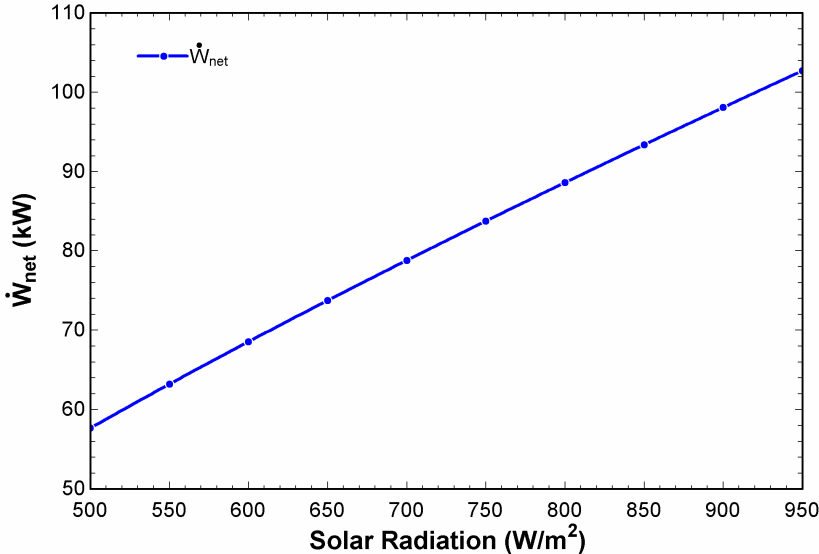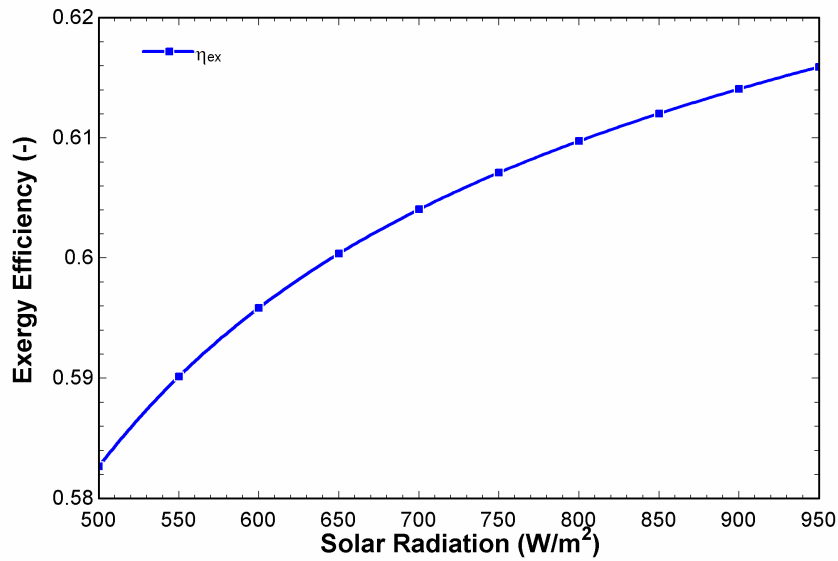Figure 2. Impact of solar irradiation on energy efficiency of the partial cooling sCO_2 Brayton cycle

Figure 3. Impact of solar irradiation on net power generation

In Figure 4, exergy efficiency variation of partial cooling sCO_2 Brayton cycle is given as a function of solar radiation. From the figure 4, it can be seen that exergy efficiency is increasing with the solar irradiation. The behavior of exergy irreversibility with increasing solar intensity is displayed in Figure 5. As can be seen from the graph, as the solar radiation rises, the exergy destruction of the partial cooling sCO_2 Brayton cycle also increases. This high destruction rate is mainly due to the solar dish collector. The heat losses from the collector to the surrounding air are the major cause of this.

Figure 4. Impact of solar irradiation on exergy efficiency of the partial cooling sCO_2 Brayton cycle
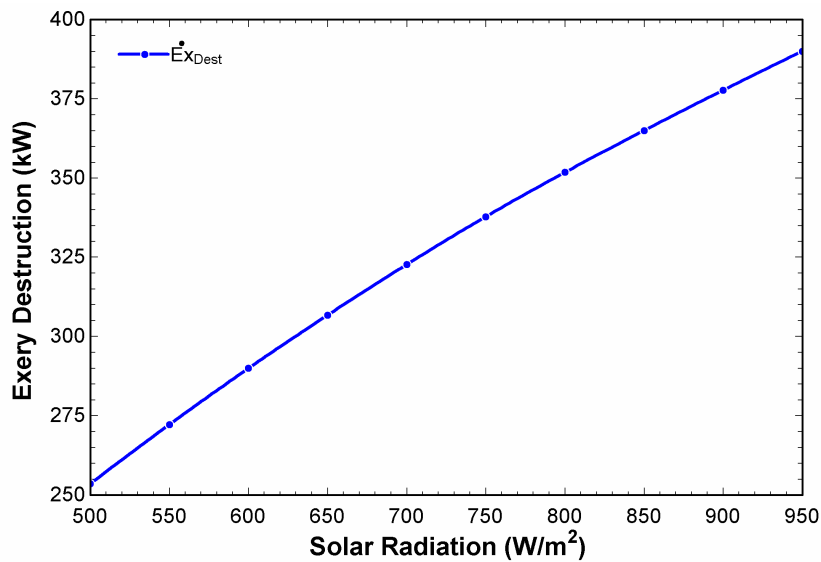
Figure 5. Impact of solar irradiation on exergy destruction rate

Another parameter that affects the cycle is the ambient temperature. Figures 6 and 7 demonstrate the effect of ambient temperature on cycle energy efficiency and net power generation. As the ambient temperature rising, the energy efficiency of the cycle rises. Similarly, with the increases in ambient temperature, the amount of net power produced from the cycle also rises. The net power generated from the cycle is increased from 106.1 kW to 108.3 kW as the ambient temperature increased from 0 ˚C to 45 ˚C.
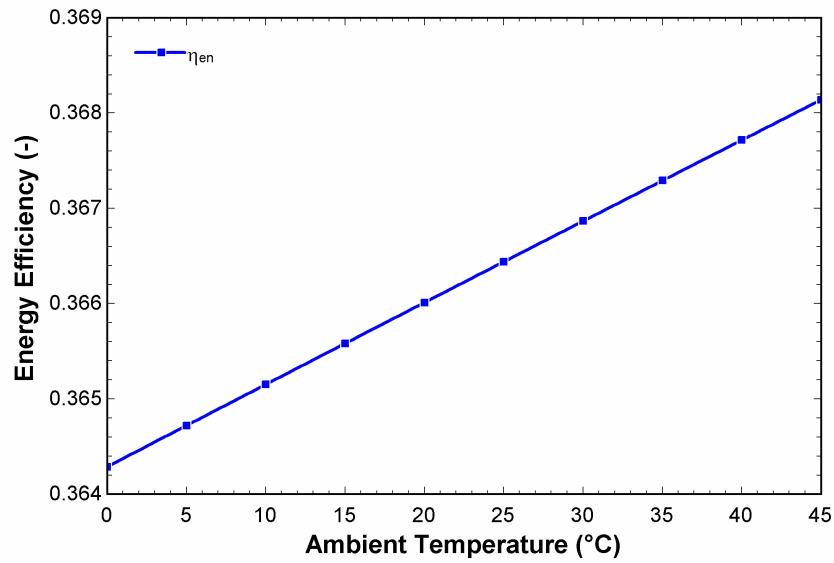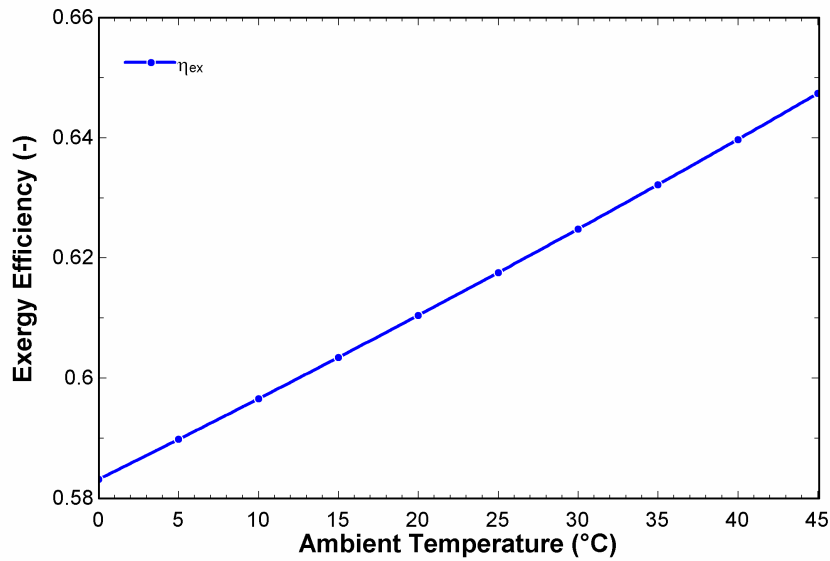
Figure 6. Impact of ambient temperature on energy efficiency of the partial cooling sCO$_2$ Brayton cycle
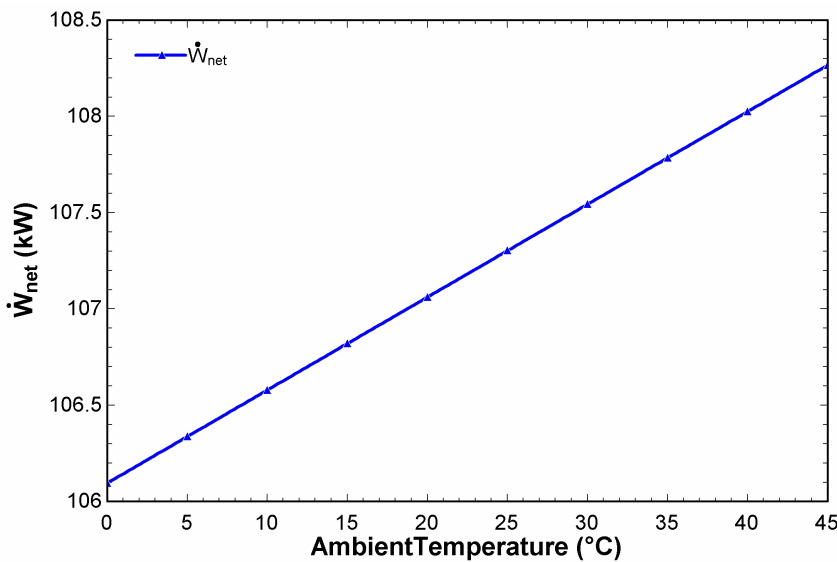
Figure 7. Impact of ambient temperature on net power generation

The effect of ambient temperature on cycle exergy efficiency and exergy destruction is depicted in Figures 8 and 9, respectively. As can be seen from Figures 8 and 9, the exergy efficiency and exergy destruction of the cycle increase linearly with the increase in ambient temperature. As the ambient temperature rises from 0 ˚C to 45 ˚C, the exergy efficiency of the cycle increases by 11 % and the cycle exergy destruction by 4.33 %.

Figure 8. Impact of ambient temperature on exergy efficiency of the partial cooling sCO$_2$ Brayton cycle
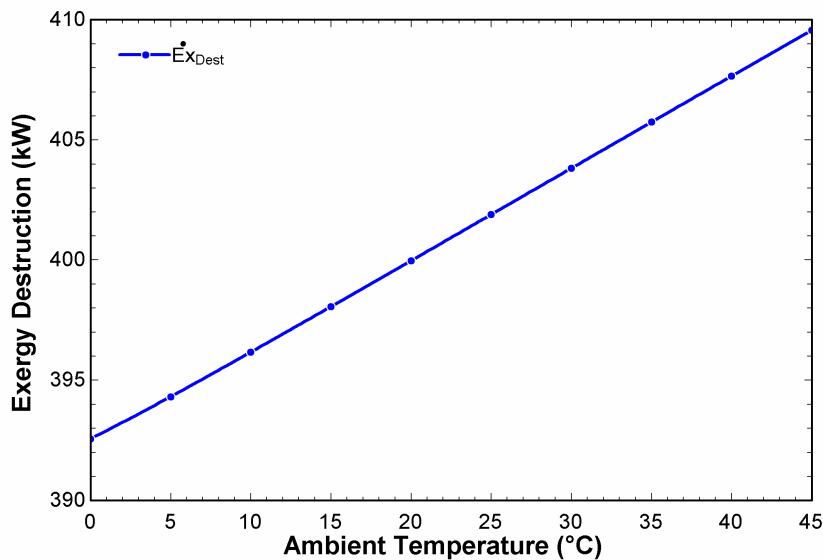
Figure 9. Impact of ambient temperature on exergy destruction rate

For the investigation of the effects of turbine and compressor inlet pressure on system performance, parametrical analyses were conducted. Figure 10 shows the effect of the turbine inlet pressure on the energy and exergy efficiencies of the partial cooling sCO$_2$ Brayton cycle. Figure 11 displays the impact of the compressor input pressure on the energy and exergy efficiencies of the cycle. As the compressor inlet pressure increased by 10000 kPa, both the energy and exergy efficiency of the cycle increased, while the energy and exergy efficiency of the cycle decreased when the compressor inlet pressure was above 10000 kPa. As seen in the Figure 11, the energy and exergy efficiencies of the partial cooling sCO$_2$ Brayton cycle increase with the increase of turbine inlet pressure. As the turbine inlet pressure increased from 15000 kPa to 25000 kPa, the energy and exergy efficiencies of the cycle increased by 23% and 19%, respectively.
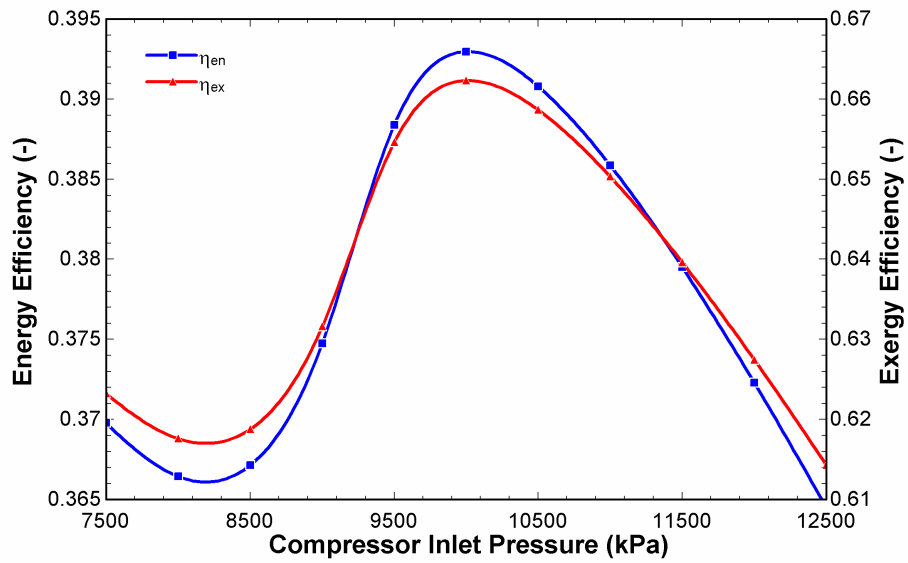
Figure 10. Impact of compressor inlet pressure on energy and exergy efficiencies of the partial cooling sCO2 Brayton cycle
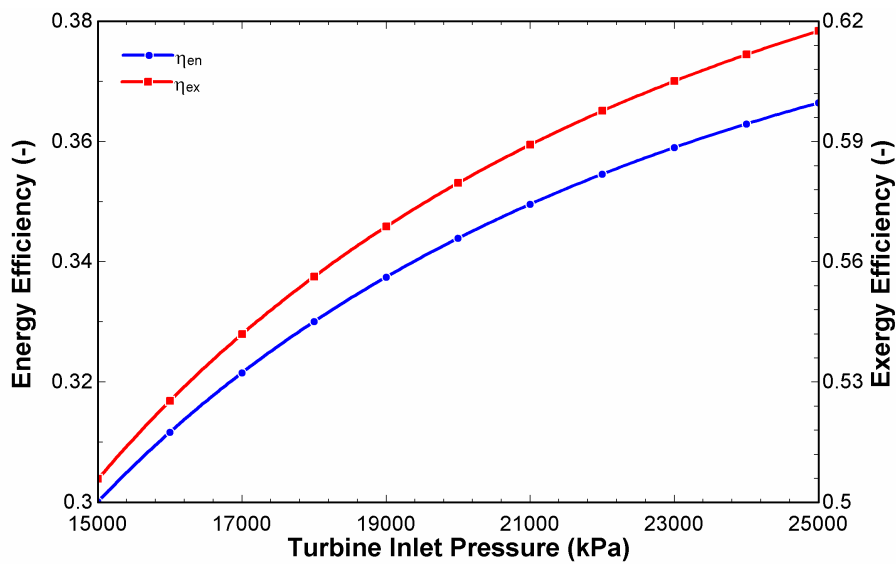

Figure 11. Impact of turbine inlet pressure on energy and exergy efficiencies of the partial cooling sCO2 Brayton cycle

Figure 12 demonstrated the exergy destruction rates of each system component of investigated Brayton system. As seen from the figure, the highest exergy destruction rate was established in the solar dish collector, with almost 87.7 % of the total irreversibility. In the absence of solar dish collector, the highest exergy destruction was calculated in the HTR with 47%.
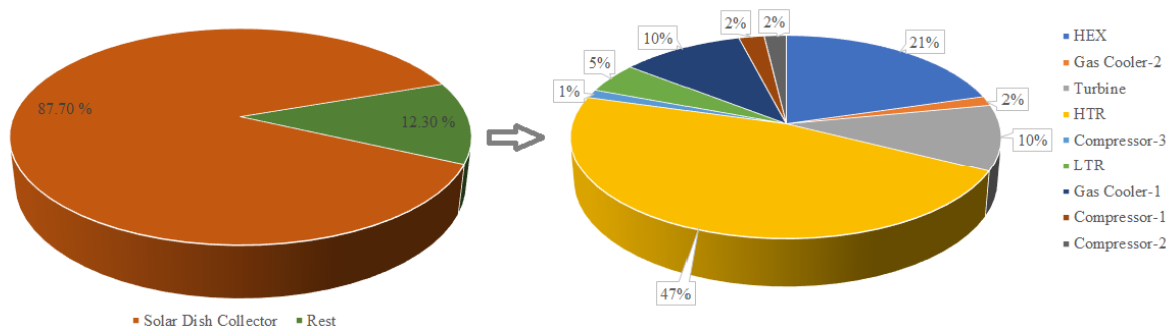
Figure 12. Exergy destruction rate of the whole components of the partial cooling sCO$_2$ Brayton cycle

5. Discussion and Conclusions

In this study, as an alternative, clean and sustainable solution, the partially cooled sCO$_2$ Brayton cycle based on solar energy was designed and the thermodynamic analysis of the cycle was investigated. In addition, various parametric studies have been carried out to determine the effects of solar radiation, ambient temperature, turbine, and compressor inlet pressure on system performance. According to the results of the study, the important findings are summarized as follows:

- The energy and exergy efficiencies of the cycle under operating parameters were calculated as 36.64% and 61.76%, respectively.
- The increase in solar intensity from 500 W/m^2 to 950 W/m^2 increased the electricity production, energy efficiency and exergy efficiency of the cycle by 78%, 40% and 5%, respectively.
- With the rise of solar radiation, the exergy destruction of the cycle increased from 253.6 kW to 390 kW.
- The energy and exergy efficiency of the cycle increased linearly with the increase in ambient temperature.
- Outputs showed that the highest exergy destruction rate take placed in solar dish collector, HTR and HEX.

References

Abid, M., Ratlamwala, T.A.H., Atikol, U., (2016). Performance assessment of parabolic dish and parabolic trough solar thermal power plant using nanofluids and molten salts. International Journal of Energy Research, 40, 550–563.

Alrobaian, A.A., (2022). Energy, exergy, economy, and environmental (4E) analysis of a multi-generation system composed of solar-assisted Brayton cycle, Kalina cycle, and absorption chiller. Applied Thermal Engineering, 204, 117988.

Al-Sulaiman, F.A., Atif, M., (2015). Performance comparison of different supercritical carbon dioxide Brayton cycles integrated with a solar power tower. Energy, 82, 61-71.

Angelino, G., (1968). Carbon dioxide condensation cycles for power production. Journal of Engineering for Power, 90 (3), 287–295.

Atif, M., Al-Sulaiman F.A., (2017). Energy and exergy analyses of solar tower power plant driven supercritical carbon dioxide recompression cycles for six different locations. Renewable and Sustainable Energy Reviews. 68, 153-167.

Bejan, A., Moran, M.J., (1996). Thermal Design and Optimization, New York: John Wiley & Sons.

Bellos, E., Korres, D., Tzivanidis, C., Antonopoulos, K.A., (2016). Design, simulation and optimization of a compound parabolic collector. Sustainable Energy Technologies and Assessments, 16, 53–63.

Cao, Y., Li, P., Qiao, Z., Ren, S., Si, F., (2022). A concept of a supercritical CO_2 Brayton and organic Rankine combined cycle for solar energy utilization with typical geothermal as auxiliary heat source: Thermodynamic analysis and optimization. Energy Reports, 8, 322-333.

Cengel, Y.A., Boles, M.A., (2015). Thermodynamics: an Engineering Approach 8th Edition.

Chen, R., Romero, M., Gonzalez-Aguilar, J., Rovense, F., Rao, Z., Liao, S., (2021). Design and off-design performance comparison of supercritical carbon dioxide Brayton cycles for particle-based high temperature concentrating solar power plants. Energy Conversion and Management, 232, 113870.

Cheng, K., Qin, J., Sun, H., Li, Heng, He, S., Zhang S., Bao, W., (2019). Power optimization and comparison between simple recuperated and recompressing supercritical carbon dioxide Closed-Brayton-Cycle with finite cold source on hypersonic vehicles. Energy, 181, 1189-1201.

Dincer, I., Rosen, M.A., (2013). Exergy: Energy, Environment and Sustainable Development.

Dostal, V., (2004). A supercritical carbon dioxide cycle for next generation nuclear reactors. PhD Thesis, Czech Technical University, Mechanical Engineering, 1–317.

Dostal, V., Driscoll, M.J., Hejzlar, P., Todreas, N.E., (2002). A supercritical CO_2 gas turbine power cycle for next-generation nuclear reactors. 10th International Conference on Nuclear Engineering, April 14-18, Virginia.

Du, B.C., He, Y.L., Zheng, Z.J., Cheng, Z.D., (2016). Analysis of thermal stress and fatigue fracture for the solar tower molten salt receiver. Applied Thermal Engineering, 99, 741-750.

Fuqiang, W., Zhennan, G., Jianyu, T., Lanxin, M., Zhenyu, Y., Heping, T., (2016). Transient thermal performance response characteristics of porous-medium receiver heated by multi-dish concentrator. International Communications in Heat and Mass Transfer, 75, 36-41.

Gavagnin, G., Sánchez, D., Martínez, G.S., Rodríguez, J.M., Muñoz, A., (2017). Cost analysis of solar thermal power generators based on parabolic dish and micro gas turbine: manufacturing, transportation and installation. Applied Energy, 194, 108–122.

Khan, M.S, Abid, M., Ali, H.M., Amber, K.P., Bashir, M.A., Javed, S., (2019). Comparative performance assessment of solar dish assisted s-CO_2 Brayton cycle using nanofluids. Applied Thermal Engineering, 148, 295-306.

Kim, Y.M., Lee, Y.D., Ahn, K.Y., (2021). Parametric study of a supercritical CO_2 power cycle for waste heat recovery with variation in cold temperature and heat source temperature, Energies, 14, 6648.

Klein, S.A., (2020). Engineering Equation Solver (EES). F-Chart.

Li, M.J., Zhu, H.H., Guo, J.Q., Wang, K., Tao, W.Q., (2017). The development technology and applications of supercritical CO_2 power cycle in nuclear energy, solar energy and other energy industries. Applied Thermal Engineering, 126, 255-275.

Li, L., Sun, J., Li, Y., (2017). Prospective fully-coupled multi-level analytical methodology for concentrated solar power plants: general modelling. Applied Thermal Engineering, 118, 171-187.

Loni, R., Kasaeian, A.B., Mahian, O., Sahin, A.Z., (2016). Thermodynamic analysis of an organic Rankine cycle using a tubular solar cavity receiver. Energy Conversion and Management 127, 494–503.

Luo, D., Huang, D., (2020). Thermodynamic and exergoeconomic investigation of various SCO_2 Brayton cycles for next generation nuclear reactors. Energy Conversion and Management, 209, 112649.

Ngo, L.C., (2013). Exergetic analysis and optimization of a parabolic dish collector for low power application. Centre for renewable and sustainable energy studies.

Prado, G.O., Vieira, L.G.M., Damasceno, J.J.R., (2016). Solar dish concentrator for desalting water. Solar Energy, 136, 659–667.

Qiu, Y., Li, M.J., Wang, K., Liu, Z.B., Xue, X.D., (2017). Aiming strategy optimization for uniform flux distribution in the receiver of a linear Fresnel solar reflector using a multi-objective genetic algorithm. Applied Energy, 205, 1394–1407.

Reddy, K.S., Veershetty, G., Vikram, T.S., (2016). Effect of wind speed and direction on convective heat losses from solar parabolic dish modified cavity receiver. Solar Energy, 131, 183–198.

Saeed, M., Kim, M.H., (2022). A newly proposed supercritical carbon dioxide Brayton cycle configuration to enhance energy sources integration capability. Energy, 239, 121868.

Turchi, C.S., Ma, Z., Neises, T.W., Wagner, M.J., (2013). Thermodynamic study of advanced supercritical carbon dioxide power cycles for concentrating solar power systems. Journal of Solar Energy Engineering, 135(4), 041007.

UNFCCC, (2015). Adoption of the Paris Agreement. Technical Report UN Framework Convention on Climate Change.

Uusitalo, A., Ameli, A., Turunen-Saaresti, T., (2019). Thermodynamic and turbomachinery design analysis of supercritical Brayton cycles for exhaust gas heat recovery. Energy, 167, 60-79.

Wang, K., Li, M.J., Guo, J.Q., Li, P., Liu, Z.B., (2018). A systematic comparison of different S-CO$_2$ Brayton cycle layouts based on multi-objective optimization for applications in solar power tower plants. Applied Energy, 212, 109–121.

Yang, J., Yang, Z., Duan, Y., (2020). Part-load performance analysis and comparison of supercritical CO$_2$ Brayton cycles. Energy Conversion and Management, 214, 112832.

Zhu, H.H., Wang, K., He, Y.L. (2017). Thermodynamic analysis and comparison for different direct-heated supercritical CO$_2$ Brayton cycles integrated into a solar thermal power tower system. Energy, 140, 144-157.

Assessment of Geothermal Energy Based Combined Power and Ejector Refrigeration Cycle working with R600a

Gamze Soytürk[1*], Serpil Çelik Toker[1], Önder Kizilkan[1]

Abstract: Low temperature heat sources, such as solar energy, geothermal energy, and low temperature waste heat, exist in the world extensively. Most of them cannot be utilized by the conventional power machines efficiently. Recently, many combined power and refrigeration cycles have been proposed to make better use of them. In this paper, a new cooling and power system is presented regarding the important role of combined cooling and power systems in increasing the efficiency of power plants, as well as the ability of organic Rankine cycle (ORC) and ejector refrigeration cycle (ERC) systems to use low to medium grade energy sources. In addition, thermodynamic and parametric analyzes of the system using R600a as the working fluid are made.

Keywords: Organic Rankine Cycle, Ejector Refrigeration Cycle, Geothermal Energy, R600a

1. Introduction

Energy and environmental issues have always been one of the main challenges facing the development of all countries over the world. These problems can be solved by increasing the share of renewable energy and improving the current energy conversion process. Reasonable utilization of renewable energy such as geothermal energy, solar energy, and various waste heat resources is an effective approach to improve process efficiency and reduce fuel consumption. In this regard, many technologies have been proposed to convert low grade heat sources into electrical energy. Among the proposed technologies, the ORC plays an important role in the development of low-grade heat sources [Liu et al., 2019], due to its simple structure, high reliability, flexible automatic control, and wide adaptability of heat sources [Lee et al., 2016]. The ORC's operation is the same as the Clausius Rankine steam power generation unit just exploits organic working fluids rather than water. This comes about in high energy performance and an extensive range of convenience for the energy resources with various temperatures. The idea of the thermodynamically study was established to portray ORC's working criteria for distinctive operating fluid considerations [The European Parliament and the Council of the European Union, 2012]. The investigations of the ORC unit were basically based on first and second laws of thermodynamics for choosing more suitable operating fluids [Bennoua et al. 2015]. Regarding this fact, Parfomak [Parfomak, 2012] analyzed an ORC system that uses organic substance R123 as a harmless unit to the environment, which integrated circulated thermosiphon to a turbine unit. He also performed an analysis of the ORC for the development of working conditions. He deduced from these experiments that the ORC performance noticeably enhances by utilizing R123 as the working fluid. Valverde et al. [Valverde et al.,

---

[1] Isparta University of Applied Sciences, Department of Mechanical Engineering, Isparta/Turkey
* Corresponding author: gamzeyildirim@isparta.edu.tr

2013] discovered that the greatest energy performance of the ORC unit with an internal heat exchanger, binary- regenerative ORC system with an internal heat exchanger, and ORC with the flash-binary could be gotten 17.65, 115.35, and 11.81 percent utilizing R123 as the operating fluid. More works have been carried out to present eco-friendly operating fluids for the organic Rankine cycle in various applications [Zakrisson, 2011]. For instance, Chen et al. [Chen et al., 2015], represented an optimal cost-effective design for the ORC utilizing geothermal heat resources with low temperatures. They assessed the highest efficiency value for the ORC for distinctive operating fluids like ammonia, R123, PF5050, and n-pentane. They also noted that the approach of optimization strategy for temperatures of condenser and evaporator would converge to a specific value.

On the other hand, ERC is highly interested in recent years because of its straightforward configuration, functioning circumstances, and most vital, operating by low-temperature resources. The ejector has been presented as an upgraded refrigeration unit because of its aim that it pursues. With this regard, Chen et al. [Chen et al.,2014] examined the working features of ejector utilizing R245fa, R141b, and R600a as the system's operating fluid. It has been illustrated that the performance of working fluids in ERC varies, whereas R141b represents the maximum coefficient of performance (COP) in comparison with others. Meantime, Ersoy et al. [Ersoy et al.,2007] explored the efficiency of the ejector refrigeration system utilizing R123 as the working fluid and evacuated-tube solar collector as the driving system in Turkey. They determined the highest total COP and cooling output of 0.197 and $-$ 178.26W/m2. In recent studies, the choice of various appropriate operating fluids has been considered to use the positive aspects of the ERC more efficiently. It is illustrated that R134 are presents the highest coefficient of performance for the ERC [Varga et al., 2013]. However, isobutane is suggested as a fascinating selection because of its low fluid inflammability and high COP.

Many works have been done to explore the combined power and refrigeration cycle to utilize the low-grade heat sources, such as industrial water heats, geothermal resources, and solar energy. Zheng and Weng [Zheng and Weng, 2010], offered an integrated power and ERC system based upon a traditional integration of the ERC and ORC utilizing low grade heat resources. In their designed system, the ERC unit was driven using the turbine exhaust to generate power and cooling output at the same time. Energetic and exergetic effectiveness was calculated by 34.1% and 56.8% by using R245fa. Habibzadeh et al. [Habibzadeh et al., 2013] conducted an analysis of the ejector cooling and power hybrid system utilizing R123, R141b, R245fa, R600a, and R601a as working fluids from the energy and exergy viewpoints. It was illustrated that R601a owns the maximum energy efficacy and minimum exergy loss. Moreover, they have represented optimal quantities for the main parameters of the proposed cycle the pump's entering pressure, evaporator temperature, and so on.

The aim of this study is to analyze the geothermal energy sourced integrated system using the first law analyze of two different outputs, namely power, and cooling. In addition, parametric studies have been carried out to examine the effects of source temperature, entrainment rate, extraction rate, turbine inlet pressure, mid pressure, evaporator, and condenser temperature on cycle performance.

2. System Description

Figure 1. schematically shows the integrated power and cooling generation system supported by geothermal energy. The system includes an ORC and an ejector refrigeration cycle. R600a is used as heat transfer fluid in all systems. The working fluid at state 1 as saturated liquid is

pumped to the operating pressure of the vapor generator. Then the working fluid enters the regenerator as compressed fluid in 2 cases, its temperature is increased at constant pressure in the regenerator before entering the boiler. The fluid, whose temperature is increased by absorbing heat in the boiler, expands in the turbine to produce work. The vapor from the turbine exits at state 5 enters the ejector as the primary fluid. The vapor from the evaporator at state 12 is entrained into the ejector as the secondary fluid. The secondary fluid mixes with the primary fluid in the mixing chamber of the ejector at a constant pressure. Then, the mixed liquid at state 13 is sent to the regenerator in state 7 by reducing its temperature and pressure in the expansion valve at constant enthalpy. Fluid leaving the regenerator with flow 8 enters the condenser. After that, the heat transfer fluid is condensed into a liquid to remove excess heat. With flow 9 is divided the condensed liquid into two, which are subsequently transferred to two distinct components. Flow 10 delivers a part of the condensed liquid to the expansion valve. Flow 11 then transports it to the evaporator to gain refrigeration capacity. The liquid R600a which is condensed in the condenser, is then pumped by the pump back into the higher-pressure condition, and the cycle recommences. (With flow 1)
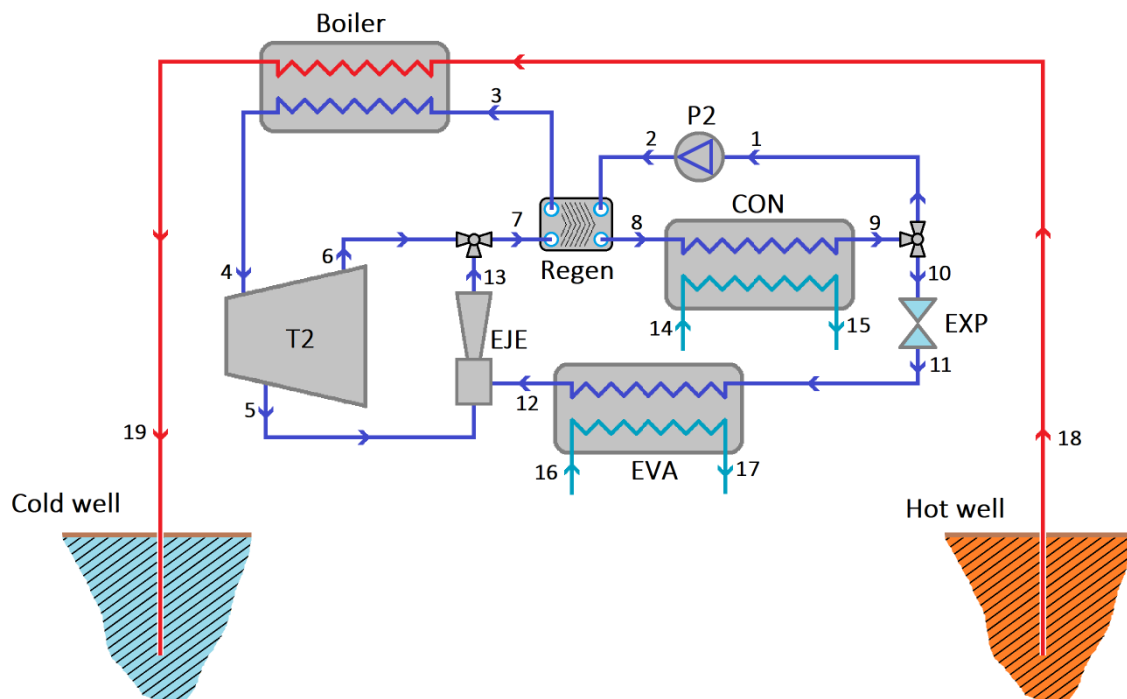

Figure 1. Schematic diagram of R600a based geothermal energy driven combined cycle.

3. Methodology

In this subchapter, a detailed definition of the thermodynamic methodology utilized in this paper is introduced. Energy analyses is performed using the EES (Engineering Equation Software) program for the performance evaluation of the system. In this paper, the thermodynamic analysis is made under the following assumptions:

- The steady-state and steady-flow conditions are chosen for all system elements.
- The energetic change for kinetic and potential energies are neglected.
- The heat losses from pumps and turbine are neglected.
- The pressure drops through the pipelines and heat exchangers are neglected.

In addition, the following assumptions have been made to estimate the performance coefficient in the ejector cooling system:

- The exit of the condenser is at a saturated liquid state.
- The fluid at the exit of the evaporator is in a saturated vapor state.
- The fluid at the exit of the generator is in a saturated vapor state.
- The expansion through the expansion value is a throttling process.
- The mixing process takes place under constant pressure.

For the performance assessment of the solar-driven system the first and second laws of thermodynamics and the principles of conservation of mass are applied to each system element.

The general mass balance equation for steady-state and steady-flow processes can be written as [Çengel, 2015]:

$$\sum \dot{m}_{in} = \sum \dot{m}_{out} \qquad (1)$$

In the above equation, $\dot{m}$ is the mass flow rate, and the subscripts in and out stand for inlet and outlet, respectively. The energy balance equation can be written as [Çengel, 2015]:

$$\dot{Q} + \sum \dot{m}_{in} h_{in} = \dot{W} + \sum \dot{m}_{out} h_{out} \qquad (2)$$

Here, $\dot{Q}$ is the rate of heat, $\dot{W}$ is the rate of work, and h is the specific enthalpy.

The cooling plant's ejector is made up of three components those are mixing chamber, nozzle, and diffuser. The steady-state energy balance of the mainstream for the nozzle component can be described as [Tukenmez et al., 2021]:

$$h_{n1} = h_{n2} + \frac{V_{n2}^2}{2} \qquad (3)$$

The nozzle performance can be determined using the following Equation (4):

$$\eta_{nz} = \frac{h_{n1} - h_{n2}}{h_{n1} - h_{n2,s}} \qquad (4)$$

Based on Equations (3) and (4), the outlet velocity of the primary stream can be determined as:

$$V_{n2} = \sqrt{2\eta_{nz}(h_{n1} - h_{n2,s})} \qquad (5)$$

One of the commonly used parameters will be used herein to characterize ejector performance, namely the '*entrainment ratio (ER)*' [Zhang et.,2016], which is defined as:

$$ER = \frac{\dot{m}_2}{\dot{m}_1} \tag{6}$$

where $\dot{m}_1$ and $\dot{m}_2$ are the inlet mass flowrates of the primary and secondary streams, respectively. The ER is considered a key indicator because it affects the performance of the entire cooling system. Based on this performance indicator, an ejector is desired with the highest possible entrainment and that maintains the highest possible discharged pressure, when operating at given conditions [Zhang et.,2016].

In the turbine, extraction ratio is defined as the extraction mass flow from the turbine divided by the turbine inlet mass flow, given by [Wang et al.,2009]:

$$R_{extr} = \frac{\dot{m}_{extr}}{\dot{m}_T} \tag{7}$$

Where $\dot{m}_{extr}$ is the extracted fluid from the turbine by the state 5 in Figure 1 and $\dot{m}_T$ is the total mass flow rated at the turbine inlet.

3. Results and Discussion

In this study, an integrated geothermal energy driven system is designed to generate power and cooling. At the same time, parametric studies were carried out to examine the effects of source temperature, drift rate, extraction rate, turbine inlet pressure, medium pressure, evaporator, and condenser temperature on cycle performance. The examinations were conducted by EES [Klein, 2022], which can calculate the thermodynamic properties of the fluids. Some assumptions were made to construct the mathematical modeling of the system. The assumed operational parameters of the proposed system are tabulated in Table 1.

Table 1. The assumed operational parameters

Design Parameters	Values
Regenerator effectiveness, ε_{reg}	0.6
Extraction ratio, R_{extr}	0.4
Entrainment ratio, ER	0.77
Isentropic pump efficiency, $\eta_{is,P}$	0.8
Isentropic turbine efficiency, $\eta_{is,T}$	0.82
Geothermal water mass flow rate, $\dot{m}_{geo}$ (kg/s)	20
Pinch point temperature, PP=(°C)	10
Turbine inlet pressure, $P_{high,ORC}$ (kPa)	1800
Turbine mid pressure, $P_{mid,ORC}$ (kPa)	600
Condenser temperature, T_{con} (°C)	30
Evaporator temperature, T_{evap} (°C)	0
Geothermal water inlet temperature, $T_{source,in}$ (°C)	140

In Figure 2, the net power is plotted against geothermal water temperature by varying it from 120 to 160 °C. In addition, energy efficiency is also drawn on the right-hand side of the plot. Increasing the geothermal water temperature has an improving effect on the net power and energy efficiency from the cycle. Because the increase in power and heat capacities obtained from the integrated system directly affects the efficiency positively.
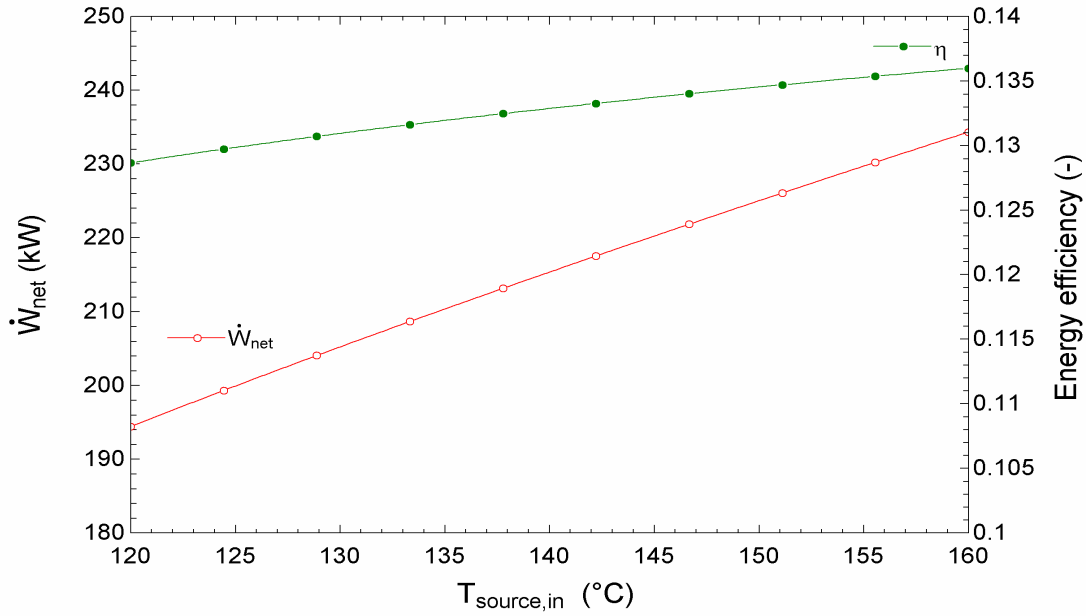
Figure 2. Variation of geothermal water temperature with net power and efficiency ($\dot{Q}_{cooling}$ remains constant at 38.57 kW)

As shown in Figure 3, while the entrainment ratio increases from 0.05 to 0.1, the primary fluid inlet pressure decreases correspondingly. However, the second fluid inlet pressure and the mixed fluid outlet pressure of the ejector do not change. Therefore, the refrigeration capacity increases from 25 to almost 48. Also, the energy efficiency shown on the right side of the axis increases with increasing entrainment ratio.
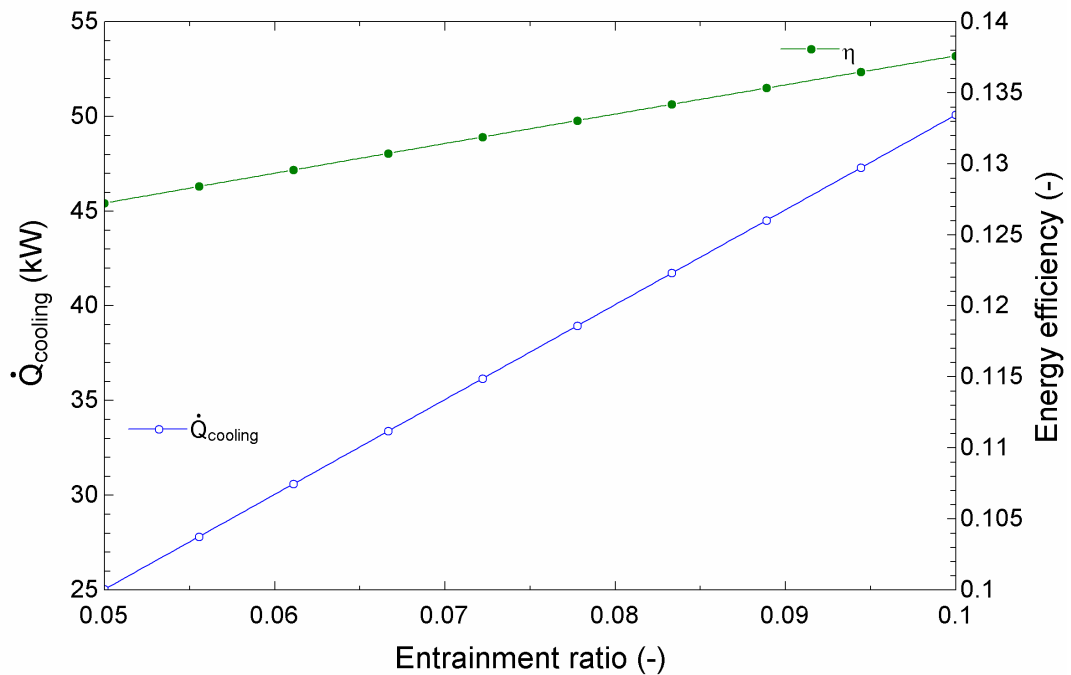
Figure 3. Variation of ejector entrainment ratio with cooling capacity and efficiency ($\dot{W}_{net}$ remains constant at 215.4 kW)

Figure 4 shows the effect of extraction ratio on the net power, refrigeration output and the energy efficiency. It is obvious that the net power decreases, and the refrigeration output increases with increasing extraction ratio. In addition, the energy efficiency increases with increasing extraction ratio.
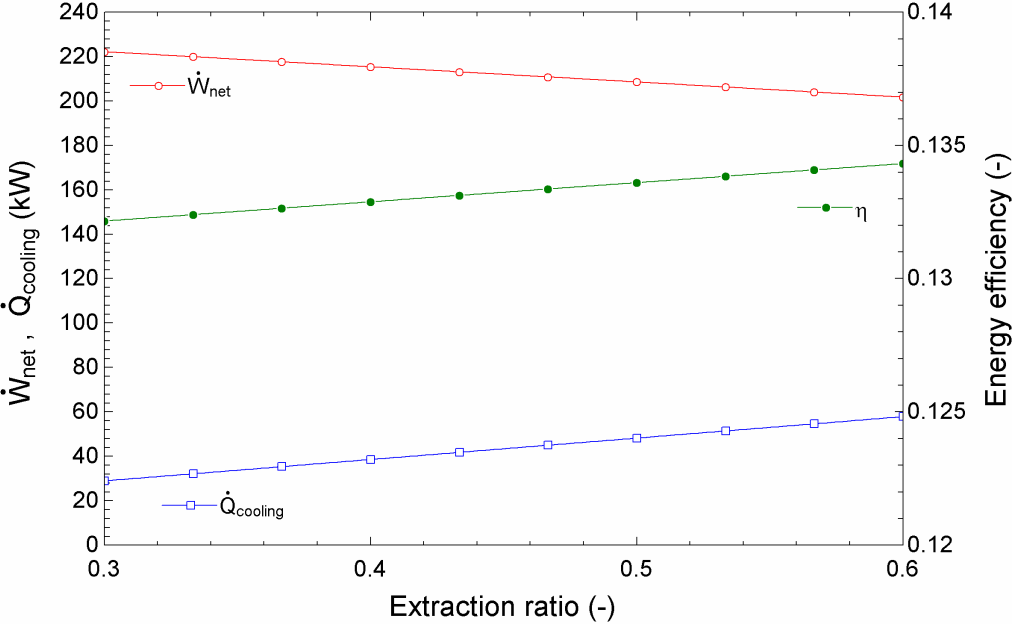

Figure 4. Variation of turbine extraction ratio with net power, cooling capacity and efficiency

Figure 5 shows the effect of turbine inlet pressure on the net power and the energy efficiency. It can be seen from the figure that with the increase of turbine inlet pressure, the net power obtained from the cycle increases. It is known that during the turbine operation, higher pressure ratio results in higher enthalpy change thus, generated power increases. This is why the net power output increases at first. It must be noted that as the turbine inlet pressure increases, the refrigeration capacity remains constant since the turbine inlet pressure does not have any effect on the refrigeration performance. As can be seen from the Figure 1, and Table 1, it is assumed that the refrigeration cycle operates between condenser and evaporator pressures. This means, the higher pressure does not have any effect on condenser and evaporator.
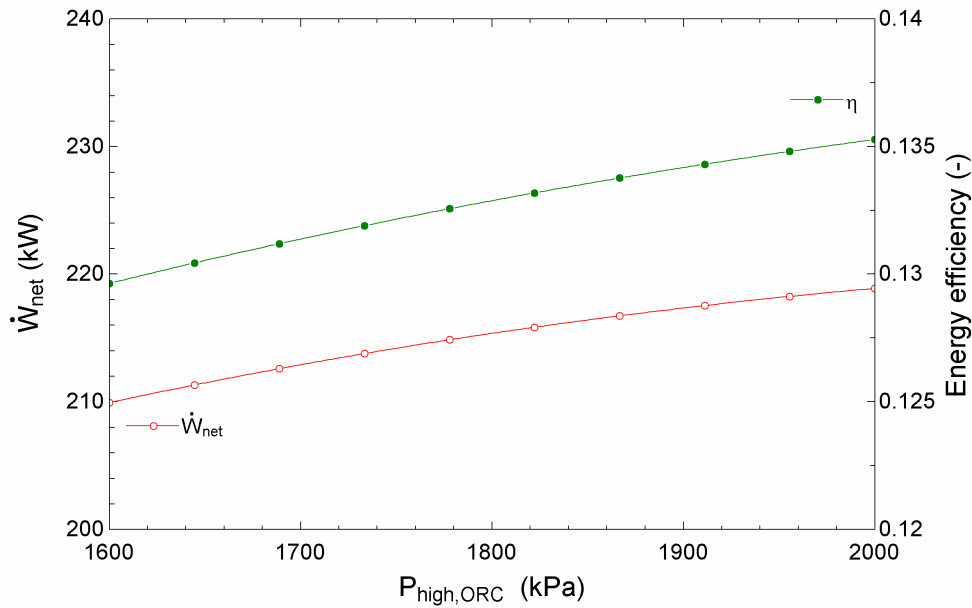
Figure 5. Variation of turbine inlet pressure with net power and efficiency ($\dot{Q}_{cooling}$ remains constant at 38.57 kW)

The effect of mid pressure, which is one of the main operating parameters of the system, on the net power and energy efficiency of the proposed power and cooling generation system is shown in Figure 6. As the plot illustrates, with mid pressure increases, the net power and energy efficiency decreases. The main reason for this is that as the mid pressure increases, the mass flow rate of generated steam for driving steam turbine decreases. Regarding this fact, the energy efficiency decreases while mid pressure increases.
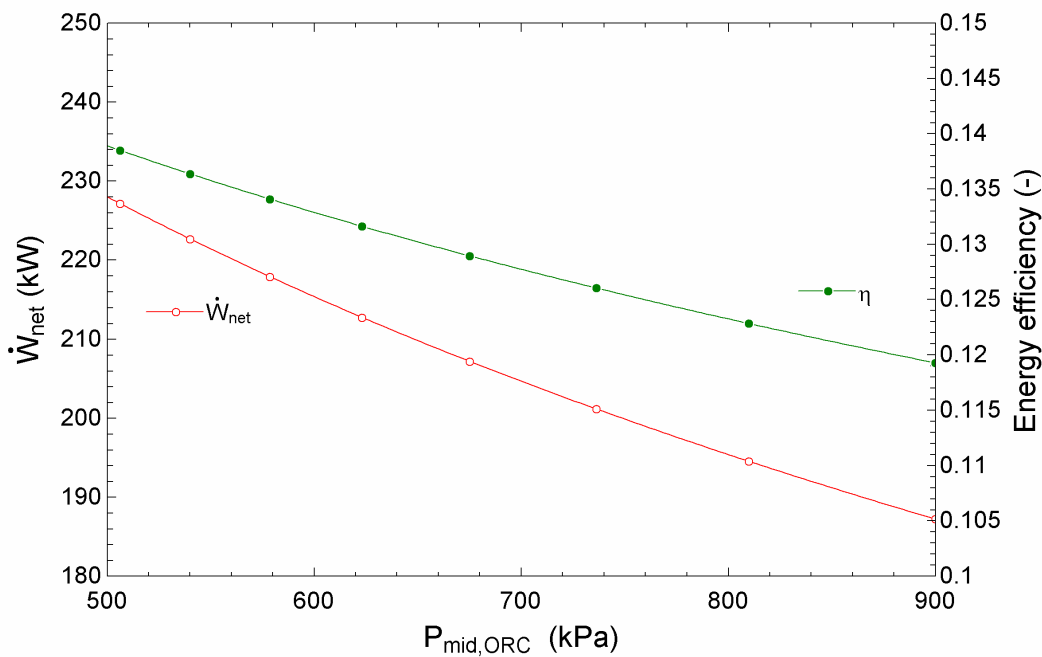

Figure 6. Variation of mid pressure with net power and efficiency ($\dot{Q}_{cooling}$ remains constant at 38.57 kW)

Figure 7 shows the effect of evaporator temperature on the refrigeration output. It is found that the turbine power output does not vary with the increasing evaporator temperature because the turbine inlet state and outlet state are not changed. As the evaporator temperature increases, the refrigeration capacity increases correspondingly. Since the pressure and mass flow rate of the primary flow remain constant, and the secondary mass flow rate increases with the increasing evaporator temperature, the refrigeration capacity of the system also increases.
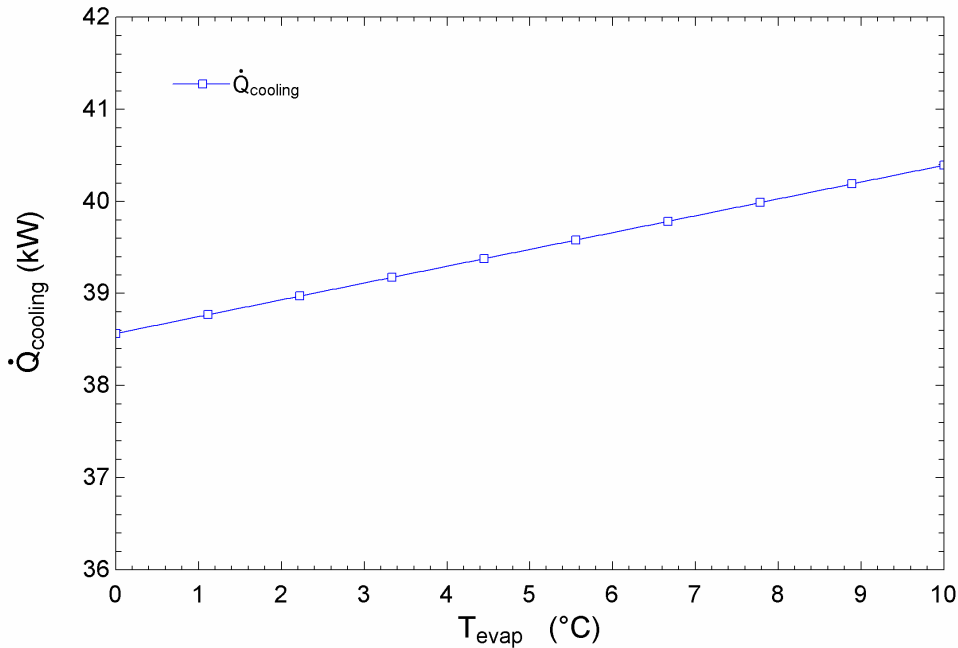

Figure 7. Variation of evaporator temperature with cooling capacity

Figure 8 shows the effect of condenser temperature on the refrigeration capacity. It is evident that the turbine power output decreases with the increasing condenser temperature because the turbine back pressure which influences turbine power output sharply increases with the increasing condenser temperature. It can also be seen that as the condenser temperature increases, the refrigeration capacity decreases. The reason for this is that as the condenser temperature increases, the back pressure on the ejector increases. Thus, the compression ratio (ratio of condenser pressure to evaporator pressure) is increased. With the constant primary vapor velocity, the entrainment of secondary vapor decreases, resulting in a decrease for the refrigeration capacity.
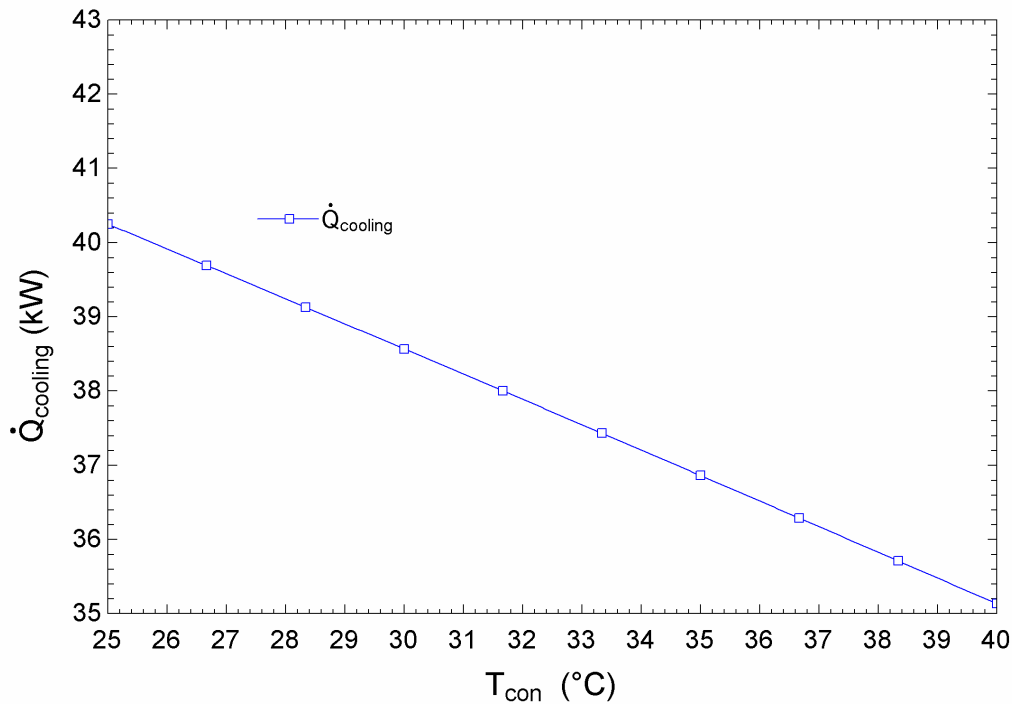
Figure 8. Variation of condenser temperature with cooling capacity

5. Conclusions

In the present study, it is aimed to examine the thermodynamic analysis of a geothermal energy supported integrated system that can produce power and cooling. For this purpose, analyses were carried out for determining the system performance indicators such as net power generation, cooling capacity and energy efficiencies. In addition, parametric studies were carried out to determine the effect of source temperature, entrainment rate, extraction rate, turbine inlet pressure, mid pressure, evaporator, and condenser temperature on system performance. According to the results of the study, the important findings are summarized as follows:

• While the net power generation of the system was calculated to be 215.4 kW, the cooling capacity was calculated to be 38.57 kW in the ejector system.

• The overall energy efficiency of the integrated system was calculated to be 13.2%

• The parametric results showed that, as the source temperature was increased, the net power production and energy efficiency were increased linearly.

• In addition, the increase in ejector entrainment ratio from 0.05 to 0.1 resulted in increase in the cooing capacity and energy efficiency of the integrated cycle.

• As the extraction rate increases from 0.3 to 0.6, energy efficiency and cooling capacity increase while net power decreases.

• As the turbine inlet pressure rises from 1600 kPa to 200 kPa, energy efficiency and net power increase while cooling capacity remains constant.

• The increase in mid pressure from 500 to 900 kPa resulted in decrease in energy efficiency, and net power production.

• As the evaporator temperature was increased, the cooling capacity were increased linearly

• Finally, as the condenser temperature was increased from 25°C to 40°C, the cooling capacity decreased linearly.

References

Bennoua, S., Le Duigou, A., Quemere, M. M., Dautremont, S., (2015). Role of hydrogen in resolving electricity grid issues. International Journal of Hydrogen Energy, 40, 7231-7245.

Chen, Jianyong., Havtun, Hans., Palm, Björn., (2014). Parametric analysis of ejector working characteristics in the refrigeration system. Applied Thermal Engineering, 69(12), 130–142.

Chen, H., Pei, P., Song, M., (2015). Lifetime prediction and the economic lifetime of proton exchange membrane fuel cells. Applied Energy, 142, 154-163.

Çengel, YA, Boles, MA., (2015). Thermodynamics: An Engineering Approach.

Ersoy, H.K., Yalcin, S., Yapici, R., Ozgoren, M., (2007). Performance of a solar ejector cooling-system in the southern region of Turkey. Applied Energy, 84(9), 971–83.
Habibzadeh, A., Rashidi, M.M., Galanis, N., (2013). Analysis of a combined power and ejector refrigeration cycle using low temperature heat. Energy Conversion and Management, 65, 381–391.

Klein, S., (2022). Engineering equation solver (EES). Academic Commercial, V11.199.3D, 2021. F-chart software, Madison, USA.

Lee, HY., Park, SH., Kim, KH., (2016). Comparative analysis of thermodynamic performance and optimization of organic flash cycle (OFC) and organic Rankine cycle (ORC). Applied Thermal Engineering, 100, 680–90.

Liu, C., Wang, S., Zhang, C., Li, Q., Xu, X., Huo, E., (2019). Experimental study of micro-scale organic Rankine cycle system based on scroll expander. Energy, 188, 115930.

Parfomak, PW., (2012). Energy storage for power grids and electric transportation: a technology assessment. Congressional Research Service, 146.

The European Parliament and the Council of the European Union, (2012). Official Journal of the Europen Union http://dx.doi.org/10.3000/19770677.L_2012.315.eng

Tukenmez, N, Koc, M, Ozturk, M., (2021). A novel combined biomass and solar energy conversion-based multigeneration system with hydrogen and ammonia generation. International Journal of Hydrogen Energy, 30, 16319-16343.

Valverde, L., Ali, D., Abdel-Wahab, M., Guerra, J., Hogg, DF., (2013). A technical evaluation of wind hydrogen (WH) demonstration projects in Europe. 4th International Conference on Power Engineering, Energy Electrical Drives, 1098- 1104.

Varga, Szabolcs., Lebre, P.S., (2013). Oliveira Armando C. Readdressing working fluid selection with a view to designing a variable geometry ejector. International Journal of Low-Carbon Technologies, 10(3), 205–215.

Zakrisson E., (2011). The effect of start/stop strategy on PEM fuel cell degradation characteristics. Engineering, Environmental Science.

Zheng, B., Weng, YW., (2010). A combined power and ejector refrigeration cycle for low temperature heat sources. Solar Energy, 84(5), 784–791.

Zhang, K., Chen, X., Markides, CN., Yang, Y., Shen, S., (2016). Evaluation of ejector performance for an organic Rankine cycle combined power and cooling system. Applied Energy, 184, 404-412

Wang, J., Dai, Y., Sun, Z., (2009). A theoretical study on a novel combined power and ejector refrigeration cycle. International Journal of Refrigeration, 32(6), 1186-1194.

Traces of History and Rural Economy for the Enhancement of Buscemi (SR), Italy

Fernanda Cantone[1*], Francesca Castagneto[2]

Abstract: The small municipalities make up about 54% of the Italian territory, but only 17% of the national population lives in these places and it has been calculated that in the inner areas there are 64 inhabitants/Kmq. A characterizing element probably at the base of the low specific weight that these territories manage to have with respect to the priorities assumed by the policy. According to an A.N.C.I. survey on ISTAT data, from 1971 to 2015, 115 municipalities have recorded an exodus of residents of more than 60%. Unemployment is not the only cause of depopulation. It should be stressed that the lack of infrastructure in the area, the absence of welfare and the remoteness of politics are submerged but decisive factors in the process of marginalization.

From these premises was addressed the theme of the redevelopment of the village of Buscemi in the province of Syracuse that with Palazzolo Acreide, Ferla, Cassaro, Buccheri and Canicattini Bagni, is part of the union of the municipalities "Valle degli Iblei", a network set up to promote the development of the local communities that make it up. A redevelopment project that takes on the value of a strategy that goes beyond the limits of urban buildings to enhance and strengthen the roots in the municipal territory and the role in the Iblea network.

Keywords: Urban Rehabilitation, Resilient Communities, Slow Living, Internal Areas, Cultural Heritage

1. Introduction

The small municipalities, settled in fragile territories, are characterized by depopulation and abandonment of the building patrimony, marginalization and reduction of essential services. The causes of these dynamics are countless. First of all, the lack of job opportunities that drives the residents of these small villages to migrate to the cities.

The VIII National Report Small Municipalities edited in 2017 for Legambiente indicates how in small municipalities you count an empty house every two occupied. Fewer inhabitants and older people in a difficult environment. The little attractiveness of these small villages is due to the difficulty of reaching essential services, such as schools and health resorts and in carrying out some work activities, related to intellectual and cultural work in technologically isolated territories. Furthermore, the geographical position of most small municipalities discourages telecommunications operators to offer fast Internet connection services and this determines a digital divide. In this way, countless opportunities are lost for inserting these small villages into many innovative sectors, such as digital craftsmanship, e-commerce and all those activities that need technology.

[1] University of Catania, SDS Architecture, Department DICAR, Syracuse, Italy
[2] University of Catania, SDS Architecture, Department DICAR, Syracuse, Italy
* Corresponding author: fernanda.cantone@unict.it

The recession of 2008, which affected not only Italy but the whole world, has often highlighted the ability of small Italian municipalities to better address the crisis compared to larger municipalities, finding less exposure to the risk of poverty, especially in cases where the whole community has been able to network, innovate and look at sustainability, so much so that they can define these as resilient communities. Resilience means the ability of a system not to adapt to the changes in progress, but to change by designing innovative and effective social, economic and environmental responses that allow it to withstand in the long run external stresses.

Figure 1. Aerial view of Buscemi and an important old building.

In Italy, the SNAI (National Strategy for Internal Areas) is an innovative tool to enhance and protect the values of the built through the sizing and distribution of services. The Strategy therefore applies a new method, imposing a change of culture and a new public action "aimed at people in places" (place-based). This is the crux of the strategy, to bend sectoral public intervention - on health, on school, on mobility - to the specific needs of people in the territories. This is possible only when objectives and actions are conceived and implemented in a participatory way, through a broad comparison between all the public and private subjects. It can increase the tourist vocation, indicated as a driving element of a new organization of local economies. The objective is clearly to respond to depopulation and physical degradation with innovative forms of residency, generally of short and medium duration. Recovery at different scales can also attract new residents interested in both new work patterns and a comfortable urban environment. The Urban Space Project, both public and private, ensures constant levels of use and maintenance as a result of the interventions.

The principles of the Green Economy can orient the use of economic resources allocated in various ways and, in this regard, it seems particularly fitting the statement of Fabrizio Barca: "If you want to revive a territory you do not have to invent strange things. You have to start with what he has. At the same time, you cannot be content for what is there but you must add the flywheel of transformation. You must innovate" (ANCE, 2017). The aim is to transmit the identity of the territory and the possible ways of fruition, to be imagined flexible for the ever more rapid change of needs and social and economic organization. In this sense the design must imagine a new relationship between the local characters and the future perspective.

In the 2017, SNAI introduces new modalities of multilevel governance and promotes the Law n. 158/2017 called "Salva-Borghi" titled «Measures for the support and enhancement of small municipalities, as well as provisions for the redevelopment and recovery of the historic centers of the same municipalities»; it, which was approved in the same year, set up a fund of EUR 100 million to invest in the rehabilitation of small villages.

On September 14th 2021 the Italian Official Gazette published the list of 5518 municipalities that fall under the actions provided for by Law 158/2017 and among them is Buscemi. The objectives that the law sets itself concern mainly interventions of valorization through:

- land maintenance (upgrading of existing buildings and disused areas, measures to reduce hydrogeological risk);
- upgrading of road infrastructure and public buildings (especially schools);

- increasing the energy efficiency of public buildings and the construction of plants for the production and distribution of energy from renewable sources;
- urban redevelopment of old town centres, including for the construction of hotels.

2. Research Objectives

The research intends to propose strategies of requalification through the study and the comparison between the existing planning tools, the initiatives in place, often promoted by local associations, and the objectives of the SNAI and the consequent regulatory provisions (Salva Borghi law, 2017). A comparison of regulatory instruments may highlight the prevailing orientations and highlight inconsistencies and critical issues.

Villages located in inland areas have a number of common characters, although they have differences of single local differences. These are aspects that concern the original settlement methods, the building transformations that have taken place over time, the demographic transformations, the relationship with the territory, the economic and productive development, the quality and morphology of architecture. These aspects are able to describe the existing and constitute a framework of knowledge indispensable to develop proposals adapted to the contemporary. Proposals facing the following problems:
- Accessibility;
- Installation of new functions and morphology of the built;
- Technological adaptation (equipment)
- Protection of the environment and the landscape;
- Public space project;
- Modes of densification.

The research aims to counteract depopulation, to stimulate interest in the territory of Buscemi, to return public space to the community and to create a network between citizens and institutions.

The actions resulting from these objectives concern the limitation of damage from abandonment, the repair of the urban fabric, public space interventions, slow living interventions.
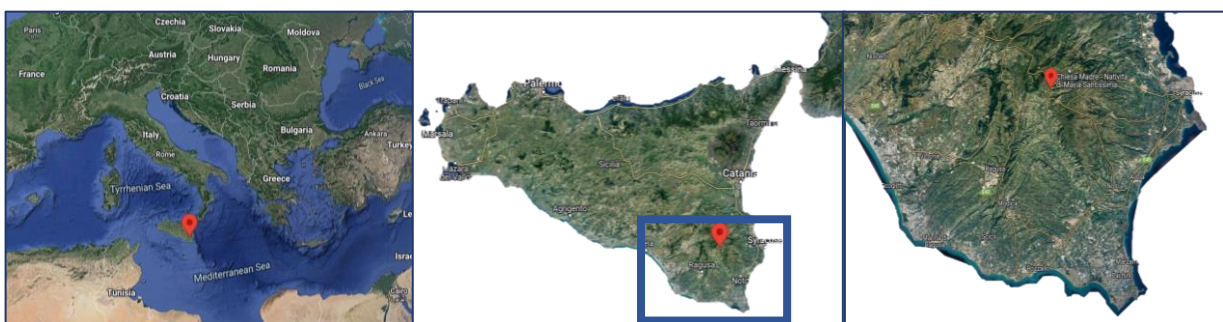
3. Study Case

Figure 2. Territorial framework: Italy, Sicily, district of Syracuse and Buscemi.

Buscemi is a small village 50 kilometers from the capital Syracuse, located on a hill at 760 meters above sea level. Buscemi was founded as a Greek colony in 644 A. C. with the name of Casmene. The term comes from an Arabic word meaning fortress or castle. In more recent times, the first historical sources date back to the Arab domination (827-1091 AD) but in the Norman period (1061-1198) Buscemi had an important fortification, the castle of the Counts Ventimiglia whose structure, today a ruin, is still partially visible. Here, in 1763, was built the convent of the Capuchin Fathers, now abandoned. Before the seventeenth century, Buscemi

stood on Mount S. Niccolò. The catastrophic earthquake of 1693 destroyed the village and caused the death of just under half of the population. Buscemi was rebuilt in another site where today you can admire valuable examples of religious and civil Baroque architecture. Only a part of the medieval site, the one to the northwest and a strip of the southern part, was incorporated into the new urban center. The difference between the old urban area and the central area of the Northeast is still visible in the urban fabric.

Figure 3. Sant'Antonio from Padova Church and Requisenz Building

The new post-earthquake layout consists of two main streets parallel to each other, heading east - west and an orthogonal one, heading north - south, and smaller streets that define a regular urban grid. There are important religious and civil buildings, almost all built after the earthquake of 1693. Eighteenth-century buildings such as Palazzo Italia and Palazzo Requisenz emerge for formal and dimensional baroque characters. Among the religious buildings, the Chiesa Madre, the church of Sant'Antonio da Padova and the church of Carmine were rebuilt after the earthquake.

A speech apart deserves the rupestrian settlements. The prehistoric necropolis on Mount San Nicolò and the quarry of San Giorgio are two important examples of these ancient sites.

Arcosolium tombs, rupestrian churches and cemetery complexes define the Oratory of Saint Peter. It is an important complex built between the fifth and seventh centuries AD; in the following centuries it was annexed to the Benedictine monastery of Santo Spirito. This site is one of the few important Byzantine traces of eastern Sicily.

Figure 4. Requisenz Castle, then Cappuccini Convent

In recent times, the eighteenth-century nucleus of urban center has remained fairly intact even if it appears less defined moving away from the center, due to the orographic irregularity of the site; here "the places of house" are aggregated on levels at different altitudes. Finally, the cementification of the last 30 years has erased the surrounding rural reality, proposing an expansion leaving fortunately enough intact the central core.

The urban development monitoring instrument, the General Development Plan (PRG) is from 2003 and photographs the conditions of the town in the 1990s. It provides recovery plans for the redevelopment of the building stock, accommodation facilities to encourage tourism, a craft area for productive settlements, some areas for public park, equipment and sports facilities, equipment and services of common and social interest. The PRG plans not to further expand the urban area. It also provides for a less serious demographic decline than then occurred, in fact in 2020 the actual number of residents is 997, while the plan provided for 1350. Given the forecasts and the time elapsed since its approval, the PRG appears dated and since 2008 the municipalities have identified new objectives: to combat phenomena of abandonment of the historic center and the agricultural territory, to improve the quality of the settlement and stimulate the participation of the community and care for the public space, multiplying the exchange of ideas and opportunities for retraining.

Figure 5. Buscemi, historical pictures.

3. Results: The research and the project

The research aims to counteract depopulation, to stimulate interest in the territory of Buscemi, to return public space to the community and to create a network between citizens and institutions. It aims to limit the damage caused by the abandonment to places through a series of links that connect the urban fabric of the eighteenth century with the oldest part of the country. In this way, the community will be able to enjoy the benefits of the development of its urban center. Having studied the context, deepened the phase of knowledge, the research proposes strategies of intervention through the construction of a "network", between the actors of the process from the individual citizen to the institutions, on the model of an active citizenship based on social cohesion.

Within this framework, it seems clear that the goal is to counter marginality and depopulation, trying to make Buscemi a place to live.

As said before, the actions must start from what you have, mainly from the ethno-anthropological itinerary called The Places of Peasant Work, that in 2020 was recognized by the Regional Department of Sicilian Cultural Heritage and Identity, Ecomuseum of Regional Interest. In addition to the rural matrix of the territory, the research aims to enhance the traces of the past, the ancient rock settlements, the baroque monuments made during the post-earthquake reconstruction of 1693. These are important pre-existing features that demonstrate the strategic importance of Buscemi in the past.

Figure 6 and 7. Paths of the Ecomuseum.
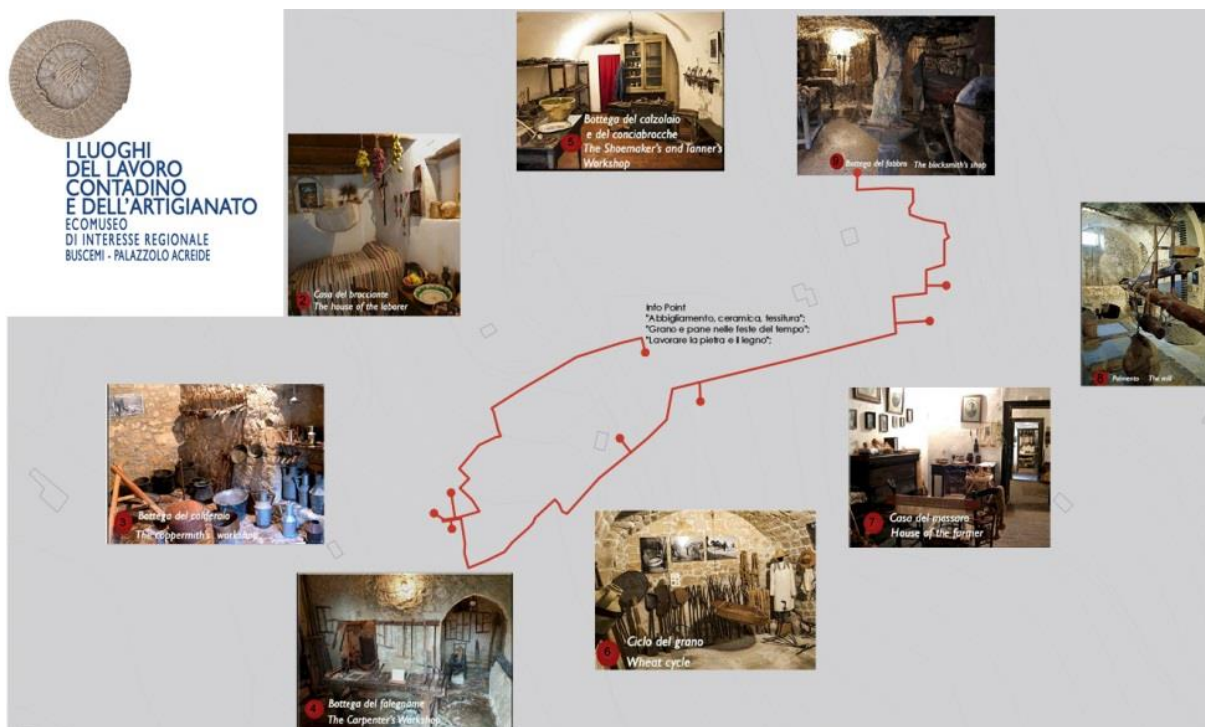
Through its previous intentions, the study proposes interventions in three areas:
• Strengthening of the Ecomuseum;

• Nature and hiking trails;
• Slow living.
The project therefore provides for more general measures:
• Network system between institutions (ecomuseum, new Iblei Park, Gal, etc);
• Restoration and implementation of nature trails and hiking;
• Recovery of the built:
       Historical-rupestrian buildings;
       Residential buildings, multi-buildings hotel (Barbi, 2014);
       rural buildings;
• Redevelopment of built fronts.
The redevelopment project is based on the reading of the settlement system; it recognizes the progressive transformation of the territorial morphology in a residential agglomeration, articulated on terraces and facing south, linked to agricultural land use and craft activities.
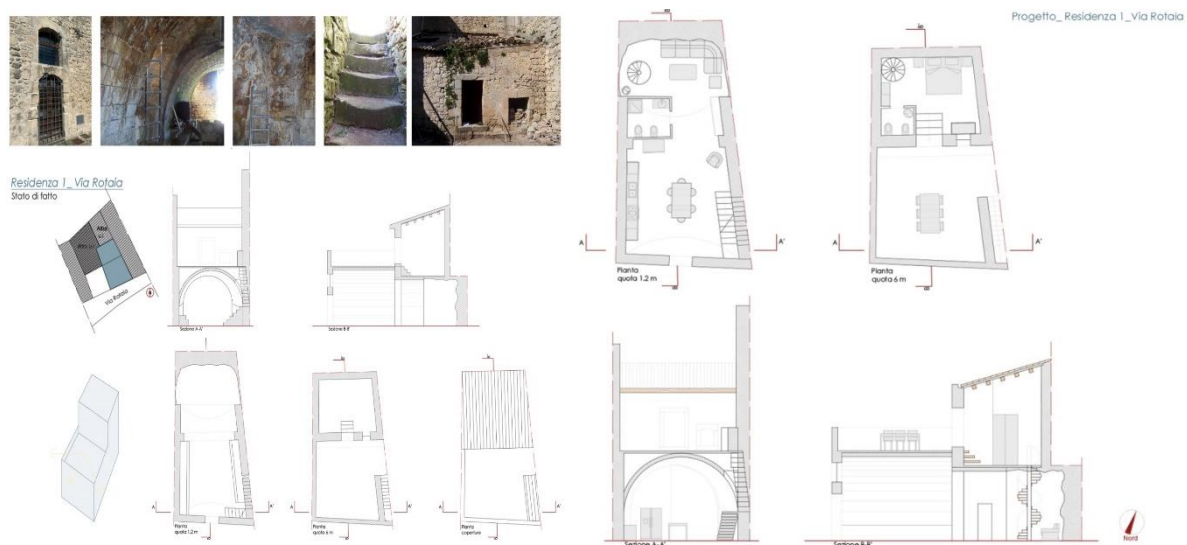

Figure 8. Terraced building unit, survey and project

The different building and architectural structures derive almost entirely from the transformation and the extension in height of shelters in the cave and have given rise to aggregated housing models in a row of two or three floors, with openings on the road in front, internal or external staircase, wooden floors. The types with the greatest development in height, deriving from the aggregation of different building units, have entrances also on the upper road. The recovery of these houses is based on the conservation of the original morphology and on the elimination of inconsistent superfetazioni. The goal is to reconfigure the original urban skyline. The residential function can be maintained and enhanced as a form of housing also temporary (short - medium term), which can meet the needs of sustainable tourism (Multi-building hotel) and innovative forms of work (smart working). In particular, the Ecomuseum is one of the most attractive, if not the only, elements for tourism in Buscemi. Considering the fact that the itinerary crosses the historic center, you can think of strengthening it by including new paths, thus succeeding in telling and making known the reality of Buscemi baroque age.
The idea of symbiosis between man and nature, is the basis of the creation of nature trails and hiking. Starting from the ancient history of the place and the morphology of the territory you can imagine to reactivate the old rural paths, still present in the collective memory, for the tourist use of the territory.

4. Discussion and Conclusions

Through the design of the individual areas, this complex and stratified historical frame highlights identities and differences, redefines public space and concretely traces paths of fruition of the territory. In essence, the historical-cognitive process and the pre-existing elements become the response to depopulation, the economic crisis and marginalization.
The Project in fact connects past and present, restores the right cultural values and enhances the heritage.
The interventions on the construction scale offer different models inspired by Slow Living: the residences designed for long periods and the possibility of a multi-building hotel are the elements to focus on. Bringing to light the original houses, typical of the rural reality of Buscemi, offers the opportunity to live rural life maintaining all the standards of quality of life today.

Figure 9. Three floors building unit, survey and project.

From the point of view of the protection of architectural heritage, the restoration, conservation and recovery of valuable building heritage offers new opportunities for use, interest, life.
Today's pandemic and emergency situation has opened the doors to a new possibility of work, the Smart Working, a strong point for municipalities like Buscemi that, adapted technologically with broadband connections, can attract those who want to change their lifestyle, without changing jobs. The recovery and redevelopment hypothesis finds in the principles of slow living and green economy the conceptual references: residences designed for long periods and the possibility of a multi-building hotel are elements to focus on.

Acknowledgements

References

ANCE, (2017). I borghi d'Italia: dalla visione alla rigenerazione, https://www.ance.it/docs/docdownload.aspx?id=41557, Roma, Italy.

Barbi, C., (2014). L'albergo diffuso: a proposito di Partenariato pubblico-privato nel settore turistico. In Queste Istituzioni, 146/147, 33-46, Italy.

Calzati, V., (2016). Nuove pratiche turistiche e slow tourism. Il caso della Valnerina in Umbria, Collana Sociologia urbana e rurale, Milano: Franco Angeli Editore, Italy.

Celata, F., (2022). Overtourism and online short-term rental platforms in Italian cities. In Journal of sustainable tourism Vol. 30 N. 5, 1020-1039, Taylor & Francis, England.

Çiğdem K. A. et al. (2020). Land use suitability analysis of rural tourism activities: Yenice, Turkey," Tourism Managment, 76, Amsterdam: Elsevier, Netherland.

Delarge, A. and Ministère de la Culture, (2018). Le musée participatif. L'ambition des écomusées. Paris: La documentation Française, France.

Feng, J. (2020). Tourism-induced landscape change along China's rural-urban fringe: a case study of Zhangjiazha. Asia Pacific journal of tourism research, Vol. 25, n. 8, 914-930, Taylor & Francis, England.

Fuggetta, A., (2020). Il paese innovatore. Un decalogo per reinventare l'Italia. Milano: Egea, Italy.

Italy Law of 2017, October 6th, n. 158 (c.d. Law Small municipalities or Save villages)

Orsini, F., (2016). Perduto nella transizione. Lo spazio aperto nell'edilizia sociale: tra annotazioni di suolo e strategie di rigenerazione", in Eutopia urbana edited by Barbara Angi. Siracusa: LetteraVentidue, Italy.

Villani, T. and Dall'Ara, G., (2015). "L'Albergo Diffuso come modello di ospitalità originale e di sviluppo sostenibile dei borghi", Techne 10, Italy.